



# Natural Organic Matter Fouling of Low-Pressure Membrane Systems

Subject Area:  
High-Quality Water





---

# **Natural Organic Matter Fouling of Low-Pressure Membrane Systems**



## **About the Awwa Research Foundation**

The Awwa Research Foundation (AwwaRF) is a member-supported, international, nonprofit organization that sponsors research to enable water utilities, public health agencies, and other professionals to provide safe and affordable drinking water to consumers.

The Foundation's mission is to advance the science of water to improve the quality of life. To achieve this mission, the Foundation sponsors studies on all aspects of drinking water, including supply and resources, treatment, monitoring and analysis, distribution, management, and health effects. Funding for research is provided primarily by subscription payments from approximately 1,000 utilities, consulting firms, and manufacturers in North America and abroad. Additional funding comes from collaborative partnerships with other national and international organizations, allowing for resources to be leveraged, expertise to be shared, and broad-based knowledge to be developed and disseminated. Government funding serves as a third source of research dollars.

From its headquarters in Denver, Colorado, the Foundation's staff directs and supports the efforts of more than 800 volunteers who serve on the board of trustees and various committees. These volunteers represent many facets of the water industry, and contribute their expertise to select and monitor research studies that benefit the entire drinking water community.

The results of research are disseminated through a number of channels, including reports, the Web site, conferences, and periodicals.

For subscribers, the Foundation serves as a cooperative program in which water suppliers unite to pool their resources. By applying Foundation research findings, these water suppliers can save substantial costs and stay on the leading edge of drinking water science and technology. Since its inception, AwwaRF has supplied the water community with more than \$300 million in applied research.

More information about the Foundation and how to become a subscriber is available on the Web at **[www.awwarf.org](http://www.awwarf.org)**.

# Natural Organic Matter Fouling of Low-Pressure Membrane Systems

Prepared by:

**Jim Lozier and Lisa Cappucci**

CH2M HILL , 2625 South Plaza Drive, Suite 300, Tempe, AZ 85282

**Gary Amy**

UNESCO-IHE, 2601 DA Delft, The Netherlands

**NoHwa Lee**

University of Colorado, Boulder, CO 80309

**Joe Jacangelo, Haiou Huang, and Thayer Young**

Johns Hopkins University, Baltimore, MD 21205

**Chandra Mysore, Christophe Emeraux, and Jeremie Clouet**

Veolia Water North America, Norcross, GA 30092

**Jean-Philippe Croué**

University of Poitiers, 86022 Poitiers, France

and

**Bas Heijmann**

Kiwa Water Research, Nieuwegein, The Netherlands

Jointly sponsored by:

**Awwa Research Foundation**

6666 West Quincy Avenue, Denver, CO 80235-3098

and

**U.S. Environmental Protection Agency**

Washington, D.C.

Published by:



Distributed by:



## **DISCLAIMER**

This study was jointly funded by the Awwa Research Foundation (AwwaRF) and the U.S. Environmental Protection Agency (USEPA) under Cooperative Agreement No. R-82967901. AwwaRF and USEPA assume no responsibility for the content of the research study report in this publication or for the opinions or statements of fact expressed in the report. The mention of trade names for commercial products does not represent or imply the approval or endorsement of either AwwaRF or USEPA. This report is presented solely for informational purposes.

Copyright © 2008  
by Awwa Research Foundation

**ALL RIGHTS RESERVED.**  
No part of this publication may be copied, reproduced  
or otherwise utilized without permission.

ISBN 978-1-60573-007-3

Printed in the U.S.A.



Printed on recycled paper

# CONTENTS

LIST OF TABLES .....	ix
LIST OF FIGURES .....	xv
FORWARD.....	xxv
ACKNOWLEDGMENTS .....	xxvii
EXECUTIVE SUMMARY .....	xxix
CHAPTER 1 INTRODUCTION, BACKGROUND, AND OBJECTIVES.....	1
Background.....	1
Research Approach.....	2
Research Objectives.....	2
Report Organization.....	3
CHAPTER 2 LITERATURE SURVEY.....	5
Characteristics of Natural Organic Matter.....	5
Effects of NOM on Membrane Fouling.....	6
The Basics of Membranes.....	7
Mechanisms of Membrane Fouling.....	8
Membrane Characterization.....	9
CHAPTER 3 EXPERIMENTAL METHODS AND PROCEDURES.....	11
Source Waters.....	11
Identities and Rationale for Selection.....	11
Pre-Filtration Step.....	12
Membranes.....	12
Flat-sheet Membranes.....	12
Hollow-Fiber Membranes.....	13
Water Quality Characterization.....	15
Natural Organic Matter.....	15
General, Inorganic, and Microbial Compounds.....	18
Membrane Characterization and Morphology.....	18
Scanning Electron Microscopy.....	22
Streaming Potential.....	22
Contact Angle Measurement.....	24
Atomic Force Microscopy.....	25
Pyrolysis – Gas Chromatography/Mass Spectrometry.....	25
Membrane Foulant Characterization.....	26
Dissolved Organic Carbon and Total Nitrogen Analyses.....	26
High-Pressure Size-Exclusion Chromatography/Ultraviolet Analysis.....	27
Fourier Transformed Infrared Analyses.....	27
Pyrolysis Gas Chromatography/Mass Spectrometry.....	27

Thermochemolysis Gas Chromatography/Mass Spectrometry .....	28
Membrane Testing .....	28
Bench-Scale Simulations .....	30
Pilot Units .....	39
Full-Scale Plants .....	76
Unified Modified Fouling Index Concept.....	80
Concept .....	80
Calculation and Utility of UMFI.....	81
 CHAPTER 4 FEED WATER CHARACTERISTICS AND MEMBRANE PROPERTIES .....	 85
Feed Water Characteristic.....	85
Membrane Properties .....	90
Flat-Sheet (Disk) Specimens.....	90
Virgin Membrane Hollow-Fiber Characterization.....	91
 CHAPTER 5 BENCH-SCALE MEMBRANE FILTRATION RESULTS .....	 103
Stirred-Cell Unit Tests .....	103
Hollow-Fiber Quality Control Tests .....	121
Effect of Pre-filtration on Fouling Rate .....	121
Effect of storage time on the fouling rate (pre-filtered samples).....	122
Effect of storage time on fouling rate (unfiltered samples) .....	123
Hollow-Fiber Unit 1.....	124
Baseline Study Results.....	124
Special Testing.....	137
Characterization of Fouled Membrane Fibers .....	148
Hollow-Fiber Unit 2.....	152
Comparison of fouling rate of Membrane C on different source waters .....	153
Comparison of fouling rate of different membranes on Twente Canal water .....	153
Impact of coagulation on fouling rate – Membrane C .....	154
Impact of changing source quality on fouling .....	156
DOC characterization.....	157
Conclusions.....	160
Integration of Bench-Scale Results via UMFI Concept .....	161
 CHAPTER 6 PILOT- AND FULL-SCALE MEMBRANE FILTRATION RESULTS .....	 163
Tier 1 Pilot Studies.....	163
Tampa Bay Pilot Study .....	163
Indianapolis Pilot Study.....	172
Scottsdale Pilot Study .....	195
Vitens Pilot Study .....	207
Tier 2 Pilot Studies.....	216
Tuscaloosa.....	216
Minneapolis.....	218
North Bay.....	222
Full-Scale Results .....	225
Parsons, Kansas.....	225

Manitowoc .....	226
Characterization of Fouled Fibers from Pilot- and Full-Scale Modules.....	227
Morphology of Fouled Pilot- and Full-Scale Membrane Fibers.....	227
Contact Angle of Fouled Pilot- and Full-Scale Membranes.....	229
AFM of Fouled Pilot- and Full-Scale Membranes .....	231
Characterization of Foulant from Fouled Pilot- and Full-Scale Membrane Modules.....	233
Integration of Pilot- and Full-Scale Results via the UMFI Concept.....	249
 CHAPTER 7 SYNTHESIS AND INTEGRATION OF ALL RESULTS.....	 251
Statistical Analyses .....	251
Correlation Matrices .....	251
Probability Frequency Distribution Diagrams .....	256
Multiple Linear Regression Equations.....	257
Principal Component Analysis .....	259
Scale-Up Via UMFI Concept.....	267
Matched Pair Data Analysis: Stirred-cell versus Bench-Scale Hollow-Fiber Tests .....	267
Matched Pair Data Analysis: Bench-Scale Hollow-Fiber versus Pilot Tests .....	269
 CHAPTER 8 SUMMARY AND APPLICATION TO UTILITIES.....	 271
Summary of Project Results.....	271
Feed Water Characteristics .....	271
Membrane Properties .....	272
Unified Modified Fouling Index Concept.....	272
Bench-Scale Membrane Filtration Tests.....	273
Pilot-Scale Testing and Full-Scale Plant Operations .....	275
Membrane Autopsies .....	278
Statistical Analyses .....	278
Simple Linear Correlation/Correlation Matrices .....	279
Probability Frequency Distributions .....	279
Multiple Linear Regression.....	279
Principal Component Analysis .....	279
UMFI Comparability and Scale-Up.....	280
Stirred-Cell versus Hollow-Fiber Bench-Scale Results.....	280
Hollow-Fiber Bench-Scale versus Pilot-Scale Results .....	281
Application to Utilities.....	281
Applications Potential.....	282
Recommendations for Future Research .....	282
What is the Take Home Message?.....	282
What is/are the problematical NOM foulant(s)?.....	283
What is the NOM-related fouling potential of different types of waters? .....	283
Which foulant(s) contribute(s) to hydraulically reversible versus irreversible fouling? .....	283
Which foulant(s) contribute(s) to chemically reversible versus irreversible fouling? .....	284

How do membrane properties affect fouling? .....	284
What pretreatment options can reduce NOM fouling? .....	284
How do membrane operating conditions affect NOM fouling? .....	284
APPENDIX: PROJECT DATABASE .....	285
REFERENCES .....	287
ABBREVIATIONS .....	293

## TABLES

3.1	Source (feed) waters: tier location and name.....	11
3.2	Characteristics of flat-sheet membranes used in the stirred-cell unit .....	13
3.3	Characteristics of hollow-fiber membranes used in bench- and Tier 1 pilot-scale Testing.....	14
3.4	Membrane products and their characteristics – Tier 2 pilot studies and full-scale Plants.....	14
3.5	In-plant water quality analyses – Tier 1 pilot studies .....	16
3.6	Inorganic parameters and associated analytical methods .....	19
3.7	Specific pyrolysis fragments of biopolymers considered in this study.....	28
3.8	Location and testing matrix .....	29
3.9	Membrane and foulant characterization matrix .....	29
3.10	Operational fluxes for baseline testing, all values given as $L/m^2 \cdot hr$ .....	34
3.11	Number of runs performed for each time-dose combination in the CT experiments .....	35
3.12	Characteristics of the Hollow-Fiber Unit 2 membrane module.....	38
3.13	Coagulation experimental matrix.....	38
3.14	Experimental conditions for Hollow-Fiber Unit 2 testing .....	38
3.15	Experimental matrix for Hollow-Fiber Unit 2 testing .....	39
3.16	General raw water quality characteristics.....	41
3.17	Characteristics of the Membrane B module.....	44
3.18	Tampa Bay pilot study experimental matrix.....	45
3.19	Monitored water quality parameters and process locations.....	46
3.20	Schedule of sampling for NOM characterization .....	47
3.21	General White River raw water quality characteristics (2004 average).....	48
3.22	Characteristics of the Membrane A module .....	50

3.23	Indianapolis pilot study experimental matrix .....	55
3.24	Monitored water quality parameters and sampling frequencies .....	56
3.25	Schedule of the sampling for NOM characterization .....	57
3.26	Schedule of fiber collection .....	57
3.27	Representative quality for tertiary effluent from Scottsdale Water Campus .....	58
3.28	Characteristics of Membrane D1 module .....	60
3.29	Scottsdale pilot study experimental matrix .....	62
3.30	Water quality parameters monitored during testing.....	62
3.31	NOM characterization sample collection.....	63
3.32	Membrane characteristics of Xiga membrane module (UFCM5) (Membrane C).....	67
3.33	Vitens pilot study experimental matrix.....	69
3.34	Membrane characteristics .....	70
3.35	Pilot system operating conditions for runs analyzed in study.....	72
3.36	NOM characterization sample collection.....	72
3.37	Characteristics of Ionics/Norit X-Flow S225 module .....	74
3.38	Operating conditions for Minneapolis pilot study .....	74
3.39	Characteristics of Siemens MEMCOR CMF-s module.....	76
3.40	Representative Labette Creek water quality .....	77
3.41	Lake Michigan water quality (Manitowoc WTP).....	79
3.42	CMF membrane module characteristics .....	80
3.43	Explanation of the various types of fouling indices used in this report.....	83
4.1	XAD 8/4 resin fractionation.....	85
4.2	Water quality data for bench- and pilot-scale source (feed) waters.....	89
4.3	Additional water quality data for pilot-scale source (feed) waters .....	90

4.4	Characteristics of flat-sheet membranes used in stirred-cell units.....	91
4.5	Physical characteristics of the hollow-fiber membranes .....	92
4.6	Contact angle and surface roughness of the hollow-fiber membranes .....	96
4.7	Roughness (Ra and Rq [RMS]) of the virgin hollow-fiber membranes .....	96
4.8	Streaming potential (SP) and isoelectric point (IEP) of the PVDF and PES Membranes.....	99
5.1	Initial water permeability or specific flux ( $J_{S0}$ ) and feed pressure for stirred-cell filtration tests .....	103
5.2	DOC, UVA <sub>254</sub> , and SUVA values in membrane filtration.....	111
5.3	Normalized flux, $J/J_0$ , and UMFI of each water source with various membrane Filtrations .....	112
5.4	Predominant fouling mechanisms in stirred-cell filtration tests .....	116
5.5	DOC levels of SEC chromatogram NOM fractions (polysaccharides, humic substances, and low molecular weight acids) for stirred-cell filtration tests as calculated by peak integration .....	119
5.6	Correlation of determination ( $r^2$ ) values obtained in the calculation of UMFI for each fouling experiment .....	125
5.7	PS-DOC levels (mg/L) from SEC-DOC chromatogram for Hollow-Fiber Unit 1 filtration tests as calculated by peak integration.....	138
5.8	Collected fouling indices for single- and multi-cycle experiments .....	147
5.9	Contact angle of hollow fibers measured after fouling tests.....	148
5.10	Modification of the roughness (Ra and Rq [RMS]) of Membrane A after filtration of the Scottsdale tertiary effluent and White River water.....	149
5.11	Modification of the roughness (Ra and Rq [RMS]) of Membrane B after filtration of the Scottsdale tertiary effluent and White River water.....	150
5.12	Streaming potential and IEP of Membrane A and B bench-scale fouled modules.....	151
5.13	Iron dose, fouling slope calculated from <a href="#">Figure 5.47</a> , and pH .....	155
6.1	Operating conditions for Runs 1, 2, and 3: baseline run and runs with variable backwash conditions .....	164

6.2	Source water quality parameters during Runs 1, 2, and 3 .....	164
6.3	Operating conditions for Runs 1, 4, 5, and 9: baseline run and runs with chemical wash .....	166
6.4	CT conditions for Run 9 chemical washes .....	166
6.5	Source water quality data for Runs 1, 4, 5, and 9 .....	167
6.6	Operating conditions for Runs 1, 6, 7, and 8: impact of coagulation .....	168
6.7	Source water quality data for Runs 6, 7, and 8 .....	169
6.8	Distribution of DOC and NOM fractions in feed, permeate, and backwash sample collected during Runs 1 and 7.....	172
6.9	Source water quality data during Runs 1, 2, and 3 .....	174
6.10	Source water quality data for Runs 1, 4, 5, and 6 .....	176
6.11	J <sub>SO</sub> recovery resulting from different chemical washes.....	178
6.12	Full-scale plant clarification conditions used during Run 8 .....	179
6.13	Source water quality data for Runs 1, 7a, 7b, 7c, and 8.....	180
6.14	Full-scale water treatment plant clarification conditions during Runs 8, 9, and 10 .....	181
6.15	Source water quality data for Runs 8, 9, and 10 .....	182
6.16	Full-scale water treatment plant clarification conditions for Runs 8, 11, 12, 13, and 17.....	183
6.17	Source water quality data for Runs 8, 11, 12, 13, and 17 .....	185
6.18	Specific flux recovery from different chemical wash regimes .....	186
6.19	Full-scale water treatment plant clarification conditions for Runs 8, 9, and 10 .....	188
6.20	Source water quality data for raw and clarified White River (Indianapolis) water - Runs 1, 2, 3, 8, 9, and 10.....	189
6.21	Full-scale water treatment plant clarification conditions for Runs 11, 12, and 13 .....	191
6.22	Source water quality data for raw and clarified White River (Indianapolis) water - Runs 4, 5, 6, 11, 12, and 13.....	191

6.23	Distribution of DOC and NOM fractions in feed, permeate, and backwash samples collected during Runs 1 and 7A.....	194
6.24	Feed water quality data for Runs 1 and 2 .....	197
6.25	Feed water quality data for Runs 1 and 3 .....	199
6.26	Feed water quality data for Runs 1, 5, and 6 .....	201
6.27	Feed water quality data for Runs 1, 7, 8, and 9 .....	203
6.28	CT Conditions for Run 12.....	204
6.29	Distribution of DOC (mg/L) and NOM fractions in permeate and backwash samples during baseline and coagulation runs.....	208
6.30	First series of data collected from samples taken from the pilot on September 17, 2006 .....	212
6.31	First series of data collected from samples taken from the pilot on September 26, 2006 .....	213
6.32	Different cleaning steps in relation to the components they remove from the Membrane .....	215
6.33	NOM characteristics for Membrane B samples.....	218
6.34	DOC and NOM SEC-DOC fractions for Mississippi River water and UF feed .....	222
6.35	XAD-8/-4 fractions for Mississippi River water and UF feed.....	222
6.36	DOC and NOM SEC-DOC fractions for North Bay pilot water samples .....	224
6.37	Contact angle of fouled membrane fibers from pilot-scale testing.....	230
6.38	Roughness parameters (Ra and Rq) of fouled Membrane A fibers operated on White River water (Indianapolis).....	232
6.39	Roughness parameters (Ra and Rq) of fouled Membrane D1 fibers operated on Scottsdale effluent.....	233
6.40	Carbon and nitrogen content of foulants isolated from fouled fibers during pilot-scale full-scale testing.....	234
7.1	Nomenclature of parameter abbreviations used in statistical analyses.....	252
7.2	Correlation matrix (r values) for stirred-cell test data .....	253

7.3	Correlation matrix (r values) for Hollow-Fiber Unit 1 test data.....	254
7.4	Correlation matrices (r values) for pilot test data .....	255
7.5	Comparison of UMF <sub>I</sub> corresponding to 50 percentile and 90 percentile cumulative frequencies .....	257

## FIGURES

3.1	Schematic diagram of XAD-8/-4 resin fractionation.....	16
3.2	Typical EEM spectra (left: humic acid, right: protein).....	17
3.3	Hollow-fiber pilot-scale unit used for streaming potential measurements.....	23
3.4	Determination of the isoelectric point of Membrane D2.....	23
3.5	Contact angle equipment and method.....	24
3.6	Material isolated from Membrane A.....	26
3.7	Dead-end, stirred-cell filtration unit.....	30
3.8	Mini-module potted with membrane fibers supplied by the manufacturer.....	31
3.9	Hollow-Fiber Unit 1.....	32
3.10	Hollow-Fiber Unit 2.....	36
3.11	Direction of flow through Hollow-Fiber Unit 2 for both operational modes.....	37
3.12	Schematic of the Tampa Bay Regional Water Treatment Plant.....	41
3.13	Membrane B pilot unit process schematic.....	42
3.14	Membrane B pilot unit as installed at the Tampa Bay Regional Water Treatment Plant.....	43
3.15	Membrane B module.....	43
3.16	The White River upstream of the intake.....	48
3.17	Schematic of the Indianapolis White River Water Treatment Plant.....	49
3.18	Membrane A module (end view and fiber bundle).....	49
3.19	Process schematic of the Indianapolis pilot unit.....	51
3.20	Indianapolis pilot unit.....	51
3.21	Schematic of the Indianapolis pilot setup while working with clarified water.....	52
3.22	Indianapolis pilot unit treating clarified water.....	53

3.23	Scottsdale pilot unit.....	59
3.24	Scottsdale pilot unit schematic.....	60
3.25	Quality characteristics of Twente Canal feed water .....	64
3.26	Twente Canal pilot unit.....	66
3.27	Process and instrumentation diagram for the Twente Canal pilot unit.....	67
3.28	Pall MF pilot system schematic (Tuscaloosa) using Membrane E.....	71
3.29	Simplified process schematic for CMF-s pilot unit (Tuscaloosa) using Membrane .....	71
3.30	Zenon ZeeWeed 1000 pilot system (Tuscaloosa) using Membrane B.....	73
3.31	Ionics/Norit X-Flow pilot unit schematic (Membrane C).....	74
3.32	Process flow diagram for full-scale Pall Microza MF system at Parsons, Kan.....	77
3.33	Pall Microza MF skids as installed at Parsons, Kan.....	78
4.1	HPSEC-DOC/UV of feed (source) waters (I).....	86
4.2	HPSEC-DOC/UV of feed (source) waters (II) .....	87
4.3	EEM spectra of source waters.....	88
4.4	FESEM image of the Membrane D1 PES/PVP fiber.....	92
4.5	FESEM images of the outer surface of the five membrane fibers used in bench and Tier 2 pilot studies.....	93
4.6	FESEM images of the inner (feed-side) surface of Membrane C and D2 fibers.....	94
4.7	FESEM cross-sections of Membrane A and D2 fibers.....	94
4.8	Topographic AFM 3D image of Membranes A and D.....	98
4.9	Pyrochromatogram (300° C) of hollow-fiber membranes.....	100
4.10	Pyrochromatogram (300° C) of hollow-fiber membranes (continued).....	101
4.11	Pyrochromatogram (300° C) of hollow-fiber membranes (end) .....	102
5.1	Flux decline tests with PES UF membrane based on filtered water volume.....	104

5.2	Flux decline tests with PAN MF/UF membrane based on filtered water volume .....	105
5.3	Flux decline tests with PVDF MF membrane based on filtered water volume .....	106
5.4	Flux decline tests with PES UF membrane based on delivered DOC .....	108
5.5	Flux decline tests with PAN MF/UF membrane based on delivered DOC .....	109
5.6	Flux decline tests with PVDF MF/UF membrane based on delivered DOC .....	110
5.7	Comparison between J/J <sub>0</sub> (at 150 L/m <sup>2</sup> ) and UMFI values .....	113
5.8	Intermediate pore blockage fitting of Tampa Bay water data.....	114
5.9	Complete pore blockage fitting of Twente Canal water data .....	115
5.10	Cake formation fitting of Scottsdale water data .....	115
5.11	SEC-DOC chromatograms of Indianapolis water with PES UF membrane.....	117
5.12	SEC-DOC chromatograms of Scottsdale water with PES UF membrane.....	117
5.13	SEC chromatograms of Scottsdale water with PAN MF/UF membrane.....	118
5.14	SEC chromatograms of Tampa Bay water with PVDF MF membrane.....	118
5.15	Effect of pre-filtration of Tampa Bay water on the fouling of Membrane B .....	121
5.16	Comparison of flux decline rate of Membrane C on unfiltered and pre-filtered Twente Canal water .....	122
5.17	Effect of storage time on fouling rate of Membrane C using raw and pre-filtered Twente Canal water .....	123
5.18	Fouling curves for Membrane C on unfiltered Twente Canal water .....	124
5.19	UMFI (open) and UMFI <sub>R</sub> (solid) values for Membrane A obtained with Scottsdale (triangle), Twente Canal (circle), Tampa Bay (diamond), and Indianapolis (square) waters .....	126
5.20	UMFI (open) and UMFI <sub>R</sub> (solid) values for Membrane B obtained with Scottsdale (triangle), Twente Canal (circle), Tampa Bay (diamond), and Indianapolis (square) waters .....	127
5.21	UMFI (open) and UMFI <sub>R</sub> (solid) values for Membrane C obtained with Scottsdale (triangle), Twente Canal (circle), Tampa Bay (diamond), and Indianapolis (square) waters .....	127

5.22	UMFI (open) and UMFI <sub>R</sub> (solid) values for Membrane D2 obtained with Scottsdale (triangle), Twente Canal (circle), Tampa Bay (diamond), and Indianapolis (square) waters .....	128
5.23	UMFI/DOC (open) and UMFI <sub>R</sub> /DOC (solid) values normalized to feed water DOC for Membrane A obtained with Scottsdale (triangle), Twente Canal (circle), Tampa Bay (diamond), and Indianapolis (square) waters.....	129
5.24	UMFI/DOC (open) and UMFI <sub>R</sub> /DOC (solid) values normalized to feed water DOC for Membrane B obtained with Scottsdale (triangle), Twente Canal (circle), Tampa Bay (diamond), and Indianapolis (square) waters.....	129
5.25	MFI/DOC (open) and UMFI <sub>R</sub> /DOC (solid) values normalized to feed water DOC for Membrane C obtained with Scottsdale (triangle), Twente Canal (circle), Tampa Bay (diamond), and Indianapolis (square) waters.....	130
5.26	UMFI/DOC (open) and UMFI <sub>R</sub> /DOC (solid) values normalized to feed water DOC for Membrane D2 obtained with Scottsdale (triangle), Twente Canal (circle), Tampa Bay (diamond), and Indianapolis (square) waters.....	130
5.27	Effects of backwash flux and NOM type on the hydraulically irreversible fouling of Membrane A.....	132
5.28	Effects of backwash flux and NOM type on the hydraulically irreversible fouling Membrane B.....	132
5.29	Effects of backwash flux and NOM type on the hydraulically irreversible fouling of Membrane C .....	133
5.30	Effects of backwash flux and NOM type on the hydraulically irreversible fouling of Membrane D2.....	133
5.31	Relative decrease of specific flux as a function of permeate backwash flux.....	134
5.32	SEC-DOC/UV responses of Twente Canal water samples filtered with Membrane A...136	
5.33	Impact of CT on membrane cleaning efficiency.....	139
5.34	Effect of CT on UMFIcleaning in virgin membranes.....	139
5.35	Impact of various cleaning conditions on the restoration of membrane permeability.....	140
5.36	Fouling profile comparison between multi-cycle and single-cycle operation using Scottsdale water as feed water .....	142
5.37	Fouling profile comparison between multi-cycle and single-cycle operation using Indianapolis water as feed water.....	142

5.38	Fouling indices for multi-cycle tests with Scottsdale water .....	143
5.39	Fouling indices for multi-cycle tests with Indianapolis water .....	143
5.40	Fouling indices for single-cycle tests with Scottsdale water .....	144
5.41	Fouling indices for single-cycle tests with Indianapolis water .....	145
5.42	Comparison of multi-cycle and single-cycle fouling indices for tests with Scottsdale water .....	146
5.43	Comparison of multi-cycle and single-cycle fouling indices for tests with Indianapolis water .....	147
5.44	Pyrochromatogram of the hollow fiber harvested from the bench-scale module fed with Tampa Bay WTP influent .....	152
5.45	$J_s/J_{s0}$ for Membrane C treating the four Tier 1 source waters .....	153
5.46	$J_s/J_{s0}$ as a function of the permeated volume through four different ultrafiltration membranes with Twente Canal water .....	154
5.47	$J_s/J_{s0}$ of Membrane C as a function of the permeated volume of Twente Canal water coagulated with different dosages of $FeCl_3$ .....	155
5.48	Fouling slope as a function of the iron dose .....	155
5.49	$J_s/J_{s0}$ of Membrane C as a function of the permeate throughput of Twente Canal water sampled on September 14 and October 5, 2004 .....	156
5.50	$J_s/J_{s0}$ of Membrane C as a function of the permeate throughput of Twente Canal water sampled on January 14 and April 26, 2005 .....	157
5.51	SEC-DOC/UV chromatograms for Twente Canal filtration with Membrane A (Series B) .....	158
5.52	SEC-DOC/UV chromatograms for Twente Canal filtration with Membrane B (Series B) .....	158
5.53	SEC-DOC/UV chromatograms for Twente Canal filtration with Membrane C (Series B) .....	159
5.54	SEC-DOC/UV chromatograms for Twente Canal filtration with Membrane D2 (Series B) .....	159
5.55	SEC-DOC/UV chromatograms for Twente Canal filtration with Membrane C (Series C) .....	160

5.56	Frequency distribution plot of bench-scale UMFJ values.....	162
6.1	Normalized net specific flux profile for Run 1 operated with raw water at 70, 80, and 90 L/m <sup>2</sup> -hr flux.....	163
6.2	Normalized net specific flux profiles for Runs 1, 2, and 3.....	165
6.3	Normalized net specific flux profile for Runs 1, 4, 5, and 9.....	167
6.4	Normalized net specific flux profile for Runs 1, 6, 7, and 8.....	169
6.5	SEC-DOC/UV chromatogram – filtration of Tampa Bay water with PVDF Membrane B (Run 1).....	170
6.6	SEC-DOC/UV chromatogram – filtration of coagulated Tampa Bay water with PVDF Membrane B (Run 7).....	171
6.7	Normalized net specific flux profile for baseline run (Run 1) operated with raw water at 90 L/m <sup>2</sup> -hr flux. Recovery = 95 percent.....	173
6.8	Normalized net specific flux profile for Run 1 following data “smoothing”.....	173
6.9	Normalized net specific flux profile for Runs 1, 2, and 3.....	175
6.10	Normalized net specific flux profile for Runs 1, 4, 5, and 6.....	177
6.11	Normalized net specific flux and fouling-related feed water quality parameters for Runs 1 and 4.....	178
6.12	Normalized net specific flux profile for Runs 1, 7a, 7b, 7c, and 8.....	180
6.13	Normalized net specific flux profile for Runs 8, 9, and 10.....	182
6.14	Normalized net specific flux profiles for Runs 8, 11, 12, 13, and 17.....	184
6.15	Normalized net specific flux profile for Runs 1, 2, 3, 8, 9, and 10.....	187
6.16	Normalized net specific flux profile for Runs 4, 5, 6, 11, 12, and 13.....	190
6.17	SEC-DOC/UV chromatogram – filtration of White River water by Membrane A during Indianapolis pilot testing (Run 1).....	192
6.18	SEC-DOC/UV chromatogram – filtration of coagulated White River water by Membrane A during Indianapolis pilot testing (Run 7A).....	193
6.19	Run 1 (baseline) normalized net specific flux of Membrane D1 during Scottsdale pilot study.....	195

6.20	Impact of decreased flux on net normalized specific flux decline of Membrane D1 during Scottsdale pilot study operating on Scottsdale effluent.....	196
6.21	Impact of feed water recovery on net normalized specific flux decline of Membrane of Membrane D1 during Scottsdale pilot study .....	198
6.22	Impact of chemical wash on net normalized specific flux decline D1 during Scottsdale pilot study.....	200
6.23	Impact of coagulation on net normalized specific flux decline of Membrane D1 during Scottsdale pilot study.....	202
6.24	Impact of CT on flux decline of Membrane D1 during Scottsdale pilot study.....	204
6.25	Impact of CT on specific flux recovery of Membrane D1 during Scottsdale pilot study .....	205
6.26	SEC-DOC/UVA chromatogram from NOM samples collected during Run 1 (baseline run) of Scottsdale pilot study.....	206
6.27	SEC-DOC/UVA chromatogram from NOM samples collected during Run 8 (low PACl dose coagulation run) of Scottsdale pilot study.....	206
6.28	Transmembrane pressure, flux, and temperature as a function of time (calendar date) for Membrane C during Vitens pilot testing .....	208
6.29	Net normalized specific flux vs. permeate throughput during Vitens pilot study .....	209
6.30	Net normalized specific flux as a function of permeate throughput for Membrane C operation at baseline conditions (with and without coagulation) and at increased flux – Vitens pilot study.....	210
6.31	Net normalized specific flux and frequency of CIP as a function of permeate throughput for Vitens pilot study .....	211
6.32	Analysis of feed water before and after coagulation .....	213
6.33	Analysis results for permeate (upper left), backwash concentrate (upper right), acidic cleaning concentrate (lower left), and caustic cleaning concentrate (lower right) relative to feed water values.....	214
6.34	Normalized net specific flux for Membrane B during Tuscaloosa pilot study.....	216
6.35	Normalized net specific flux for Membrane E during Tuscaloosa pilot study .....	217
6.36	Normalized net specific flux for Membrane A during Tuscaloosa pilot study.....	217

6.37	Run 1 normalized net specific flux during Minneapolis pilot study.....	219
6.38	Run 2 normalized net specific flux for Membrane C during Minneapolis pilot study....	219
6.39	Run 3 normalized net specific flux for Membrane C during Minneapolis pilot study....	220
6.40	SEC-DOC/UVA chromatogram for raw water for Runs 1, 2, and 3 – Minneapolis pilot study using Membrane C.....	221
6.41	SEC-DOC/UVA chromatogram for UF feed water for Runs 1, 2 and 3 – Minneapolis pilot study using Membrane C.....	221
6.42	Normalized net specific flux profile for the Membrane A pilot unit at North Bay, Ontario .....	223
6.43	SEC-DOC/UVA chromatogram for NOM samples collected during the Membrane A pilot study at North Bay, Ontario.....	224
6.44	Normalized net specific flux profile for one of the full-scale Membrane E units at Parsons, Kansas.....	226
6.45	Normalized net specific flux profile for the full-scale Membrane A skid at Manitowoc .....	227
6.46	SEM of fouled Membrane B fiber from Tampa Bay pilot study (Run 9).....	228
6.47	SEM of fouled Membrane A fiber from Indianapolis pilot study (Run 3).....	228
6.48	SEM of fouled Membrane A fiber from Indianapolis pilot study (Run 7).....	228
6.49	SEM of fouled Membrane D1 PES fiber from Scottsdale pilot study (end of study, baseline conditions) .....	229
6.50	SEMs of Membrane F fiber from module treating Lake Michigan water .....	230
6.51	HPSEC/UV-260 of foulant material isolated from Run 14 of Indianapolis (Run 14) and Scottsdale pilot studies, Manitowoc full-scale plant (Lake Michigan) and Marne River water.....	235
6.52	HPSEC/UVA 260 profiles of foulant harvested from membrane modules operated during Runs 1, 3, 4, and 7a of the Indianapolis pilot study (Membrane A) .....	236
6.53	FTIR spectra of NOM fractions isolated from Marne River water .....	237
6.54	FTIR spectra of foulants isolated from Membrane A fibers operated during the Indianapolis pilot study.....	238

6.55	FTIR spectra for foulants isolated from Membrane D1 fibers (Scottsdale) and Membrane F fibers (Manitowoc WTP [Lake Michigan]).....	239
6.56	Pyrochromatograms of foulant isolated from Membrane B (Tampa Bay) and Membrane A (Indianapolis) fibers.....	240
6.57	Pyrochromatograms of foulant isolated from Membrane B (Indianapolis) fibers.....	241
6.58	Pyrochromatograms of foulant isolated from Membrane D1 (Scottsdale) and Membrane F (Manitowoc) fibers.....	242
6.59	Relative distribution of the main biopolymers present in the foulant material from isolate from Tampa Bay, Indianapolis, and Scottsdale pilot and Manitowoc (Lake Michigan) full-scale plant membrane fibers.....	244
6.60	Thermochemolysis–TMAH/GC-MS chromatograms of the hollow-fiber foulants .....	247
6.61	Thermochemolysis –TMAH/GC-MS chromatograms of the hollow-fiber foulants (end) .....	248
6.62	Cumulative frequency distribution diagram of UMFI values for the pilot-scale studies .....	250
7.1	Probability frequency distribution of various filtrations.....	256
7.2	Component loading (NOM characteristics and filtration performance) by stirred-cell test results.....	260
7.3	Ordination results for stirred-cell test results with respect to NOM characteristics and filtration performance.....	261
7.4	Component loading (NOM characteristics and filtration performance) by the Hollow-Fiber Unit 1 bench test results .....	262
7.5	Ordination results for Hollow-Fiber Unit 1 bench test results with respect to NOM characteristics and filtration performance .....	262
7.6	Component loading (membrane property and filtration performance) by stirred-cell test results .....	263
7.7	Ordination results for stirred-cell test results with respect to membrane property and filtration performance.....	264
7.8	Component loading (membrane property and filtration performance) for Hollow-Fiber Unit 1 bench test results .....	265

7.9	Ordination results for Hollow-Fiber Unit 1 bench test results with respect to membrane property and filtration performance .....	265
7.10	Component loading by pilot test results.....	266
7.11	Ordination results for pilot test results.....	267
7.12	Matched pair analysis of UMF1 results between flat-sheet and bench-scale Hollow-Fiber Unit 1 end-of-run backwash tests.....	268
7.13	Matched pair analysis for three membrane-water combinations between Hollow-Fiber Unit 1 and the corresponding pilot-scale units.....	270
7.14	Correspondence between Hollow-Fiber Unit 1 and pilot-scale operation for three membrane-water combinations .....	270

## FOREWORD

The Awwa Research Foundation (AwwaRF) is a nonprofit corporation that is dedicated to the implementation of a research effort to help utilities response to regulatory requirements and traditional high-priority concerns of the industry. The research agenda is developed through a process of consultation with subscribers and drinking water professionals. Under the umbrella of a Strategic Research Plan, the Research Advisory Council prioritizes the suggested projects based upon current and future need, applicability, and past work; the recommendations are forwarded to the Board of Trustees for final selection. The foundation also sponsors research projects through an unsolicited proposal process; the Collaborative Research, Research Applications, and Tailored Collaboration programs; and various joint research efforts with organizations such as the U.S. Environmental Protection Agency, the U.S. Bureau of Reclamation, and the Association of California Water Agencies.

This publication is a result of one of these sponsored studies, and it is hoped that its findings will be applied in communities throughout the world. The following report serves not only as a means of communicating the results of the water industry's centralized research program, but also as a tool to enlist the further support of the nonmember utilities and individuals.

Projects are managed closely from their inception to the final report by the foundation's staff and a large cadre of volunteers who willingly contribute their time and expertise. The foundation performs a planning and management function, and awards contracts to other institutions such as water utilities, universities, and engineering firms. The funding for this research comes primarily from the Subscription Program, through which water utilities subscribe to the research program and make an annual payment proportionate to the volume of water they deliver and consultants and manufacturers subscribe based on their annual billings. The program offers a cost-effective and fair method for funding research in the public interest.

A broad spectrum of water supply issues is addressed by the foundation's research agenda: resources, treatment and operations, distribution and storage, water quality and analysis, toxicology, economics, and management. The ultimate purpose of the coordinated effort is to assist water suppliers to provide the highest possible quality of water economically and reliably. The true benefits are realized when the results are implemented at the utility level. The foundation's trustees are pleased to offer this publication as a contribution to that end.

David E. Rager  
Chair, Board of Trustees  
Awwa Research Foundation

Robert C. Renner, P.E.  
Executive Director  
Awwa Research Foundation



## ACKNOWLEDGMENTS

The authors are indebted to Awwa Research Foundation (AwwaRF) and the U.S. Environmental Protection Agency (USEPA) for funding this project. The authors wish to thank Alice Fulmer, AwwaRF Project Manager; Jason Allen, former AwwaRF Project Manager; and the following members of the Project Advisory Committee: Samer Adham, MWH; Michelle Chapman, U.S. Bureau of Reclamation; Isabel Escobar, University of Toledo, Ohio; Nilaksh Kothari, Manitowoc Public Utilities, Wisconsin; and Charles Liu, Pall Corporation.

The authors would like to acknowledge and thank the Joint Research Programme of the Dutch Water Sector (BTO), who provided funding for the portion of the research conducted by Bas Heijman of Kiwa.

The authors wish to acknowledge and thank the following participating water utilities that provided water for bench testing, site facilities, assistance for pilot testing, and data for full-scale case studies:

Annika Bankston, Minneapolis Water Works, Minnesota  
Derek Clevenger, City of Parsons, Kansas  
David Hackworth, Veolia Water North America (at Tampa Bay Water, Florida)  
Nilaksh Kothari, Manitowoc Public Utilities, Wisconsin  
Dan Moran, Veolia Water North America (at City of Indianapolis, Indiana)  
Arthur Nunez and Mike Helton, City of Scottsdale, Arizona  
John Simmonds, City of North Bay, Ontario, Canada  
Maurice Sledge, City of Tuscaloosa, Alabama

The authors would also like to thank the following individuals and their respective companies for provided membrane samples, equipment, and technical and field assistance during the bench and pilot testing phases of this project:

Dave Faber and Ryan Furukawa, Hydranautics  
Jack Jordan, Norit Americas  
Paul Gallagher and Jason Siefert, Siemens Water Technologies  
Pierre Cote and Craig Hotchkies, Zenon (of GE Water and Process Technologies)

Finally, the authors would like to acknowledge the work of Mike Blair, Pamela Carlson, Jennifer Chang, Jane Mailand, Paul Mueller, and Dana Raughton from CH2M HILL.



# EXECUTIVE SUMMARY

## INTRODUCTION

The use of low-pressure membranes, microfiltration (MF) and ultrafiltration (UF), has increased dramatically over the last decade in response to new drinking water regulations focused on increased control of pathogens and disinfection byproducts (DBPs), and reduced membrane costs. More cost-effective, and therefore expanded, applications of MF and UF are currently constrained by fouling, in particular fouling by natural organic matter (NOM). NOM fouling is poorly understood because of the complexity of both NOM and of the membranes used in MF and UF treatment. NOM includes *allochthonous* NOM, derived from terrestrial sources (e.g., leaf litter and debris) within a watershed and consisting primarily of humic and fulvic acids. NOM derived from algae is considered *autochthonous* or algal organic matter (AOM), consisting of intracellular and extracellular organic materials and cell fragments (cellular debris). Effluent organic matter (EfOM) associated with wastewater treated to a secondary (biological) level consists of NOM associated with the original drinking water source plus soluble microbial products (SMPs) produced during biological treatment. All three types of NOM are believed to contribute to low-pressure membrane fouling, but to different degrees.

MF and UF membranes used in the drinking water industry are primarily polymeric materials that are, somewhat analogous to NOM, chemically complex in terms of monomer and surface functional group compositions. The majority of MF and UF membranes are of a hollow-fiber configuration, either symmetric (uniform composition) or asymmetric (variable composition and pore structure). Individual hollow fibers are potted and bundled together within a pressure vessel to create an element or module that can be operated in either a dead-end mode (dominant) or cross-flow mode with either outside-in flow (dominant) or inside-out flow. An important attribute of hollow-fiber elements, in contrast to spiral-wound elements, is that they can be hydraulically backwashed in addition to chemically cleaned. In present practice, backwashing is automated (typically augmented with feed-side air scour) and cleaning can occur either during a regularly scheduled, more frequent maintenance cleaning or during a cleaning-in-place (CIP) cycle that is generally triggered by a target transmembrane pressure (TMP) increase. The specific backwashing and cleaning conditions can be expected to significantly influence operational definitions of reversible versus irreversible fouling.

In the mid-1990s, low-pressure membrane technology was most often employed in a direct filtration mode, with source water applied directly to the membrane with only pre-screening where particle removal is the primary treatment objective. The practice has gradually evolved and pretreatment in the form of chemical coagulation, either alone or succeeded by clarification, has now become more common and has led to such hybrid technologies as coagulation-microfiltration (C-MF). C-MF addresses the need to reduce DBP precursor concentrations and reduce solids loading to the membranes in addition to providing high-level microbial removal. While some degree of fouling reduction can be realized by C-MF, primarily by adsorption of dissolved fouling NOM into the floc, there is no consistent understanding that emerges from the literature. Incorporating sedimentation between coagulation and MF/UF further decreases solids loading, but its benefit on membrane fouling (compared with C-MF) has not been adequately quantified. Another hybrid technology, powdered activated carbon (PAC)-UF, has been more common in Europe, most notably France, where pesticide and other synthetic

organic compound removals are required. There is no consensus on whether PAC pretreatment provides fouling reduction.

Fouling potential has been shown to be impacted by pretreatment, particularly by coagulation and less so by PAC. The progression from direct to hybrid treatment has produced benefits in terms of membrane fouling reduction by NOM through coagulation and by solids through clarification, however the fouling reduction mechanisms are poorly understood. The research conducted in this study was intended to help elucidate NOM fouling mechanisms through the study of NOM and membrane characteristics at bench-, pilot-, and full-scale tests using a variety of pretreatment and other fouling management techniques so that more cost-effective and reliable application of low-pressure membranes can be achieved.

## **PROJECT GOALS AND OBJECTIVES**

The overall goal of this project was to investigate the specific contributions of the different types of NOM to MF/UF fouling with the intent to develop a surrogate test or index that could be used to predict NOM fouling at low cost through a combination of source water characterization and rapid bench-scale testing. The specific objectives were to:

- Identify and quantify problematical NOM foulant(s).
- Contrast NOM-related fouling potential for different types of waters.
- Differentiate between hydraulically reversible versus irreversible fouling.
- Distinguish between chemically reversible versus irreversible fouling.
- Determine the influence of membrane properties on fouling.
- Evaluate pretreatment options to reduce NOM-related fouling.
- Determine how membrane operating conditions influence fouling.
- Develop a predictive tool(s), either a surrogate parameter(s) or a fouling index, to estimate fouling potential

## **SUMMARY OF PROJECT RESULTS**

### **Feed Water Characteristics**

A number of different feed waters were selected for membrane testing, primarily based on different types of NOM:

- Allochthonous (terrestrially derived) NOM
- Autochthonous (microbially derived) NOM
- Wastewater EfOM

These different NOM types were distinguished through analytical *signatures* including the following:

- (i) dissolved organic carbon (DOC)
- (ii) dissolved organic nitrogen (DON)
- (iii) specific UV absorbance (SUVA)

- Size-exclusion chromatography with on-line dissolved organic carbon detection (SEC-DOC), providing a molecular weight (MW) distribution and classification according to polysaccharide-like NOM (PS-DOC), humic substances (HS-DOC), and low molecular weight acids (LMA-DOC)
- Fluorescence excitation emission matrix (3-D spectrum), differentiating humic-like NOM from protein-like NOM and providing a fluorescence index (FI) distinguishing allochthonous NOM from autochthonous NOM
- XAD-8/-4 resin chromatography, fractionating NOM according to hydrophobic NOM (HPO-DOC), transphilic NOM (TPI-DOC), and hydrophilic NOM (HPI-DOC).

The hypothesis to be tested was that *character* is more important than *amount* of NOM; and that foulant attributes correspond to higher DON, lower SUVA, higher PS-DOC, greater protein-like NOM, higher FI, and higher HPI-DOC (i.e., non-humic NOM).

Source (feed) waters included (i) the White River (Indianapolis, Ind.); (ii) a secondary effluent (Scottsdale, Ariz.), (iii) the Hillsborough River (Tampa Bay, Fla.); and (iv) the Twente Canal (Netherlands); a more limited amount of testing was done with a Tuscaloosa, Ala. source. Based on the above hypothesis, the secondary effluent (low SUVA, high FI, high HPI-DOC) was expected to have a high fouling potential as an EfOM source; the Hillsborough River (high DON) and the Twente Canal (high PS-DOC) were anticipated to have a medium fouling potential; and the White River was expected to have a low fouling potential (it was originally selected as a potential autochthonous source, but an anticipated algal bloom did not occur to the desired degree during the period of testing).

## Membrane Properties

Three flat-sheet membranes were tested as disk specimens in stirred-cell testing. Properties determined included (i) pore size/molecular weight cutoff (MWCO); (ii) pure water permeability (PWP); (iii) contact angle, an index of surface hydrophobicity; (iv) zeta potential, an index of surface charge; and (v) surface roughness by atomic force microscopy (AFM). The specific membranes—a PVDF MF a PAN MF/UF, and a PES UF—were selected as flat-sheet analogs of hollow-fiber membranes tested at both the bench- and pilot-scales. The PVDF exhibited the largest pore size, highest PWP, greatest contact angle, and highest roughness. The PAN MF/UF exhibited a pore size intermediate to classical definitions of MF and UF, and the highest zeta potential.

Four hollow-fiber membranes were tested at both the bench- and pilot-scale: (i) membrane A, a PVDF MF; (ii) membrane B, a PVDF UF; (iii) membrane C, a PES/PVP UF; and (iv) membrane D, a PES UF tested in earlier (D1) and later (D2) product forms. These membranes were also characterized according to pore size/MWCO, PWP, contact angle, and roughness. Streaming current was used to estimate isoelectric point (IEP) and material composition was probed by pyrolysis GC/MS. Membrane A exhibited the largest pore size and greatest roughness; Membrane A and B exhibited the lowest IEP, corresponding to the greatest (negative) charge, and Membranes C and D1 exhibited the most hydrophilic character. Given a comparison of the properties of flat-sheet versus hollow-fiber properties, it was concluded that the flat-sheet PVDF MF was a good analog of membrane A, the flat-sheet PAN MF/UF was a poor analog of the Membrane B, and the flat-sheet PES UF was a fair analog of membranes C and D. The hypothesis was that attributes of a low fouling membrane would include higher

surface charge and lower contact angle. Prediction of the impact of membrane pore size on NOM fouling tendency was not considered a priority in this research.

### **Unified Modified Fouling Index Concept**

Because the traditional modified fouling index (MFI) was developed for constant-pressure filtration, the concept of a unified MFI (UMFI) was derived to quantify the fouling rate encountered not only in constant pressure, but also in constant flux filtration; moreover, the UMFI provides a basis for comparison of results derived from different units (e.g., stirred-cell versus hollow-fiber bench-scale units) and different scales (e.g., bench- versus pilot-scale). A value of UMFI ( $\text{m}^2/\text{L}$ ) can be estimated from a data plot of inverse normalized specific flux ( $J_s/J_{s0}$ ) versus hydraulic throughput ( $\text{L}/\text{m}^2$ ). There are several versions of the UMFI, as discussed below.

The general UMFI is calculated for experiments with a single longer period of filtration, specifically bench-scale testing with the flat-sheet stirred-cell unit, and the hollow-fiber unit with a single end-of-run backwash operational mode. The UMFI is a measure of the total fouling capacity but does not take the effects of backwashing or chemical washing into account. The  $\text{UMFI}_i$  is used to assess the total fouling potential of a water for operational protocols involving multiple, short periods of filtration, specifically hollow-fiber bench scale multicycle tests with multiple backwashes, as well as pilot- and full-scale operation. The  $\text{UMFI}_i$  is calculated for the first filtration cycle of an experiment; thus, the  $\text{UMFI}_i$  and UMFI are equivalent in concept, except that  $\text{UMFI}_i$  represents a shorter period of filtration. The short-term hydraulically irreversible portion of fouling is described by the  $\text{UMFI}_{150}$ , corresponding to results over a volumetric throughput of  $150 \text{ L}/\text{m}^2$ , for operational protocols involving multiple cycles of filtration interspersed by backwashing, namely multicycle bench scale as well as pilot- and full-scale operation. Long-term hydraulically irreversible fouling is described by the  $\text{UMFI}_{3000}$  for pilot- and full-scale operation;  $\text{UMFI}_{3000}$  is similar to  $\text{UMFI}_{150}$ , except that the volumetric throughput is  $3000 \text{ L}/\text{m}^2$ . A major advantage of the  $\text{UMFI}_{3000}$  is that it includes at least one cleaning cycle for pilot scale runs for which chemical washing was performed; the  $\text{UMFI}_{150}$  does not. Short-term hydraulically irreversible fouling in the hollow-fiber bench scale tests with a single end-of-run backwash operational mode is described by the  $\text{UMFI}_R$ , and is comparable to the  $\text{UMFI}_{150}$  or  $\text{UMFI}_{3000}$  of multicycle bench-, pilot-, and full-scale operation. Chemically irreversible fouling is described by the  $\text{UMFI}_{\text{cleaning}}$  for the bench scale end-of-run backwash operational mode. The  $\text{UMFI}_{\text{cleaning}}$  can be compared to the  $\text{UMFI}_{3000}$  for multicycle runs with chemical washing included in the protocol.

### **Bench-Scale Membrane Filtration Tests**

Bench-scale membrane filtration tests were performed using two approaches: stirred-cell tests with disk specimens of flat-sheet membranes, operated under a constant pressure/declining flux mode of operation, and hollow-fiber tests using two different units (1 and 2), operated under a constant flux, increasing pressure mode of operation. Fouling trends were defined in terms of the unified modified fouling index (UMFI) as a means of comparing different units and scales of testing.

### ***Stirred-Cell Tests***

Stirred-cell experiments were performed with five source waters (Indianapolis, Scottsdale, Tampa Bay, Twente Canal, and Tuscaloosa) and one clarified water (Tuscaloosa), under a constant pressure/declining flux mode of operation, using three membranes (PVDF MF, PAN MF/UF, and PES UF). For all three membranes evaluated as a function of volumetric throughput ( $L/m^2$ ), the Scottsdale, Tampa Bay, and Twente Canal waters imparted significant flux decline while the Indianapolis water and both the untreated and clarified Tuscaloosa waters showed less flux decline. These results may be due to the high content of DOC in the Tampa Bay water and the presence of problematical NOM components in the Scottsdale and Twente Canal waters (PS-DOC and/or HPI-DOC). Among the three membranes, the PVDF MF showed the least flux decline. Little benefit was realized in clarification based on limited testing because the subject water (Tuscaloosa) contained low foulant levels. For all three membranes evaluated as a function of delivered DOC ( $mg/m^2$ ), the same general trends were observed with the following exceptions: (i) a lesser degree of fouling for the (high DOC) Tampa Bay water except for the PAN MF/UF where Tampa Bay water still showed significant fouling and (ii) a benefit of clarification was observed for the PVDF MF membrane with the Tuscaloosa water. An evaluation of fouling mechanisms showed a dominance of cake formation. In all cases, cake formation dominated for the PES UF while, in several cases, pore constriction played a role in fouling of the PVDF MF, and to a lesser extent, the PAN MF/UF. The PES UF and PAN MF/UF membranes showed that high molecular weight components were accumulated in the cell within the retentate during filtration, or on the membrane surface and later recovered in a simulated backwash. The PVDF MF membrane did not indicate significant accumulation of high molecular components, likely because of its relatively larger pore size.

The qualitative trends indicated above were supported by corresponding UMFI values ( $m^2/L$ ) and trends. Over an order of magnitude in difference was observed for UMFI values, with higher values for the Scottsdale, Twente Canal, and Tampa Bay source waters, and the PES UF and PAN MF/UF membranes.

### ***Hollow-Fiber Unit 1***

The experimental matrix tested with Hollow-Fiber Unit 1 included four source waters (Scottsdale, Tampa Bay, Indianapolis, and Twente Canal) and four membranes (A, B, C, and D2). Regardless of the permeate flux, UMFI values were the greatest for Membranes B and C when the Tampa Bay water was filtered, and the least when the Indianapolis water was filtered. For Membranes A and D2, the Indianapolis water also yielded the lowest UMFI values for the four waters tested. However, the greatest UMFI values for Membrane A were observed with the Scottsdale water, not the Tampa Bay water. In comparison, UMFI values were similar and the highest when the Scottsdale and Tampa Bay waters were filtered by Membrane D2. The results suggest that Scottsdale water and/or Tampa Bay water in general caused the greatest total fouling for all four membranes tested, while the Indianapolis water caused the least.

The trend for  $UMFI_R$  was somehow different from that for UMFI. The  $UMFI_R$  was the greatest for the Tampa Bay water and the least for the Indianapolis water with Membranes A, C, and D2. Membrane B performed differently from the others in this case.  $UMFI_R$  values for Membrane B did not differ extensively with the four waters studied, although the values were slightly higher with the Scottsdale water. These results indicate that the hydraulically irreversible fouling was the worst for all membranes when the Tampa Bay water was filtered under the

hydraulic conditions investigated, except for Membrane B. Interestingly, the Tampa Bay water appeared to be extremely problematic for Membrane A, the only microfiltration membrane tested in the study.

However, because the natural waters tested contained different concentrations of DOC, membrane fouling trends were also examined in terms of delivered DOC ( $\text{mg}/\text{m}^2$ ), in addition to volumetric throughput ( $\text{L}/\text{m}^2$ ) that serves as the basis for the UMFI concept. Unlike the difference in UMFI and  $\text{UMFI}_R$  observed with different membranes, a consistency in the relationship between total fouling and NOM source was found with all membranes tested from the perspective of delivered DOC. Regardless of the type of membrane, the Scottsdale water NOM resulted in the most severe fouling; the Tampa Bay water NOM produced the least. Considering the dominant NOM component of the waters, these data suggest that, under conditions employed in the study, EfOM exhibited the highest fouling potential; allochthonous NOM had the lowest fouling potential; and autochthonous NOM lay between the two. However, given the Tampa Bay source, NOM *amount* (concentration) is also influential.

An increase of permeate flux usually resulted in a slight increase of UMFI and  $\text{UMFI}_R$ , indicating a positive relationship between membrane fouling (both total and hydraulically irreversible) and the permeate flux. However, the type or source of the NOM had a greater impact on membrane fouling than operating fluxes. This finding is different from earlier studies with respect to a critical flux in membrane fouling, a result likely attributable to differences in the properties of the major foulants and the range of permeate fluxes tested.

The hydraulic reversibility of NOM fouling reflects the possibility of fouling reduction using permeate backwash, with an operational definition of hydraulically irreversible fouling (HIF).  $\text{UMFI}_R$  values were calculated based on the recovery of the permeate flux immediately after the first hydraulic backwash of a single cycle experiment. In these and subsequent backwash flux experiments, the restoration of specific flux varied to different extents according to NOM source. Experiments were conducted to evaluate the effects on membrane fouling by single versus multiple backwash cycles. Generally, multicycle backwashing yielded similar levels of hydraulically irreversible fouling compared to single cycle. The similarity in the permeability of the membranes after the first minute of filtration following backwash of the single cycle and the first minute of filtration of the final cycle in the multicycle experiments suggest that the simpler single-cycle, end-of-run backwash protocol can be used to *simulate* multiple cycle results.

Further assessment of the similarity of multi- and single-cycle bench scale operations was performed by comparing various unified modified fouling indices. The total fouling is described by UMFI for single cycle and  $\text{UMFI}_i$  for multicycle experiments. The hydraulically irreversible portion of the fouling is expressed as  $\text{UMFI}_R$  for single cycle and  $\text{UMFI}_{150}$  for multicycle experiments. There was a good correspondence observed between each pair of UMFI values, furthering supporting the proposition that the bench-scale, end-of-run backwash protocol does an equally good job of estimating hydraulically irreversible fouling as does the multicycle operation.

## ***Hollow-Fiber Unit 2***

The Hollow-Fiber Unit 2 was used to test four source waters (primarily Twente Canal with limited work on Scottsdale, Tampa Bay, and Indianapolis) and four membranes (primarily Membrane C, with limited work on membranes A, B, and D2). The main attribute of Unit 2

versus Unit 1 is its fully automated backwash capabilities; its major deficiency compared to Unit 1 is that it can be operated only at a single constant flux (120 L/m<sup>2</sup>-hr).

Based on work with membrane C and the four source waters, the fouling rate was lowest for the secondary effluent of the Scottsdale Wastewater Treatment Plant, higher for the Twente Canal and the White River (Indianapolis), and far highest for the Tampa Bay water. These results differ from other bench-scale results in terms of a lower relative fouling potential for the Scottsdale water and a higher relative fouling potential for the Indianapolis water, possibly an artifact of shipping these waters across the Atlantic for testing in the Netherlands (only the Twente Canal water was a local source). Based on work with the Twente Canal water and the four membranes, it was observed that the two PVDF-membrane types (A and B) have similar fouling properties. However, the fouling rate of the two PES membranes (C and D2) is very different, likely due to a difference in material composition (Membrane C is made with a blend of PES and PVP). These results are generally similar to results observed in other bench-scale testing. In evaluating pretreatment, the fouling properties of the Twente Canal water tested with Membrane C revealed an optimum coagulant dose of 2.5 mg Fe/L; at this concentration, there was little irreversible fouling.

## **Pilot-Scale Testing and Full-Scale Plant Operations**

### ***Tier 1 Pilot Studies***

Tier 1 pilot-scale testing was performed at three sites using four source waters and three hollow-fiber membrane types:

- Tampa Bay (Fla.)/Hillsborough River - PVDF UF (Membrane B)
- Indianapolis (Ind.)/White River – PVDF MF (Membrane A)
- Scottsdale (Ariz.)/secondary effluent – PES UF (Membrane D1)
- Vitens/Twente Canal – PES UF (Membrane C)

Tampa Bay testing included raw and coagulated waters; and different flux rates, backwash flows, feedwater recoveries and chemical wash regimes. Indianapolis testing included raw, coagulated and clarified waters; and different flux rates, feedwater recoveries, coagulant doses and chemical wash regimes. The Scottsdale testing comprised raw and coagulated waters; and different flux rates, feedwater recoveries, coagulants, coagulant doses and chemical wash regimes.

At baseline flux and recovery conditions (90 L/m<sup>2</sup>-hr and 95 percent recovery at Tampa Bay and Indianapolis, and 80 L/m<sup>2</sup>-hr and 90 percent recovery at Scottsdale; 50 L/m<sup>2</sup> and 60 percent recovery at Vitens), the rate of fouling was highest at Scottsdale (despite the less challenging operating conditions) and lower DOC when compared to Tampa Bay. Similarly, the fouling rate was next highest at Vitens despite the least challenging operating conditions of flux and recovery. These results are generally consistent with the greater fouling potential of the PS, hydrophilic NOM fractions present in the Scottsdale effluent, White River, and Twente Canal waters although the lower fouling potential result for Tampa Bay differs from that observed in bench tests. Moreover, calcium, which has been shown to increase NOM fouling, was significantly higher in the Scottsdale, Indianapolis (White River), and Vitens (Twente Canal) sources, another possible explanation for higher fouling potential.

Increasing flux and feedwater recovery for tests conducted on raw water increased fouling rate in all studies except Vitens, with the greatest impact observed at Scottsdale (wastewater effluent source). At Tampa Bay and Indianapolis (PVDF membranes), increased flux and recovery (relative to baseline conditions) caused comparable losses of normalized net specific flux, although the higher rate of fouling was temporary; long-term fouling rate was comparable to baseline conditions. Backwash flow rate (at equal recovery) did not materially affect the rate of fouling. For PES Membrane D1 tested at Scottsdale, higher recovery caused a much greater rate of fouling than did higher flux, suggesting that the backwash regime used with the inside-out flow configuration (no air scour) is not as effective in managing fouling from solids accumulation. For PES Membrane C piloted at Vitens, no increase in fouling rate was observed when flux was increased by 50 percent (from 50 to 75 L/m<sup>2</sup>-hr).

Of the different chemical wash regimes evaluated with Tampa, Indianapolis, and Scottsdale studies, the most significant reduction in fouling was observed using chlorine (sodium hypochlorite), followed by caustic (in combination with acid). Acid (citric) alone provided little or no benefit. An evaluation of different CT conditions (that is, combinations of chlorine dose and contact (soak) time) during chemical washing showed a non-linear relationship between flux recovery and CT, with a 10-fold increase in CT (from 1500 to 15,000 mg min/L) required to achieve a doubling of flux recovery at Indianapolis. The greater effectiveness of chlorine (which oxidizes a range of NOM compounds) versus caustic (which is effective at solubilizing (desorbing) the humic substance fraction) is consistent with industry's predominant use of hypochlorite chemical washes. The single chemical wash regime (HCl followed by caustic) was not employed on a fixed permeate throughput basis, but instead at a trigger TMP (30 kPa) and was effective in stabilizing flux when used with increasing frequency.

Coagulation had a beneficial effect on NOM fouling in all studies, but the effect was dependent on coagulant dose and feedwater recovery. For Tampa Bay, ferric coagulation reduced flux decline at 90 percent recovery but increased it at 95 percent recovery. Incorporating a phosphoric chemical wash with coagulation allowed for improved performance at the higher recovery. For Indianapolis, alum coagulation reduced fouling at a low dose (5-15 mg/L), but increased it at a high dose (30 mg/L). At Scottsdale, coagulation using polyaluminum chloride (PACl) was beneficial at low and high doses (15 and 85 mg/L), with the greater dose providing the highest fouling reduction. Ferric chloride coagulation (25 mg/L) provided a reduction intermediate to the two PACl doses. Considering the high solids loading resulting from 85 mg/L PACl dosing, it was surprising the PES membrane showed such a significant fouling reduction considering the negative impact observed when this membrane was operated at high (95 percent) recovery. For Vitens, a very low dose of coagulant (1/mg/L Al) showed only a temporary benefit (300 L/m<sup>2</sup>) permeate throughput on specific flux.

Vitens testing examined the impact of flux, coagulation, and chemical wash regimes on NOM fouling rate. Operation at 50 percent higher flux (with 1 mg/L Al coagulation) showed no increase in fouling; likewise, operation at baseline with the absence of coagulation had little impact after a low coagulant dose (1 mg/L Al) showed decreased fouling rate in the short term (initial 300 L/m<sup>2</sup>).

As expected, clarification (alum coagulation, flocculation, and sedimentation) was more effective in reducing NOM fouling than coagulation alone (at Indianapolis [PVDF]). Specific flux loss was reduced by more than 50 percent at 5000 L/m<sup>2</sup> of permeate throughput. Although clarification reduced fouling (compared to no pretreatment), extent to which fouling was increased by increased flux and recovery was more pronounced on clarified versus raw water.

When clarification was coupled with chemical washing, the relative benefits of acid, caustic, and chlorine washing on flux recovery were similar to that observed with raw water; however, the degree of benefit derived from chlorine washing was reduced.

NOM characterization by SEC-DOC of feed, permeate, and backwash streams from the three pilot studies were consistent. PS is the only NOM fraction appreciably retained by the MF and UF membranes. Upon backwashing, this fraction is readily displaced and highly concentrated in the backwash water, indicating that PS fouling is hydraulically reversible. Coagulation is very effective in converting a significant portion of all three SEC fractions (PS, HS, and LMA) from soluble to particulate, thereby reducing the amount of soluble NOM available to cause membrane fouling.

### ***Tier 2 Pilot Studies***

Tier 2 pilot studies were limited to three locations (Tuscaloosa, AL; Minneapolis, MN and North Bay, Ontario) where testing was conducted with either multiple (two MF [A and E] and one UF PVDF [B] at Tuscaloosa) or single membrane types (PES UF at Minneapolis and PVDF MF [A] at North Bay). The source waters at these locations contained predominantly allochthonous NOM. At Tuscaloosa, the tighter UF membrane showed a higher rate of fouling than the two MF membranes, possibly due to a greater amount of PS retention. Size-exclusion chromatography with on-line dissolved organic carbon detection (SEC-DOC) analyses showed significant PS and lesser HS retention by the UF membrane, with both fractions highly concentrated in the backwash water. At Minneapolis, lime softening/recarbonation/clarification was effective for reducing all three SEC/DOC NOM fractions, but reduction was greatest for PS, considered to be the most fouling. Increased frequency of chemical washing was shown to be beneficial in reducing the rate of fouling. For North Bay, the use of high CT chlorine washes was very effective in reversing NOM flux loss. SEC-DOC NOM fractionation results were consistent with those from other bench and pilot studies: the PS fraction was well retained by the MF membrane and effectively removed during backwashing.

### ***Full-Scale Plant Operations***

Evaluation of NOM fouling contribution and impacts on performance of full-scale MF plants at Manitowoc, Wis. (Membrane F) and Parsons, Kan. (Membrane E) was constrained by the absence of NOM characterization data. The rate of fouling in both plants was low, however. Although NOM levels in Parson's raw water supply are significant (8 to 12 mg/L), chemical clarification reduces these levels to < 2 mg/L. Although SEC-DOC characterization was not performed on the MF process samples, it is assumed that the PS DOC fraction removal was very high, thereby resulting in a low NOM fouling potential for the clarified water. NOM (DOC) levels in the Manitowoc plant feed (Lake Michigan) are low (< 2mg/L), suggesting that NOM fouling potential is low.

## Membrane Autopsies

Autopsies were performed on membrane fibers harvested from both bench- and pilot-scale testing of hollow-fiber membranes. Autopsy tools included:

- Contact angle
- Field emission scanning electron microscopy (FESEM), providing a visualization of foulant deposition
- Fourier transform infrared spectroscopy (FTIR)
- Pyrolysis GC/MS of extracted foulant
- Elemental (carbon [C] and nitrogen [N]) composition of extracted foulant

As a general rule, there were only small changes in contact angle before and after fouling. In bench-scale testing with less severely fouled membranes, the contact angle slightly decreased when fouled with autochthonous NOM or EfOM for more hydrophobic membranes. A slight increase was observed when membranes were fouled with allochthonous NOM. In pilot testing with more severely fouled membranes, contact angle slightly increased for a hydrophobic membrane and either an autochthonous or an allochthonous NOM source. It was concluded that contact angle measurement does not provide relevant information.

FESEM images were made of both the external and internal surfaces of the fibers autopsied after fouling. For Membrane B (outside-in configuration) with an allochthonous source, FESEM images did not show clear evidence of an organic deposit at the external surface (filtration surface) of the fibers. For an autochthonous source conducted with Membrane A (outside-in configuration), results led to the same observation. More surprisingly, for both the allochthonous and autochthonous sources, a deposit was observed at the inner surface of the fibers, with material possibly corresponding to microbial entities (algae or/and bacteria), particularly for the autochthonous source where algae were observed during the period of testing. For Membrane D1 (inside-out configuration), there was some evidence of microbial accumulation on the inner surface.

Fouling material was recovered from hollow fibers using sonication in Milli-Q water and lyophilization. Material isolated from fouled membranes was found to be relatively poor in organic material. NOM present in natural waters typically has a carbon content ranging from 40 to 55 percent; material isolated from fouled membranes did not exceed 15 percent of organic carbon. A high N/C ratio was found in foulant extracted from membrane D1, fouled with secondary effluent. Most of the FTIR spectra of extracted foulant indicated the presence of organic matter derived from bacterial origin (aminosugars, proteins, lipids). All of the pyrolysis GC/MS chromatograms of extracted foulant showed strong indicators of the presence of natural biopolymers with the presence of peaks that are produced from the thermal degradation of proteins, sugars, aminosugars, and lignin-type structures.

The autopsy results are generally supportive of the findings related to feed-water NOM composition in which EfOM or autochthonous NOM characteristics were found to correspond to a higher fouling potential.

## **Statistical Analyses**

From the different scales of membrane filtration tests (stirred-cell tests, bench-scale (Hollow-Fiber Unit 1) tests, and pilot tests), several parameters from NOM characteristics and membrane properties were identified and quantified for statistical analyses. Statistical analysis was employed to determine which parameters contribute most significantly to low-pressure membrane fouling by NOM. Methods used for the statistical analyses included simple linear correlation matrix, probability frequency distribution, multiple linear regression, and principal component analysis (PCA).

### ***Correlation Matrices***

Simple linear correlation matrices based on stirred-cell test data showed that PS-DOC and HPI-DOC are more highly correlated to UMFI than other independent variables. HS-DOC and HPO-DOC are poorly correlated with UMFI. These results confirm the greater influence of non-humic over humic NOM in low pressure membrane fouling. No clear trends emerged in term of the influence of membrane properties on UMFI. Correlation matrices based on hollow-fiber bench tests demonstrated the highest (inverse) correlation between zeta potential and both UMFI, an index of total fouling, and  $UMFI_R$ , an index of (short-term) hydraulically irreversible fouling. This inverse relationship suggests the merits of a (negatively) charged membrane. No clear trends emerged from correlation matrices based on data from pilot tests.

### ***Frequency Distributions***

Probability frequency distributions of UMFI values among the various tests revealed that pilot testing results show a more narrow distribution of UMFI than stirred-cell or hollow-fiber bench tests. This reflects the fact that stirred-cell and hollow-fiber (bench) UMFI values represent total membrane fouling (which have higher values) versus pilot  $UMFI_{150}$  and  $UMFI_{3000}$  values, which represent hydraulically reversible fouling only. Hollow-fiber (bench)  $UMFI_{150}$  values are intermediate because of shorter-term, hydraulically reversible fouling. The narrower distribution for pilot-scale results indicate that reversible fouling is quite consistent (in terms of fouling rate) across all the source water types.

### ***Multiple Regression***

Multiple linear regression analysis based on stirred-cell tests show that UMFI is best explained by PS-DOC, fluorescence intensity (FI) (a higher FI value reflects autochthonous [microbially derived] NOM), and (inverse) zeta potential. These results confirm some of the correlation matrix trends. Multiple regression analysis based on hollow-fiber bench tests indicates that HPI-DOC, (inverse) zeta potential, and surface roughness best explain UMFI.

### ***Principal Component Analysis***

PCA was used to address three questions:

- Which feed water NOM characteristics most affect membrane fouling?
- Which membrane properties most influence fouling?
- Which membrane operating conditions most influence fouling?

The Scottsdale and Twente Canal feed waters clustered together and corresponded with higher UMFI values, inferring higher fouling tendency. These waters reflect significant levels of PS-DOC, HPI-DOC, and/or DON. Even though the Tampa Bay feed water has a high DOC concentration (~17 mg/L), its fouling tendency is less than the Scottsdale and Twente Canal waters. Thus, PS-DOC and HPI-DOC are closely related to UMFI values and relate to significant membrane fouling. This is consistent with the multiple linear regression analysis.

Based on PCA analysis of membranes tested in stirred-cell tests, clustering of results suggests that the PES UF exhibited the highest fouling tendency followed by the PAN MF/UF and the PVDF MF membrane, with the progression toward a larger pore size. Zeta potential appears to be inversely related to UMFI. Thus, fouling appears to be dominantly affected by pore size of the membrane in stirred-cell tests (without backwashing). Based on membranes tested in hollow-fiber membranes, smaller pore size and a less negatively charged membranes correspond to higher UMFI and UMFI<sub>R</sub> values, indicating a higher fouling tendency. Membrane D2 has the highest fouling tendency, and also has the smallest pore size and the lowest zeta potential. In contrast, Membrane A shows the least fouling tendency, and has the largest pore size (0.1 μm) and the highest zeta potential.

Based on PCA analysis of pilot test results, different backwash flux (high and normal) conditions and pretreatments by alum coagulation and ferric coagulation were evaluated. Data clustering suggested that high backwash flux reduces membrane fouling through removal of a reversible cake layer from the membrane surface, and a high recovery condition increases membrane fouling. Most data points corresponding to filtration with pretreated water were clustered to regions corresponding to low fouling tendency.

### **UMFI Comparability and Scale-Up**

Matched paired analyses was used to address important scale-up questions: (i) do UMFI values derived from stirred-cell tests simulate (predict) UMFI trends based on hollow-fiber (Unit 1) bench-scale tests and (ii) do UMFI values derived from hollow-fiber bench-scale (Unit 1) tests simulate (predict) UMFI trends based on pilot-scale tests?

#### ***Stirred-Cell versus Hollow-Fiber Bench-Scale Results***

Matched pair analysis was used to compare stirred-cell, flat-sheet results and hollow-fiber bench-scale results corresponding to end-of-run backwash experiments. Three sets of comparisons were performed, based on membrane type. Membrane pairings were the PVDF Membrane B, with the PAN MF/UF; the PVDF Membrane A, with the PVDF MF; and the PES Membranes C and D1, with the PES UF. The highest flux run for each membrane/source water combination in Hollow-Fiber Unit 1 baseline testing was used for comparison, as it best approximated the flux range used in the constant pressure/declining flux operational mode of the flat-sheet, stirred-cell unit. The hollow-fiber and flat-sheet tests were found to be statistically different in all cases. While there was still a (statistically) significant difference between the results from tests on Membrane B and PAN MF/UF, the results from this pair are closest among all the pairs. These comparisons support the assertion that flat-sheet membranes chosen for this research do not serve as good surrogates of the hollow-fiber membranes tested at the bench scale.

## ***Hollow-Fiber Bench-Scale versus Pilot-Scale Results***

Matched pair analysis was used to compare UMFI results from hollow-fiber bench-scale versus pilot-scale experiments for each of three membrane/source water combinations. The experiments with Scottsdale water show a distinct difference between pilot and bench scale, with consistently higher index values for the bench-scale unit. This difference is likely attributable to the properties of the D2 and D1 membranes, used at the pilot and bench scales, respectively, with the D2 membrane exhibiting higher fouling potential due to the absence of polyvinyl pyrrolidene (PVP) co-polymer. No difference was observed between bench and pilot scale for the Tampa Bay/Membrane B combination. The best correspondence between bench and pilot was observed with the Indianapolis water/Membrane A tests. The results from the bench to pilot comparisons generally support the premise that bench-scale testing can be used to successfully predict fouling behavior at the pilot scale.

## **CONCLUSIONS**

Low-pressure, hollow-fiber (LPHF) membranes are subject to fouling by natural organic matter (NOM) during the filtration of natural waters. The fouling results were quantified using a new concept called the “UMFI.” The development of the UMFI enabled the comparison of results between these differing levels of experimental complexity. The bench-scale work showed that flat-sheet membranes do not serve as a good surrogate of hollow-fiber membranes at bench scale. Conversely, using the UMFI concept, the results from the bench to pilot comparisons support the idea that bench-scale testing can be used to successfully predict fouling behavior at pilot scale.

It was found that 1) the high molecular weight PS fraction of NOM was potentially the major organic foulant; 2) the magnitude of fouling, however, was more specific to each membrane/water combination, than hydrodynamic conditions of filtration; 3) most of the fouling was hydraulically reversible, indicating low binding of the majority of the organic foulant on membrane surface; 4) the foulant resistant to hydraulic cleaning appeared to be reactive with chlorine, thereby chemically removable under proper conditions; and 5) other NOM fractions, comprising more than 90 percent of DOC in natural waters, seemed less important to fouling. Moreover, the analysis of UMFI suggested that the observed fouling usually followed a pseudo-cake formation type of fouling.

The potential for fouling reduction was also investigated from the perspective of membrane selection, hydrodynamic conditions (permeation flux, backwashing flux and frequency), and chlorine cleaning. Selection of proper membranes appeared to be an important first step in fouling reduction; their fouling was related to multiple membrane properties, such as material, pore size rating, and surface charge. In terms of hydrodynamics, decreasing permeate flux usually reduced fouling, but the variation was generally less than what was observed between different membrane or NOM types. Moreover, backwashing flux and frequency showed little impacts on the fouling of submerged LPHF membranes; comparatively, higher backwashing flux was beneficial to the hydraulic cleaning of pressurized outside-in membranes. Finally, chlorine cleaning of a fouled membrane was effective in the reduction of hydraulically irreversible fouling; however, the efficiency was dependent on the “CT” value, i.e., chlorine dose and contact time.



# CHAPTER 1

## INTRODUCTION, BACKGROUND, AND OBJECTIVES

### BACKGROUND

Fouling represents the major constraint to the more cost-effective, and therefore expanded, application of membrane technology in drinking water and wastewater reclamation/reuse. Fouling can take several forms and can vary in type from high- to low-pressure membranes. Fouling by organic matter—more specifically, natural organic matter (NOM)—is poorly understood, particularly for low-pressure membranes. An Awwa Research Foundation (AwwaRF)-sponsored study on NOM fouling of high-pressure membranes has already been completed (Amy et al., 2001).

NOM is a heterogeneous mixture of naturally occurring organic components consisting of humic substances (humic and fulvic acids), as well as various non-humic biochemicals such as proteins and carbohydrates. Adding further complexity is the fact that NOM varies significantly depending on its source. NOM resulting from terrestrial sources (e.g., leaf litter and vegetative debris) within a watershed is called *allochthonous* NOM. NOM derived from algae, considered *autochthonous* and also referred to as algal organic matter (AOM), consists of intracellular and extracellular organic materials and cell fragments. AOM dominates in eutrophic water supplies and may vary in magnitude during algal blooms. Still another form of NOM is effluent organic matter (EfOM) associated with wastewater treated to a secondary (biological) level. EfOM consists of NOM contributed by the drinking water source plus soluble microbial products (SMPs) produced during biological treatment, and has relevance from the perspective of wastewater reclamation and reuse or effluent-impacted drinking water sources. Based on significant chemical differences, fouling potential varies according to the *type* of NOM.

The use of low-pressure membranes, i.e., microfiltration (MF) and ultrafiltration (UF), has increased dramatically over the last decade in response to new drinking water regulations focused on the increased control of pathogens and disinfection byproducts (DBPs), and reduced membrane costs. MF and UF membranes used in the drinking water market are primarily polymeric materials that are, somewhat analogous to NOM, chemically complex in terms of monomer and surface functional group compositions. The majority of MF and UF membranes are of a hollow-fiber configuration, either symmetric (uniform composition) or asymmetric (variable composition and pore structure). Individual hollow fibers are potted and bundled together within a pressure vessel to create an element or module that can be operated in either a dead-end mode (dominant) or cross-flow mode with either outside-in flow or inside-out flow (dominant). An important attribute of hollow-fiber elements, in contrast to spiral wound elements, is that they can be hydraulically backwashed in addition to chemically cleaned. In present practice, backwashing is automated (typically augmented with feed-side air scour) and cleaning can occur either during a regularly scheduled, more frequent maintenance cycle or during a clean-in-place (CIP) cycle that is generally triggered by a target transmembrane pressure (TMP) increase. The specific backwashing and cleaning conditions can be expected to significantly influence operational definitions of reversible versus irreversible fouling.

In the mid-1990s, low-pressure membrane technology was most often employed in a direct filtration mode, with source water applied directly to the membrane with only pre-screening and where particle removal is the primary treatment objective. The practice has gradually evolved and pretreatment in the form of chemical coagulation, either alone or

succeeded by clarification, has now become more common and has led to such hybrid technologies as coagulation-microfiltration (C-MF). C-MF addresses the need to reduce DBP precursor concentrations and reduce solids loading to the membranes in addition to providing high-level microbial removal. While some degree of fouling reduction can be realized by C-MF, there is no consistent understanding that emerges from the literature. Incorporating sedimentation between coagulation and MF/UF further decreases solids loading, but its benefit on membrane fouling (as compared with C-MF) has not been adequately quantified. Another hybrid technology, powdered activated carbon (PAC)-UF, has been more common in Europe, most notably France, where pesticide and other synthetic organic compound removals are required. There is no consensus on whether PAC pretreatment provides fouling reduction.

Fouling potential has been shown to be impacted by pretreatment, particularly for coagulation and less so for PAC. The progression from direct to hybrid treatment (e.g., coagulation/sedimentation/C-MF) has produced benefits in terms of membrane fouling reduction by solids. However, these methods have shown variable benefits relative to NOM fouling. The research proposed within this study is intended to help elucidate NOM fouling mechanisms so that more cost-effective and reliable application of low-pressure membranes can be achieved.

## **RESEARCH APPROACH**

The research approach involved a comprehensive testing program consisting of complementary sets of bench-, pilot-, and full-scale membrane filtration tests. Several different types of bench tests were employed to contribute to the development of a surrogate test to predict fouling. These tests were supported by intensive analytical characterization of both water quality and membrane properties, and were augmented by membrane autopsies involving new diagnostic techniques. Innovative NOM characterizations were evaluated as predictors of fouling potential.

## **RESEARCH OBJECTIVES**

The primary research objectives of this study were:

- Identify and quantify problematical NOM foulant(s)
- Contrast NOM-related fouling potential for different types of waters
- Differentiate between hydraulically reversible versus irreversible fouling
- Distinguish between chemically reversible versus irreversible fouling
- Evaluate pretreatment options to reduce NOM-related fouling
- Determine how membrane operating conditions influence fouling
- Develop a predictive tool(s), either a surrogate parameter(s) or a fouling index, to estimate fouling potential.

In addition, and as a secondary objective, this study was to determine the influence of membrane properties on fouling.

## REPORT ORGANIZATION

This report is organized in these eight chapters:

- 1.0 Introduction, Background, and Objectives
- 2.0 Literature Survey
- 3.0 Experimental Methods and Procedures
- 4.0 Feed Water Characteristics and Membrane Properties
- 5.0 Bench-Scale Membrane Filtration Results
- 6.0 Pilot- and Full-Scale Membrane Filtration Results
- 7.0 Synthesis and Integration of All Results
- 8.0 Summary and Application to Utilities

Chapter 2 provides a brief overview of the present knowledge base of low-pressure membrane fouling by NOM.

Chapter 3 first defines the innovative analytical approaches used to characterize NOM in an attempt to define a surrogate parameter(s) as a predictor of fouling potential; it then depicts innovative techniques to define membrane properties that contribute to an integrated understanding of NOM-membrane interactions.

Chapter 4 summarizes the water quality, NOM characteristics, and routine parameters of several natural source waters and corresponding pretreated waters used as feed waters in various experiments, as well as membrane properties measured as part of this project and those provided by the respective manufacturer. The feed waters were selected to encompass a range of NOM types and were tested in corresponding bench- and pilot-scale tests. The hollow-fiber membranes selected for study were based on those used in commercial, full-scale drinking water and reuse facilities. Flat-sheet membranes were selected as potential analogs of hollow-fiber membranes with similar properties.

Chapter 5 begins with a summary of bench-scale testing protocols, stirred cell units with flat-sheet (disk specimen) membranes, and two different hollow-fiber units. Results derived from each testing unit are presented with associated discussion on the influence of operating conditions, pretreatment, backwashing, and cleaning. Results from characterization of fouled bench-scale membrane fibers are then presented. The chapter culminates with a derivation of a *unified modified fouling index (UMFI)* as a means of comparing results from different bench-scale protocols as well as results from the pilot- and full-scale studies presented later.

Chapter 6 presents results from the pilot testing using several source waters and several membranes. Results from each pilot test are presented with associated discussion on the influence of operating conditions, pretreatment, backwashing, and cleaning. The resultant data are then represented in terms of the UMFI concept. Results from the characterization of fouled fibers harvested from membrane modules operated in the pilot trials, together with foulant material extracted from these fibers, is then presented. The chapter culminates with a discussion of the full-scale results from other pilot studies using additional feed waters and membrane types.

Chapter 7 synthesizes the results from Chapters 4, 5, and 6. Various statistical tools are used to probe linkages between fouling (e.g., UMFI values) and NOM characteristics and/or membrane properties and/or operating conditions. The chapter then addresses scale-up issues to ascertain whether bench-scale simulations can predict larger-scale (i.e., pilot-scale) fouling. The

chapter culminates with an examination of whether there is a consistency between NOM feed water characteristics and NOM foulant deposited on membrane surfaces.

Chapter 8 presents an overall summary, conclusions, and recommendations for future research.

## CHAPTER 2

### LITERATURE SURVEY

#### CHARACTERISTICS OF NATURAL ORGANIC MATTER

NOM is a heterogeneous mixture with wide ranges in molecular weight (size) and functional groups. The mixture of NOM is formed by allochthonous input such as terrestrial vegetative debris and autochthonous input such as algae and associated cellular products. NOM has been shown to be aesthetically undesirable and to adversely impact public health through the formation of carcinogenic compounds. In particular, the chlorination of humic substances fraction of NOM with high aromaticity leads to DBP formation (Singer 1999).

NOM is difficult to quantify due to its complexity. For practical purposes, organic matter is quantified by measuring organic carbon concentrations such as total organic carbon (TOC), particulate organic carbon (POC), and dissolved organic carbon (DOC). In general, total organic matter (TOM), particulate organic matter (POM), and dissolved organic matter (DOM) constitute approximately twice the mass of TOC, POC, and DOC. The boundary between POC and DOC is 0.45  $\mu\text{m}$ ; DOC is operationally defined as organic carbon passing through 0.45  $\mu\text{m}$  filter (Thurman 1985).

Generally, NOM can be separated into three fractions by the XAD-8/-4 fractionation technique: the hydrophobic (HPO) fraction, which is XAD-8 adsorbable; the transphilic (TPI) fraction, which is XAD-4 adsorbable; and the hydrophilic (HPI) fraction, which passes through the XAD-8/-4 resin without any adsorption. The hydrophobic fraction that represents ~50 percent of DOC consists of larger molecular weight (MW)/low-charge density NOM acids such as humic and fulvic acids; the transphilic fraction that composes ~25 percent of the DOC includes medium MW/medium-charge density acids such as simple organic acids or sugar acids; and the hydrophilic fraction that comprises ~25 percent of DOC includes lower MW/high-charge density acids such as carboxylic acids as well as NOM bases and neutrals. The hydrophilic fraction is an operationally defined, non-humic fraction comprising bio-chemicals (proteins, polysaccharides, amino acids, etc.). Hydrophobic and transphilic neutrals, typically very minor constituents, adsorb onto XAD-8 and XAD-4 resins, respectively, while hydrophilic neutrals pass through both resins (Aiken et al. 1988; Thurman, Malcolm, and Aiken 1978; Aiken and Leenheer 1993; Aiken, et al. 1992; Aiken, et al. 1979). Humic substances have typically weak anionic polyelectrolytic properties (O'Melia, et al. 1999) due to carboxylic and phenolic functional groups. The anionic functional groups impart solubility, metal complexation, and buffer capacity. Humic and fulvic acids exhibit both aromatic and aliphatic characteristics. As a representative example, the molecular weights of Suwannee River humic and fulvic acids show ~1061 and ~800 molecular weight, respectively (Averett, et al. 1994).

Natural organic matter includes ~40-60 percent of fluorescent organic matter generally comprising organic acids and proteins. The acids are derived from the decomposition of plants and animals. Baker (2001) reported on high protein-like and fulvic-like fluorescence intensities in sewage treatment works (STW) discharge and the downstream flow of a sewage-impacted river. Esparza-Soto and Westerhoff (2001) used excitation emission matrix (EEM) spectroscopy to characterize organic matter of bacterial origin in wastewater treatment operations. They found three peaks from extracellular polymer substances (EPS) fractions: two peaks were protein-like substances, and one peak was a humic-like substance.

## EFFECTS OF NOM ON MEMBRANE FOULING

The different organic fractions have different hydrophobicities, molecular weights/sizes, and charge densities. Thus, different interactions in membrane filtration are expected. Bian et al. (1999) reported that UF membranes having a 50 kilo Dalton (kD) to 200 kD molecular weight cutoff remove only large-size humic substances, and pre-coagulation enhanced the removal efficiency of humic substances. Wiesner and Aptel (1996) reported that hydrophobic interactions might increase the accumulation of NOM on membranes with adsorptive fouling. Previous researchers (Combe, et al. 1999; Jones and O'Melia 2000) have indicated that NOM is responsible for membrane fouling by interacting with the membrane surface and structure. Yuan and Zydney (1999) found that NOM adsorbed both inside the pores and on the membrane surface, and formed a gel layer. The physical and chemical characteristics of humic acid can affect MF membrane fouling. For example, Aldrich humic acid with a lower functional group (i.e., carboxylic acids) content caused more significant flux decline than Suwannee River humic acid, which was more negatively charged and hydrophilic. The aromaticity of NOM can be an important factor in flux decline of UF membranes while it affects nanofiltration (NF) membranes less (Cho, et al. 1999). Her, et al. (2000) reported that significant flux decline is dependent on high DOC, high divalent cations (i.e., Fe and Al), high alkalinity, and low temperature in natural water for NF membranes.

Braghetta and co-authors (1997) described the relationship between ionic strength, pH, and flux decline of nanofiltration membranes. Low pH and high ionic strength caused compaction of membrane pores with a concomitant reduction of pure water permeability, allowing the molecules to accumulate more densely at the membrane surface by charge neutralization and shifting macromolecules to a smaller apparent macromolecular size range. These trends have been demonstrated for protein fouling of hydrophobic UF membranes. Her et al. (2002) investigated high-performance liquid chromatography (HPLC), size-exclusion chromatography (SEC) with ultraviolet absorbance (UVA), and on-line DOC detectors. The on-line DOC detector is capable of providing molecular weight distribution of non-aromatic, as well as aromatic, carbon compounds. Huber and Gluschke (1998) identified molecules (e.g., polysaccharides, humics, acids, and amphiphilics) contained in feed water for reverse osmosis (RO) membrane treatment with liquid chromatography with high-sensitivity organic carbon detection. Lee, et al. (2002) found that macromolecules (i.e., polysaccharides and proteins) that have a large-size molecular weight and a low ultraviolet (UV) response corresponding to the first peak of the high-pressure size-exclusion chromatography with an online connection of DOC and UV detectors (SEC-DOC/UV) were attributable to significant low-pressure membrane (MF/UF) fouling. Ng, et al. (2004) investigated the organic fouling of RO membranes using bovine serum albumin (BSA) and sodium alginate as representatives of proteins and polysaccharides. The fouling of sodium alginate was more significant than BSA and increased as the calcium (Ca) concentration increased. Habarou, et al. (2005) reported that the major organic foulant on membrane surfaces after backwashing and chemical cleaning is a mixture of biopolymers, especially aminosugars and polysaccharides, which are major constituents of membrane foulants.

Metal ions affect flux decline during membrane filtration. Hong and Elimelech (1997) studied the chemical and physical aspects of NOM fouling in nanofiltration (NF). Membrane fouling was increased with increased electrolyte (NaCl), decreased solution pH, and the addition of Ca<sup>2+</sup>; the rate of fouling is controlled by interplay between permeation drag and electrostatic double layer repulsion in NF. The influence of calcium presence has been investigated by many researchers as well. Calcium-induced charge neutralization by the divalent cation interacting

with the carboxylic functional groups of humic substances increased deposition of NOM on membrane surface (Maartens, et al. 1999; Cho, et al. 2000; Fan, et al. 2001).

Many researchers suggest that humic substances might play a role in the irreversible fouling of membranes (Combe, et al. 1999; Jones and O'Melia 2000; Yuan and Zydney 1999). Hydrophobic interactions between the hydrophobic NOM fraction and a hydrophobic membrane may cause more flux decline than that of a hydrophilic membrane associated with adsorptive fouling. However, recent studies suggest that neutrals and hydrophilic materials contribute more significant membrane flux decline (Cho, et al. 1998; Amy 2000; Lin, et al. 2000) and that low-aromatic hydrophilic neutral compounds determined the rate and extent of flux decline (Fan, et al. 2001; Carroll, et al. 2000).

From the research conducted by Chan, et al. (2002), the retention of larger-size proteins formed a dynamic layer that contributes considerable hydraulic resistance and increasing transmembrane pressure at the apparent critical flux. However, smaller proteins were mainly observed by mass spectrometry in fouled membranes, indicating that these proteins are retained in pores and membrane structures. Marwah, et al. (2005) reported that the major size range of foulants during filtration of Chattahoochee River water is 100,000 Da  $\sim$  1  $\mu$ m and that coagulation is effective in reducing membrane fouling.

## THE BASICS OF MEMBRANES

Membranes are classified by their operational driving force, separation mechanism, chemical nature, configuration, morphology, and geometry. MF, UF, NF, and RO membranes are pressure-driven membranes for which the driving force is a pressure difference across the membrane (known as TMP). MF and UF membranes are porous membranes that separate molecules based on their size. RO membranes are non-porous. NF membranes can be placed between porous and non-porous membranes due to consideration of diffusion and electrostatic effects. Membranes are made with two different mechanical structures: symmetric and asymmetric. An asymmetric membrane consists of two layers; one is a thin top layer comprising a polymer that has selectivity and a supporting layer that has more porous media and negligible resistance. Another form of asymmetric membrane is a composite membrane, i.e., a membrane composed of two identical membrane materials. The top layer is the same as any other asymmetric membrane; the support layer is another single asymmetric membrane.

Membranes are made of various organic or inorganic materials. Early organic membranes were made of cellulose, a natural material. Cellulose and its derivatives offer good chlorine resistance, but are subject to acid or alkaline hydrolysis, whose rate increases with temperature, and to biological degradation. Polyacrylonitrile (PAN) is also used for UF membranes, but not used for MF, NF, or RO. Polysulphone (PSF) and polyethersulphone (PES) are used for UF membranes and serve as a support for composite NF and RO membranes. Other hydrophobic membranes are constructed of polytetrafluoroethylene (PTFE), polyvinylidene fluoride (PVDF), polyethylene (PE), polycarbonate (PC), or isotactic polypropylene (PP). PP and PVDF are commonly used for MF membranes. PVDF has excellent chlorine resistance; PP does not.

For inorganic membranes, ceramics (e.g., alumina ( $\gamma$ -Al<sub>2</sub>O<sub>3</sub>,  $\alpha$ -Al<sub>2</sub>O<sub>3</sub>), zirconia (ZrO<sub>2</sub>), titania (TiO<sub>2</sub>), ceria (CeO<sub>2</sub>), glass (i.e., silicon dioxide (SiO<sub>2</sub>)), and metal (e.g., sintered steel fibers or powders in thin or thick film deposits on various support media) are used. Inorganic membranes are generally brittle and more expensive than organic membranes (Aptel and Buckley 1996, Amy 2000).

## MECHANISMS OF MEMBRANE FOULING

MF and UF membranes are porous, and they separate solutes mainly by size (steric) exclusion. MF membranes have been used for reducing turbidity/particles and larger microbials (protozoa, bacteria) from natural waters (Jacangelo and Buckley 1996), while UF membranes have been used to remove inorganic and organic particles/colloids and smaller microbials (viruses).

MF and UF membrane filtration rejects particulates/colloids and/or macromolecular solutes primarily by size exclusion. The accumulated molecules in, on, and near a membrane cause flux decline through the resistance of the fouled membrane. MF and UF membrane fouling can be explained by cake/gel layer formation, pore blockage, and/or adsorptive fouling.

Darcy's law describes the permeate flux in a clean membrane (Eq. 2.1).

$$J = \frac{\Delta P}{\mu R_m} \text{-----} (2.1)$$

Where, J: Permeate flux (m/second)

$\Delta P$ : Transmembrane pressure drop (kg/m<sup>2</sup>)

$\mu$ : The absolute viscosity of the water (kg/m-second)

$R_m$ : The hydraulic resistance of the clean membrane (m<sup>-1</sup>)

Membrane fouling can be described by the progressive saturation of adsorption sites of the membrane material by NOM. It has been shown that irreversible fouling of a hydrophobic membrane (e.g., polysulfone, polypropylene, etc.) is more significant due to chemical bonds with higher energy (Wiesner and Aptel 1996). Bowen, et al. (1995) elucidated the consecutive steps of membrane blocking in flux decline during protein microfiltration: the smallest pores were blocked by all particles arriving at the membrane for the initial blocking process, then the inner surfaces of bigger pores were covered, and afterwards, some particles covered other pre-existing particles while others directly blocked some of the pores, and finally, a cake layer started to build.

Colloidal substances and protein also cause MF and UF membrane fouling by deposition or forming of a cake/gel layer (Schäfer, et al. 2000; Ho 2001). Waite et al. (1999) suggested that the Carmen-Kozeny equation appeared to provide a reasonable description of the proportional differences in specific resistances that might be expected for cakes formed from aggregates of differing sizes and fractal dimensions in colloidal fouling. Jonsson and Jonsson (1995) calculated electrostatic interaction by the Poisson-Boltzmann equation, and dispersion forces and solid sphere interaction by the Carnahan-Starling equation to explain the interaction between the particles and the concentration polarization phenomena of colloidal dispersions in UF. Ho and Zydney (2000) developed a mathematical model for elucidating initial fouling in MF membrane filtration due to pore blockage and subsequent fouling due to the growth of a protein cake or deposit over the initially blocked area. Continuous membrane filtration leads to flux decline by pore blockage or cake/gel layer formation. Gray et al. (2005) indicated that a hydrophilic membrane provides less fouling than a hydrophobic membrane, and interaction between organic compounds leads to NOM adsorption on the membrane surface and blockage of membrane pores.

## MEMBRANE CHARACTERIZATION

Microscopy represents a powerful technique to visualize directly the structural appearance of MF and UF. Optical microscopy (OM), transmission electron microscopy (TEM), scanning electron microscopy (SEM), and atomic force microscopy (AFM) have been used for membrane characterization.

SEM has been widely used for surface analysis. It produces topographical images of the membrane surface and direct, practical, and instant structural membrane information (Zeman and Zydny 1996). Madaeni (1997) employed field emission scanning electron microscopy (FESEM) to better understand the critical flux mechanism in MF membrane filtration. Cake layer formation was not observed with a latex suspension. However, a small deposition occurred due to intermittent pore blockage or obstruction. Lee et al. (2003) provided morphological analysis with SEM and AFM for low-pressure (MF/UF) membranes fouled by NOM. They found that membrane fouling was caused by pore blockage and cake/gel layer formation with NOM and that the fouling was affected by the roughness and structure of membrane. Kim, et al. (1999) employed AFM to analyze pore size in comparison to SEM analysis. The pore diameters obtained from AFM are larger than those from SEM, and AFM analysis is considered to be more accurate due to its non-coating preparation of samples. Zeng, et al. (2003) investigated surface morphology and the nodule formation mechanism of cellulose acetate membranes with AFM and found that temperature and variation of the solvent environment are major factors for nodule formation on the membrane. AFM was used to investigate surface pore structures of MF and UF membranes and provided quantitative information on surface pore structure such as pore size, pore density, and porosity (Dietz, et al. 1992; Bowen, et al. 1996).

The measurement of contact angle explains the hydrophobicity/hydrophilicity of the membrane surface. Previous research has shown that a hydrophobic membrane can be changed in its hydrophobicity/hydrophilicity due to adsorption of foulants on the membrane surface (Cho, et al. 1998).

Attenuated Total Reflection-Fourier Transform Infrared Spectroscopy (ATR-FTIR) analysis provides valuable information related to the chemical structure of NOM and membrane surface by recognizing functional groups of molecules. Using FTIR, Jarusutthirak (2002) and Her (2002) found that a functional group such as alcohol and amide came from polysaccharides and proteins on fouled membranes, and those macromolecules cause significant NF membrane fouling. Belfer, et al. (2000) also investigated the functional group of modified PES ultrafiltration membranes and adsorption of albumin on the surface of the membrane. Croué, et al. (2003) employed FTIR, pyrolysis gas chromatography/mass spectrometry (GC/MS), and <sup>13</sup>C nuclear magnetic resonance (NMR) spectroscopy for autopsy of a nanofiltration membrane obtained from full-scale filtration. The organic phase was the major foulant. Calcium, iron, and aluminum are major inorganic constituents in fouling. Itoh and Magara (2004) found by membrane autopsy that citric acid is effective as a cleaning agent for a high content of inorganic foulant, especially one that has a high concentration of calcium.



## CHAPTER 3 EXPERIMENTAL METHODS AND PROCEDURES

### SOURCE WATERS

#### Identities and Rationale for Selection

The rate and extent of low-pressure membrane fouling by NOM is strongly influenced by the type and concentration of NOM that is present in the feed water. For the purposes of the bench- and pilot-study portions of this study, several natural waters were selected to obtain the full complement of NOM types: allochthonous (terrestrial) NOM, autochthonous (algal) NOM (also referred to as AOM), and wastewater EfOM. Four primary source waters (also referred to as feed waters) were chosen for use in the bench and Tier 1 pilot testing portions of the experimental work conducted (see Table 3.1). The Indianapolis water, as characterized by historical water quality, represented a supply that contained both autochthonous and allochthonous NOM, the former present in particular during the spring months during periodic algal blooms. The Scottsdale secondary effluent was selected to represent an effluent organic matter-dominated source having SMPs from the biological wastewater treatment process. The Twente Canal and Tampa Bay waters both represented sources that are dominated by allochthonous NOM, with the Tampa Bay water having very high levels of DOC and humic substances, as evidenced by its high color.

**Table 3.1**  
**Source waters: tier location and name**

Tier	Source water location	Source water name
1	Indianapolis (Ind.)	White River, raw and clarified
1	Scottsdale (Ariz.)	Filtered secondary effluent
1	Tampa Bay (Fla.)	Tampa Bypass Canal, Alafia River, and Hillsborough River
1	Enschede, The Netherlands	Twente Canal
2	Tuscaloosa (Ga.)	Lake Nicol, raw and clarified*
2	Minneapolis (Minn.)	Mississippi River, clarified†
2	North Bay, Ont., Canada	Trout Lake, raw
2	Parsons WTP (Kan.)	Labette Creek, clarified‡
2	Manitowoc (Wis.)	Lake Michigan, raw

\*Lake water is coagulated with lime and ferric chloride and then settled. Settled water is then dosed with caustic and potassium permanganate for manganese oxidation.

†River water is softened and coagulated with lime and alum, recarbonated, settled, re-coagulated with ferric chloride, and resettled. PAC is added to the recarbonation influent and either PAC or potassium permanganate is added to the raw water.

‡River water is treated prior to membrane filtration as follows: oxidation using potassium permanganate, taste and odor (organics) adsorption using PAC, coagulation/flocculation using polyaluminum chloride, sedimentation, and 500- $\mu$ m screening.

Also listed in [Table 3.1](#) are the five source waters associated with the Tier 2 pilot study and full-scale plant portions of the study. The Tuscaloosa pilot tests were conducted with both raw and clarified water from Lake Nichol, a predominantly allochthonous source. Minneapolis (Water Works) piloting was conducted with Mississippi River water, a highly allochthonous supply that had been first treated using lime softening (with alum addition) and recarbonation followed by ferric coagulation and settling. PAC is added to the recarbonation influent and either PAC or potassium permanganate is added to the raw water; all PAC is added upstream of the filter plants. The Parsons, Kan. full-scale water treatment plant is fed by water from Labette Creek, which is dominated by allochthonous NOM. This supply was treated as follows prior to membrane filtration: oxidation using potassium permanganate, PAC and polyaluminum chloride addition, coagulation/flocculation/sedimentation in an upflow flocculation blanket clarifier, and 500- $\mu\text{m}$  filtration. The second full-scale plant included in this project, the Manitowoc Public Utilities microfiltration plant, treated water obtained directly from Lake Michigan following 500- $\mu\text{m}$  screening.

### **Pre-Filtration Step**

Each sample was pre-filtered with a 0.45- $\mu\text{m}$  filter (PVDF filter [HVLP, Millipore]) prior to water quality analysis to comply with requirements of the analytical instruments and protocols. A 1.2- $\mu\text{m}$  filter (GF/C, Whatman) was used prior to bench-scale experiments (both stirred-cell tests and hollow-fiber unit tests) to remove particulate matter, but not colloidal (<1  $\mu\text{m}$ ) matter that might contribute to fouling. Because the pre-filtered samples still contained particulate organic matter, control experiments were performed to demonstrate that 1.2  $\mu\text{m}$  prefiltration had little, if any, impact on membrane fouling and would not have to be considered when comparing fouling rates between bench and pilot results (1.2- $\mu\text{m}$  prefiltration was not conducted with the pilot studies).

## **MEMBRANES**

A variety of membrane materials are used in the manufacture of hollow-fiber, low-pressure membrane filtration for drinking water production. The most common materials currently in use include PVDF and PES. PES is predominantly used in “inside-out” flow mode and in UF membranes. In contrast, PVDF is manufactured in both MF and UF membranes and predominantly used in “outside-in” flow configuration. For purposes of this research, hollow-fiber membranes comprising both materials were selected for testing.

A primary objective of this research was to develop a fouling surrogate test or index that could be used to quickly, yet accurately, assess the fouling characteristics of a given membrane on a given source water. In addition to the testing of hollow-fiber membranes, flat-sheet membranes were also evaluated to assess the applicability of a stirred-cell test as a fouling surrogate.

### **Flat-Sheet Membranes**

Three different types of flat-sheet MF/UF membranes were selected as a potentially equivalent simulation of commercial hollow-fiber membranes ([Table 3.2](#)) for use in NOM fouling studies conducted using the dead-end, stirred-cell unit. Two of the membranes were hydrophilic and one membrane was hydrophobic based on specifications from the manufacturer

**Table 3.2**  
**Characteristics of flat-sheet membranes used in the stirred-cell unit**

Membrane	Material	Pore size/ MWCO	HPO/HPI*	Manufacturer	Corresponding hollow-fiber membrane
VVLP	PVDF	0.1-0.2 $\mu\text{m}$	HPI	Millipore	Siemens MEMCOR
MX500	PAN	0.05 $\mu\text{m}$	HPI	Osmonics	ZeeWeed Zenon (pore size only, not material)
PES100	PES	100 KD	HPO	Amicon	Hydra-cap/ Hydranautics; XIGA/Norit

\*Specified by manufacturer and/or inferred from material

and/or inferred from the polymeric material. The hydrophobic membrane was a UF membrane made of PES. Each membrane was anticipated to show different trends of membrane fouling depending on NOM characteristics and membrane properties.

### **Hollow-Fiber Membranes**

#### ***Bench and Tier 1 Pilot Studies***

Two primary types of membrane materials were utilized in the bench and Tier 1 pilot studies—PES and PVDF—as they represent the dominant materials in use in commercial MF/UF systems for drinking water. These materials were provided by four different membrane suppliers in hollow fibers, operated in two different flow patterns (from feed to filtrate): outside-in and inside-out. The names of the membranes, their suppliers, as well as the characteristics of each product, are shown in [Table 3.3](#). For the HYDRA-cap product, two different versions of the PES UF membrane were used. The “new” version was used in the bench studies, while the “old” version was used in the Tier 1 pilot study (on Scottsdale effluent). This use of the two different versions was not by design. Hydranautics did not inform the research team of the differences in the products until a majority of the bench studies were completed and after the pilot study had been completed. Unfortunately, this prevented a direct comparison of fouling results between bench- and pilot-scale. It did, however, permit a comparison of fouling between the two formulations on the same water (Scottsdale effluent) using the unified modified fouling index.

#### ***Tier 2 Pilot Studies***

The three Tier 2 pilot studies used the membrane products as shown in [Table 3.4](#). These included products used in the bench and Tier 1 studies as well as products not tested in these studies, but employing the same membrane material and flow pattern. For purposes of this study, hydrophilic refers to a contact angle greater than 50 degrees and hydrophobic refers to a contact angle less than 50 degrees.

**Table 3.3**  
**Characteristics of hollow-fiber membranes used in bench- and Tier 1 pilot-scale testing\***

Designation	Membrane	Supplier	Type	Material	Pore size/ MWCO	Flow pattern	Surface characteristic
A	CMF-L	Siemens MEMCOR	MF	PVDF	0.1 μm	Outside-in	Hydrophobic
B	ZW-1000	Zenon	UF	PVDF	0.02 μm	Outside-in	Hydrophobic
C	XIGA	Ionics/Norit		PES/PVP†	100 kD	Inside-out	Hydrophilic
D1	HYDRA-cap - old	Hydranautics	UF	PES/ PVP†	0.025 μm/ 150 kD	Inside-out	Hydrophilic
D2	HYDRA-cap - new	Hydranautics	UF	PES	100 kD/ 0.020 μm	Inside-out	Hydrophobic
E	Microza	Pall Corporation	MF	PVDF	0.1 μm	Outside	Hydrophobic
F	CMF	Siemens MEMCOR	MF	PP	0.2 μm	Outside	Hydrophobic

\*As specified by the supplier.

†PVP is incorporated into the membrane structure to increase the hydrophilicity of the PES.

**Table 3.4**  
**Membrane products and their characteristics – Tier 2 pilot studies and full-scale plants**

Scale	Location	Membrane	Supplier (Membrane Designation)	Type	Material	Pore size/ MWCO	Flow pattern	Surface characteristic
T2P*	Tuscaloosa	CMF-s	Siemens MEMCOR (A)	MF	PVDF	0.1 μm	Outside-in	Hydrophilic
		ZW-1000	Zenon (B)	UF	PVDF	0.02 μm	Outside-in	
		Microza	Pall (E)	MF	PVDF	0.1 μm	Outside-in	
T2P	North Bay	CMF-s	Siemens MEMCOR (A)	MF	PVDF	0.1 μm	Outside-in	Hydrophilic
T2P	Minneapolis	XIGA	Ionics/Norit (C)	UF	PES	100 kD	Inside-out	Hydrophilic
FS†	Parsons	Microza	Pall (E)	MF	PVDF	0.1 μm	Outside-in	Hydrophobic
FS	Manitowoc	CMF	Siemens MEMCOR (A)	MF	PP‡	0.2 μm	Outside-in	Hydrophobic

\*Tier 2 pilot studies

†Full-scale plant

‡Polypropylene

## ***Full-scale Plant Studies***

The two full-scale plants used the membrane products as shown in [Table 3.4](#). The PP membrane in use at the Manitowoc facility represents an older material that was commonly employed by Siemens MEMCOR in the 1990s when the Manitowoc facility was constructed. The Parsons facility uses Microza modules manufactured by Asahi (Japan) and incorporated into a complete system by Pall Corporation. These modules use fibers composed of PVDF, the same material used with two of the four fibers tested at bench- and pilot-scale.

## **WATER QUALITY CHARACTERIZATION**

NOM characterization was conducted by the University of Colorado (or under its direction) using the following methods: DOC, UV absorbance at 254 nm ( $UVA_{254}$ ), specific UV absorbance ( $SUVA = UVA_{254}/DOC$ ), XAD-8/-4 resin fractionation of DOC, SEC-DOC/UV, a three-dimensional (3D) fluorescence EEM, and dissolved organic nitrogen (DON). Both DOC and DON measurements were performed on 0.45  $\mu\text{m}$  filtered samples. Routine water quality parameters tested included turbidity, pH, hardness, and alkalinity. Inorganic constituents tested included cations (Ca, Fe, Mn), anions ( $\text{Br}^-\text{PO}_4^{3-}$ ,  $\text{SO}_4^{2-}$ ), and  $\text{SiO}_2$  that were also analyzed at the University of Colorado.

[Table 3.5](#) lists the water quality analyses that were conducted for the Tampa Bay, Scottsdale, and Indianapolis source waters by the in-plant laboratories during pilot testing.

### **Natural Organic Matter**

#### ***XAD-8/-4 Resin Fractionation***

XAD-8/-4 resin fractionation (adsorption chromatography) was performed using a sequence of XAD-8 adsorption (white colored beads [40 to 60 mesh size]) followed by XAD-4 adsorption (amber colored beads [20 to 60 mesh size]). Using this protocol, NOM can be separated into three fractions according to DOC: the HPO fraction, which is XAD-8 adsorbable; the TPI fraction, which is XAD-4 adsorbable; and the HPI fraction, which passes through the XAD-8/-4 resins without any adsorption. The organic colloid fraction ends up in the hydrophilic fraction when pre-dialysis is not used (as was the case in this study); thus, organic colloids are classified as hydrophilic. This fraction also includes hydrophilic macromolecules such as polysaccharides and proteins. The waters were first adjusted to pH 2.0 before being passed through XAD-8 and XAD-4 in sequence ([Figure 3.1](#)). Each fraction was determined by performing a DOC mass balance across XAD-8/-4 resin columns.

**Table 3.5**  
**In-plant water quality analyses – Tier 1 pilot studies**

Membrane product	Characteristics
General	Temperature, pH, total hardness, conductivity, TDS, turbidity, particle count*, color†, alkalinity
Metals	Calcium, iron (total and dissolved), manganese (total and dissolved)
Organics	TOC, UVA <sub>254</sub>
Microbial	Heterotrophic Plate Count (HPC)†, chlorophyll <u>a</u> *

\*For Indianapolis only.

†For Tampa Bay and Indianapolis only.

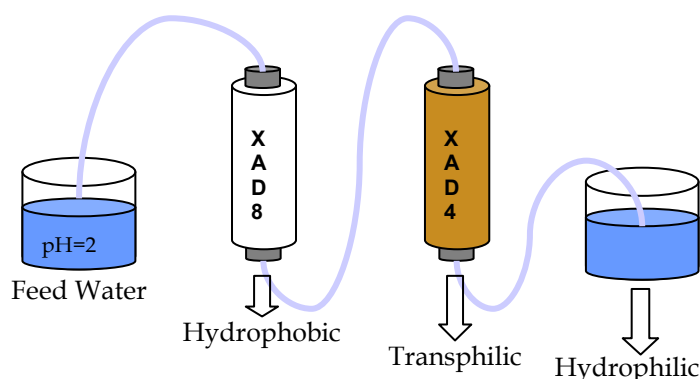


**Figure 3.1 Schematic diagram of XAD-8/-4 resin fractionation**

### ***High-Pressure Size-Exclusion Chromatography***

Apparent MW distributions were determined using an SEC method. An HPLC (LC600 Shimadzu) was used with a UVA detector (SPD-6A Shimadzu) and an on-line DOC detector (modified Sievers Turbo Total Organic Carbon Analyzer) following size separation by a HW-50S column. The column packing material was a Toyopearl resin (semi-rigid, spherical beads) with a hydrophilic surface that is synthesized by co-polymerization of ethylene glycol and methacrylate-type polymers (GROM, Denmark). The separation range of the column was 100 to 18,000 Daltons based on polyethylene glycols (PEGs), and 500 to 80,000 Daltons based on globular proteins. The DOC detector was connected to the UVA detector waste line sequentially. UVA and DOC data were recorded every 6 seconds by a modified Labview software. The SEC column separated compounds based on hydrodynamic molecular size. The average retention time was affected by the effective size and structure of the molecules. Consequently, larger and linear-shaped molecules were excluded earlier than smaller and globular shape molecules. Polyethylene glycols were used for calibration of the relationship between MW and retention time. Samples with a DOC of 1 to 10 mg/L samples were analyzed with this instrument; samples with over 10 mg/L DOC were diluted with Milli-Q (DOC-free) water. The UV (254 nm) detector was effective in recognizing aromatic (humic) substances but was poor in detecting aliphatic

(non-humic) substances. Conversely, the DOC detector recognized all organic matter. A typical SEC-DOC chromatogram revealed a PS peak consisting of polysaccharides, proteins, and organic colloids; a humic substances (HS) peak; and a low molecular weight acids (LMA) peak. To quantify the SEC results, individual peaks were integrated using a trapezoidal method and expressed as DOC.

### ***Fluorescence Excitation Emission Matrix***

A JY-Horiba/Spex Fluoromax-2 fluorometer with a xenon lamp as an excitation source was used for measuring the 3D EEM matrices (spectra) of NOM sources (Jobin-Yvon-Horiba, Edison, NJ). Three-dimensional EEM spectra were obtained by collecting excitation (Ex) and emission (Em) spectra over a range (200 to 500 nm). Data were analyzed with DataMax software and displayed on a contour map (Figure 3.2). Spectral subtraction was performed to remove blank spectra mainly caused by Raman scattering. Through knowledge of EEM mapping of known compounds/substances, EEM regions can be identified because they correspond to humic-like NOM (peak at higher Em/Ex) versus protein-like NOM (peak at lower Ex/Em). Quantitative data can be extracted from EEM by estimation of a fluorescence index (FI) employed to identify NOM properties corresponding to origin/source. FI is the ratio of fluorescence intensity at Em 50 nm to fluorescence intensity at Em 500 nm, at Ex 370 nm. Fluorescence index values generally range from about 1.4 for plant/terrestrially derived (allochthonous) NOM to about 1.9 for algal/microbial-derived (autochthonous) NOM (AOM or EfOM) (McKnight et al., 2001).

### ***Dissolved Organic Nitrogen***

DON was analyzed by two methods. The first is LC-OND (liquid chromatography with organic nitrogen detection) performed by a laboratory in Germany. This method is similar to SEC-DOC except that it uses a total nitrogen (TN) detector to detect organic nitrogen chromatographically separated from inorganic nitrogen. The second involves an initial dialysis step using a 100 D (cellulose ester) dialysis bag (Spectra/Por, Spectrum Laboratories Inc., Calif.) with continuous recirculation of Milli-Q water to eliminate inorganic nitrogen, followed by direct DON measurement of the material retained within the bag by a TN analyzer.

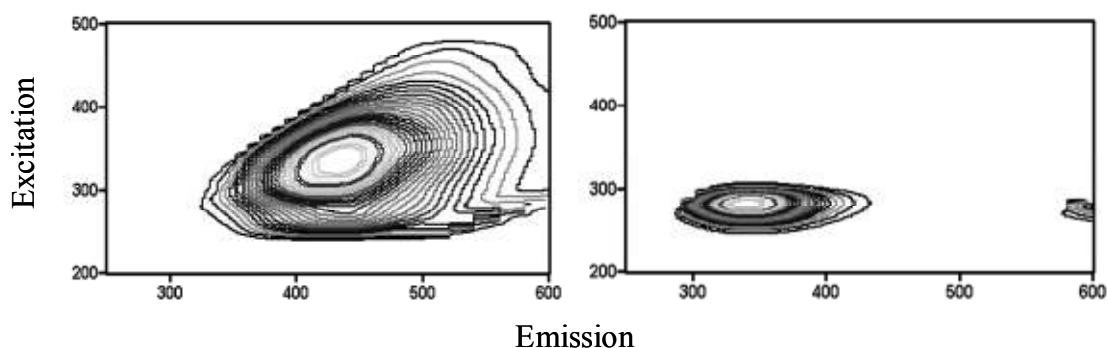


**Figure 3.2 Typical EEM spectra (left: humic acid, right: protein)**

## General, Inorganic, and Microbial Compounds

Inorganic compounds are also important in membrane fouling. Metal ions (e.g.,  $\text{Ca}^{2+}$ ) can contribute to fouling by forming NOM complexes and neutralizing NOM charge, and to precipitative (e.g., Fe and Mn) fouling (scaling). The presence of Ca in water is a very important factor; while it has a lower binding constant than other divalent heavy metals (e.g.,  $\text{Cu}^{2+}$ ), it is much more abundant in natural waters. Anions are more influential in coagulation or adsorption in water treatment. However, in the case of a hybrid system with a low-pressure membrane, the presence of anions is also important factor.

pH can influence membrane surface properties such as the zeta potential (charge), as well as the steric configuration and charge of humic substances (humic and fulvic acids).

Methods, instruments, and associated controls used for the analysis of the inorganic parameters monitored in both the bench and Tier 1 pilot portions of the study are presented in [Table 3.6](#). Samples collected in the field (pilot) and laboratory (bench) were labeled clearly and legibly with the following information:

- Parameter
- Any preservative agent present
- Laboratory analyzing sample
- Date and time of sample collection
- Facility where sample collected
- Sample location within facility
- Sample number
- Replicate (A, B, or C, whenever appropriate)

Chain-of-custody forms were used to track sample handling to ensure compliance with accepted sample holding times and to report sample conditions upon receipt. Where practical, samples were collected during the early part of the week to prevent storage of samples through the weekend. All samples were shipped via overnight delivery to ensure that travel times were kept to a minimum. Where appropriate, travel blanks and standards were included in the sample shipment.

## MEMBRANE CHARACTERIZATION AND MORPHOLOGY

Membrane hollow fibers harvested from pilot-scale modules were first preserved in 1 M sodium bisulfite to prevent microbial growth, cooled, and then shipped by express courier in an iced cooler to the University of Poitiers, France.

**Table 3.6**  
**Inorganic parameters and associated analytical methods**

Parameter	Method/reference	Instrument	Controls		Calibration
			Negative	Positive	
Alkalinity	Standard Method 2320 B. (APHA 2005)	None (glassware only)	None: A standard is run at the beginning and end of each sample batch as calibration checks.	None A standard is run at the beginning and end of each sample batch as calibration checks.	Standardize the acid against a sodium carbonate solution.
Ammonia	Standard Method 4500-NH <sub>3</sub> E. (APHA 2005)	Orion EA 940 Expandable Ion Analyzer		A calibration curve is run with every sample batch; 10% of samples are spiked.	Per Method
Calcium	U.S. Environmental Protection Agency (EPA) Method 200.7 (EPA 1999)	VARIAN ICP	Per Method	Per Method	Per Method
Hardness	Standard Method 2340 C. (APHA 2005)	Standard glassware	A standard is run at the beginning and end of each sample batch as calibration checks	A standard is run at the beginning and end of each sample batch as calibration checks	
Nitrite/nitrate	Standard Method 4110 B. (APHA 2005); EPA Method 300.0 (EPA 1999)	DIONEX DX500	Milli-Q water	Standards prepared from chemicals in both Milli-Q and matrix addition	Seven-point calibration curve

(continued)

**Table 3.6 (Continued)**

Parameter	Method/reference	Instrument	Controls		Calibration
			Negative	Positive	
pH	Standard Method 4500-H+ B. (APHA, 2005)	Orion 250 A pH meter	None	None	Commercial pH calibration buffers, pH 4,7,10. Calibrated prior to analyzing any batch of samples. Electrode solution verified prior to analysis.
Temperature	Standard Method 2550 B. (APHA 2005)	Certified thermometer	None	None	Checked against NIST-certified thermometer once per year
Total Nitrogen	EPA Method 300.00 (EPA 1999)	DIONEX DX500	Per Method	Per Method	Per Method
TOC	EPA Method 415.3 (EPA 1999)	Total Organic Carbon Analyzer, Model 80, Sievers	Milli-Q water	None	Potassium hydrogen phthalate (KHP) standard
Turbidity	Standard Method 2130 B. (APHA 2005) EPA Method 180.1 (EPA 1999)	Hach 2100N turbidimeter	Milli-Q water	None	As specified in manufacturer's instructions with Hach's formazin standards

(continued)

**Table 3.6 (Continued)**

Parameter	Method/reference	Instrument	Controls		Calibration
			Negative	Positive	
UVA254 nm	EPA Method 415.3 (EPA 1999)	UV Spectropho meter, Shimadzu UV-VIS Model UV- 160/CL-750	Milli-Q water	None	Not applicable
Iron	EPA Method 200.7 (EPA 1999)	VARIAN ICP	Per Method	Per Method	Per Method
Manganese	EPA Method 200.7 (EPA 1999)	VARIAN ICP	Per Method	Per Method	Per Method

## Scanning Electron Microscopy

Scanning electron microscopy (SEM) analyses were performed with a JSM-6301 F JEOL apparatus to characterize the surface and physical characteristics of the hollow-fiber membranes (pore size and structure, inner and outer diameter, wall thickness, and surface appearance). The operational conditions were as follows:

- Pressure = 10<sup>-7</sup> torr, electron beam energy 3 to 5 keV, secondary electrons used
- Magnification of 100 to 50,000
- Resolution ≈ 20 nm

Before analysis, the membranes were rinsed with Milli-Q water to remove the bisulfite used for preservation, and the membranes were coated with a thickness of less than 2 nm of carbon using a vacuum chamber process.

## Streaming Potential

Following the experimental approach developed by Habarou et al. (2005), streaming potential measurements were conducted using the equipment shown in [Figure 3.3](#). The streaming potential measurement across the membrane provides an indication of the surface charge in the membrane pores.

The streaming potential is determined as the slope (K) of the curve resulting from the linear regression between the difference of potential between two Ag-AgCl electrodes ( $\Delta\Phi = E_2 - E_1$ , mV) and the pressure applied ( $\Delta P$ , mV/mbar):

$$\Delta\Phi = K(\Delta P)$$

with electrode E2 immersed in the permeate,  
electrode E1 immersed in the feed water

The streaming potential is directly proportional to zeta potential,  $\zeta$ , and is inversely proportional to conductivity according to the Helmholtz-Schmoluchovsky equation. Using low concentration electrolytes (10<sup>-3</sup> M), zeta potential can be determined from the streaming potential measurement as follows:

$$\zeta = 1.406(\Delta\Phi/\Delta P)(\rho)$$

$\zeta$ : zeta potential (mV)

$\rho$ : electrical conductivity ( $\mu\text{S}/\text{cm}$ )

Streaming potentials of the different membranes were determined using a KCl 2.10<sup>-4</sup> M solution at pH 6.5. The isoelectric point was determined from the plot of the streaming potential determined at different pH levels as shown on [Figure 3.4](#).

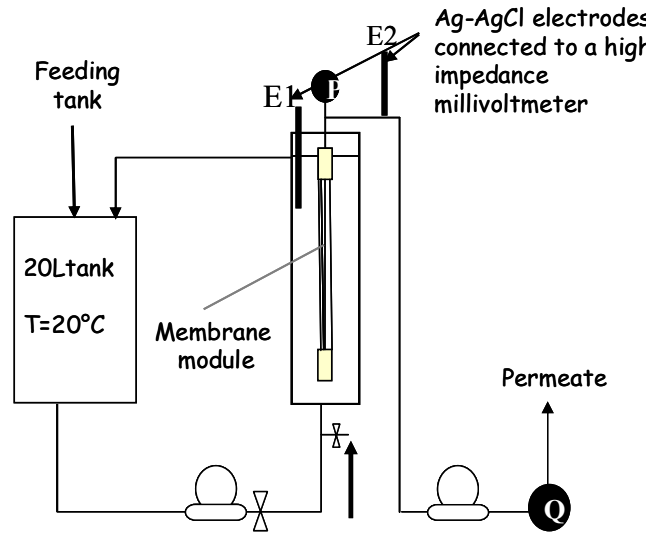


Figure 3.3 Hollow-fiber pilot-scale unit used for streaming potential measurements

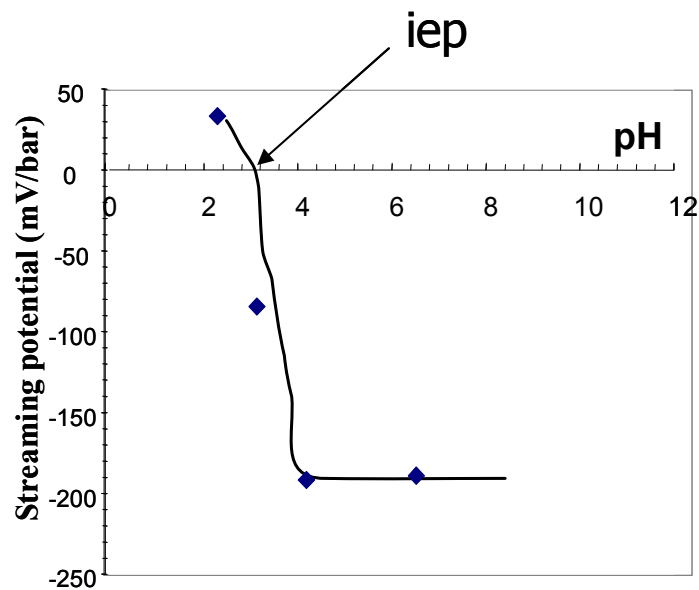


Figure 3.4 Determination of the isoelectric point of Membrane D2

## Contact Angle Measurement

Contact angle measurements were determined using a Kruss G 10 Goniometer (monitored with DSA software, version 1.9). A photo of the equipment used is shown in [Figure 3.5](#). The experimental protocol consists of the deposition of a 2- $\mu$ L drop of Milli-Q water at the surface of the membrane. A photo is immediately taken (image capture occurred in less than 1 second) and used to measure the contact angle that characterized the shape of the drop at the membrane surface. The higher the contact angle, the stronger the hydrophobic character of the membrane surface. Although there is no industry consensus, a contact angle of greater than or less than 50° is generally considered HPO or HPI, respectively.

The contact angle was determined for hollow-fiber and flat-sheet membranes. Only the contact angle of the outer surface could be determined for the hollow fibers given their small diameter. However, measurement of the inner surface was attempted, first by splitting and flattening the fibers and then by applying a drop of water to the flattened surface. This technique was not successful due to the shape and size of the fibers. The water drop was too large for the fibers and the shape of the fiber after slicing (concave) could not be accurately photographed with the Goniometer. Consequently, only contact angles for the outside-in flow hollow-fiber membranes, where the angle of the filtration surface of the fiber could be measured, are reported herein.

For virgin membranes, contact angle measurements were performed with membranes as received or after several rinses with Milli-Q water over 48 hours. The membrane was dried in a dry chamber for 12 hours before analysis. Membranes isolated from a pilot unit and stored in bisulfite for shipment were carefully rinsed with Milli-Q water and dried using the same protocol specified above.

All contact angle values reported herein were the average value of 8 to 10 measurements conducted with several fibers.

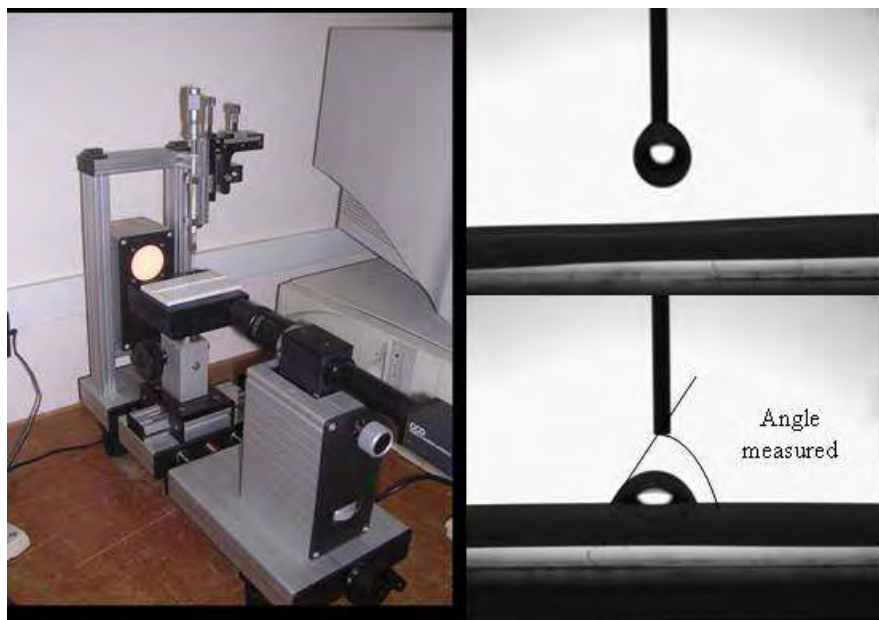


**Figure 3.5 Contact angle equipment and method**

## Atomic Force Microscopy

AFM analysis was conducted using the tapping mode (implemented in ambient air) with dry membrane. A siliceous tip at a 300 Hz (NCHR-W, VEECO) resonant frequency was used. The scanning frequency was fixed to 0.6 Hz. Based on preliminary tests, two distinct scanning areas were chosen for outside-in and inside-out depending on the membrane status. All virgin membranes were compared with the AFM scan of  $5.0 \times 2.5 \mu\text{m}^2$ . Roughness analysis of inside-out membranes was also conducted with an AFM scan of  $20 \times 10 \mu\text{m}^2$  to compare virgin and fouled hollow fiber membranes. The spatial resolution was 10 nm laterally and  $<0.1$  nm vertically.

Roughness analysis was conducted on the filtering surface of each membrane: the outer surface of the outside-in membrane and on the inner surface of the inside-out membrane (the membrane was sliced and gently flattened to perform the inner AFM scan). Ra (arithmetic average roughness) is the most commonly used parameter to describe the average surface roughness and is defined as an integral of the absolute value of the roughness profile measured over an evaluation length:

$$Ra = \frac{1}{l} \int_0^l |z(x)| dx$$

The average roughness is the total area of the peaks and valleys divided by the evaluation length. The total area of the peaks above the mean line should be equal to the total area of the valleys below the mean line.

The Rq roughness (statistical approach) is the root mean squared (RMS) value of all vertical deviations from the mean surface level.

$$R_{ms} = \sqrt{\frac{\sum (Z_i - Z_m)^2}{N_p}}$$

with  $Z_i$  = peak height,  $Z_m$  = average peak height,  $N_p$  = number of measurements

## Pyrolysis – Gas Chromatography/Mass Spectrometry

Low-temperature (300° C) pyrolysis-GC/MS analysis was performed directly on hollow-fiber fragments. The objective of this analysis was to develop a better understanding of the chemical nature of the membrane surface, in particular to determine if a hydrophilic coating material was utilized to increase the hydrophilicity of the membrane (e.g., PVP). The instrument used was a Pyroprobe 2000 (Chemical Data Systems, Oxford, Pa.) filament pyrolyzer. An approximately 1-cm long fiber fragment was deposited into each 100- $\mu\text{L}$  quartz tube. The quartz tube was then placed into the platinum filament of the pyrolysis probe that was inserted into the pyrolysis oven. This oven was connected to the split/splitless injection port of a Hewlett Packard G1800 gas chromatography detector (GCD) system equipped with an electron ionization detector. The pyrolysis was performed in a platinum filament that was programmed to a final temperature of 300° C at a rate of 20° C/ms, with a final hold for 20 seconds. The use of higher temperature produces more complex pyrochromatograms that are difficult to interpret. After flash pyrolysis, the thermal degradation fragments were separated by GC. A 30-m DB-Wax

(J&W Scientific) fused-silica capillary column was temperature-programmed from 30 to 220° C at a rate of 3° C/min. The fragments were then identified by a mass spectrometer operated at 70 eV scanning from 20 to 450 amu at 1 scan/second.

## MEMBRANE FOULANT CHARACTERIZATION

Hollow fibers extracted from bench- and pilot-scale modules following testing were thoroughly rinsed with Milli-Q water to remove residual sodium bisulfite. Fibers were cut into 5 to 10 cm long fragments, immersed in Milli-Q water, and sonicated using a BRANSON sonication stick at 15 W (2 pulses/second) for 30 minutes at room temperature. The temperature was found to increase by 2 to 3° C during sonication. After sonication, the membranes were removed and the solution was lyophilized to recover the organic foulant that was resolubilized. [Figure 3.6](#) shows the material isolated from hollow fibers harvested from the Indianapolis pilot modules.

Isolated material was characterized using:

- DOC + TN analysis and SEC coupled with a UV detector analysis after the isolate was redissolved in Milli-Q water.
- FTIR analyses and Pyrolysis gas chromatography/mass spectrometry and thermochemolysis gas chromatography/mass spectrometry analyses on the dry material.

### Dissolved Organic Carbon and Total Nitrogen Analyses

To obtain DOC and TN measurements, the solution of foulant material was analyzed using a Shimadzu TOC-VCSH/CSN analyzer.



**Figure 3.6 Material isolated from Membrane A**

## High-Pressure Size-Exclusion Chromatography/Ultraviolet Analysis

SEC-DOC/UV 260 analysis was performed on a BIOSEP SEC-2000 (7.8 x 300 mm, MW range 800 – 300,000 Da, particle size: 5  $\mu\text{m}$ ) using a flow rate of 1 mL/min. The mobile phase was a 10 mM sodium acetate solution adjusted at pH 7 with acetic acid. The UV detection was performed using Photodiode array detector (Waters 996).

## Fourier Transformed Infrared Analyses

Infrared spectra were collected using few mg of material in potassium bromide (KBr) pellets. Spectra were recorded at ambient temperature from 400 to 3000  $\text{cm}^{-1}$  using a NICOLET 750 Magna-IR<sup>TM</sup> FTIR spectrophotometer with a 2  $\text{cm}^{-1}$  resolution.

## Pyrolysis Gas Chromatography/Mass Spectrometry

Isolated foulants were submitted to flash pyrolysis–GC/MS according to the method described by Bruchet et al. (1990) using the same equipment as described previously. Approximately 1 mg of each dry sample was deposited into 100  $\mu\text{L}$  quartz tubes. Quartz wool was used at both ends of the tubes to prevent the samples from escaping during their introduction into the pyrolysis interface. The pyrolysis oven was preheated to 200° C. The final temperature of the temperature program was 650° C with a rate of 20° C/ms and a final hold of 20 seconds. The thermal degradation fragments were analyzed as described previously.

Upon rapid heating at a high temperature, natural and synthetic biopolymers degrade into a large number of low molecular-weight thermal decomposition products that were volatile enough to be separated and identified by GC/MS. Only the major pyrolysis fragments most commonly encountered in pyrochromatograms from aquatic NOM were considered in this study (see [Table 3.7](#)).

The relative abundance of each biopolymer was determined as the sum of its corresponding pyrolysis fragments listed in [Table 3.7](#) divided by the sum of all the fragments considered for this study. By contrast with previous work by Bruchet et al. (1990), no correction factors were applied to address the relative abundance of the different major biopolymers. It is important to note that the pyrolysis fragments produced from the degradation of the membrane at elevated temperatures were not taken into account (e.g., acetic acid, pyrrolidinones, pyrrolidones, and fluorocompounds).

**Table 3.7**  
**Specific pyrolysis fragments of biopolymers considered in this study**

Type	Pyrolysis fragments
Polyhydroxyaromatics	Phenol, p-Cresol, m-Cresol, C <sub>2</sub> -Phenol, methoxy phenols
Other aromatics	Benzene, alkylbenzene, naphthalene, indene
Proteins	Acetonitrile, benzonitrile, phenylacetonitrile, pyridine, methylpyridine, pyrrole, methylpyrrole, indole, methylindole, toluene, styrene
Polysaccharides	Methylfuran, furfural, furaldehyde, acetylfuran, benzofuran, methylfurfural, levoglucosenone, hydroxypropanone, cyclopentenone, methylecyclopentenone, acetophenone, benzaldehyde
Aminosugars	Acetamide, <i>N</i> -methylacetamide, propanamide
Bacterial origins	Furfuryl alcohol, Butenoic acid, fatty acids

### Thermochemolysis Gas Chromatography/Mass Spectrometry

For thermochemolysis, a 2- to 3-mg sample was placed in a tube and moistened with 100  $\mu$ L of a methanol 25 percent w/w solution of tetramethyl ammonium hydroxide (TMAH) overnight at 70° C. The sample was then placed in a quartz pyrolysis tube and subjected to flash pyrolysis (Pyroprobe 2000) conducted at 400° C as a final temperature and a hold of 20 seconds. The thermochemolysis by-products were analyzed by GC/MS. GC separation was carried out with a Hewlett Packard 6890 gas chromatograph using a HP-5 (Hewlett Packard) capillary column (30 m long). The temperature of the column was programmed from 60 to 300° C at 5° C/min. GC/MS was performed with a ThermoFinnigan Automass Solo mass spectrometer.

### MEMBRANE TESTING

Testing to characterize the effect of NOM on membrane fouling and the impact of different foulant management strategies was conducted at bench and pilot scale. This testing comprised the following:

- Bench testing using flat-sheet membranes and a dead-end, stirred-cell unit
- Bench testing using hollow-fiber membranes and a dead-end test unit employing both end-of-run and periodic backwashing (Hollow-Fiber Unit 1)
- Bench testing using hollow-fiber membranes and a dead-end unit employing periodic backwashing (Hollow-Fiber Unit 2)
- Pilot testing using four different vendor-supplied pilot units

Additionally, operational data on the performance of membrane filtration units from the two full-scale facilities were analyzed in conjunction with characterization of the units' feed water NOM and fouled membrane fibers.

Table 3.8 presents a matrix of the locations where each type of testing was conducted. Table 3.9 shows a characterization matrix for the virgin and fouled membranes and membrane foulant.

**Table 3.8**  
**Location and testing matrix**

Location	Bench – flat sheet, stirred cell	Bench – Hollow-Fiber Unit 1	Bench – Hollow Fiber Unit 2	Pilot	Full-scale
Tampa Bay	X	X	X	X	
Scottsdale	X	X	X	X	
Indianapolis	X	X	X	X	
Twente Canal	X	X	X	X	
Tuscaloosa	X			X	
Minneapolis				X	
North Bay				X	
Parsons					X
Manitowoc					X

**Table 3.9**  
**Membrane and foulant characterization matrix**

Designation	Membrane	Virgin*	Fouled	Foulant
A	CMF-s	BS	BS, PS	PS
B	ZW-1000	BS	BS, PS	PS
C	XIGA	BS		
D1	HYDRA-cap (old)	PS	PS	PS
D2	HYDRA-cap (new)	BS		
E	Microza			
F	CMF		FS†	FS
NA‡	VVLP	SC		
NA	MX-500	SC		
NA	PES-100	SC		

\*BS – from Hollow-Fiber Unit 1 tests, PS – from pilot-scale tests, SC – stirred-cell units

†FS – from full-scale plant.

‡NA – not applicable

## Bench-Scale Simulations

### *Dead-End Stirred-Cell Unit*

NOM flux decline tests were performed using a dead-end, stirred-cell filtration unit (Amicon Div., W.R. Grace, Mass.) under constant pressure. Dead-end, stirred-cell tests provide realistic filtration conditions to investigate NOM impacts on membrane fouling. One L of feed water was filtered until 150 mL of retentate remained in the cell. For backwashing, the membrane was turned over (face down) and filtered with 150 mL of permeate at the same flux. Thus, feed, permeate, retentate, and backwash samples were collected from each membrane filtration. The contents of the cell were stirred at 200 rpm. The flux was recorded automatically with a computer by measuring the weight of permeate with a balance. Figure 3.7 is a schematic diagram of the dead-end stirred-cell unit. Locations for the source water foulant characterizations that were conducted are shown in Table 3.8.

### *Hollow-Fiber Units*

Two different bench-scale units were employed to test hollow-fiber membranes. Hollow-Fiber Units 1 and 2 were designed, constructed, and operated by JHU and Kiwa, respectively. Hollow Fiber Unit 1 was operated under two protocols: “end-of-run backwash” mode and “alternating filtration/backwash” mode. End-of-run backwash, similar to the stirred-cell apparatus, was operated in a continuous filtration cycle to a pre-determined loss of specific flux, and backwashed with filtrate and chemical solutions. This protocol was used for the purpose of determining both hydraulically reversible and chemically reversible fouling. Alternating filtration/backwash mode tests were conducted with alternating filtration and backwash cycles to assess differences in hydraulically reversible fouling arising from backwash frequency. Hollow-Fiber Unit 2 was used to test hollow-fiber membranes in an alternating filtration/backwash mode only.

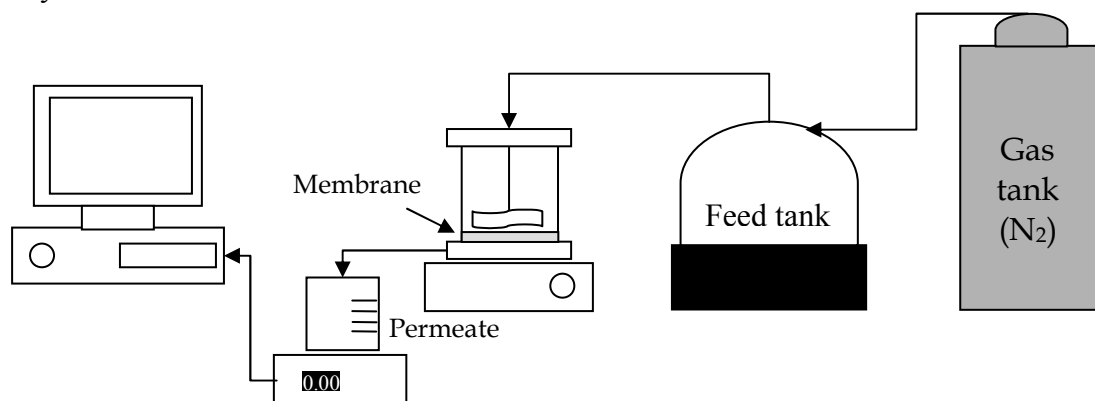


**Figure 3.7** Dead-end, stirred-cell filtration unit

**Feed waters used by Hollow-Fiber Unit 1.** Locations for the source (feed) waters that were evaluated using Hollow-Fiber Unit 1 are shown in [Table 3.8](#). A 5-gal (18.9-L) aliquot of each type of source water was collected, cooled, and then shipped to Johns Hopkins University (JHU) by overnight courier. Upon arrival, the samples were prefiltered as described previously. Prior to a conduct of a fouling experiment, the water sample was allowed to warm to ambient room temperature (18.5 – 22° C).

**Membranes and membrane modules used by Hollow-Fiber Unit 1.** Hollow-fiber membranes A, B, C, and D2 were used for testing with Hollow-Fiber Unit 1. Membranes A and B were operated in submerged outside-in configuration, while Membranes C and D2 were operated in submerged inside-out configuration. Loose fibers supplied by the manufacturers were potted into direct flow mini-modules with membrane surface areas between 0.0055 and 0.0060 m<sup>2</sup>, an example of which is shown in [Figure 3.8](#). Membrane D2 fibers were provided as prefabricated mini-modules with a surface area of approximately 0.0060 m<sup>2</sup>. All new modules were rinsed by filtering a minimum of 2 L of ultra-pure water prior to use in fouling experiments.

**Hollow-Fiber Unit 1 operational design.** Hollow-Fiber Unit 1 comprised two parallel channels that allowed two membranes to be tested simultaneously. Both channels were operated under constant flux in either an inside-out or submerged outside-in flow configuration. Each channel consisted of a clear polycarbonate shell with a length of 300 mm, a disposable membrane module, and a digital compound pressure gauge (Cecomp Electronics, DGP100B +/- 15PSIG-5) used to measure the hydraulic pressure in the permeate line. For selected studies, a pressure transducer was added to each channel (Cole Parmer, A-68075-32), and data were collected with a personal computer using a Personal Daq 55 data acquisition system and PersonalDaqViewXL 2.0.4 software (Iotech, Cleveland, Ohio). Cumulative permeate mass was measured with a top-loading electronic balance (Mettler Toledo, PG3001-S).

Measurements of hydraulic pressure and permeate mass were used for the determination of temporal variations of permeate specific flux ( $J_s$ ). Constant flux was achieved using a dual-channel digital peristaltic pump (Cole Parmer, Masterflex model 7523-60) with one channel for each of the membrane units. This pump was used as both the filtration and the backwashing pump. In the inside-out configuration, the pump pressurized the feed-water line during filtration,



**Figure 3.8 Mini-module potted with membrane fibers supplied by the manufacturer**

and backwashed using vacuum. For the outside-in submerged configuration, the pump used vacuum during filtration and pressure during backwashing. In the submerged outside-in membrane configuration, a second dual-channel peristaltic pump (Cole Parmer, Masterflex 7554-80) was used to feed raw water into the PC feed-water column. This configuration was open to the atmosphere, and the water level was maintained at a constant level by allowing excess feed-water to overflow to a drain. The diagram for both filtration configurations is shown in Figure 3.9.

**Experimental protocol.** The protocol used to conduct tests with Hollow-Fiber Unit 1 consists of the following steps:

- **Determination of  $J_{S0}$ .** The clean membrane-specific flux ( $J_{S0}$ ) of each membrane module was determined at constant flux prior to fouling experiments. Ultrafiltered, UV-treated water from a Barstead Nanopure Diamond deionization system (D11931) (laboratory organic free water) was filtered through the membrane for a period of 30 min at the same permeate flux as that to be used for the fouling experiment. The TMP and permeate mass were recorded, and the  $J_{S0}$  calculated. This procedure was repeated until a stable baseline TMP was achieved.
- **Fouling of clean membranes.** Membranes were fouled by filtration of feed water at constant flux. TMP and permeate mass were measured to be used for calculation of specific flux ( $J_S$ ). Unless otherwise noted, filtration was stopped when a decrease in  $J_S/J_{S0}$  of 0.5 was achieved. The total volume of water filtered varied depending on the ability of the feed water to cause fouling. The maximum TMP of an experiment was less than 12 pounds per square in (psi) (82.74 kPa) and often below 6 psi (41.37 kPa).
- **Permeate backwashing.** Permeate backwashing was manually initiated at the end of each filtration experiment and was achieved by reversing the direction of permeate flow under constant flux conditions. Permeate collected in the previous filtration step

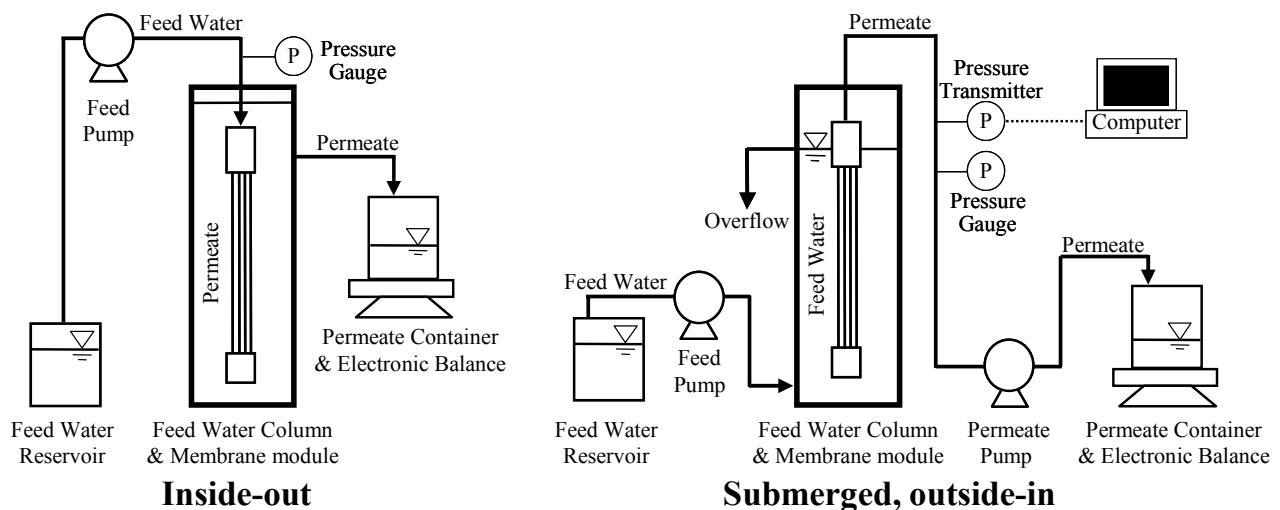


**Figure 3.9 Hollow-Fiber Unit 1. The unit consisted of two channels that allowed two membranes to be tested in parallel. The unit configuration is flexible and can be used to test either inside-out or submerged outside-in flow configurations.**

was reversed either from inside to outside (for outside-in membranes) or from outside to inside (for inside-out membranes). The duration of backwashing was controlled at 1 minute. At the end of the backwash, filtration of feed water was again manually initiated to determine the efficiency of the backwash at restoring specific flux. This was done by comparing the initial specific flux after backwashing and the final specific flux before backwashing. This difference also served as a measure of hydraulically irreversible fouling. The flux of filtration following permeate backwashing was always the same as the flux of filtration in the fouling experiment. The flux of permeate backwashing was evaluated at different levels in the baseline testing experiments, as described in section 3.5.1.2.5, and maintained equal to the flux of filtration for the remaining experiments.

- **Chemical washing and soaking.** Following permeate backwashing, the modules were subjected to chemical washing to further characterize the foulants that contributed to hydraulically irreversible fouling. Chemical washes consisted of backwashing and soaking the membrane in caustic and/or chlorine-containing solutions. A chemical wash was conducted similarly to a permeate backwash, with a period of soaking in the chemical solution, before determining the efficiency of restoration of permeate flux by the chemical wash. Caustic solutions were prepared by adjusting the pH of laboratory organic free water with 1 mM reagent-grade sodium hydroxide (NaOH) to a final pH of 10.3-10.5. This pH range was selected to maximize solubility of NOM while remaining below the maximum allowable pH permitted for the PVDF membranes. Chlorine solutions were diluted in a laboratory organic free water from a 4 to 6 percent stock solution of purified grade sodium hypochlorite (NaOCl). Free chlorine concentration was determined using the DPD Colorimetric assay for free chlorine (Standard Method 4500-Cl G DPD) using a Hach DR/890 Colorimeter.
- **Water sampling for NOM characterization.** Samples of each water stream were collected from select experiments run on Hollow-Fiber Unit 1. The samples were cooled and shipped to the University of Colorado by overnight courier for NOM characterization. The water streams that were collected were feed water, permeate, retentate, permeate backwash water, and caustic backwash water. It was not possible to sample the retentate from the inside-out membrane configuration.
- **Preparation of virgin and fouled membrane module samples for fiber and foulant characterization.** Membrane samples were packaged in 2.5-percent sodium bisulfite (American Chemical Society [ACS] grade) and shipped using express courier to the University of Poitiers, France for fiber and foulant characterization.
  - **Virgin fibers.** Virgin modules of each of the four hollow-fiber membrane types used in the bench-scale experiments were prepared as previously described. Membranes were washed thoroughly with purified water before packaging and shipment.
  - **Fouled and backwashed fibers.** Membranes A and B were fouled with Tampa Bay water (two membrane-water combinations) and backwashed with permeate, as previously described, before packaging and shipment.
  - **Fouled fibers.** Membranes A and B were fouled with either Indianapolis or Scottsdale water (four membrane-water combinations) before packaging and shipping. Membranes were not backwashed.

**Hollow-Fiber Unit 1 baseline testing.** A 4 x 4 x 3 experimental matrix was established to determine the effects of membrane type, source (feed) water, and flux on membrane fouling. This matrix consisted of 16 membrane-water combinations tested at each of three separate filtration fluxes. Fluxes were chosen based upon the recommendations of the manufacturer and preliminary testing. The preset flux levels for submerged outside-in membranes and for the inside-out flow configuration membranes are presented in [Table 3.10](#).

Three permeate backwash cycles were performed following each filtration experiment. Each of these permeate backwashing cycles was performed at a different backwashing flux in order of increasing flux (as shown in [Table 3.11](#)).

The permeate backwash cycles were followed by a caustic backwash cycle and a chlorine backwash cycle. The caustic backwash did not include a period of soaking. The chlorine cycle included a 30-minute soaking period with a free chlorine concentration of 100 mg/L for Membrane C and D2 and 500 mg/L for Membranes A and B. Caustic and chlorine solutions were prepared in double-filtered RO water. If the specific flux of membranes after cleaning was close to that of clean membranes, i.e., within 95 percent of the latter, the module was reused in a subsequent experimental run. Otherwise, the module was soaked in ultrafiltered water for 12 hours to several days before the permeability was re-tested. If the final  $J_S/J_{S0}$  was still less than 0.95, the module was replaced with a new module.

Samples were collected for NOM analysis as previously described.

**Free chlorine vs. time (contact time) experiments.** A study of the interaction of chlorine dose and contact time (CT) was undertaken with a Membrane B module fouled with Tampa Bay water. The module was fouled to a  $J_S/J_{S0}$  of 0.6 before undergoing a permeate backwashing cycle and then subjected to a chlorine backwash and soaking cycle.

[Table 3.11](#) shows the initial free chlorine concentration and soaking time experimental matrix for the CT experiments. Solutions were prepared in 80 mM sodium phosphate buffer, pH 7, using laboratory organic free water.

Residual chlorine concentration was determined as a function of soaking time in selected experimental runs of different initial chlorine concentrations. The resulting chlorine decay curves were used to express CT in terms of the integrated residual over the soaking period.

**Additional cleaning condition experiments.** A study was conducted to explore the added benefit of using chlorine in combination with the following additional cleaning conditions: caustic pH, elevated temperature, and shear stress.

**Table 3.10**  
**Operational fluxes for baseline testing, all values given as L/m<sup>2</sup> • hr**

Membrane flow configuration	Filtration flux	Permeate 1 <sup>st</sup>	Backwash 2 <sup>nd</sup>	flux 3 <sup>rd</sup>	Caustic BW* flux	Chlorine BW flux
Submerged Outside-In	55	109	163	218	218	218
Submerged Outside-In	82	109	163	218	218	218
Submerged Outside-In	110	109	163	218	218	218
Pressurized Inside-Out	70	136	204	272	272	272
Pressurized Inside-Out	102	136	204	272	272	272
Pressurized Inside-Out	140	136	204	272	272	272

\*BW – backwash

**Table 3.11**  
**Number of runs performed for each time-dose combination in the CT experiments**

		Initial free Cl <sub>2</sub> concentration (mg/L)				
		0	1	10	100	500
Time (min)	5		2	2	2	2
	30		1	1	1	1
	180					1
	360			1	2	4
	720	1				1
	1440					1

**Caustic pH.** Conditions were the same as in the CT experiments except that the pH of the chlorine solution was adjusted to 10.3, and the soaking time was set to 30 min. Chlorine solutions contained either zero or 520 mg/L initial free chlorine. Reagent-grade hydrochloric acid was used to adjust the pH of the high-dose caustic chlorine.

**Elevated temperature.** Conditions were the same as in the CT experiments except that the test solution was warmed to 42 °C in a water bath that also served as the feed for a re-circulating water jacket surrounding the feed water column. Two runs were performed, with chlorine solutions of 0 and 106 mg/L initial free chlorine. After the 5-minute soaking period, the chlorine solution was drained into a pre-warmed flask, and the temperature determined to be 32 °C in both.

**Shear stress.** Conditions were the same as in the CT experiments except that the chlorine solution was re-circulated during the 5-minute soaking time by using a peristaltic pump to pull the solution from the bottom of the column and reintroduce it at the top through the overflow. Two such runs were performed, with 0 and 105 mg/L initial free chlorine. The average flow rate of recirculation was 15.3 mL/min.

**Alternating filtration backwash mode experiments.** To relate the standard end-of-run backwashing protocol applied to Hollow-Fiber Unit 1, as used in the above-described experiments, to the “alternating filtration/backwash” mode used with Hollow-Fiber Unit 2 and the pilot- and full-scale systems, a series of tests were conducted using the alternating filtration/backwash operating mode.

The operational protocol for the unit was the same as for the CT study, with the following three modifications: 1) each run consisted of 8 or 9 cycles, 2) each cycle was composed of 15 minutes of filtration followed by 1 minute of permeate backwashing, and 3) no chemical wash was performed in these experiments.

A total of four membrane-water combinations were tested. Membranes A and B were each tested with Indianapolis and Scottsdale water. For each membrane-water combination, a run of unit permeate throughput comparable to that used for the end-of-run backwash protocol was conducted.

## ***Hollow-Fiber Unit 2***

***Hollow-Fiber Unit 2 operational design.*** Figure 3.10 shows a photograph of Hollow-Fiber Unit 2, consisting of a syringe pump, a pressure difference sensor, a four-way valve, and a backwash water reservoir. Membrane modules with a length of 20 cm, a diameter of 2.4 cm, and an active membrane area of 0.0125 m<sup>2</sup> were employed with this unit.

For tests conducted in this study, the unit was operated in alternating filtration/backwash mode. Cycling between filtration and backwash was performed automatically using the four-way valve, as shown in Figure 3.11.

Filtration and backwash periods were fixed at 15 minutes and 1 minute, respectively. Filtrate and backwash flow rates were also fixed and equivalent at 25 mL/min. All experiments were conducted at constant flux, with filtration and backwash fluxes equivalent. (For most commercial MF/UF systems, backwash flux is typically 150 to 200 percent greater than filtration flux.) During filtration, the syringe pump pumps feed water through the hollow fibers. During backwash, the 4-way valve is rotated and filtrate is introduced from a storage tube into the pump suction and backwash is implemented. The volume of the tube is approximately 50 mL, which corresponds to a 2-minute backwashing interval at 25 mL/min.



**Figure 3.10 Hollow-Fiber Unit 2**

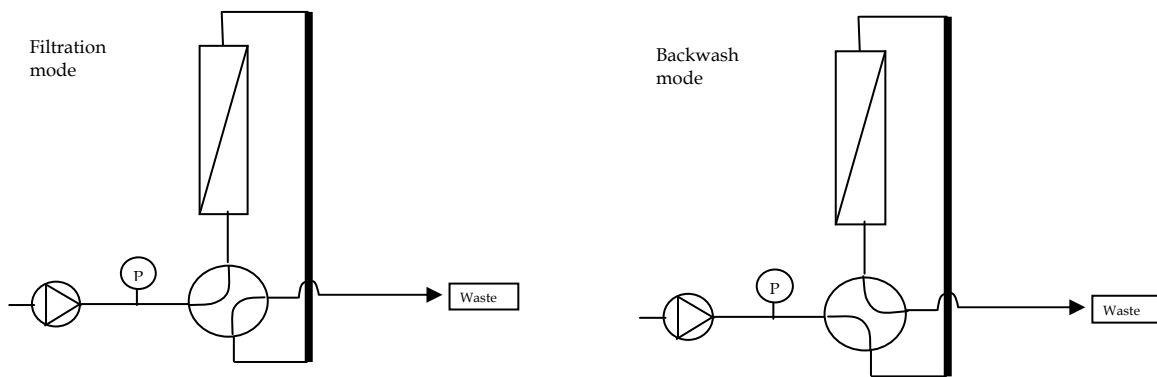


**Figure 3.11 Direction of flow through Hollow-Fiber Unit 2 for both operational modes**

Membrane feed pressure, as monitored by a pressure transmitter on the pump discharge, was continuously recorded by a laptop computer to calculate TMP.

**Hollow-Fiber Unit 2 membrane module.** The characteristics of the hollow-fiber membrane module used with Hollow-Fiber Unit 2 are shown in Table 3.12. Fibers from each of the manufacturers listed in Table 3.3 were used to pot modules for testing. A module fabricated using Membrane C, with which a majority of the testing with Hollow-Fiber Unit 2 was performed, contained 0.0125 m<sup>2</sup> (0.135 ft<sup>2</sup>) of membrane area (based on filtering surface).

**Hollow-Fiber Unit 2 feed water.** For membrane preparation and cleaning, Milli-Q water was used.

The baseline water used for the majority of the experiments was Twente Canal water. The water was collected at the Elsbeekweg Water Treatment Plant at Enschede, The Netherlands. The water was transported to Kiwa's facilities, 1.2- $\mu$ m prefiltered, and then cooled and stored (maximum of 2 weeks). Prior to each experiment, an aliquot of the water was allowed to warm to ambient room temperature.

In addition to experiments with Twente Canal water, single or duplicate experiments were performed with Scottsdale secondary effluent, White River water, and Tampa Bay raw water.

**Prefiltration.** All samples were prefiltered upon arrival at the Kiwa facilities using Whatman glass microfiber filters with a pore size of 1.2  $\mu$ m (Whatman, Cat No. 1822 047). The water was filtered at a flow rate of 5 L/h. Filters were changed when the pressure drop reached 1 MPa.

To check the effect of prefiltration on membrane fouling, some experiments were also carried out with both raw and prefiltered samples.

**Ferric pre-coagulation.** In one series of experiments, coagulation of the Twente Canal water prior to membrane filtration was conducted using ferric chloride (FeCl<sub>3</sub>). A calculated amount of FeCl<sub>3</sub> was first added to the water sample and stirred at a high rate (rapid mix) for 30 seconds. The coagulated water was then slowly stirred (flocculated) for 30 minutes and then processed by the Hollow-Fiber Unit 2. During filtration, the coagulated water was continuously stirred. No pH correction was performed, resulting in different coagulation pH values for different coagulation doses. Ferric dose and resulting coagulant pH values are given in Table 3.13.

**Experimental conditions.** In Table 3.14, the experimental conditions used with Hollow-Fiber Unit 2 are shown using Membrane C as an example. Table 3.15 summarizes all of the experiments and shows the parameters that are different than the standard conditions. During each experiment, filtration and backwash were conducted at a flux of 120 L/m<sup>2</sup>h.

**Table 3.12**  
**Characteristics of the Hollow-Fiber Unit 2 membrane module**

Property	Value
Supplier	Filtrix, Utrecht, The Netherlands
Material	PP and PE
Potting material	Epoxy
Length	20 cm
Outside diameter	24 mm
Number of fibers	50

**Table 3.13**  
**Coagulation experimental matrix**

Iron dose, mg/L as Fe	pH, units
0.0	8.02
1.1	7.63
2.5	7.39
4.8	7.08
12.5	6.55

**Table 3.14**  
**Experimental conditions for Hollow-Fiber Unit 2 testing**

Property	Value
Membrane type	C
Flow direction	Inside-out
Water type	Twente Canal
Pretreatment	Filtration with glass fiber filter
Filtration time	15 min
Backwash time	1 min
Flow	25 mL/min
Flux	120 L/m <sup>2</sup> h
Temperature	20° C
Number of experiments with identical conditions	Duplicate

**Table 3.15**  
**Experimental matrix for Hollow-Fiber Unit 2 testing**

Test series	Purpose	Source water location	Membrane
1	Baseline	Twente Canal	C
2	Impacts of holding time and prefiltration (replicate runs)	Twente Canal	C
3	Fouling rate comparison on different source waters (duplicate runs)	Twente Canal, Scottsdale, Tampa Bay, Indianapolis	C
4	Fouling rate comparison on different membrane types (duplicate runs)	Twente Canal	A, B, C, D2
5	Impact of coagulant dosing on fouling rate (see <a href="#">Table 3.8</a> for test conditions)	Twente Canal	C

**Sampling and analysis.** Samples of permeate and backwash water were collected for NOM characterization by the University of Colorado. No general, inorganic, or microbial analyses were performed as part of this testing.

Feed and backwash water samples only were analyzed from Series 3. Feed, permeate, and backwash samples from Series 4 were analyzed. Permeate samples were collected over an 8-minute period during the third filtration cycle of the experiment.

### Pilot Units

As described in Section 1, pilot-scale testing was conducted to quantify NOM fouling impacts on the same hollow-fiber membranes tested at bench-scale, but using an operating system that incorporated the same fouling management strategies employed at full-scale. This testing included the following:

- Evaluation of the impact of different fouling control strategies on membrane performance, including flux, backwashing with and without chemical enhancement, (chemical) pretreatment, and CIP
- Correlation of performance changes with the NOM character of the pilot unit feed, permeate, backwash and chemical wash samples, as well as NOM present on membrane fibers harvested at the completion of the pilot testing period

The pilot-scale studies are intended to bridge the gap between bench-scale tests focusing on variable membrane materials and backwashing strategies conducted using controlled NOM water matrices.

The objectives of the pilot testing were to:

- Investigate the fouling profiles of a select number of membrane systems and membrane materials treating natural waters with characteristically different NOM profiles

- Evaluate the impact of different fouling control strategies on membrane performance, including reversible and irreversible fouling predominated by NOM, using hydraulic, hydro-pneumatic, and chemical-based strategies
- Characterize the relative contribution of NOM to membrane fouling and flux loss and the benefit of each fouling control approach using advanced analytical techniques

The proposed pilot study phase of this research was developed to address these objectives using different low-pressure membrane systems/materials under various pre-treatment conditions, water qualities, and operating conditions as directed by the results of the bench-scale studies. The pilot-scale studies also investigated the effectiveness of backwashing in restoring flux decline associated with NOM fouling, as well as the efficiency of the chemical cleaning as identified by bench-scale studies. The pilot-testing phase also aimed to validate findings from the bench-scale studies, including the efficacy of a NOM fouling index. These objectives were accomplished by performing pilot-scale studies specifically designed to evaluate the membrane fouling behavior in a systematic way, using varying water quality conditions and different membrane systems/materials at participating utility sites. Pilot studies were conducted using selected pre-treatment conditions identified and tested at bench scale. The participating utilities represented those that currently have full-scale low-pressure membrane systems or are implementing pilot projects intended to lead to full-scale system installation. The various utilities encompassed surface water and wastewater reuse facilities. The pilot testing program was designed to distinguish between three types of NOM-based fouling:

- Hydraulically reversible fouling: fouling that can be removed by backwashing with filtrate, either alone or in conjunction with air scour (hydropneumatically)
- Chemically reversible fouling: fouling not removable by hydraulic or hydropneumatic means that can be removed by application of chemicals
- Irreversible fouling, fouling that cannot be removed by hydraulic, hydropneumatic, or chemical means

The level of fouling is quantified and monitored by the decline in temperature-corrected specific flux and other operating and water quality parameters that were identified in the bench-scale studies. To differentiate NOM fouling from particulate and colloidal fouling, advanced analytical methods such as SEC-DOC were employed and contrasted with techniques specific to inorganic constituents, such as inductively coupled plasma (ICP) spectrophotometry. General, inorganic, and microbial characterization of feed, permeate, backwash and chemical wash streams were conducted during each pilot run as described in section 3.2.2 using samples collected by field staff and analyzed by in-plant laboratory personnel.

Two tiers of pilot-scale studies were conducted. Tier 1 pilot studies were more intensive and employed source waters selected to capture the three NOM classes (i.e., NOM, AOM, and EfOM). Tier 2 pilot studies included those that leveraged “other project” studies underway at the time that the pilot study phase was being performed and that feature a variety of pre-treatment methods and NOM source waters. Tier 2 pilot studies represent opportunities to conduct targeted investigations that reflect knowledge gained during the bench-scale phase and that complement and expand the knowledge base to be developed from Tier 1 pilot studies.

**Tier 1**

**Tampa Bay.** The first of the four Tier 1 pilot studies was conducted at the Tampa Bay Regional Water Treatment Plant (TBRWTP) using a pilot unit employing Membrane B. The TBRWTP raw water supply, comprising a blend of Tampa Bypass Canal, Alafia River, and Hillsborough River water, served as the feed water to the pilot unit. As shown in Table 3.16, the composite source is characterized by high color, TOC, and hardness and dominated by allochthonous NOM. TBRWTP employs a sand-ballasted clarification process (Actiflo), ozonation, and biological filtration using granular activated carbon (as shown in Figure 3.12) to produce drinking water.

**Table 3.16**  
**General raw water quality characteristics**

Parameter	Range	Average
Temperature (°C)	10-30	23
pH	7.5-7.8	7.6
Alkalinity (mg CaCO <sub>3</sub> /L)	40-200	110
Color (platinum cobalt unit [PCU])	23-300	100
Bromide (µg/L)	110-120	100
TOC (mg/L)	3.9-32	12
Turbidity (NTU)	0.6-10	1.9
Iron (mg/L)	0.01-1.2	0.35
Total Nitrogen (mg/L)	0.2-1.6	0.8
Total Organic Nitrogen (mg/L)	8-40	12
Total Hardness (mg CaCO <sub>3</sub> /L)	190-210	203
Calcium Hardness (mg CaCO <sub>3</sub> /L)	180-220	203

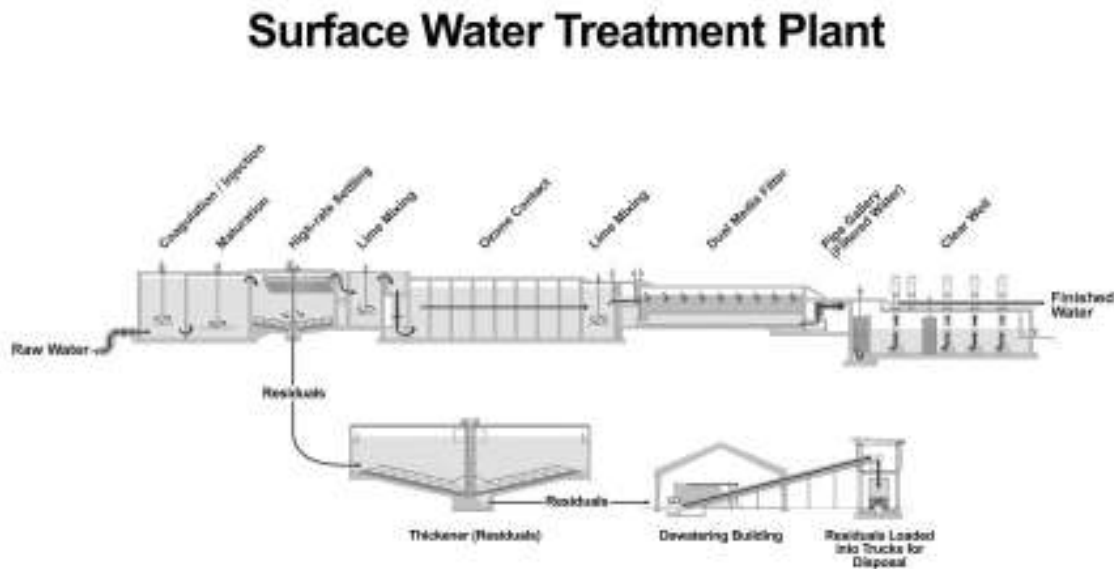


**Figure 3.12 Schematic of the Tampa Bay Regional Water Treatment Plant**

**Pilot unit description.** A pilot unit provided by Zenon Environmental, Inc., fitted with Membrane B modules and operating in submerged mode, was installed at TBRWTP in September 2004. Following installation and commissioning, the unit was operated for a period of 4 months, from October 28, 2004 until February 19, 2005. A vacuum of between 3 and 11 psig (20 to 76 kPa), developed by a permeate pump, was applied to the lumen of the fibers, which pulled feed water through the fiber wall to create permeate. The product operated in outside-in flow configuration and direct (or dead-end) filtration mode. Backwash was conducted using filtrate reverse flow combined with low-pressure air scour. Following backwash, the contents of the membrane tank were drained to remove displaced solids.

The pilot unit consisted of the following major components:

- Two 500- $\mu\text{m}$  basket strainers to prevent the entry of larger particles that could damage the hollow fibers
- Three membrane modules, mounted vertically, each containing 46.5 m<sup>2</sup> (500 ft<sup>2</sup>) of membrane surface area
- Permeate pump
- Air compressor to operate the valve pneumatic actuators of the pilot unit, to provide compressed air for membrane integrity testing (Pressure Decay Test), and to supply air for backwash air scour
- Backwash/CIP tank

Figure 3.13 shows the flow diagram of the pilot unit in the filtration mode. Figures 3.14 and 3.15 are photographs of the pilot unit as installed at the TBRWTP and of the membrane module, respectively. Table 3.17 lists the characteristics of the membrane used during the study.

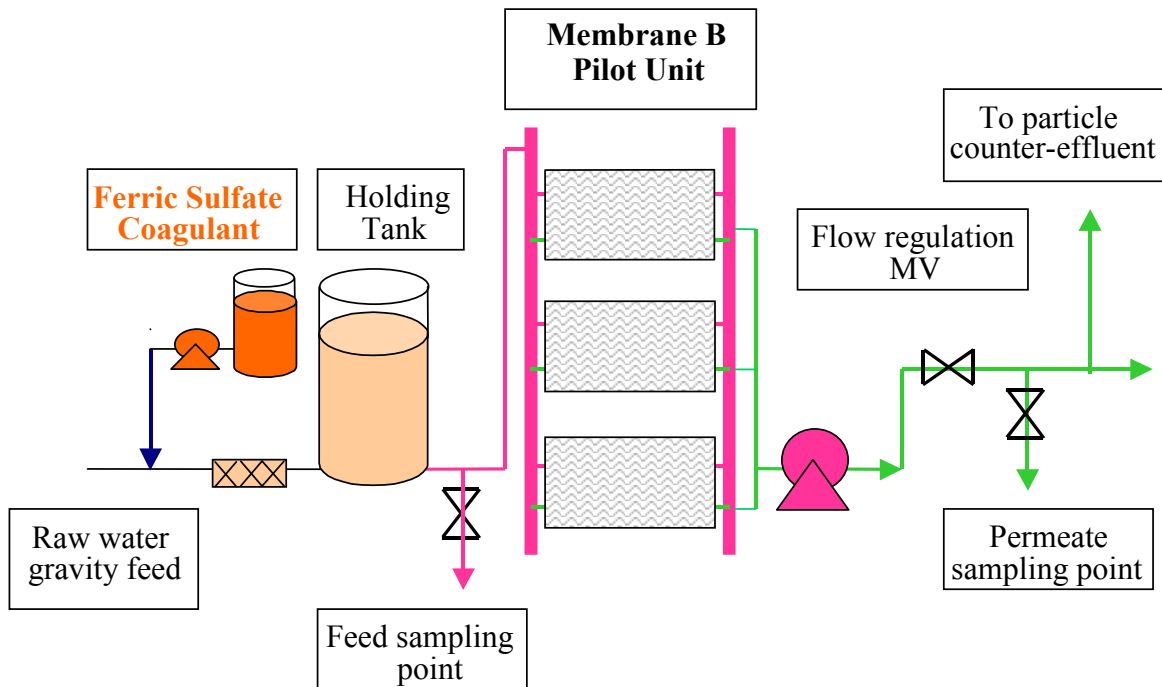


**Figure 3.13 Membrane B pilot unit process schematic**



**Figure 3.14 Membrane B pilot unit as installed at the Tampa Bay Regional Water Treatment Plant**



**Figure 3.15 Membrane B module**

**Table 3.17**  
**Characteristics of the Membrane B module\***

Property	Value
Membrane Type	Hollow-Fiber
Membrane Material	PVDF
Flow Direction	Outside-In
Active Module Surface Area	500 ft <sup>2</sup> (46.5 m <sup>2</sup> )
Maximum TMP	11 psi (75.84 kPa)
Fiber Inside Diameter (mm)	0.31
Fiber Outside Diameter (mm)	0.65
Number of Fibers (per module) (approx.)	14,500
Active Fiber Length	3.3 ft (1 m)
Nominal Pore Size (μm)	0.02
Surface Characteristics	Hydrophobic
Surface Charge	Neutral

\*As reported by the manufacturer.

**Operations.** During filtration, UF feed water flowed by gravity through the holding tank and into the membrane tank where permeation through the Membrane B modules was achieved by the permeate pump. Filtrate was directed to the backpulse/CIP tank until filled, after which it was discharged to the plant drain.

At the end of a filtration cycle, a backwash was performed that was initiated either automatically or manually. The backwash consisted of these successive steps:

1. Close feed valve.
2. Stop filtration pump.
3. Aerate membrane modules (for predetermined time period).
4. Aerate and backpulse membrane modules (with permeate for predetermined time period).
5. Backpulse modules only for predetermined time period.
6. Drain membrane tank.
7. Refill the membrane tank with feed water.

The duration of backpulse and aeration, and backpulse flux varied during the testing (see [Table 3.18](#)) in accordance with recovery and flux rate.

**Table 3.18**  
**Tampa Bay pilot study experimental matrix**

Run no.	Feed water type	Flux (L/m <sup>2</sup> -hr)	Parameter evaluated	Filtration period (min)	Back-pulse duration(s)	Backpulse flow	Recovery (%)	Chemical wash type
1	Raw water	70 - 80 - 90	Baseline	15	30	Same as filtration	95	none
2	Raw water	90	Increased recovery	30	21	Same as filtration	97.5	none
3	Raw water	90	Increased backwash flowrate	15	20	150% of the filtration flow	95	none
4	Raw water	90	NaOH wash	15	30	Same as filtration	95	NaOH
5	Raw water	90	Citric acid wash	15	30	Same as filtration	95	Citric acid
9	Raw water	90	NaOCl wash	15	30	Same as filtration	95	NaOCl
6	Coagulated water	90	Baseline	15	30	Same as filtration	95	none
7	Coagulated water	90	Reduced recovery	7	30	Same as filtration	90	none
8	Coagulated water	90	Phosphoric acid wash	15	30	Same as filtration	95	Phosphoric acid

During selected runs, a chemical wash (CW) was conducted to evaluate the removal of NOM and other foulants from the membrane fibers using different chemicals. The CW procedure was as follows:

- Adding designated chemical(s) to the backwash tank after filling the tank with permeate and thoroughly mixing the contents.
- Draining the membrane tank and filling it with the backwash tank solution.
- Recirculating the cleaning solution through the membranes for 30 minutes.
- Draining the membrane tank, refilling it with raw water, and then restarting production.

**Experimental approach.** Table 3.18 lists the experimental matrix for testing conducted with the pilot unit at TBRWTP. Runs 1 through 5 were conducted using raw water as feed between October 29 and December 16, 2004. Runs 6 through 8 were conducted using raw water pre-coagulated with 25 mg/L ferric sulfate (Fe<sub>2</sub>(SO<sub>4</sub>)<sub>3</sub>) from January 12 to February 20, 2005. Run 9 was conducted with raw water (following the completion of Run 8) to assess the impact of chemical washing using sodium hypochlorite on flux restoration.

Initial testing (Run 1) was conducted to establish a “baseline” flux and recovery that would result in a significant loss in specific flux (between 40 and 60 percent) after a permeate throughput of between 6000 and 7000 L/m<sup>2</sup> (about 5 days of continuous operation) at a recovery of 95 percent. Runs 2 and 3 were conducted to evaluate the impact of increased recovery and increased backwash flow rate, respectively, on the rate of hydraulically reversible fouling. Runs 4 and 5 were conducted to determine the benefit, if any, of once-per-day washing with alkaline and acid chemicals on flux restoration. Runs 6 through 8 evaluated the impact on the flux decline rate of pre-coagulation at baseline flux and reduced recovery.

Following the completion of each run, the membrane modules were cleaned first with a 2 percent by weight citric acid solution and then with a 500-ppm solution of sodium hypochlorite in accordance with manufacturer’s standard recovery cleaning protocol. The citric acid solution was supplemented with muriatic acid to maintain the solution pH at 2.2. Each CIP included both a recirculation and soaking step. Prior to and following the hypochlorite CIP, a permeability test was conducted to determine cleaning efficiency.

**Water quality sampling analysis.** Samples of pilot unit feed, permeate, and backwash water were collected and analyzed by the TBRWTP laboratory to measure parameters relevant to membrane system performance and determine the basic foulant properties of the feed water. A listing of process locations within the pilot at which samples were collected and associated water quality parameters analyzed are presented in [Table 3.19](#). All samples were collected on a “grab” basis. In addition, feed and permeate turbidity and particle counts were monitored on a continuous basis using on-line instrumentation provided with the pilot unit.

**Table 3.19**  
**Monitored water quality parameters and process locations**

Constituent	Process location*
General	
pH	Feed, Permeate, Backwash
Temperature	Feed, Permeate, Backwash
Electrical Conductivity	Feed, Permeate, Backwash
Total Hardness (as CaCO <sub>3</sub> )	Feed, Permeate, Backwash
Calcium Hardness (as CaCO <sub>3</sub> )	Raw
Alkalinity (as CaCO <sub>3</sub> )	Feed, Permeate, Backwash
Color	Feed, Permeate, Backwash
Particulate	
Turbidity	Feed, Permeate, Backwash
Organics	
UVA <sub>254</sub>	Feed, Permeate, Backwash
Total Organic Carbon	Feed, Permeate, Backwash
Metals	
Total Iron	Feed, Permeate, Backwash
Dissolved Iron	Feed, Backwash
Total Manganese	Feed, Permeate, Backwash
Dissolved Manganese	Feed, Backwash
Microbial	
HPC (every 2 weeks)	Feed, Permeate, Backwash

\*Samples collected weekly except where indicated.

**NOM characterization.** For each run, grab samples were also collected and shipped by overnight courier to the University of Colorado for NOM characterization. NOM was characterized according to DOC, SUVA, XAD-8/-4 fractionation, SEC-DOC/UV, and 3-D fluorescence EEM. [Table 3.20](#) lists the schedule for which NOM samples were collected for each run.

**Fouled membrane and foulant fiber characterization.** At the completion of Runs 1, 3, 4, and 7, the membrane tank was drained, opened, and approximately 100 membrane fibers harvested from the one of the three membrane modules by cutting the fibers approximately 2 inches (5 cm) from the pot. These fibers were placed in a quart plastic bottle to which a 2 percent solution of sodium bisulfite was added. The fibers were then shipped by 2-day courier to the University of Poitiers in France for fouled membrane and foulant characterization. The damaged module was then replaced by a new one before starting the following run.

**Indianapolis.** The second Tier 1 pilot study was conducted at the City of Indianapolis (Ind.) White River Water Treatment Plant (WTP). This source was selected based on the historical presence of high levels of algal-derived (autochthonous) NOM during the spring and summer months in the plant source water, the White River. (The river water also contains baseline levels of allochthonous NOM). Quality characteristics of the White River as measured at the WTP intake are shown in [Table 3.21](#).

A photo of the river taken just upstream of the intake is shown in [Figure 3.16](#).

**Table 3.20**  
**Schedule of sampling for NOM characterization**

Run	Feed	Permeate	Backwash	Chemical wash
1	X	X	X	
2		X	X	
3	X	X	X	
4	X		X	X
5				X
7	X	X	X	
8				X
9				X

**Table 3.21**  
**General White River raw water quality characteristics (2004 average)**

Parameter	Units	Raw Water
Temperature	°C	15.5
pH	SU	8.1
Hardness	mg/L CaCO <sub>3</sub>	320
Alkalinity	mg/L CaCO <sub>3</sub>	224
Turbidity	NTU	7.6
TKN	mg/L	0.6
BOD	mg/L	2
COD	mg/L	9.9
TOC	mg/L	3.8
Color	PCU	30
Iron	mg/L	0.7
Manganese	mg/L	0.04



**Figure 3.16 The White River upstream of the intake**

Treatment processes in use at the WTP to produce drinking water comprised coagulation (using alum), flocculation, sedimentation, dual media filtration, and chloramination (Figure 3.17). Powdered activated carbon is periodically added during the summer months to remove taste and odor compounds (geosmin and 2-Methylisoborneol [MIB]) that enter the WTP in the source water. The taste and odor compounds originate from algae in the reservoir located on the river upstream of the WTP intake.

**Pilot Unit Description.** A continuous microfiltration-low pressure (CMF-L) unit, provided by Siemens MEMCOR and fitted Membrane A modules, was installed at the Indianapolis White River WTP in March 2005 and used to conduct the pilot testing. The pilot unit was placed into service April 2005 and was operated until the end of March 2006.

The CMF-L unit is a pressurized MF unit that utilizes four Membrane A modules. A feed pump provides the pressure necessary to force-feed water through the hollow fibers from outside to inside in direct (dead-end) filtration mode. Backwash is conducted using filtrate together with low-pressure air applied to the feed side of the fibers. Following backwash and air scour, the filtrate with suspended solids is drained by gravity from the membrane modules. Characteristics of the hollow-fiber membrane and membrane module are shown in [Table 3.22](#).

[Figure 3.18](#) shows the end of a membrane module with potted fibers as well as a portion of the fiber bundle.

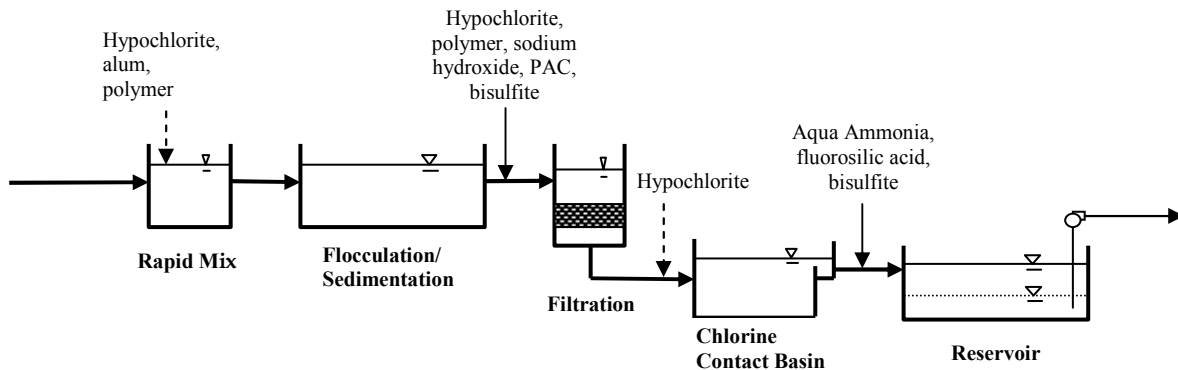


**Figure 3.17 Schematic of the Indianapolis White River Water Treatment Plant**



**Figure 3.18 Membrane A module (end view and fiber bundle)**

**Table 3.22**  
**Characteristics of the Membrane A module\***

Property	Value
Membrane Type	Hollow-Fiber
Membrane Material	PVDF
Flow Direction	Outside to Inside
Active Module Surface Area	251.9 ft <sup>2</sup> (23.4 m <sup>2</sup> )
Maximum TMP	22 psi (151.68 kPa)
Total Number of Fibers (approx.)	9600
Active Fiber Length	40 in (1.0 m)
Fiber Inside Diameter (mm)	0.5
Fiber Outside Diameter (mm)	0.8
Nominal Pore Size (μm)	0.1
Surface Characteristics	Hydrophilic
Surface Charge	Neutral

\*As reported by the manufacturer.

The pilot unit consisted of the following major components:

- 500-μm wye strainer to prevent the entry of larger particles that could damage the hollow fibers
- Three membrane modules, mounted vertically, each containing 23.4 m<sup>2</sup> (252 ft<sup>2</sup>) of membrane surface area
- Feed tank and pump
- Air compressor to operate the valve pneumatic actuator of the pilot unit and provide compressed air for membrane integrity testing (Pressure Decay Test) and backwash air scour.

Feed water was sampled directly from the feeding tank of the pilot as there was no sampling port for the feed. A sampling point was provided on the permeate piping for permeate sampling. Samples of backwash were collected as the solution exited the membrane modules through a drain line. Samples of chemical wash solutions were collected directly from the feeding tank of the pilot at the end of the chemical wash.

During the first portion of the testing, the pilot unit was installed at the WTP intake and operated using raw river water as feed water (Runs 0 through 7). During this period of operation, a raw water receiving tank was used to store and provide head to a transfer pump that conveyed the river water to the pilot unit feed tank. This was necessary because the pilot unit was installed at a higher location (head) than the discharge head of the intake pumps. A process schematic for the pilot unit as operated on river water is shown in [Figure 3.19](#). Photos of the unit installed at the intake are shown in [Figure 3.20](#).

During the second portion of testing (Runs 8 through 15), the pilot unit was relocated to the main building of the WTP and operated on settled (clarified) water from the Actiflo unit. A transfer pump installed in the clarified water channel conveyed the clarified water directly to the pilot unit feed tank.

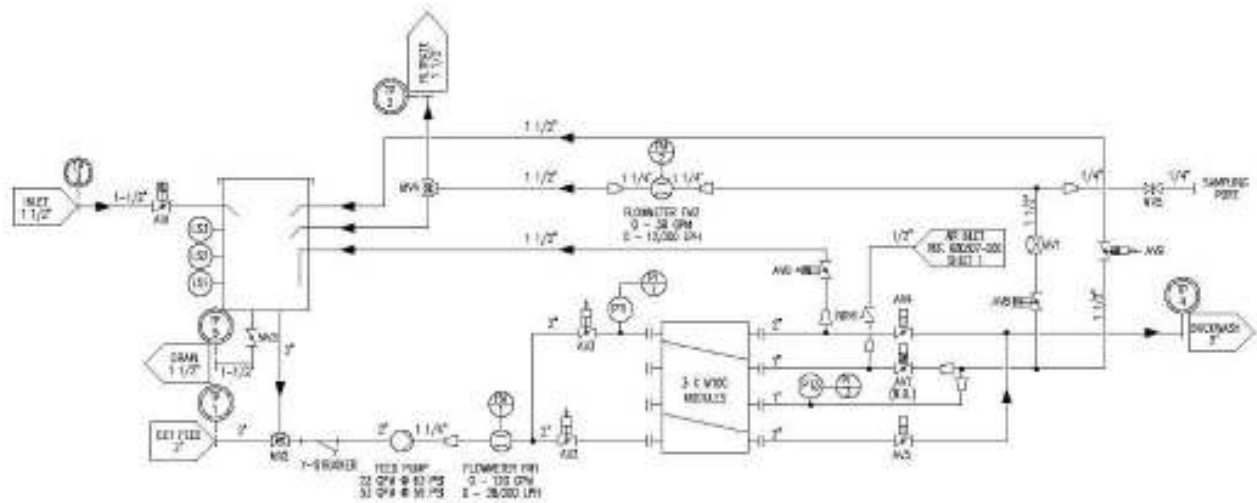


**Figure 3.19 Process schematic of the Indianapolis pilot unit**



**Figure 3.20 Indianapolis pilot unit**

The water was continuously pumped from the wet well of the intake to feed tank 1, which was on the first floor of the intake. A pipe was provided at the top of the feed tank to carry any overflowing water to the drain. The water was then pumped to feed tank 2 of the pilot unit when the level in feed tank 1 was above mid-level. From feed tank 2, the water was pumped to the membrane modules. In normal filtration, the feed flow entered the top and bottom of each membrane module. Inside the membrane module, water flowed around the hollow membrane fibers. The flow passed through the walls of the membrane fibers (outside-in) to the inside of the fiber (lumen). Filtered water then exited via the top and bottom of each module through the clean module manifold. In normal filtration, the permeate was finally sent to the drain.

During CIP and chemical wash events, the permeate was recycled to feed tank 2 to provide a source of filtered water for the chemical solution.

Due to hydraulic limitations, it was not possible to have a flow large enough to feed the three modules, so the pilot operated with only two filtration modules.

Figures 3.21 and 3.22 show the pilot unit and associated process schematic during operation on clarified water.

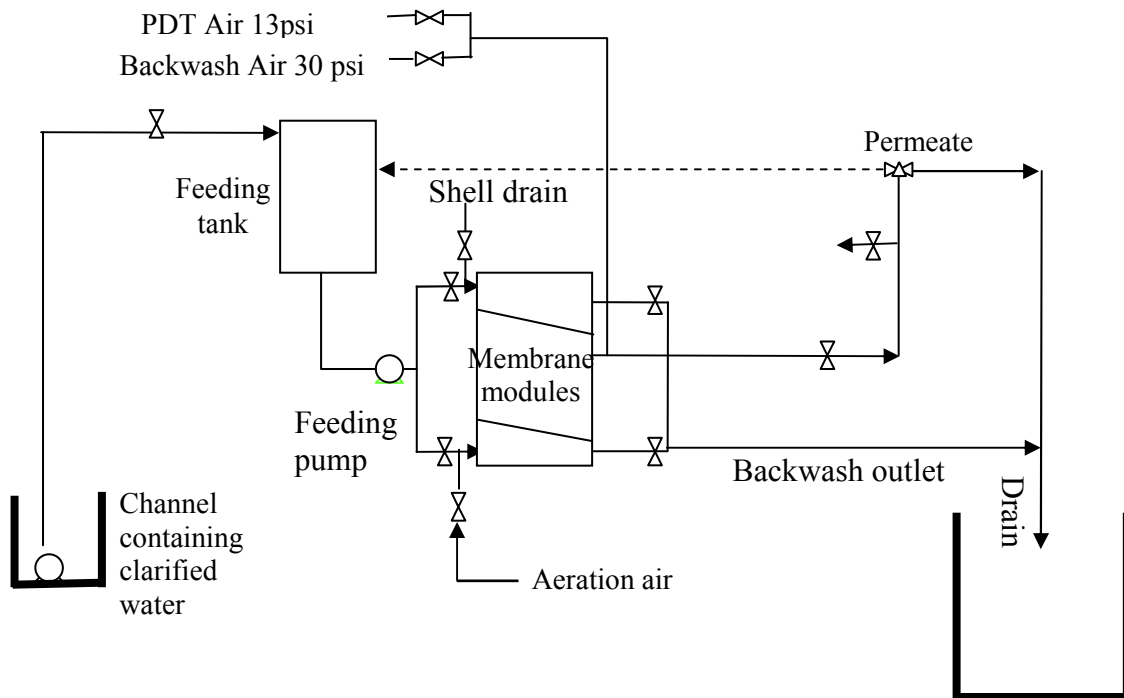


Figure 3.21 Schematic of the Indianapolis pilot setup while working with clarified water



**Figure 3.22 Indianapolis pilot unit treating clarified water**

**Operations.** During filtration, MF feed water flowed from the feed tank through the feed pump and through the hollow fibers. Permeate was discharged to the plant drain.

At the end of a filtration cycle, a backwash was performed to remove accumulated solids using both filtrate and feed-side air scour. The backwash was initiated automatically and consisted of the following successive steps:

- Filter to backwash level: an air pressure of 30 psig (207 kPa) was applied to the shell side. The filtration occurred until a set volume was reached (1.6 gallons/module). The liquid level was lowered on the shell side to enhance the system recovery.
- Aeration and air-assisted liquid backwash: the aeration rate was 3.8 standard cubic feet per minute (SCFM) (0.1 cubic feet per meter) per membrane module. The air pressure was 30 psig (207 kPa) for air-assisted liquid backwash.
- Post-aeration at 3.8 SCFM (0.1 cubic feet per meter) per module
- Drain down
- Fill shell
- Fill lumen

The duration of backpulse and aeration was varied during the testing (see [Table 3.18](#)) in accordance with recovery and flux rate.

During selected runs, a chemical wash was conducted to evaluate the removal of NOM and other foulants from the membrane fibers using different chemicals. The CW procedure was as follows:

- Recycling and filling feed tank with permeate
- Adding designated chemicals to the feed tank
- Recycling the chemical solution between the tank and the membrane modules with permeation for 30 minutes
- Soaking modules in solution for 30 minutes
- Recycling solution on the feed side for 60 minutes
- Draining the feed tank, refilling it with feed water, and backwashing (twice)
- Resuming filtration

**Experimental approach.** Table 3.23 lists the experimental matrix for testing conducted with the pilot unit at Indianapolis. Runs 0 through 6 were conducted using raw water as feed between October 29 and December 16, 2004. Run 7 was performed using raw water to which alum was dosed (pre-coagulation run). Alum was added to the line conducting raw water from the wet well to feed tank 1. The coagulation system was composed of a pump adding alum to the line and a holding tank. After the alum was added, a static mixer was used to ensure proper mixing. Runs 8 through 17 were conducted using clarified water from January 12 to February 20, 2005.

Initial testing (Run 0) was conducted to establish a “baseline” flux and recovery that would result in a significant loss in specific flux (between 40 and 60 percent) after a permeate throughput of between 6000 and 7000 L/m<sup>2</sup> (about 5 days of continuous operation) at a recovery of 95 percent, similar to what was done with the Tampa Bay pilot. Subsequently, Run 1 was performed to establish the fouling rate at the baseline operating conditions. Runs 2 and 3 were then conducted to evaluate the impact of increased flux and recovery, respectively, on fouling rate. Runs 4 through 6 were conducted to assess the benefit of different once-per-day chemical washes on reduction in fouling rate. Run 7 was performed to determine the benefit of differing alum doses on fouling rate in the absence of settling. With clarified water, Runs 8 through 12 were conducted at conditions identical to Runs 1 through 4 on raw water to determine the impact of clarification on fouling rate reduction. Run 13 was conducted to determine the impact of both chlorine contact times and concentrations (“CT” study) as applied during once-per-day chemical wash in a manner that could permit comparison of CT conditions between pilot-scale and bench-scale (as performed by JHU). Run 14 was conducted at increased recovery to accelerate the accumulation of organic foulants on the membrane surface prior to the harvesting of fouled fibers for fouled membrane and foulant characterization. Runs 15 and 16 were ancillary runs conducted to assess the rate of fouling at conditions established by the manufacturer as appropriate for full-scale plant design on clarified water.

Between Runs 10 and 11, the WTP began blending groundwater from local wells with White River water at the plant intake. The blending was not realized until completion of Run 12. Comparison of specific flux decline curves between Run 8 and Runs 11 and 12 indicated that the blended water caused a higher rate of fouling, most likely from the increased calcium levels contained in the hard groundwater. (Calcium has been shown to increase NOM fouling by causing bridging and destabilization of NOM molecules.) Consequently, Run 17 was performed to determine the rate of fouling at baseline conditions with the blended, clarified water to be able to accurately interpret the results from Runs 11 through 14.

**Table 3.23**  
**Indianapolis pilot study experimental matrix**

Run no.	Feed water	Parameter evaluated	Coagulant/dose	Flux (L/m <sup>2</sup> -hr)	Recovery (%)	CW type	CW frequency (hr)	CW duration (min)
0	River	Preliminary	None	80, 90, 100	95	None	--	--
1	River	Baseline	None	90	95	None	--	--
2	River	High flux	None	110	95	None	--	--
3	River	High recovery	None	90	97.5	None	--	--
4	River	Acid wash	None	90	95	HCl; pH 2.0	24	30
5	River	Caustic/acid wash	None	90	95	Caustic, pH 11; HCl, pH 2.0	24	30/30
6	River	Hypo wash	None	90	95	50 ppm hypochlorite acidified to pH 7.0	24	30
7	River	Alum coagulation	30	90	95	None	--	--
7b	River	Alum coagulation	5	90	95	None	--	--
7c	River	Alum coagulation	15	90	95	None	--	--
8	Clarified	Baseline	None	90	95	None	--	--
9	Clarified	High flux	None	110	95	None	--	--
10	Clarified	High recovery	None	90	97.5	None	--	--
11	Clarified	Acid wash	None	90	90	HCl, pH 2.0	24	30
12	Clarified	Caustic/acid wash	None	90	95	Caustic, pH 11; HCl, pH 2.0	12	30/30
13	Clarified	CT study	None	90	95	Cl <sub>2</sub> CT matrix	24	--
14	Clarified	Characterization of the foulants	None	90	95-98.5%	--	--	--
15	Clarified	Full-scale plant parameters	None	68	97	50 ppm hypochlorite	24	30
16	Clarified	Full-scale plant parameters	None	68	99	100 ppm hypochlorite	24	30
17	Clarified	Impact of blended water	None	90	95	None	--	--

Notes

- 1: Runs 11 to 17, the feed consisted of clarified water blended with ground water (20 to 30 percent).  
 2: Runs 15 and 16, the unit was operated until terminal TMP was reached (23 psi [158.59 kPa]).

For the clarified water runs (8 through 17), the river water was coagulated at pH 7.0 to 7.8 with alum at doses ranging from 31 to 78 mg/L, depending upon the river water quality. A cationic polymer was also used to promote floc settling.

Following the completion of each run, the membrane modules were cleaned first with a 500-ppm solution of sodium hypochlorite at 25° C followed by a 2 percent by weight citric acid/200 mL hydrochloric acid at 40° C in accordance with the manufacturer's requirements. The citric acid solution was supplemented with muriatic acid to maintain solution pH at 2.2. After completion of each CIP, a permeability test was conducted to determine cleaning efficiency.

**Water quality analysis.** The water quality parameters that were monitored, along with sampling frequencies and locations, are presented in Table 3.24. The pilot unit was equipped with an on-line turbidimeter and particle counter for both feed and permeate flows.

**Table 3.24**  
**Monitored water quality parameters and sampling frequencies**

Parameters	Unit	Feed	Permeate	Backwash	Chemical wash
<b>General</b>					
pH		2*	2	1	1
Total Hardness	mg/L as CaCO <sub>3</sub>	2	--	1	1
Calcium	mg/L	2	--	1	1
Alkalinity	mg/L as CaCO <sub>3</sub>	2	--	--	--
True Color	mg/L	2	2	1	1
<b>Particulate</b>					
Total Dissolved Solids (TDS)	mg/L	2	--	--	--
Particle Count	counts/mL	C†	C	--	--
Turbidity	NTU	C	C	1	1
<b>Organics</b>					
Total Organic Carbon	mg/L	2	2	1	1
UVA	1/cm	2	2	1	1
Algae‡	count/mL	2	--	1	--
Chlorophyll a‡	ppb	1	--	--	--
HPC	colony/mL	1	1	1	--
<b>Metals</b>					
Iron, Dissolved	mg/L	2	--	1	1
Iron, Total	mg/L	2	2	1	1
Manganese, Dissolved	mg/L	2	--	1	1
Manganese, Total	mg/L	2	2	1	1

\*Indicates number of samples collected per run.

†Continuous

‡Algae counts and chlorophyll a analyses were conducted on membrane feed water for Indianapolis pilot only based on the autochthonous content of this source water.

**NOM characterization.** For each run, samples were sent to the University of Colorado for NOM characterization. NOM was characterized using DOC, SUVA absorbance, XAD-8/-4 fractionation, SEC-DOC/UV, and 3-D fluorescence EEM.

Table 3.25 shows the schedule of the sampling.

**Membrane fiber characterization.** Membrane fibers were also collected and sent to the University of Poitiers (France) for autopsy, as shown in Table 3.26.

**Table 3.25**  
**Schedule of the sampling for NOM characterization**

Run	Feed	Permeate	Backwash	Chemical wash
0				
1	X	X	X	
2		X	X	
3	X	X	X	
4			X	
5	X			X
6				X
7a	X	X	X	
7b	X	X	X	
7c	X	X	X	
8	X	X	X	X
9		X	X	
10	X	X	X	
11				X
12				X
13	X	X	X	X
14				
15				
16				
17	X	X	X	

**Table 3.26**  
**Schedule of fiber collection**

Run no.	Post-filtration	Post-backwash	Post-chemical wash	No. of samples
1	X			1
3		X		1
4			X	1
7a	X			1
14	X			1

The fiber collection protocol was as follows:

- Stop the pilot filtration.
- Take a module out of the pilot.
- Cut the plastic matrix of the membrane to be able to collect the fibers.
- Cut 100 fibers, paying attention to obtaining the longest fibers possible.
- Rinse the fibers with de-ionized (DI) water.
- Store the fibers in DI water with 2 percent bisulfite.

This protocol results in the destruction of one module per fiber collection.

**Scottsdale pilot-scale testing.** The third Tier 1 pilot study was conducted at the City of Scottsdale (Ariz.) Water Campus (SWC) using clarified, filtered secondary effluent. This source represented an effluent NOM-based supply for testing. Representative quality characteristics for the Scottsdale effluent are showing [Table 3.27](#). The effluent used as pilot plant feed water originates as drinking water derived from treatment of local (groundwater and Salt River Project water) and imported (Central Arizona Project) water supplies that is converted to wastewater by domestic, commercial, and light industrial use. The wastewater is treated using primary and secondary treatment, biological nutrient removal (nitrification and denitrification), gravity clarification and cloth disk filtration.

**Table 3.27**  
**Representative quality for tertiary effluent from Scottsdale Water Campus\***

Parameter	Units	Raw water
Temperature	°C	20-30
pH	SU	7.2
TKN	mg/L	1.5
BOD	mg/L	<10
COD	mg/L	<20
TOC	mg/L	6.2
SUVA	L/mg-m	1.6
Hardness	mg/L CaCO <sub>3</sub>	296
Alkalinity	mg/L CaCO <sub>3</sub>	172
Turbidity	NTU	0.8
Calcium	mg/L	73
Iron	mg/L	0.7
Manganese	mg/L	0.05
TDS	mg/L	970

\*From data collected during the 2004 calendar year.

**Pilot unit operations.** The Membrane D1 pilot unit was installed in the microfiltration building at SWC on January 18, 2005. The pilot plant unit was a skid-mounted system that included all instrumentation and components necessary to provide a complete set of data required for a membrane pilot plant performance study. The pilot system components are described below:

- Raw water feed tank with level control and on/off inlet valve.
- 150 micron feed water strainer.
- A single UF module. The module is identical in all aspects to those used in existing full-scale Hydranautics plants, including length, diameter, fiber, and other materials of construction. The membrane used in the module is Membrane D1.
- 100-gal (378.5 L) product tank with an overflow connected to a drain.
- Backwash pump.
- Two chemical feed systems, caustic and sulfuric acid, to enhance backwash effectiveness.
- A coagulant feed upstream of the membrane to enhance removal of organics and DBP precursors.
- Air from the SWC for valve control and integrity testing.
- A manual cleaning system consisting of a storage tank and pump.
- Main control panel mounted on the skid with a programmable controller and Man Machine Interface display panel.
- Data collection laptop computer with connection to an Allen Bradley PLC.

Figure 3.23 is a photograph of the pilot system setup.

Table 3.28 lists specific characteristics of the Membrane D1 module. Figure 3.24 presents the flow diagram of the pilot unit in the filtration mode.



Figure 3.23 Scottsdale pilot unit



initiated automatically or manually. The automatic backwash was programmed to begin at an interval necessary to obtain the percent recovery identified for each run. The first step of the backwash cycle was a “co-current” flow that is directed from the product tank through the hollow-fiber membrane outside-in at a rate of 50 gpm, exiting through the concentrate (top) side of the module for a duration of 25 seconds.

The second step of the backwash cycle was a “counter-current” flow that is directed from the product tank through the hollow-fiber membrane outside-in at a rate of 50 gpm, exiting through the feed (bottom) side of the module for a duration of 25 seconds.

Chemicals were added to the backwash flow periodically to enhance the effectiveness of the membrane cleaning (chemical wash). The CW was programmed to begin once a day using caustic, acid, or both. During the CW, the membranes soaked for a period of 30 minutes to allow contact time of the backwash chemical with the foulants on the membranes. Following the soak period, the system went into a 15-second rinse mode where the backwash water was fed through the membrane and released through both the top and bottom of the module.

At the completion of each run, a CIP was performed following the manufacturer’s recommended procedure. The CIP consisted of two separate chemical cleanings performed in succession. The first was conducted using a 50 mg/L sodium hypochlorite solution to which sufficient caustic soda was added to achieve a solution pH of 12-13. The second cleaning was conducted using citric acid at a target pH of 2-3. Each CIP comprised recirculating the chemical solution through the membranes for 90 minutes followed by a rinse and backwash cycle.

**Experimental protocol.** After some troubleshooting of the pilot system, the first run was initiated on March 22, 2005. Run No. 1 was designated as the “baseline” run and operating conditions (flux and recovery) were selected to achieve a minimum specific flux decline ( $J_s/J_{s0}$ ) of 50 percent after a permeate throughput of approximately 8000 L/m<sup>2</sup> with or without chemical wash. These parameters were selected to achieve a reasonable degree of NOM membrane fouling during each run prior to sample collection for NOM characterization. Baseline run flux and recovery values were established based on flux decline results observed during a preliminary run conducted prior to March 22 and to account for lower flux reductions that might occur when enhanced fouling management strategies were employed (e.g., chemical wash, pre-coagulation).

Except for the first run, the duration of each run was established to achieve a minimum permeate throughput of 8000 L/m<sup>2</sup>. After this throughput was achieved, the pilot run was stopped, a CIP performed, and the next run started. [Table 3.29](#) shows the pilot study schedule between March 22 and October 5, 2005.

**Water quality characterization.** The water quality parameters that were monitored along with the sampling frequencies and locations are presented in [Table 3.30](#).

The number of samples that were collected for NOM characterization is presented in [Table 3.31](#).

**Table 3.29**  
**Scottsdale pilot study experimental matrix**

Run no.	Test condition	Flux (L/m <sup>2</sup> -hr)	Recovery (%)	Chemical wash type
1	Baseline	80	90	None
2	Low flux	60	90	None
3	Low recovery	80	80	None
4	High recovery	80	95	None
5	Acid wash	80	90	Acid
6	Caustic/acid wash	80	90	Caustic, pH 11; HCl, pH 2.0
7	Coagulation with PACl* (85 mg/L as product; 10 mg/L as Al)	80	90	None
8	Coagulation with PACl (14.5 mg/L as product; 1.8 mg/L as Al)	80	90	None
9	Coagulation with ferric chloride (25 mg/L as product; 3.5 mg/L as Fe)	80	90	None
10	Baseline	80	90	None
11	Acid wash	80	90	HCl; pH 2.0
12	CT study	80	90	Cl <sub>2</sub> CT study

\*Polyaluminum chloride

**Table 3.30**  
**Water quality parameters monitored during testing**

Parameter	Feed	Permeate	Backwash	Chemical wash
<b>General</b>				
pH	2*	2	1	1
Total hardness (mg/L CaCO <sub>3</sub> )	2	-	1	1
Calcium (mg/L)	2	-	1	1
Alkalinity (mg/L CaCO <sub>3</sub> )	2	-	-	-
<b>Particulate</b>				
TDS	2	-	-	-
Turbidity (NTU)	Continuous	Continuous	1	1
<b>Organics</b>				
Total organic carbon (mg/L)	2	2	1	1
UVA (1/cm)	2	2	1	1
<b>Metals</b>				
Iron, dissolved (mg/L)	2	-	1	1
Iron, total (mg/L)	2	2	1	1
Manganese, dissolved (mg/L)	2	-	1	1
Manganese, total (mg/L)	2	2	1	1

\*Indicates number of samples collected per run.

**Table 3.31**  
**NOM characterization sample collection**

Run no.	Feed*	Permeate	Backwash	Acid wash	Caustic wash	Chlorine wash
1	2	2	2			
3	2	2	2			
6	1		1	1	1	
7	1	1				
8	1	1	1			
9	1	1	1			
10	1	1	1			
11			1	1		
12						4

\*Indicates number of samples collected per run.

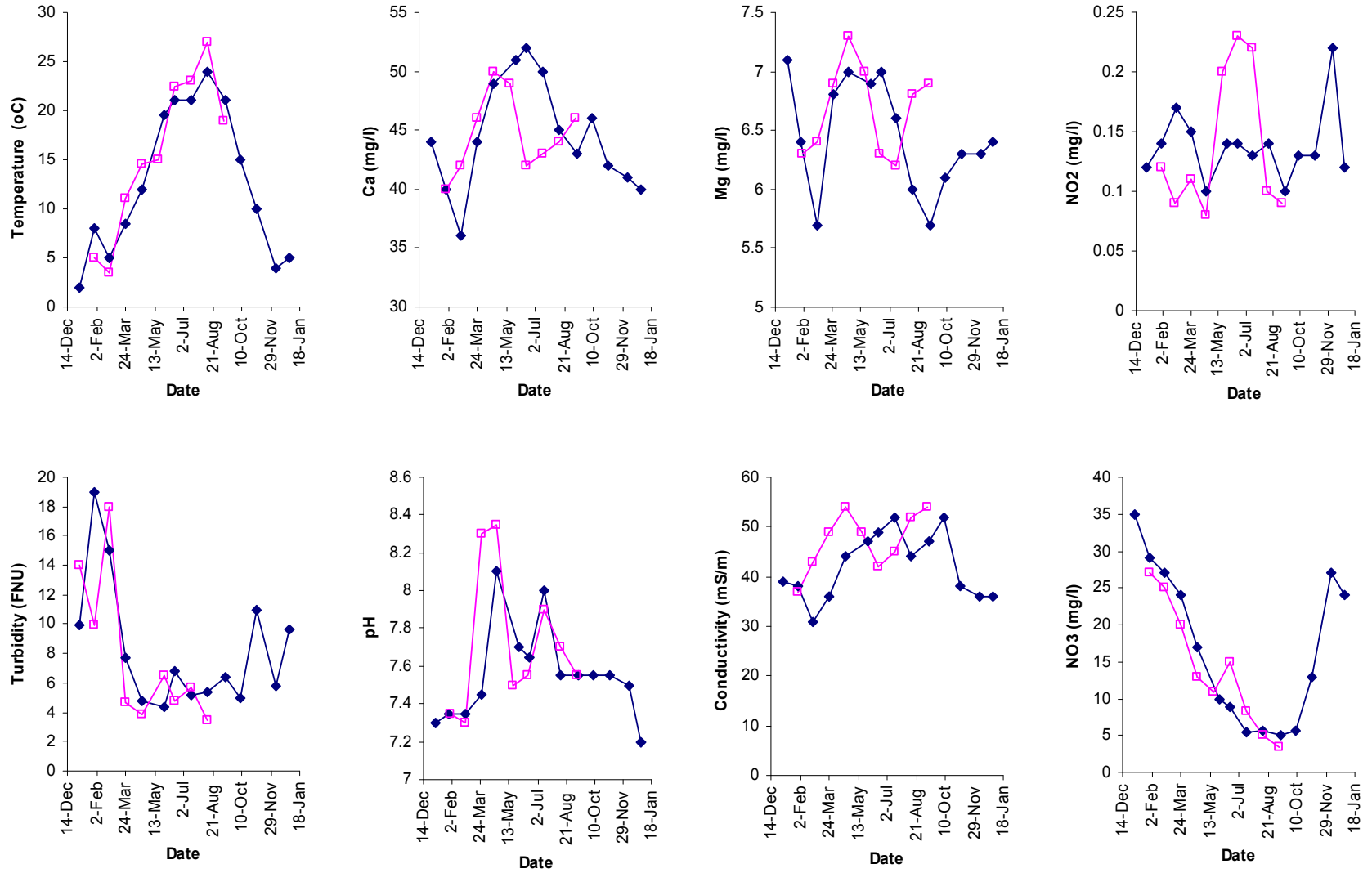
**Vitens pilot-scale testing.** The fourth Tier 1 pilot study was conducted with Twente Canal feed water. The selected feed water source is known for its relative high TOC/DOC content predominated by allochthonous NOM (about 10 ppm).

Representative quality characteristics for the Twente Canal feed water (over a 2-year evaluation period) are shown in [Figure 3.25](#).

**Pilot unit operations.** The pilot unit, owned by Vitens Water, was operated during from July through October 2006. The pilot plant unit contained all instrumentation and components necessary to provide a complete set of data required for a membrane pilot plant performance study. The main pilot system components are described below:

- Raw water feed tank
- 200-micron feed water pre-filter (Udimatic)
- A single UF module using Membrane C
- 1.5-m<sup>3</sup> permeate tank
- Filtration pump
- Backwash pump
- Three chemical cleaning tanks and dosing pumps
- Coagulant dosing system
- Indicators for temperature, pH, turbidity, conductivity, flow and pressure
- National Instruments control panel
- Data collection computer with MEFIAS (Vito) software

In [Figure 3.26](#), a photographic overview of the pilot system setup is shown. In [Figure 3.27](#), a process and instrumentation diagram of the setup is presented. In [Table 3.32](#), the specifications of the Membrane C module are presented.



(continued)

Figure 3.25. Quality characteristics of Twente Canal feed water

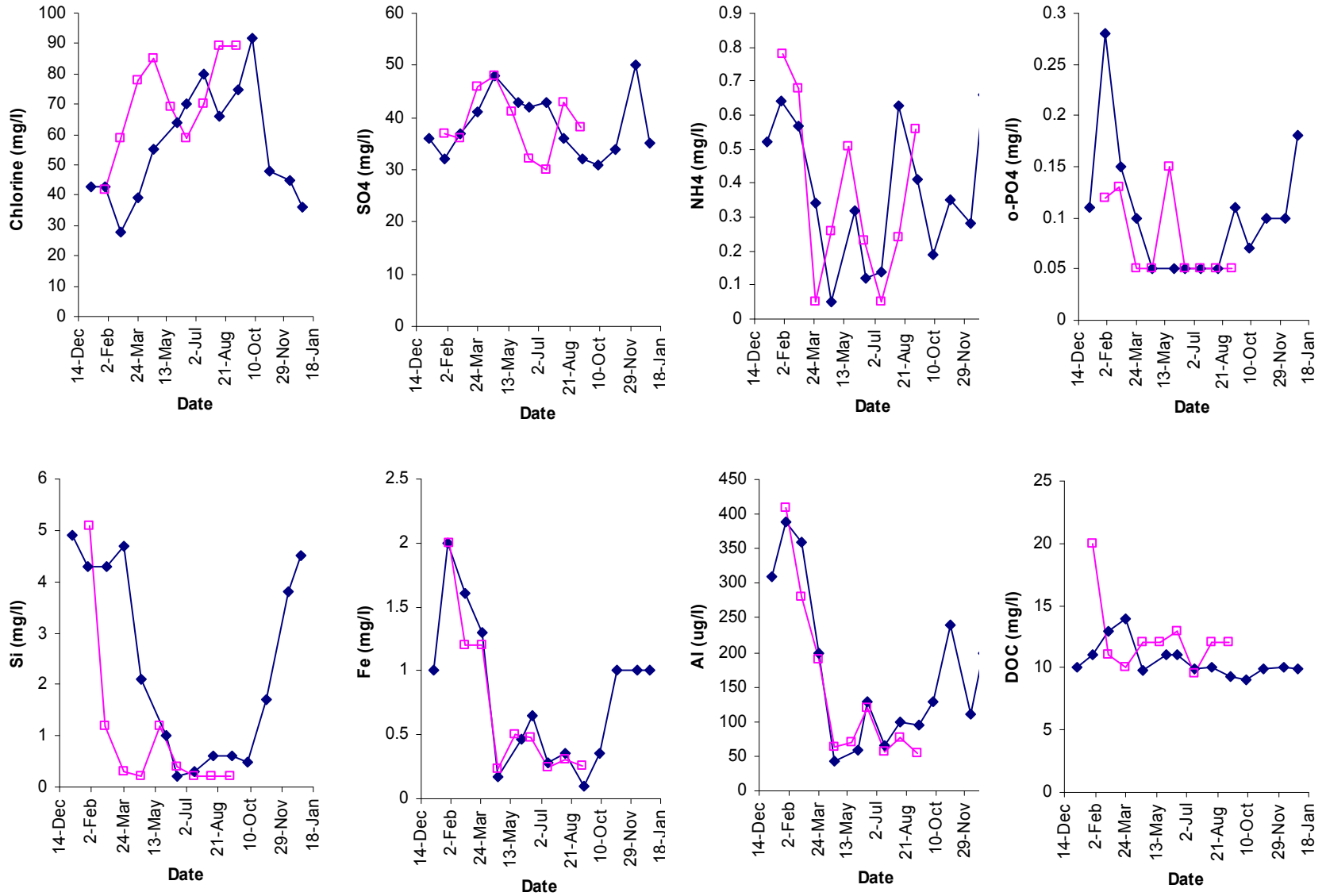
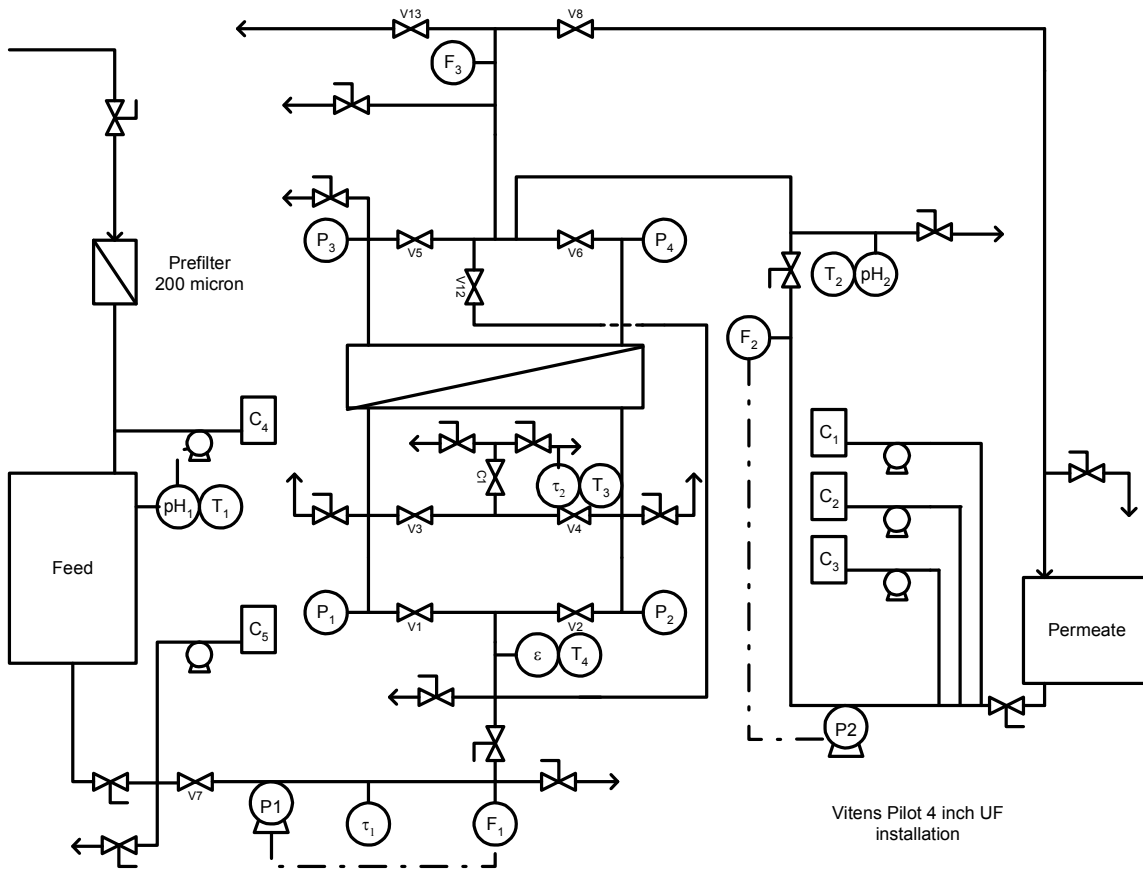


Figure 3.25. (Continued)



**Figure 3.26 Twente Canal pilot unit**



Legend:

PX pump

VX valve

C<sub>x</sub> chemical tank

P<sub>x</sub> pressure indicator

F<sub>x</sub> flow indicator

T<sub>x</sub> temperature indicator

pH<sub>x</sub> pH meter

τ<sub>x</sub> turbidity meter

ε conductivity meter

Note: X = a numeral (1, 2, 3, etc.)

**Figure 3.27 Process and instrumentation diagram for the Twente Canal pilot unit**

**Table 3.32**

**Membrane characteristics of Xiga membrane module (UFCM5) (Membrane C)**

Property	Value
Membrane material	PES
Flow direction	Inside-Out
Active module surface	65 ft <sup>2</sup> (6.2 m <sup>2</sup> )
Fiber outer diameter	0.8 mm
Length	1015 mm
Molecular weight cutoff	200 kD
Surface characteristic	Hydrophilic
Structure	Asymmetric
Maximum filtration TMP	300 kPa
Maximum backwash TMP	200 kPa

The pilot can be operated in three different modes: a production or filtration mode, a backwash or hydraulic cleaning mode, and a chemical cleaning mode.

During the production mode, the system processed feed water into permeate using pressure from the feed pump (P1) and delivered it to the permeate tank. The permeate flux through the UF module during operation was selected from between 30 and 75 L/h/m<sup>2</sup>. During filtration, flocculant may be added to the feed water as a coagulant (e.g., aluminum or iron). A typical filtration run lasted 10 to 30 minutes.

The permeate tank also served as the backwash tank to provide UF permeate for the periodic backwash cycle in the backwash mode. Permeate is flushed back through the module using the backwash pump (P2). A backwash is executed at a backwash flux of 150 to 200 L/h/m<sup>2</sup> for 2 minutes. The 2 minutes of backwashing were required to flush foulant from the system. The original pilot was designed to operate membranes with higher membrane surface. Pilot plant feed water recoveries were considerably lower than typical for a full-scale plant due to oversized piping (and greater hold-up volumes) that was sized to accommodate larger sized membrane modules.

**Experimental protocol.** After preparation of the installation, pre-flush of the module to flush out membrane conservation chemicals, clean water flux measurements, and check up of the installation, the pilot was started on July 3, 2006. The main objective of this study was to investigate whether a stable operation could be achieved with minimal coagulant dosing for feed water containing a relative high TOC/DOC. If this objective could be achieved, it would imply that NOM fouling can be controlled. The second objective was to establish a relationship between feed water composition, membrane foulant, and the removal of foulant during cleaning. Over a 3-month period, the testing schedule listed in [Table 3.33](#) was executed.

Each run was executed in cycles of 22 minutes. For 20 minutes, permeate was produced at a constant operating flux of 50 L/h/m<sup>2</sup>, followed by a backwash of 2 minutes at a flux of 200 L/h/m<sup>2</sup>. In principle, a backwash of 1 minute should be sufficient, but, due to a high system volume, a larger volume of backwash water is required to flush the released fouling from the system. As a result, the recoveries presented in [Table 3.33](#) are quite low. For each run, the membrane feed water was dosed with 9 mg/L of PACl (1.0 mg/L as Al). Coagulant was not fed for a 24-hour period beginning on September 24 (Run 5).

In this study, chemical cleaning was performed as soon as the TMP during production reached a level of 4.4 psi (30.34 kPa). The chemical cleaning procedure was executed as follows: 5 minutes flushing with hydrochloric acid (0.1M), then 5 minutes soaking, 5 minutes flushing with sodium hydroxide (0.1M), then 5 minutes soaking, and finally a 5 minutes flush with permeate to flush out the remaining chemicals.

The membrane was operated in dead-end mode. Filtration, as well as backwashing, was done by feeding the module from both sides.

**Table 3.33**  
**Vitens pilot study experimental matrix**

Run	Period	Test	Flux (L/h/m <sup>2</sup> )	Recovery (%)
1	3 Jul. – 12 Sept.	“Stable operation”	50	60
2	12 September	24 hours without coagulant	50	60
3	15 Sept. – 16 Sept.	24 hours at higher filtration flux	75	75
4	17 Sept.	Sampling sessions	50	60
5	17 Sept. – 25 Sept.	“Stable operation”	50	60
6	26 Sept.	Sampling session	50	60
7	26 Sept. – 3 Oct.	“Stable operation”	50	60

### ***Tier 2***

Tier 2 pilot studies consisted of studies that were completed for the purpose of other projects. These pilot studies included studies performed by project team members CH2M HILL or Veolia Water North America for municipal clients investigating low-pressure membrane systems for the purpose of full-scale plant design and construction. This interface provided the project team with the opportunity to leverage additional pilot data and water quality analysis during the planned 1-year pilot study period of this project. Three pilot studies were selected for incorporation into this project. Information obtained from these studies included the following:

- Membrane performance data to quantify rate of fouling, response to backwashing (with and without chemical aid), and chemical cleaning
- Samples of feed water, backwash water, and spent cleaning solutions to characterize for NOM and other constituents
- Performance and analytical data to assess degree of NOM fouling

***Tuscaloosa.*** 3.5.2.2.1.1 *Pilot unit operations.* CH2M HILL and the City of Tuscaloosa initiated pilot testing of three MF/UF systems (Pall Microza, Siemens MEMCOR CMF-s, and Zenon ZW-1000) to select the most appropriate low-pressure membrane technology and develop design data for a water treatment plant expansion.

Table 3.34 presents specific membrane characteristics of the three membrane systems that were piloted. The Microza module and CMF-s module characteristics are similar with respect to membrane material, pore size, and flow configuration.

**Table 3.34**  
**Membrane characteristics**

	Siemens MEMCOR		
	Pall Microza	CMF-s	Zenon ZW-1000
Membrane designation	E	A	B
Membrane material	PVDF	PVDF	PVDF
Flow direction	Outside-in	Outside-in	Outside-in
Active module service area	538 ft <sup>2</sup> (50 m <sup>2</sup> )	300 ft <sup>2</sup> (27.9 m <sup>2</sup> )	500 ft <sup>2</sup> (46.5 m <sup>2</sup> )
Maximum TMP	43.5 psi (299.93 kPa)	4.6 psi (31.72 kPa)	10.9 psi (75.16 kPa)
Nominal pore size	0.1 μm	0.1 μm	0.02 μm
Surface characteristics	Hydrophobic	Hydrophobic	Hydrophobic
Surface charge	--	Neutral	

**Pall.** The schematic of the Pall MF system is as shown in [Figure 3.28](#).

In filtration mode, the feed pump drew water from the feed tank and pumped it into the bottom port of the module, with most (~90 percent) of the flow permeating the fibers. The remainder exited the module through the top port as concentrate and was recycled back to the suction side of the feed pump. To remove accumulated solids from the fiber bundle, filtration mode was stopped and a simultaneous air scrubbing and reverse filtration (SASRF) step was conducted. This was followed by a forward flush with feed water in which the feed pump drew water stored in the feed tank through the membrane filter at the upper discharge port. In addition, daily chemical washes (referred to as enhanced flux maintenance [EFM]) were also used with either a chlorine or acid solution.

**Siemens MEMCOR.** The CMF-s pilot system consisted of the following major components:

- Raw water low-lift pump
- 500-micron inlet strainer
- Membrane process tank
- Four S10V using Membrane A modules
- Permeate pump
- Filtrate storage tank
- Air compressor
- Data logger

[Figure 3.29](#) shows a simplified process schematic for the CMF-s pilot unit.

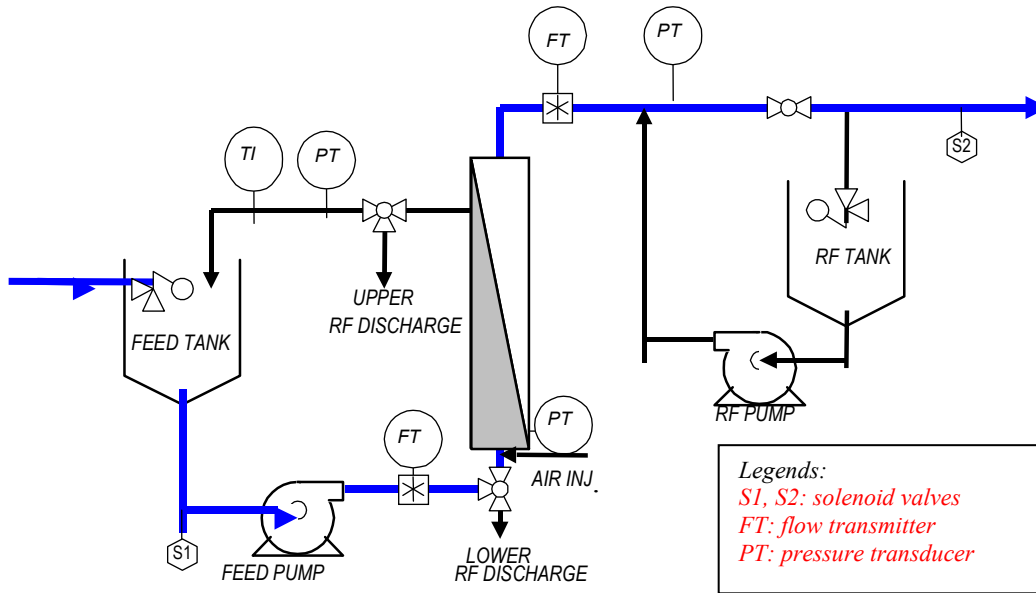


Figure 3.28 Pall MF pilot system schematic (Tuscaloosa) using Membrane E

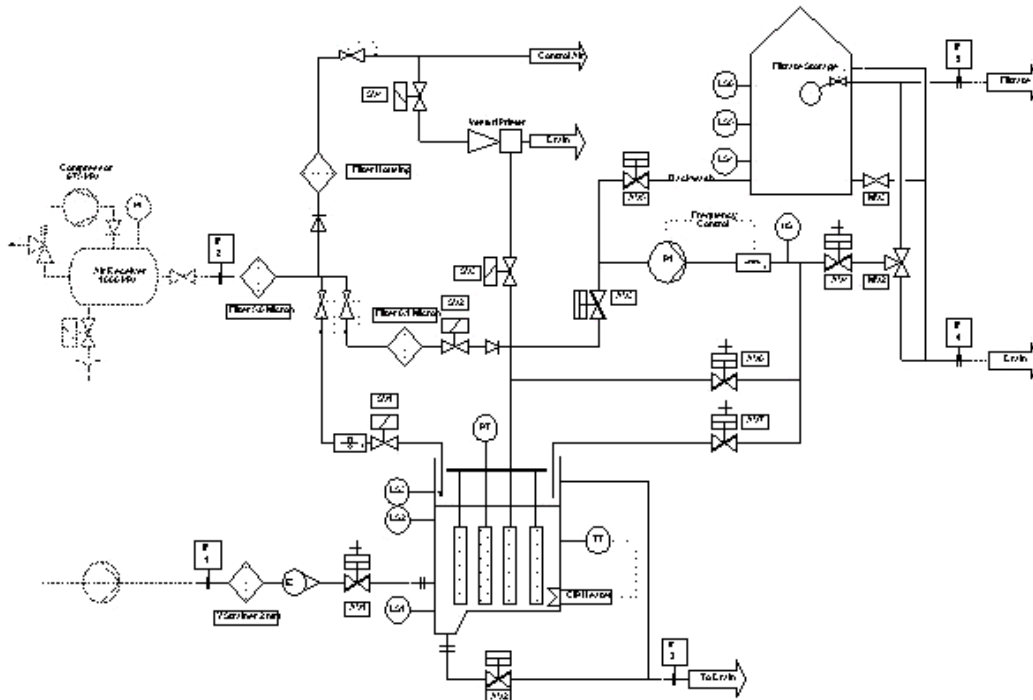


Figure 3.29 Simplified process schematic for CMF-s pilot unit (Tuscaloosa) using Membrane A

During filtration, water was drawn through the membrane by the permeate pump. The filtrate flow was maintained at a constant rate regardless of TMP through the use of a variable frequency drive on the permeate pump and a permeate flow feedback loop. Periodically, the membrane modules were backwashed using reverse flow of permeate with simultaneous application of low-pressure air scour on the feed side of the membrane. Chemical washes were initially conducted every 48 hours, then increased to every 24 hours using a variety of chemicals to reduce the rate of fouling (see Table 3.35 for a list of the chemicals used). When the TMP reached approximately 12 psi (82.74 kPa), a clean-in-place was performed.

**Zenon.** Figure 3.30 shows the ZW-1000 pilot system as set up at the Tuscaloosa site.

Permeate was achieved by pulling a vacuum on the submerged hollow-fiber membranes using the permeate pump. Backpulsing was performed every 15 to 60 minutes, using permeate stored in the backpulse tank. A low-pressure air scour was applied to the fibers on the feed side in conjunction with backpulsing. Chemical washes were performed approximately once per day (see Table 3.34 for a list of the chemicals used). CIPs using both hypochlorite and citric were conducted when the TMP reached approximately 11 psi (75.85 kPa). During the CIP, the tank was drained, filled with permeate, and dosed with a chemical solution that was recirculated for 10 to 20 minutes.

**Experimental protocol.** The data obtained from the pilot runs listed in Table 3.36 will be used in the discussion of this study.

**3Water quality characterization.** The number and type of samples that were collected for NOM characterization are presented in Table 3.36.

**Table 3.35**  
**Pilot system operating conditions for runs analyzed in study**

	Run no.	Flux (L/m <sup>2</sup> -hr)	Recovery (%)	Chemical wash type
Pall	4	123	96	Chlorine, acid
Siemens MEMCOR	6a	51.4	91	Citric, hydrochloric acid, chlorine
Zenon	4	34.3	95	NaOCl

**Table 3.36**  
**NOM characterization sample collection**

	Run no.	Feed	Permeate	Raw	Backwash
Pall	4	1			
Siemens MEMCOR	6a	1			
Zenon	4	1	1	1	1



**Figure 3.30 Zenon ZeeWeed 1000 pilot system (Tuscaloosa) using Membrane B**

*Minneapolis.* The pilot plant was provided on lease from the Ionics Division of GE to the Minneapolis Water Works, who operated the plant for the purposes of design and procurement of a 70-mgd (26.5-ML/d) ultrafiltration system currently being commissioned at the Columbia Heights Water Filtration Plant.

The Ionics/Norit X-Flow pilot unit included the following components:

- 500-gal (1892.7 L) feed tank
- 100- $\mu$ m in-line strainer
- Feed pump
- Two 8-inch diameter by 40-inch long Norit X-Flow modules in a single housing (using Membrane C)
- 500-gal (1892.7 L) filtrate tank
- Backwash pump
- Sodium hypochlorite dosing system
- Hydrochloric acid dosing system
- On-line turbidimeter for both feed stream and filtrate
- On-line filtrate particle counter

The pilot unit used a PLC and included valves, pressure gauges, and flow meters for monitoring and controlling the system. [Table 3.37](#) presents the specific characteristics of the Ionics/Norit X-Flow S225 membrane module. [Figure 3.31](#) shows the flow diagram of the pilot unit in the filtration mode.

The membrane operation cycle comprised both filtration and backwash steps. The filtration step consisted of the movement of feed water from one end of the housing horizontally through the fiber bundles in a unilateral direction at the flux presented in Table 3.38. Water moved through the fibers and was collected in the central filtrate channel where it was then sent to the filtrate tank. The system operated in dead end mode. The backwash steps were automatic and lasted 45 seconds at a flux presented in Table 3.38.

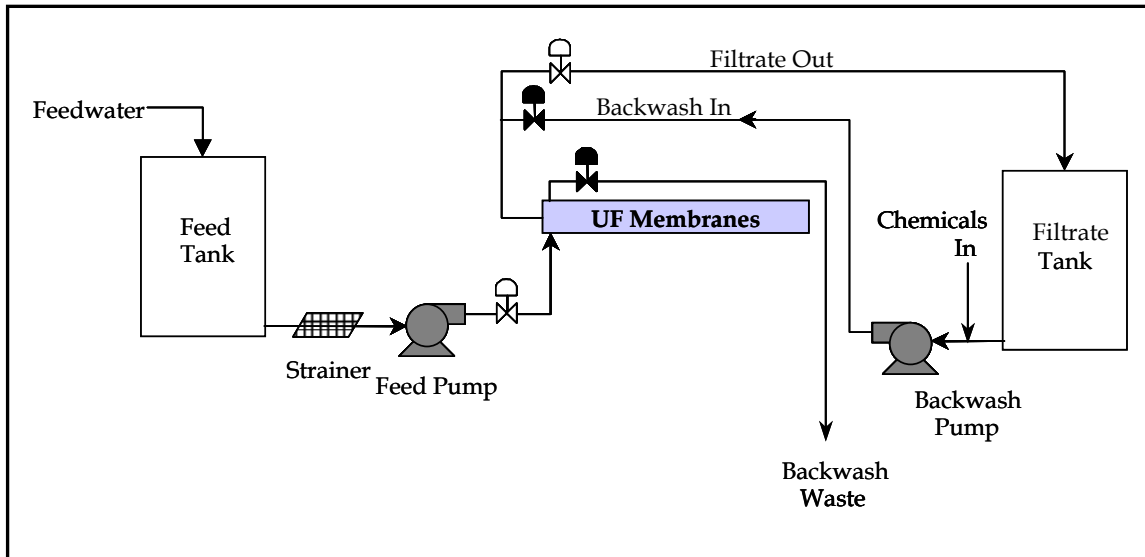


Figure 3.31 Ionics/Norit X-Flow pilot unit schematic (Membrane C)

**Table 3.37**  
**Characteristics of Ionics/Norit X-Flow S225 module**

Property	Value
Membrane type	Ionics/Norit X-Flow S225
Membrane designation	C
Membrane material	PES, modified with PVP
Flow direction	Inside-out, horizontal
Active module service area	377 ft <sup>2</sup> (35 m <sup>2</sup> )
Maximum TMP	36 psi (248.21 kPa)
Total no. of fibers (approx.)	10,000
Nominal retention	100k Daltons
Surface characteristics	Hydrophilic

**Table 3.38**  
**Operating conditions for Minneapolis pilot study**

Run no.	Flux (gfd [L/m <sup>2</sup> -hr])	Backwash flux (gfd [L/m <sup>2</sup> -hr])
1	40 (61)	110
2	42 (71)	110
3	45 (76)	110

Chemicals were periodically added to the backwash water to enhance the removal of membrane foulants through a chemical wash-cleaning (CW). The CW regime employed was as follows:

- Chemical wash 1 – sodium bisulfite at 300 mg/L and hydrochloric acid at 800 mg/L with target pH < 2. Soak time of 10 minutes. Conducted once every 36 backwash cycles.
- Chemical wash 2 – sodium hypochlorite at 200 mg/L. Soak time of 10 minutes. Conducted once every 216 backwash cycles.

Operational data from the pilot used in this study to conduct three fouling runs was limited to a period from March 21 to April 14, 2005, when the Mississippi River water quality was undergoing relatively rapid increases in NOM content associated with snowmelt (spring thaw). Pilot plant operation during the previous season had shown that the increased NOM content increased the rate of membrane fouling. Samples of the untreated river water and UF pilot feed water (following softening and ferric clarification) were collected within this period of operation for NOM characterization.

To better manage fouling caused by the increased NOM levels during the spring thaw, the frequencies of CWs 1 and 2 were increased from every 36 backwash cycles to every 18 backwash cycles and from 216 backwash cycles to every 108 backwash cycles, respectively, between the first and second runs.

**North Bay.** The Ontario Clean Water Agency (OCWA), City of North Bay, Ontario and CH2M HILL conducted a pilot-scale study for the purposes of developing information required for MF/UF system prequalification and equipment procurement, including design and operation parameters, to supply a full-scale membrane treatment system at the Trout Lake site. Four membrane manufacturers participated: Pall, Siemens MEMCOR, Zenon, and Ionics. The pilot units were operated at the City's Water Treatment Plant from October 22 to December 21, 2003. The feed water to the pilot systems was raw water collected from Trout Lake.

For the purposes of this study, results from the operation of the Siemens MEMCOR CMF-s unit will be presented because NOM characterization was only performed with samples collected from this skid (at the request of Siemens MEMCOR). It should be noted that at the conclusion of the pilot testing/pre-qualification/procurement process, a Pall MF system was selected for full-scale implementation by the City based on the best combination of price and performance.

Table 3.39 presents specific characteristics of the CMF-s module.

**Pilot operations.** During filtration mode, feed water under vacuum created by the permeate pump was drawn through the fiber walls and directed to the permeate tank or to the drain. The flux was set at 37 gfd (63 L/m<sup>2</sup>-hr) during the run discussed in this study. PLC-initiated backwashes were conducted after a 30-minute period of filtration. The backwash frequency and duration resulted in a 92 percent recovery rate. Backwashing was conducted using permeate in combination with low-pressure air scour applied to the feed side of the fibers. CIP was accomplished using either an acid- or caustic-based cleaning solution.

Chemical washing was conducted every 16 hours using a sodium hypochlorite dose of 150 mg/L for a contact time of 51 minutes at temperatures of 10 to 25° C.

**Table 3.39**  
**Characteristics of Siemens MEMCOR CMF-s module**

Property	Value
Membrane type	Hollow fiber
Membrane designation	A
Membrane material	PVDF
Flow direction	Outside-in
Active module service area	271 ft <sup>2</sup> (25.2 m <sup>2</sup> )
Maximum TMP	12 psi (82.74 kPa)
Active fiber length	41 in (1.0 m)
Fiber inside diameter	500 μm
Fiber outside diameter	800 μm
Nominal pore size	0.1 μm

## Full-Scale Plants

### *City of Parsons*

**Introduction.** The City of Parsons, Kan. currently operates a 4.5-mgd (17.0 ML/d) water treatment facility to treat water from Labette Creek. The facility consists of the following unit operations and processes:

- Chemical addition (caustic, potassium permanganate, aluminum chlorohydrate, and PAC) for pH adjustment, iron and manganese oxidation, coagulation, and taste and odor control
- Upflow solids contact reactors (Claricones™) for flocculation and sedimentation
- Membrane feed tank for flow balance between Claricones and MF units
- Fine screening
- Pall Microza MF units
- Chlorine disinfection, ground storage, and high-service pump

A process flow diagram of the WTP is shown in [Figure 3.32](#). The WTP was originally constructed with a 3-mgd (11.4-ML/d) UF system provided by another manufacturer in 2001, but the system failed to produce the design capacity. The system was removed and replaced with the Pall Microza system in 2004 and 2005 to provide the current 4.5-mgd (17.0-ML/d) capacity.

**Materials and methods.** Characteristics for Labette Creek water quality are shown in [Table 3.40](#). The creek water is characterized by high TOC levels, variable and often very high turbidity, and elevated levels of iron and manganese.

The Pall Microza system includes:

- Two AP-4 skids containing (40 membrane module)
- Feed tank
- Backwash tank
- Pumps
- Process instrumentation and Control Valves

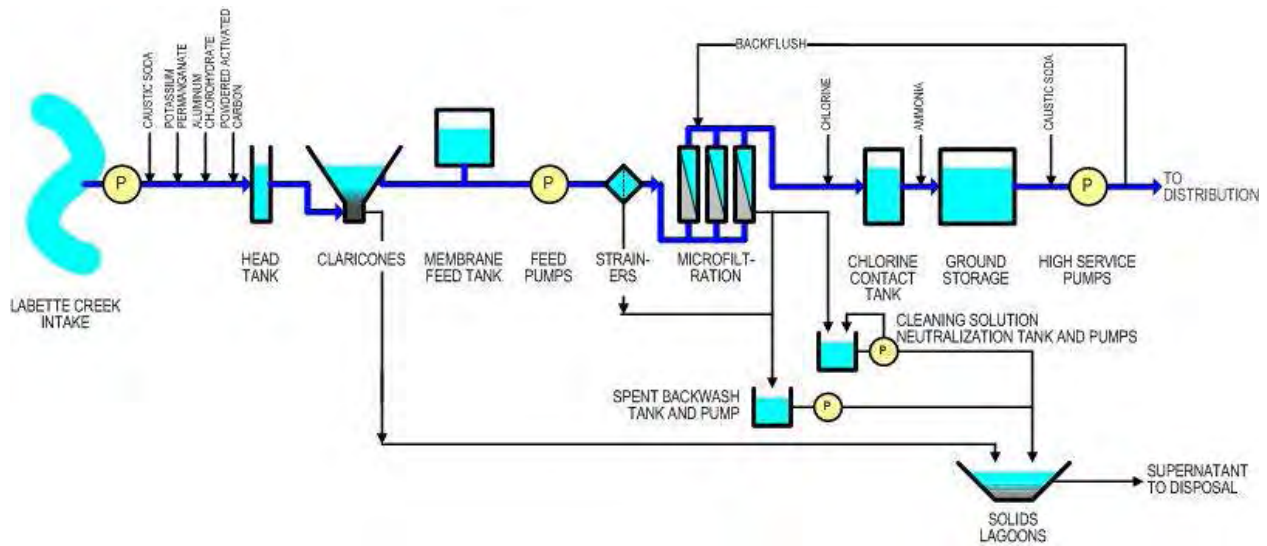


**Figure 3.32 Process flow diagram for full-scale Pall Microza MF system at Parsons, Kan.**

**Table 3.40  
Representative Labette Creek water quality**

Parameter	Units	Range
Turbidity	NTU	10 - 1000
TOC	mg/L	8 - 12
Temperature	°C	4.5 - 28
Alkalinity	mg/L as CaCO <sub>3</sub>	80 - 120
pH	Units	7.0 - 8.0
Iron	µg/L	500 - 1500
Manganese	µg/L	100 - 500
Silica	mg/L	8 - 10

Characteristics of the Microza module are identical to those shown in [Table 3.32](#). The hollow-fiber membrane characteristics are similar to those of the CMF-s modules used in the Indianapolis pilot study with respect to membrane material and nominal pore size. A photo of the three Pall MF skids is shown in [Figure 3.33](#).



**Figure 3.33 Pall Microza MF skids as installed at Parsons, Kan.**

**Full-scale operations.** The full-scale process schematic is provided in [Figure 3.32](#). The basis of design was based on producing 4.3 mgd (16.3-ML/d) net at 25° C, feed turbidity < 2 ntu, and feed TOC = 4 mg/L. The filtration cycle duration is approximately 45 minutes. Chemical washes (EFMs) are performed at 10,000,000 gallons (37,850 ML) gross permeate production per rack. This translates to about 9 days of operation between CWs at the design conditions, 65 gfd (110 L/m<sup>2</sup>-hr) flux at 95.4 percent recovery.

### ***City of Manitowoc***

**Introduction.** Manitowoc Public Utility (MPU) was a participating utility in this study with the intent of gaining a better understanding of how the NOM in their water supply (Lake Michigan) was impacting the performance of their membrane system. The MPU membrane facility employs polypropylene-based hollow-fiber modules; consequently, information gleaned from the analysis of their system's performance, feed water NOM, and membrane characterizations could not be compared with results from the bench and pilot portions of this study.

MPU commissioned a 14-mgd (53.0 ML/d) microfiltration plant in 1999 to replace a conventional treatment train (rapid mix, flocculation, sedimentation, and granular media filtration). The plant has been operated on a more or less continuous basis since commissioning. Operating data for one of the thirteen membrane skids was provided to the project team for the purpose of calculating the rate of fouling (as measured by UMFI and discussed in Section 3.6).

**Materials and methods.** Lake Michigan is the raw water source for the MF plant. Quality for this source is presented in [Table 3.41](#).

The MF plant contains the following major components:

- Thirteen CMF units, each comprising 90 M15C CMF modules (the thirteenth skid was added in 2001 to more effectively provide firm capacity)

- Chemical CIP system including two 5000-gal (18,927-L) solution tanks, circulation pumps, bulk chemical storage tanks, heating and control system
- Air backwash system, including three compressors and two horizontal air-receiving tanks

Table 3.42 lists the characteristics of the CMF modules used with the Manitowoc MF system. The membrane material used in this module is designated “Membrane F” as listed in Table 3.3.

**Full-scale operations.** In filtration mode, feed water is first pretreated with 3 mg/L polyaluminum chloride (Sumalchlor-50). Raw water is pumped through the membrane fibers from outside to inside using the feed pump, with the permeate conveyed to disinfection, storage, and distribution. Pressure is approximately 30 psi (206.85 kPa), and the filtration cycle is between 25 and 45 minutes. The membrane modules are backwashed using high-pressure air (90 to 95 psi [620.55 to 655.03 kPa]) applied from the inside of the fiber to the outside to displace accumulated solids. The displaced solids are then flushed from the feed side of the module using unidirectional flow of feed water from the bottom of module to the top. The air-feed water backwash is between 120 and 150 seconds. Chemical CIP is conducted by circulating either a citric acid or caustic solution (with proprietary cleaning agents) through the modules followed by soaking for 90 minutes with a typical total CIP time of 2 to 3 hours. No chemical washes are employed.

**Table 3.41**  
**Lake Michigan water quality (Manitowoc WTP)**

Parameter	Result
Alkalinity, total as CaCO <sub>3</sub>	110
Calcium	38
Chloride	9.2
Copper, ppb	3.2
Fluoride	0.035
Hardness (calculation) as CaCO <sub>3</sub>	140
Iron	0.0027
Lead, ppb	2
Magnesium	11
Nitrate	0.1
pH, units	7.6–8.1
Silica/silicate	0.29
Sodium	6.1
Sulfate	21
Total organic carbon	0.6–1.8
Turbidity (NTU)	1.0–100
Total coliform (count per 100 mL)	0–130
Cryptosporidium	ND
Giardia	ND

ND-Non Detect

**Table 3.42**  
**CMF membrane module characteristics**

Property	Value
Membrane type	Hollow fiber
Membrane designation	CMF
Membrane material	PP
Flow direction	Outside-in
Active module service area	161.4 ft <sup>2</sup> (15 m <sup>2</sup> )
Maximum TMP	10 psi (68.95 kPa)
Active fiber length	41 in (1.0 m)
Nominal pore size	0.2 μm

The CMF system was designed to operate over a flux range of 71 to 90 gfd (121 to 153 L/m<sup>2</sup>-hr), but has operated in the range of 28 to 57 gfd (48 to 97 L/m<sup>2</sup>-hr) with an average CIP interval of 5.5 days. Attempts to operate the units closer to the design flux has resulted in unacceptably short CIP intervals.

## UNIFIED MODIFIED FOULING INDEX CONCEPT

### Concept

Because the traditional membrane-fouling index (MFI) was derived for constant pressure filtration, the concept of unified MFI (UMFI) was developed as a key analytical tool for this project to quantify the fouling rate encountered not only in constant pressure, as used with the bench-scale stirred-cell tests, but also in constant flux filtration as employed in the hollow-fiber bench- and pilot-scale testing, as well as the operation of the full-scale membrane systems.

The foundation of UMFI is Darcy's law and the resistant-in-series model, which is written as:

$$J_s = \frac{J}{P} = \frac{1}{\mu(R_m + R_c)} \text{ (fouled membrane)}$$

$$J_{s0} = \frac{1}{\mu R_m} \text{ (clean membrane)}$$

where  $J_s$  is the specific flux,  $\mu$  is the dynamic viscosity of water at a given temperature, and  $R_m$  and  $R_c$  are the membrane resistance and fouling resistance, respectively. These two equations apply to both constant pressure and constant flux filtration. An important assumption made herein is that the fouling is solely ascribed to the formation of a cake layer on the membrane surface. If the temperature is the same,  $J_{s0}$  can be normalized to  $J_s$ , and the following linear relationship is established:

$$\frac{1}{J'_s} = \frac{J_{s0}}{J_s} = 1 + \frac{R_c}{R_m} = 1 + \frac{\alpha_c m_c}{R_m}$$

where  $\alpha_c$  is the specific cake resistance and  $m_c$  is the mass of foulants per unit membrane surface area. If the concentration of the foulants in the feed water is constant throughout the filtration, the equation above can be converted to another linear form using  $m_c = C_f V_S$ :

$$\frac{1}{J_s'} = 1 + \left( \frac{\alpha_c C_f}{R_m} \right) V_s$$

where  $J_s'$  [dimensionless] is as defined previously, and  $V_S$  [L/m<sup>2</sup>] is the unit permeate throughput. Based on this relationship, UMFI [m<sup>2</sup>/L] is defined as follows:

$$\text{UMFI} = \frac{\alpha_c C_f}{R_m}$$

For a filtration without hydraulic backwash, UMFI is related to the hydraulic property of the cake layer ( $\alpha_c$ ), the concentration of total foulants ( $C_f$ ), and the hydraulic property of the clean membrane ( $R_m$ ). Its value is not affected by operating mode. Temperature effects are also canceled out through the normalization of specific fluxes. If the concept is applied to a filtration with either frequent hydraulic backwashes or chemical cleaning (as with the pilot systems), the UMFI can still be calculated as a measure of the rate of hydraulically irreversible fouling or chemically irreversible fouling that occurs within certain unit permeate throughputs. However, the consistency of the calculated UMFI is dependent on whether the concentration of foulants that cannot be removed hydraulically or chemically remains constant during the test.

### Calculation and Utility of UMFI

To fully describe the diversity of data collected during this project, eight fouling indices are used. The method of calculation and the utility of each index are described in this section. [Table 3.43](#) summarizes the details for each of the indices.

#### ***UMFI***

The UMFI is calculated for experiments with a single long period of filtration, specifically bench-scale testing with the flat-sheet stirred-cell unit, and the hollow-fiber end-of-run backwash operational modes. The UMFI is a measure of the total fouling capacity of a 1.2- $\mu\text{m}$  prefiltered water sample. The UMFI does not take into account the effects of backwashing or chemical washing. The UMFI is defined as the slope of the least squares linear regression line fit to the reciprocal of the normalized specific flux ( $1/J_s'$ , dimensionless) as the dependant variable, and the unit permeate throughput,  $V_S$  (L/m<sup>2</sup>), as the independent variable, at each measurement interval of the filtration cycle. A graphical representation of this calculation is represented by the open squares and triangles in [Figure 5.40](#) of section 5.2.2.3. The hollow symbols represent data used for the calculation of UMFI. It is important to note that each fouling index described in this report is equal to the slope of the regression line that describes the plot of  $1/J_s'$  versus  $V_S$ . The units for each index, being the units of the slope of the regression line, are the reciprocal of the units for permeate throughput, namely m<sup>2</sup>/L.

### ***UMFI<sub>i</sub>***

The  $UMFI_i$  is used to assess the total fouling capacity of a water for operational protocols involving multiple short periods of filtration, specifically bench-scale multicycle, pilot-scale, and full-scale operation. The  $UMFI_i$  is calculated for the first filtration cycle of an experiment using the same procedure as that used for the  $UMFI$ .  $UMFI_i$  and  $UMFI$  are equivalent, except that  $UMFI_i$  represents a shorter period of filtration. The gray symbols in [Figure 5.38](#) of section 5.2.2.3 represent data used for the calculation of  $UMFI_i$ .

### ***UMFI<sub>150</sub>***

The short-term hydraulically irreversible portion of fouling is described by the  $UMFI_{150}$ , corresponding to data over a  $V_S$  of  $150 \text{ L/m}^2$  for operational protocols involving multiple cycles of filtration interspersed by backwashing, namely multicycle bench-scale, pilot-scale, and full-scale operation. Two methods of calculation of  $UMFI_{150}$ , described here, were necessitated by differences in the frequency of data collection between pilot-scale operational protocols.

***UMFI<sub>150</sub> Method 1.*** The  $1/J_S'$  at the start of each filtration cycle within the first  $150 \text{ L/m}^2$  of unit permeate throughput are used to calculate the  $UMFI_{150}$  Method 1. The solid black symbols in [Figure 5.38](#) of section 5.2.2.3 represent data used for the calculation of  $UMFI_{150}$  Method 1. Method 1 has the advantage of considering the behavior of each cycle.

***UMFI<sub>150</sub> Method 2.*** The  $1/J_S'$  at the start of the first and final cycle within the first  $150 \text{ L/m}^2$  of unit permeate throughput are used to calculate  $UMFI_{150}$  Method 2. This method is calculated in an identical manner as  $UMFI_{150}$  Method 1 except that intervening filtration cycles are not considered. Method 2 has the advantage of minimizing the effects of high variability between cycles during a run.

### ***UMFI<sub>3000</sub>***

Long-term hydraulically irreversible fouling is described by the  $UMFI_{3000}$  for pilot-scale and full-scale operation.  $UMFI_{3000}$  Method 1 and Method 2 are calculated as corresponding to  $UMFI_{150}$ , except that the unit permeate throughput cutoff is  $3000 \text{ L/m}^2$ . A major advantage of the  $UMFI_{3000}$  is that it includes at least one cleaning cycle for pilot-scale runs for which chemical washing was performed. The  $UMFI_{150}$  does not.

### ***UMFI<sub>R</sub>***

Short-term hydraulically irreversible fouling in the bench-scale end-of-run backwash operational mode is described by the  $UMFI_R$ , and is comparable to the  $UMFI_{150}$  or  $UMFI_{3000}$  of multicycle bench-scale, pilot-scale, and full-scale operation. This index is calculated using the  $1/J_S'$  at the start of the fouling filtration cycle and the start of filtration following permeate backwashing. As such the  $UMFI_R$  is calculated as the slope of the regression line between two data points. The two outlined, grey-shaded squares in [Figure 5.40](#) of section 5.2.2.3 represent the data used for the calculation of  $UMFI_R$ .

**Table 3.43**  
**Explanation of the various types of fouling indices used in this report**

	UMFI	UMFI <sub>i</sub>	UMFI <sub>150M1</sub>	UMFI <sub>150M2</sub>	UMFI <sub>3000M1</sub>	UMFI <sub>3000M2</sub>	UMFI <sub>R</sub>	UMFI <sub>cleaning</sub>
Bench, pilot or both	Bench	Both	Both	Both	Pilot	Pilot	Bench	Bench
Single or multicycle	Single	Multi	Multi	Multi	Multi	Multi	Single	Single
Stirred-cell, hollow-fiber, or both	Both	Hollow	Hollow	Hollow	Hollow	Hollow	Hollow	Hollow
Takes permeate backwashing into account?			Yes	Yes	Yes	Yes	Yes	Yes
Takes chemical cleaning into account (if done)?					Yes	Yes		Yes
Calculation performed using:								
two points?				Yes		Yes	Yes	Yes
more than two points?	Yes	Yes	Yes		Yes			
all of the points in the first cycle?	Yes	Yes						
the following unit permeate throughput cutoff:			150 L / m <sup>2</sup>	150 L / m <sup>2</sup>	3000 L/m <sup>2</sup>	3000 L/m <sup>2</sup>		
the first point from each cycle within any applicable cutoff?			Yes		Yes		Yes	Yes
the first point from the first and the last cycles? (for bench scale consider permeate and chemical backwashing cycles)				Yes		Yes	Yes	Yes
Index describes	Total Fouling		Hydraulically* Irreversible Fouling		Hydraulically* or Chemically (if done) Irreversible Fouling		Hydraulic.* Irreversible Fouling	Chemically Irreversible Fouling
Equivalent bench/pilot index for comparison	UMFI <sub>i</sub>	UMFI	UMFI <sub>R</sub>	UMFI <sub>R</sub>	UMFI <sub>R</sub> , UMFI <sub>cleaning</sub>	UMFI <sub>R</sub> , UMFI <sub>cleaning</sub>	UMFI <sub>150M1</sub> , UMFI <sub>150M2</sub> , UMFI <sub>3000M1</sub> , UMFI <sub>3000M2</sub>	UMFI <sub>3000M1</sub> , UMFI <sub>3000M2</sub>

\* Note Indianapolis pilot used air scour during permeate backwashing

### ***UMFI<sub>cleaning</sub>***

Chemically irreversible fouling is described by the  $UMFI_{cleaning}$  for the bench-scale end-of-run backwash operational mode. The  $UMFI_{cleaning}$  can be compared to the  $UMFI_{3000}$  for multicycle runs with chemical washing included their protocol. The  $UMFI_{cleaning}$  is calculated using the  $1/J_s'$  at the start of the fouling filtration cycle and the start of filtration following chemical washing. As such, the  $UMFI_{cleaning}$  is calculated as the slope of the regression line between two data points.

## CHAPTER 4

### FEED WATER CHARACTERISTICS AND MEMBRANE PROPERTIES

#### FEED WATER CHARACTERISTICS

Each of the feed waters tested at the various scales of membrane filtration was characterized according to NOM properties as well as potentially influential inorganic constituents. NOM characterization included SEC-DOC/UV chromatograms, fluorescence EEM, DON, and XAD-8/-4 fractionation. Quantitative information was also extracted from the various NOM characterizations. The SEC PS and HS peaks were integrated to provide DOC-based concentrations of PS-DOC (mg/L) and HS-DOC (mg/L). FI values were extracted from the EEM spectra. Based on a DOC mass balance, values of HPO-DOC, TPI-DOC, and HPI-DOC were derived from the XAD fractionation. Supplementing these organic parameter were various inorganic characteristics, including pH, conductivity, Ca<sup>2+</sup>, and Fe.

Table 4.1 provides XAD-8/-4 resin fractionation results according to a DOC mass balance. The Tampa Bay water exhibited a high content of HPO-DOC, while the Indianapolis and Scottsdale waters showed a high content of HPI-DOC. Generally, the hydrophilic fraction of natural waters contains macromolecules, such as polysaccharides and proteins, and organic colloids (if not pre-isolated as was the case in this study); our hypothesis is that HPI-DOC is a problematic fraction in low-pressure membrane fouling. The HPO-DOC corresponds to an operational definition of humic substances and, in the absence of high levels of calcium (which forms complexes with humic substances), is hypothesized to play only a small role in fouling. The Tuscaloosa water exhibited a high percentage of HPO-DOC and a relatively low amount of TPI-DOC.

**Table 4.1**  
**XAD 8/4 resin fractionation**

Feed water	Hydrophobic DOC (%) (mg/L)	Transphilic DOC (%) (mg/L)	Hydrophilic DOC (%) (mg/L)
Indianapolis	39.0 (1.53)	25.0 (0.98)	36.0 (1.41)
Scottsdale	32.0 (1.92)	28.0 (1.68)	40.0 (2.4)
Tampa Bay	60.0 (10.32)	22.0 (3.78)	17.0 (3.10)
Twente Canal	45 (4.26)	23 (2.18)	32 (3.03)
Tuscaloosa (raw)	49 (1.18)	16 (0.38)	35 (0.84)
Tuscaloosa (clarified)*	52 (0.87)	10 (0.17)	38 (0.63)

\*As described in Chapter 3.

Figures 4.1 and 4.2 are SEC-DOC/UV chromatograms of the feed waters evaluated in bench-scale testing. The first chromatographic peak corresponds to the so-called polysaccharide (PS) peak consisting of polysaccharides and proteins in macromolecular and/or (organic) colloidal forms and having a large molecular weight (MW) greater than  $\sim 10,000$  Daltons, the second peak corresponds to humic substances having a moderate MW of  $\sim 1,000$  to  $\sim 10,000$  Daltons, and the third peak corresponds to simple carboxylic and amino acids designated as low molecular weight acids (LMA) with a MW less than  $\sim 1,000$  Daltons. In the case of the Tampa Bay water, the sample was diluted three-fold with Milli-Q water due to its high DOC concentration. A high response of HS correlates with a high SUVA value. Our hypothesis is that a feed water containing a high PS-DOC concentration would correlate with a higher fouling rate for low-pressure membranes.

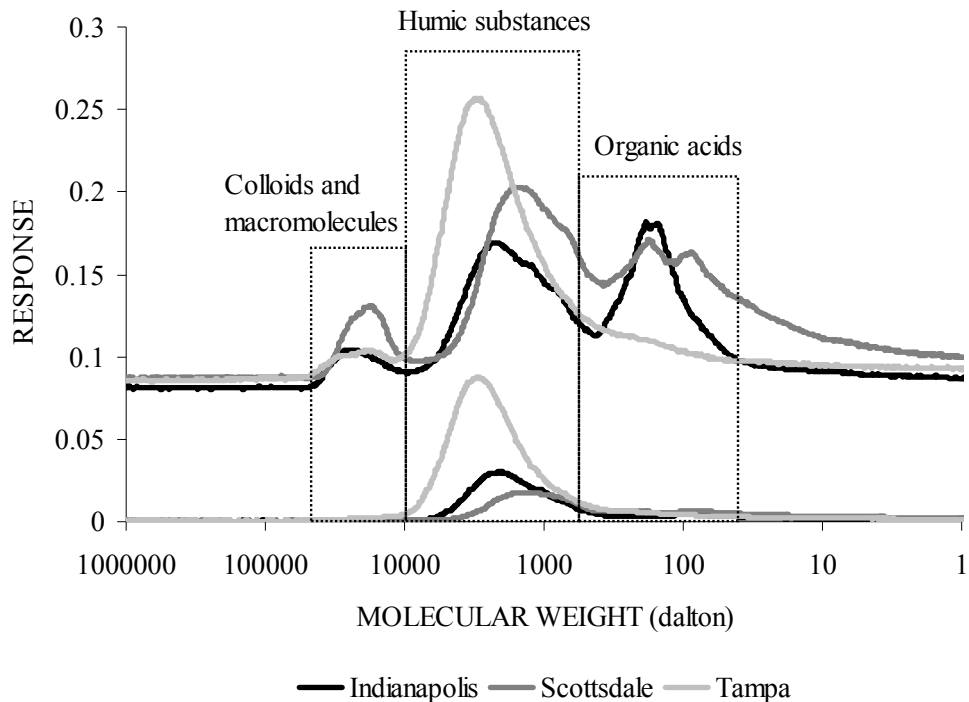


**Figure 4.1 SEC-DOC/UV of feed waters (I)**

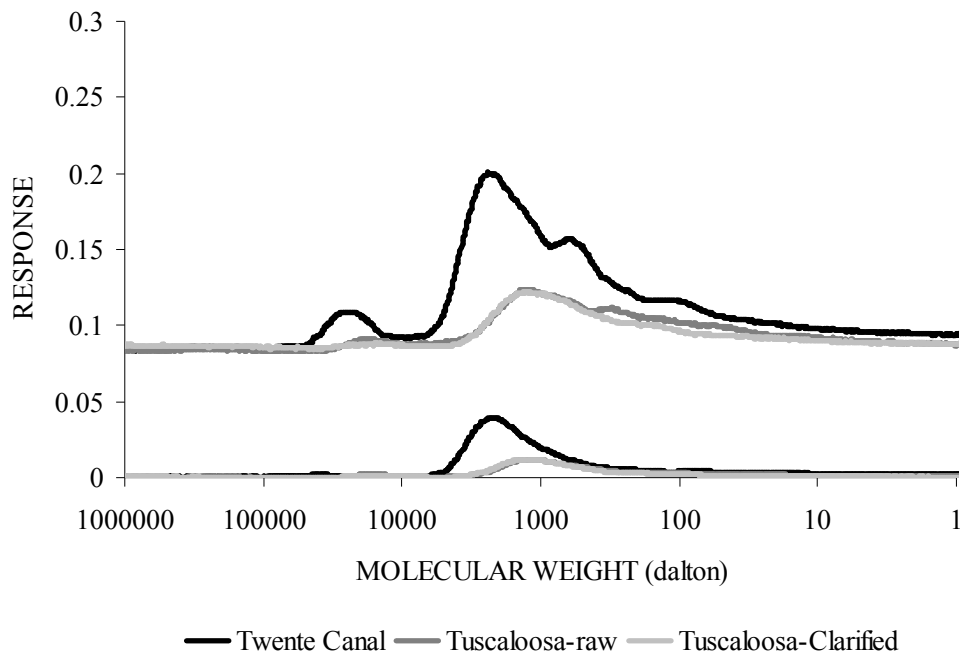


**Figure 4.2 SEC-DOC/UV of feed waters (II)**

Figure 4.3 depicts the fluorescence EEM spectra of six feed waters. Generally, a peak at higher excitation/emission wavelengths is representative of humic-like organic matter (e.g., ex = 278~282 nm and em = 304~353 nm) while a peak at lower excitation/emission wavelengths is characteristic of protein-like organic matter (e.g., ex = 250~300 nm, em = 300~350 nm). All source waters exhibit humic substance peaks; however, the Scottsdale, Twente Canal, and Tuscaloosa waters also exhibit the signature of protein-like substances. The Tuscaloosa-clarified water also shows protein-like substances despite its low DOC concentration; this may be due to protein-like substances not removed by coagulation. As derived from the respective EEM, the FI values of feed waters are provided in Table 4.2. Our hypothesis is that protein-like substances and/or a high value of FI correlate with higher membrane fouling potential.

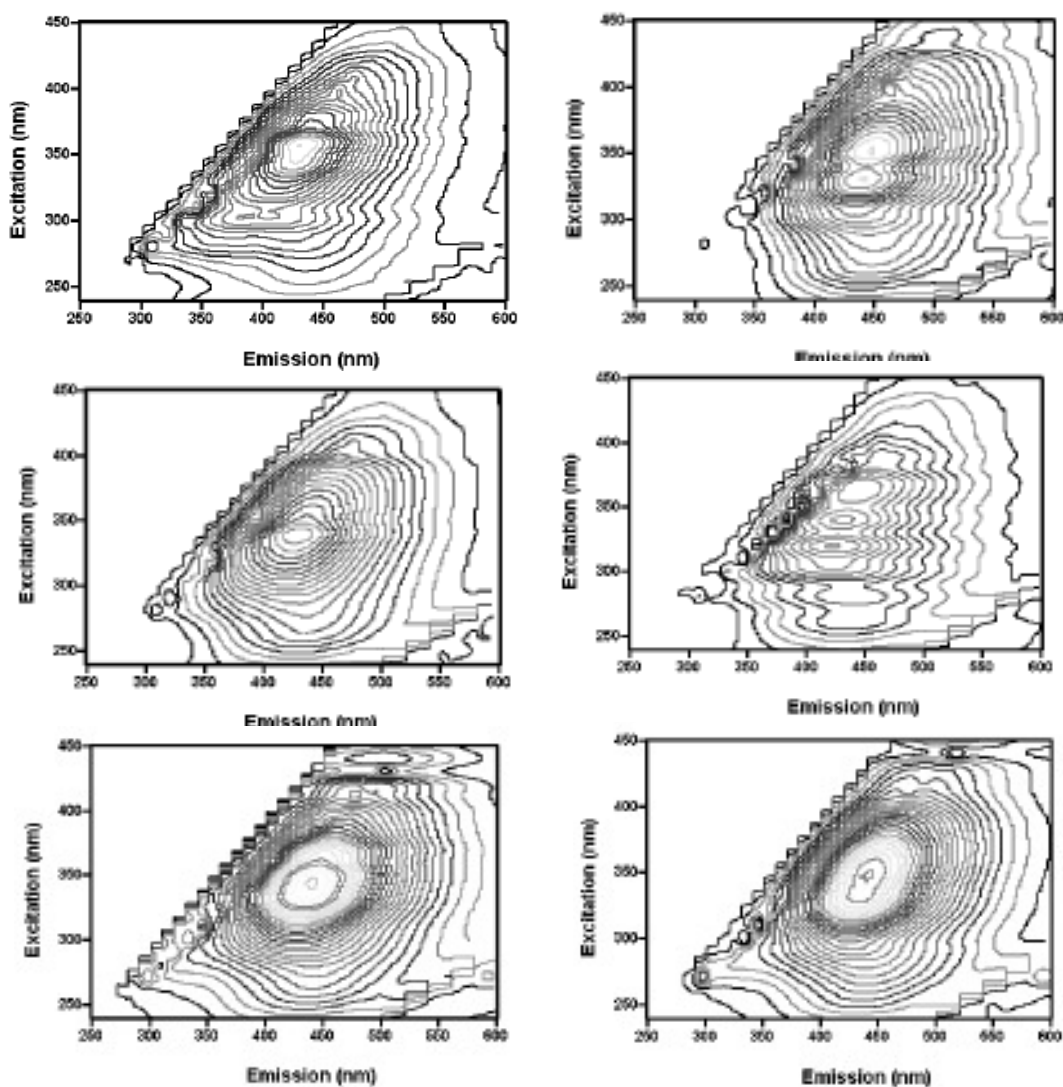


**Figure 4.3 EEM spectra of feed waters (left column: Scottsdale, Twente Canal, Tuscaloosa-raw; right column: Tampa Bay, Indianapolis, Tuscaloosa-clarified)**

From the various NOM analyses, quantitative data can be extracted for use in better evaluating the NOM membrane fouling character of the feed waters. These data are tabulated in [Table 4.2](#) along with general and inorganic data. NOM in the Tampa Bay water, which exhibits the highest DOC concentration, is mostly humic substances, as revealed by XAD-8/-4 resin fractionation. The Twente Canal water also has a high content of DOC. With respect to the HPI-DOC:HPO-DOC ratio (reflecting the relative fraction of hydrophilic to hydrophobic NOM), all feed waters are similar except for Tampa Bay, which has a ratio that is nearly one-tenth as low. Tuscaloosa, despite having the lowest DOC level, also has a significantly lower HPI:HPO ratio. The PS-DOC:HS-DOC ratios are identical for Indianapolis and Scottsdale waters, despite their origin differences, while the PS-DOC:HS-DOC ratios for Tampa Bay, Twente Canal, and Tuscaloosa waters are much lower. These comparisons illustrate that the NOM present in the Tampa Bay water is clearly dominated by hydrophobic humic substances, whereas the Scottsdale, and Twente Canal waters have higher fractions of hydrophilic and PS NOM, with

Tuscaloosa being intermediate. It is interesting to note that the Twente Canal water is unique in that it has a high HPI-DOC:HPO-DOC ratio but a low PS-DOC:HS-DOC ratio, which is unexpected.

**Table 4.2**  
**Water quality data for bench- and pilot-scale feed waters\***

Parameter	Indianapolis†		Scottsdale		Tampa Bay		Twente Canal	Tuscaloosa-Raw (clarified)
	Bench	Pilot	Bench	Pilot	Bench	Pilot		
DOC (mg/L)	3.92	3.77	6	7.72	17.2	8.42	9.46	2.4 (1.67)
UVA (cm <sup>-1</sup> )	0.091	0.12	0.102	0.13	0.743	0.29	0.236	0.071 (0.048)
SUVA (L/mg-m)	2.3	2.01	1.7	1.63	4.32	3.33	2.49	2.96 (2.87)
DON (mg/L)	0.48	--	0.48	--	0.82	--	0.70	0.56
TN (mg/L)	3.1	--	6.44	--	1.03	--	2.86	0.52
DON/DOC	0.12	--	0.08	--	0.05	--	0.07	0.23
PS-DOC (mg/L)	0.21	0.22	0.39	0.57	0.44	0.35	0.51	0.09 (0.02)
HS-DOC (mg/L)	2.08	1.33	2.74	3.29	16.76	6.59	8.95	2.31 (1.65)
HPI-DOC (mg/L)	1.41	--	2.4	--	3.1	--	3.03	0.84 (0.63)
HPO-DOC (mg/L)	1.53	--	1.92	--	10.32	--	4.26	1.18 (0.87)
HPI-DOC:HPO-DOC	1.16	--	1.29	--	0.3	--	1.33	0.72 (0.72)
PS-DOC:HS-DOC	0.16	--	0.16	--	0.027	--	0.06	0.040 (0.012)
FI	1.57	--	2.07	--	1.37	--	1.65	1.5 (1.5)
pH	8	7.96	6.91	7.19	7.02	7.72	8	7.13
Conductivity (µS/cm)	868	--	1757	--	315	--	704	46.2
Ca (mg/L)	79.2	79.22	81.8	75.87	47	142.79	48.54	1.63
Fe (mg/L)‡	<MDL	0.581	0.048	0.27	0.106	0.141	0.004	0.312
Mn (mg/L)‡	<MDL	0.039	0.035	0.055	0.001	0.012	0.001	0.007
Si (mg/L)	1.4	--	6.02	--	2.7	--	4.099	3.211
Br <sup>-</sup> (mg/L)	0.048	--	0.244	--	0.069	--	0.075	0.004
PO <sub>4</sub> <sup>3-</sup> (mg/L)	<MDL	--	3.292	--	0.521	--	0.113	0.079
SO <sub>4</sub> <sup>2-</sup> (mg/L)	47.8	--	256.2	--	43.1	--	48.92	4.22
Turbidity (NTU)	--	13.6	--	0.5	--	2.8	---	8.5 (7.3)

\*The data presented here were obtained from samples taken at a different time than the data presented in Table 5.5.

† Algal Counts: 1600 – 26,000/mL, Chlorophyll a: 2.6 – 10.8 µg/L

‡MDL: method detection limit (0.002 ppm for Fe; 0.001 ppm for Mn)

As expected, Scottsdale water contains very high level of total nitrogen due to characteristics of wastewater treatment effluent; however, its DON concentration is similar to the other feed waters. The DON of Tampa Bay water is similar to that of the other feed waters, despite its much higher DOC, reflecting the origin of its NOM (terrestrial, vegetative debris). A high FI value indicates that the Scottsdale water contains microbially derived (nitrogen-containing) organics. The Indianapolis source was originally selected as an autochthonous (algal-impacted) source; however, at the time of sampling, there was only a modest algal bloom. This is reflected by its relatively low DON and FI.

Table 4.3 summarizes the additional water quality data from in-plant sampling and analysis performed in conjunction with the Tier 1 pilot studies. A complete tabularization of these data can be found in Appendix A.

## MEMBRANE PROPERTIES

### Flat-Sheet (Disk) Specimens

Flat-sheet membranes used for stirred-cell tests were characterized according to pure water permeability (PWP), contact angle, zeta potential, and roughness (Table 4.4). The PVDF MF membrane exhibits high PWP as well as a high surface roughness value due to its large pore size, while the PES UF membrane shows the lowest PWP. Based on zeta potential, all three membranes are negatively charged at neutral pH. The contact angle for the PAN MF/UF membrane is low, indicating that this membrane is hydrophilic, while the other two are hydrophobic. For the PVDF MF, a relatively high contact angle was measured in contrast to the expectation of a more hydrophilic character based on material.

**Table 4.3**  
**Additional water quality data for pilot-scale feed waters**

Source water	Units	Scottsdale	Tampa Bay	Indianapolis-raw	Indianapolis-clarified*
		Avg	Avg	Avg	Avg
TDS	mg/L	994.9	NP	417.8	538.4
Alkalinity	mg/L as CaCO <sub>3</sub>	173.6	97.0	216.5	235.2
Total hardness	mg/L as CaCO <sub>3</sub>	305.3	181.6	311.8	397.1
Iron, dissolved	mg/L	0.220	0.068	0.048	0.109
Manganese, dissolved	mg/L	0.050	0.005	0.022	0.083
TOC	mg/L	6.34	7.32	3.65	2.69
Aluminum	mg/L	6.34	0.00	0.00	0.00

\*As described in Chapter 3.

**Table 4.4**  
**Characteristics of flat-sheet membranes used in stirred-cell units**

Membrane	Pore Size/ MWCO	PWP (L/m <sup>2</sup> ·hr-kPa)	Contact angle (°)	Zeta potential (mV) (at pH7.0, 10 mM KCl)	Rough- ness (nm)
PVDF MF	0.1-0.2 μm	1435	93	-35	173
PAN MF/UF	0.05 μm	871	20	-42	39
PES UF	100 KD	235	75	-38	15

## Virgin Membrane Hollow-Fiber Characterization

### *Morphology*

FESEM analysis was used to determine the respective inner and outer diameter and thickness of the hollow fibers. Figure 4.4 is an example of the FESEM image of the Membrane D1 as received (virgin) from the supplier. Table 4.5 lists the results obtained for the virgin fibers.

All PES membranes (C, D1, and D2) are characterized by similar outer and inner diameters, nearly 0.7 mm and 1.0 mm, respectively. The wall of Membrane D1 is thicker than that of both the other two PES fibers. Generally, the PES fibers have a larger outer diameter and a thicker wall than the PVDF fibers, reflecting their inside-to-out flow configuration. FESEM images of the outer surface of the fibers are shown in Figure 4.5. The outer surface is the feed surface of the PVDF membranes (out-in filtration mode), while the outer surface is the permeate surface for the PES membranes (inside-out filtration mode). Membrane D1 fiber shows very large pores at the immediate surface (1 to 2 μm in diameter), significantly larger than the pores of Membrane D2 fiber. Although this does not indicate potential differences in the filtration (inside) surface of the two membranes, it does suggest differences in the membrane casting process. The Membrane C fiber permeate-side pores are intermediate in size, falling between the two Membrane D fibers. Membrane A and B (PVDF) fibers are very different from the PES fibers in terms of pore distribution and morphology, reflecting the differences between filtration (feed) surface and permeate surface.

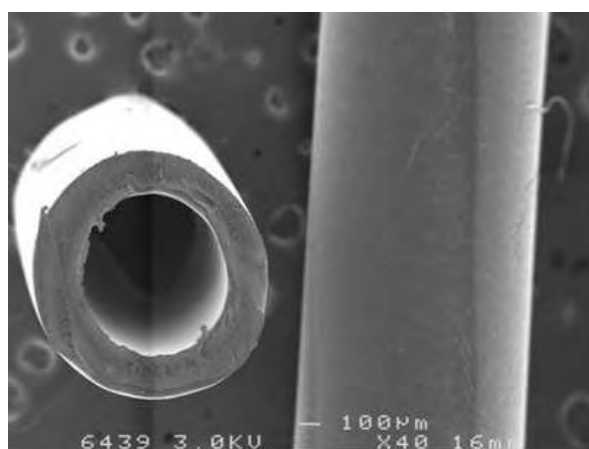
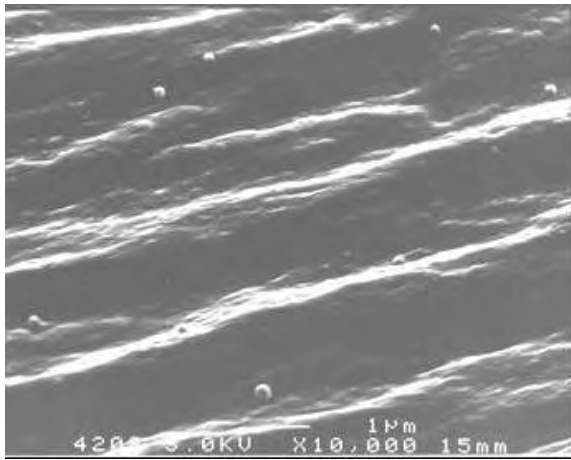


**Figure 4.4 FESEM image of the Membrane D1 PES/PVP fiber**

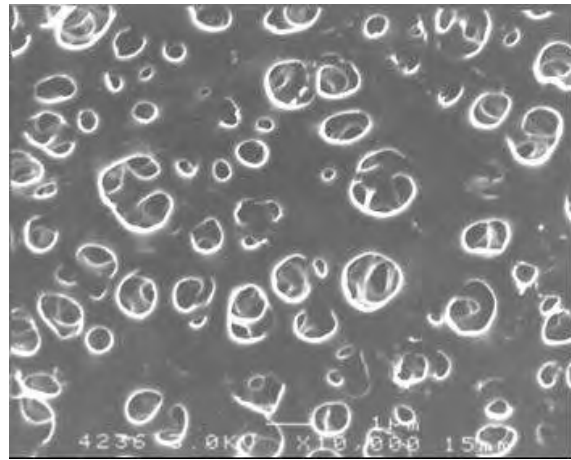
**Table 4.5  
Physical characteristics of the hollow-fiber membranes**

Membrane designation	Material	Outer diameter (µm)	Inner diameter (µm)	Wall thickness (µm)
A	PVDF	815	492	162
B	PVDF	821	479	171
C	PES (PVP*)	1172	735	219
D1	PES (PVP)	1200	700	250
D2	PES	1050	725	163

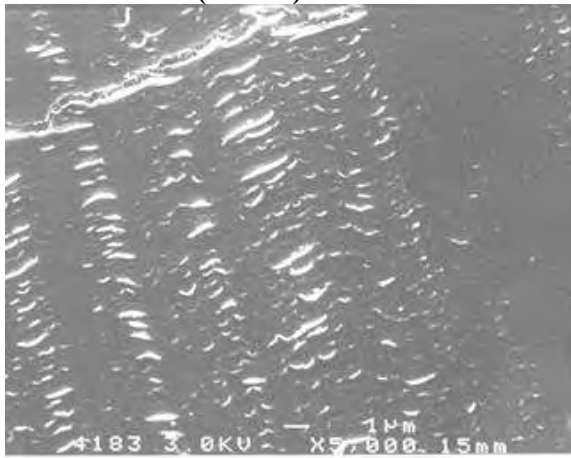
\*PVP incorporated into the PES membrane.



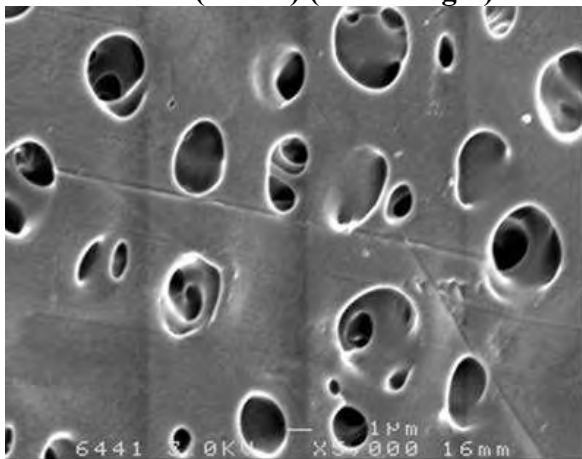
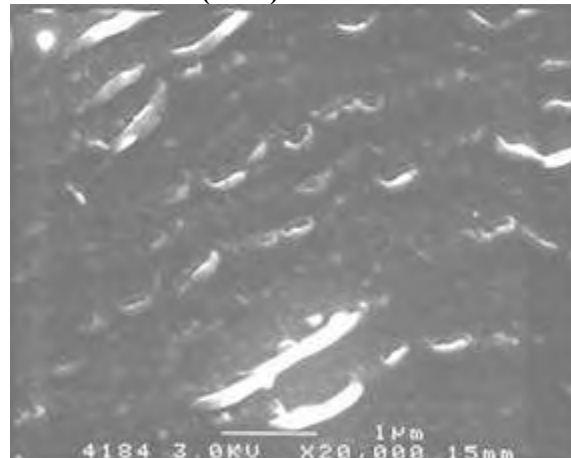
**Membrane A (PVDF)**



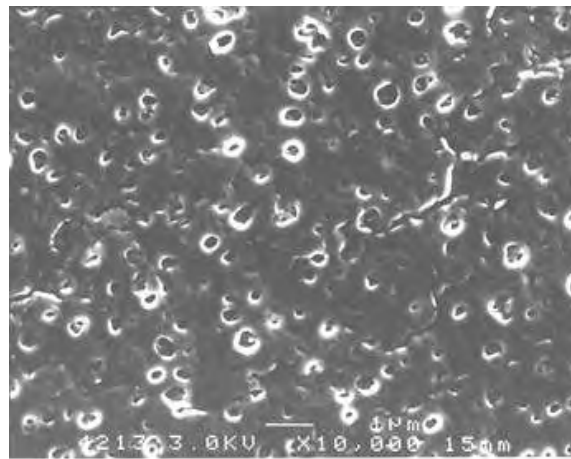
**Membrane C (PES)**



**Membrane B (PVDF) (both images)**



**Membrane D1 (PES)**

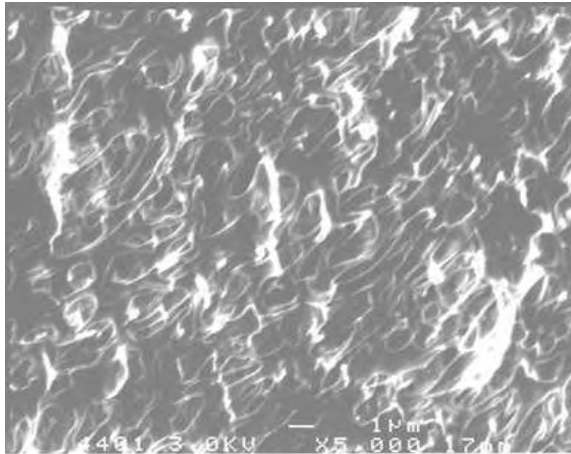


**Membrane D2 (PES)**

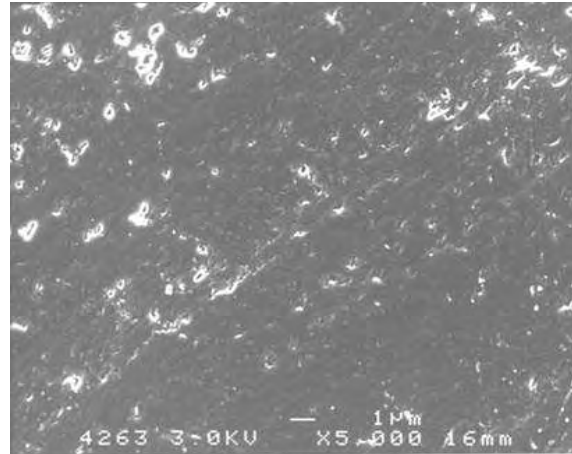
**Figure 4.5 FESEM images of the outer surface of the five membrane fibers used in bench and Tier 2 pilot studies**

FESEM images of the internal (feed-side) surface of Membranes C and D2 PES membranes are shown in Figure 4.6. The feed-side surface has a very different morphology as compared to the permeate-side surface. Pores can still be observed, but the overall morphology appears more similar to the feed-side surface of the PVDF membranes.

Figure 4.7 shows FESEM cross-sections of Membranes A and D2. Cross-sections of Membranes B, C, and D1 fibers look similar to that of Membrane D2 cross-section. In contrast, the Membrane A cross-section shows large vacuoles connected to the pores on the feed-side surface of the fiber.

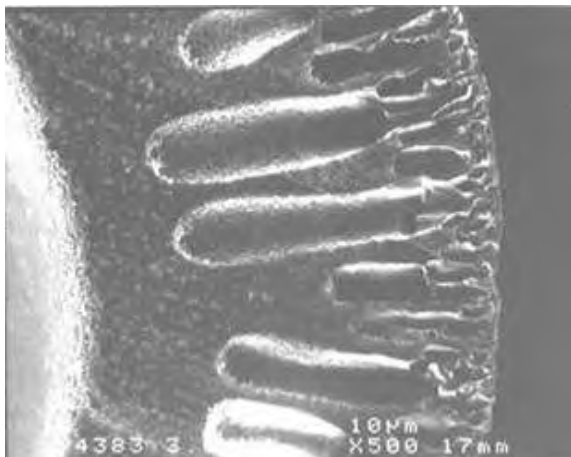


**Membrane C (PES)**

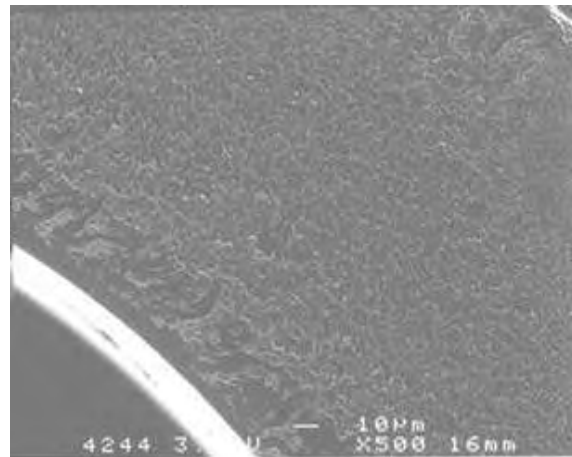


**Membrane D2 (PES)**

**Figure 4.6 FESEM images of the inner (feed-side) surface of Membrane C and D2 fibers**



**Membrane A (PVDF)**



**Membrane D2 (PES)**

**Figure 4.7 FESEM cross-sections of Membrane A and D2 fibers**

## **Contact Angle**

Contact angles of the studied virgin membranes are given in [Table 4.6](#). It is generally accepted that contact angle measurements are method and operator dependent. For similar membranes, different authors using different methods have published different contact angle (Jucker and Clark, 1994; Kim et al., 1999). However, it is also accepted that based on a well-defined and reproducible protocol, this tool can be used to compare the hydrophobic character of low-pressure membranes on a *relative* basis. Membrane surface with a contact angle ranging from 0 to 50° are considered hydrophilic, while above 50°, membrane surface are considered hydrophobic. Membrane roughness also affects contact angle.

A contact angle of zero corresponds to the immediate disappearance of the water droplet (i.e., total wetting). After cleaning, the Membrane A, B, and D2 fibers have similar hydrophobicity with a contact angle around 80°. The increase in the hydrophobicity of the Membrane A fiber after Milli-Q cleaning is attributed to the removal of the glycerin used as a membrane preservative (and detected by pyrolysis GC/MS).

It is worth noting that Membranes C and D1, both PVP-modified PES membranes, show contact angles equal to zero (total wetting). The characteristic, which is not displayed by the Membrane D2 PES membrane, may be related to the greater hydrophilicity imparted by the PVP or by the larger diameter of the pores on the permeate side of the fibers ([Figure 4.5](#)). The rather high contact angle for Membrane A is in contrast to the more hydrophilic character claimed by the manufacturer.

## **Surface Roughness**

[Table 4.6](#) also presents the surface roughness (Ra) for the four hollow-fiber membranes evaluated at bench scale. These results indicate that Membrane A is significantly rougher than the other membranes. This may be due differences in the membrane fabrication process or due to the larger pore size of this MF membrane. The roughness of Membrane B is the lowest of the three UF membranes, even though it has the largest pore size.

[Table 4.7](#) also presents the surface roughness (Ra and Rq) of the studied hollow-fiber membranes. These results indicate that Membrane A (MF membrane) is significantly rougher than the other membranes. The roughness of Membrane B is the lowest of the four UF membranes, even though it has the largest pore size. This may be due to differences in the membrane fabrication. Membranes C, D1, and D2 are characterized by similar roughness, intermediate between Membranes A and B. Topographic two-dimensional (2D) AFM images clearly show the structural differences between membranes. Black areas are probably pores, larger for Membrane A as compared to Membrane B. The filamentous structure of the inner surface of Membrane C, D1, and D2 differs from the rough surface of Membrane A. The morphological difference of the surface of these two membranes is well shown on the topographic AFM three-dimensional (3D) images ([Figure 4.8](#)).

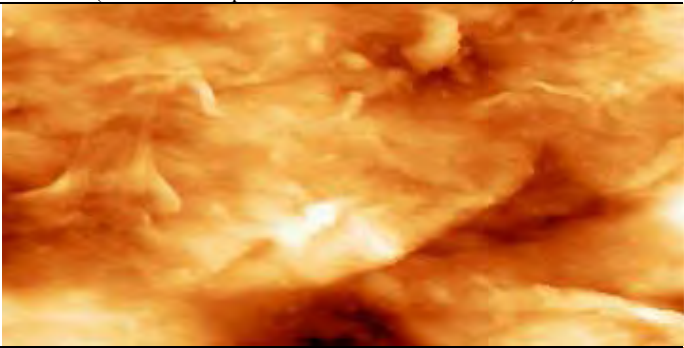
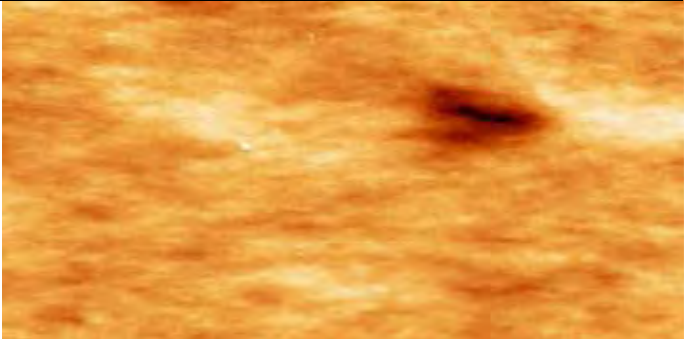
**Table 4.6**  
**Contact angle and surface roughness of the hollow-fiber membranes**

Membrane designation	Material	Contact angle (°) before Milli-Q cleaning	Contact angle (°) after Milli-Q cleaning	Surface roughness (Ra) (nm) (10 μm x 10 μm)*
A	PVDF	82 ± 4	83 ± 5	45.9
B	PVDF	63 ± 5	80 ± 4	3.9
C	PES (PVP)†	0	0	14
D1	PES (PVP)	(total wetting) 0	(total wetting) 0	15.9
D2	PES	(total wetting) 82 ± 4	(total wetting) 84 ± 5	15.5

\*Average measurement of Ra values detailed in Table 4.7.

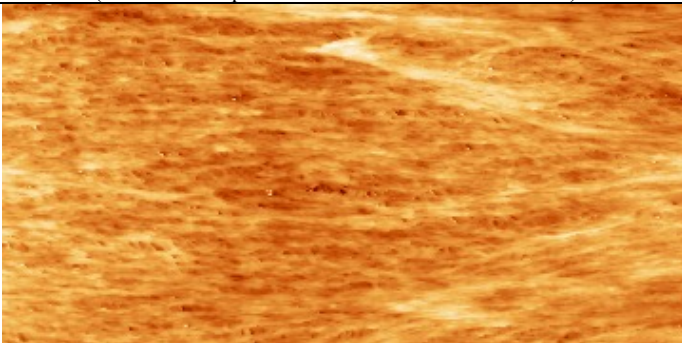
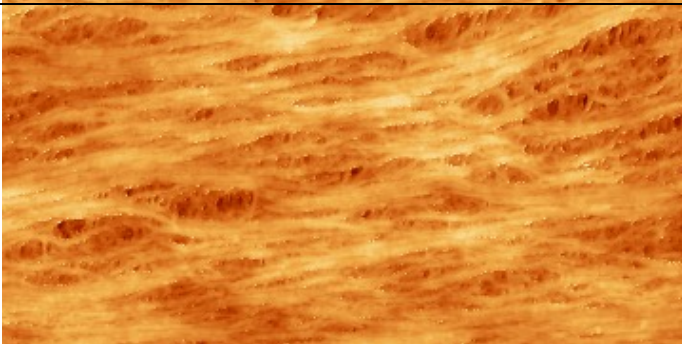
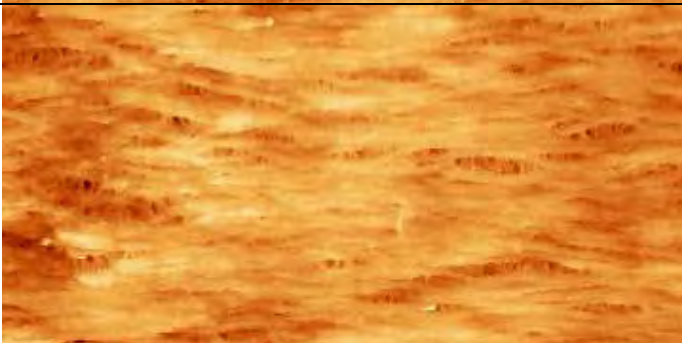
†PVP incorporated into the PES membrane.

**Table 4.7**  
**Roughness (Ra and Rq [RMS]) of the virgin hollow-fiber membranes**

Membrane	Rq (nm)	Ra (nm)	Topographic AFM 2D image (White area = protuberance / Black area = hollow)
A Outside-In Virgin Outer surface Scan 5×2.5 μm <sup>2</sup>	60.9 61.8 54.2	48.2 48.5 41.2	
B Clean Out-In Virgin Outer surface Scan 5×2.5 μm <sup>2</sup>	5.7	3.9	

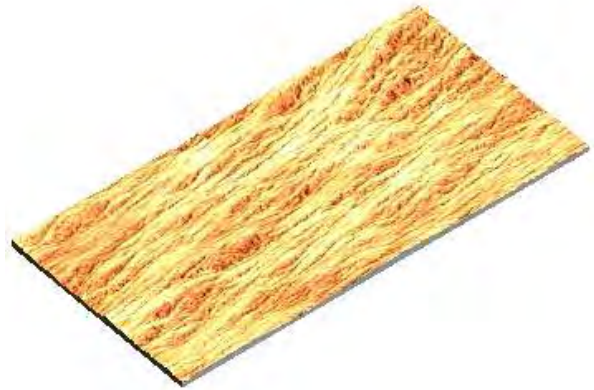
(continued)

**Table 4.7 (continued)**

Membrane	Rq (nm)	Ra (nm)	Topographic AFM 2D image (White area = protuberance / Black area = hollow)
C	17.7	13.9	
Inside-Out	18.1	14.1	
Virgin Inner surface Scan 5×2.5 μm <sup>2</sup>			
D1	19.9	15.9	
Inside-Out			
Virgin Inner surface Scan 5×2.5 μm <sup>2</sup>			
D2	19.4	15.5	
Inside-Out	19.8	15.6	
Virgin Inner surface Scan 5×2.5 μm <sup>2</sup>			



Membrane A (outer surface)



Membrane D1 (inner surface)

**Figure 4.8 Topographic AFM 3D image of Membranes A and D1**

### ***Surface Charge***

Table 4.8 summarizes the streaming potential and isoelectric point (IEP) of the four hollow-fiber membranes evaluated at bench scale.

All membranes are negatively charged at pH 6.5, with potentially a higher degree of charges for PES Membranes C and D2 as compared to the PVDF membranes. The presence of negative charges on the surface of the pores for the PVDF membrane is surprising but already observed by Habarou, et al. (2005). The presence of chemicals coated or grafted at the surface of the membrane to increase the hydrophilic character might be responsible for the presence of a negatively charged surface. This same remark may explain that an isoelectric point could not be determined ( $<2$ ) for the PVDF membranes (below pH 2, the conductivity of the solution may affect the determination of the IEP, which explained why no values were collected below this pH). The two PES membranes showed similar IEP.

**Table 4.8**  
**Streaming potential (SP) and isoelectric point (IEP) of the PVDF and PES membranes**

Membrane designation	Material	SP (mV/ kPa) (KCl = $2 \times 10^{-4}$ M); pH = 6.5	IEP
A	PVDF	$- 65 \pm 5$	$< 2$
B	PVDF	$- 80 \pm 5$	$< 2$
C	PES (PVP)*	$- 126 \pm 5$	$2.8 \pm 0.5$
D2	PES	$- 190 \pm 5$	$2.8 \pm 0.5$

\*PVP incorporated into the PES membrane.

### ***Chemical Composition***

Pyrolysis GC/MS was conducted at low temperature to investigate the chemical composition of the membranes. Pyrograms of the studied membranes are provided in [Figures 4.9](#) through [4.11](#).

At an elevated temperature (300° C), all PES membranes release sulfur dioxide (SO<sub>2</sub>) and phenol that are produced from the thermal degradation of the polymer. Membrane C fiber is preserved with glycerin, which is probably the precursor of hydroxypropanone (also observed with Membrane B fiber). Pyrrolidinone compounds are clearly identified in the pyrochromatograms of PES membranes. These compounds are potentially remaining manufacturing solvents or coated agents used to hydrophilize the membrane surface. It is interesting to observe that Membranes D1 and D2 do not provide similar fingerprints with a larger presence (proportionally speaking) of methyl pyrrolidinone in the new version (Membrane D2).

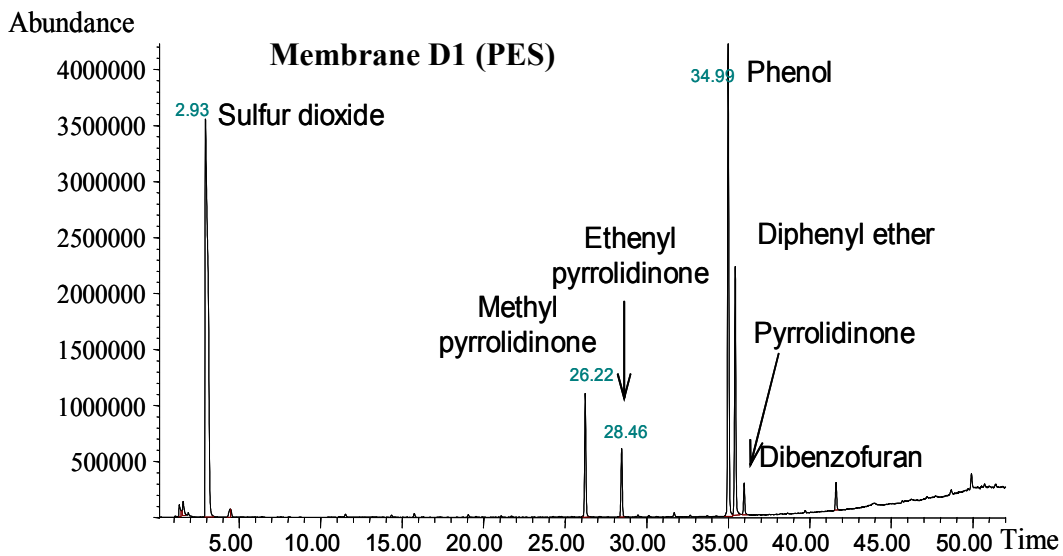
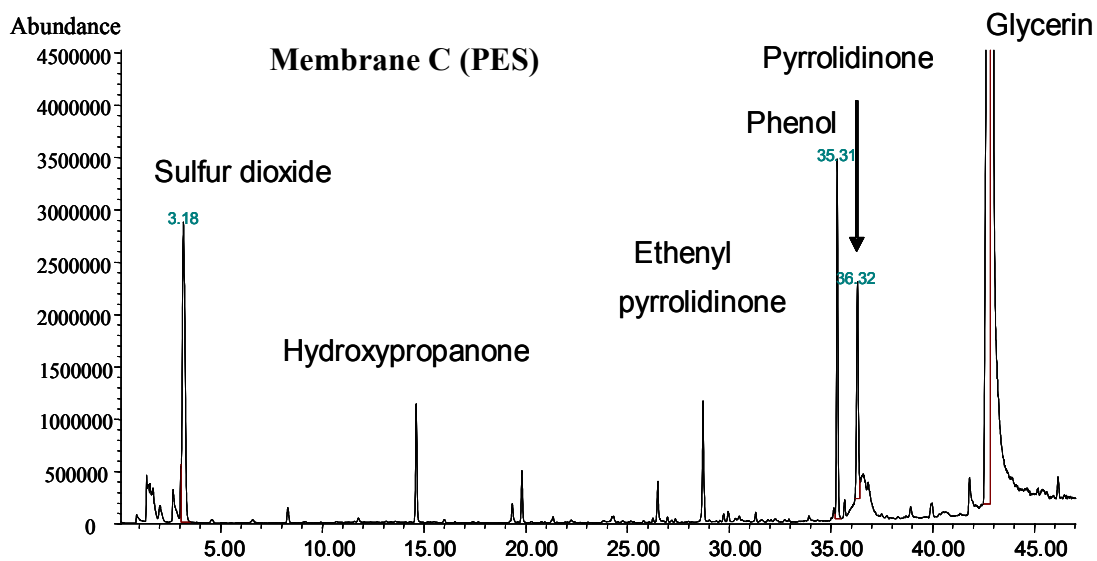


**Figure 4.9 Pyrochromatogram (300° C) of hollow-fiber membranes**

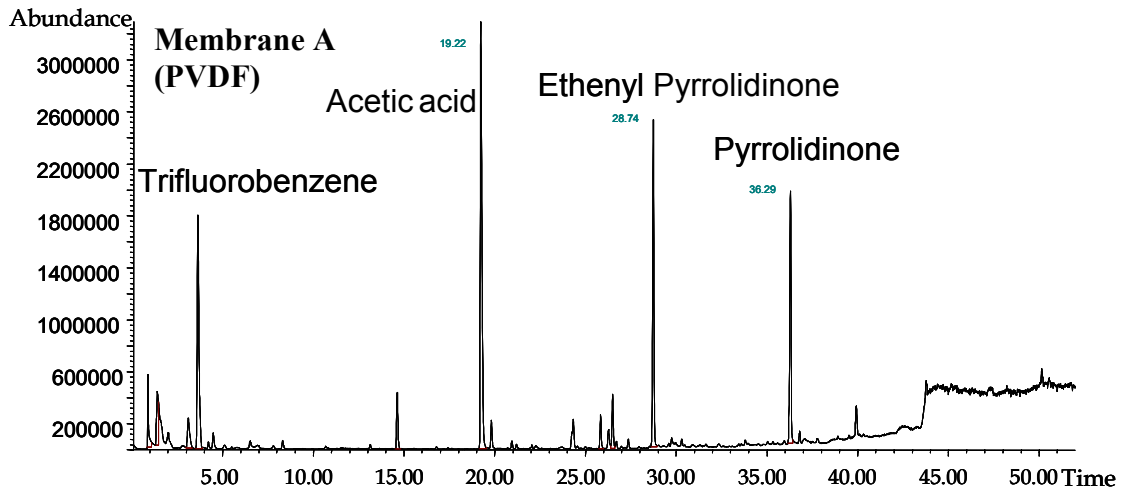
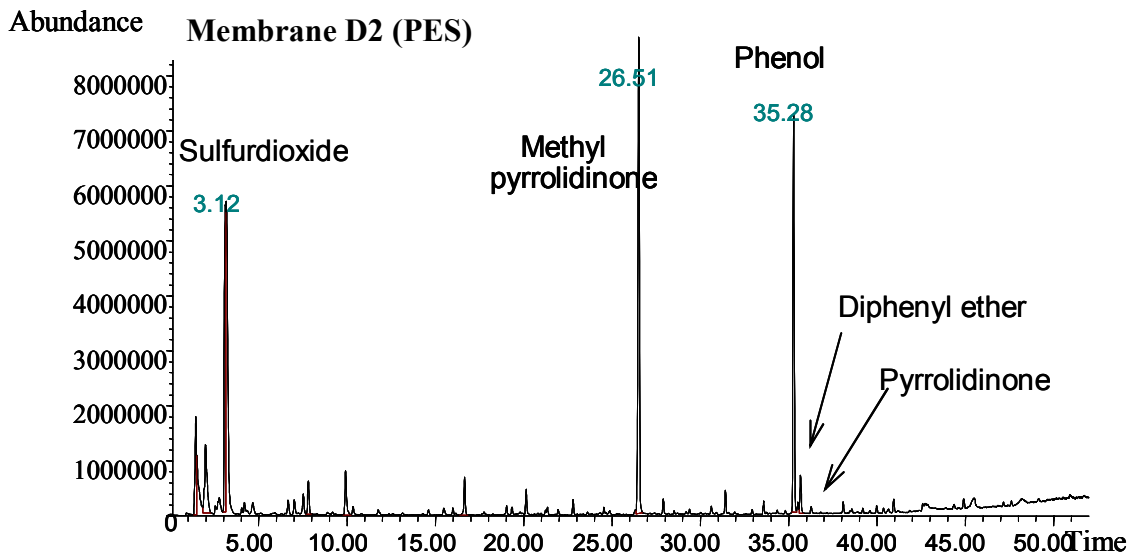
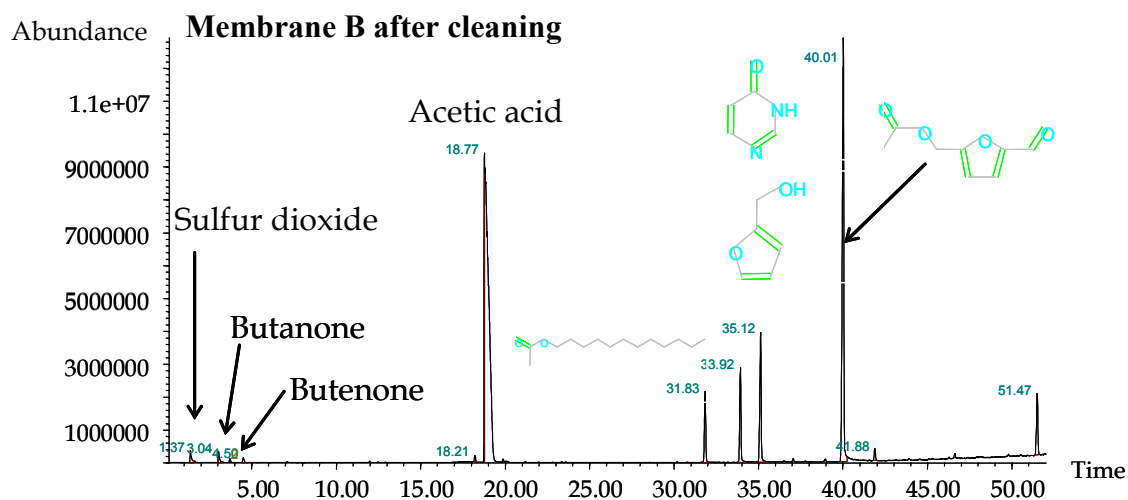


Figure 4.10 Pyrochromatogram (300° C) of hollow-fiber membranes (continued)

## Membrane B (PVDF)



**Figure 4.11 Pyrochromatogram (300° C) of hollow-fiber membranes (end)**

PVDF membranes produce trifluorobenzene, a compound that may be produced from the cyclization and rearrangement of  $(-\text{CH}_2\text{-CF}_2)_n$  polymer chains released at elevated temperature. Other fluorinated compounds are detected at trace levels.

Pyrochromatograms obtained from Membrane B show a distinct fingerprint. The presence of glycerin is well observed but disappears after cleaning the membrane with a 50/50 percent by volume (v/v) methanol water solution. This is consistent with the manufacturer's use of glycerin for membrane preservation. No pyrrolidinone derivatives are found; however hydroxyaromatics and ketones are identified, compounds that can be produced from the thermal degradation of a different hydrophilic agent.

## CHAPTER 5

### BENCH-SCALE MEMBRANE FILTRATION RESULTS

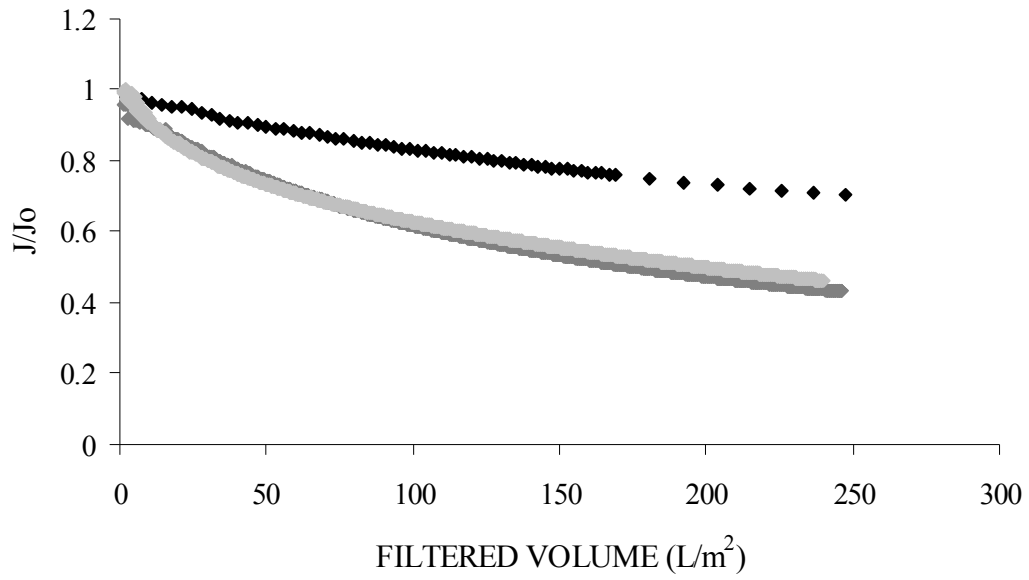
#### STIRRED-CELL UNIT TESTS

Stirred-cell experiments were performed with five water sources, with limited testing of one clarified water source with pretreatment by coagulation and settling. Table 5.1 shows the initial membrane permeability or specific flux,  $J_{S0}$ , corresponding to the applied pressure for various membrane and water combinations. Higher feed pressure was required for the PES UF membrane because of greater resistance associated with its MWCO (UF, 100 kilo Dalton (kD)). Likewise the PVDF MF membrane has the highest  $J_{S0}$  due to its larger pore size (0.1  $\mu\text{m}$ ).

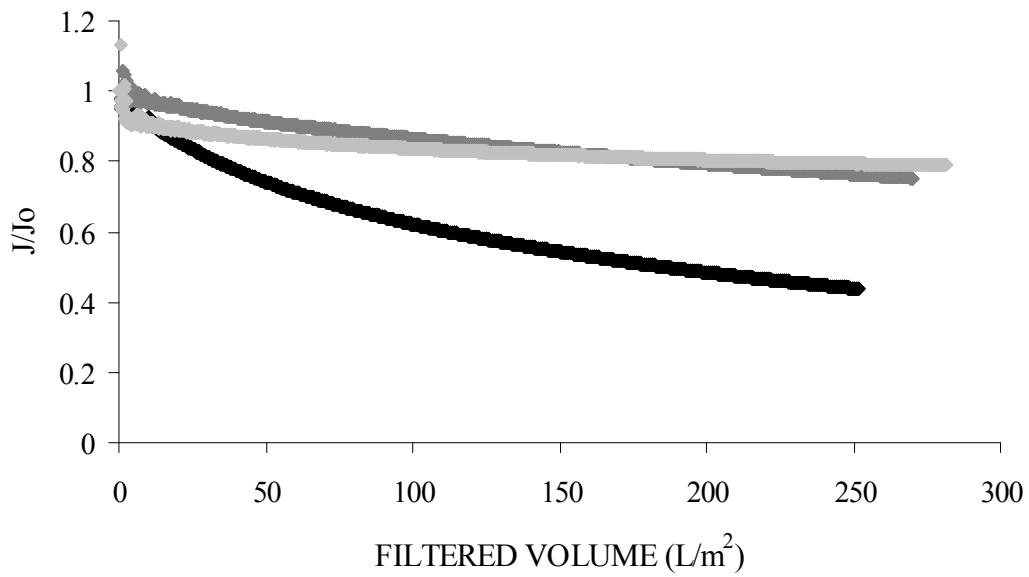
Figures 5.1, 5.2, and 5.3 show the normalized flux decline profiles ( $J/J_0$ ) for the three membranes operated on three of the four source waters. Specific flux decline with Scottsdale and Tampa Bay waters was significant (over 50 percent) for each membrane type, while the Indianapolis water produced less flux decline with all three membranes. These results may be due to the high content of DOC in the Tampa Bay water and the presence of problematical wastewater components in the Scottsdale water. With the Twente Canal water, both PAN MF/UF and PES UF membranes showed significant flux decline (up to 60 percent) while the PVDF MF membrane showed less flux decline. The Tuscaloosa-clarified water showed the least flux decline (less than 20 percent) among all source water due to the removal of NOM by coagulation and sedimentation. Overall, the Scottsdale, Twente Canal, and Tampa Bay waters caused significant fouling as a consequence of a high content of hydrophilic DOC fraction, a high amount of large molecular weight compounds (i.e., PS-DOC), and/or a high DOC content.

**Table 5.1**  
**Initial water permeability or specific flux ( $J_{S0}$ ) and**  
**feed pressure for stirred-cell filtration tests**

Membrane	Pressure (psi [kPa])	Water	$J_{S0}$ (L/m <sup>2</sup> ·hr·bar)
PES UF	25 (1.79)	Indianapolis	124
		Scottsdale	133
		Tampa Bay	98.6
		Twente Canal	90.8
		Tuscaloosa-Raw	66.6
		Tuscaloosa-Clarified	122
		PAN MF/UF	5 (0.36)
Scottsdale	731		
Tampa Bay	541		
Twente Canal	610		
Tuscaloosa-Raw	448		
Tuscaloosa-Clarified	662		
PVDF MF	4 (0.29)		
		Scottsdale	822
		Tampa Bay	940
		Twente Canal	822
		Tuscaloosa-Raw	617
		Tuscaloosa-Clarified	822

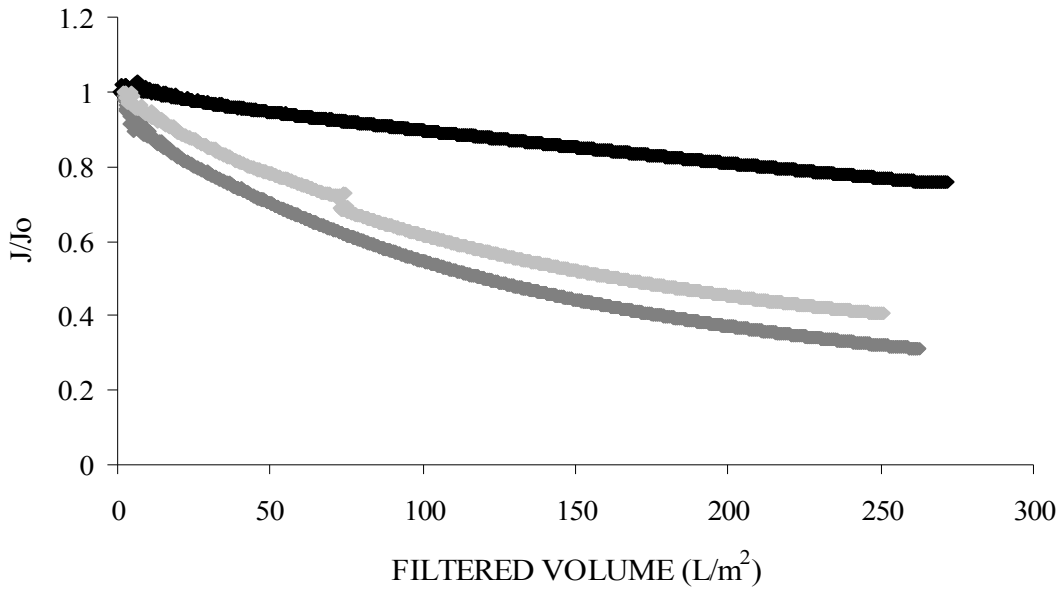


◆ Indianapolis ◆ Scottsdale ◆ Tampa

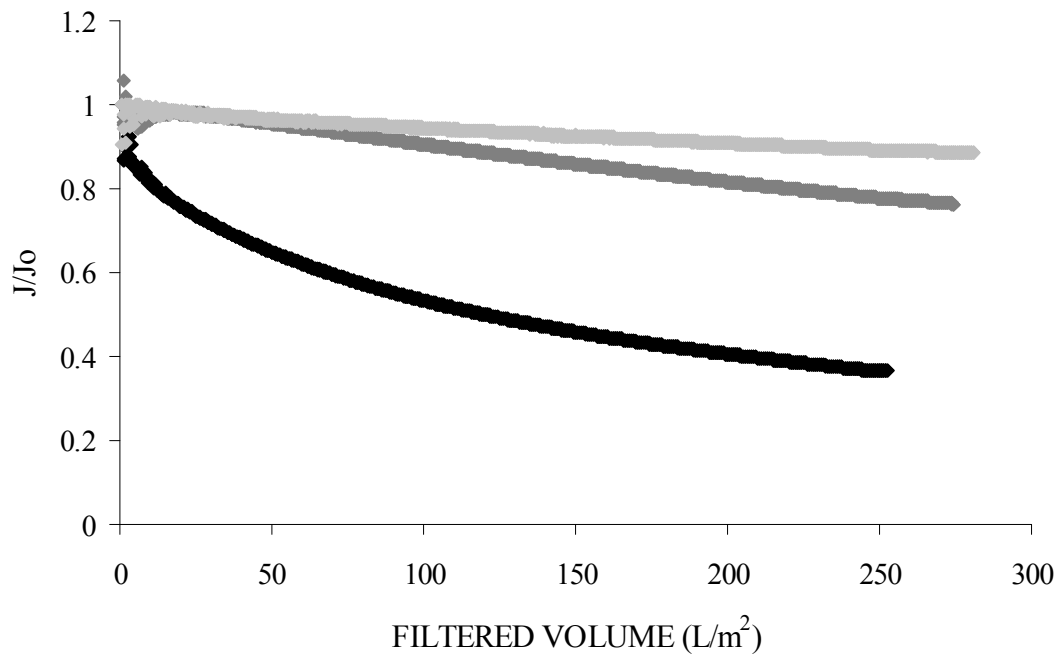


◆ Twente Canal ◆ Tuscaloosa-raw ◆ Tuscaloosa-clarified

**Figure 5.1 Flux decline tests with PES UF membrane based on filtered water volume**

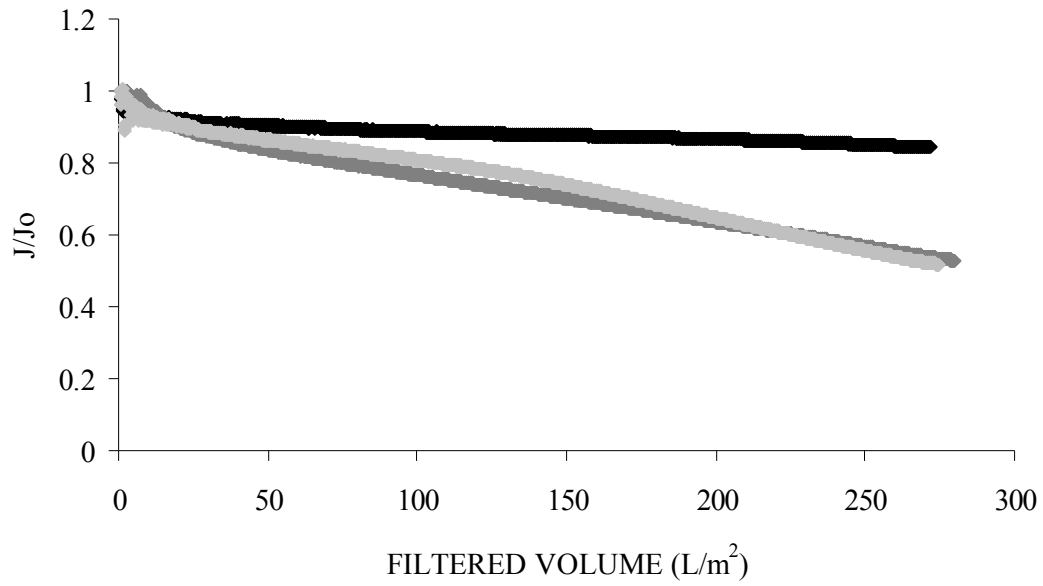


◆ Indianapolis ◆ Scottsdale ◆ Tampa

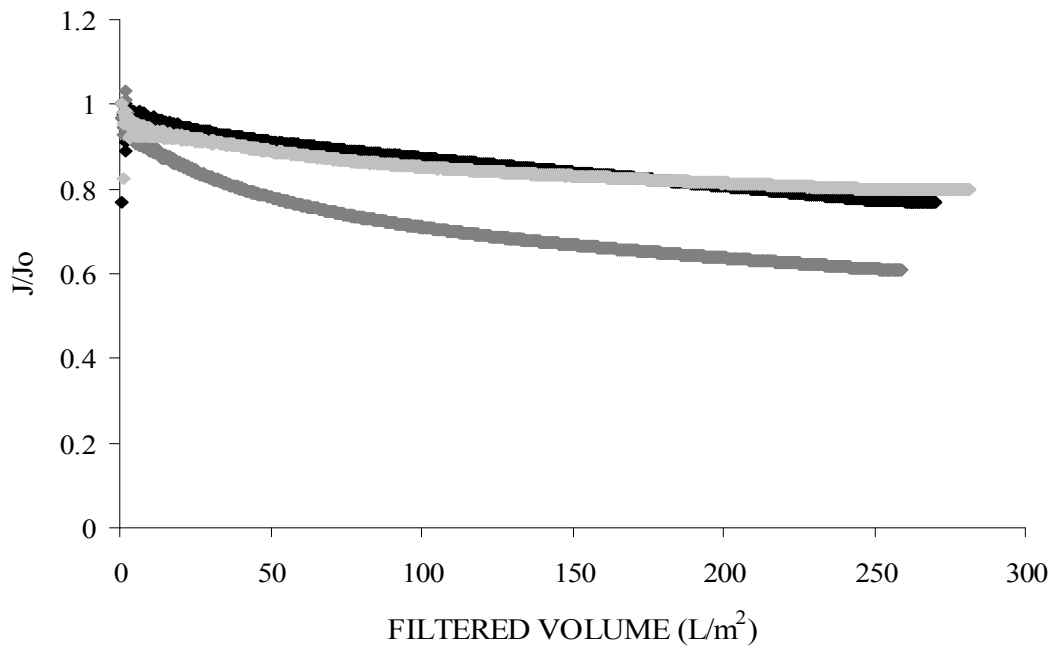


◆ Twente Canal ◆ Tuscaloosa-raw ◆ Tuscaloosa-clarified

**Figure 5.2 Flux decline tests with PAN MF/UF membrane based on filtered water volume**



◆ Indianapolis ◆ Scottsdale ◆ Tampa



◆ Twente Canal ◆ Tuscaloosa-raw ◆ Tuscaloosa-clarified

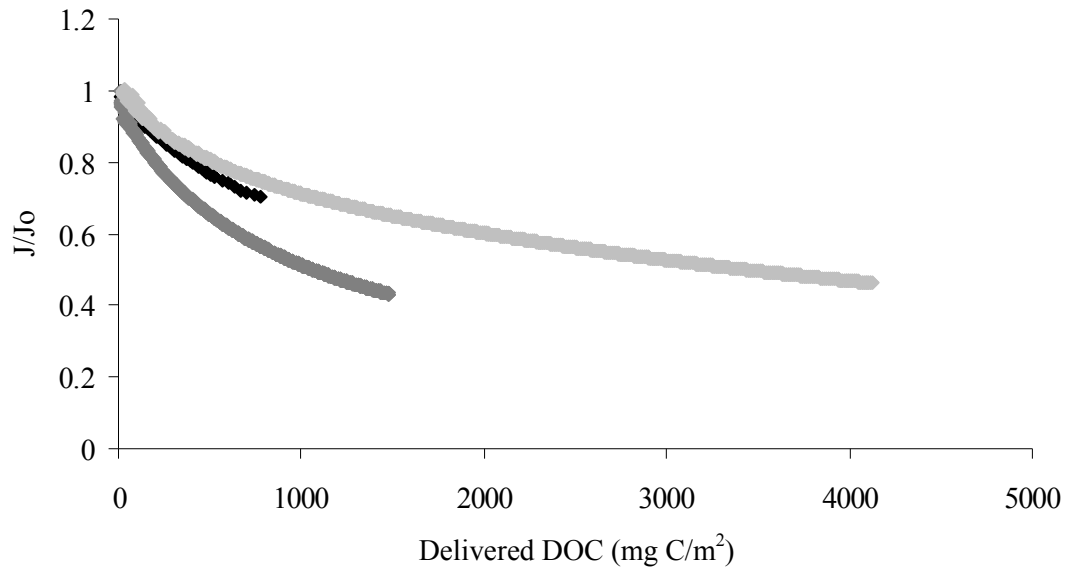
**Figure 5.3 Flux decline tests with PVDF MF membrane based on filtered water volume**

Figures 5.4, 5.5, and 5.6 show flux decline curves based on delivered DOC.

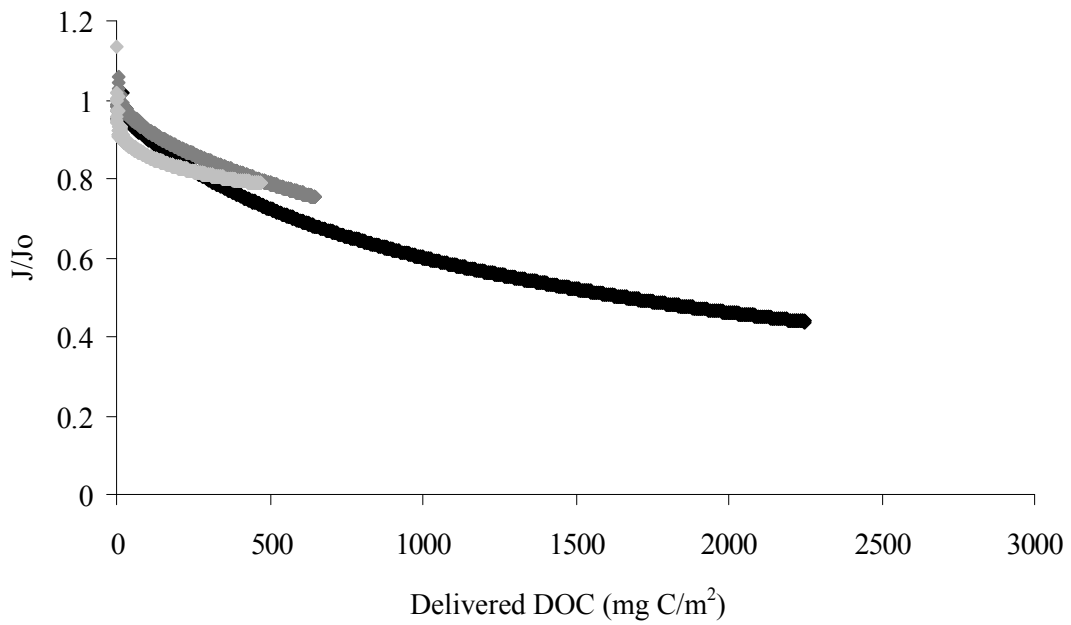
The Tampa Bay water delivered a high amount of DOC for a given permeate throughput because of its much higher DOC content. Over the delivered DOC ranges tested, the overall flux decline of the Tampa Bay water is much higher than the Indianapolis water, but the two waters show similar flux decline trends at less than 1000 mg/m<sup>2</sup> delivered DOC. It is likely that a high delivered DOC imparts significant fouling during overall filtration; however, over a shorter time period, the characteristics of NOM are more influential in fouling. This is important because the flux decline over a shorter time period is closely related to the frequency of backwashing. The Tampa Bay water also shows similar or less flux decline than the Scottsdale water over a comparable filtration time even though the Scottsdale water has a much lower DOC content. This indicates that the Scottsdale water contains problematical foulants such as macromolecules (mainly polysaccharides) and organic colloids. While delivered DOC provides a means of normalizing data for different sources with different DOC levels, it is important to recognize that the DOC content of each source still must be considered. For example, while the Tampa Bay water has a higher DOC and PS-DOC than the Indianapolis water, over an equivalent delivered DOC, there is a greater level of delivered PS-DOC for the Indianapolis water.

In the comparison among Twente Canal, Tuscaloosa-raw, and Tuscaloosa-clarified waters, the Twente Canal water generally showed a higher flux decline than other two waters except when filtered with the PVDF MF membrane. Flux decline of the Twente Canal water with PVDF MF filtration shows a similar flux decline trend to those of the Tuscaloosa waters even though the Twente Canal water contains a much higher DOC than other two waters. However, Scottsdale, Tampa Bay, and Twente Canal waters generally show more significant fouling trends than the other source waters when the results with all membranes are considered. This supports the premise that both NOM characteristics and the amount of NOM are important in low-pressure membrane fouling.

Table 5.2 compares DOC, UVA<sub>254</sub>, and SUVA of waters generated during membrane filtration. High removal efficiency is observed in PES UF membrane filtration due to its tight MWCO; the PVDF MF membrane shows the least removal. Backwash (BW) DOC reflects DOC present in the permeate used for backwashing plus any DOC removed from the membrane or cake layer during backwashing. With minor exceptions, the BW DOC was elevated relative to the feed, indicating displacement of DOC during backwashing. Except for Twente Canal and Tuscaloosa clarified waters, the concentration of DOC in the BW was highest with the PES UF (0.01 µm) membrane and lowest with the PVDF MF (0.1 µm) membrane, correlating well with the lowest DOC permeate levels in PES UF and highest in the PVDF MF. These results indicate that the tighter PES UF membrane retained more DOC in or on the membrane surface, with this DOC contributing more significantly to the DOC of the BW water.



◆ Indianapolis ◆ Scottsdale ◆ Tampa



◆ Twente ◆ Tuscaloosa-raw ◆ Tuscaloosa-clarified

**Figure 5.4 Flux decline tests with PES UF membrane based on delivered DOC**

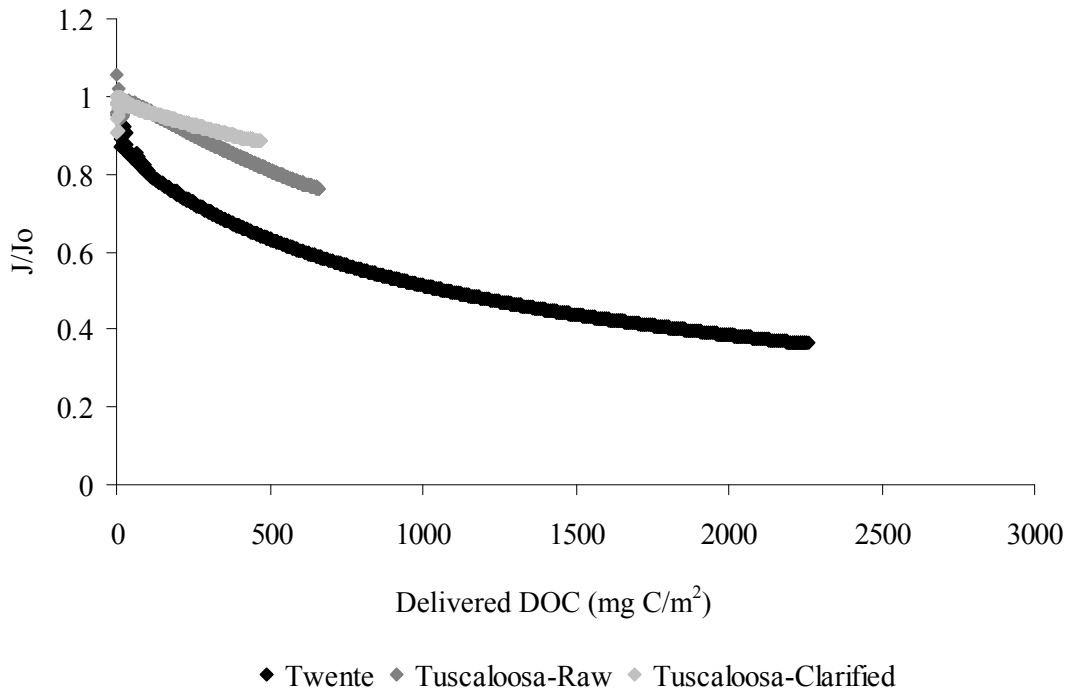
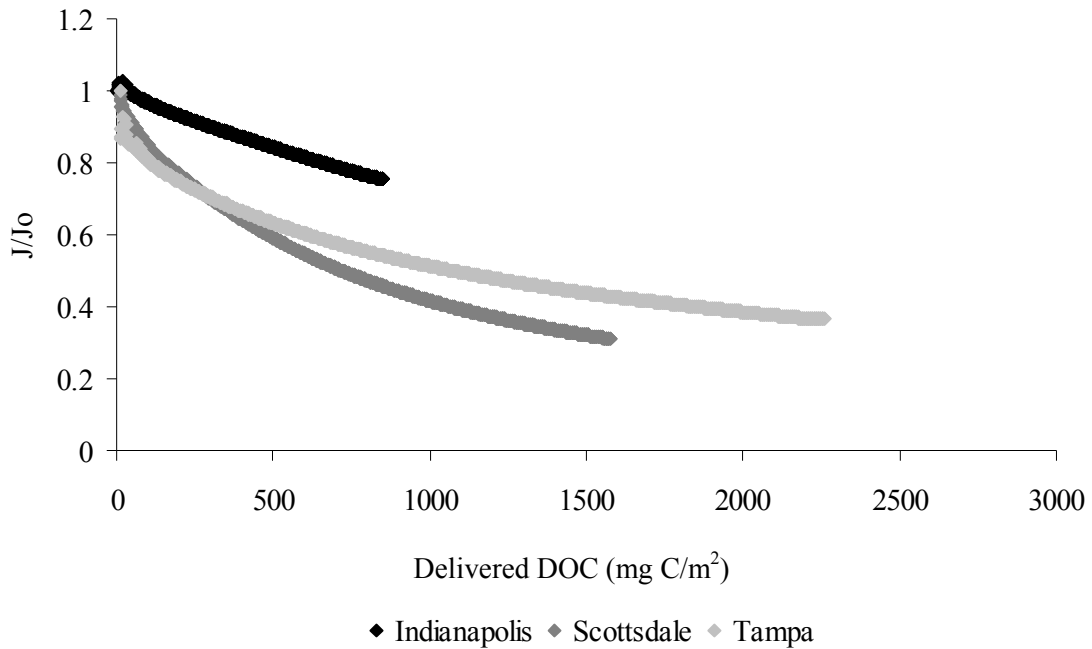


**Figure 5.5 Flux decline tests with PAN MF/UF membrane based on delivered DOC**

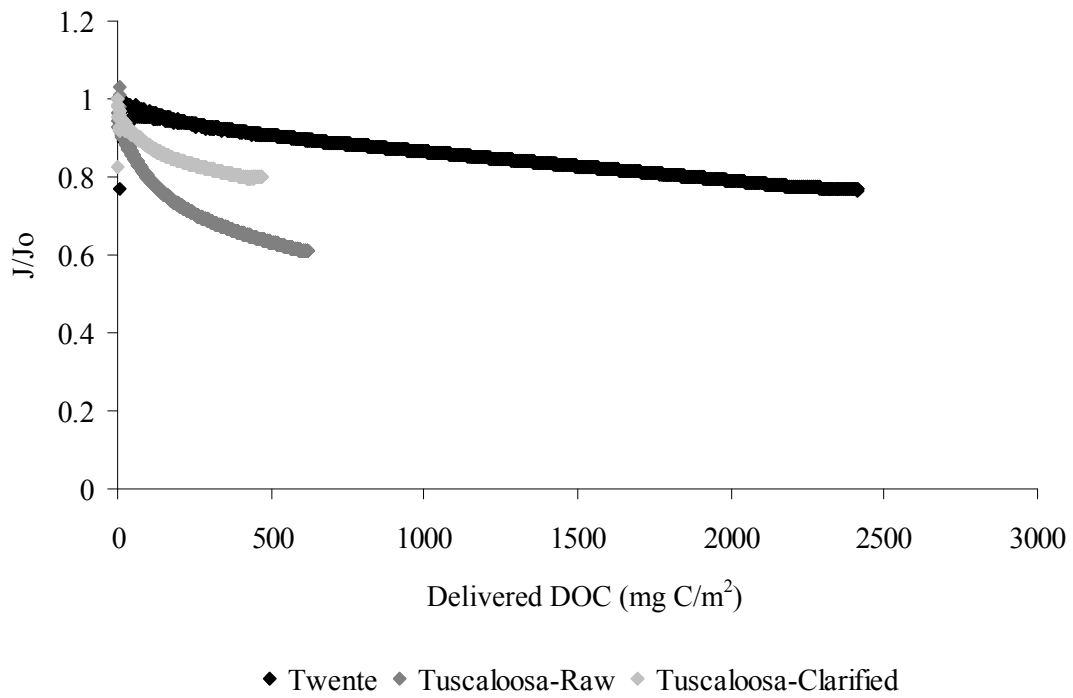
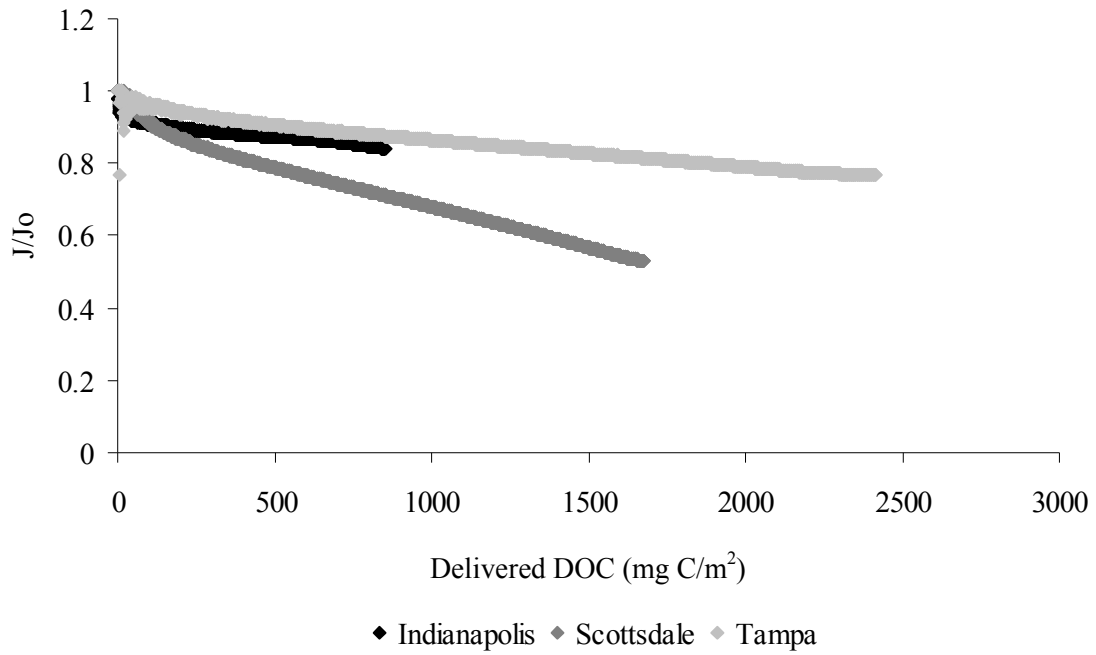


**Figure 5.6 Flux decline tests with PVDF MF/UF membrane based on delivered DOC**

**Table 5.2**  
**DOC, UVA<sub>254</sub>, and SUVA values in membrane filtration**

		Indianapolis			Scottsdale		
Membrane	Stream	DOC	UVA <sub>254</sub>	SUVA	DOC	UVA <sub>254</sub>	SUVA
PES UF	Feed	3.13	0.083	2.65	5.8	0.096	1.66
	Permeate	2.87	0.081	2.82	5.05	0.086	1.70
	Retentate	4.48	0.087	1.94	7.67	0.114	1.49
PAN MF/UF	BW	3.67	0.089	2.43	6.83	0.122	1.79
	Permeate	3.07	0.083	2.70	5.36	0.094	1.75
	Retentate	4.03	0.092	2.28	7.59	0.112	1.48
PVDF MF	BW	3.36	0.09	2.68	6.23	0.109	1.75
	Permeate	3.08	0.082	2.66	5.7	0.093	1.63
	Retentate	3.15	0.084	2.67	5.92	0.105	1.77
	BW	3.19	0.085	2.66	5.95	0.105	1.76

		Tampa Bay			Twente Canal		
Membrane	Stream	DOC	UVA <sub>254</sub>	SUVA	DOC	UVA <sub>254</sub>	SUVA
PES UF	Feed	17	0.735	4.32	8.97	0.228	2.54
	Permeate	14	0.616	4.40	7.8	0.212	2.72
	Retentate	26.2	1.174	4.48	15.6	0.322	2.06
PAN MF/UF	BW	18.6	0.724	3.89	8.34	0.214	2.57
	Permeate	15.4	0.682	4.43	8.58	0.224	2.61
	Retentate	20.6	0.898	4.36	10.5	0.254	2.42
PVDF MF	BW	18.7	0.77	4.12	9.71	0.224	2.31
	Permeate	17	0.729	4.29	8.96	0.228	2.54
	Retentate	18.4	0.774	4.21	8.98	0.224	2.49
	BW	18	0.754	4.19	9.06	0.232	2.56

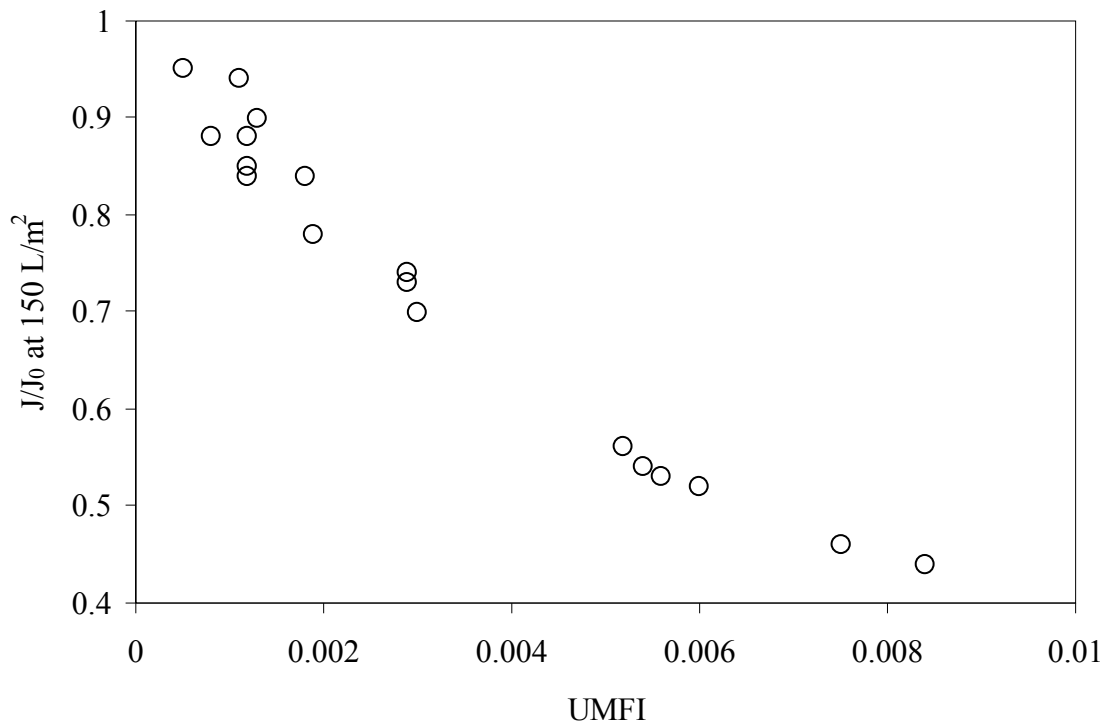
  

		Tuscaloosa (raw)			Tuscaloos (clarified)		
Membrane	Stream	DOC	UVA <sub>254</sub>	SUVA	DOC	UVA <sub>254</sub>	SUVA
PES UF	Feed	2.4	0.084	3.50	1.67	0.05	2.99
	Permeate	1.52	0.039	2.57	1.63	0.049	3.01
	Retentate	3.15	0.125	3.97	1.82	0.052	2.86
PAN MF/UF	BW	2.44	0.118	4.84	1.94	0.047	2.42
	Permeate	1.6	0.047	2.94	1.66	0.047	2.83
	Retentate	2.85	0.115	4.04	1.74	0.062	3.56
PVDF MF	BW	2.1	0.092	4.38	1.99	0.048	2.41
	Permeate	1.84	0.053	2.88	1.67	0.05	2.99
	Retentate	2.76	0.107	3.88	1.71	0.058	3.39
	BW	2.03	0.08	3.94	1.91	0.053	2.77

Table 5.3 summarizes the UMFI values and normalized flux decline ( $J/J_0$ ) at two different conditions. Scottsdale, Tampa Bay, and Twente Canal waters display high UMFI values and low values of  $J/J_0$  at  $75 \text{ L/m}^2$  permeate throughput compared with other source waters, indicating a high NOM fouling rate. The Scottsdale water has the highest value of UMFI in each set of membrane filtrations. Comparing UMFI and  $J/J_0$  at  $150 \text{ L/m}^2$  (in Figure 5.7), it can be seen that the two parameters are inversely proportional. The Scottsdale, Tampa Bay, and Twente Canal waters show the lowest  $J/J_0$  and high UMFI. These source waters, which comprise high DOC, high HPI-DOC, and high PS-DOC, produce high UMFI and low  $J/J_0$  values, (high membrane fouling rate). Moreover, the larger the membrane pore size, the higher the  $J/J_0$  and lower the UMFI values. This implies that membrane pore size does influence the NOM membrane fouling rate.

**Table 5.3**  
**Normalized flux,  $J/J_0$ , and UMFI of each water source with various membrane filtrations**

Water source	Membrane	UMFI	$J/J_0$	$J/J_0$
			@ $75 \text{ L/m}^2$	@ $450 \text{ mgC/m}^2$
Indianapolis	PES UF	0.0019	0.86	0.78
	PAN MF/UF	0.0012	0.92	0.86
	PVDF MF	0.0008	0.89	0.88
Scottsdale	PES UF	0.0056	0.67	0.67
	PAN MF/UF	0.0084	0.62	0.62
	PVDF MF	0.0030	0.8	0.80
Tampa Bay	PES UF	0.0052	0.67	0.82
	PAN MF/UF	0.0060	0.69	0.87
	PVDF MF	0.0029	0.83	0.89
Twente Canal	PES UF	0.0054	0.67	0.74
	PAN MF/UF	0.0075	0.58	0.58
	PVDF MF	0.0012	0.89	0.89
Tuscaloosa-raw	PES UF	0.0013	0.89	0.80
	PAN MF/UF	0.0011	0.91	0.83
	PVDF MF	0.0029	0.74	0.64
Tuscaloosa-clarified	PES UF	0.0018	0.85	0.79
	PAN MF/UF	0.0005	0.96	0.89
	PVDF MF	0.0012	0.87	0.80



**Figure 5.7 Comparison between  $J/J_0$  (at 150 L/m<sup>2</sup>) and UMFI values**

From a general mathematical equation explaining the relationship between filtration time and filtered volume, different fouling mechanisms can be explained depending on the value of the exponent,  $n$ , in the equation (Hermia 1982):

$$d^2t/dV^2 = k(dt/dV)^n$$

where,  $t$  = filtration time  
 $V$  = filtered volume  
 $k$  = rate (constant depending on  $n$ )  
 $n$  = filtration constant characterizing the filtration model

The flux data from the stirred-cell membrane filtration experiments were re-plotted based on different sets of characteristic x-axis and y-axis coordinates. A linear plot of each set of coordinates describes a dominant fouling mechanism as follows:

- Cake formation ( $n=0$ ):  
linear fit of filtration time/filtered volume ( $t/V$ ) versus filtered volume ( $V$ )
- Pore constriction ( $n=1.5$ ):  
linear fit of filtration time/filtered volume ( $t/V$ ) versus filtration time ( $t$ )
- Complete pore blockage ( $n=2$ ):  
linear fit of flux ( $J$ ) versus filtered volume ( $V$ )

When the data points show a linear fit ( $r^2$  approaching 1.0) for a selected set of parameters (x-axis versus y-axis), the dominant fouling mechanism can be elucidated (Figures 5.8, 5.9, and 5.10). Table 5.4 summarizes  $r^2$  values obtained from linear curve fitting using different coordinates. In most cases, cake layer formation is the predominant fouling mechanism for these data sets. Pore constriction is a significant fouling mechanism for the PVDF MF membrane because it is an MF membrane with a large pore size. Nevertheless, the high  $r^2$  values observed for the PVDF MF support applicability of the UMFI.

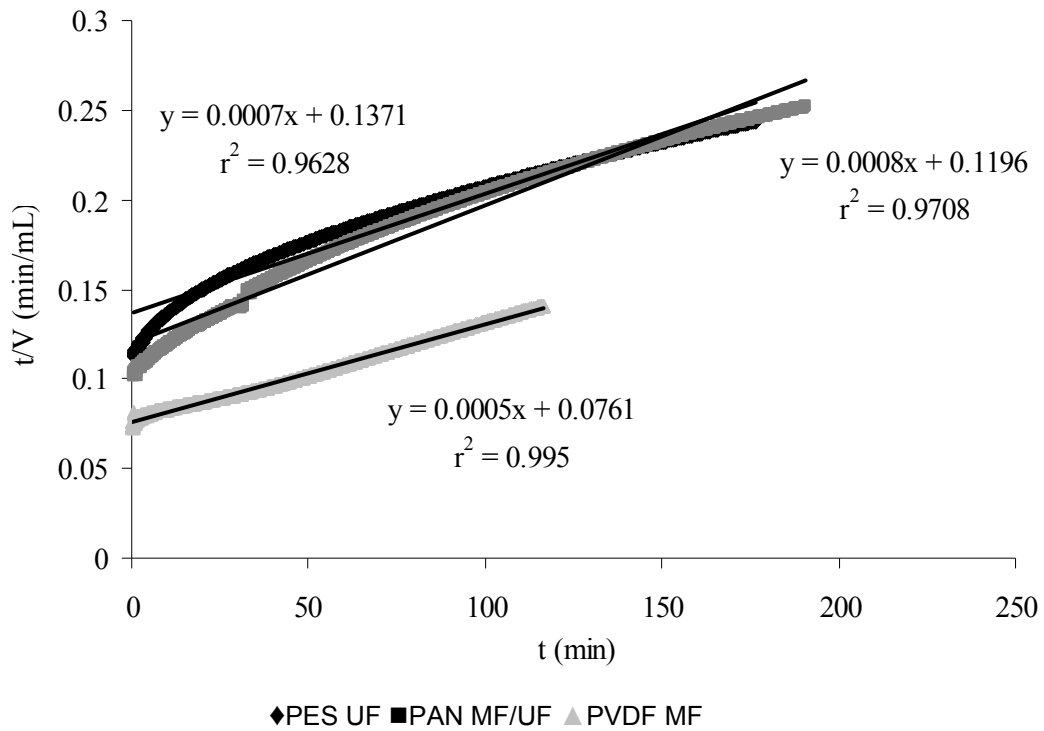


**Figure 5.8 Intermediate pore blockage fitting of Tampa Bay water data**

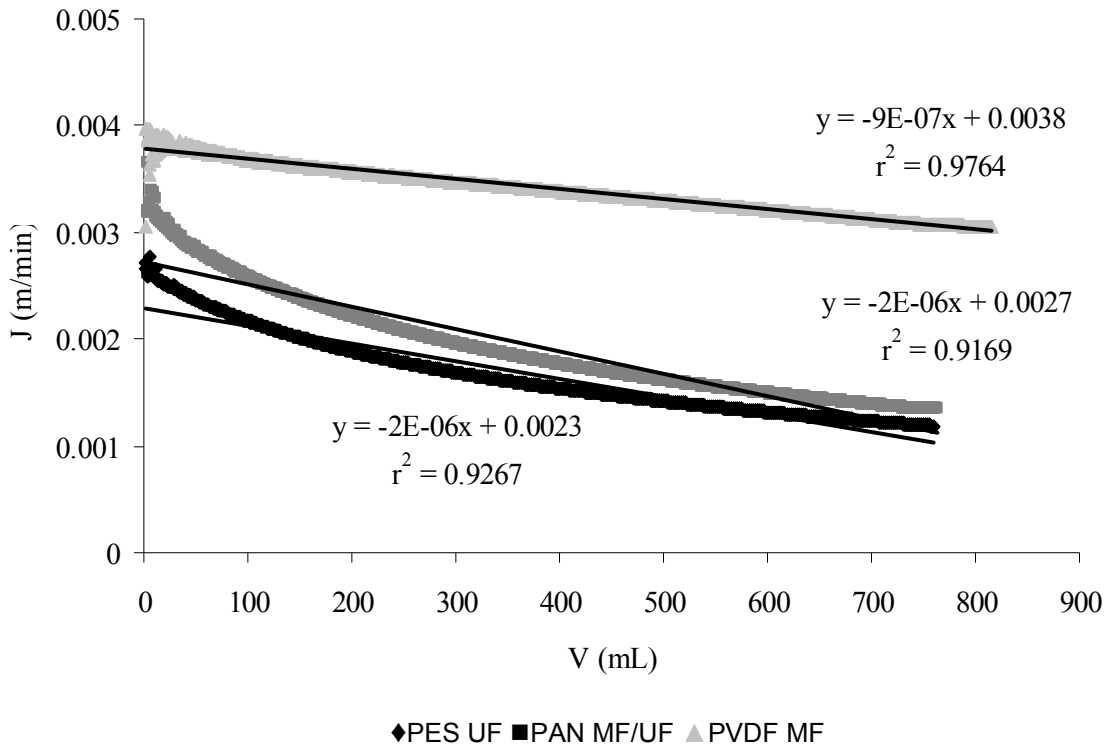


**Figure 5.9 Complete pore blockage fitting of Twente Canal water data**

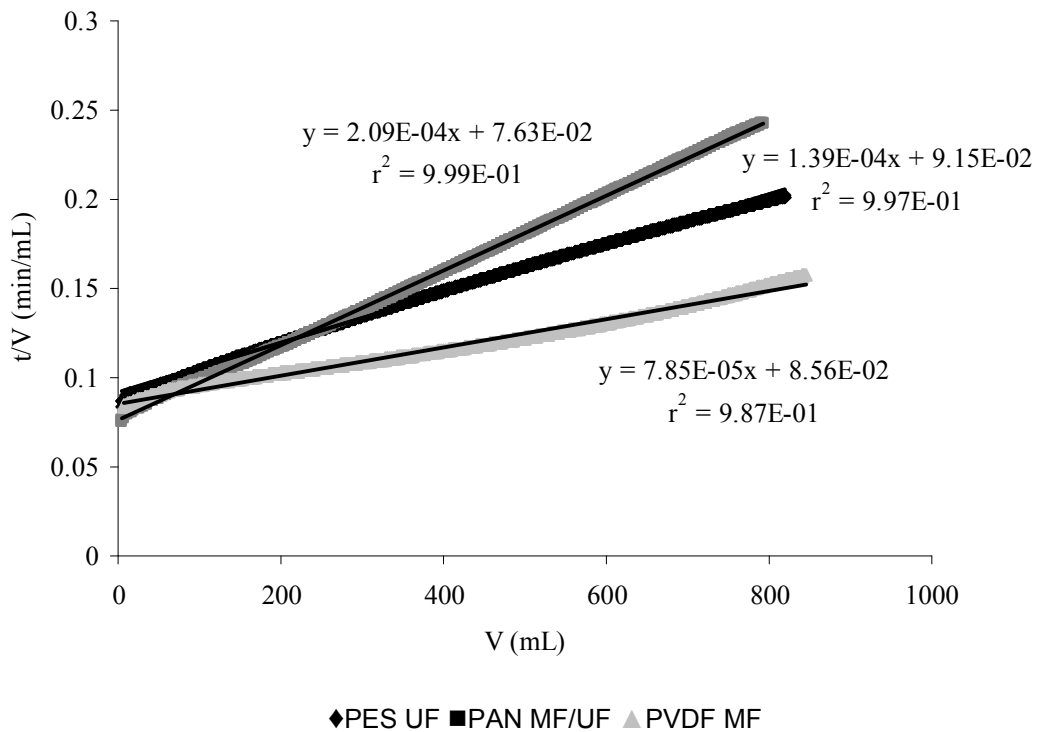


**Figure 5.10 Cake formation fitting of Scottsdale water data**

**Table 5.4**  
**Predominant fouling mechanisms in stirred-cell filtration tests**

Source water	Membrane	Pore constriction (r <sup>2</sup> value)	Complete pore blockage (r <sup>2</sup> value)	Cake formation (r <sup>2</sup> value)	Predominant fouling mechanism(s)
Indianapolis	PES UF	0.9774	0.9701	0.9943	Cake formation
	PAN MF/UF	0.9951	0.9929	0.9991	Pore constriction & cake formation
	PVDF MF	0.9354	0.9211	0.9391	Pore constriction & cake formation
Scottsdale	PES UF	0.9681	0.9309	0.9973	Cake formation
	PAN MF/UF	0.9754	0.9331	0.9995	Cake formation
	PVDF MF	0.9950	0.9862	0.9873	Pore constriction
Tampa Bay	PES UF	0.9628	0.9183	0.9920	Cake formation
	PAN MF/UF	0.9708	0.9384	0.9979	Cake formation
	PVDF MF	0.9950	0.9890	0.9443	Pore constriction
Twente Canal	PES UF	0.9658	0.9267	0.9957	Cake formation
	PAN MF/UF	0.9640	0.9169	0.9959	Cake formation
	PVDF MF	0.9812	0.9764	0.9852	Pore constriction & cake formation
Tuscaloosa (raw)	PES UF	0.9805	0.9728	0.9911	Cake formation
	PAN MF/UF	0.9934	0.9901	0.9908	Pore constriction
	PVDF MF	0.9231	0.8818	0.9488	Cake formation
Tuscaloosa (clarified)	PES UF	0.8814	0.8396	0.8920	Cake formation
	PAN MF/UF	0.9780	0.9752	0.9805	Cake formation
	PVDF MF	0.9215	0.9064	0.9325	Cake formation

Representative SEC-DOC chromatograms are presented in [Figures 5.11](#) through [5.14](#) and the concentrations of peaks by integration are tabulated in [Table 5.5](#). (The remainder of the results is presented in Appendix B).

The Scottsdale water has a high content of high molecular weight compounds corresponding to macromolecules and/or organic colloids, as revealed by SEC-DOC/UV, and produced significant flux decline with all three membrane types. The Tampa Bay water contains relatively less amounts of high molecular weight components but showed significant flux decline compared to the Indianapolis water. This result is likely due to a DOC content in the Tampa Bay water that is over three times that of other source waters; thus, the amount of NOM as well as the character are both potentially influential. The Twente Canal water also contains significant amounts of large molecular weight compounds while the Tuscaloosa water does not. Thus, waters containing high levels of macromolecules and/or organic colloids as well as high DOC content are problematical in low-pressure membrane fouling. In other words, if the focus is on throughput, the Tampa Bay water has the highest PS-DOC concentration and exhibits higher fouling potential; if the focus is on delivered DOC, the results are normalized and the Tampa Bay water does not reflect a higher fouling potential.

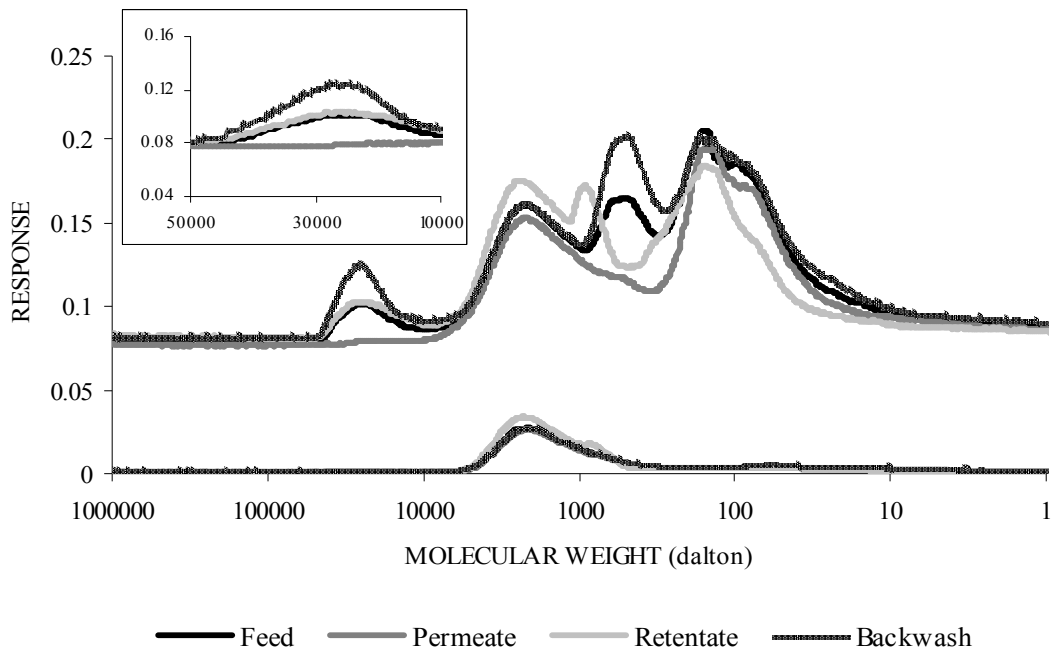


**Figure 5.11 SEC-DOC chromatograms of Indianapolis water with PES UF membrane**

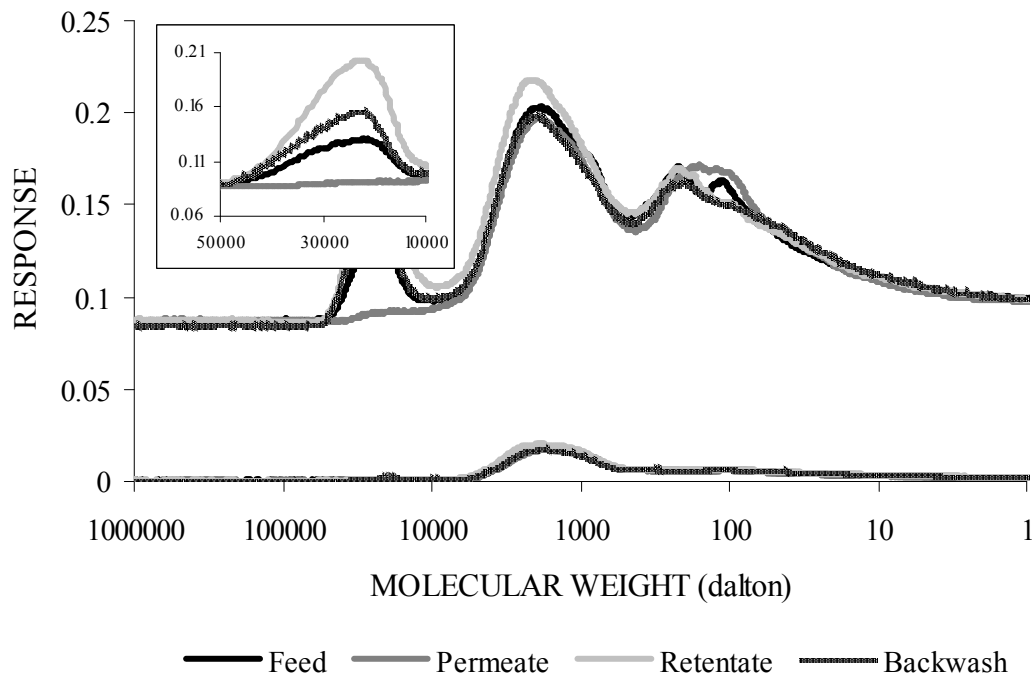


**Figure 5.12 SEC-DOC chromatograms of Scottsdale water with PES UF membrane**

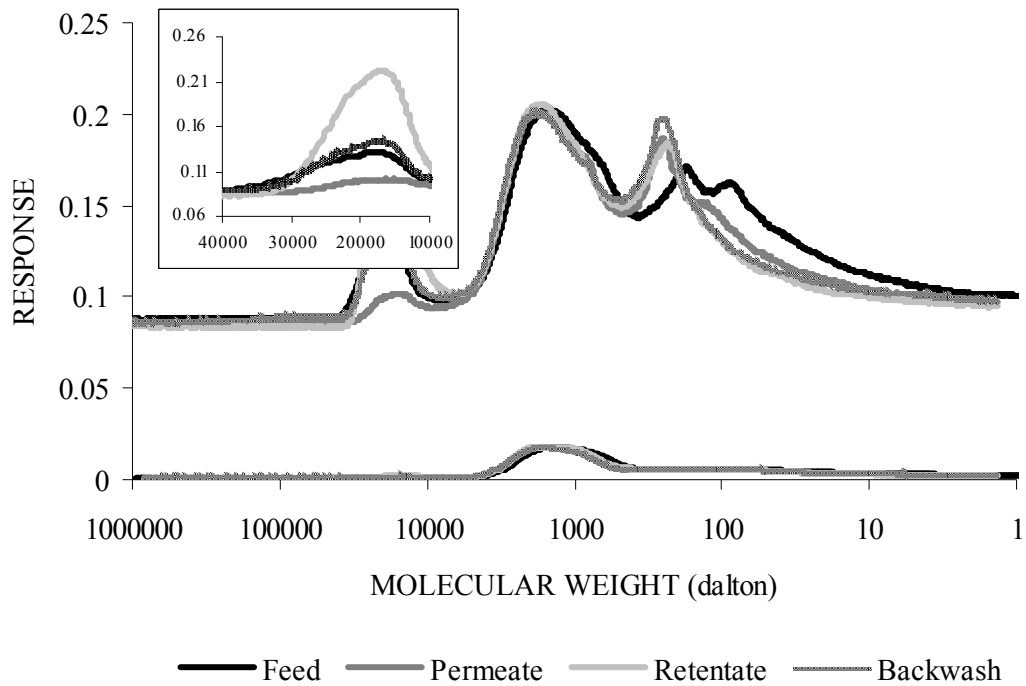


**Figure 5.13 SEC chromatograms of Scottsdale water with PAN MF/UF membrane**

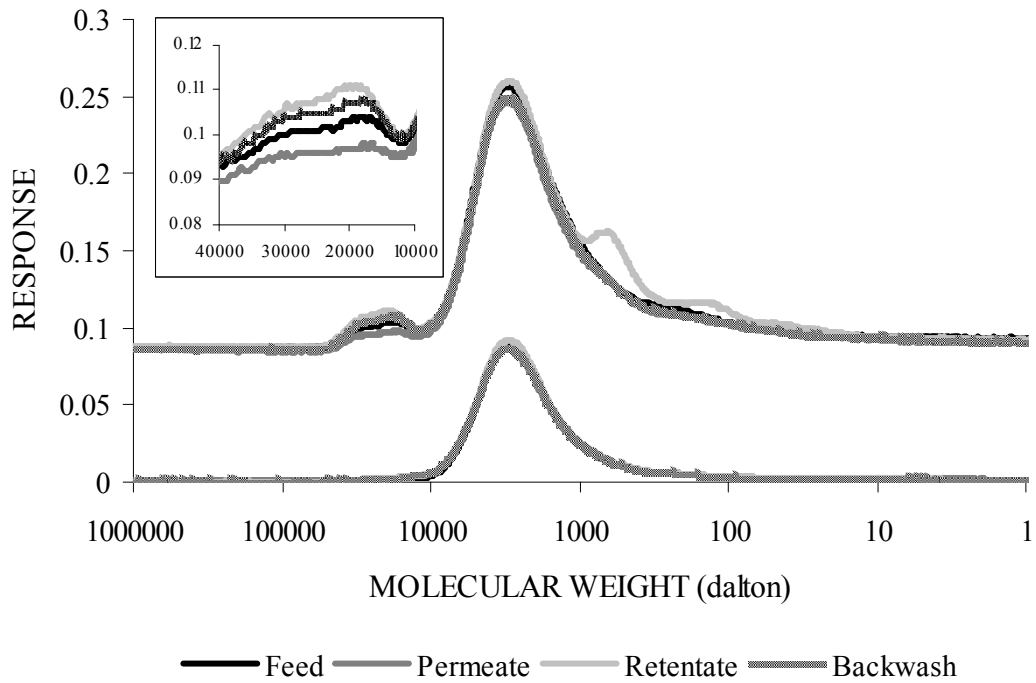


**Figure 5.14 SEC chromatograms of Tampa Bay water with PVDF MF membrane (three-fold dilution)**

**Table 5.5**  
**DOC levels of SEC chromatogram NOM fractions**  
**(polysaccharides, humic substances, and low molecular weight acids)**  
**for stirred-cell filtration tests as calculated by peak integration\***

Source water	Membrane	Stream	PS (1 <sup>st</sup> ) peak (mg/L)	HS (2 <sup>nd</sup> ) peak (mg/L)	LMA (3 <sup>rd</sup> ) peak (mg/L)	
Indianapolis	PES UF	Feed	0.13	1.29	1.71	
		Permeate	0.00	0.66	2.21	
		Retentate	0.25	2.04	2.19	
		Backwash	0.25	1.60	1.81	
	PAN MF/UF	Permeate	0.07	1.31	1.69	
		Retentate	0.54	1.56	1.93	
		Backwash	0.12	1.47	1.77	
	PVDF MF	Permeate	0.16	1.26	1.66	
		Retentate	0.15	1.27	1.73	
		Backwash	0.14	1.28	1.77	
	Scottsdale	PES UF	Feed	0.45	2.51	2.84
			Permeate	0.00	2.41	2.64
Retentate			1.30	3.24	3.13	
Backwash			0.79	2.81	3.23	
PAN MF/UF		Permeate	0.14	2.56	2.66	
		Retentate	1.63	3.01	2.95	
		Backwash	0.63	2.81	2.79	
PVDF MF		Permeate	0.45	2.59	2.66	
		Retentate	0.45	2.71	2.75	
		Backwash	0.50	2.69	2.76	
Tampa Bay		PES UF	Feed	0.69	16.31	n.q. <sup>†</sup>
			Permeate	0.08	13.92	n.q.
	Retentate		1.25	24.95	n.q.	
	Backwash		2.01	16.59	n.q.	
	PAN MF/UF	Permeate	0.09	15.30	n.q.	
		Retentate	1.42	19.18	n.q.	
		Backwash	1.64	17.06	n.q.	
	PVDF MF	Permeate	0.38	16.62	n.q.	
		Retentate	0.89	17.51	n.q.	
		Backwash	0.91	17.09	n.q.	

(continued)

**Table 5.5 (continued)**

Source water	Membrane	Stream	PS (1 <sup>st</sup> ) peak (mg/L)	HS (2 <sup>nd</sup> ) peak (mg/L)	LMA (3 <sup>rd</sup> ) peak (mg/L)
Twente Canal	PES UF	Feed	0.48	8.49	n.q.
		Permeate	0.00	7.80	n.q.
		Retentate	3.33	12.27	n.q.
	PAN MF/UF	Backwash	0.20	8.14	n.q.
		Permeate	0.31	8.27	n.q.
		Retentate	0.88	9.62	n.q.
	PVDF MF	Backwash	0.79	8.92	n.q.
		Permeate	0.64	8.32	n.q.
		Retentate	0.70	8.28	n.q.
Tuscaloosa- Raw	PES UF	Backwash	0.61	8.45	n.q.
		Feed	0.18	2.22	n.q.
		Permeate	0.00	1.52	n.q.
	PAN MF/UF	Retentate	0.31	2.84	n.q.
		Backwash	0.41	2.03	n.q.
		Permeate	0.05	1.55	n.q.
	PVDF MF	Retentate	0.11	2.74	n.q.
		Backwash	0.29	1.81	n.q.
		Permeate	0.11	1.73	n.q.
Tuscaloosa- Clarified	PES UF	Retentate	0.21	2.55	n.q.
		Backwash	0.25	1.78	n.q.
		Feed	0.04	1.63	n.q.
	PAN MF/UF	Permeate	0.02	1.61	n.q.
		Retentate	0.04	1.78	n.q.
		Backwash	0.05	1.89	n.q.
	PVDF MF	Permeate	0.02	1.64	n.q.
		Retentate	0.11	1.63	n.q.
		Backwash	0.09	1.90	n.q.
	PVDF MF	Permeate	0.03	1.64	n.q.
		Retentate	0.06	1.65	n.q.
		Backwash	0.05	1.86	n.q.

\*The data presented here were obtained from samples taken at a different time than the data presented in [Table 4.2](#).

†n.q. = not quantifiable

Filtration with the tighter PES UF and/or PAN MF/UF membranes showed greater accumulation of high molecular weight compounds in the retentate or on the membrane surface and later recovered in the backwash. The PVDF MF membrane filtration did not indicate significant accumulation of high molecular compounds, likely because the PVDF MF membrane has a relatively large pore size compared with the size of these compounds.

## HOLLOW-FIBER QUALITY CONTROL TESTS

### Effect of Pre-filtration on Fouling Rate

Experiments were conducted with Hollow-Fiber Unit 1 to assess the impact of pre-filtration on membrane fouling and response to backwash and chemical wash. This was important because the bench studies employed pre-filtration while the pilot studies did not, and it was important to assess the impact of particles greater than 1.2  $\mu\text{m}$  on fouling rate. (The use of such a fine level of filtration would both be economically impractical at pilot scale and not reflective of full-scale operation.) Testing was conducted using unfiltered and pre-filtered Tampa Bay water and a clean module containing Membrane C fibers.

Figure 5.15 illustrates the membrane fouling rate with and without pre-filtration. As expected, greater fouling was observed when raw water without prefiltration was filtered by Membrane C. The additional fouling observed could not be recovered by permeate backwashing at the end of the filtration cycle, but was removed partially by caustic backwashing and further by chlorine cleaning. The results suggest that the fouling caused by these coarse materials is hydraulically irreversible and may be affecting the fouling profile of pilot- and full-scale systems before chemical cleaning is conducted.

A second set of experiments was conducted with Hollow-Fiber Unit 2 using Twente Canal water and Membrane C. Like the tests conducted with Hollow-Fiber Unit 1, pre-filtration also reduces the rate of hydraulically reversible and irreversible membrane fouling (Figure 5.16) and indicates that the benefit of pre-filtration extends to the inside-out PES membranes. Pre-filtration removes part of the irreversible fouling substances and, as can be seen from the slope during each filtration cycle, the resistance of the cake layer is also less after pre-filtration.

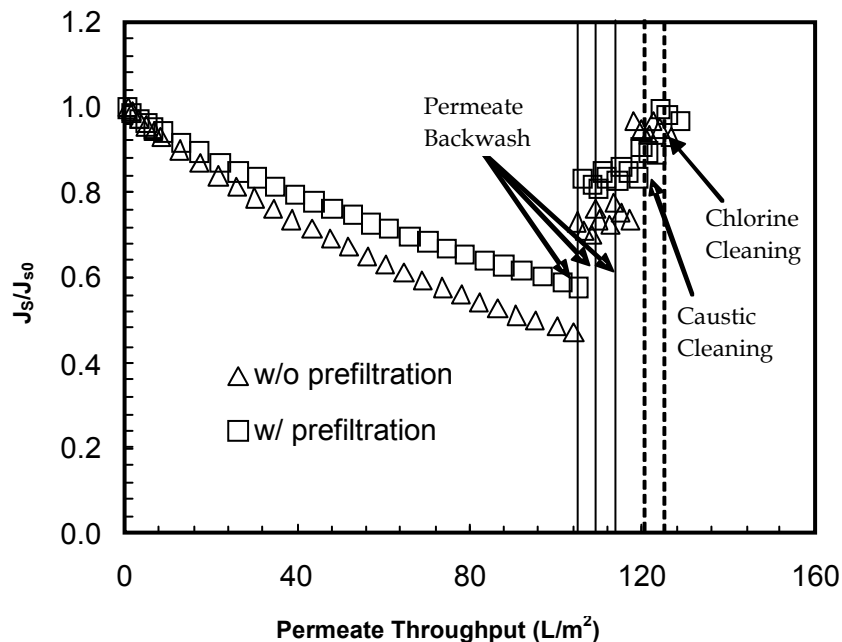
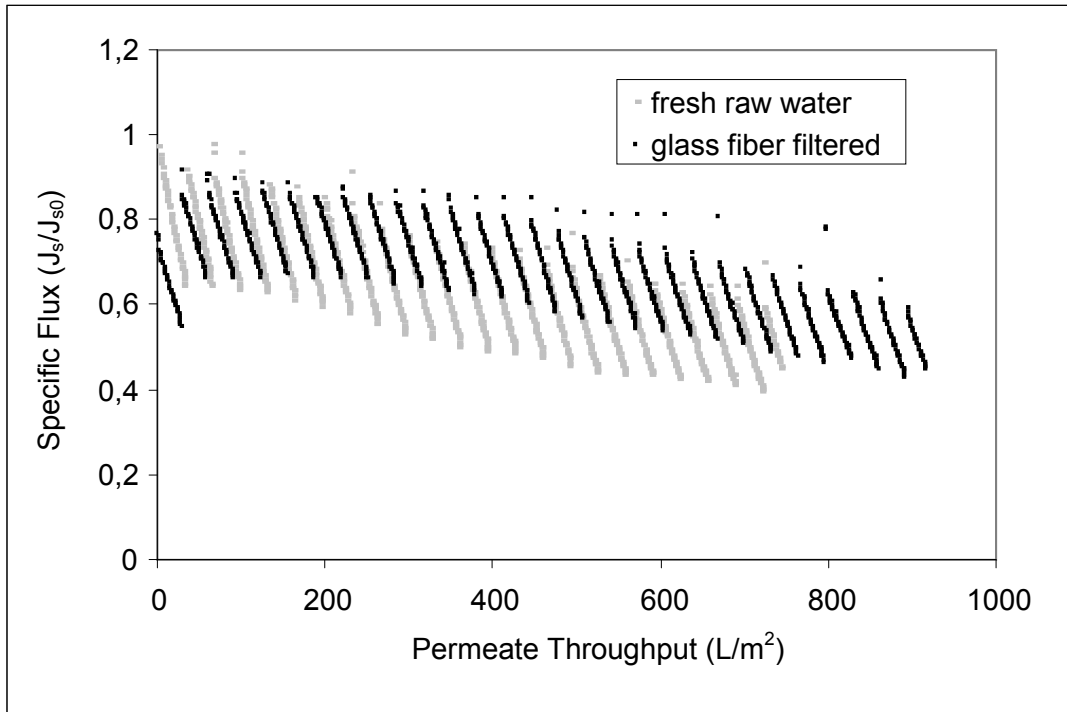


Figure 5.15 Effect of pre-filtration of Tampa Bay water on the fouling of Membrane B. The filtration was operated at a permeate flux of 54 L/m<sup>2</sup>-hr (32 gfd).



**Figure 5.16 Comparison of flux decline rate of Membrane C on unfiltered and pre-filtered Twente Canal water**

**Effect of storage time on the fouling rate (pre-filtered samples)**

Experiments were conducted with Hollow-Fiber Unit 2 to assess the impact of sample storage time and pre-filtration on fouling rate. In the first experiment, a sample of Twente Canal water that had been collected and stored at 5 °C were 1.2- $\mu\text{m}$  filtered at different times—the first, 2 days after storage and the second, 8 days after storage. Filtration runs using Membrane C were conducted immediately after pre-filtration. In the second experiment, a third aliquot of the Twente Canal sample was filtered immediately and then stored for 9 days, after which a filtration run with Membrane C was performed.

The flux decline curves for the three samples are shown in [Figure 5.17](#). Although the shapes of the three curves are slightly different, at a 600 L/m<sup>2</sup> permeate throughput the curves have nearly identical specific flux values. This result indicates that storage of raw or pre-filtered water for a week or more has no appreciable impact on fouling rate.

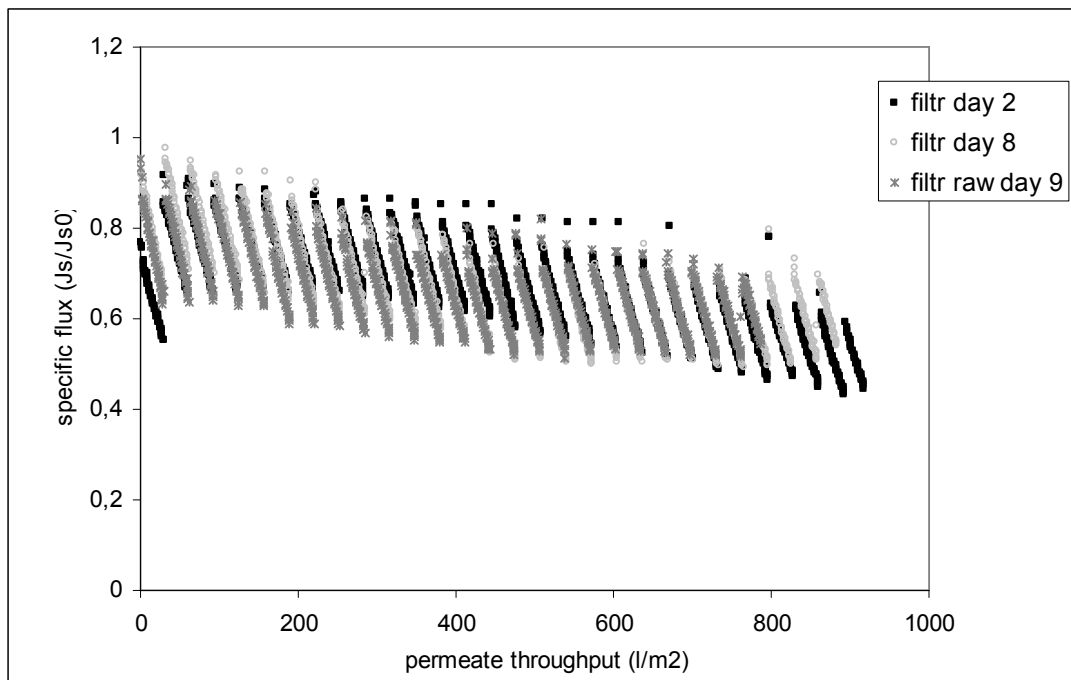


**Figure 5.17 Effect of storage time on fouling rate of Membrane C using raw and pre-filtered Twente Canal water (filtr day 2 = stored and pre-filtered on day 2; filtr day 8 = stored and pre-filtered on day 8; filtr raw day 9 – filtered immediately and stored for 9 days)**

### **Effect of storage time on fouling rate (unfiltered samples)**

A second set of flux decline experiments was performed with a new, unfiltered aliquot of Twente Canal water within 1 day of receipt and after refrigeration at 5° C for 7 days. With unfiltered water, one may expect some microbial breakdown of components, possibly changing the fouling rate.

The flux decline curves for the unfiltered sample are shown in [Figure 5.18](#). The unfiltered water experiments show some effect from storage: fresh raw water gives a slightly higher fouling rate than raw water stored for 7 days. This is confirmed by the observation of sludge at the bottom of the vessel of the stored raw water. By comparing these two graphs more carefully, we see that the maximum specific flux values are almost the same, while the minimum specific fluxes are different. The maximum specific flux is the flux just after the backwash, giving an indication of the amount of hydraulically reversible fouling. The minimum specific flux is the flux after a period of filtration in which a cake layer was built. It can be concluded that fresh raw water imparts a thicker cake layer on the membrane, but the amount of irreversible fouling substances does not change over time.

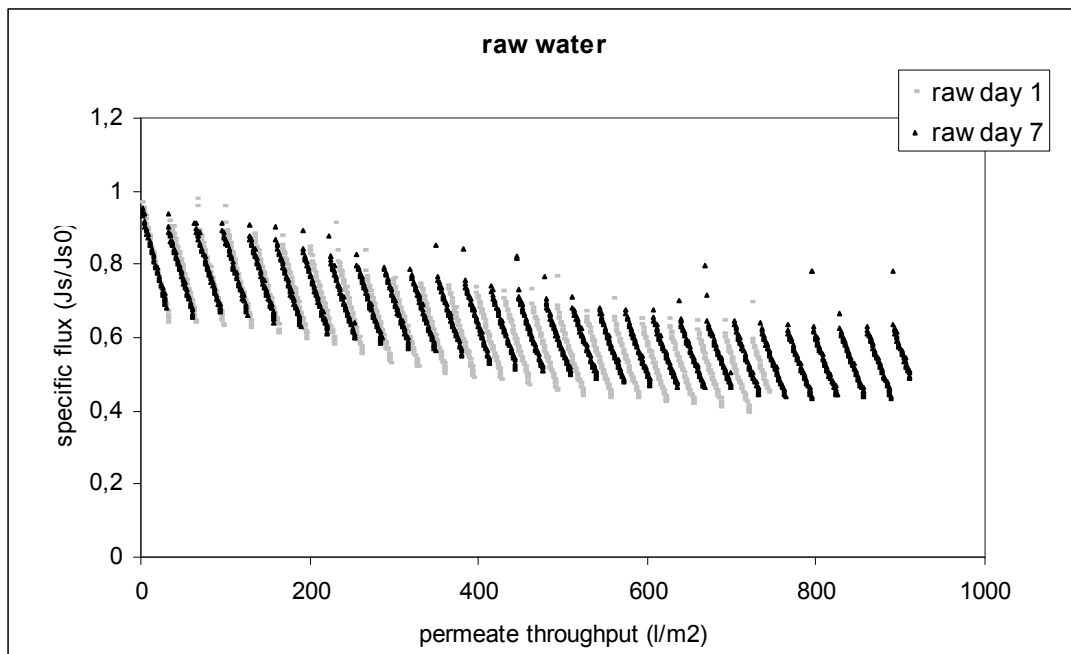


**Figure 5.18 Fouling curves for Membrane C on unfiltered Twente Canal water (after 1 day and 7 days of refrigerated storage)**

## HOLLOW-FIBER UNIT 1

### Baseline Study Results

#### *r<sup>2</sup> Values for UMFI Calculation*

Using the computing method described previously, the total fouling curve obtained in each fouling experiment can be represented using the UMFI. These UMFI values are used in the following discussions. The degree to which the UMFI provides a suitable statistical means to explain the correlation between  $1/J_S'$  ( $J_{S0}/J_S$ ) and  $V_S$  (unit permeate throughput) is quantified in the following sections using the correlation of determination ( $r^2$  value), which is the measure of how well the linear regression equations represents the data. The closer the  $r^2$  value is to one, the better the total variance in  $1/J_S'$  is explained by the linear relationship between  $1/J_S$  and  $V_S$ . As shown in [Table 5.6](#), the  $r^2$  values for all experiments ranged between 0.9686 and 0.9997, indicating an excellent accounting of variation for all membrane and water combinations. Therefore, it is statistically reasonable to use the UMFI values to describe the development of total fouling observed in corresponding experiments.

**Table 5.6****Correlation of determination ( $r^2$ ) values obtained in the calculation of UMFI for each fouling experiment**

Membrane		A			B			C			D2		
Flux (L/m <sup>2</sup> -hr)		54	82	109	54	82	109	68	102	136	68	102	136
Source	IND	0.9878	0.9952	0.9913	0.9979	0.9990	0.9993	0.9849	0.9910	0.9964	0.9979	0.9944	0.9984
Water	TP	0.9990	0.9979	0.9831	0.9953	0.9979	0.9958	0.9917	0.9894	0.9859	0.9983	0.9980	0.9912
	TC	0.9903	0.9897	0.9686	0.9961	0.9987	0.9997	0.9980	0.9980	0.9962	0.9973	0.9991	0.9912
	SCD	0.9964	0.9993	0.9819	0.9988	0.9969	0.9950	0.9909	0.9912	0.9904	0.9969	0.9971	0.9945

IND = Indianapolis, TP = Tampa Bay, TC = Tuscaloosa, SCD = Scottsdale

### Effects of Water Source on Fouling

Variations of UMFI and  $UMFI_R$  values with different water sources are plotted in Figures 5.19 through 5.22. Regardless of the permeate flux, the UMFI values were highest for Membranes B and C when the Tampa Bay water was filtered, and lowest when the Indianapolis water was filtered. For Membranes A and D2, the Indianapolis water also gave the lowest UMFI for the four waters tested. However, the highest UMFI values for Membrane A were observed with the Scottsdale water, not the Tampa Bay water. In comparison, the UMFI values were similar and the greatest when the Scottsdale and Tampa Bay waters were filtered by Membrane D2. The results suggest that Scottsdale water and/or Tampa Bay water in general caused the greatest total fouling for all four membranes tested, while the Indianapolis water caused the least.

The trend for  $UMFI_R$  was different from that for UMFI. As shown in the same figures, the  $UMFI_R$  was highest with the Tampa Bay water and lowest with the Indianapolis water for all membranes except Membrane A. The  $UMFI_R$  values for Membrane B did not differ extensively with the four waters studied, although the values were slightly higher with the Scottsdale water. These results indicate that the hydraulically irreversible fouling was the worst for all membranes when the Tampa Bay water was treated under the hydraulic conditions investigated, except for Membrane B. Interestingly, the Tampa Bay water appeared to be extremely problematic to Membrane A, the only microfiltration membrane used in the study.

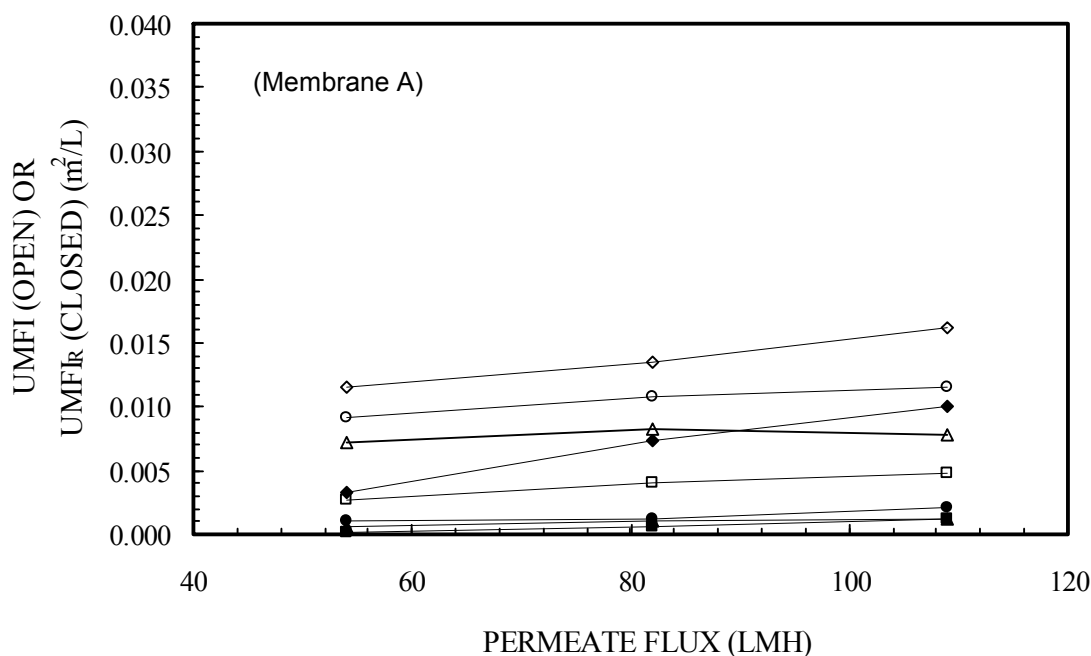


**Figure 5.19 UMFI (open) and  $UMFI_R$  (solid) values for Membrane A obtained with Scottsdale (triangle), Twente Canal (circle), Tampa Bay (diamond), and Indianapolis (square) waters**

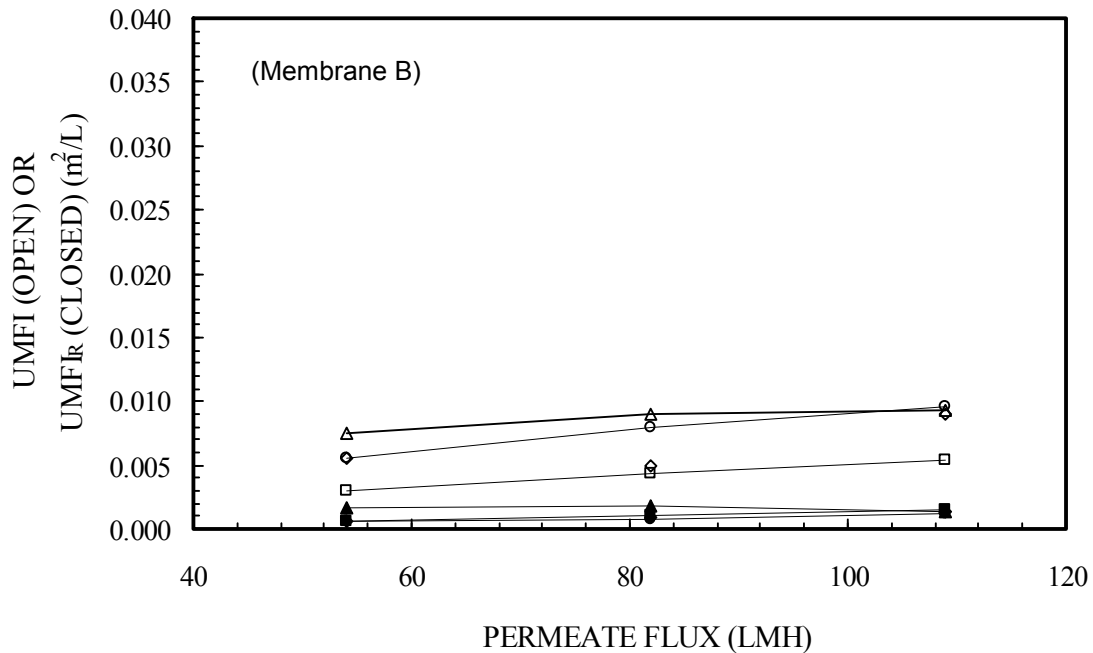


**Figure 5.20** UMFI (open) and UMFI<sub>R</sub> (solid) values for Membrane B obtained with Scottsdale (triangle), Twente Canal (circle), Tampa Bay (diamond), and Indianapolis (square) waters

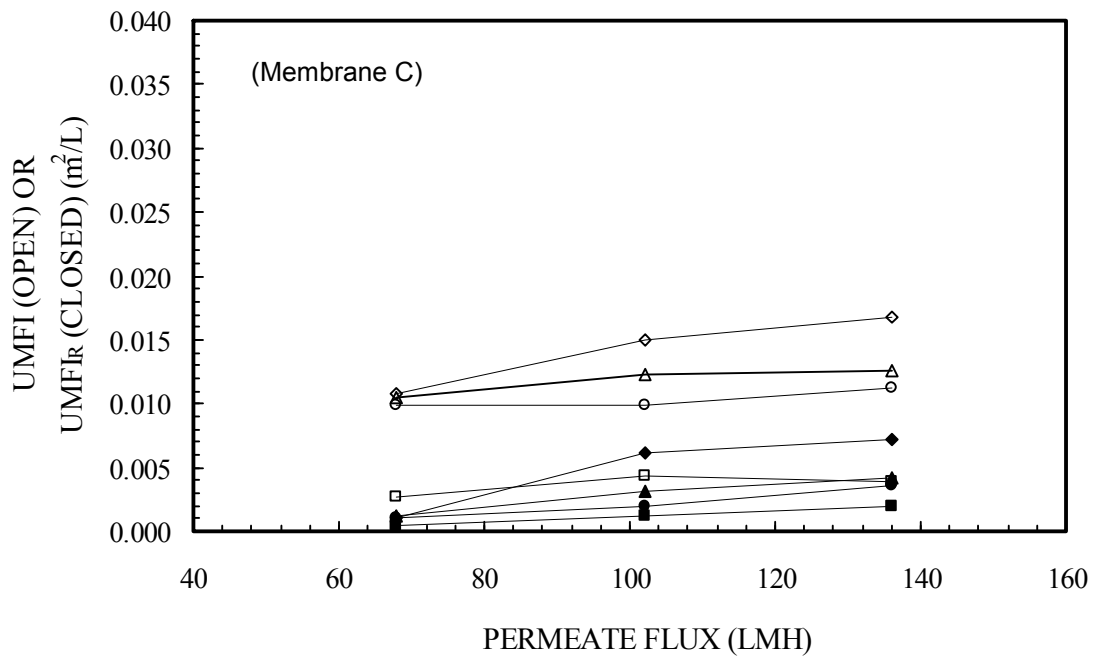


**Figure 5.21** UMFI (open) and UMFI<sub>R</sub> (solid) values for Membrane C obtained with Scottsdale (triangle), Twente Canal (circle), Tampa Bay (diamond), and Indianapolis (square) waters

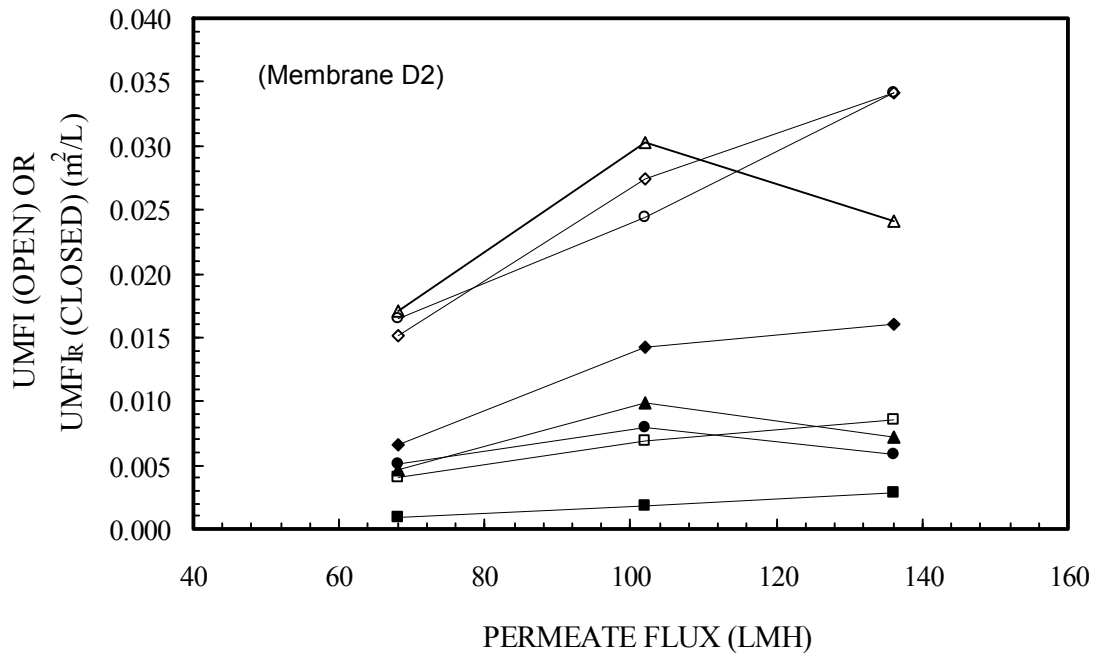


**Figure 5.22 UMFI (open) and UMFI<sub>R</sub> (solid) values for Membrane D2 obtained with Scottsdale (triangle), Twente Canal (circle), Tampa Bay (diamond), and Indianapolis (square) waters**

### *Effects of NOM Type on Fouling*

Because the natural waters used in the study contained different concentrations of DOC, it is also important to plot the membrane fouling profiles as a function of the total amount of DOC delivered per unit surface area of membrane to assess the impact of NOM type rather than total NOM (DOC). These plots are shown in Figures 5.23 through 5.26. The total amount of delivered DOC was calculated based on permeate throughput and feed DOC, and it is plotted together with the variation of membrane fouling obtained with different sources of NOM, expressed as UMFI or UMFI<sub>R</sub> per mg DOC delivered to the membrane. Unlike the difference in UMFI and UMFI<sub>R</sub> observed with different membranes, a consistency in the relationship between total fouling and NOM source was found with all membranes tested. Regardless of the type of membrane, the Scottsdale water NOM resulted in the most severe fouling (the highest UMFI/DOC values); the Tampa Bay water NOM produced the lowest. Considering the dominant NOM component of the waters, these data suggest that, under conditions employed in the study, EfOM exhibited the highest fouling potential; “allochthonous” NOM had the lowest fouling potential on the low-pressure hollow-fiber (LPHF) membranes tested; and “autochthonous” NOM usually lay between the two.

On the other hand, there was no clear trend for the UMFI<sub>R</sub>/DOC values of all membranes as illustrated in the figures. For instance, EfOM caused the greatest UMFI<sub>R</sub>/DOC for the two PES membranes (Membranes C and D2), but not for the two PVDF membranes (Membranes A and B).

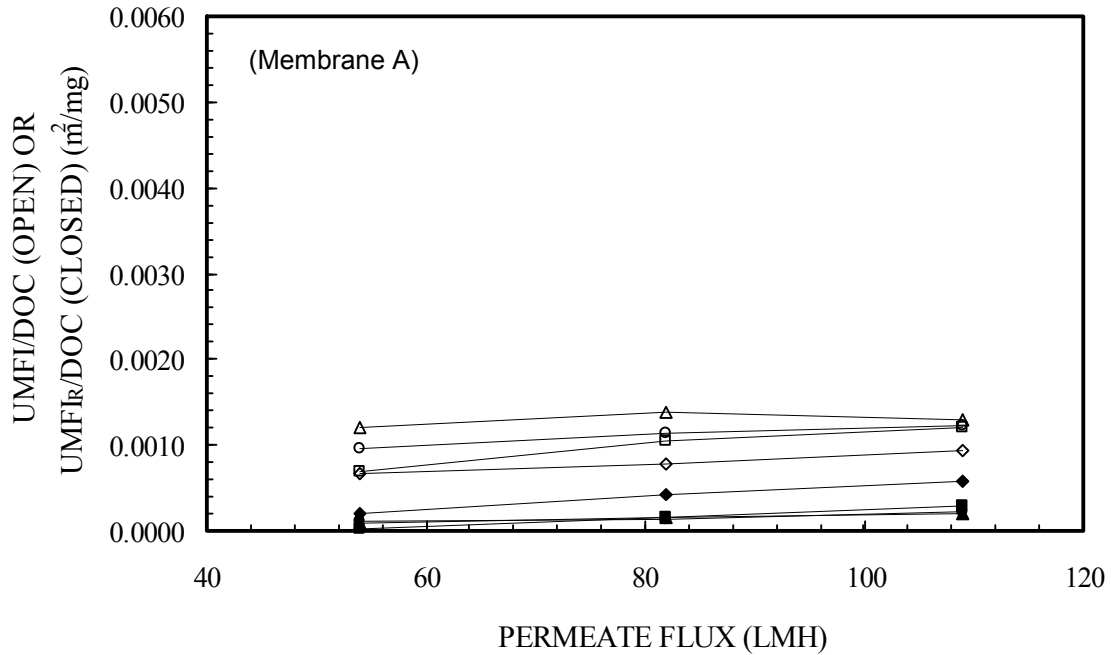


**Figure 5.23 UMFI/DOC (open) and UMFI<sub>r</sub>/DOC (solid) values normalized to feed water DOC for Membrane A obtained with Scottsdale (triangle), Twente Canal (circle), Tampa Bay (diamond), and Indianapolis (square) waters**

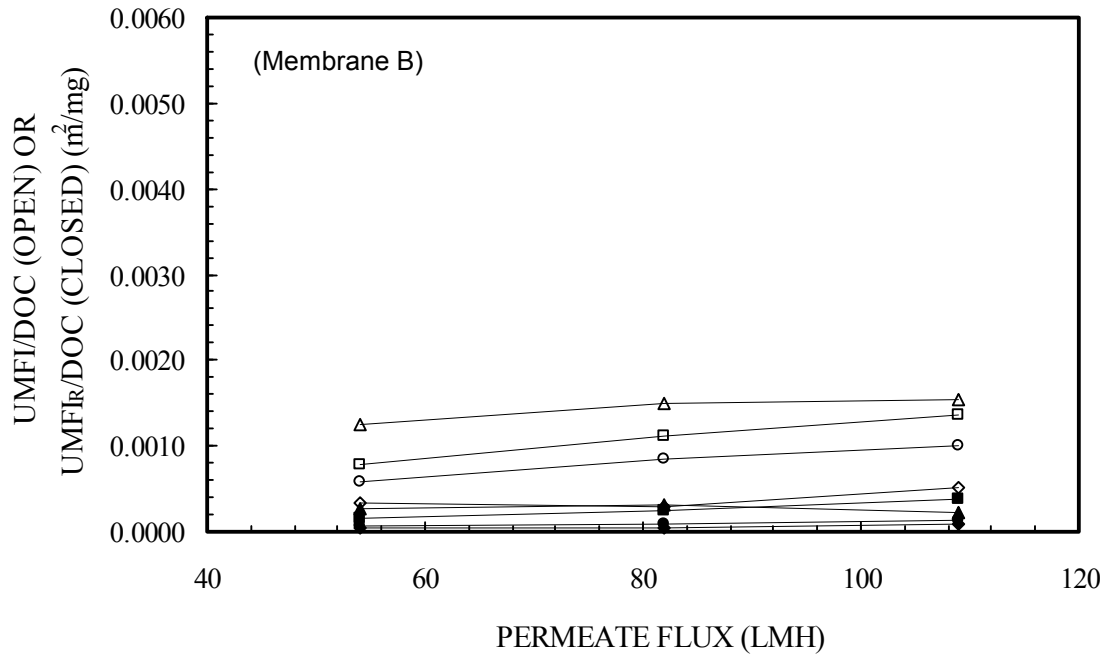


**Figure 5.24 UMFI/DOC (open) and UMFI<sub>r</sub>/DOC (solid) values normalized to feed water DOC for Membrane B obtained with Scottsdale (triangle), Twente Canal (circle), Tampa Bay (diamond), and Indianapolis (square) waters**

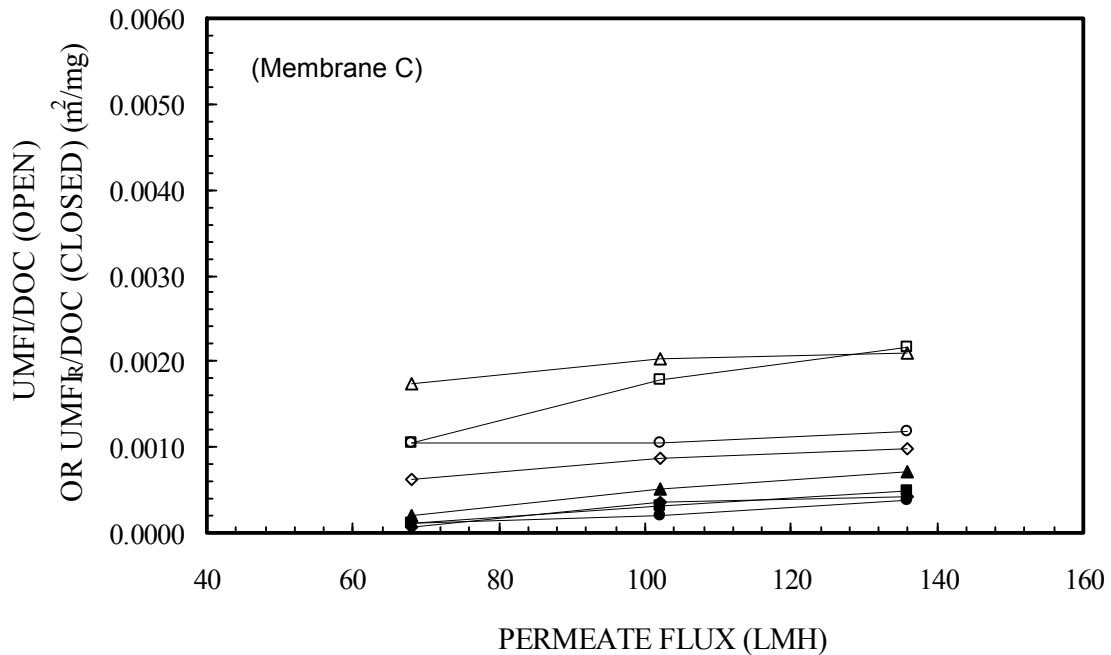


**Figure 5.25 UMFI/DOC (open) and UMFI<sub>r</sub>/DOC (solid) values normalized to feed water DOC for Membrane C obtained with Scottsdale (triangle), Twente Canal (circle), Tampa Bay (diamond), and Indianapolis (square) waters**

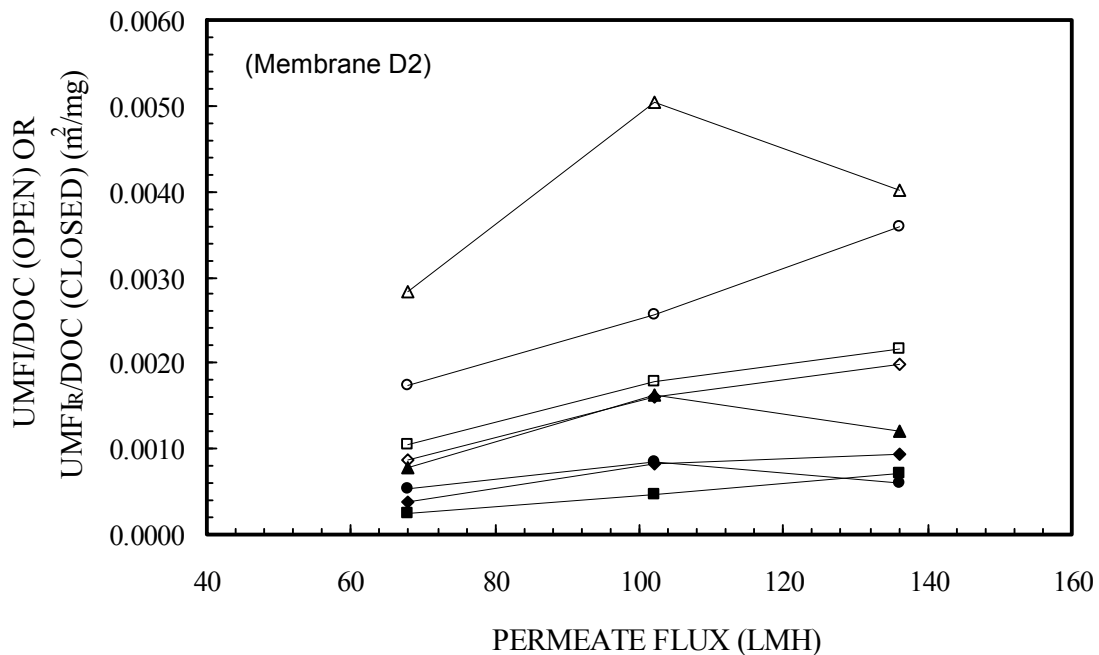


**Figure 5.26 UMFI/DOC (open) and UMFI<sub>r</sub>/DOC (solid) values normalized to feed water DOC for Membrane D2 obtained with Scottsdale (triangle), Twente Canal (circle), Tampa Bay (diamond), and Indianapolis (square) waters**

### ***Effects of Permeate Flux on Fouling***

As shown in Figures 5.19 through 5.22 and 5.23 through 5.26, an increase of permeate flux from 54 to 109 L/m<sup>2</sup>-hr (for PVDF membranes) or 68 to 136 L/m<sup>2</sup>-hr (for PES membranes) usually resulted in a slight increase of UMFI and UMFI<sub>R</sub>, indicating a positive, although weak, relationship between membrane fouling (both total and hydraulically irreversible) and permeate flux. In comparison, the increase was usually more extensive for UMFI than for UMFI<sub>R</sub>. The increase in UMFI or UMFI<sub>R</sub> values with increasing permeate fluxes sometimes also changed the order of their values for the fouling by different sources of NOM (see Figure 5.25 as an example). A more important observation in these figures was the relative importance of NOM source in membrane fouling. For instance, for the fouling of Membrane B by Tampa Bay and Indianapolis waters, the UMFI values increased from 0.012 to 0.016 m<sup>2</sup>/L and from 0.0027 to 0.0047 m<sup>2</sup>/L, respectively, as the permeate flux increased two-fold (see Figure 5.20). In comparison, the difference in UMFI values when comparing the two waters directly at any given flux was substantially greater. Similar trends were found with most of other membrane/water combinations. Thus, the type of water or the source of NOM had a greater impact on membrane fouling than operating fluxes. This finding is different from earlier studies with regard to the presence of critical flux in membrane fouling as discussed in Chapter 2. The difference is likely to result from the differences in the properties of the major foulants.

### ***Effects of Backwash Flux on Hydraulically Irreversible Fouling***

Hydraulic reversibility of NOM fouling reflects the possibility of fouling reduction using permeate backwash. The impacts of NOM types and water sources on hydraulically irreversible fouling (HIF) have been discussed in previous sections, where HIF is defined as  $J_s/J_{s0}$  at some given permeate throughput or DOC delivered, where  $J_s$  is measured after the completion of the backwash cycle. It should be pointed out, however, that the UMFI<sub>R</sub> values were calculated based on the recovery of the permeate flux immediately after the first hydraulic backwash (the one at the lowest backwashing flux) of the single-cycle experiment. In these and subsequent backwash flux experiments, the restoration of  $J_s/J_{s0}$  varied to different extents for water/NOM sources. Figures 5.27 and 5.28 illustrate the HIF of the two PVDF membranes as a function of backwash flux. The normalized specific flux ( $J_s/J_{s0}$ ) after backwash varied over the range of 0.80 to 0.92 for Membrane A and 0.60 to 0.92 for Membrane B with different sources of water. In comparison, and as shown in Figures 5.29 and 5.30, a maximum specific flux of approximately 0.92 was observed for Membrane B (fouled by Tampa Bay water) and Membrane A (fouled by Twente Canal water), respectively, as backwash flux was altered. Likewise, the HIF of two PES membranes was also affected by the NOM type, although the effect of backwash flux was slightly more pronounced in some cases than that observed for the two PVDF membranes (see Figure 5.30). The most dramatic decrease of HIF was observed in the fouling of the Membrane D2 membrane by Tampa Bay water, where the specific flux increased by approximately 0.18 with increasing backwash flux. However, it was still less than that caused by the variation of water source, i.e., approximately 0.20 for Membrane D2 and 0.26 for Membrane C.

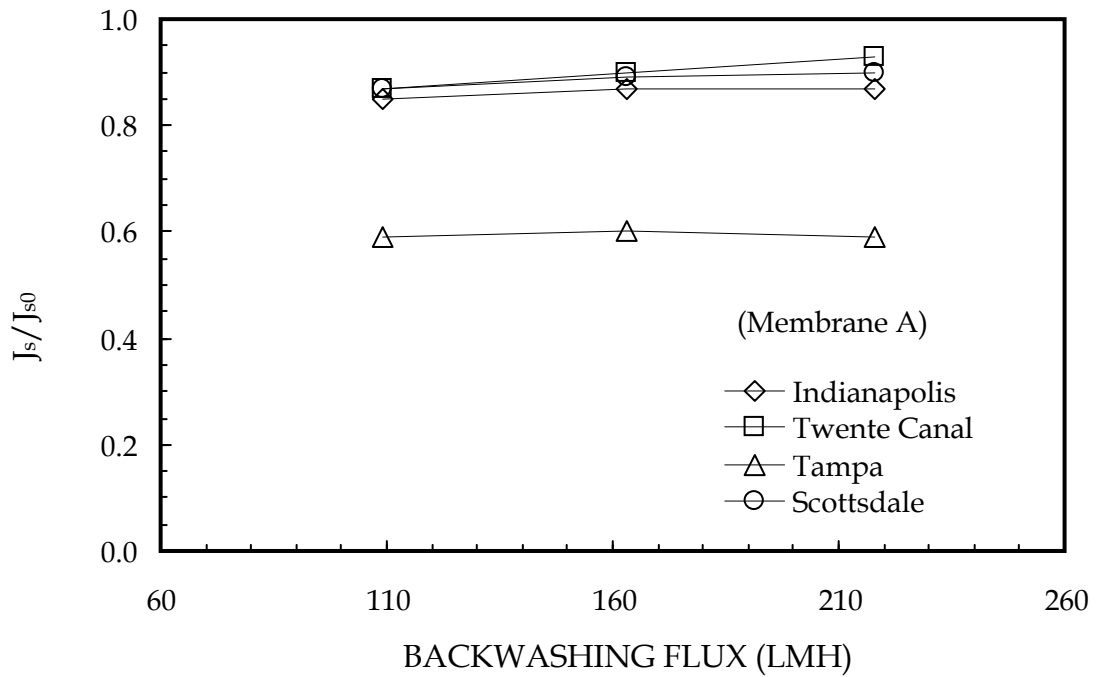


**Figure 5.27 Effects of backwash flux and NOM type on the hydraulically irreversible fouling of Membrane A. All runs were conducted at a permeate flux of 109 L/m<sup>2</sup>-hr or 64 gfd.**

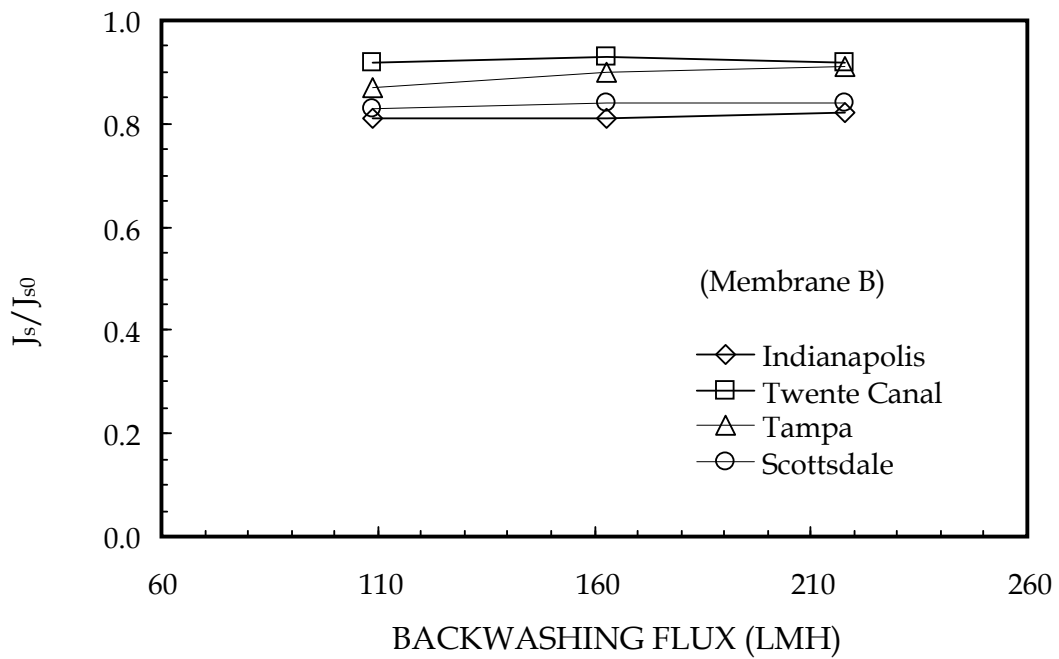


**Figure 5.28 Effects of backwash flux and NOM type on the hydraulically irreversible fouling of Membrane B. All runs were conducted at a permeate flux of 109 L/m<sup>2</sup>-hr or 64 gfd.**

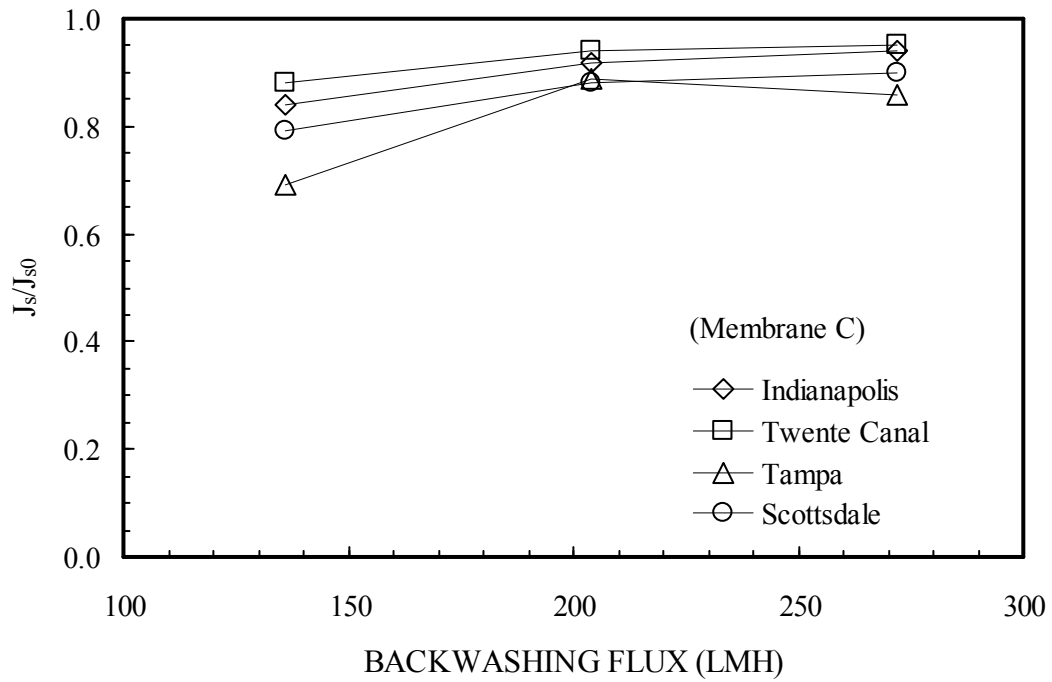


**Figure 5.29** Effects of backwash flux and NOM type on the hydraulically irreversible fouling of Membrane C. All runs were conducted at a permeate flux of 102 L/m<sup>2</sup>-hr or 60 gfd.

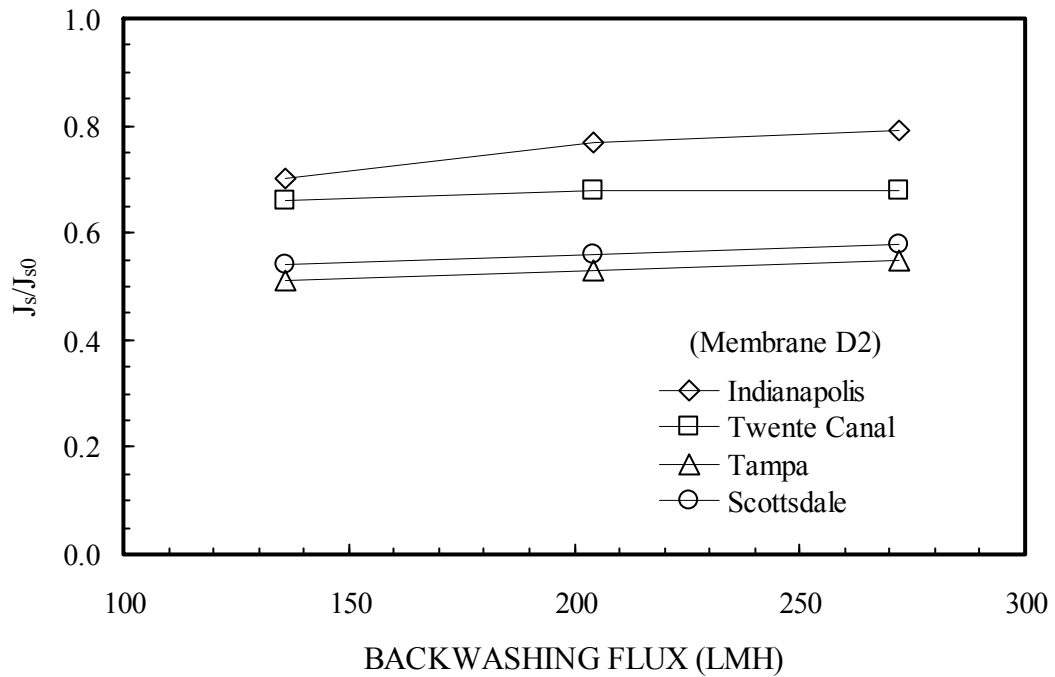


**Figure 5.30** Effects of backwash flux and NOM type on the hydraulically irreversible fouling of Membrane D2. All runs were conducted at a permeate flux of 102 L/m<sup>2</sup>-hr or 60 gfd.

HIF directly reflects the loss of membrane permeability immediately after permeate backwash. It also impacts the fouling of membrane systems in the subsequent filtration of natural waters. In other words, the decay of the specific flux observed for a fouled membrane after a permeate backwash was sometimes faster than that for a clean membrane. This effect was assessed by calculating the decrease of specific flux within 5 minutes after backwash and normalizing it to that observed with the clean membrane at the beginning 5 minutes of the filtration. The greater the value is, the faster the specific flux declines compared to a clean membrane. The results from experiments conducted at a permeate flux of 102 to 109 L/m<sup>2</sup>-hr (60 to 64 gfd) are presented in Figure 5.31. As shown in the figure, the two PES and the two PVDF membranes responded differently to the variation of backwash fluxes. The relative decrease of specific flux was reduced by a factor of 2 to 5 as the backwash flux doubled (from 136 to 272 L/m<sup>2</sup>-hr, or 80 to 160 gfd) in the case of PES membranes. In comparison, the relative decrease of specific flux remained at around one for the two PVDF membranes, regardless of the variation of backwash flux (ranging from 109 to 218 L/m<sup>2</sup>-hr, or 64 to 128 gfd). This difference between PVDF and PES membranes was observed consistently with all natural waters evaluated in the study. Therefore, the difference appeared not to be a result of the type of NOM, but a difference in membrane configuration (inside out versus outside in) or materials (PES versus PVDF). This finding implies that optimization of backwashing flux is more critical to inside-out, PES membranes than to outside-in, PVDF membranes in regard to fouling reduction.

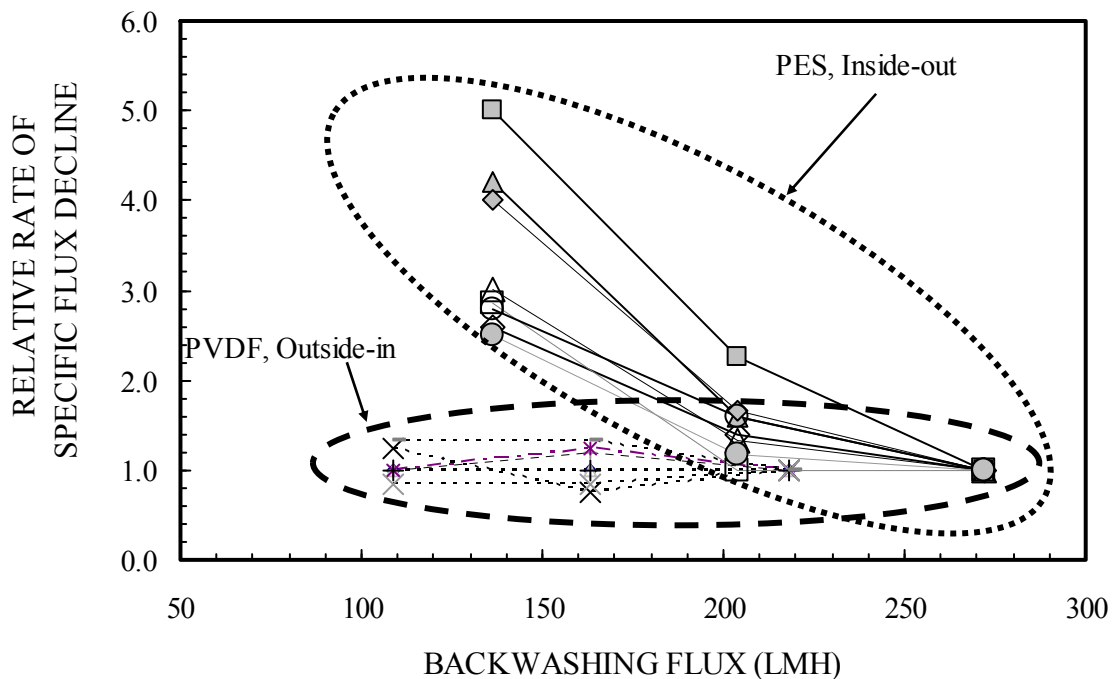


**Figure 5.31** Relative decrease of specific flux as a function of permeate backwash flux. The two circles indicate two distinctive regions for PVDF and PES membranes, respectively.

### ***Behaviors of PS-NOM in Membrane Fouling***

Figure 5.32 is an example of the SEC-DOC/UV responses of different samples collected in the fouling experiments. As shown in the figure, the most extensive differences were observed for the high MW or PS peak, while the other two peaks remained relatively stable. During the filtration of Twente Canal water, PS-NOM in the feed was partially retained by Membrane A, observed as a decrease of the high MW peak from the feed raw water to the permeate. Meanwhile, for this submerged membrane, some PS rejected by the membrane did not attach to the membrane surface, but remained in the bulk liquid phase, resulting in the elevated concentration of PS-NOM in the retentate sample. Thereafter, backwashing of the fouled membrane removed some of the PS-NOM on the membrane surface as the high MW peak increased dramatically for the backwash water sample. The remaining PS-NOM was further removed from the membrane surface during the caustic backwash, evidenced by the appearance of a distinctive high MW peak in the chromatograph. On the other hand, the medium and the low MW peaks were fairly consistent for all samples. Similar trends were observed with other membrane and water combinations. These results (except for the chemical wash) are generally consistent with the bench-scale stirred-cell tests, although permeate backwashing with the stirred-cell tests were not adequately optimized.

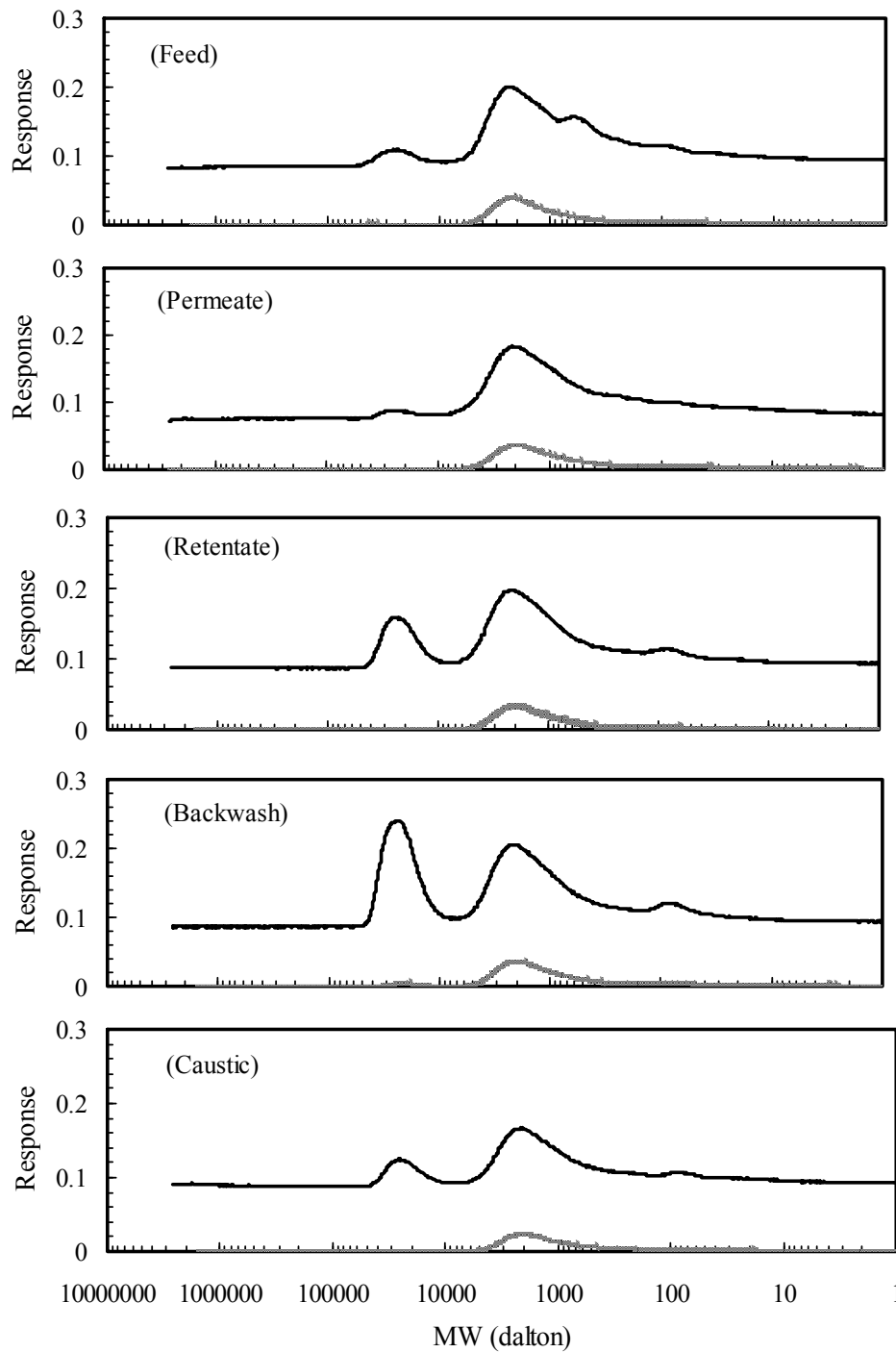


**Figure 5.32 SEC-DOC/UV responses of Twente Canal water samples filtered with Membrane A. Upper and lower curves in each graph represent DOC and UV<sub>254</sub> responses, respectively.**

Table 5.7 summarizes the peak area of the PS-NOM for all water samples measured in the Hollow-Fiber Unit 1 baseline study. It clearly shows that the trend observed during the filtration of Twente Canal water using Membrane A was similar for all other membrane and water combinations, suggesting that the relevance of PS-NOM in the fouling of LPHF membranes is likely to be universal for the LPHF membranes used in water treatment. Since the retention and the removal of PS-NOM were always coincident with the loss and the restoration of membrane specific flux (i.e., permeability), it is probable that PS-NOM was most responsible for the hydraulically irreversible fouling of the LPHF membranes evaluated in this study. PS-NOM may also play an active role in the chemically reversible fouling as suggested by the coincidence of the effectiveness of caustic backwash in restoring membrane permeability and the appearance of PS-NOM in the caustic backwash water.

## Special Testing

### *Free Chlorine vs. Time (CT) Experiments*

Membrane cleaning efficiency was found to increase gradually at low CT and, to a greater extent, at the highest levels of CT evaluated. This relationship can be observed in Figure 5.33 in terms of  $J_S/J_{S0}$ , and in Figure 5.34 in terms of  $UMFI_{\text{cleaning}}$  for virgin membranes. CT is presented as the integrated residual over time for each run. Both  $J_S/J_{S0}$  and  $UMFI_{\text{cleaning}}$  show a gradual increase in the recovery of permeability with increasing CT. At about 100,000 mg/L-min, an increase to  $J_S/J_{S0}$  values as high as 0.97 was observed.

Figure 5.34 presents the  $UMFI_{\text{cleaning}}$  values, solid black symbols, for runs with applied free chlorine, plotted with respect to the CT value of that application. The  $UMFI$  observed before backwashing or cleaning for each experiment is plotted at the same CT value, for reference, as gray symbols. The same is done with open black symbols for the  $UMFI_R$ , the permeability of the membrane after backwashing, but before chlorine cleaning. Trend lines for  $UMFI$  and  $UMFI_R$  display the reproducibility of the fouling and backwashing steps. Decreasing  $UMFI_{\text{cleaning}}$  is indicative of increased membrane cleaning efficiency, which was observed at the highest CT values, approximately 100,000 mg  $Cl_2$ /L-min.

**Table 5.7**  
**PS-DOC levels (mg/L) from SEC-DOC chromatogram**  
**for Hollow-Fiber Unit 1 filtration tests as calculated by peak integration**

Membrane	Membrane A				Membrane B				Membrane C				Membrane D2			
	IND	TC	TP	SCD	IND	TC	TP	SCD	IND	TC	TP	SCD	IND	TC	TP	SCD
Water	IND	TC	TP	SCD	IND	TC	TP	SCD	IND	TC	TP	SCD	IND	TC	TP	SCD
Feed	0.21	0.51	0.44	0.39	0.21	0.51	0.44	0.39	0.21	0.51	0.44	0.39	0.21	0.51	0.44	0.39
Retentate	0.95	1.38	na	na	0.68	1.22	na	na	na	na	na	na	na	na	na	na
Permeate	0.19	0.29	na	0.16	na	0.28	na	0.23	0.18	0.28	0.28	0.24	0.18	0.29	0.18	0.30
Backwash	3.47	2.95	na	4.52	3.47	3.01	na	3.17	1.79	2.63	2.65	4.39	2.18	2.93	3.16	3.70
Caustic	na	0.66	na	0.47	na	0.72	na	0.40	na	1.01	1.02	0.74	na	1.09	3.21	0.81

Abbreviations: IND (Indianapolis), TC (Twente Canal), TP (Tampa Bay), SCD (Scottsdale); na (not available)

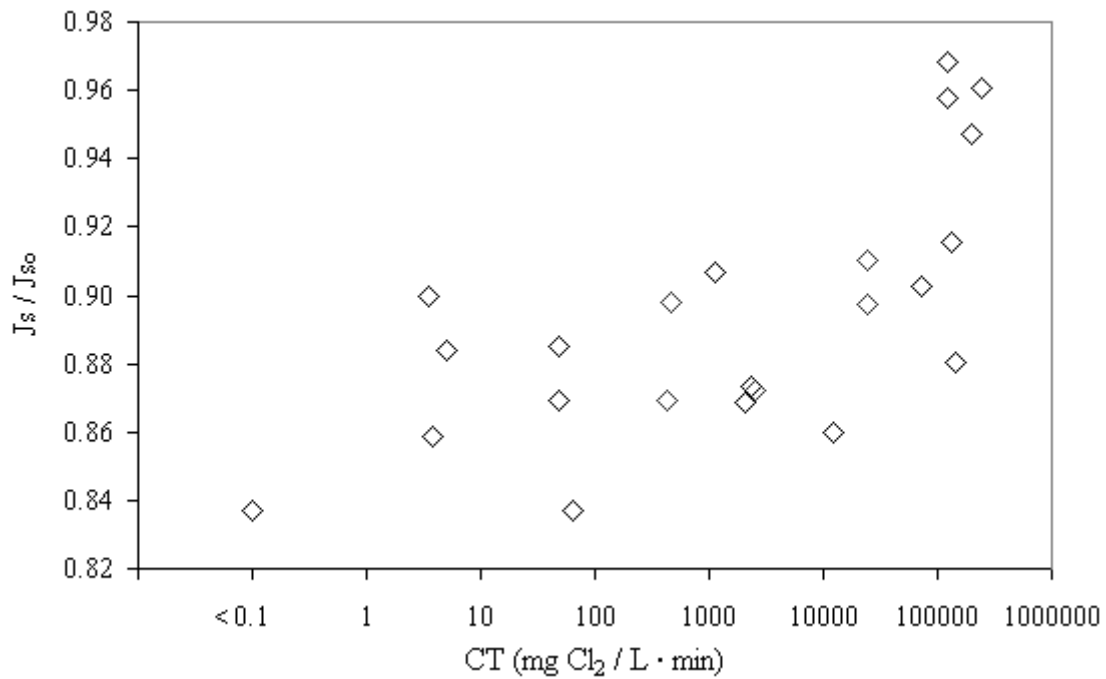


Figure 5.33 Impact of CT on membrane cleaning efficiency

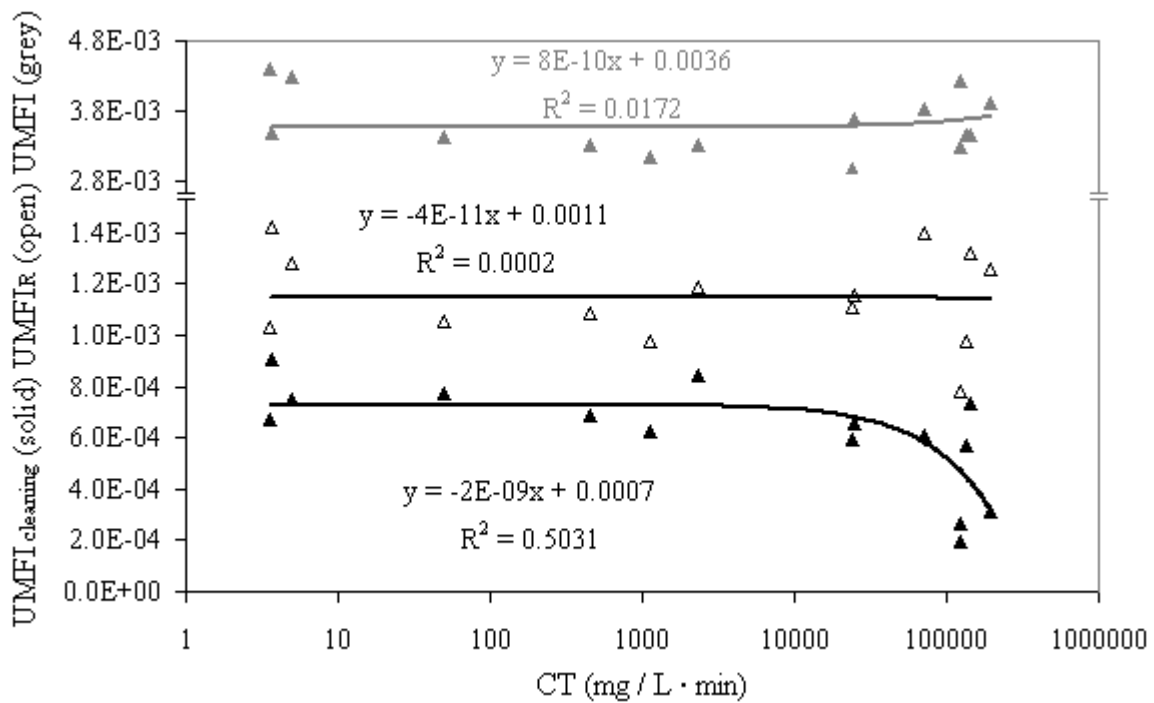
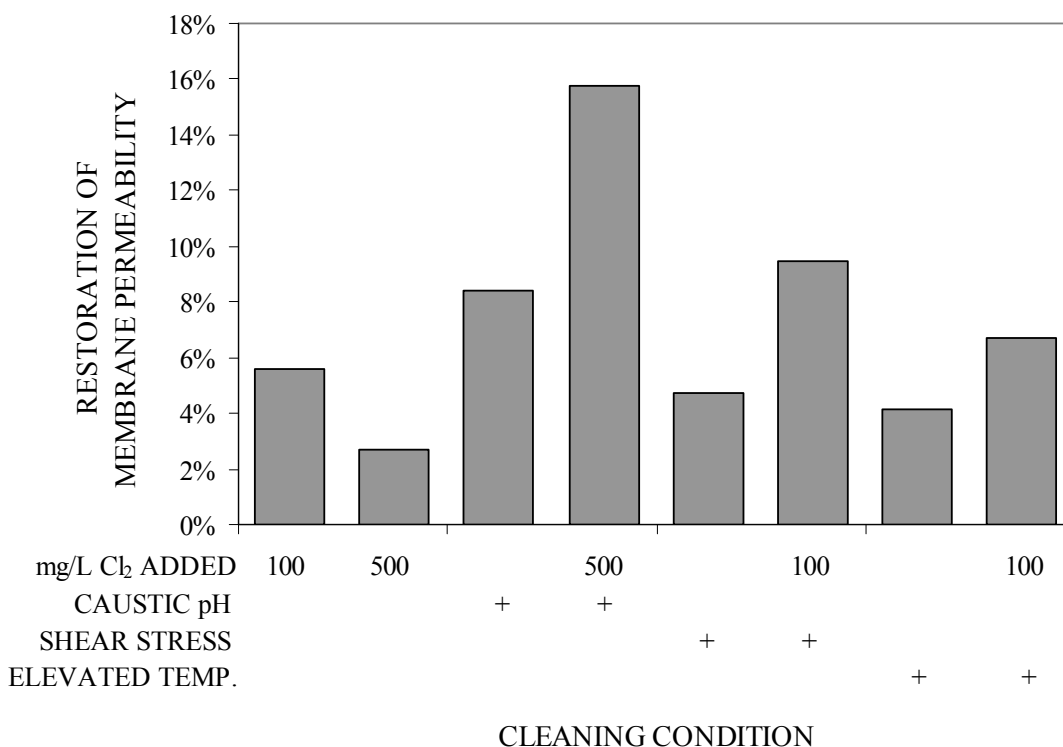


Figure 5.34 Effect of CT on UMFICleaning in virgin membranes. UMFICleaning is represented by black solid symbols. The UMFIR and UMFIR for the steps preceding the CT exposure are shown for reference purposes only, and are represented by solid gray, and open black solid symbols, respectively.

***Additional Cleaning Condition Experiments:***

The impacts of various cleaning conditions on membrane permeability, relative to control, are shown in Figure 5.35. Pertinent results from the CT study are shown for reference as to the effect of the addition of chlorine alone. The caustic condition created an added recovery of 8.4 percent over the control. The chlorinated caustic run had an added recovery of 16 percent over the control and 13 percent compared to chlorine alone. Shear stress added 4.8 percent to the recovery, and chlorinated shearing, 9.5 percent (3.9 percent vs. chlorine alone). Elevated temperature added 4.1 percent to the recovery compared to the control. Chlorinated elevated temperature added 6.7 percent to the recovery, only 1.1 percent versus chlorine alone. Because the differences in recovery were small, additional experiments would need to be conducted to determine any statistical significance. However, the most effective cleaning regime was a combination of chlorine and caustic.



**Figure 5.35 Impact of various cleaning conditions on the restoration of membrane permeability. The restoration is relative to control (no added Cl<sub>2</sub>, pH 7, no shear stress, ambient temperature). The cleaning condition reads vertically from the corresponding column of the table below each bar. Specific details are given in Section 3.5.1.2.7.**

### ***Multi-cycle Backwash Experiments***

Experiments were conducted to evaluate the effects on membrane fouling by single versus multiple backwash cycles. [Figures 5.36](#) and [5.37](#) present the fouling profiles for both multi-cycle and single-cycle experiments using Scottsdale and Indianapolis waters, respectively. The data show that the multi-cycle backwashing yielded similar levels of HIF to single cycle for Hollow-Fiber Unit 1.

Membrane A and B were found to behave similarly in the single-cycle mode with both waters tested. Little difference between the membranes was observed in the multi-cycle mode for Indianapolis water. The Scottsdale water showed greater irreversible fouling of Membrane B in the multi-cycle mode when compared to membrane A.

The similarity in the permeability of the membranes after the first minute of filtration following backwash of the single cycle and the first minute of filtration of the final cycle in the multi-cycle experiments suggest that the simpler single-cycle end-of-run backwash protocol can be used to simulate multiple cycle results.

Further assessment of the similarity of multi- and single-cycle bench-scale operations was performed by comparing various UMFI's, the calculation of which has been described previously. The total fouling capacity of prefiltered water is described by UMFI for single-cycle and  $UMFI_i$  for multi-cycle experiments. The hydraulically irreversible portion of the fouling is expressed as  $UMFI_R$  for single-cycle and  $UMFI_{150}$  Method 1 for multi-cycle experiments. Plots showing the data points from which the fouling indices,  $UMFI_i$  and  $UMFI$ , were calculated for the multi-cycle experiments with Scottsdale and Indianapolis waters are presented in [Figures 5.38](#) and [5.39](#), respectively. Corresponding fouling indices,  $UMFI$  and  $UMFI_R$ , from the single-cycle experiments conducted with Scottsdale and Indianapolis waters are presented in [Figures 5.40](#) and [5.41](#), respectively. The regression lines from which comparable multi- and single-cycle fouling indices were generated are overlaid for Scottsdale and Indianapolis waters in [Figures 5.42](#) and [5.43](#), respectively. The values of each of the indices are presented in [Table 5.8](#).

The  $UMFI_{150}$  and  $UMFR$  values show good correspondence ( $r^2 = 0.75$  for  $n = 4$  pairs), indicating that the bench-scale end-of-run backwash protocol is a reasonably effective means of estimating hydraulically irreversible fouling as measured by multi-cycle operation.

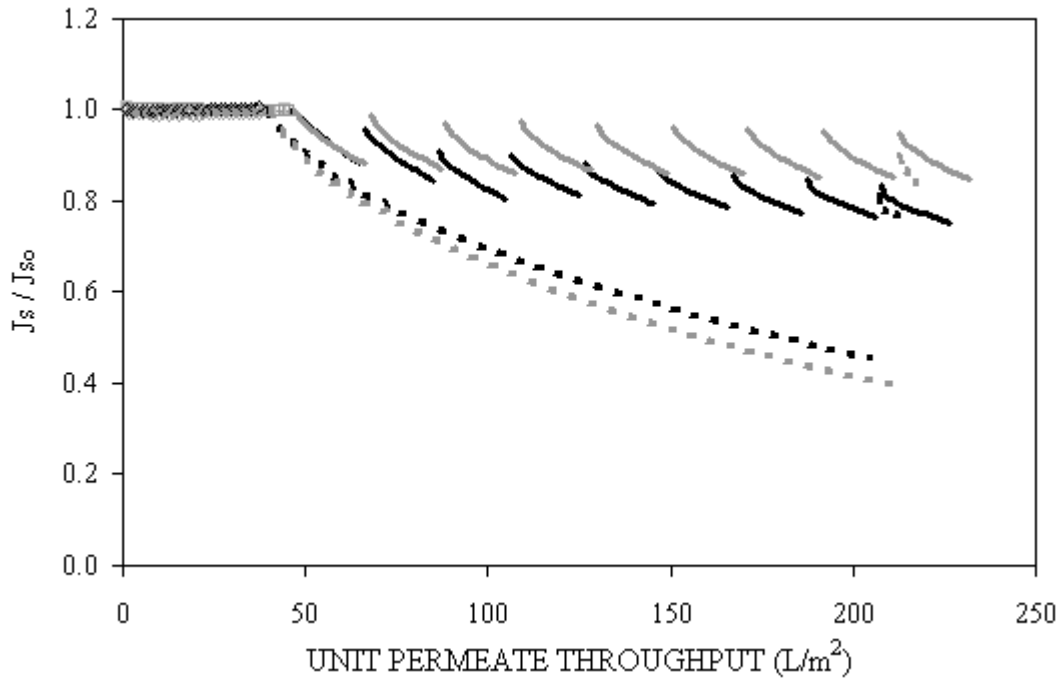


**Figure 5.36 Fouling profile comparison between multi-cycle and single-cycle operation using Scottsdale water as feed water. Multi-cycle (solid), single-cycle (dotted), Membrane A (gray), Membrane B (black).**

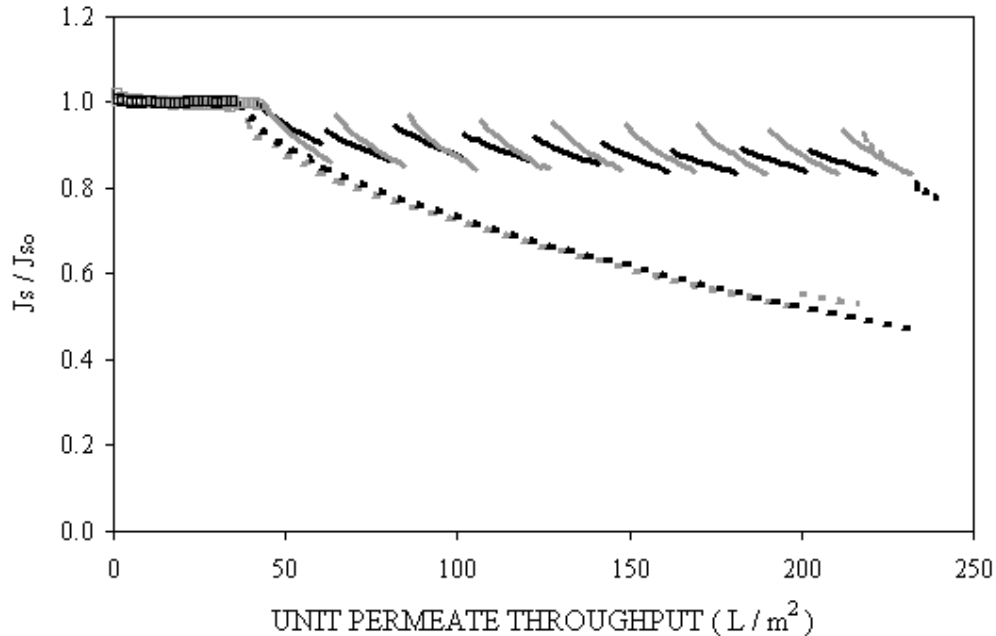


**Figure 5.37 Fouling profile comparison between multi-cycle and single-cycle operation using Indianapolis water as feed water. Multi-cycle (solid), single-cycle (dotted), Membrane A (gray), Membrane B (black).**

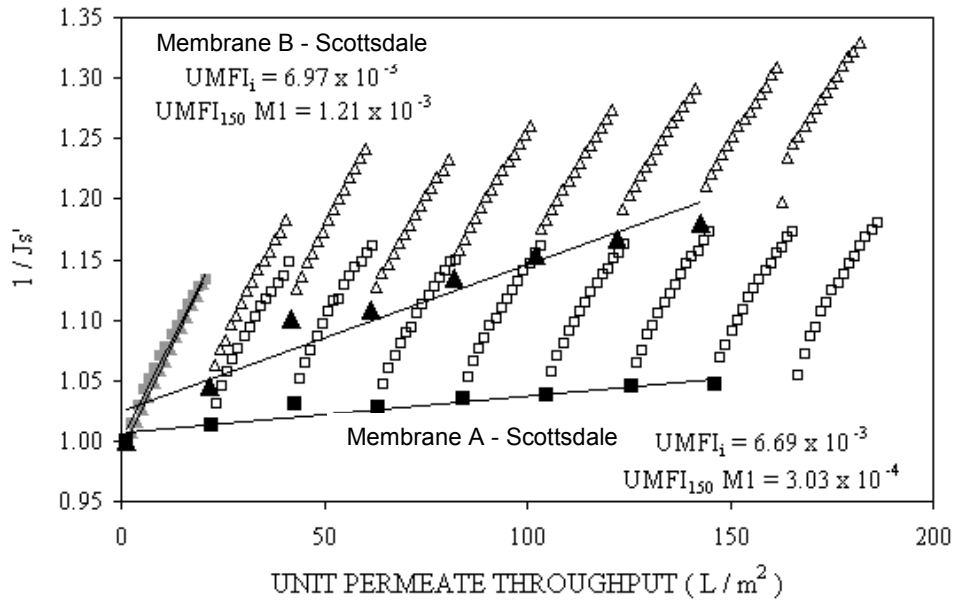


**Figure 5.38 Fouling indices for multi-cycle tests with Scottsdale water. Membrane A (squares), Membrane B (triangles). Data represented by gray shaded symbols were used for calculation of  $UMFI_i$ , black solid symbols were used for calculation of  $UMFI_{150}$ , and open symbols are shown for illustrative purposes only.**

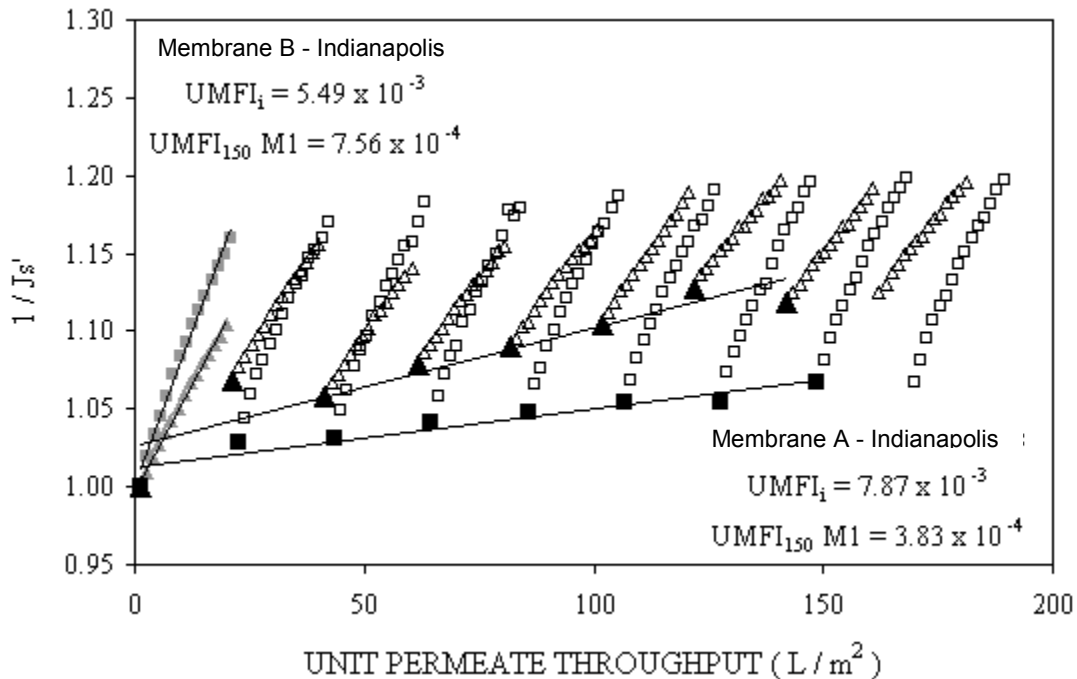


**Figure 5.39 Fouling indices for multi-cycle tests with Indianapolis water. Membrane A (squares), Membrane B (triangles). Data represented by gray shaded symbols were used for calculation of  $UMFI_i$ , black solid symbols were used for calculation of  $UMFI_{150}$ , and open symbols are shown for illustrative purposes only.**

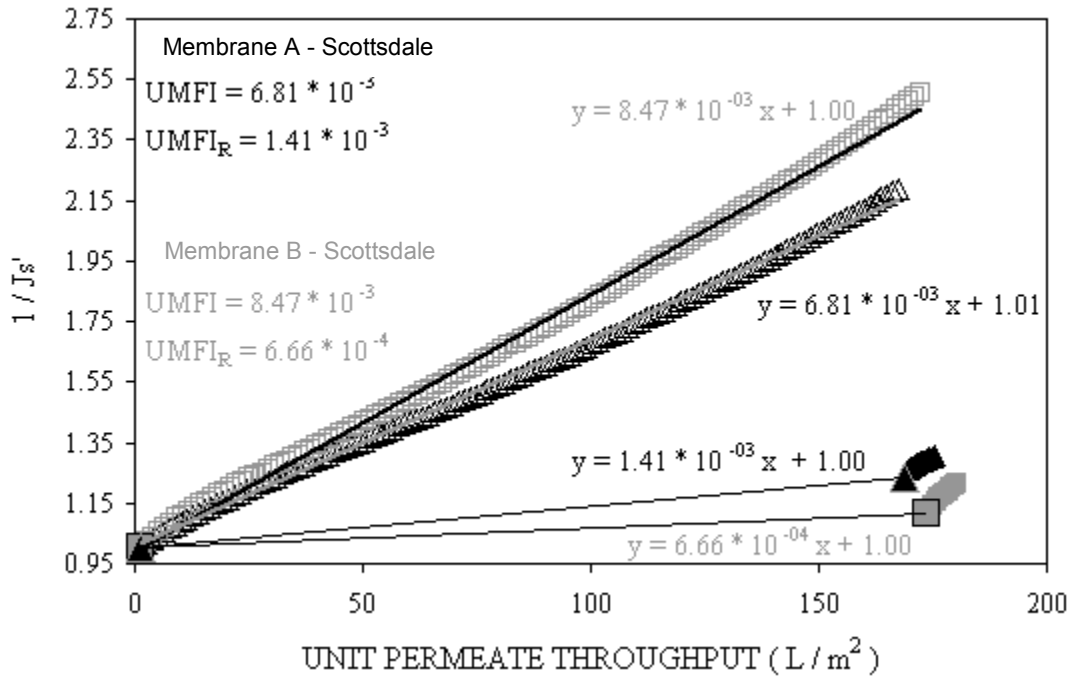


**Figure 5.40 Fouling indices for single-cycle tests with Scottsdale water. Membrane A (gray squares), Membrane B (black triangles). Cycles of fouling and filtration after backwashing are shown in order of increasing unit permeate throughput. Data represented by open symbols were used for calculation of UMFI, solid outlined symbols were used for calculation of UMFI<sub>R</sub>, and solid symbols not outlined are shown for illustrative purposes. UMFI trendlines are shown in contrasting shade.**

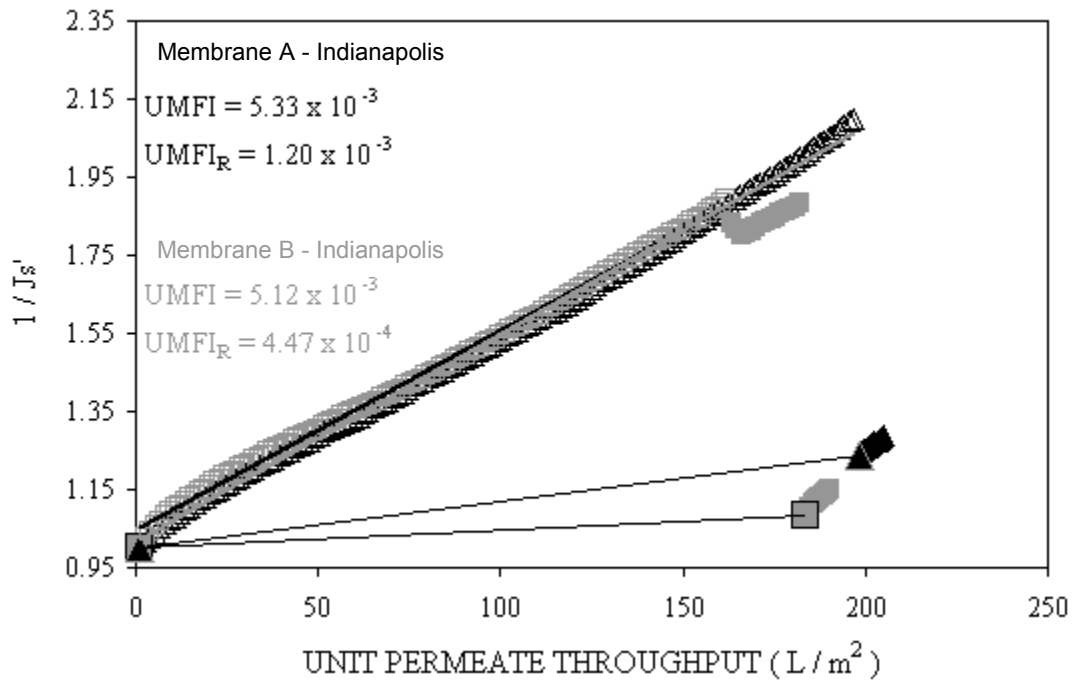


**Figure 5.41 Fouling indices for single-cycle tests with Indianapolis water. Membrane A (gray squares), Membrane B (black triangles). Cycles of fouling and filtration after backwashing are shown in order of increasing unit permeate throughput. Data represented by open symbols are used for calculation of UMFI, solid outlined symbols are used for calculation of  $UMFI_R$ , and solid symbols not outlined are shown for illustrative purposes. UMFI trendlines are shown in contrasting shade.**

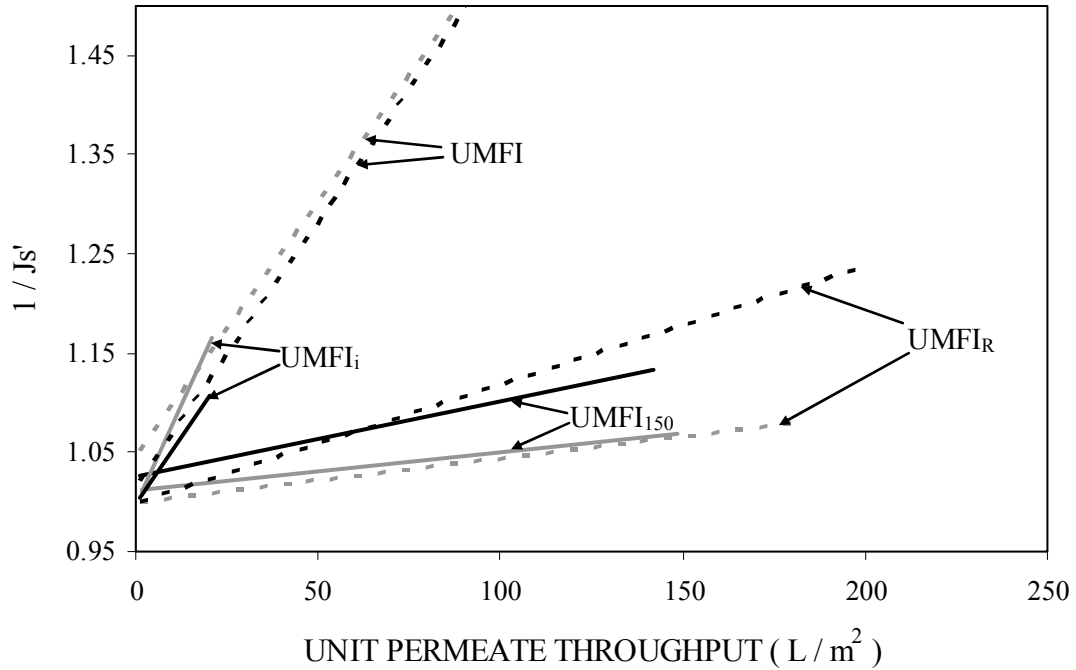


**Figure 5.42 Comparison of multi-cycle and single-cycle fouling indices for tests with Scottsdale water. Displayed are the least squares regression trend lines for each index. The index is equal to the slope of the corresponding regression line. Data points have been omitted for clarity. Membrane A (gray), Membrane B (black), multi-cycle (solid), single-cycle (dotted).**

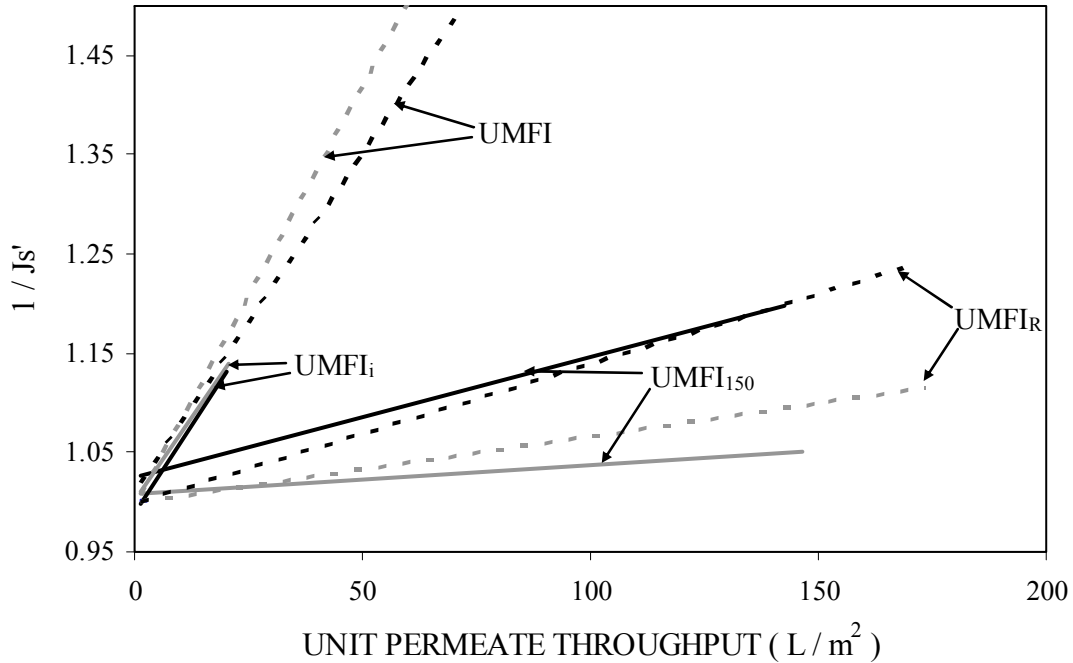


**Figure 5.43 Comparison of multi-cycle and single-cycle fouling indices for tests with Indianapolis water. Displayed are the least squares regression trend lines for each index. The index is equal to the slope of the corresponding regression line. Data points have been omitted for clarity. Membrane A (gray), Membrane B (black), multi-cycle (solid), single-cycle (dotted).**

**Table 5.8**

**Collected fouling indices for single- and multi-cycle experiments.**

**UMFI<sub>i</sub> and UMFI are measures of the total fouling of the prefiltered water;**

**UMFI<sub>150</sub> Method 1 and UMFI<sub>R</sub> are measures of the hydraulically irreversible fouling**

Membrane	Water	Multi-cycle operation		Single-cycle operation	
		UMFI <sub>i</sub>	UMFI <sub>150</sub> Meth.1	UMFI	UMFI <sub>R</sub>
A	Scottsdale	$6.69 \times 10^{-3}$	$3.03 \times 10^{-4}$	$8.47 \times 10^{-3}$	$6.66 \times 10^{-4}$
B	Scottsdale	$6.97 \times 10^{-3}$	$1.21 \times 10^{-3}$	$6.81 \times 10^{-3}$	$1.41 \times 10^{-3}$
A	Indianapolis	$5.49 \times 10^{-3}$	$7.56 \times 10^{-4}$	$5.33 \times 10^{-3}$	$1.20 \times 10^{-3}$
B	Indianapolis	$7.87 \times 10^{-3}$	$3.83 \times 10^{-4}$	$5.12 \times 10^{-3}$	$4.47 \times 10^{-4}$

## Characterization of Fouled Membrane Fibers

### *Contact angle*

Contact angle characterization was conducted with fibers extracted from fouled Membrane A and B outside-in flow PVDF modules used in selected test runs conducted with Hollow-Fiber Unit 1. Table 5.9 summarizes the results from these characterizations. At the end of the filtration cycle, the Membrane B module operated with Tampa Bay water was backwashed prior to contact angle measurement. For the Indianapolis and the Scottsdale tests, no backwash was conducted prior to contact angle measurement.

Results show differing degrees of contact angle modification from filtration.

- For Membrane A, a decrease in contact angle was observed with both Indianapolis (White River water) and Scottsdale effluent. The decrease was more significant for the latter source.
- For Membrane B, filtration caused a decrease in contact angle from filtration of White River water but no (statistically significant) change in angle from filtration of Scottsdale effluent.
- Following filtration and backwash with Tampa Bay water, contact angle increased.

These results show that NOM deposition decreases the hydrophobicity of these PVDF membranes, most likely through accumulation of compounds that are more hydrophilic than the membrane surface. It appears, however, that backwashing preferentially displaces these hydrophilic compounds, leaving behind more hydrophobic NOM. Interestingly, post-filtration contact angle is inversely correlated to  $J_S/J_{S0}$  (at the end of the filtration cycle).

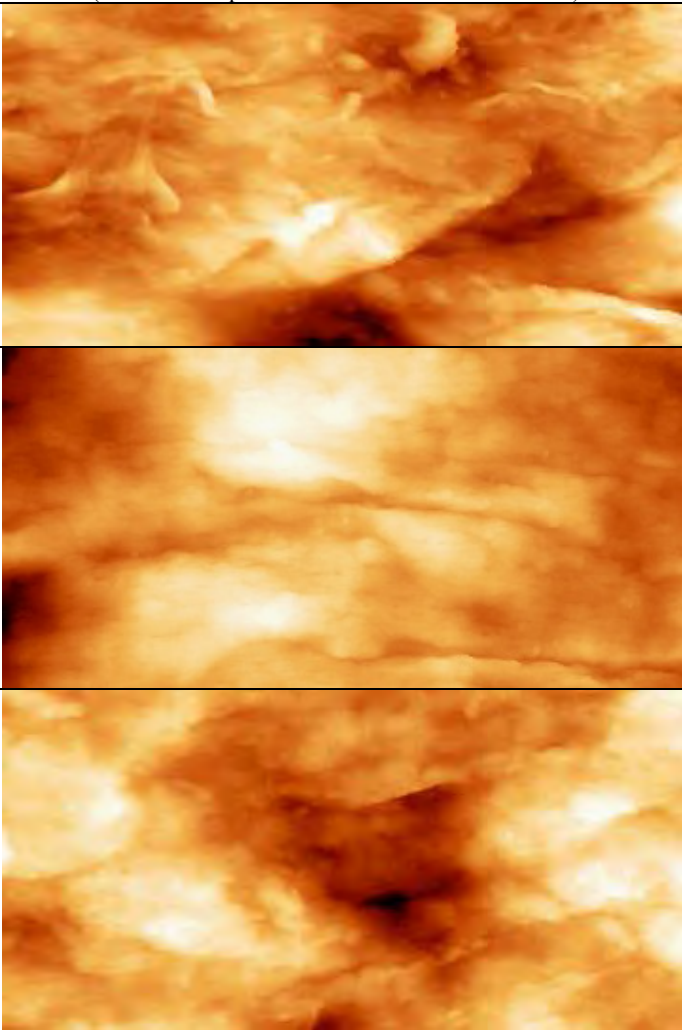
**Table 5.9**  
**Contact angle of hollow fibers measured after fouling tests**

Membrane	Feed water	Flux (gfd [L/m <sup>2</sup> -hr])	BW duration (min)	$J_S/J_{S0}$	Contact angle (°)	
					Virgin	Fouled
A	Indianapolis	48 (81)	0	0.40	83 ± 5	76 ± 1
A	Scottsdale	48 (81)	0	0.25	83 ± 5	72 ± 2
B	Tampa Bay	32 (54)	1	0.63	80 ± 4	92 ± 3
B	Indianapolis	48 (81)	0	0.34	80 ± 4	71 ± 1
B	Scottsdale	48 (81)	0	0.27	80 ± 4	79 ± 1

## Atomic Force Microscopy

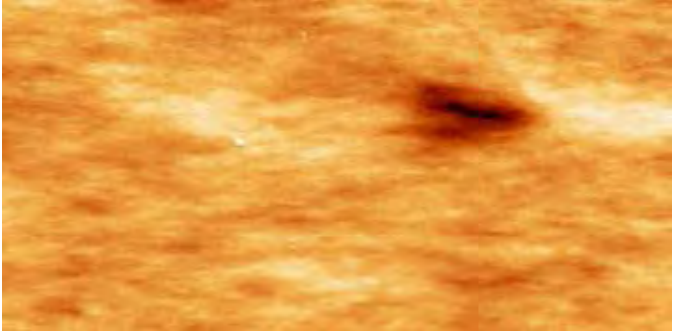
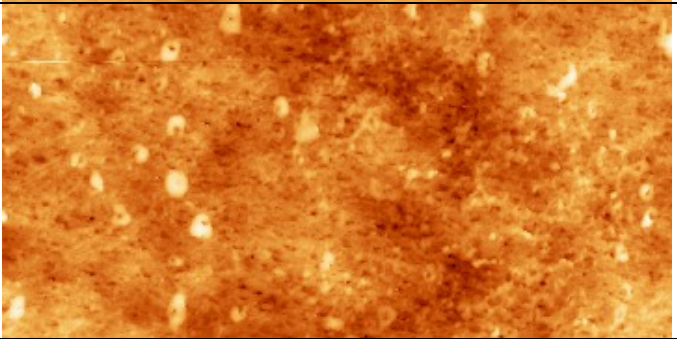
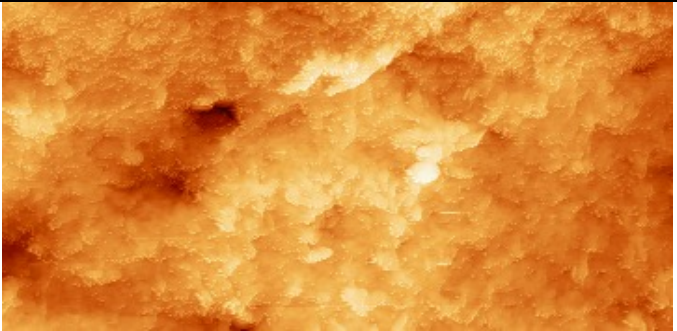
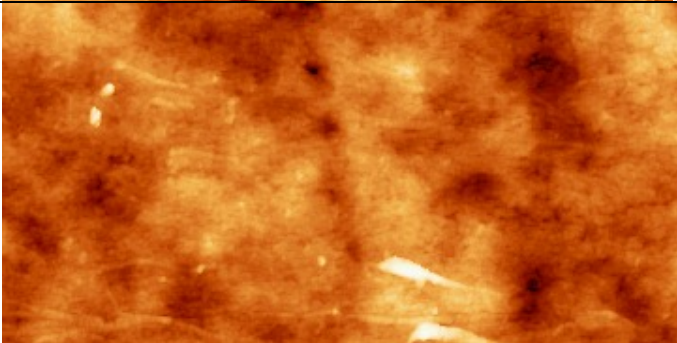
The same hollow fibers used for contact angle measurement were subjected to AFM analysis. Table 5.10 shows the results obtained for Membrane A fibers. While no significant change was noticed after filtration of the Scottsdale tertiary effluent, the roughness of Membrane A decreased after filtration of the White River water. Decreased roughness does correlate with higher post-filtration flux.  $J_s/J_{s0}$  was considerably greater at the end of the filtration cycle for White River water than for Scottsdale effluent. However, decreased roughness is poorly correlated with hydrophilicity. Contact angle was reduced more from filtration of Scottsdale effluent than for White River. Other work has shown that for rough membranes, foulants can accumulate in the “valleys” and reduce the roughness of the membrane (Vrijenhoek et al., 2001; Makdissy et al., 2005).

**Table 5.10**  
**Modification of the roughness (Ra and Rq [RMS]) of Membrane A after filtration of the Scottsdale tertiary effluent and White River water**

Membrane A	Rq (nm)	Ra (nm)	Topographic AFM 2D image (White area = protuberance / Black area = Hollow)
<b>Virgin</b>	60.9	48.2	
	61.8	48.5	
Outer surface	54.2	41.2	
Scan 5×2.5 μm <sup>2</sup>			
<b>Scottsdale</b>	60.3	48.2	
	64.6	51.8	
Outer surface			
Scan 5×2.5 μm <sup>2</sup>			
<b>White River</b>	44.7	35.9	
	56.4	45.1	
Outer surface			
Scan 5×2.5 μm <sup>2</sup>			

In the case of Membrane B, originally very smooth as compared to the Membrane A, the filtration of all waters generates an increase of the roughness of the membrane (Table 5.11).

**Table 5.11**  
**Modification of the roughness (Ra and Rq [RMS]) of Membrane B after filtration of the Scottsdale tertiary effluent and White River water**

Membrane B	Rq (nm)	Ra (nm)	Topographic AFM 2D image (White area = protuberance / Black area = Hollow)
Virgin  Outer surface Scan 5×2.5 μm <sup>2</sup>	5.7	3.9	
Scottsdale  Outer surface Scan 5×2.5 μm <sup>2</sup>	11.6 14.1	9.1 10.4	
Tampa Bay  Outer surface Scan 5×2.5 μm <sup>2</sup>	41.4 43.1	32.5 34.7	
White River  Outer surface Scan 5×2.5 μm <sup>2</sup>	9.5 9.9 11.7	7.5 8.0 8.9	

The increase remains small for the Scottsdale tertiary effluent and White River water; however, for the former and to lesser degree for the latter, small nodules were observed by AFM (20-40 nm height; 200-300 nm width). A larger increase of the roughness was observed with the Tampa Bay water with the presence of tiny particles (40-50 nm height; 10-20 nm width) swept off by the tip during scanning. The much greater roughness increase for the post-backwash Tampa Bay sample correlates with the greater hydrophobicity (contact angle) but not with post-filtration flux. Although not shown in Table 5.9, post-backwash flux for Tampa Bay is much higher than post-filtration flux for White River water and Scottsdale effluent, suggesting that, for humic-dominated source waters like the Tampa Bay water, backwash is effective in displacing the NOM that causes flux loss, but leaves behind foulants that cause both increased surface roughness and hydrophobicity.

### ***Streaming Potential and Isoelectric Point***

Table 5.12 lists the streaming potential and IEP of the bench-scale fouled modules. For all cases the reduction in permeability, i.e., membrane fouling, corresponds to a decrease of the streaming potential and an increase of the iso-electric point. These parameters are more related to fouling phenomenon inside the porosity of the membrane; however, as we observed for the AFM results, the filtration of the Tampa Bay WTP influent has a significant impact on the membrane properties. This observation is not in accordance with the reduction in permeability (see Table 5.9).

**Table 5.12**  
**Streaming potential and iso-electric point**  
**of Membrane A and B bench-scale fouled modules**

Membrane	Feed water	SP (mV/kPa) KCl = 3. 10 <sup>-4</sup> M pH: 6.5			
		IEP		Virgin	Fouled
A	Tampa Bay WTP influent	- 65 ± 5	- 11.4	<2.5	3.2 ± 0.5
A	White River water (Indianapolis)	- 65 ± 5	- 65 ± 5	<2.5	3.2 ± 0.5
A	Scottsdale effluent	- 65 ± 5	NM	<2.5	<2.5
B	Tampa Bay WTP influent	- 80 ± 5	- 40 ± 5	<2.5	5 ± 1
B	White River water (Indianapolis)	- 80 ± 5	- 50 ± 5	<2.5	3 ± 0.5
B	Scottsdale effluent	- 80 ± 5	- 35 ± 5	<2.5	3.5 ± 0.5

NM: not measured

## Pyrolysis GC/MS

Pyrolysis GC/MS analyses were conducted directly on fouled fibers by inserting small pieces of hollow fiber in the quartz tube introduced into the pyrolyser. The temperature of pyrolysis did not exceed 400° C to avoid the combustion of the membrane and consequently the presence of numerous and large peaks in the chromatograms. Results were poor with little evidence of the presence of foulants. However, this result was expected due to the small quantity (i.e., membrane surface) introduced into the pyrolyser. Figure 5.44 shows the pyrochromatogram of the pyrolysis of Membrane B fibers from the Tampa Bay pilot. The major peaks are membrane derivatives; however, tracers of foulant (i.e., furfural, methyl furfural produced from polysaccharides, and methyl pyrrole from proteins) were detected.

## HOLLOW-FIBER UNIT 2

During Hollow-Fiber Unit 1 experiments, TMP values were recorded over time during flushing of the membrane with Milli-Q water and during the experiment. The “clean water TMP at the start of the experiment” was determined by averaging the pressure values during the last 30 minutes of the preparation of the membrane module. The data were plotted using the following standardized method:

- The x-axis is represented by the volume permeated through one square meter (m<sup>2</sup>) of membrane area. This value is calculated from the time after starting the experiment, using the membrane area and the (constant) flow value.
- The y-axis is represented by normalized specific flux, or  $J_s/J_{s0}$ .

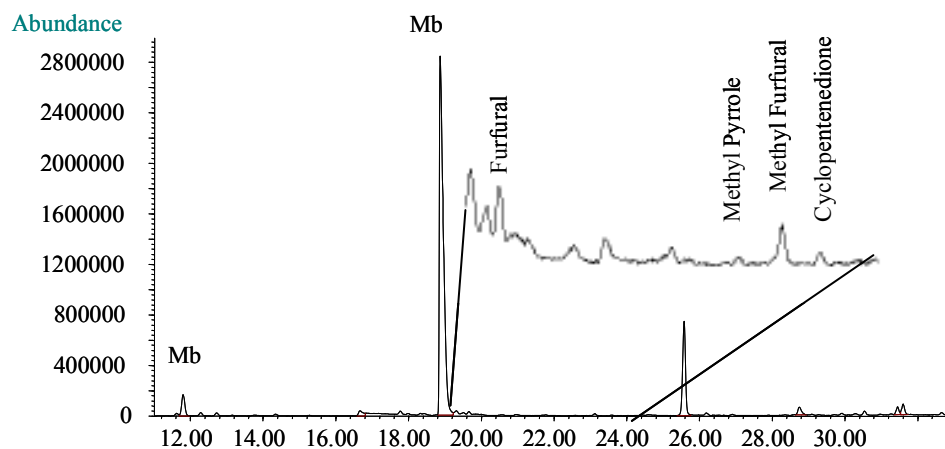


**Figure 5.44 Pyrochromatogram of the hollow fiber harvested from the bench-scale module fed with Tampa Bay WTP influent**

### Comparison of fouling rate of Membrane C on different source waters

The four Tier 1 source waters were tested with Membrane C. Figure 5.45 shows the results of one experiment of each water type. Appendix C also presents this and other figures in this section with duplicate runs. For Indianapolis, only one experiment was carried because of insufficient water volume. During this single run, air bubbles were observed in the test apparatus at the start of the experiment, which may have impacted the fouling curve. The testing protocol was refined for subsequent runs to prevent air entrainment in the equipment during the experiment.

The fouling rate was lowest for the Scottsdale effluent, increasing with the Twente Canal and the Indianapolis waters, and highest for the Tampa Bay water. Multi-cycle fouling experiments were not conducted with Hollow-Fiber Unit 1 using Membrane C; however, the  $UMFI_R$  values for the single-cycle tests show reasonably good correlation to these results. As shown in Figure 5.21, hydraulically reversible fouling rate was highest for Tampa Bay water and lowest for Indianapolis water, with both Twente Canal and Scottsdale waters intermediate.

### Comparison of fouling rate of different membranes on Twente Canal water

Each membrane type was tested using a common source water (Twente Canal water). The resulting fouling curves are shown in Figure 5.46.

The two PVDF-membrane types (Membranes A and B) exhibited nearly identical fouling rates. In contrast, fouling rates of the two PES membranes (C and D2) are quite different. This is most likely due to a difference in material composition (PVP/PES versus PES only). Because contact angles of the feed surface of these membranes could not be directly measured, it cannot be determined if the fouling rate was influenced by differences in contact angle. However, this is suspected because PVP is a hydrophilizing agent. Both membranes have a comparable IEP.

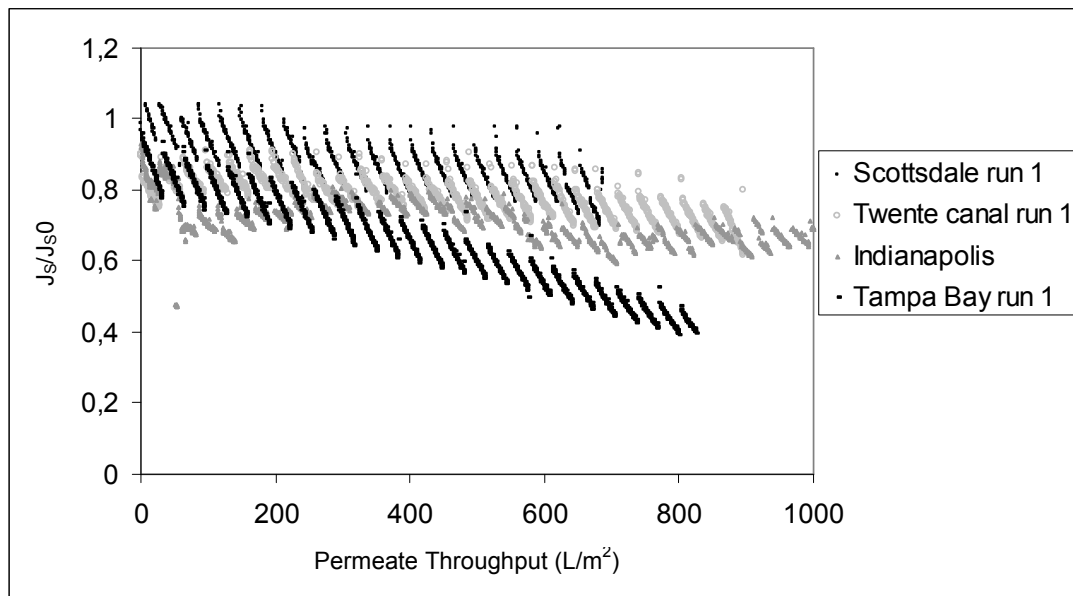
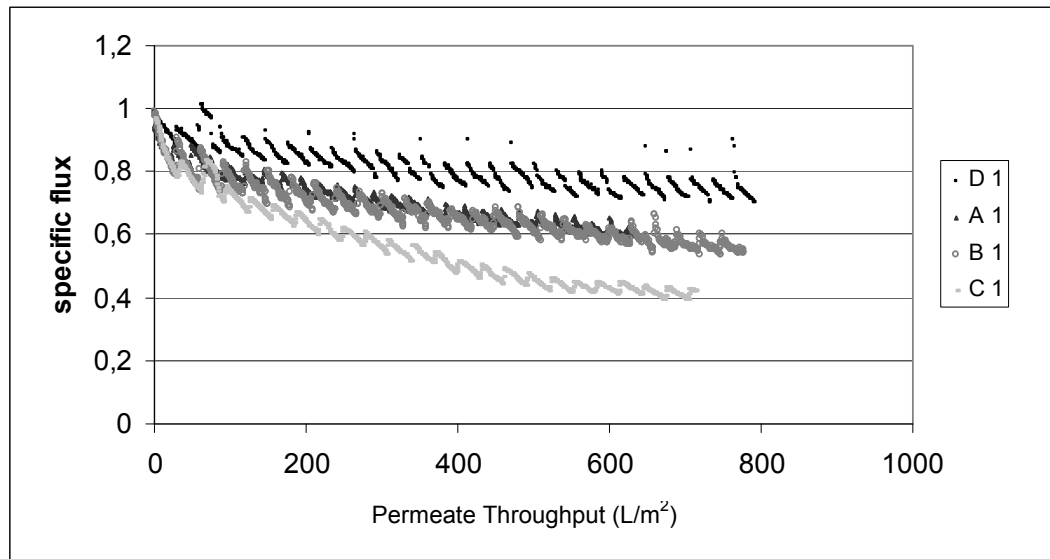


Figure 5.45  $J_s/J_{s0}$  for Membrane C treating the four Tier 1 source waters



**Figure 5.46  $J_s/J_{s0}$  as a function of the permeated volume through four different ultrafiltration membranes with Twente Canal water. (See Table 3.3 for membrane designation).**

#### **Impact of coagulation on fouling rate – Membrane C**

The effect of coagulation with different doses of ferric chloride on the fouling properties of Membrane C treating Twente Canal water is shown in Figure 5.47. Coagulation is beneficial up to a certain dose, after which it increases fouling. This threshold effect most likely results from (1) coagulation of fouling NOM moieties at low dose and (2) increased fouling from high solids loading at high dose. From the data in Figure 5.47, the fouling rates were calculated from the averaged slopes of the curves (Table 5.13). These fouling rates were plotted against the iron dose to determine the optimum iron dose for NOM fouling reduction (Figure 5.48). There appears to be a clear optimum dose at 2.5 mg Fe/L. At this concentration, irreversible fouling was minimal (Figure 5.48).

It should be noted that the solution pH was not controlled during the pre-coagulation experiments and decreased with increasing ferric dose (Table 5.13). Consequently, it cannot be determined if solution pH had a beneficial or detrimental impact on fouling rate.

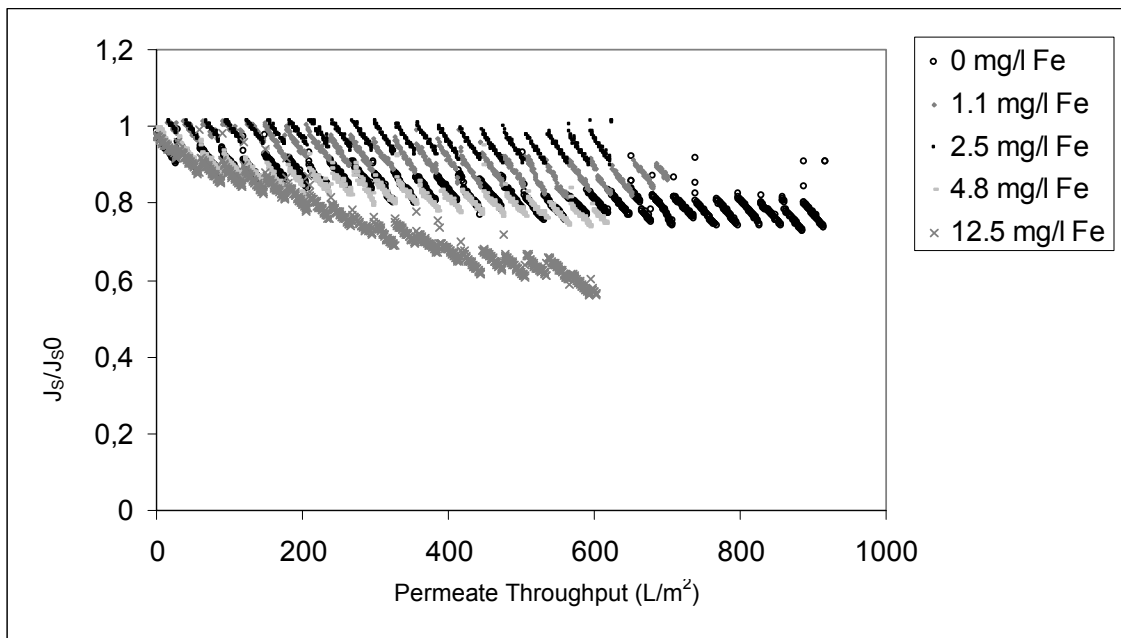


Figure 5.47  $J_s/J_{s0}$  of Membrane C as a function of the permeated volume of Twente Canal water coagulated with different dosages of  $FeCl_3$

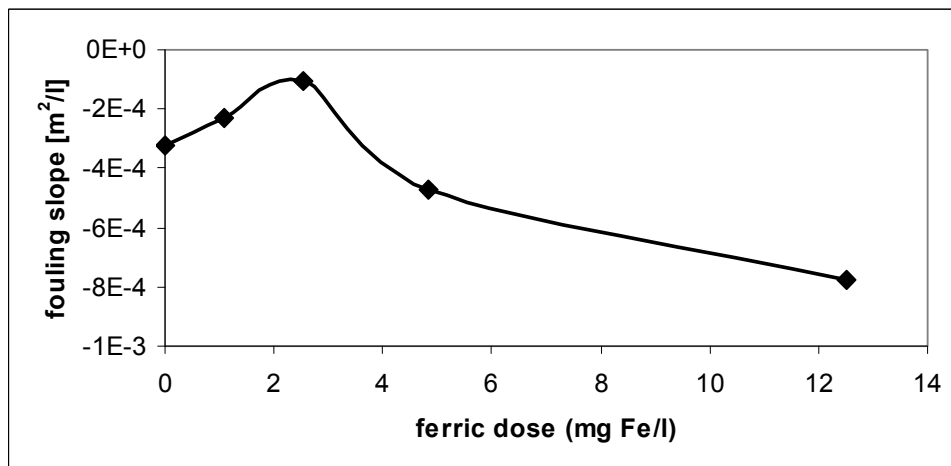


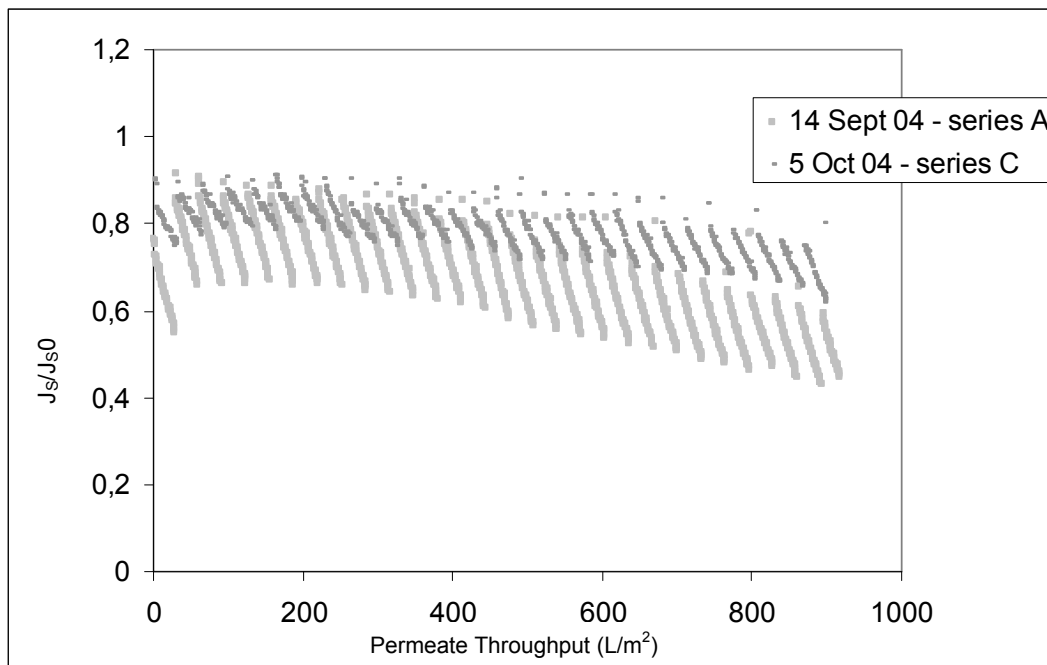
Figure 5.48 Fouling slope as a function of the iron dose

Table 5.13  
Iron dose, fouling slope calculated from Figure 5.47, and pH

Dosage (mg/L Fe)	Fouling slope ( $m^2/L$ )	pH (-)
0.00	-3.20E-4	8.02
1.09	-2.28E-4	7.63
2.53	-1.03E-4	7.39
4.83	-4.69E-4	7.08
12.50	-7.76E-4	6.55

## Impact of changing source quality on fouling

Samples of Twente Canal water were collected from September 2004 through April 2005 (a 7-month period) and filtered using Membrane C. In each experimental series (listed in Table 3.4), a “standard” experiment was carried out with Twente Canal water and Membrane C. Figure 5.49 illustrates the impact of sampling date on membrane fouling rate. Two samples, collected 3 weeks apart, show measurable differences in membrane flux decline rate over a permeate throughput of 900 L/m<sup>2</sup>. The September sample produced a higher rate of flux decline than the October sample. Further, a comparison of filtration curves in Figure 5.49 and Figure 5.50, which present curves for samples collected in winter and spring, shows a much greater initial flux decline for the summer and fall samples. Based on historical data for the Twente Canal, it is known that NOM levels are highest in the spring and summer. Although the fall samples showed higher initial flux decline, the spring sample shows the highest rate of irreversible flux decline.



**Figure 5.49  $J_s/J_{s0}$  of Membrane C as a function of the permeate throughput of Twente Canal water sampled on September 14 and October 5, 2004**

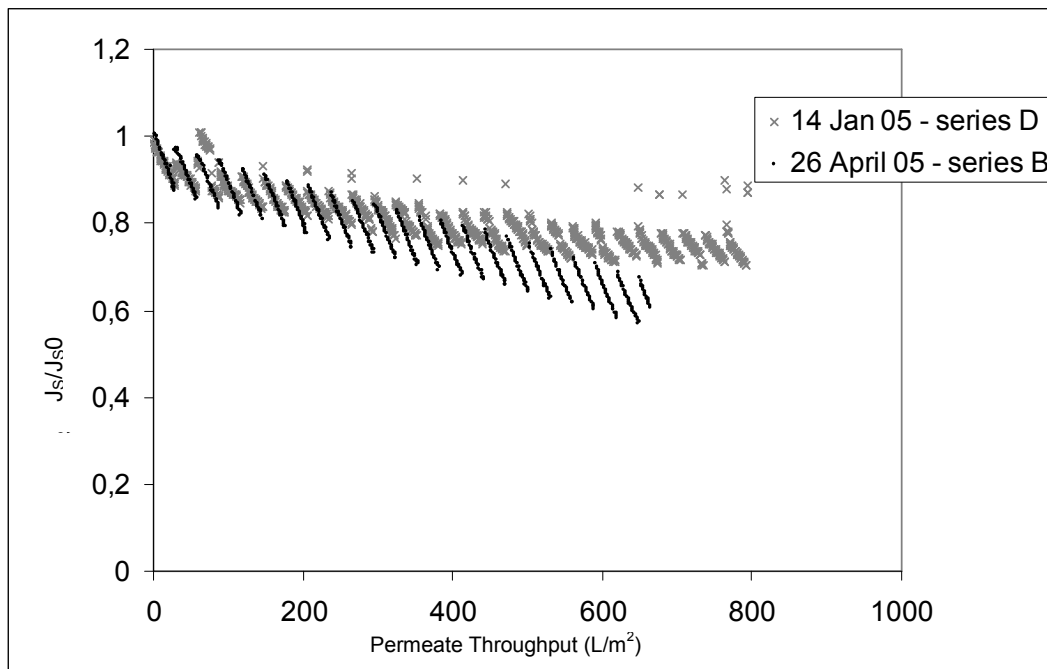


**Figure 5.50  $J_s/J_{s0}$  of Membrane C as a function of the permeate throughput of Twente Canal water sampled on January 14 and April 26, 2005**

### DOC characterization

During the experiments with the four membrane types, samples were collected for SEC-DOC/UV measurements. Three different samples were collected: feed water, permeate, and backwash. In all of the experiments, the transmembrane pressure after the collection of a backwash sample for 8 minutes was lower than the transmembrane pressure just prior to backwash. This illustrates that a significant portion of the foulant was removed through backwashing. However, complete reversal of TMP increase was not achieved indicating that some of the fouling was not hydraulically reversible.

Figures 5.51 through 5.54 present the SEC-DOC/UV chromatograms from filtration of Twente Canal water with all four membrane types (Series B). Figure 5.55 shows the chromatogram for Membrane C filtration of Twente Canal water (from Series C), but with duplicate backwashing.

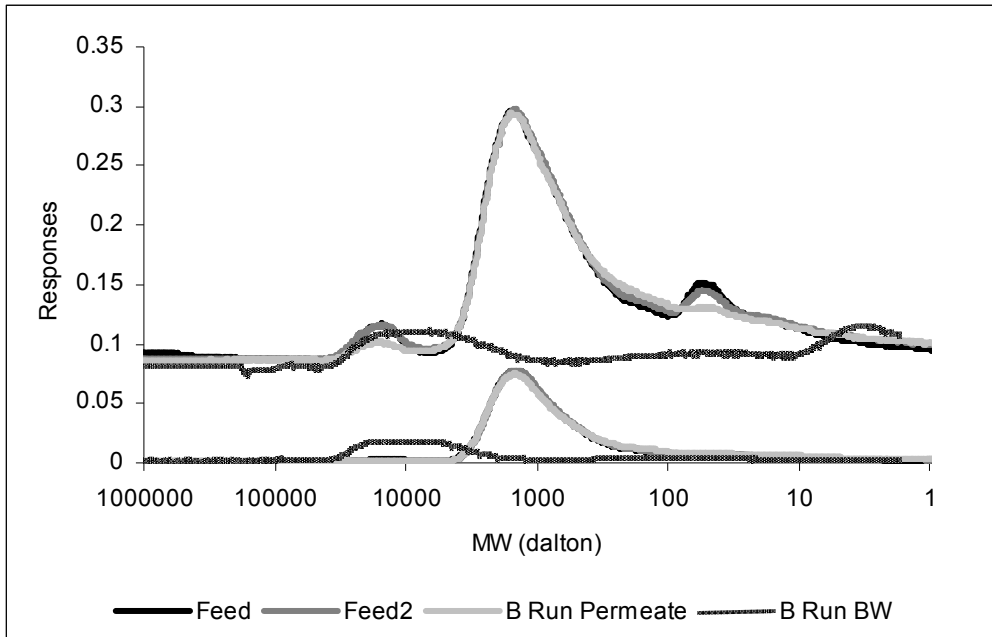


**Figure 5.51 SEC-DOC/UV chromatograms for Twente Canal filtration with Membrane A (Series B)**

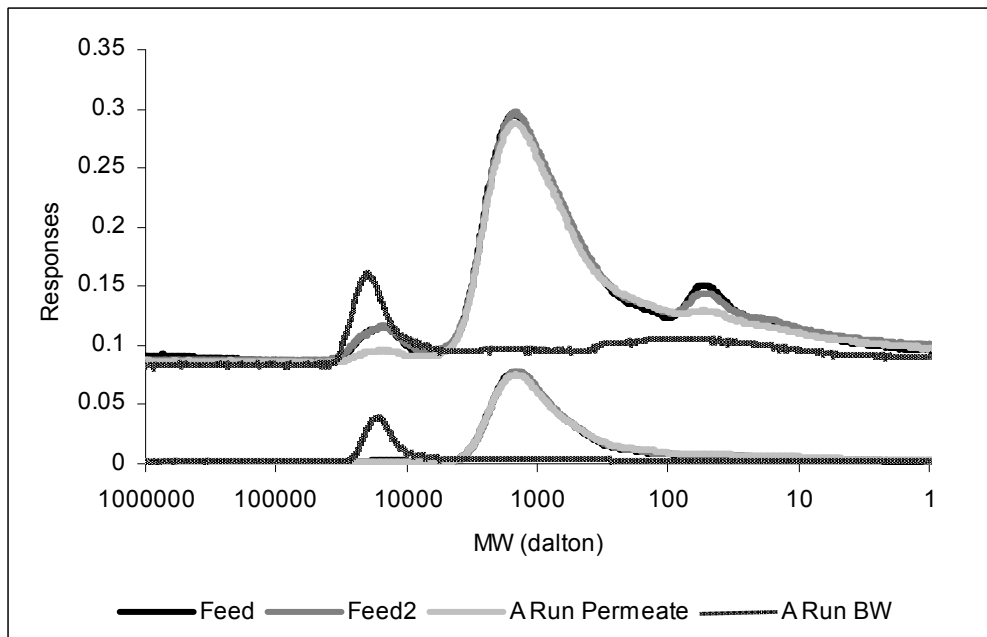


**Figure 5.52 SEC-DOC/UV chromatograms for Twente Canal filtration with Membrane B (Series B)**

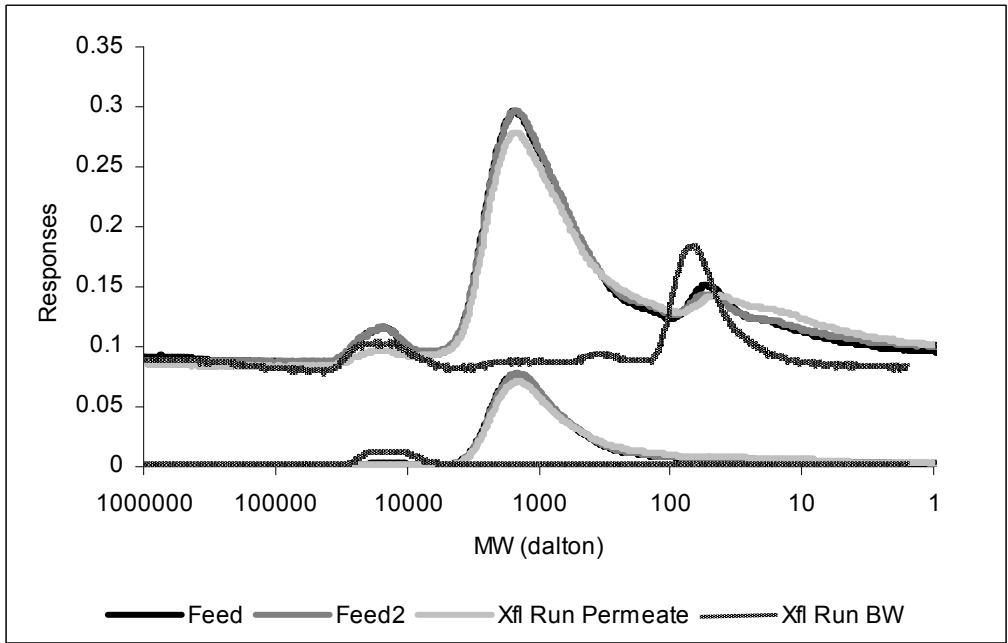


**Figure 5.53 SEC-DOC/UV chromatograms for Twente Canal filtration with Membrane C (Series B)**

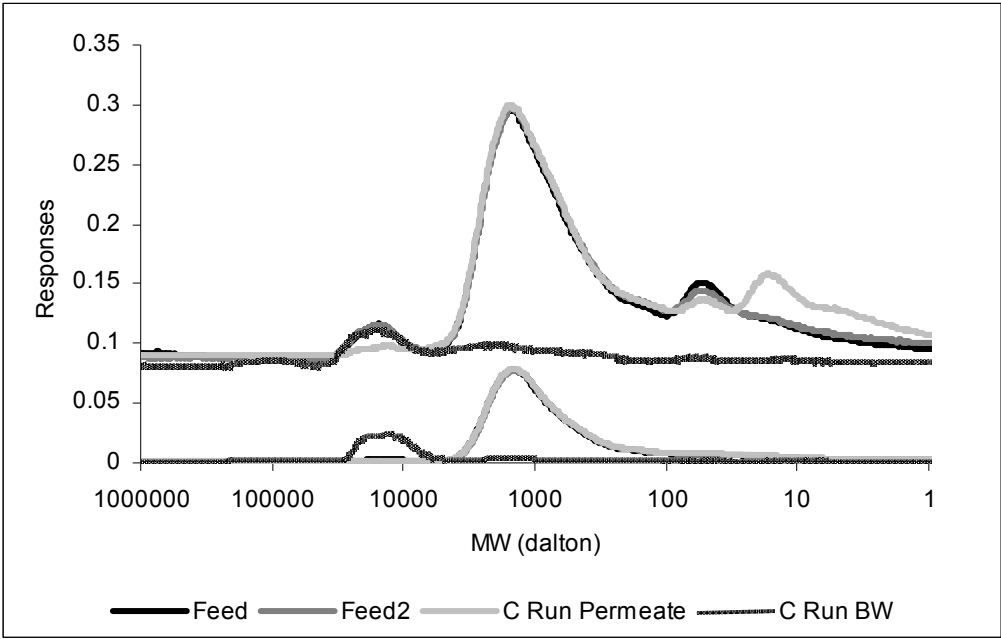


**Figure 5.54 SEC-DOC/UV chromatograms for Twente Canal filtration with Membrane D2 (Series B)**

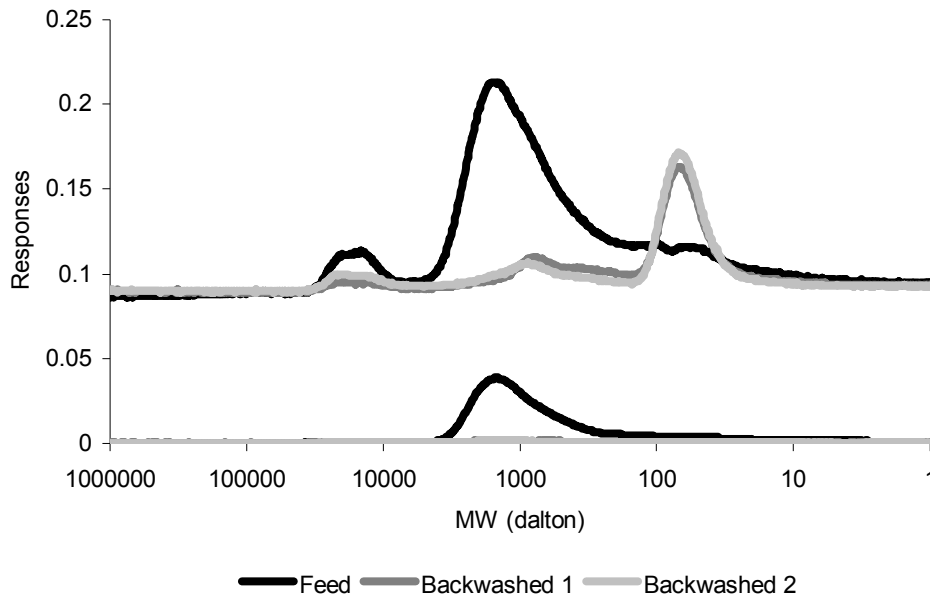


**Figure 5.55 SEC-DOC/UV chromatograms for Twente Canal filtration with Membrane C (Series C)**

As has been observed with the stirred-cell and Hollow-Fiber Unit 1 experiments, these figures show that the high MW fraction plays a dominant role in the membrane fouling process: With all membranes, a significant portion of the high MW NOM fraction is removed by the membrane during filtration (the difference between feed and permeate chromatograms). For Membranes A, B and D2, this fraction is elevated in the backwash water (relative to the feed), showing that the high MW NOM fraction is retained during filtration and displaced during backwash. The amount of the high MW fraction displaced during backwash varies by membrane type. It is highest for Membrane B shows the largest displacement and lowest for Membranes A and D2. This result is unexpected given that Membrane D2 has a smaller pore size and would be expected to retain more NOM. However, the two membranes do have different chemistry (PVDF versus PES) and this may explain the difference. For Membrane C, which has a slightly larger pore size, than Membrane D2, the high MW NOM fraction in the backwash water is less than in the feed, an unexpected result. Likewise, Membrane C backwash water contained an elevated level of the low MW fraction, a result not seen with the other membranes. This unique NOM backwash characteristic may be related to the presence of the PVP co-polymer in Membrane C.

## Conclusions

In this research, we established a protocol for fouling experiments with the Hollow-Fiber Unit 2 system. With this system, reproducible results were obtained. Further, the method is sensitive: experiments with different conditions give different fouling curves.

Pre-filtration of the raw water with a glass fiber filter (1.2  $\mu\text{m}$ , included in the protocol) removes part of the irreversible fouling components. Nevertheless, experiments with different conditions can still be compared, although it should be kept in mind that part of the fouling fraction (presumably the larger molecules) is not present in the feed water.

Both pre-filtered and raw Twente Canal water could be stored at 5° C without any change in water quality affecting the fouling during ultrafiltration.

The secondary effluent of the wastewater treatment plant at Scottsdale gives the least amount of fouling with Membrane C. Twente Canal and White River water (Indianapolis) result in slightly more fouling, and the fouling with Tampa Bay water with this membrane type is the worst.

Two different commercially available PVDF membranes (one MF, one UF) resulted in the same fouling rate. One of the PES-membranes (Membrane C) showed a lower fouling rate, while the other PES-membrane (Membrane D2) had a much higher fouling rate. Irreversible fouling was for all membranes caused by a fraction of DOC with a molecular size of approximately 20 kD. However, in the extended-backwash sample in the experiment with Membrane C, smaller-sized NOM (approximately 80 Da) was also found.

As expected, the water quality of the Twente Canal water, and probably of any surface water, changes during the seasons. In experiments in September and October 2004, there was a rapid drop in the specific flux at the start of the experiment, which cannot yet be explained.

The Hollow-Fiber Unit 2 system may be used for pre-treatment studies, which is shown by the Fe-dosage optimization curve.

Thus, experiments with the Hollow-Fiber Unit 2 system are inexpensive and prove to be useful in showing different fouling behavior under different conditions. This system may be used to compare water qualities or membrane types, or to study different pre-treatment options for a specific water type. If the water quality changes during the year, a quick optimization of the pre-treatment in several seasons may be useful.

## INTEGRATION OF BENCH-SCALE RESULTS VIA UMFI CONCEPT

Figure 5.56 presents a cumulative frequency plot\* of UMFI values resulting from the various filtration runs conducted with the stirred-cell unit, Hollow-Fiber Unit 1, and Hollow-Fiber Unit 2 systems.

The following observations were made regarding the data in Figure 5.56:

- The decrease in UMFI after backwash was implemented in the bench-scale runs clearly shows the difference in total fouling and hydraulically reversible fouling.
- There was a good correlation of hydraulically reversible fouling between the single-cycle and multi-cycle bench-scale runs.
- The total fouling measured by the flat-sheet surrogate was consistently less than the fouling of the hollow-fiber membranes runs, exhibiting a reasonable correlation with the hydraulically reversible fouling of the hollow-fiber bench-scale runs.

---

\*A general definition of cumulative frequency distribution is a plot of the number of observations falling in or below an interval.

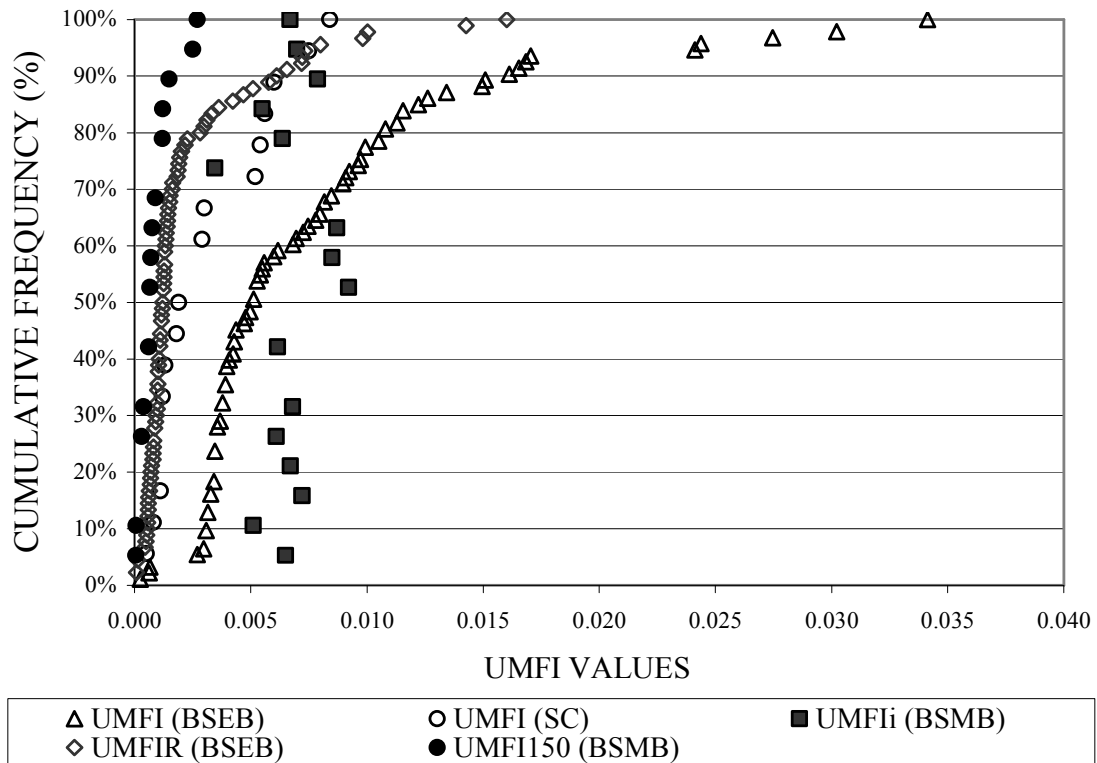


**Figure 5.56** Frequency distribution plot of bench-scale UMFI values

# CHAPTER 6

## PILOT- AND FULL-SCALE MEMBRANE FILTRATION RESULTS

### TIER 1 PILOT STUDIES

#### Tampa Bay Pilot Study

Eight separate runs were conducted with Membrane B during the Tampa Bay pilot study to evaluate the impact of different operating conditions and the contribution of NOM to membrane fouling. These impacts are discussed in the following sections. Refer to [Table 3.19](#) for a tabulation of the operating conditions used for each run. Unless otherwise indicated, all runs were conducted using a filtration period of 15 minutes, a backwash duration of 30 seconds, and a backwash flux equal to the filtration flux.

A baseline run (Run 1) was first completed to establish a flux that would provide a reasonable degree of specific flux loss after 6000–7000 L/m<sup>2</sup> permeate throughput. [Figure 6.1](#) presents the decline in normalized net specific flux over 13,000+ L/m<sup>2</sup> of permeate throughput where three different flux rates were evaluated. Based on these results, a flux of 90 L/m<sup>2</sup>-hr (53 gfd) at 95 percent feed water recovery was selected to represent baseline conditions. The curve is characterized by a moderate and fairly linear loss of specific flux compared to the curves obtained with the other pilots.

Turbidity, TOC, and HPC values for feed water grab samples collected during Run 1 are also shown on [Figure 6.1](#).

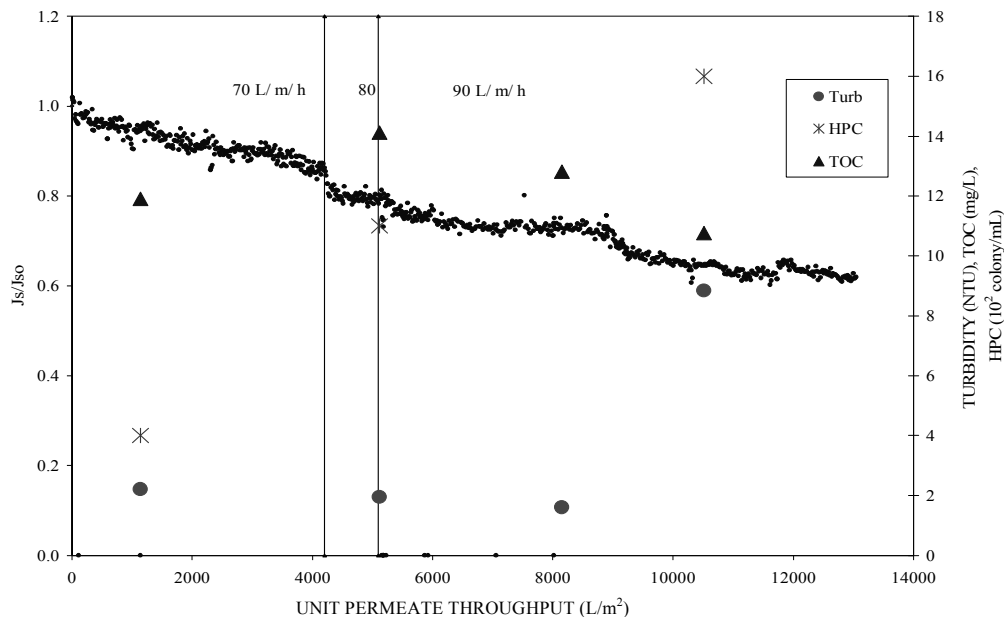


**Figure 6.1 Normalized net specific flux profile for Run 1 operated with raw water at 70, 80, and 90 L/m<sup>2</sup>-hr flux. Backwash every 15 min at the same flux as production. Recovery = 95 percent.**

### ***Effect of Backwashing (Comparing Runs 1, 2 and 3)***

Comparison of differences in the rate of decline in normalized net specific flux for Runs 1, 2, and 3 permit a determination of the impact of increased feed water recovery and increased backwash flow rate on fouling. Table 6.1 lists the significant operating parameters for Runs 1, 2, and 3. In Run 2, recovery was increased by decreasing duration of backpulse (permeate backwash). In Run 3, backpulse flow rate was increased and backwash duration decreased (relative to Run 1).

Table 6.2 shows water quality data associated with Runs 1, 2, and 3. The only significant changes in feed water quality between Run 1 and Runs 2 and 3 were a 33 percent decrease in the TOC, a 70 percent decrease in iron, and a 50 percent decrease in manganese. These changes were anticipated to reduce the degree of membrane fouling.

**Table 6.1**  
**Operating conditions for Runs 1, 2, and 3:**  
**baseline run and runs with variable backwash conditions**

Run no.	Flux (L/m <sup>2</sup> -hr)	Parameter evaluated	Backpulse duration (seconds)	Recovery (%)	Chemical wash type
1	70 - 80 - 90	Baseline	30	95	none
2	90	Increased recovery	21	97.5	none
3	90	Increased back- wash flowrate	20	95	none

**Table 6.2**  
**Source water quality parameters during Runs 1, 2, and 3**

Parameter	Unit	Run 1	Run 2	Run 3
Temperature	° C	25.1	22.8	22.1
pH	su	7.4	7.7	7.72
Turbidity	NTU	3.70	2.75	2.71
Conductivity	µS	384	517	554
Alkalinity	mg/L as CaCO <sub>3</sub>	80	114	97
Hardness	mg/L as CaCO <sub>3</sub>	154	184	188
UVA	cm <sup>-1</sup>	0.558	0.316	0.301
TOC	mg/L	12.40	8.25	8.18
Calcium	mg/L as CaCO <sub>3</sub>	123	150	140
Color	pcu	124	80	60
Iron total	mg/L	0.316	0.123	0.141
Iron (dissolved)	mg/L	0.182	0.050	0.042
Manganese (total)	mg/L	0.021	0.011	0.0097
Manganese (dissolved)	mg/L	0.009	0.004	nd
HPC	colonies/mL	1033	nd	480

Figure 6.2 shows the normalized net specific flux profile for Runs 1, 2, and 3.

Increased feed water recovery (Run 2) increased the fouling rate during most of the run (throughput from 0 to 4000 L/m<sup>2</sup>, operating time from 0 to 30 hours). After a throughput of 4000 L/m<sup>2</sup>, the specific flux of Runs 1 and 2 are similar. Although the fouling rate at a higher feed water recovery is more rapid initially, the degree of flux loss at the end of the run (6100 L/m<sup>2</sup> throughput) is very similar to that of the baseline run. This suggests that operating at a lower recovery provides only temporary benefit and that long-term benefits on the fouling rate for Membrane B with Tampa Bay water is marginal.

Increasing backwash flow (decreased backwash duration) resulted in a higher rate of flux decline, similar to that at a higher feed water recovery. From this, it can be concluded that backwash duration has more impact on fouling rate than backwash flow rate.

It should be noted that the increased fouling observed in Runs 2 and 3 occurred despite the reduced levels of feed water TOC, iron, and manganese.

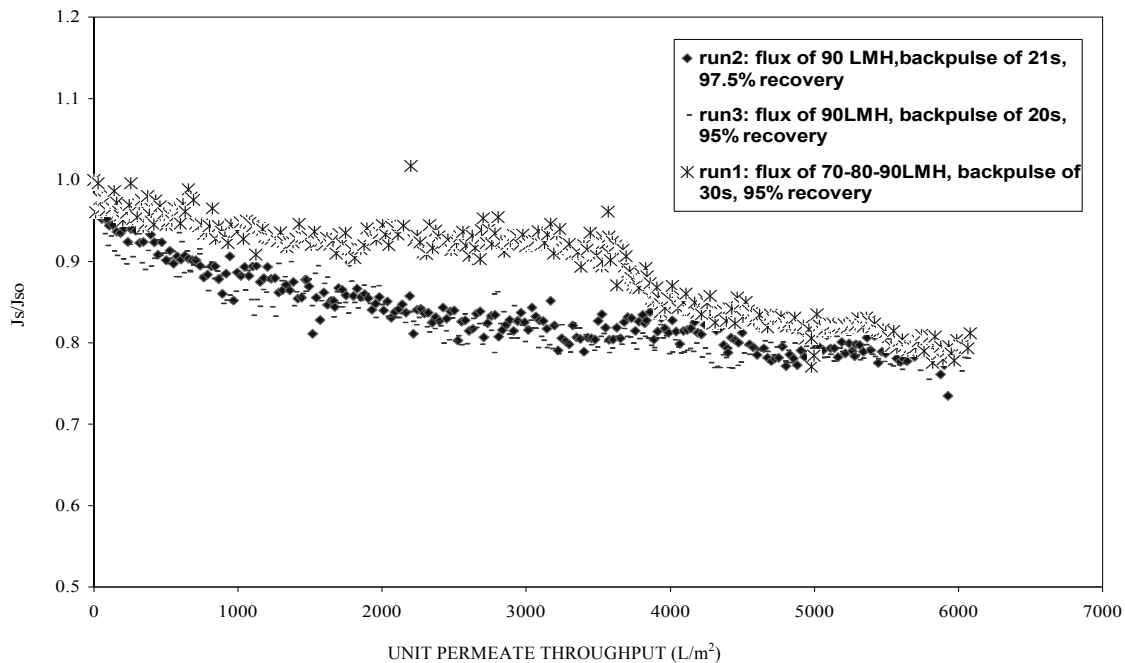


Figure 6.2 Normalized net specific flux profiles for Runs 1, 2, and 3

## Impact of Chemical Wash

The impact of different types of chemical washes on NOM fouling can be evaluated by comparing the flux decline curves from Runs 4, 5, and 9 with Run 1. [Table 6.3](#) lists the significant operating parameters for these four runs. During Runs 4, 5, and 9, a CW (as described in 3.5.2.1.1.2) was initiated every 24 hours of filtration.

In Run 9, the protocol changed slightly, as some muriatic acid was used to reduce the pH of the hypochlorite solution to avoid precipitation of CaCO<sub>3</sub>. The target pH for the citric acid wash was 2.2 (using a 2 percent-by-weight solution) and 10.5 for the sodium hydroxide wash. Run 9 included washes at four different CT conditions, as shown in [Table 6.4](#).

Feed water quality as measured from grab samples collected during the four runs are shown in [Table 6.5](#). NOM-related parameters for Runs 4, 5 and 9 are significantly lower than for Run 1, as are iron and manganese and, to a lesser extent, turbidity. Calcium is higher, however, for Runs 4 and 5.

[Figure 6.3](#) shows normalized net specific flux as a function of permeate throughput for Runs 1, 4, 5, and 9.

**Table 6.3**  
**Operating conditions for Runs 1, 4, 5, and 9: baseline run and runs with chemical wash**

Run no.	Flux (L/m <sup>2</sup> -hr)	Parameter evaluated	Backpulse duration (seconds)	Recovery (%)	Chemical wash type
1	90	Baseline	30	95	None
4	90	NaOH wash	30	95	Sodium hydroxide (NaOH)
5	90	Citric acid wash	30	95	Citric acid
9	90	NaOCl wash	30	95	Hypochlorite (NaOCl)

**Table 6.4**  
**CT conditions for Run 9 chemical washes**

NaOCl wash	First	Second	Third	Fourth
Contact time, min	2	30	2	30
Initial NaOCl Conc., mg/L	50	50	500	500
CT, mg/L-min	100	1500	1000	15,000

**Table 6.5**  
**Source water quality data for Runs 1, 4, 5, and 9**

Parameter	Unit	Run 1	Run 4	Run 5	Run 9
Temperature	° C	25.1	22.2	18.8	17.5
pH	su	7.40	7.81	7.80	8.19
Turbidity	NTU	3.7	1.77	1.95	2.24
Conductivity	µS	384	416	534	541
Alkalinity	mg/L as CaCO <sub>3</sub>	80	110	111	114
Hardness	mg/L as CaCO <sub>3</sub>	154	230	238	nd
UVA	cm <sup>-1</sup>	0.558	0.128	0.146	0.121
TOC	mg/L	12.40	5.36	4.84	4.38
Calcium	mg/L as CAaO <sub>3</sub>	123	180	200	69
Color	pcu	124	50	50	50
Iron (total)	mg/L	0.316	0.068	0.065	0.058
Iron (dissolved)	mg/L	0.182	0.024	0.014	0.015
Manganese (total)	mg/L	0.021	0.0076	0.0075	0.0058
Manganese (dissolved)	mg/L	0.009	0.0011	0.001	0.0007
HPC	colonies/mL	1033	nd	470	1000

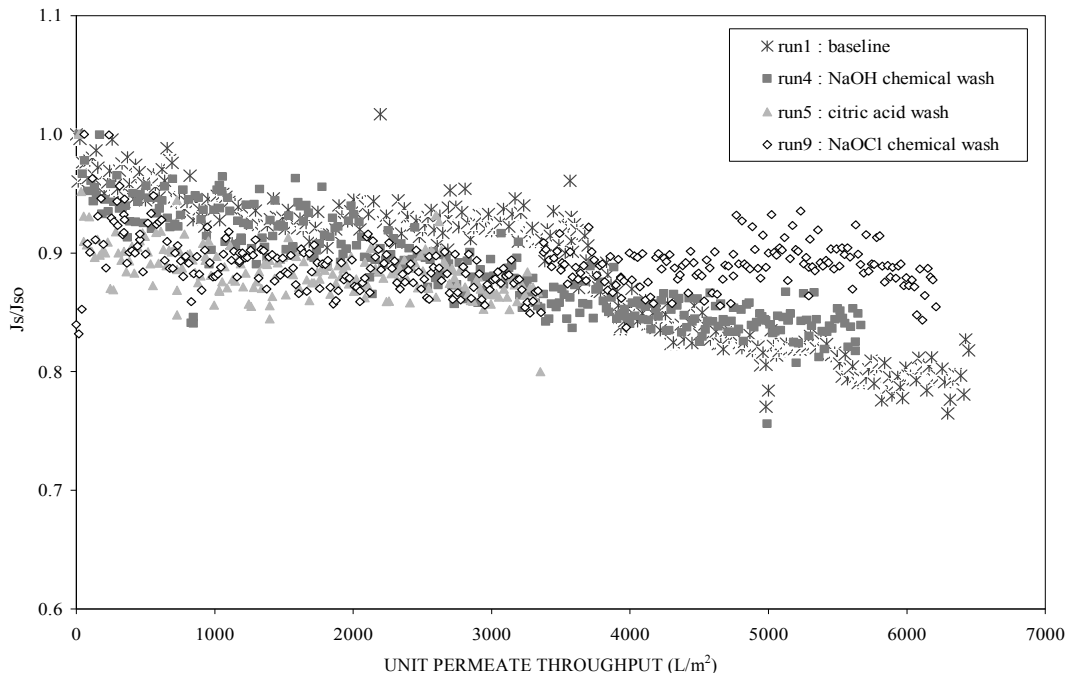


**Figure 6.3 Normalized net specific flux profile for Runs 1, 4, 5, and 9**

As there is no discernable difference in the rate of flux decline between Runs 1, 4, and 5, the use of NaOH and citric chemical washes was judged to have little benefit on the reduction of NOM fouling at the operating conditions employed. In contrast, the use of hypochlorite reduced flux decline, particularly in the latter portion of the run. The flattening of the curve after 4000 L/m<sup>2</sup> suggests that the hypochlorite was effectively oxidizing the NOM on the surface and in the pores of the Membrane B PVDF fibers. The benefit from the hypochlorite cannot be attributed to the lower feed water NOM concentration (compared to Run 1) because no improvement was seen in Runs 4 and 5 where the feed water quality was also improved.

***Impact of Coagulation***

During Runs 6, 7, and 8, the membrane feed water was dosed with ferric chloride with the intent to coagulate NOM and colloidal matter to reduce their fouling impact. In these tests, ferric sulfate was dosed at 25 mg/L, and the pilot unit operated at baseline conditions (Run 6), at decreased feed water recovery (Run 7), and with a daily phosphoric acid chemical wash. Table 6.6 shows the operating conditions for each the coagulated water runs along with Run 1. Table 6.7 presents the UF feed water during the coagulated runs. The data in Table 6.7 reflects the quality of the Tampa Bay water following coagulant addition. Relative to Run 1, NOM levels (as measured by TOC, UVA, and color), as well as iron and manganese, were lower.

Figure 6.4 shows the normalized net specific flux profile for Runs 1, 6, 7, and 8.

**Table 6.6  
Operating conditions for Runs 1, 6, 7, and 8: impact of coagulation**

Run no.	Flux (L/m <sup>2</sup> -hr)	Parameter evaluated	Filtration period (min)	Recovery (%)	Chemical wash type	Ferric sulfate concentration (mg/L)
1	90	Baseline	15	95	None	0
6	90	Baseline	15	95	None	25
7	90	Reduced recovery	7	90	None	25
8	90	Phosphoric acid wash	15	95	Phosphoric acid	25

**Table 6.7**  
**Source water quality data for Runs 6, 7, and 8**

Parameter	Unit	Run 6	Run 7	Run 8
Temperature	° C	21.9	18.4	17.5
pH	su	7.81	7.20	8.19
Turbidity	NTU	2.58	7.44	2.24
Conductivity	µS	583	420	541
Alkalinity	mg/L as CaCO <sub>3</sub>	118	84	114
Hardness	mg/L as CaCO <sub>3</sub>	ND	116	ND
UVA	cm <sup>-1</sup>	ND	0.086	0.121
TOC	mg/L	2.19	5.25	4.38
Calcium	mg/L as CaCO <sub>3</sub>	ND	170	ND
Color	pcu	35	30	50
Iron total	mg/L	ND	ND	0.058
Iron (dissolved)	mg/L	ND	0.012	0.015
Manganese (total)	mg/L	ND	0.017	ND
Manganese (dissolved)	mg/L	ND	0.012	ND
HPC	colonies/mL	ND	370	ND

\*ND = not detected

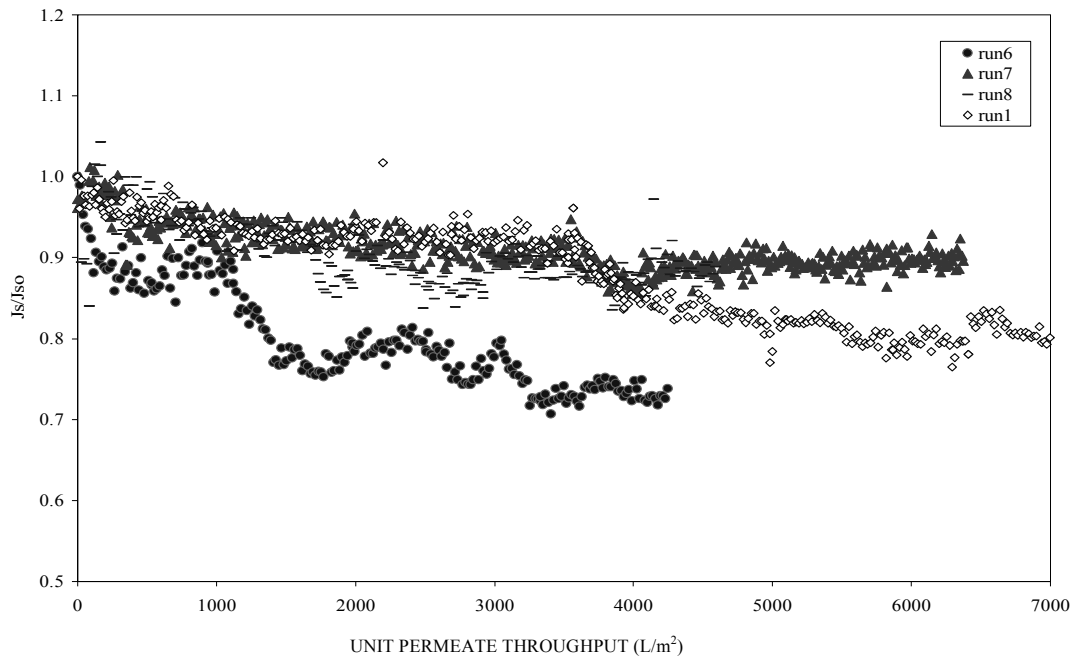


**Figure 6.4 Normalized net specific flux profile for Runs 1, 6, 7, and 8**

Rate of flux decline rate was significantly greater for Run 6 (with coagulant addition) than for Run 1 (without). The higher rate of fouling observed in Run 6 suggests that at high recovery (95 percent), the higher solids loading from coagulant addition was more dominant in determining fouling rate than any reduction that might have occurred from adsorption of soluble NOM onto the ferric hydroxide floc.

Reducing feed water recovery and solids loading during the filtration period (Run 7) dramatically reduced the rate of fouling, indicating that NOM adsorption onto the ferric hydroxide is an effective means to reduce NOM fouling, provided that solids loading to the membrane module is managed. When a daily phosphoric acid chemical wash is utilized in conjunction with coagulation (Run 8), the wash is effective in controlling the adverse impact of higher coagulant (solids) loading, thereby allowing for NOM fouling reduction at high recovery.

### ***Bulk Sample NOM Characterization and Impact on Fouling***

As discussed in Sections 5.0 and 5.1, the Tampa Bay feed water has a very high DOC content, with a predominant hydrophobic (humic) fraction that produced a significant flux decline in the bench-scale experiments. As presented and discussed below, the NOM characterization and operational data from the pilot study also support this finding.

Figures 6.5 and 6.6 show SEC-DOC/UVA chromatograms from NOM present in samples collected during Run 1 (baseline run) and Run 7 (coagulation run). The chromatograms show that, of the three NOM fractions, (1) backwashing was most effective in displacing the high MW PS material accumulated on the membrane surface and (2) the level of (dissolved) PS and HS fractions is lower when the feed water is first coagulated.

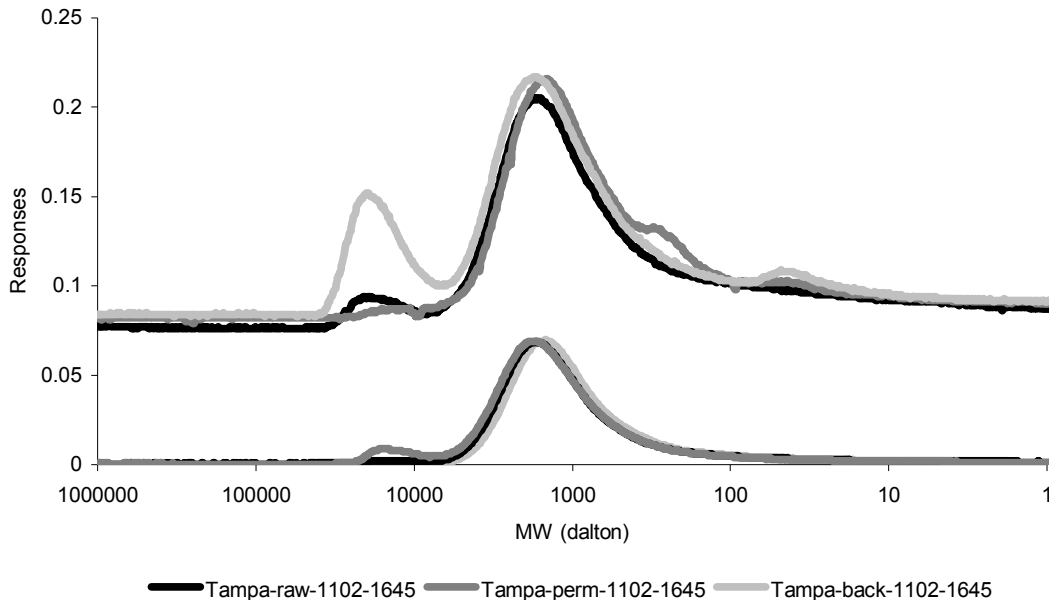


**Figure 6.5 SEC-DOC/UV chromatogram – filtration of Tampa Bay water with PVDF Membrane B (Run 1)**

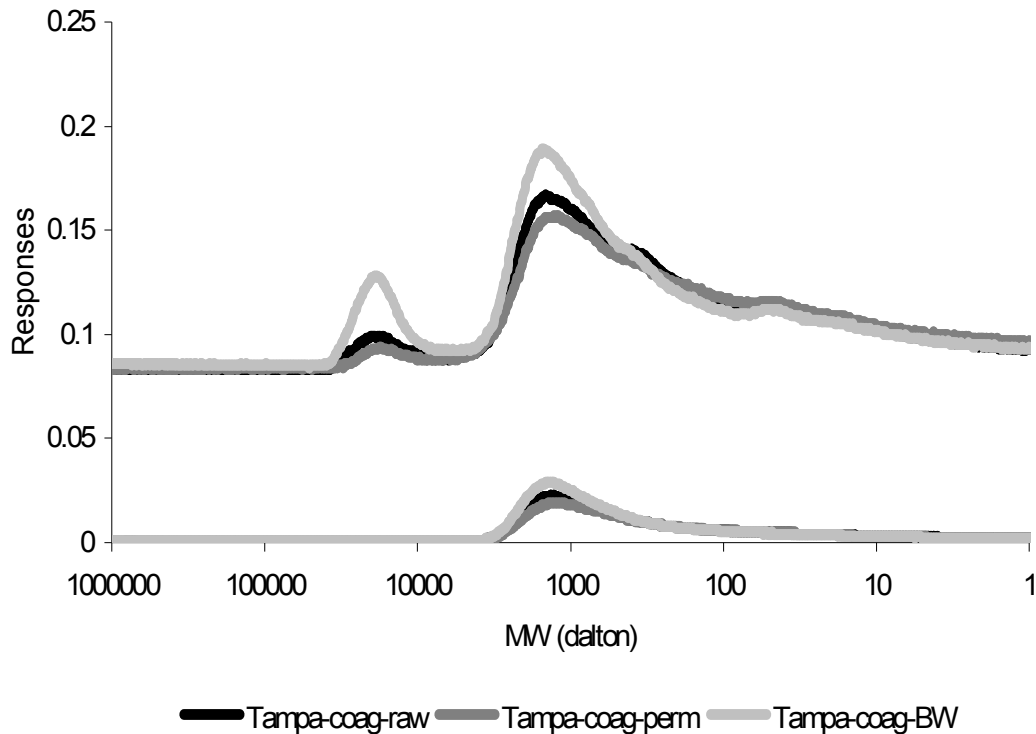


**Figure 6.6 SEC-DOC/UV chromatogram – filtration of coagulated Tampa Bay water with PVDF Membrane B (Run 7)**

Table 6.8 presents the DOC and NOM fractions (PS, HS, and LMA) present in the feed, permeate, and backwash samples collected during Runs 1 and 7. The data in Table 6.8 show the following:

- Although the smallest NOM fraction (by percentage of DOC), the PS is the fraction that is most highly retained by Membrane A (the difference between feed and permeate concentrations). Only five percent of the HS fraction is retained and none of the LMA fraction is retained.
- The PS is the most highly concentrated fraction in the backwash, indicating that backwashing is very effective for removing this fraction from the membrane surface.
- Coagulation removes a significant portion (75 percent) of the DOC, thereby reducing the amount of PS (and HS) material that is available to foul the membrane.

**Table 6.8**  
**Distribution of DOC and NOM fractions in feed, permeate, and backwash samples**  
**collected during Runs 1 and 7**

Run	Feed (mg/L)				Permeate (mg/L)				Backwash (mg/L)			
	DOC	PS*	HS*	LMA*	DOC	PS*	HS*	LMA*	DOC	PS*	HS*	LMA*
1 (Baseline)	14.4	0.5	11.3	2.6	14	0.5	10.7	2.9	18	3.1	12	2.9
7 (Coagulation, 25 mg/L Ferric)†	3.77	0.2	2.5	1.0	3.5	0.1	2.2	1.1	4.6	0.5	3	1.0

\*Values based on integration of SEC-DOC chromatogram peaks.

†Samples were filtered through a 0.45-micron filter prior to analysis.

These observations suggest that the PS fraction is primarily responsible for membrane fouling through accumulation at the membrane surface or in the membrane pores and that both coagulation and backwashing are effective in mitigating PS fouling. Backwash fouling mitigation was clearly demonstrated in Chapter 5 with the hollow-fiber bench-scale test. Reduction in fouling by coagulation was demonstrated in this pilot testing, provided that solids loading is not excessive.

### Indianapolis Pilot Study

During the pilot testing at Indianapolis, the impact of different operating conditions on NOM fouling with raw and coagulated water was similarly evaluated; however, testing was also conducted using clarified water. This resulted in a total of seventeen runs, not including a preliminary run. Test conditions for each run are shown in [Table 3.24](#). It should be noted that, for Runs 11 through 17, the clarified water serving as feed to the pilot unit was a blend of White River water and groundwater rather than only White River water.

The baseline run (Run 1) was conducted at 90 L/m<sup>2</sup>-hr (53 gfd) flux, feed water recovery of 95 percent, and a backwash frequency of 10 minutes. Normalized net specific flux decline for Run 1 is presented in [Figure 6.7](#). Feed water TOC and turbidity as measured from grab samples are also shown in the figure.

The flux decline curve for Run 1 is typical, with a higher rate of decline during the initial filtration period, becoming more gradual with increasing throughput. The peak in flux observed at a throughput of 3500 L/m<sup>2</sup> was caused by a brief shutdown (~2 hours) for pilot unit maintenance. To reduce the impact of this non-feed water quality/non-operational event, the flux curve was adjusted using a “smoothing” algorithm to better illustrate the degree of flux decline that would have occurred without the shutdown. The data points between 3200 and 3500 L/m<sup>2</sup> were discarded and data points after 3500 L/m<sup>2</sup> were smoothed by using the algorithm. The smoothed curve was used for more accurate comparison with other runs ([Figure 6.8](#)).

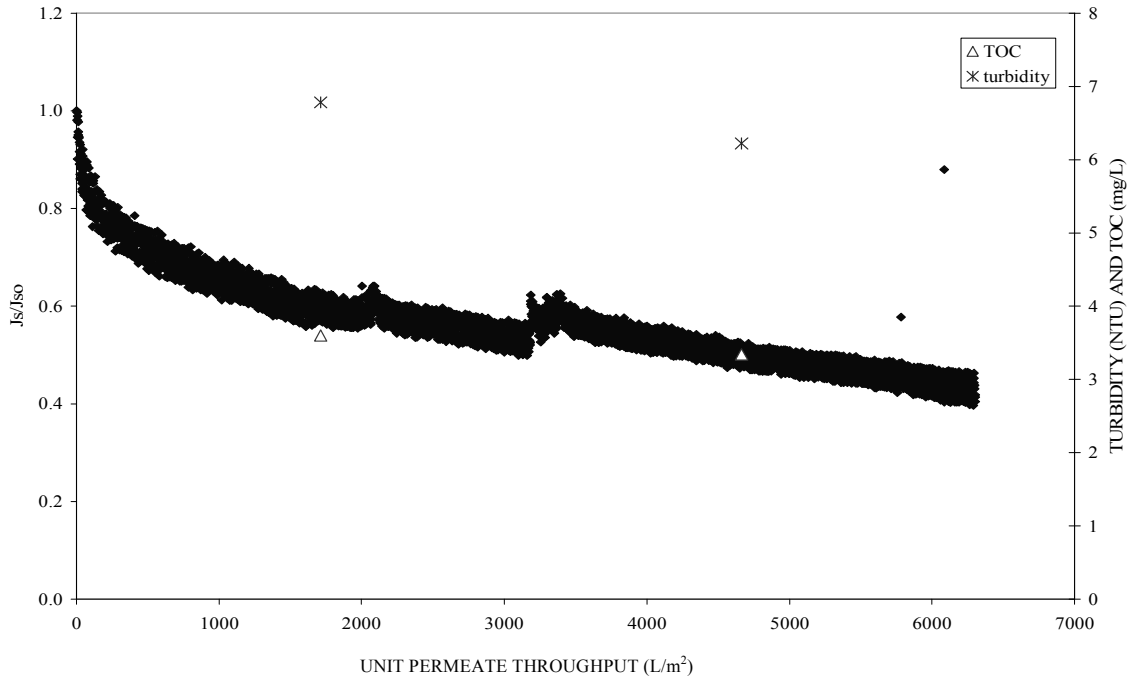


**Figure 6.7 Normalized net specific flux profile for baseline run (Run 1) operated with raw water at 90 L/m<sup>2</sup>-hr flux. Recovery = 95 percent.**

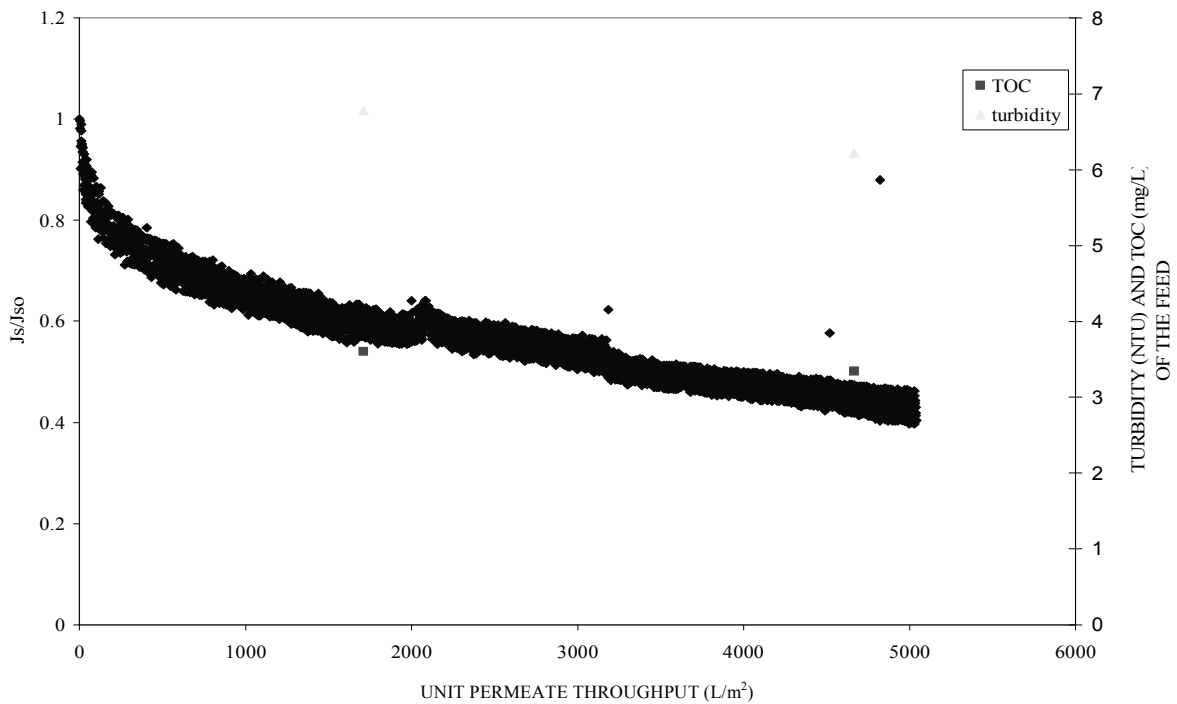


**Figure 6.8 Normalized net specific flux profile for Run 1 following data "smoothing"**

### ***Effect of Flux and Recovery***

A comparison of flux decline curves for Run 1 with those for Runs 2 and 3 illustrate the impact of flux and recovery, respectively, on fouling. The operating parameters for these three runs were as follows:

- Run 1: flux of 90 L/m<sup>2</sup>-hr, 95 percent recovery
- Run 2: flux of 110 L/m<sup>2</sup>-hr, 95 percent recovery
- Run 3: flux of 90 L/m<sup>2</sup>-hr, 97.5 percent recovery

Table 6.9 shows feed water quality during these runs. Quality was consistent for all three runs with the following exceptions: (1) algae count and alkalinity was significantly higher for Run 2 and (2) UVA was lower for Run 1. The higher algal count for Run 2 could have resulted in higher NOM fouling rate due to the presence of higher concentrations of soluble microbial products (SMP) NOM.

**Table 6.9**  
**Source water quality data during Runs 1, 2, and 3**

Parameters	Units	Run 1	Run 2	Run 3
pH	su	8.90	8.17	8.20
Total hardness	mg/L as CaCO <sub>3</sub>	316	335	331
Calcium	mg/L	79.5	85	82
Alkalinity	mg/L as CaCO <sub>3</sub>	219	345	238
True color	pcu	20	20	22.5
TDS	mg/L	384	421	455
Particle count	#/mL (particle size: 2-750 microns)	12900	11500	16600
Turbidity	NTU	6.5	7.55	4.21
TOC	mg/L	3.47	3.2	3.47
UVA	cm <sup>-1</sup>	0.092	0.2	0.179
Algae	count/mL	7600	22400	8400
Chlorophyll a	ppb	10.8	6.21	7.36
HPC	colonies/mL	2600	1100	4100
Iron (dissolved)	mg/L	< 0.02	0.061	0.02
Iron (total)	mg/L	0.33	0.28	0.23
Manganese (dissolved)	mg/L	< 0.02	<0.02	<0.02
Manganese (total)	mg/L	0.030	0.036	0.035

Figure 6.9 presents normalized net specific flux versus permeate throughput for Runs 1 through 3.

Higher recovery (longer backwash interval) operation increased fouling rate, most notably during the early portion of the run; with increased run time, the difference is less apparent. Operating at a higher flux also increased the initial fouling rate, however after 5000 L/m<sup>2</sup> throughput, the loss of membrane permeability is equivalent. Consequently, recovery appears to have a stronger impact on fouling than flux. This is not unexpected in that increasing recovery from 95 to 97.5 percent doubles the solids loading (particulate and dissolved matter) to the membrane modules, whereas the flux increase for 90 to 110 L/m<sup>2</sup>-hr only increases solids loading (particulate and dissolved matter) by 22 percent. Operation at either relatively extreme condition (for an outside-in flow configuration) did not result in a critical flux condition.

### ***Effect of Chemical Wash***

With Runs 4, 5, and 6, chemical washes were performed to assess impact on NOM fouling as follows:

- Run 4: citric acid wash at pH 2
- Run 5: caustic wash at pH 11 followed by a citric acid wash at pH 2
- Run 6: 50 mg/L hypochlorite wash acidified to pH 7

Table 6.10 shows feed water quality during these runs.

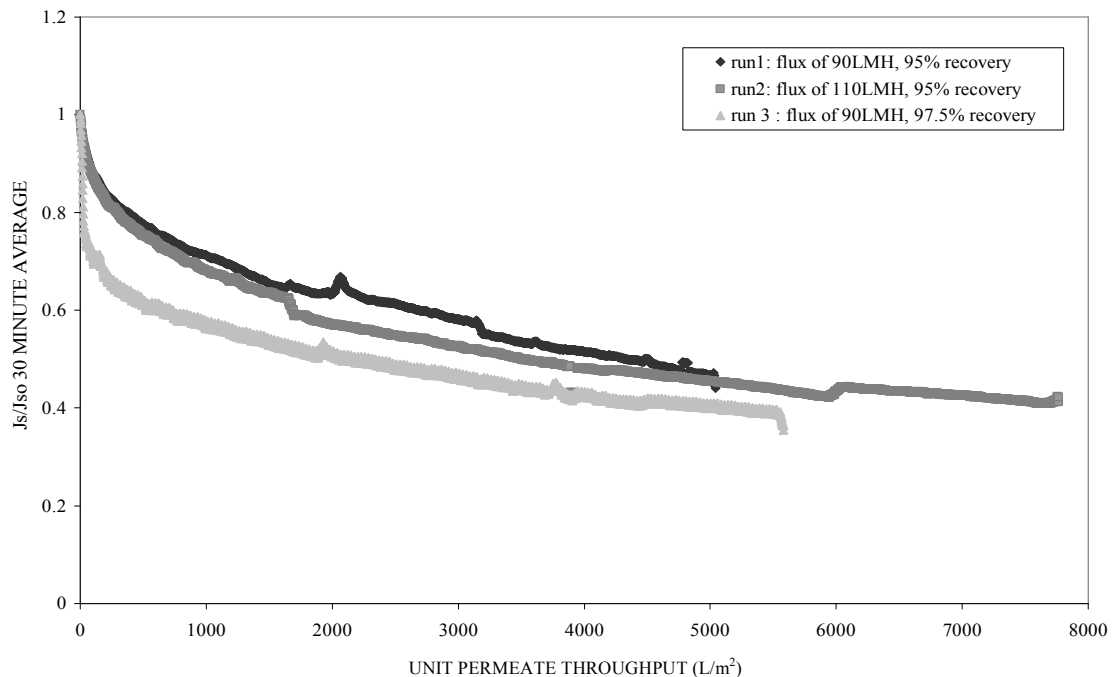


**Figure 6.9 Normalized net specific flux profile for Runs 1, 2, and 3**

**Table 6.10**  
**Source water quality data for Runs 1, 4, 5, and 6**

Parameters	Units	Run 1	Run 4	Run 5	Run 6
pH	su	8.9	8.0	8.1	8.0
Total hardness	mg/L as CaCO <sub>3</sub>	316	243	332	300
Calcium	mg/L	79.5	61.8	93	76
Alkalinity	mg/L as CaCO <sub>3</sub>	219	161	225	224
True color	pcu	20	67.5	20	38
TDS	mg/L	384	295	448	388
Particle Count	#/mL (size range: 2-750 microns)	12,900	11,600	11,800	8240
Turbidity	NTU	6.5	38	8.8	4.0
TOC	mg/L	3.47	4.6	3.4	3.7
UVA	cm <sup>-1</sup>	0.092	0.180	0.090	0.120
Algae	count/mL	7600	20,400	10,400	2,400
Chlorophyll a	ppb	10.8	13.3	9.04	2.57
HPC	colonies/mL	2600	4100	2100	3400
Iron (dissolved)	mg/L	< 0.02	0.02	< 0.02	< 0.02
Iron (total)	mg/L	0.33	1.9	0.49	0.49
Manganese (dissolved)	mg/L	< 0.02	< 0.02	< 0.02	< 0.02
Manganese(total)	mg/L	0.03	0.08	0.04	0.04

Figure 6.10 presents normalized net specific flux curves for Runs 1, 4, 5 and 6 as a function of permeate throughput.

The data in Figure 6.10 indicate that the caustic/acid and hypochlorite washes were beneficial and reduced the rate of fouling, while acid alone was not. To quantify these effects, percent recovery of flux from chemical wash was calculated. The calculation was made as follows:

$$J_{s\text{RECOVERY}} = (J_{s\text{CWA}} - J_{s\text{CWB}})/J_{s0} \times 100,$$

where:

$J_{s\text{CWA}}$  = average of  $J_s$  data for the 30 minutes after chemical wash

$J_{s\text{CWB}}$  = average of  $J_s$  data for the 30 minutes before chemical wash

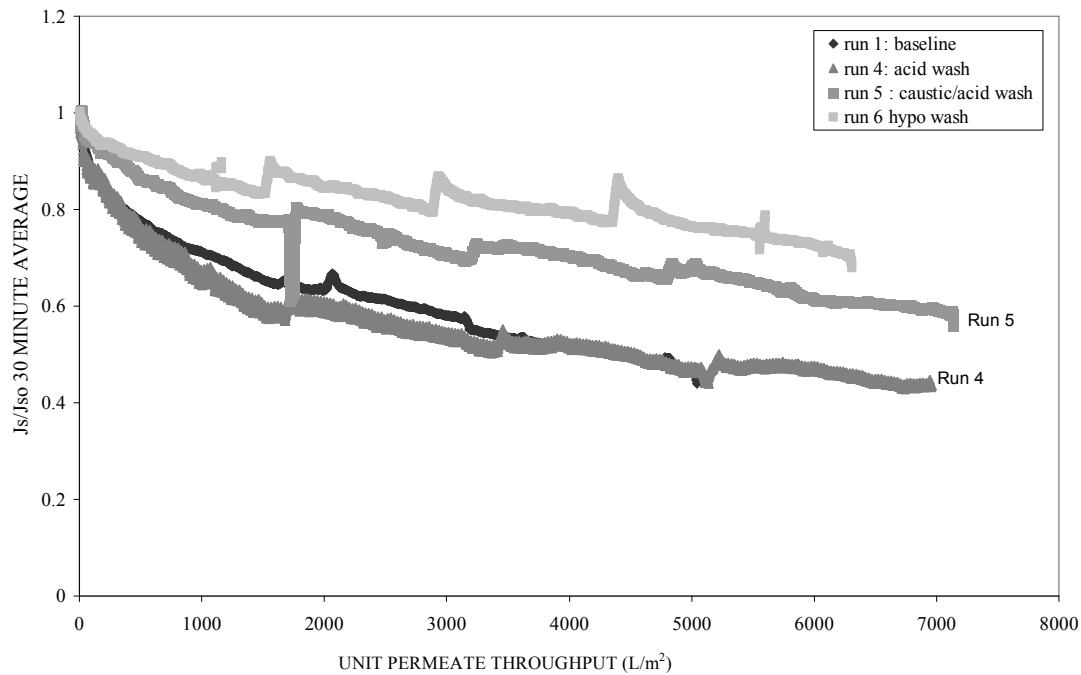


**Figure 6.10 Normalized net specific flux profile for Runs 1, 4, 5, and 6**

The hypochlorite wash (Run 6) is the most effective, exhibiting an average flux recovery of 7.6 percent. This can be partly explained by the fact that hypochlorite oxidizes algae and organics, in contrast to the two other chemical washes, which only solubilize inorganics (citric acid) and organics (caustic). The sequencing of caustic and acid washes proved more effective than acid alone. Normalized specific flux recovery increased to 3.1 percent on average. The acid wash (Run 4) appeared to have little benefit; however, feed water quality during this run was worse than during Run 1 (Figure 6.11 and Table 6.11). The higher fouling rate of Run 4 (relative to Runs 5 and 6) could be explained by the high TOC, turbidity, and algae count in the feed during this run. The total iron is also high, with the potential of precipitating as scale, which could foul the membrane more quickly.

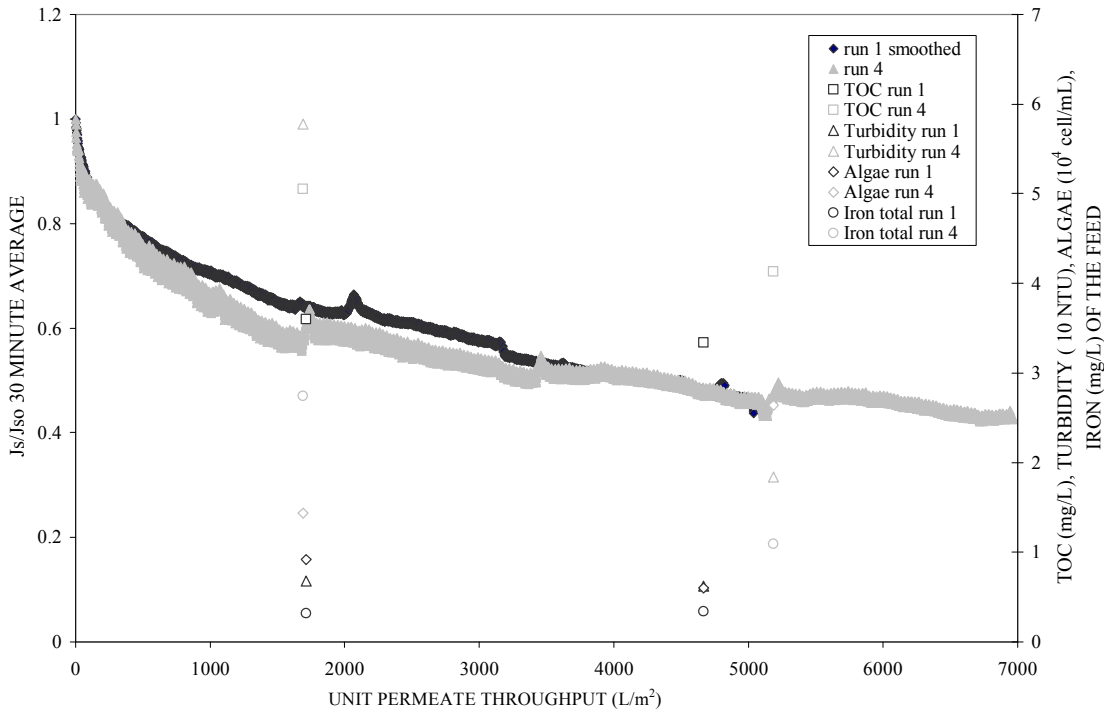


**Figure 6.11 Normalized net specific flux and fouling-related feed water quality parameters for Runs 1 and 4**

**Table 6.11**  
 **$J_{S0}$  recovery resulting from different chemical washes**

Run 4—citric acid wash			
	$J_{SCWB}$ (gfd/psi [L/m <sup>2</sup> -hr/kPa] @ 20° C)	$J_{SCWA}$ (gfd/psi [L/m <sup>2</sup> -hr/kPa] @ 20° C)	$J_{Srecovery}$ (%)
1st wash	6.58 (77.02)	7.04 (82.40)	2.6
2nd wash	5.72 (66.95)	6.21 (72.69)	2.8
3rd wash	5.44 (63.68)	5.71 (66.84)	1.5
Run 5—caustic/citric acid wash			
	$J_{SCWB}$ (gfd/psi [L/m <sup>2</sup> -hr/kPa] @ 20° C)	$J_{SCWA}$ (gfd/psi [L/m <sup>2</sup> -hr/kPa] @ 20° C)	$J_{Srecovery}$ (%)
1st wash	11.8 (138.12)	12.3 (143.97)	4.3
2nd wash	10.9 (127.58)	11.2 (131.10)	2.8
3rd wash	10.2 (119.39)	10.5 (112.90)	2.2
Run 6—hypochlorite wash			
	$J_{SCWB}$ (gfd/psi [L/m <sup>2</sup> -hr/kPa] @ 20° C)	$J_{SCWA}$ (gfd/psi [L/m <sup>2</sup> -hr/kPa] @ 20° C)	$J_{Srecovery}$ (%)
1st wash	9.33 (109.21)	10.03 (117.40)	6.3
2nd wash	8.81 (103.12)	9.7 (113.54)	8
3rd wash	8.68 (101.60)	9.61 (112.49)	8.4

The data in [Table 6.11](#) above show that the effectiveness of the acid and caustic/acid washes decreased as fouling progressed. However, it remained the same or improved for the hypochlorite wash.

### ***Effect of Coagulation and Sedimentation***

To ascertain the influence of these pretreatment processes on membrane fouling rate, a number of runs were performed using raw water that was either coagulated only or coagulated, flocculated, and settled (clarified) prior to membrane filtration. Pretreatment conditions are shown below and in [Table 6.12](#). Clarification was conducted using the full-scale WTP, whereas coagulation only was done at pilot scale.

- Run 7b: low dosage of alum (5 mg/L).
- Run 7c: medium dosage of alum (15 mg/L).
- Run 7a: high dosage of alum (30 mg/L, dose normally added at the WTP).
- Run 8: clarified water. Parameters of the clarification process at the treatment plant during Run 8 are shown in the [Table 6.12](#).

[Table 6.13](#) presents membrane feed water quality during the baseline run and four pretreatment runs.

[Figure 6.12](#) shows the profiles of the normalized net specific flux of Runs 1, 7a, 7b, 7c, and 8.

**Table 6.12**  
**Full-scale plant clarification conditions used during Run 8**

Run no.	Alum dose (mg/L)	Polymer dose (mg/L)	Sedimentation rate (L/min/m <sup>2</sup> )
8	78.1	0.258	13.9

**Table 6.13**  
**Source water quality data for Runs 1, 7a, 7b, 7c, and 8**

Parameters	Units	Run 1	Run 7a	Run 7b	Run 7c	Run 8
pH	su	8.90	7.10	8.02	7.92	7.09
Total hardness	mg/L as CaCO <sub>3</sub>	316	321	356	328	310
Calcium	mg/L	79.5	78.5	88.1	81.8	86.3
Alkalinity	mg/L as CaCO <sub>3</sub>	219	188	243	237	154
True color	pcu	20	20	22.5	35	27.5
TDS	mg/L	384	456	512	500	415
Particle count	#/mL (size range: 2-750 microns)	12,900	9000	7900	16,500	590
Turbidity	NTU	6.5	0.87	1.2	1.49	1.73
TOC	mg/L	3.47	3.4	3.3	3.4	4.15
UVA	cm <sup>-1</sup>	0.092	0.057	0.079	0.082	0.093
Algae	count/mL	7600	84,000	72,000	10,000	14,000
Chlorophyll a	ppb	10.8	ND*	4.26	3.64	(< 1 ppb)
HPC	colonies/mL	2600	4600	3100	860	173
Iron (dissolved)	mg/L	< 0.02	0.05	0.03	< 0.02	< 0.02
Iron (total)	mg/L	0.33	0.538	0.25	0.301	0.148
Manganese (dissolved)	mg/L	< 0.02	< 0.02	< 0.02	< 0.02	0.15
Manganese (total)	mg/L	0.03	0.026	< 0.02	< 0.02	0.183

\*ND = not detected

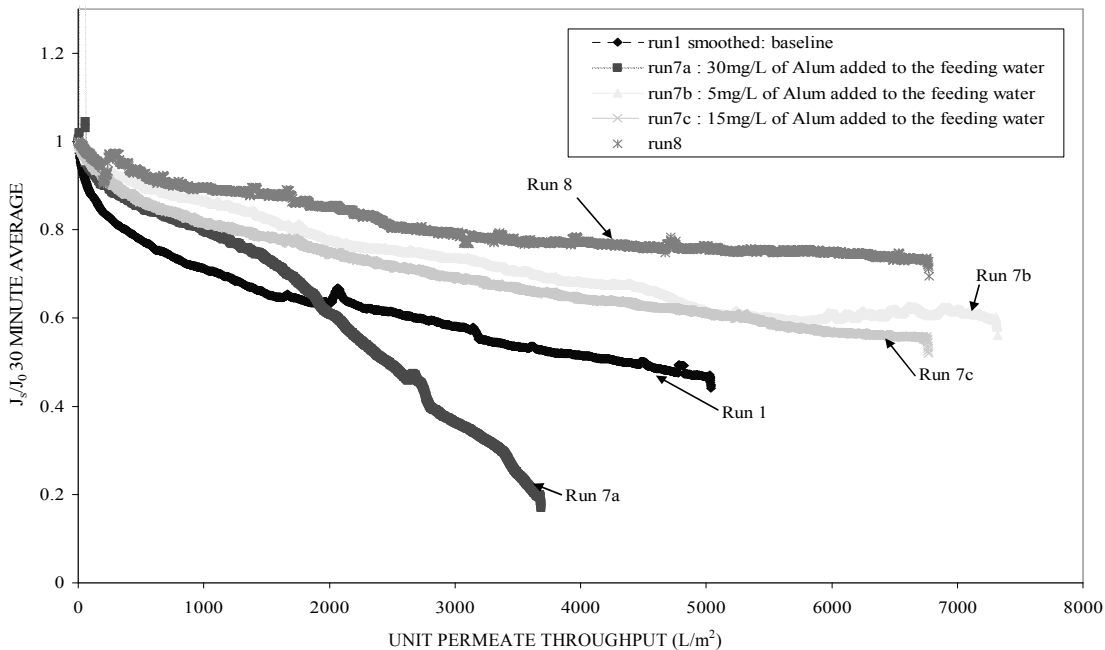


**Figure 6.12 Normalized net specific flux profile for Runs 1, 7a, 7b, 7c, and 8**

For Run 7a, the high alum dose caused a severe rate of fouling due to high solids loading, with specific flux declining by 80 percent after only 3700 L/m<sup>2</sup>. Based on the increasing rate of fouling with time, the critical flux was exceeded. Although the dose was only slightly higher than that used during the Tampa Bay pilot coagulation tests (25 mg/L), the fouling of the Membrane A modules was much more pronounced.

With lower alum doses used in Runs 7b and 7c, the fouling rate was reduced relative to the baseline. At these doses, the benefit of NOM adsorption was realized without the detrimental impact of higher solids loading.

By further reducing the solids loading through clarification, fouling rate was further reduced, indicating that optimal fouling control is obtained by maximizing NOM adsorption followed by solids removal through sedimentation so that solids loading to the membrane is minimized.

### ***Effect of Flux and Recovery with Clarified Water***

The impact of flux and recovery on fouling during clarified water operation was evaluated in Runs 8, 9 and 10. Clarification parameters at the WTP during these runs are shown in [Table 6.14](#). Operation conditions were as follows:

- Run 8: flux of 90 L/m<sup>2</sup>-hr, 95 percent recovery
- Run 9: flux of 110 L/m<sup>2</sup>-hr, 95 percent recovery
- Run 10: flux of 90 L/m<sup>2</sup>-hr, 97.5 percent recovery

[Table 6.15](#) presents source water quality during these runs. Source water quality was similar except during Run 8, where particle counts and HPC were lower, and algae counts, turbidity, metals, and TOC values are higher.

[Figure 6.13](#) shows normalized net specific flux for Runs 8, 9, and 10 as a function of permeate throughput.

**Table 6.14**  
**Full-scale water treatment plant clarification conditions during Runs 8, 9, and 10**

Run no.	Alum dose (mg/)	Polymer dose (mg/)	Sedimentation rate (L/min/m <sup>2</sup> )
8	78.1	0.258	13.9
9	41.9	0.074	15.3
10	30.8	0	15.9

**Table 6.15**  
**Source water quality data for Runs 8, 9, and 10**

Parameters	Units	Run 8	Run 9	Run 10
pH	su	7.09	7.66	7.84
Total Hardness	mg/L as CaCO <sub>3</sub>	310	333	359
Calcium	mg/L	86.3	87.7	90.6
Alkalinity	mg/L as CaCO <sub>3</sub>	154	243	267
True color	pcu	27.5	22.5	22.5
TDS	mg/L	415	464	550
Particle Count	#/mL	590	4015	4460
Turbidity	NTU	1.73	1.20	1.55
TOC	mg/L	4.15	3.06	2.71
UVA	cm <sup>-1</sup>	0.093	0.073	0.066
Algae	count/mL	14000	< 4000	< 4000
Chlorophyll a	ppb	(< 1 ppb)	(< 1 ppb)	(< 1 ppb)
HPC	colonies/mL	173	800	740
Iron (dissolved)	mg/L	<0.02	<0.02	0.15
Iron (total)	mg/L	0.148	0.027	0.047
Manganese (dissolved)	mg/L	0.15	0.025	0.049
Manganese (total)	mg/L	0.183	0.047	< 0.02

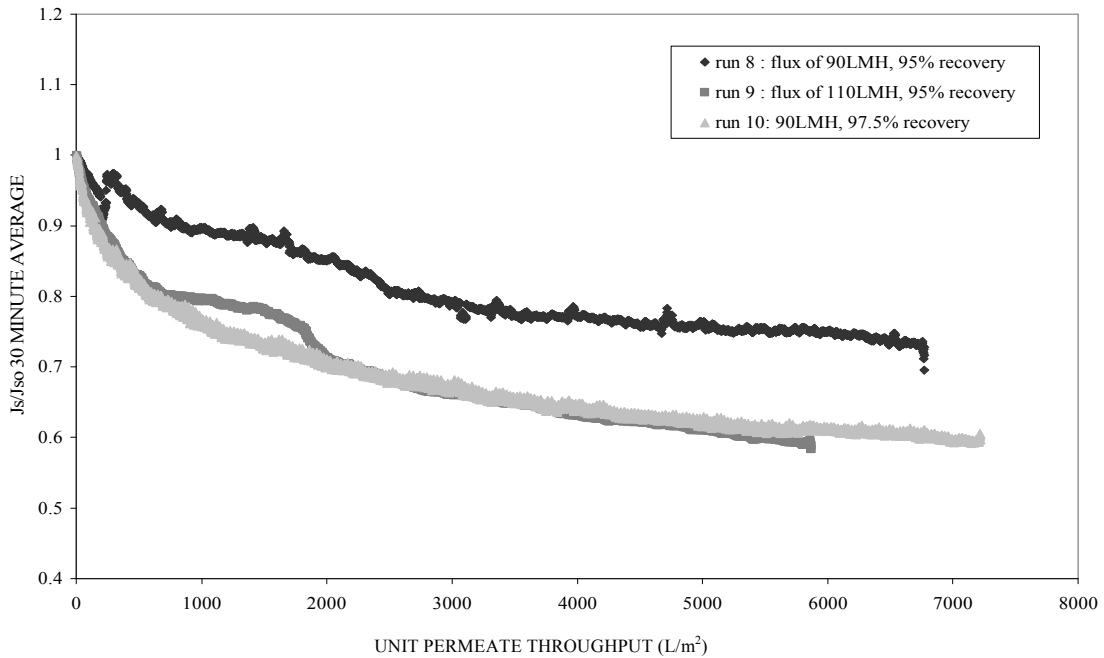


**Figure 6.13 Normalized net specific flux profile for Runs 8, 9, and 10**

Higher flux and feed water recovery increased fouling rate to a similar extent. Contrary to runs conducted with raw water, hydraulic conditions impacted both short- and long-term fouling. Indicative of severe fouling, specific flux was ~80 percent less at higher flux and recovery than the baseline run (Run 8) after a throughput of 6000 L/m<sup>2</sup>. This is counterintuitive in that high flux and high recovery increase solids loading to the membrane, which should have a greater (negative) impact on membrane fouling for runs conducted with the higher turbidity raw water versus the lower turbidity settled water. This may be partly explained by a change in MF feed water particle size and fouling potential. Clarified water would contain a higher number of smaller particles that are more likely to cause pore blocking. The fouling rate of the smaller particles may more significantly increase fouling by increased solids loading than larger particles.

### ***Effect of Chemical Wash with Clarified Water***

A comparison of flux decline profiles for Runs 11, 12, and 13 with the baseline run (Run 10) permits an evaluation of the impact of the following chemical wash regimes on membrane performance:

- Run 11: citric acid wash at pH 2
- Run 12: caustic wash at pH 11 followed by citric acid wash at pH 2
- Run 13: hypochlorite wash at pH 7, with different contact times and different chlorine concentrations (CT values)

Because the WTP influent for Runs 11, 12, and 13 was a blend of 20 percent groundwater and 80 percent surface water rather than the 100 percent surface water used during the first ten runs, the fouling profile of Runs 11 through 13 are compared with that of Runs 8 and 17, the former representing the clarified baseline run on 100 percent surface water and the latter representing the clarified baseline run on the ground-surface water blend.

The clarification conditions used at the WTP during Runs 8, 11 through 13, and 17 are listed in [Table 6.16](#). The normalized net specific flux profiles for these runs are presented in [Figure 6.14](#).

**Table 6.16**  
**Full-scale water treatment plant clarification conditions for Runs 8, 11, 12, 13, and 17**

Run no.	Alum dose (mg/L)	Polymer dose (mg/L)	Sedimentation rate (L/min/m <sup>2</sup> )
8	78.1	0.258	13.9
11	30.9	0	15.8
12	54.6	0.118	12.6
13	39.5	0.15	12.0
17	44.2	0.068	19.7

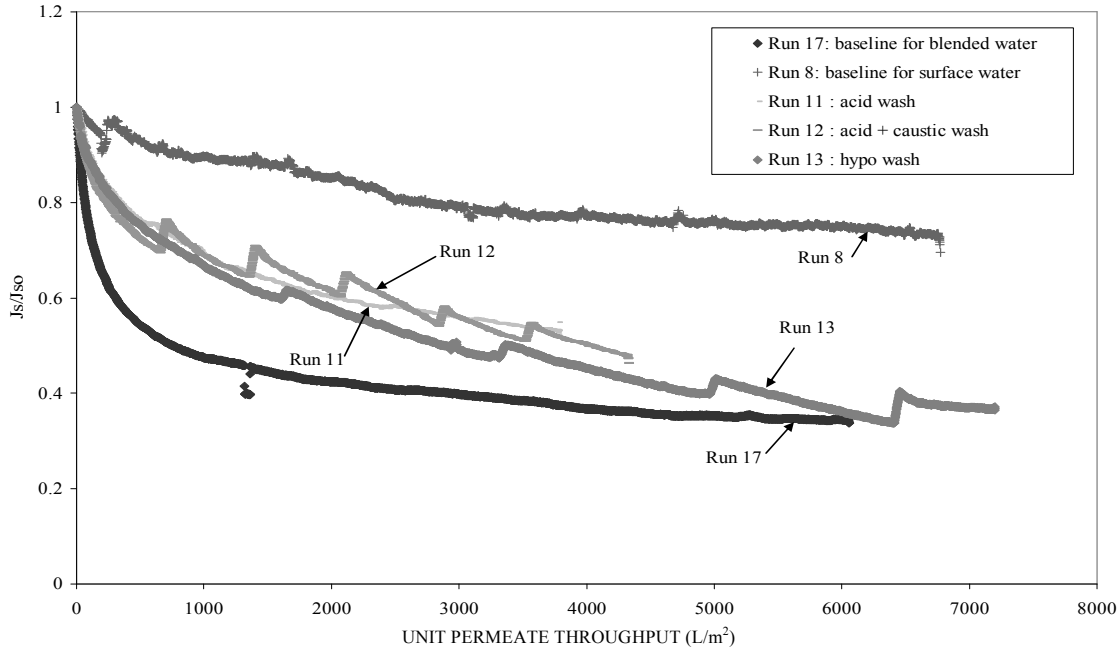


**Figure 6.14 Normalized net specific flux profiles for Runs 8, 11, 12, 13, and 17**

Run 17, which is the baseline for clarified blended water, shows severe fouling at the beginning of the run, while after a throughput of 1000 L/m<sup>2</sup>, fouling moderates. Specific fluxes for runs using a daily chemical wash are higher than for Run 17, but lower than for Run 8. This can be attributed to the difference in water quality between clarified surface water and clarified blend water, as shown in Table 6.17. The data in the table reveals that the ground/surface water blend has lower NOM concentrations, but higher levels of inorganics (TDS, calcium, alkalinity, iron, and manganese) and turbidity than the surface water. The increased degree of fouling for runs performed using the blend is most likely attributable to the higher calcium and ionic strength of the groundwater causing bridging and agglomeration of NOM despite lower NOM levels. Iron fouling, either as oxides or as combined with Ca and NOM, may also be a contributor.

**Table 6.17**  
**Source water quality data for Runs 8, 11, 12, 13, and 17**

Parameters	Units	Run 8	Run 11	Run 12	Run 13	Run 17
pH	su	7.09	7.72	7.33	7.51	7.53
Total Hardness	mg/L as CaCO <sub>3</sub>	310	441	387	456	408
Calcium	mg/L	86.3	117	106	124	112
Alkalinity	mg/L as CaCO <sub>3</sub>	154	282	208	263	238
True color	pcu	27.5	17.5	22.5	17.5	18
TDS	mg/L	415	657	540	617	581
Particle count	#/mL (size range: 2-750 microns)	590	2950	2200	2215	2150
Turbidity	NTU	1.73	2.33	3.0	2.65	1.9
TOC	mg/L	4.15	2.49	3.24	2.78	2.33
UVA	cm <sup>-1</sup>	0.093	0.055	0.07	0.056	0.044
Algae	count/mL	14,000	< 4000	< 4000	< 4000	ND*
HPC	colonies/mL	172.5	860	5100	290	90
Iron (dissolved)	mg/L	< 0.02	0.015	0.19	0.12	0.024
Iron (total)	mg/L	0.148	0.253	0.41	0.82	0.318
Manganese (dissolved)	mg/L	0.15	0.07	0.10	0.12	0.046
Manganese (total)	mg/L	0.183	0.07	0.11	0.11	0.067

\*ND = not detected

The effect of the chemical wash regimes for specific flux restoration (or flux recovery) can be better determined by comparing specific flux values in the filtration cycle directly before and after a wash event. These are shown in [Table 6.18](#), where  $J_{sCWB}$  is the specific flux measured directly before a chemical wash,  $J_{sCWA}$  is the specific flux measured directly after a chemical wash, and flux recovery ( $J_{sRECOVERY}$ ), expressed as a percentage, is defined as:

$$J_{sRECOVERY} = \frac{J_{sCWA} - J_{sCWB} \times 100\%}{J_{sCWB}}$$

**Table 6.18**  
**Specific flux recovery from different chemical wash regimes**

Run 11				
Citric acid wash at pH 2.0		$J_{sCWB}$ (gfd/psi [L/m <sup>2</sup> - hr/kPa] @ 20° C)	$J_{sCWA}$ (gfd/psi [L/m <sup>2</sup> - hr/kPa] @ 20° C)	$J_{Srecovery}$ (%)
1st wash		9.96 (116.58)	9.86 (115.41)	0
2nd wash		8.7 (101.83)	8.65 (101.25)	0
3rd wash		8 (93.64)	7.97 (93.29)	0
Run 12				
Caustic wash at pH 11/citric acid wash at pH 2.0		$J_{sCWB}$ (gfd/psi [L/m <sup>2</sup> - hr/kPa] @ 20° C)	$J_{sCWA}$ (gfd/psi [L/m <sup>2</sup> - hr/kPa] @ 20° C)	$J_{Srecovery}$ (%)
1st wash		9.75 (114.12)	10.68 (125.01)	6
2nd wash		8.98 (105.11)	9.9 (115.88)	5.9
3rd wash		8.51 (99.61)	9.16 (107.22)	4.2
4th wash		7.54 (88.26)	8.17 (95.63)	4.1
5th wash		7.17 (83.92)	7.66 (89.66)	3.2
Run 13				
Hypochlorite wash regime (CT condition)		$J_{sCWB}$ (gfd/psi [L/m <sup>2</sup> - hr/kPa] @ 20° C)	$J_{sCWA}$ (gfd/psi [L/m <sup>2</sup> - hr/kPa] @ 20° C)	$J_{Srecovery}$ (%)
1st wash	2 minute contact time at 50 mg/L Cl <sub>2</sub> (100 mg/L-min CT)	8.98 (105.11)	9.26 (108.39)	2.3
2nd wash	2 minute contact time at 500mg/L Cl <sub>2</sub> (1000 mg/L-min CT)	7.16 (83.81)	7.53 (88.14)	3
3rd wash	30 minute contact time at 50 mg/L Cl <sub>2</sub> (1500 mg/L-min CT)	5.98 (70.00)	6.38 (74.68)	3.2
4th wash	30 minute contact time at 500 mg/L Cl <sub>2</sub> (15,000 mg/L-min CT)	5.07 (59.34)	5.99 (70.11)	7.4

$J_{sCWB}$  = specific flux measured directly before chemical wash

$J_{sCWA}$  = specific flux measured directly after chemical wash

Although the run using a citric acid wash (Run 11) had the lowest flux decline of all runs conducted on the blended source water, this result can be attributed to a lower feed water recovery (90 percent) than used with Runs 12, 13, 14, and 17 (95 percent). No flux recovery was observed from the acid wash step as shown in the table. The acid may have provided some measurable specific flux recovery if the run had been performed at the higher feed water recovery, but this was not determined.

The caustic/acid wash combination (Run 12) produced a significant flux recovery of 4.7 percent, but as the membrane became more fouled, flux recovery lessened. This is consistent with the results from the Tampa Bay pilot.

For Run 13, flux recovery increased with increasing CT. Flux recovery was low during the initial portion of the run, particularly compared with that obtained using an acid-caustic wash. However, flux recovery increased as permeate throughput increased, to a maximum value

of 7.4 percent at 6,300 L/m<sup>2</sup> throughput with the use of a hypochlorite wash having a CT of 15,000 mg/L-min,. This was the best recovery obtained for all chemical wash regimes. Again, this is consistent with the results from Tampa Bay and illustrates the effectiveness of chlorine in managing NOM fouling. However, the higher flux recovery observed with hypochlorite did not produce a lower overall fouling rate than with caustic and acid.

It is interesting that the hypochlorite wash was the least effective chemical wash regime with respect to long-term fouling rate, which contrasts with its effect on the high NOM Tampa Bay source water. This may be due to a dominant inorganic fouling element, for which the acid wash would be most effective as a solubilizing agent.

### ***Effect of Clarification on Changes in Flux and Recovery***

By comparing the fouling profiles from Runs 1 through 3, performed with White River (Indianapolis) water, with Runs 8 through 10, conducted with clarified river water, the impact of clarification can be evaluated with respect to both changes in flux and feed water recovery of Membrane A. Normalized net specific flux profiles for these six runs are shown in [Figure 6.15](#). The specific operating parameters for these runs were as follows:

- Runs 1 and 8: flux of 90 L/m<sup>2</sup>-hr and recovery of 95 percent
- Runs 2 and 9: flux of 110 L/m<sup>2</sup>-hr and recovery of 95 percent
- Runs 3 and 10: flux of 90 L/m<sup>2</sup>-hr and recovery of 97.5 percent

[Table 6.19](#) lists the clarification conditions used at the full scale WTP during Runs 8, 9, and 10.

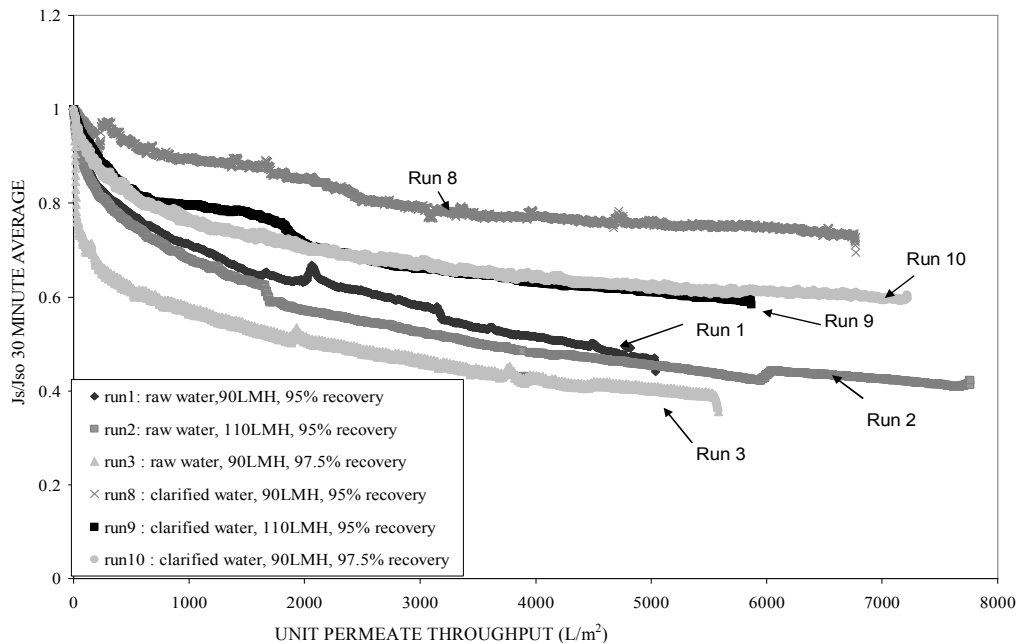


**Figure 6.15 Normalized net specific flux profile for Runs 1, 2, 3, 8, 9, and 10**

**Table 6.19**  
**Full-scale water treatment plant clarification conditions for Runs 8, 9, and 10**

Run no.	Alum dose (mg/L)	Polymer dose (mg/L)	Sedimentation rate (L/min/m <sup>2</sup> )
8	78.1	0.258	13.9
9	41.9	0.074	15.3
10	30.8	0	15.9

It is clear that clarification of the river water decreased fouling; however, when Membrane A operated on clarified river water at higher flux and recovery, fouling increased to a greater degree compared to the same hydraulic conditions used with direct river water treatment. It is important to note, however, that even at the higher flux and recovery, the rate of fouling over the total period of permeate throughput was still less than with river water at baseline conditions. This clearly indicates that the Membrane A system design can be optimized when solids and NOM loading to the membrane is reduced.

Water quality for the raw and clarified river water shown in [Table 6.20](#) is based on grab samples collected during the three raw and three clarified runs. There is very little difference in the NOM levels as indicated by TOC, UVA, and color; however, there are significant reductions in particle count and turbidity. This suggests that the improvements observed from clarification may be due primarily to reduction in solids loading to the membrane rather than in NOM. However, as described later in this chapter, coagulation does reduce the level of the high molecular weight (polysaccharide) NOM fraction, which is not necessarily reflected in the TOC or UVA results in [Table 6.20](#), and this reduction is instrumental in reducing membrane fouling.

**Table 6.20**  
**Source water quality data for raw and clarified White River (Indianapolis) water -**  
**Runs 1, 2, 3, 8, 9, and 10**

Parameters	Units	Raw			Clarified		
		Run 1	Run 2	Run 3	Run 8	Run 9	Run 10
pH	su	8.90	8.2	8.2	7.1	7.7	7.8
Total Hardness	mg/L as CaCO <sub>3</sub>	316	335	331	310	333	359
Calcium	mg/L	79.5	85	82	86	88	91
Alkalinity	mg/L as CaCO <sub>3</sub>	219	345	238	154	243	267
True color	pcu	20	20	23	28	23	23
TDS	mg/L	384	421	455	415	464	550
Particle count	#/mL (size range: 2-750 microns)	12,900	11,500	16,600	590	4000	4460
Turbidity	NTU	6.5	7.6	4.2	1.7	2.0	1.5
TOC	mg/L	3.5	3.2	3.5	4.2	3.0	2.7
UVA	cm <sup>-1</sup>	0.09	0.2	0.18	0.09	0.07	0.07
Algae	count/mL	7600	22,400	8400	14,000	< 4000	< 4000
HPC	colonies/mL	2600	1100	4100	170	800	740
Iron (dissolved)	mg/L	< 0.02	0.06	0.02	< 0.02	< 0.02	(0.15)*
Iron (total)	mg/L	0.33	0.28	0.23	0.15	0.03	0.05
Manganese (dissolved)	mg/L	< 0.02	0.01	< 0.02	0.15	0.03	(0.05)*
Manganese (total)	mg/L	0.03	0.04	0.04	0.18	0.05	< 0.02

\*High result is from sample contamination.

### ***Effect of Clarification on Fouling Management by Chemical Wash***

A comparison of the fouling profiles of Runs 4, 5, and 6 (river water filtration) with those of Runs 11, 12, and 13 (clarified river water filtration) permits an evaluation of the impact of clarification on the effectiveness of chemical washing in managing fouling. The normalized net specific flux profiles for these six runs are presented in [Figure 6.16](#) as a function of permeate throughput. All runs were operated at the same flux (90 L/m<sup>2</sup>-hr) and feed water recovery (95 percent) conditions except for Run 11, for which recovery was 90 percent.

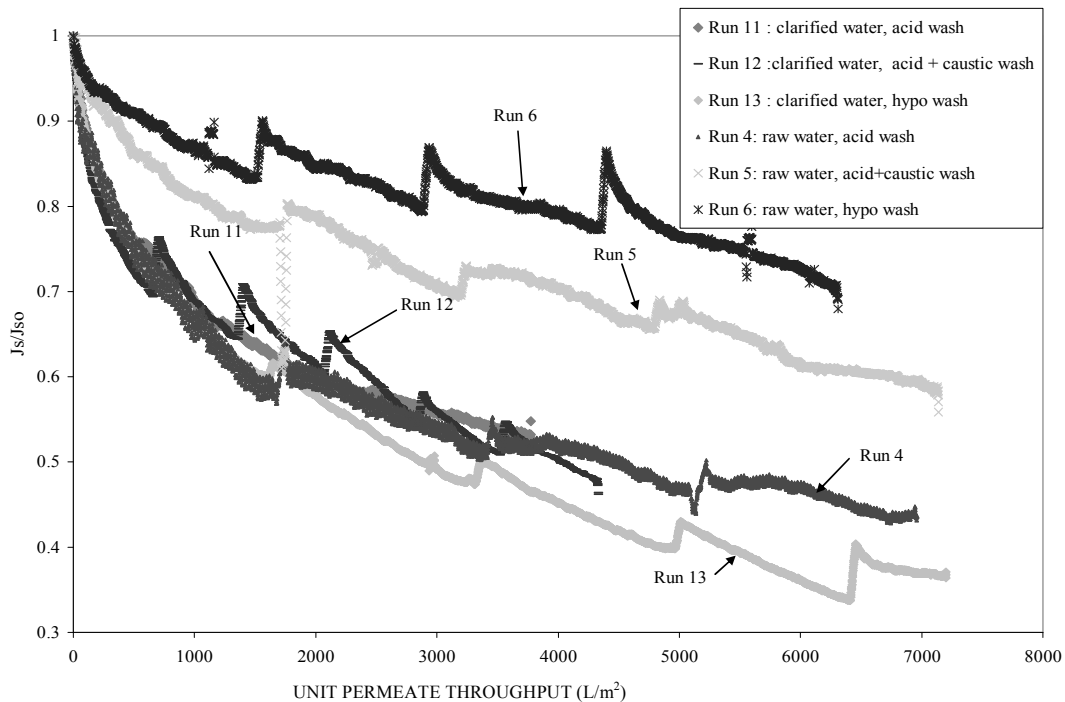


**Figure 6.16 Normalized net specific flux profile for Runs 4, 5, 6, 11, 12, and 13**

The chemical wash regime for the paired runs was as follows:

- Runs 4 and 11: daily citric acid wash.
- Runs 5 and 12: daily caustic wash followed by citric acid wash.
- Runs 6 and 13: daily hypochlorite wash. For Run 6, all washes used a soak time of 30 minutes and an initial HOCl concentration of 50 ppm. For Run 13, a CT matrix was used having different contact times and hypochlorite concentrations.

Table 6.21 shows the clarification conditions used at the full-scale WTP during Runs 11 through 13.

Following are the average flux recovery provided by these different chemical washes as calculated previously in this chapter:

- Run 4: 2.3 percent
- Run 5: 3.1 percent
- Run 6: 7.6 percent
- Run 11: 0 percent
- Run 12: 4.7 percent
- Run 13\*: 3.2 percent

---

\*Contact time of 30 minutes and a hypochlorite concentration of 50 ppm (same as during Run 6).

The acid wash was the least effective wash for both source waters. The caustic/acid wash was slightly more effective with clarified water. The major difference is apparent with the HOCl wash. This wash was much more effective with the river water. This could be due to the reduced level of organic matter in the clarified water (Table 6.22); TOC, algae counts, and HPC values were consistently higher in the river water, providing more organic substrate for the chlorine to oxidize and from which to reduce the fouling impact.

**Table 6.21**  
**Full-scale water treatment plant clarification conditions for Runs 11, 12, and 13**

Run	Alum dose	Polymer dose	Sedimentation rate (L/min/m <sup>2</sup> )
11	31	0	15.8
12	55	0.12	12.6
13	40	0.15	12.0

**Table 6.22**  
**Source water quality data for raw and clarified White River (Indianapolis) water -  
Runs 4, 5, 6, 11, 12, and 13**

Parameters	Units	River water			Clarified river water		
		Run 4	Run 5	Run 6	Run 11	Run 12	Run 13
pH	su	8.0	8.1	8.0	7.7	7.3	7.5
Total Hardness	mg/L as CaCO <sub>3</sub>	243	332	300	441	387	456
Calcium	mg/L	61.8	93	76	117	106	124
Alkalinity	mg/L as CaCO <sub>3</sub>	161	225	224	282	208	263
True color	pcu	68	20	38	18	23	18
TDS	mg/L	295	448	388	657	540	617
Particle count	#/mL (size range: 2-750 microns)	11,550	11,800	8242	2950	2200	2215
Turbidity	NTU	38	8.8	4.0	2.3	3.0	2.7
TOC	mg/L	4.6	3.4	3.7	2.5	3.2	2.8
UVA	cm <sup>-1</sup>	0.18	0.09	0.12	0.06	0.07	0.06
Algae	count/mL	20,400	10,400	2400	< 4000	< 4000	NM*
HPC	colonies/mL	4100	2100	3400	860	5100	290
Iron (dissolved)	mg/L	0.02	< 0.02	< 0.02	0.02	0.19	0.12
Iron (total)	mg/L	1.9	0.49	0.49	0.25	0.41	0.82
Manganese (dissolved)	mg/L	< 0.02	< 0.02	< 0.02	0.07	0.1	0.12
Manganese (total)	mg/L	0.08	0.04	0.04	0.07	0.11	0.11

\*NM = not measured

## ***Bulk Sample NOM Characterization and Impact on Fouling***

As discussed in Chapter 4, the White River (Indianapolis) water contained a moderated DOC level with a high hydrophilic or polysaccharide NOM fraction. Figures 6.17 and 6.18 present SEC-DOC/UVA chromatograms for NOM present in feed, permeate, and backwash samples collected during Run 1 (baseline run) and Run 7a (ferric coagulation run). The chromatograms show that, (1) of the three NOM fractions, the PS fraction was more effectively retained by the MF membrane and more effectively removed from the membrane surface by backwashing than the smaller HS and LMA fractions; and (2) the magnitude of the PS and HS fractions was reduced by coagulation prior to filtration.

Table 6.23 shows the distribution of DOC and NOM fractions (PS, HS, and LMA) in the feed, permeate, and backwash samples collected during Runs 1 and 7a. The data in Table 6.23 indicate that the high MW compounds (PS fraction) were rejected or adsorbed by Membrane A during filtration as indicated by the decreased concentration of these compounds in the permeate. Backwash samples showed an elevated PS fraction (relative to the feed), indicating that the high MW compounds were hydraulically displaced from the membrane or with the foulant layer. Some retainage and backwash concentration of the smaller HS and LMA fractions is evident, but to a much lower degree than for the HS fraction. Coagulation reduces the DOC present in the White River (Indianapolis) water, which in turn reduces the level of all NOM fractions in the membrane feed, resulting in lower rate of fouling as shown in the normalized net specific flux profile for the coagulated run with lower solids loading.

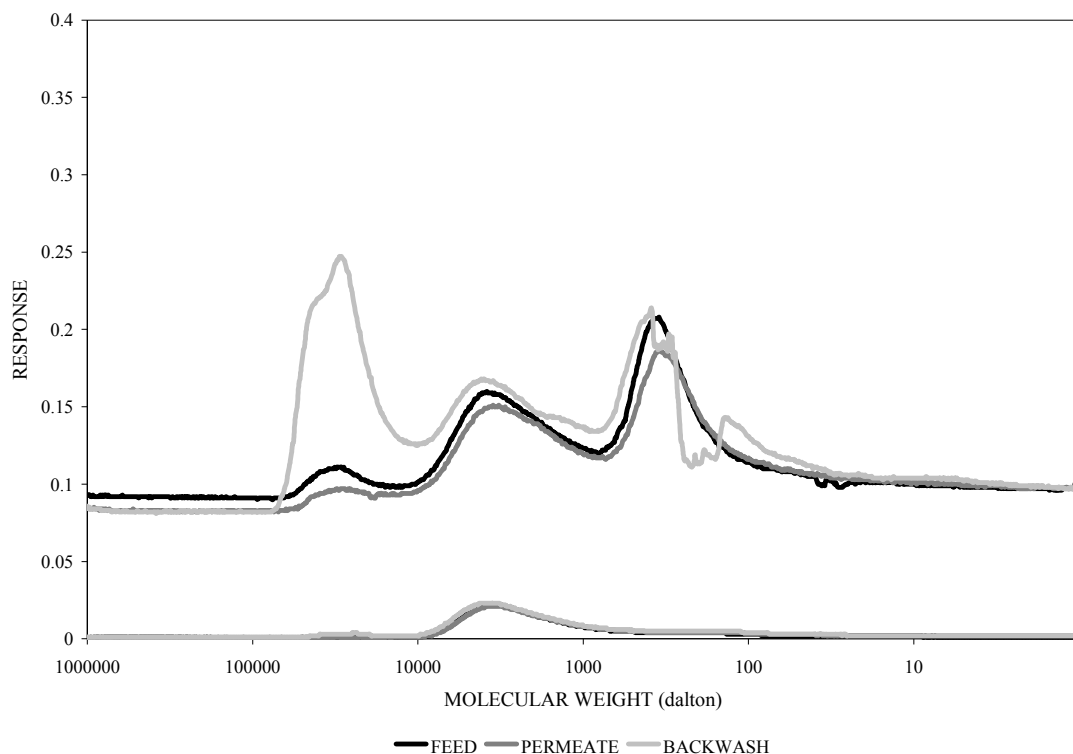


**Figure 6.17 SEC-DOC/UV chromatogram – filtration of White River water by Membrane A during Indianapolis pilot testing (Run 1)**

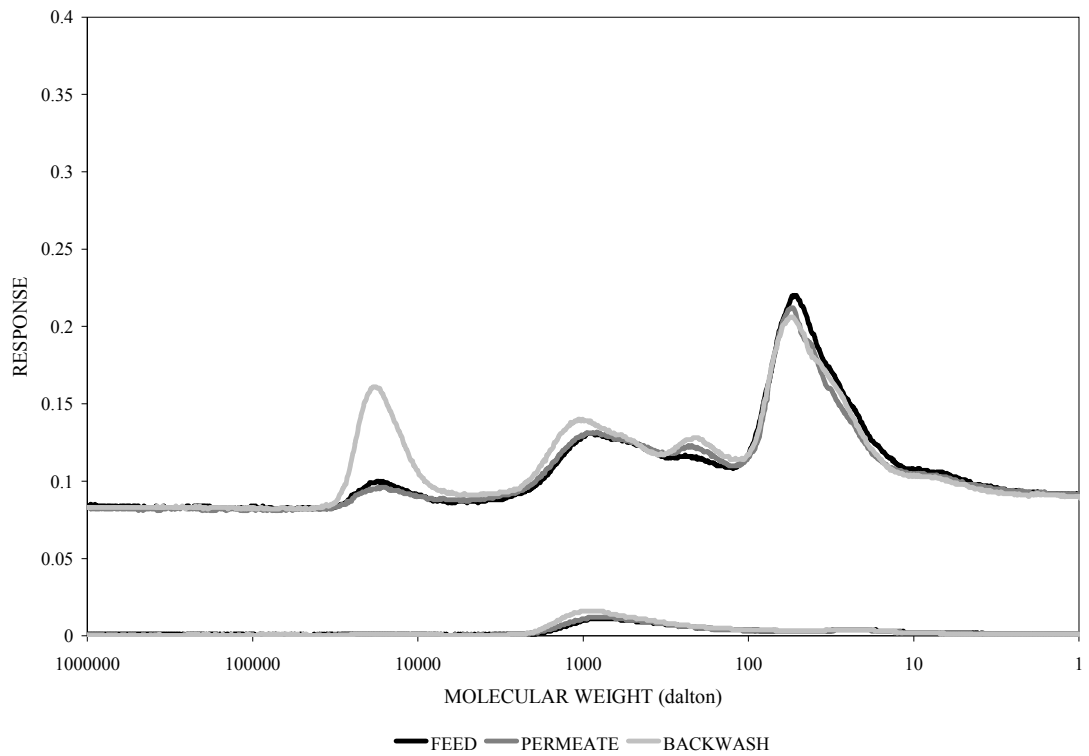


**Figure 6.18 SEC-DOC/UV chromatogram – filtration of coagulated White River water by Membrane A during Indianapolis pilot testing (Run 7A)**

**Table 6.23****Distribution of DOC and NOM fractions in feed, permeate, and backwash samples collected during Runs 1 and 7A**

Run	Feed (mg/L)				Filtrate (mg/L)				Backwash (mg/L)			
	DOC	PS*	HS*	LMA*	DOC	PS*	HS*	LMA*	DOC	PS*	HS*	LMA*
1 (Baseline)	4.45	0.27	1.66	2.5	3.54	0.15	1.21	2.2	9.5	2.79	2.56	4.1
7a (Coagulant, 30 mg/L alum)†	2.95	0.15	0.92	1.9	2.69	0.13	0.96	1.6	4.5	0.76	1.54	2.2

\*Values based on integration of SEC-DOC chromatogram peaks.

†Samples were filtered through a 0.45-micron filter prior to analysis.

## Scottsdale Pilot Study

To develop a method of comparing different impacts on performance of Membrane D1 by varying operating conditions, a baseline run was first completed. The baseline conditions consisted of the following: flux of  $80 \text{ L/m}^2\text{-hr}$  (47 gfd), a backwash frequency of 30 minutes at a flow rate at 50 gpm, and feed water recovery of 90 percent.

The normalized net specific flux decline for the baseline run (Run 1) is presented in Figure 6.19. The curve is characterized by a rapid loss of specific flux during the initial  $4000 \text{ L/m}^2$  of permeate throughput, followed by a gradual increase in flux during the remaining  $6000+$   $\text{L/m}^2$  of throughput. This type of curve is not characteristic of MF/UF fouling; flux does not typically generally decline and then increase without some significant improvement in feed water quality that would reduce the foulant load to the membrane. The feed water quality data for the Scottsdale effluent presented in Chapter 4 does not support a reduction in fouling load caused by reduction in EfOM levels to the membrane. To assess whether such flux increases could be caused by variations in UF feed water solids levels, UF feed water turbidity was also plotted in Figure 6.19. The turbidity trend shows no major decrease in turbidity during the duration of the run. As such there is no feed water quality-based explanation for the cyclic pattern in specific flux during the run.

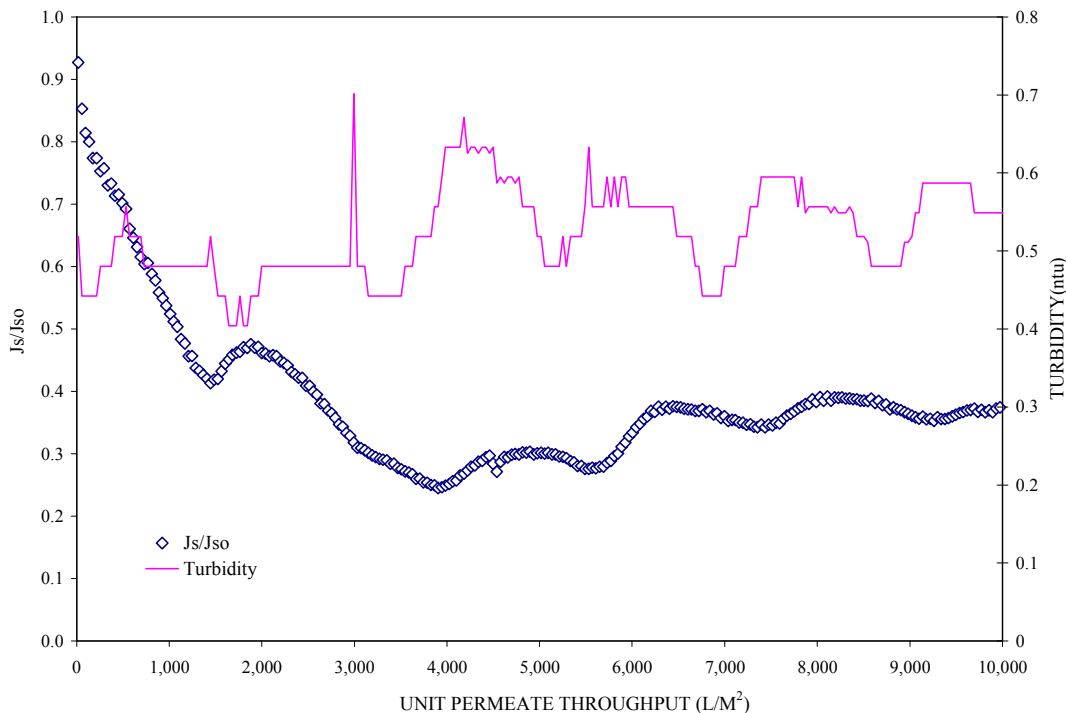


**Figure 6.19 Run 1 (baseline) normalized net specific flux of Membrane D1 during Scottsdale pilot study (flux =  $80 \text{ L/m}^2\text{-hr}$ ; recovery = 90 percent)**

### Impacts of Varying Flux

The second run was conducted to demonstrate the impact of flux on membrane fouling. This run was performed with a flux of 60 L/m<sup>2</sup>-hr (35 gfd). The normalized net specific flux graph is presented in Figure 6.20. The fouling rate for the low flux run was slightly lower (7 percent) than for the baseline run ( $J_s/J_{s0}$  of 0.30 versus 0.25, respectively). This is not particularly significant given the 25 percent reduction in flux during the run and suggests that flux has only a minor impact on the NOM fouling rate of the PES Membrane D1 on filtered secondary effluent. The atypical increase in specific flux seen during the latter part of the baseline run was more accentuated at lower flux.

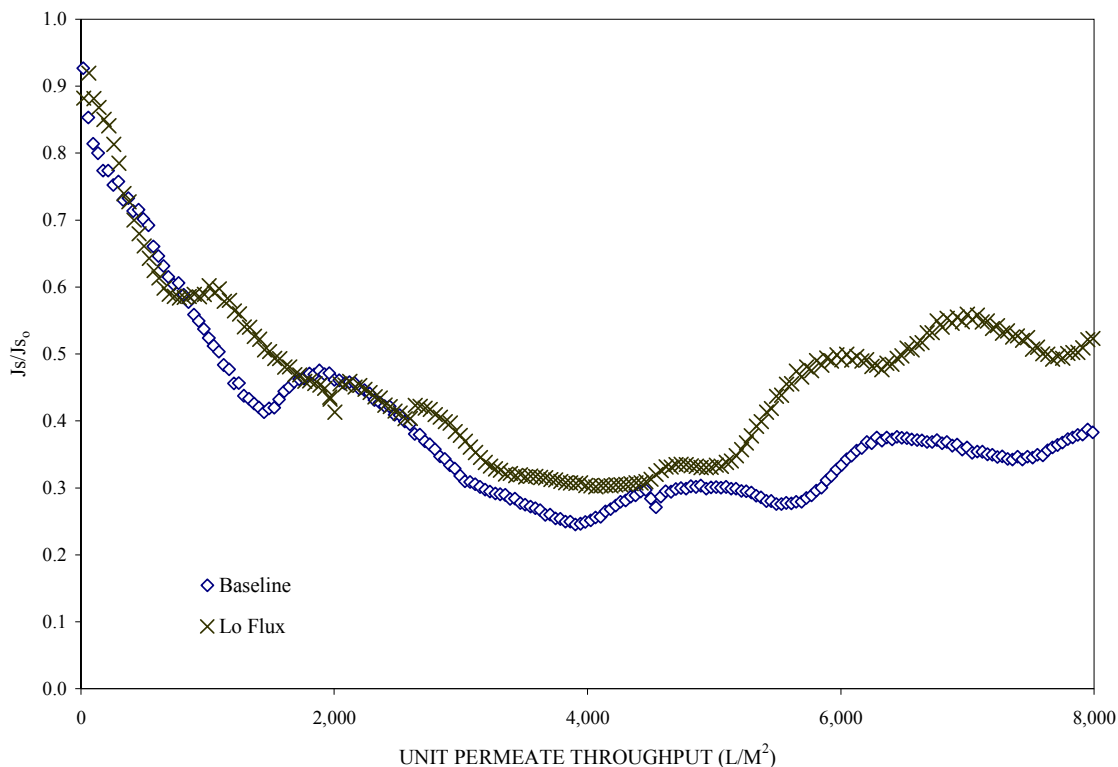


**Figure 6.20 Impact of decreased flux on net normalized specific flux decline of Membrane D1 during Scottsdale pilot study operating on Scottsdale effluent (baseline flux = 80 L/m<sup>2</sup>-hr and lo flux = 60 L/m<sup>2</sup>-hr; recovery = 90 percent)**

To compare variability in water quality between runs, the grab sample water quality analysis is presented in [Table 6.24](#). It should also be noted that feed TOC and UVA<sub>254</sub> levels during Run 2 were somewhat lower than Run 1, which would have reduced the EfOM loading to the membrane.

**Table 6.24**  
**Feed water quality data for Runs 1 and 2**

Parameter	Unit	Run*			
		1	1	2	2
TDS	mg/L	1020	1010	993	888
Alkalinity	mg/L as CaCO <sub>3</sub>	150	186	160	206
Calcium	mg/L	87.9	76.1	78.9	70.4
Total Hardness	mg/L as CaCO <sub>3</sub>	345	190	320	287
Iron, Total	mg/L	0.35	0.14	0.10	0.72
Iron, Dissolved	mg/L	0.05	0.057	0.041	0.056
Manganese, Total	mg/L	0.052	0.039	0.034	0.051
Manganese, Dissolved	mg/L	0.038	0.037	0.029	0.042
pH	units	7.1	7.3	7.2	7.1
TOC	mg/L	7.1	6.7	6.6	6.6
UVA-254	cm <sup>-1</sup>	0.137	0.143	0.123	0.135

\*Two grab samples were collected during each run.

### ***Impacts of Varying Percent Recovery***

Runs 3 and 4 were conducted to demonstrate the effect that a lower or higher feed water recovery rate would have on the rate of membrane fouling. The recovery rate was decreased to 80 percent (a 10 percent reduction) during Run 3 by increasing backwash frequency to once every 15 minutes and increased to 95 percent during Run 4 by decreasing backwash frequency to once every 60 minutes while maintaining the flux at the baseline level of 80 L/m<sup>2</sup>-hr (47 gfd). The normalized net specific flux trends for these runs, along with that for Run 1, are presented in [Figure 6.21](#).

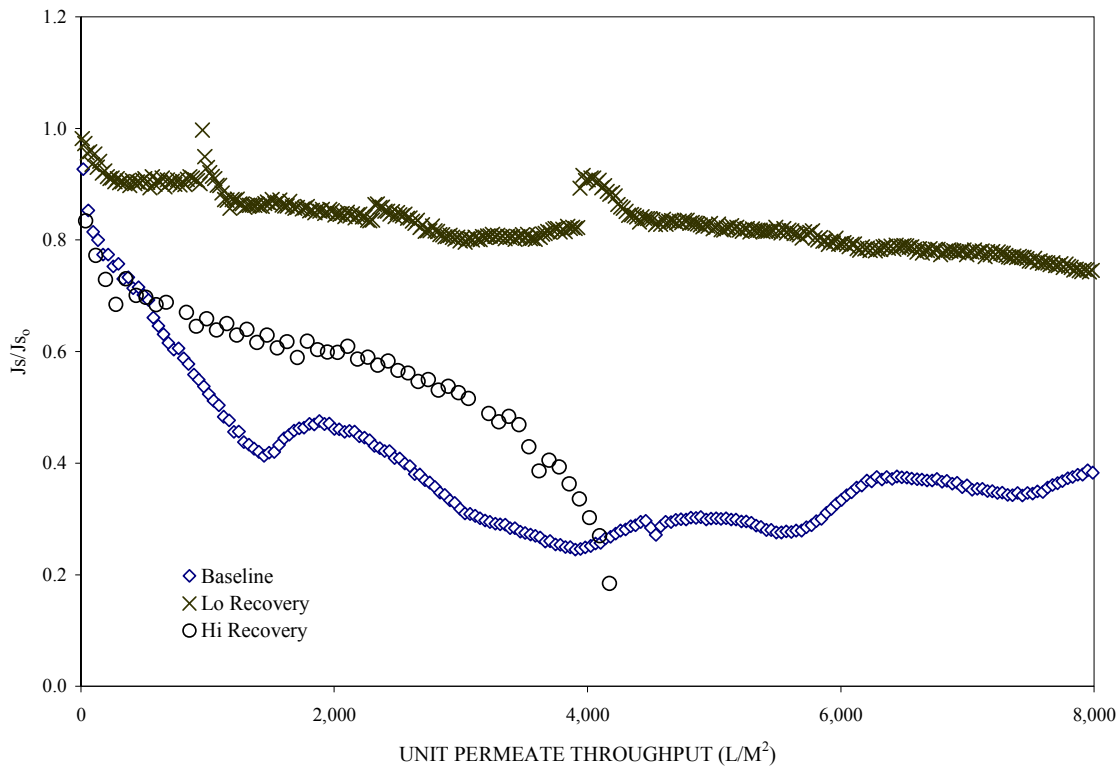


**Figure 6.21 Impact of feed water recovery on net normalized specific flux decline of Membrane D1 during Scottsdale pilot study (baseline recovery = 90 percent; lo recovery = 80 percent; hi recovery = 95 percent)**

These data indicate that feed water recovery (solids loading during the filtration cycle) has a much greater impact on fouling of Membrane D1 than flux. If NOM fouling is the predominant cause of flux decline in this source water, this data would suggest that increasing backwash frequency is very effective in controlling the rate of effluent organic matter (EfOM) (and particulate) fouling and has a greater impact on rate of fouling than the rate of EfOM loading to the membrane surface (i.e., flux). Due to the rapid rate of fouling of Run 4, the unit was shut down based on high TMP and remained down for 2 days before City of Scottsdale personnel could attend to it. Consequently, no conventional or NOM characterization samples could be collected during the abbreviated run period. To compare variability in water quality between runs, the grab sample water quality analysis is presented in [Table 6.25](#).

**Table 6.25**  
**Feed water quality data for Runs 1 and 3**

Parameter	Unit	Run*			
		1	1	3	3
TDS	mg/L	1020	1010	925	976
Alkalinity	mg/L as CaCO <sub>3</sub>	150	186	192	200
Calcium	mg/L	87.9	76.1	77.7	76
Total Hardness	mg/L as CaCO <sub>3</sub>	345	190	310	312
Iron, Total	mg/L	0.35	0.14	0.12	0.10
Iron, Dissolved	mg/L	0.05	0.057		
Manganese, Total	mg/L	0.052	0.039	0.045	0.034
Manganese, Dissolved	mg/L	0.038	0.037		
pH	units	7.1	7.3	7.4	7.4
TOC	mg/L	7.1	6.7	5.7	5.9
UVA-254	cm <sup>-1</sup>	0.137	0.143	0.13	0.122

\*Two grab samples were collected during each run.

### ***Impacts of Chemical Cleaning of Membranes***

Runs 5 and 6 were conducted to demonstrate the effect of performing low and high pH chemical washes (conducted for a soak period of 30 minutes once per day) on the rate of membrane fouling. These runs were performed at baseline operating conditions (flux of 80 L/m<sup>2</sup>-hr (47 gfd) and recovery of 90 percent). Run 5 employed an acid wash (using HCl at pH 2), while Run 6 consisted of an acid wash followed by a caustic wash at pH 11 (acid solution was backwashed out of the membrane module before the caustic solution was applied). The normalized net specific flux trends for these two runs, together with the baseline run (Run 1), are presented in [Figure 6.22](#).

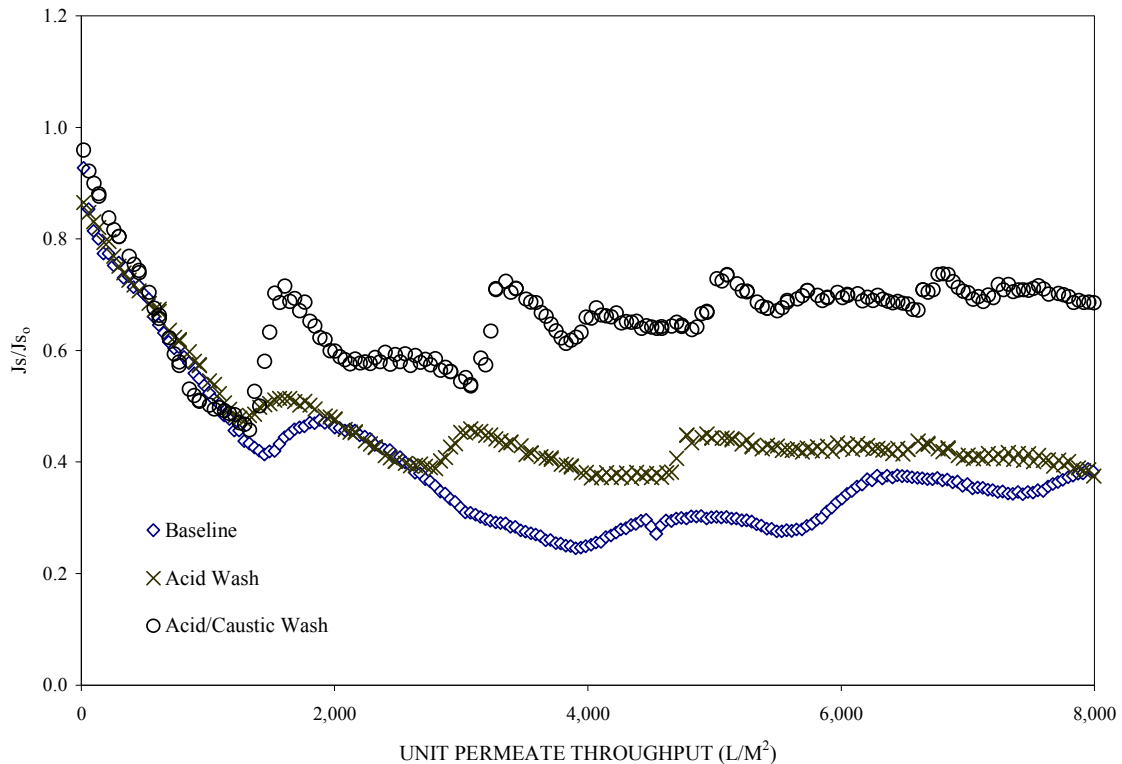


**Figure 6.22 Impact of chemical wash on net normalized specific flux decline of Membrane D1 during Scottsdale pilot study (baseline: no chemical wash; acid wash: hydrochloric acid at pH 2; caustic wash at pH 11)**

The use of daily acid washes resulted in temporary increases in specific flux; however, the effectiveness of the washes diminished with increasing throughput. The second acid wash conducted at approximately 3,000 L/m<sup>2</sup> permeate throughput increased normalized specific flux about 0.05, resulting in a 50 percent recovery in flux compared to that of the baseline run. However, after 8,000 L/m<sup>2</sup>, specific flux for both baseline and acid wash runs were equivalent, indicating that once-per-day acid washes are not an effective long-term NOM fouling management strategy, at least for Membrane D1 operating on an effluent-dominated NOM source. The result is not unanticipated because most NOM is not effectively solubilized at low pH.

In contrast, the sequential use of caustic wash, followed by acid wash, produced a significant beneficial impact on specific flux and membrane fouling. Beginning with its use at approximately 3,000 L/m<sup>2</sup> permeate throughput, this combination of chemical washes produced a steady increase in specific flux following the initial steep decline. The extent of specific flux improvement lessened with increasing run time; however, this is due primarily to the increased flux (which reduced the amount of foulant subject to removal by chemical wash). The post-wash specific flux remained consistent throughout the run. The combination of acid and caustic wash would address the removal (solubilization) of both precipitated inorganic material (by acid) and biological/organic contaminants (by caustic). Because the caustic wash was more effective (that

is, the difference between acid wash alone versus acid and caustic together), this would indicate that organic matter is the predominant foulant in the effluent. UF feed water quality was consistent between the three runs, including turbidity (not shown [Figure 6.22](#)); however, iron levels were variable both within runs and between runs. While iron levels were highest during the run employing acid wash, iron fouling should have been more effectively controlled than other types of fouling (turbidity or NOM). Hence, the increased iron level is not considered a significant contributor to the low effectiveness of the acid wash. Because of the undulating nature of the baseline run specific flux, the ability to clearly discern the impacts of acid and acid/caustic washes on fouling is made more difficult. However, it is reasonable to conclude that caustic wash has a greater benefit than acid wash in controlling NOM fouling.

To compare variability in water quality between runs, the grab sample water quality analysis is presented in [Table 6.26](#).

**Table 6.26**  
**Feed water quality data for Runs 1, 5, and 6**

Parameter	Unit	Run*					
		1	1	5	5	6	6
TDS	mg/L	1020	1010	1042	1036	960	971
Alkalinity	mg/L as CaCO <sub>3</sub>	150	186	160	172	198	178
Calcium	mg/L	87.9	76.1	80	96.3	69.3	70.4
Total Hardness	mg/L as CaCO <sub>3</sub>	345	190	333	396	289	290
Iron, Total	mg/L	0.35	0.14	0.09	0.401	0.157	0.25
Iron, Dissolved	mg/L	0.05	0.057	0.082	0.369	0.152	0.254
Manganese, Total	mg/L	0.052	0.039	0.031	0.1	0.067	0.09
Manganese, Dissolved	mg/L	0.038	0.037	0.029	0.089	0.066	0.087
pH	units	7.1	7.3	7.1	7.4	7.3	7.2
TOC	mg/L	7.1	6.7	5.9	6.8	6.2	6.1
UVA-254	cm <sup>-1</sup>	0.137	0.143	0.110	0.119	0.138	0.130

\*Two grab samples were collected during each run.

## Impacts of Coagulation

Runs 7, 8, and 9 were conducted to demonstrate the effect of coagulation on NOM fouling on Membrane D1. These runs were performed at baseline operating conditions (flux of 80 L/m<sup>2</sup>-hr (47 gfd) and recovery of 90 percent). The normalized net specific flux trends for these runs, together with Run 1, are presented in Figure 6.23.

Specific flux decreased at a slower rate with the addition of a coagulant. This would indicate that coagulation is in fact changing the fouling characteristics of the NOM, as expected. (This will be discussed more in the following NOM characterization section.) The coagulant dose was not optimized as part of this pilot study; however, a higher coagulant dose was more effective in mitigating fouling. While there was no appreciable difference in the effect of coagulant type at comparative metal ion dose (i.e., coagulation with a ferric dose intermediate to the two aluminum doses produced an intermediate degree of fouling reduction), the characteristic of the ferric chloride flux curve varied from that of the polyaluminum chloride. The former showed a much greater initial flux but stabilized for the remainder of the run, whereas the PACl curves showed more gradual flux loss.

To compare variability in water quality between runs, the grab sample water quality analysis is presented in Table 6.27.

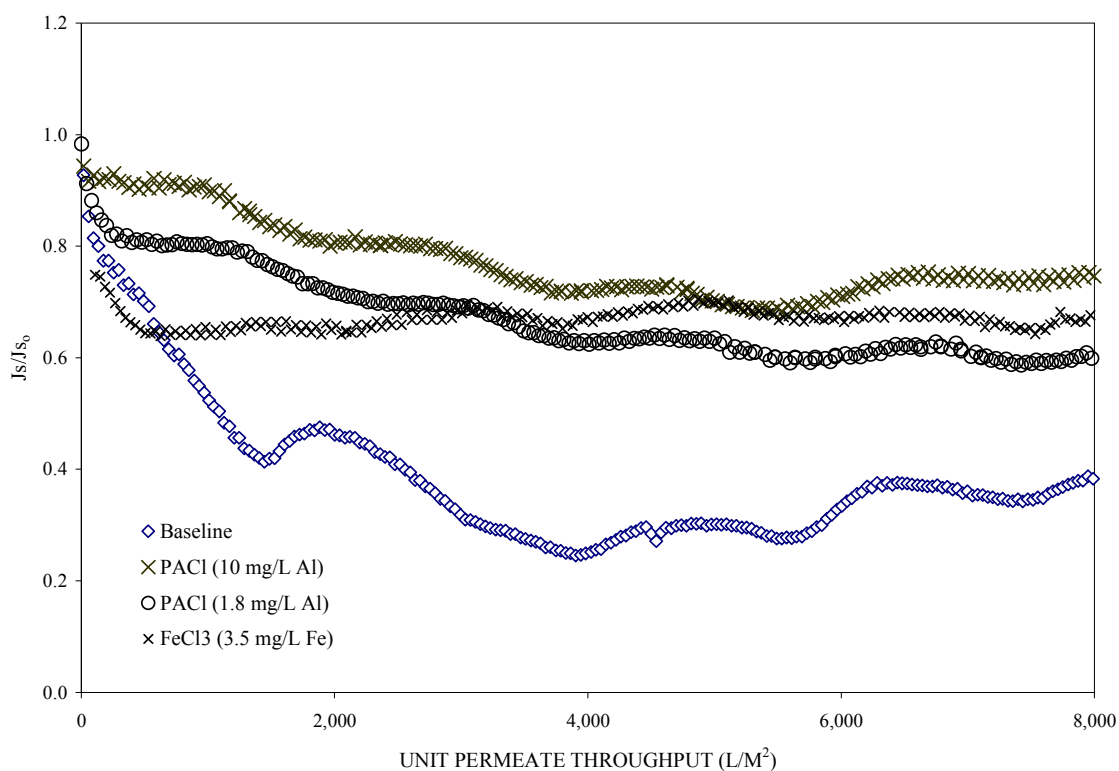


**Figure 6.23 Impact of coagulation on net normalized specific flux decline of Membrane D1 during Scottsdale pilot study (baseline: no coagulation)**

**Table 6.27**  
**Feed water quality data for Runs 1, 7, 8, and 9**

Parameter	Unit	Run							
		1	1	7	7	8	8	9	9
TDS	mg/L	1020	1010	920	920	910	960	900	950
Alkalinity	mg/L as CaCO <sub>3</sub>	150	186	200	180	170	156	166	158
Calcium	mg/L	87.9	76.1	63.5	71	64.8	70.8	63.5	63.7
Total Hardness	mg/L as CaCO <sub>3</sub>	345	190	266	298	272	296	271	271
Iron, Total	mg/L	0.35	0.14	0.12	0.234	0.066	0.109	4.21	5.16
Iron, Dissolved	mg/L	0.05	0.057	0.118	0.079	0.065	0.046	0.32	0.9
Manganese, Total	mg/L	0.052	0.039	0.046	0.062	0.035	0.045	0.063	0.078
Manganese, Dissolved	mg/L	0.038	0.037	0.042	0.049	0.033	0.039	0.059	0.069
pH	units	7.1	7.3	7.2	7.1	7.2	7.3	7.0	6.9
TOC	mg/L	7.1	6.7	6.6	5.9	5.6	5.8	6.0	5.8
UVA-254	cm <sup>-1</sup>	0.137	0.143	0.114	0.109	0.105	0.111	0.110	0.171
Aluminum	mg/L			106.0		2.1	2.7		

Note: two grab samples were collected during each run.

### ***Impact of CT***

Run 12 was conducted to demonstrate the effect of different chlorine doses and contact times to mitigate fouling using the chemical wash protocol. [Table 6.28](#) presents the CT conditions that were evaluated during this run. The CT range is fairly narrow; higher chlorine doses were intended, but could not be achieved with the dosing pumps provided with the pilot.

Run 12 was performed at baseline operating conditions (flux of 80 L/m<sup>2</sup>-hr (47 gfd) and 90 percent recovery). The normalized net specific flux profile for the run reflecting the effects of the different CT conditions is presented in [Figure 6.24](#). The permeate throughput values at which the different CT conditions were applied are also shown in [Figure 6.24](#).

Specific flux showed temporary, but consistent, increases following all of the chlorine washes. This was not significant for long-term flux sustainability because the flux increase was also followed by a rapid decline. As expected, the chlorine wash was more effective when the membrane became more fouled. The highest flux recovery was obtained during chemical washes designated B and E in [Figure 6.24](#) where the highest CT was used. During the throughput period of 2,000 to 8,000 L/m<sup>2</sup>, it was clear that the chlorine washes were effective in mitigating fouling. The sustained effectiveness of a hypochlorite wash was also demonstrated in the Tampa Bay and Indianapolis pilot studies.

Interpretation of the sustained impact of the chlorine washes on flux was complicated by a 5.5-day downtime that occurred at 10,000 L/m<sup>2</sup> permeate throughput. It is interesting to note that this downtime, in which the membrane module contained only feed water (no flushing or chemical preservation), resulted in a significant flux improvement once the unit was returned to service. This improvement can only be attributed to “relaxation” and subsequent displacement of the fouling layer.

**Table 6.28**  
**CT Conditions for Run 12**

Condition	Chlorine dose (mg/)	Contact time (min)	CT (mg·min/L)
A	45	2	90
B	45	30	1350
C	45	2	90
D	65	2	130
E	65 </tr		

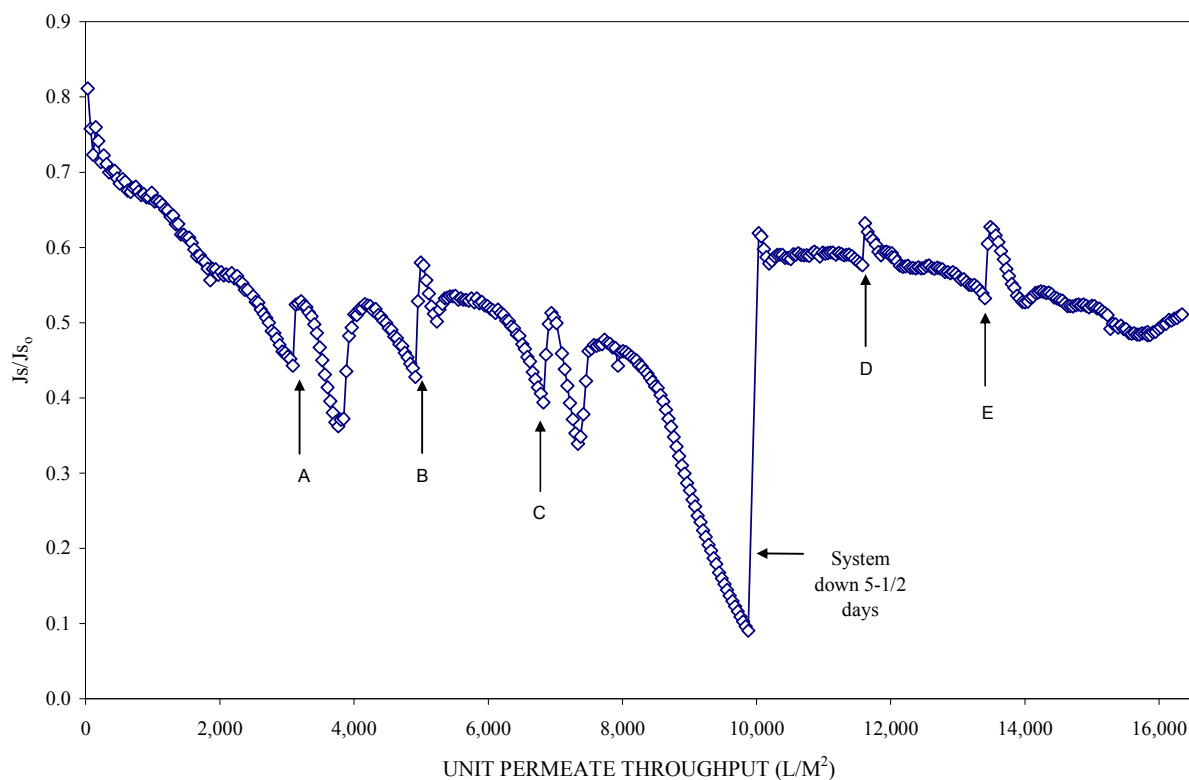


**Figure 6.24 Impact of CT on flux decline of Membrane D1 during Scottsdale pilot study**

Using the equation presented in section 6.0.2.2, specific flux recovery values were calculated for each chlorine wash. The results are presented in Figure 6.25. Over the narrow range of CT values, no correlation was observed between CT and flux recovery. This is consistent with the results presented in section 5.1 and indicates that significant flux recovery does not occur unless higher CT values are used ( $\geq 10,000$  mg/L-min) are used. Full-scale MF/UF facilities typically use CT values in the range of 3000 to 15,000 mg/L-min.

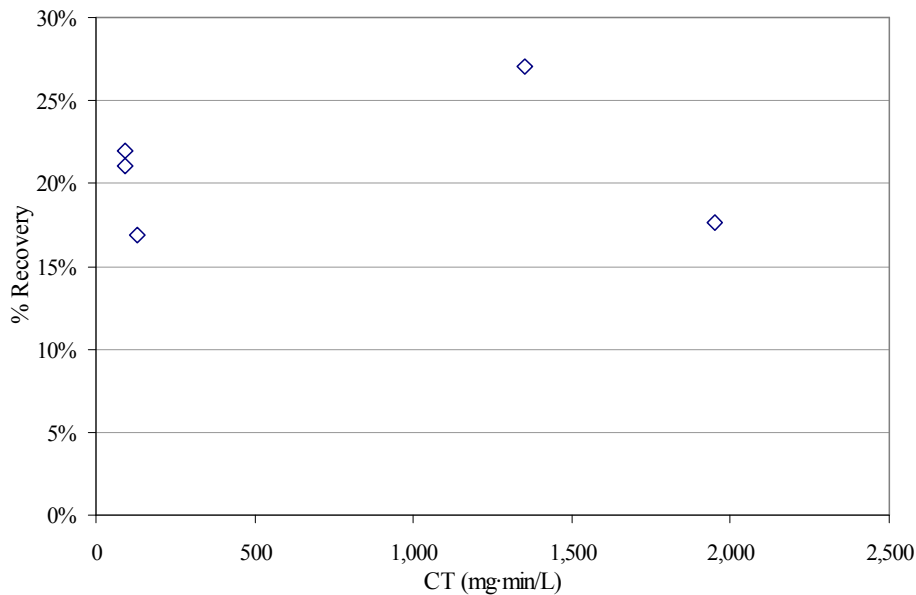


**Figure 6.25 Impact of CT on specific flux recovery of Membrane D1 during Scottsdale pilot study**

### ***Bulk Sample NOM Characterization and Impact on Fouling***

As described in Sections 5.0 and 5.1, the Scottsdale clarified and filtered secondary effluent has a significant PS fraction, corresponding to macromolecules and/or organic colloids, that resulted in a high rate of membrane fouling in the bench-scale experiments. The NOM characterization and operational data from this pilot study provide further evidence that the PS fraction is the main contributor to NOM membrane fouling.

Figures 6.26 and 6.27 present SEC-DOC/UVA chromatograms from NOM samples collected during Run 1 (baseline run) and Run 8 (low PACl dose coagulation run). The chromatograms show the following:

- The PS peak is significant in the effluent (feed). This fraction is reduced in the permeate and increased in the backwash water, indicating its retention by Membrane D1 during filtration and displacement from the membrane surface during backwash (Figure 6.26).
- When coagulation is used, the magnitude of PS peak is reduced in both the feed and permeate, while the backwash peak is increased (Figure 6.27), indicating that coagulation reduced the (soluble) PS level reaching the membrane. No reduction in HS or LMA fraction was apparent.
- Although both the HS and LMA peaks are large, there is no appreciable retention of these fractions by the membrane, either with or without coagulation. Consequently, these fractions are most likely not contributing in a meaningful way to membrane fouling.

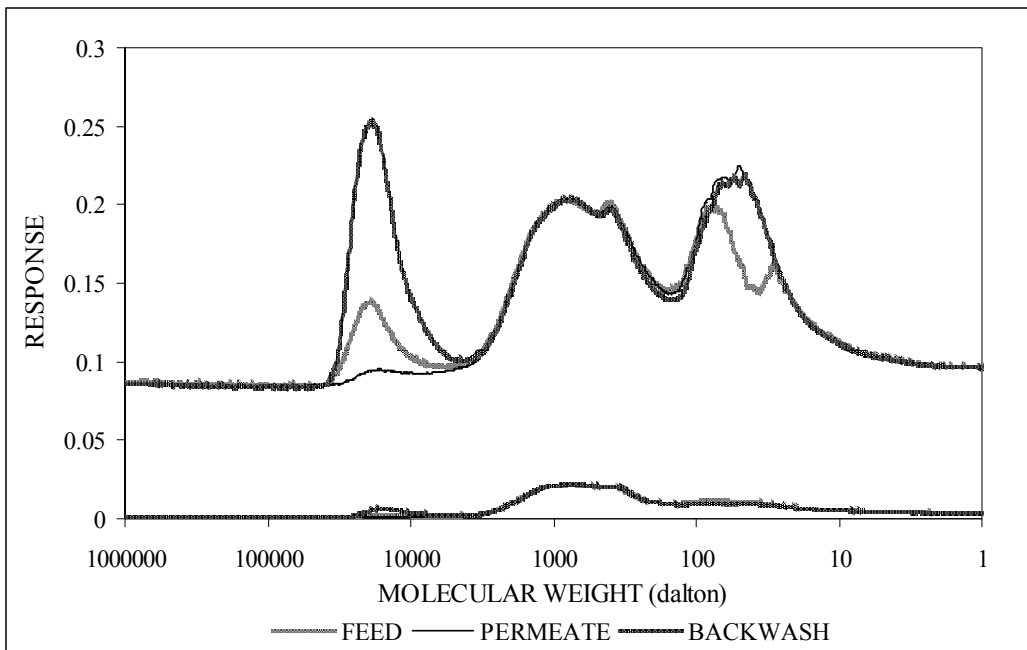


**Figure 6.26 SEC-DOC/UVA chromatogram from NOM samples collected during Run 1 (baseline run) of Scottsdale pilot study**

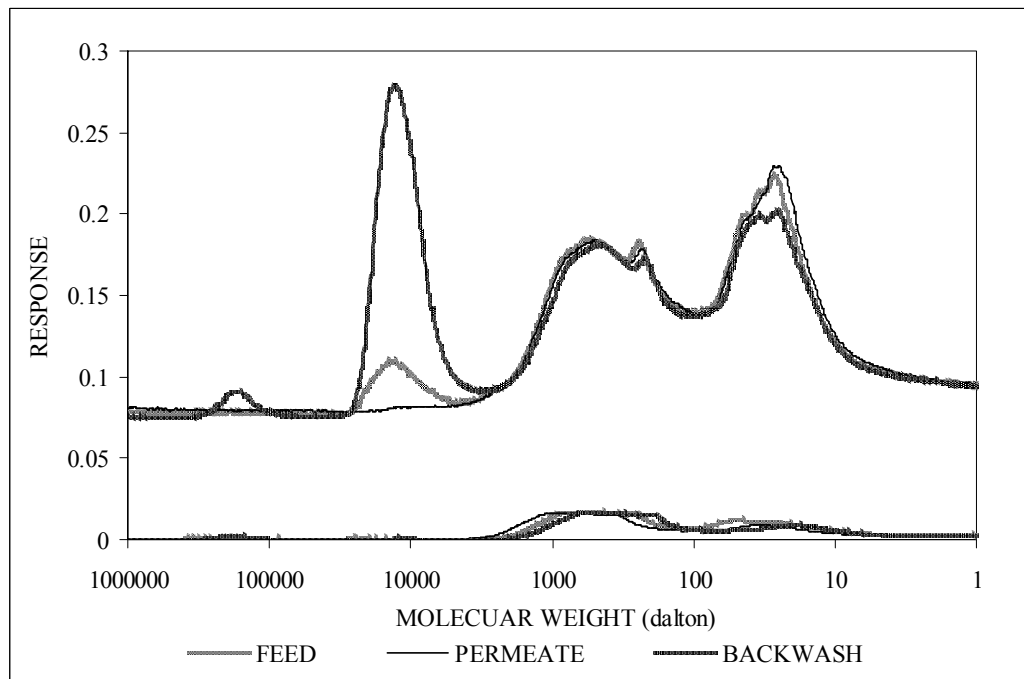


**Figure 6.27 SEC-DOC/UVA chromatogram from NOM samples collected during Run 8 (low PACl dose coagulation run) of Scottsdale pilot study**

These effects are quantitatively illustrated in [Table 6.29](#). The PS concentration in the Scottsdale effluent (feed) is 0.48 mg/L, and is reduced to 0.13 mg/L in the permeate. With coagulation at both the low and high PACl doses, the permeate PS concentrations are reduced to zero (below detection). Correspondingly, the PS level in the backwash water is significantly increased with the PACl and ferric chloride coagulation runs compared with the baseline, indicating PS adsorption onto the floc and subsequent displacement during backwash. In contrast, the reduction in HS and LMA fractions from feed to permeate and increase from feed to backwash (on a percent basis) is much lower for the HS and LMA fractions.

Based on the ratio of PS in backwash to PS in feed, ferric coagulation is not as effective as PACl coagulation on a unit-dose basis in converting PS fraction from soluble to coagulated. Although soluble-to-coagulated ratios for HS were small (1.3 to 2.0 for all three coagulation runs), conversion ratios were similar for PACl and ferric.

### **Vitens Pilot Study**

During the pilot study on Twente Canal water, the impact of operation of Membrane C filtering coagulated Twente Canal water at elevated flux was evaluated. Coagulation is the preferred method for operation of Membrane C on NOM-containing feed waters by the manufacturer; consequently, baseline testing was performed with coagulated water. In [Figure 6.28](#), the TMP is shown during the overall pilot period. In [Figure 6.29](#), the fouling status of the membrane, during the overall period of three months is presented as function of permeate throughput (L/m<sup>2</sup>) and feed water turbidity (NTU).

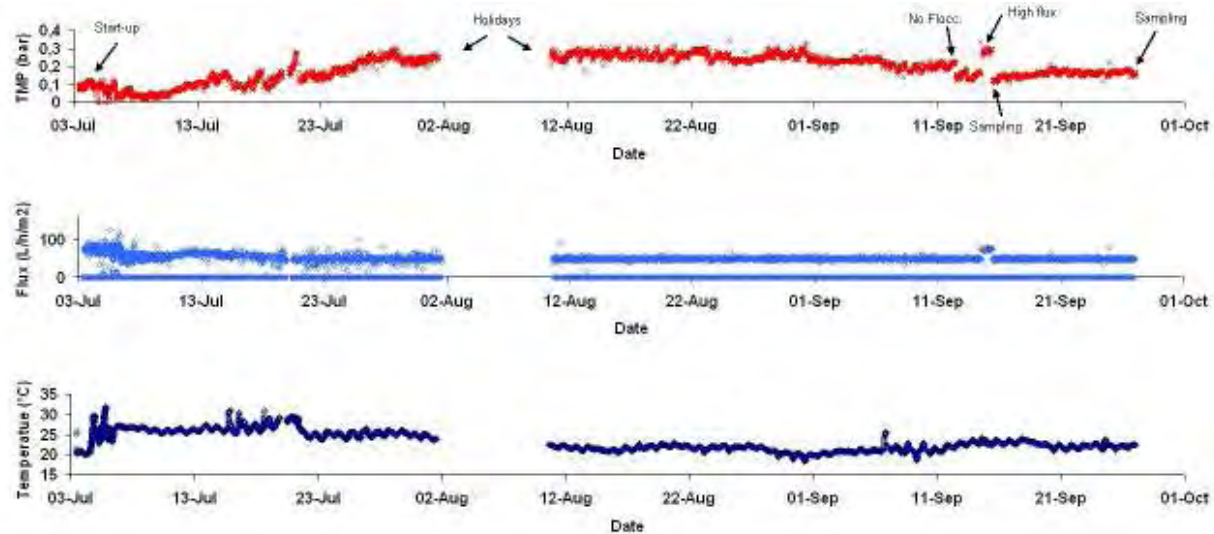
During Run 1, after one week the TMP increased to a maximum of about 26 kPa (3.7 psi), indicating that initial fouling not completely controlled by coagulation and backwashing (no CIP was performed during this period). After the pilot unit was off-line for approximately one week, followed by a CIP, fouling leveled off despite slightly higher feed turbidity and lower temperature. Specific flux remained stable or decreased slightly during the remainder of testing, even during the period of higher flux and no coagulation. These results indicate that stable performance of Membrane C on Twente Canal water could be achieved with coagulation at selected operating conditions.

**Table 6.29**  
**Distribution of DOC (mg/L) and NOM fractions in permeate and backwash samples**  
**during baseline and coagulation runs**

Run	Feed				Permeate				Backwash			
	DOC	PS*	HS*	LMA*	DOC	PS*	HS*	LMA*	DOC	PS*	HS*	LMA*
Baseline	7.46	0.48	2.98	4.00	6.83	0.13	2.99	3.71	8.57	1.10	3.11	4.37
PACl (high dose)†	5.11	0.18	2.07	2.86	4.93	0.00	1.97	2.96	11.90	4.05	4.13	3.71
PACl (low dose) †	5.64	0.35	2.51	2.78	5.56	0.00	2.55	3.01	9.18	2.45	3.19	3.54
Ferric†	5.64	0.43	2.28	2.93	5.33	0.16	2.25	2.92	9.51	2.90	3.10	3.51

\*Values based on integration of SEC-DOC/UVA chromatogram peaks

†Samples were filtered through a 0.45-micron filter prior to analysis



No Operation

**Figure 6.28 Transmembrane pressure, flux, and temperature as a function of time (calendar date) for Membrane C during Vitens pilot testing**

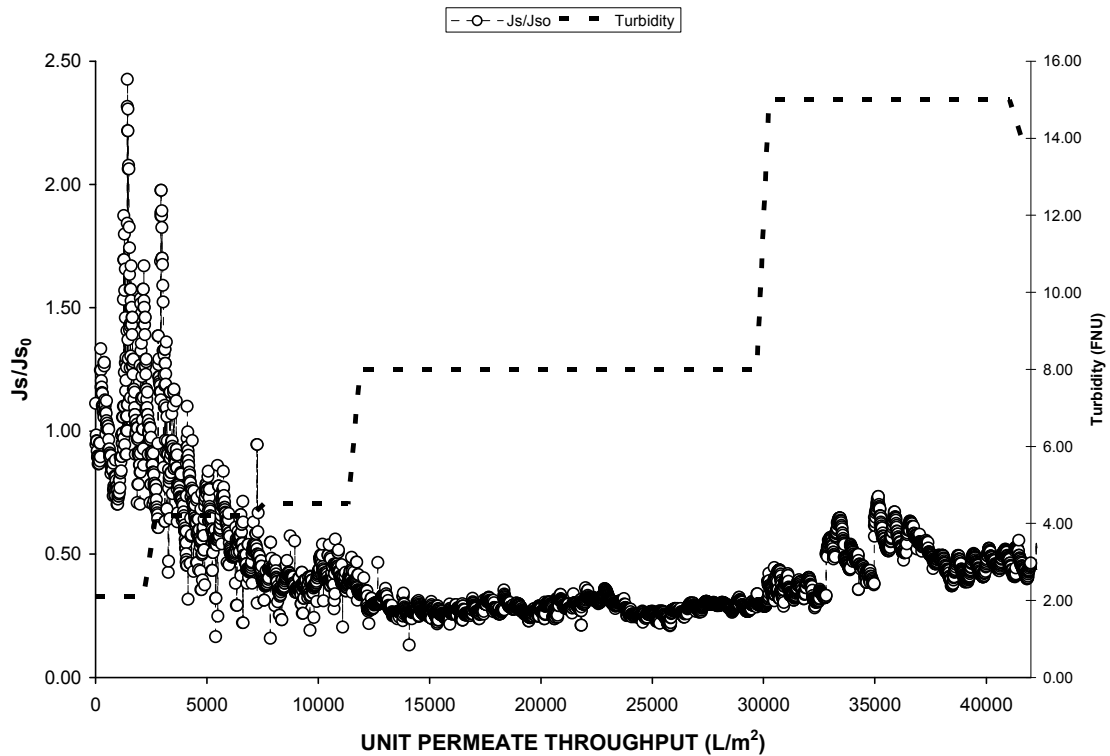


**Figure 6.29 Net normalized specific flux vs. permeate throughput during Vitens pilot study**

### ***Impact of Higher Flux***

The fouling rate for the higher flux is comparable with the fouling rate at baseline flux. To better evaluate the impact of higher flux operation of specific flux, permeate throughput was calculated at baseline flux of 50 L/m<sup>2</sup>-hr and increased flux of 75 L/m<sup>2</sup>-hr. Operation at higher flux did not cause an increase in irreversible fouling, only an increase in TMP resulting from operation at higher flux. It should be noted that direct comparison is difficult because of the fact that the runs were done subsequently, therefore changes in water quality might have influence on the result.

### Impact of Coagulation

In Figure 6.30, the impact of coagulation fouling rate is shown. Although the fouling rate is higher during the first 350 L/m<sup>2</sup> of throughput, the decrease in specific flux at 500 L/m<sup>2</sup> is equal.

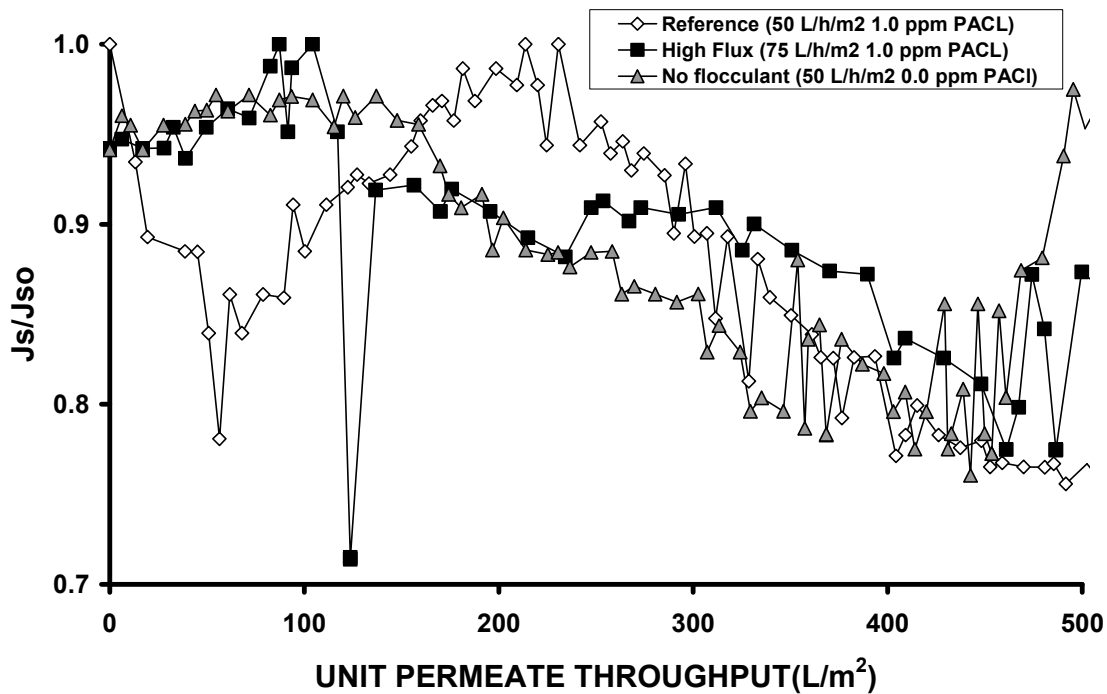


Figure 6.30 Net normalized specific flux as a function of permeate throughput for Membrane C operation at baseline conditions (with and without coagulation) and at increased flux – Vitens pilot study

### Impact of Chemical Cleaning of the Membrane

Chemical cleaning, as described earlier, was performed when the TMP exceeded the limit of 30 kPa (4.3 psi). From Figure 6.31 it can be seen that the first chemical cleaning procedure was executed after a net production of approximately 18,500 L/m<sup>2</sup>. The number of CIPs performed per volume unit then increased considerably. After 28,500 L/m<sup>2</sup> permeate throughput, the turbidity of the feed water increased significantly (see Figure 6.29). Cleaning frequency was increased accordingly to maintain specific flux at a reasonably consistent level. Note that the CIP was performed with hydrochloric acid and caustic soda, sequentially. This increased CIP frequency corresponds to a significant increase in feed water turbidity (see Figure 6.29) indicating the sensitivity of Membrane C to solids loading.

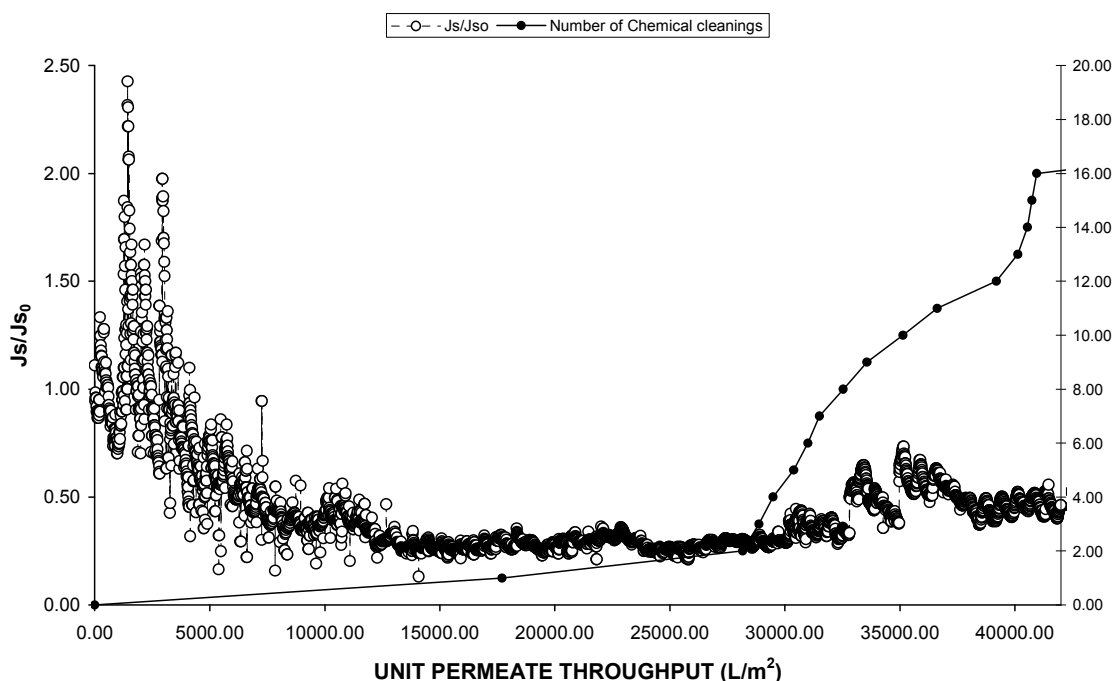


Figure 6.31 Net normalized specific flux and frequency of CIP as a function of permeate throughput for Vitens pilot study

## Chemical Analysis of Process Waters

Feed water, permeate, back wash water and cleaning solutions were sampled and analyzed for a variety of parameters. The results are presented in Tables 6.30 and 6.31 and Figure 6.32. The results of Table 6.30 are normalized to the feed water values (e.g., backwash value divided by feed value) and plotted in Figure 6.33.

**Table 6.30**  
**First series of data collected from samples taken from the pilot on September 17, 2006**

Analysis	Feed before coagulation	Average feed	Average permeate	Average backwash waste	Acid CIP waste	Caustic CIP waste
pH	7.71	7.42	7.48	7.57	2.32	11.4
Conductivity (mS/m)	54.6	54.0	54.0	54.20	392	NA*
Turbidity (NTU)	8.00	11.75	1.36	18.0	8.00	37.0
UV (1/m)	24.0	22.0	22.0	22.3	24.0	25.0
NO <sub>2</sub> (mg/L)	0.07	0.03	0.06	0.02	0.01	0.06
NO <sub>3</sub> (mg/L)	6.50	4.85	5.40	5.13	4.80	4.50
Cl (mg/L)	100	100	100	100	530	150
NH <sub>4</sub> (mg/L)	0.05	0.05	0.05	0.05	0.07	0.05
SO <sub>4</sub> (mg/L)	37	36.8	37	37	36	37
Al (µg/L)	43.8	1010	90.9	1630	3650	499
Ca (mg/L)	43.7	42.9	42.6	43.1	43.6	39.3
Mg (mg/L)	6.28	6.14	6.13	6.17	6.02	2.23
Fe (mg/L)	0.38	0.61	0.02	0.99	0.81	1.18
TOC (mg/L)	9.0	9.5	8.6	10.7	10.0	13.0
DOC (mg/L)	9.1	9.1	8.5	9.7	11.0	15.0

\*NA = not analyzed

**Table 6.31**  
**First series of data collected from samples taken from the pilot on September 26, 2006**

Analysis	Feed before coagulation	Average feed	Average permeate	Average		
				BW backwash waste	Acid CIP waste	Caustic CIP waste
pH	7.70	7.68	7.74	7.57	2.33	10.95
Conductivity (mS/m)	56.80	56.03	56.0	56.30	386	93.80
Turbidity (FNU)	14.00	13.50	0.86	29.00	13.00	46.00
UV <sub>254</sub> (1/m)	24.00	21.25	20.50	22.00	37.00	31.00
NO <sub>2</sub> (mg/L)	0.09	0.03	0.06	0.01	0.01	0.06
NO <sub>3</sub> (mg/L)	4.90	5.68	5.35	5.55	4.90	5.40
CL (mg/L)	110	110	110	110	520	150
NH <sub>4</sub> (mg/L)	0.06	0.05	0.05	0.05	0.07	0.34
o-PO <sub>4</sub> (mg/L)	0.12	0.09	0.05	0.20	0.85	0.14
Si (mg/L)	1.50	1.58	1.58	1.53	2.10	3.70
SO <sub>4</sub> (mg/L)	38	38	38	39	38	40
Al (µg/L)	89.4	1008	99.6	2098	7270	2040
Ca (mg/L)	48.6	48.4	48.4	48.9	48.6	43.6
Mg (mg/L)	6.78	6.73	6.76	6.80	6.41	2.76
Fe (mg/L)	0.73	0.83	0.02	1.46	1.53	2.85
TOC (mg/L)	9.1	9.4	8.4	11.0	13.0	17.0
DOC (mg/L)	9.0	8.8	8.3	10.0	15.0	17.0

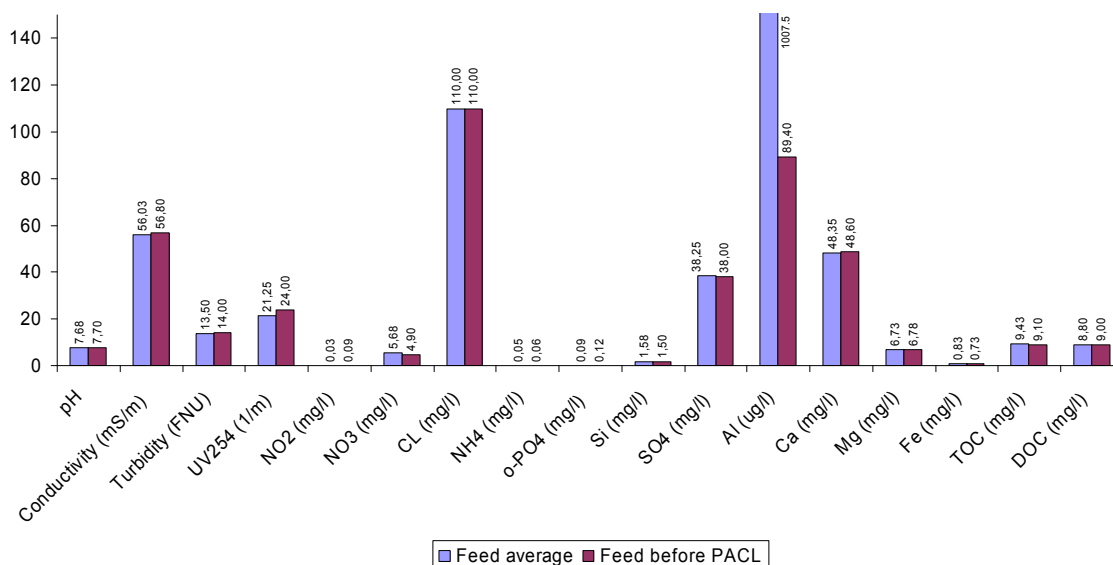


**Figure 6.32 Analysis of feed water before and after coagulation**

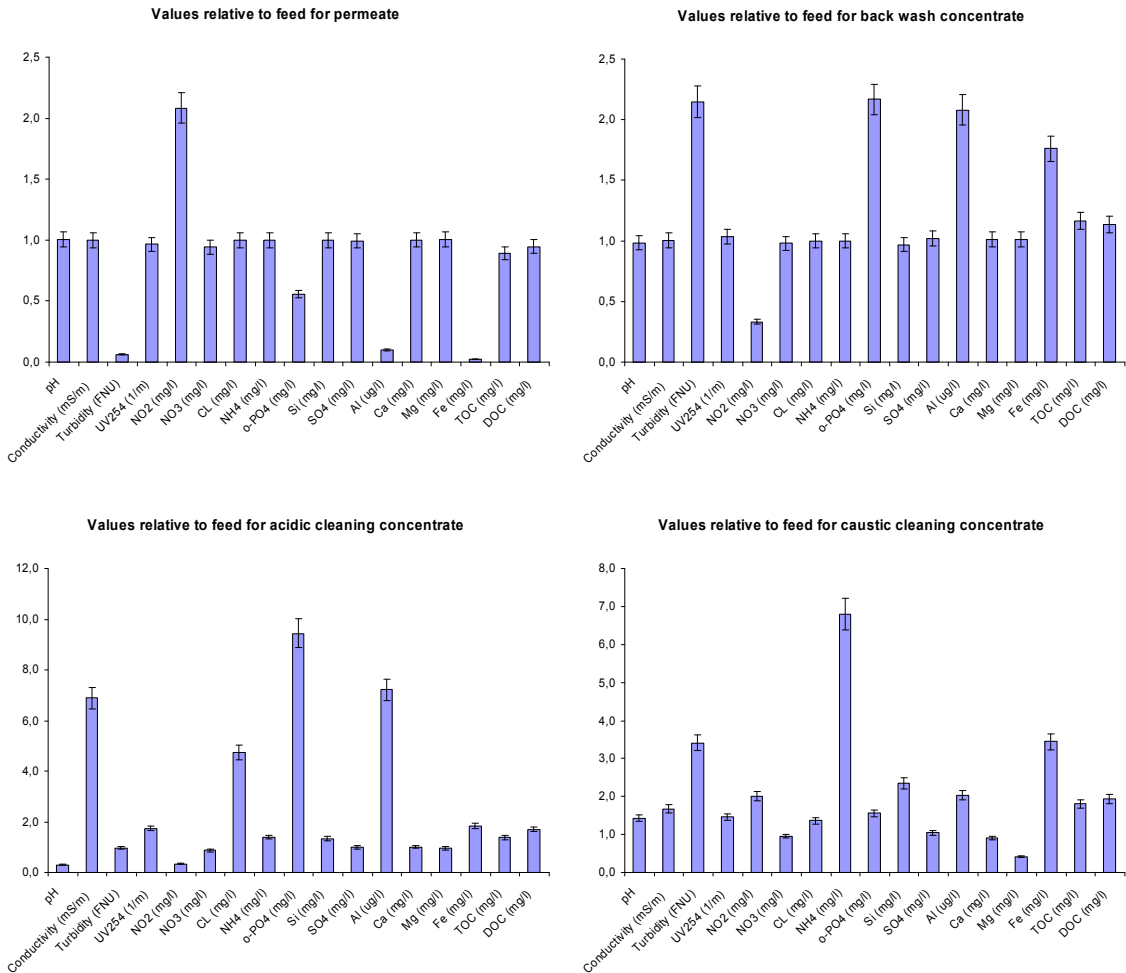


**Figure 6.33 Analysis results for permeate (upper left), backwash concentrate (upper right), acidic cleaning concentrate (lower left), and caustic cleaning concentrate (lower right) relative to feed water values**

Comparing the permeate and feed analyses (after aluminum dosing), turbidity, ortho-phosphate, aluminum, and iron were retained from the feed by the membrane. Only a small fraction of the DOC and TOC was retained. During backwashing, turbidity, ortho-phosphate, aluminum, and iron were partly removed from the membrane surface. The DOC and TOC concentrations in the backwash water were slightly higher than those of the feed water. From the analysis of the acidic- and caustic cleaning solutions, it can be seen that other components are also removed, which means that they were also retained on the membrane surface. During the acidic cleaning, mainly aluminum was removed, as well as a small portion of the DOC/TOC fouling. During caustic cleaning, ammonium (only in the case of September 17), silica, aluminum, iron, and organic matter (DOC and TOC) were removed. Based on mass balance calculations, an estimation of DOC accumulation onto the membrane was made. An average of 1 mg DOC per liter of permeate throughput was deposited on the membrane during production, and approximately 90 percent of the deposited DOC was removed by means of backwashes, suggesting that this DOC was associated with particles and the remaining 10 percent can be

removed with chemical cleaning (approximately 3 percent by acidic cleaning and approximately 7 percent by caustic cleaning). The higher values for conductivity and chlorine are a result of the cleaning agent itself (hydrochloric acid).

In Table 6.32, the different cleaning steps are compared as to the components that they removed from the membrane surface.

Organic NOM is clearly present in the membrane foulant layer; DOC values are twice as high in the caustic cleaning waste as compared to the feed. UV<sub>254</sub> were elevated in the acid cleaning waste. This result is surprising given that NOM-adsorbing UV at this frequency is typically hydrophobic (humic substances), having lower solubility at acidic pH.

**Table 6.32**

**Different cleaning steps in relation to the components they remove from the membrane**

	Backwash	Acidic cleaning	Caustic cleaning
Turbidity	+	0	++
Nitrite	-	-	-
Ammonium	0	0	++
Ortho-phosphate	+	+++	0
Silica	0	0	+
Aluminum	+	+++	+
Magnesium	0	0	-
Iron	+	+	++
TOC/DOC	0/+	+	++

- [+++] High removal rate
- [++] Medium removal rate
- [+] Low removal rate
- [0] No removal
- [-] Has negative effect

## TIER 2 PILOT STUDIES

### Tuscaloosa

Figures 6.34 through 6.36 present net normalized specific flux decline curves for pilot units using Membrane B, Membrane E, and Membrane A, respectively. The high degree of data scatter in Figure 6.36 reflects the manner in which the operating data was collected with Membrane B pilot unit. Data collection occurred on a fixed time interval, rather than at a fixed time within a filtration cycle. This results in  $J_s$  value being calculated at different degrees of fouling with the cycle (different TMP values). The flux decline curves show different degrees of fouling by the three PVDF membranes, two of which are MF (Membranes A and E) with pore size of  $0.1 \mu\text{m}$  and one UF (Membrane B) with pore size of  $0.02 \mu\text{m}$ . The tighter UF membrane showed a higher rate of flux decline (over a shorter throughput) than the MF membranes, suggesting that a greater amount of the PS fraction was retained by the tighter UF membrane.

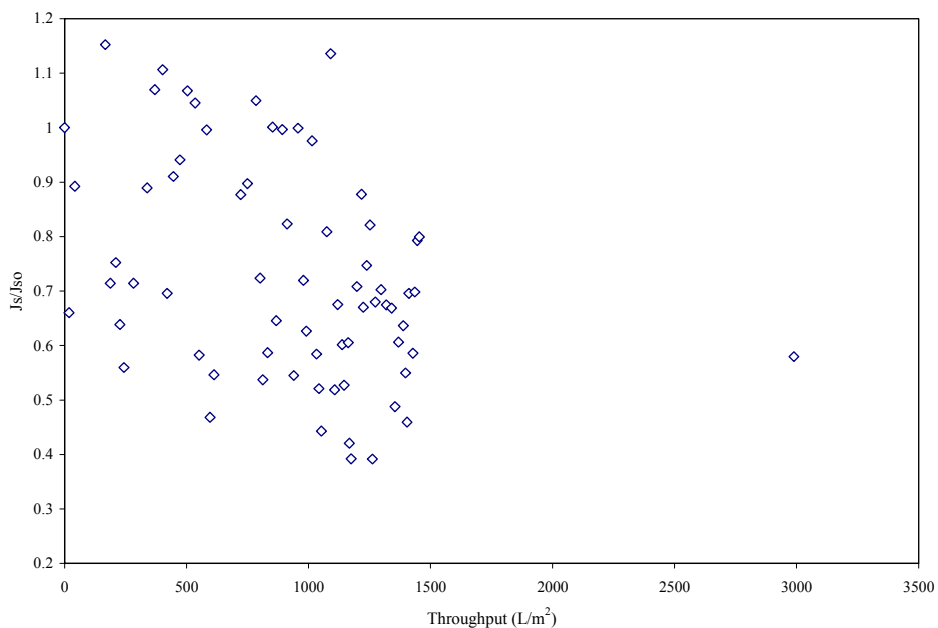


**Figure 6.34 Normalized net specific flux for Membrane B during Tuscaloosa pilot study**

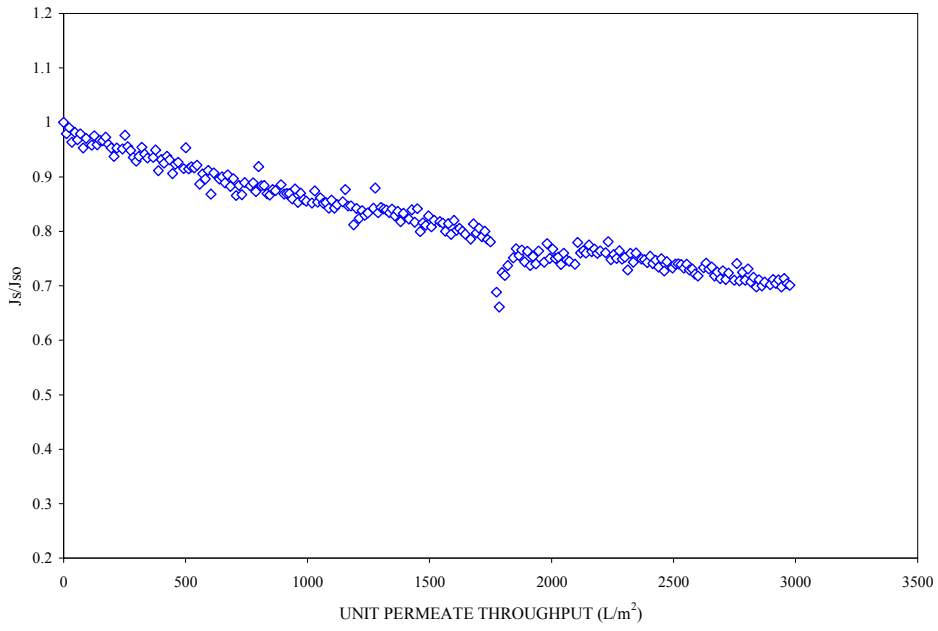


**Figure 6.35 Normalized net specific flux for Membrane E during Tuscaloosa pilot study**

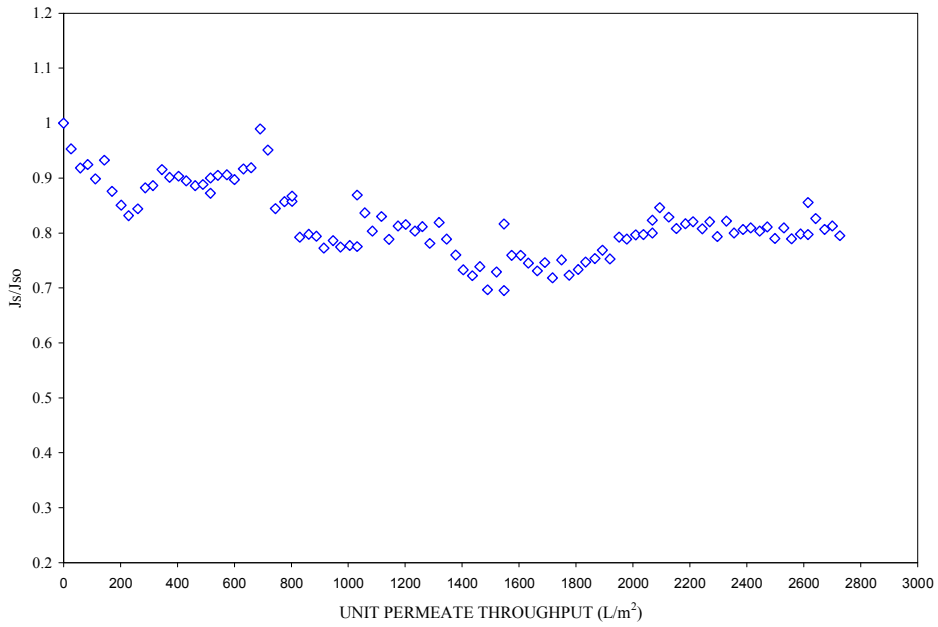


**Figure 6.36 Normalized net specific flux for Membrane A during Tuscaloosa pilot study**

Samples were collected for NOM characterization during Membrane B pilot testing. The results are shown in [Table 6.33](#). Consistent with the results from the bench and Tier 1 pilot studies, the following can be concluded from the Membrane B pilot test for NOM characterization: (1) coagulation reduced the PS fraction to a greater degree than the HS fraction (the LMA fraction was too low to quantify), and (2) the UF membrane rejected a much greater percentage of the PS fraction than the HS fraction, with the former being highly concentrated in the backwash water (by a factor of five). These results support PS as the dominant fouling fraction. The absence of NOM characterization data for the MF pilot units does not allow a determination as to whether a higher level of PS rejection by the UF membrane correlated with higher flux decline.

## Minneapolis

[Figures 6.37](#) through [6.39](#) present net normalized specific flux decline curves for three different “runs”<sup>1</sup> conducted with the Membrane C pilot unit operated on softened, recarbonated, and chemically clarified Mississippi River water. The fouling rate exhibited by this UF membrane was highest (slope of curve between chemical washes) in [Figure 6.38](#) and lowest in [Figure 6.39](#).

**Table 6.33**  
**NOM characteristics for Membrane B samples\***

Process Stream	DOC (mg/L)	PS (mg/L)	HS (mg/L)	LMA (mg/L)
Raw	2.4	0.15	2.25	ND†
Coagulated (Feed)	1.67	0.08	1.59	ND
Permeate	1.55	0.05	1.50	ND
Backwash	2.79	0.25	2.54	ND

\*PS, HS, and LMA values were obtained from the integration of respective peaks on SEC-DOC chromatograms.

†ND = not detected

---

<sup>1</sup> The data in the figures do not represent distinct runs as defined as operating periods of filtration and backwash separated by chemical cleanings (CIPs). The Membrane C pilot unit was operated over the long term with only chemical washes, whose chemical strength and soak duration varied periodically. The data included in the three runs were based on periods of operation where membrane feed water quality was different with respect to NOM levels. As such, the  $J_s/J_{s0}$  values in [Figures 6.32](#) and [6.33](#) are  $>1.0$  because the  $J_{s0}$  is less than the clean membrane  $J_s$ .

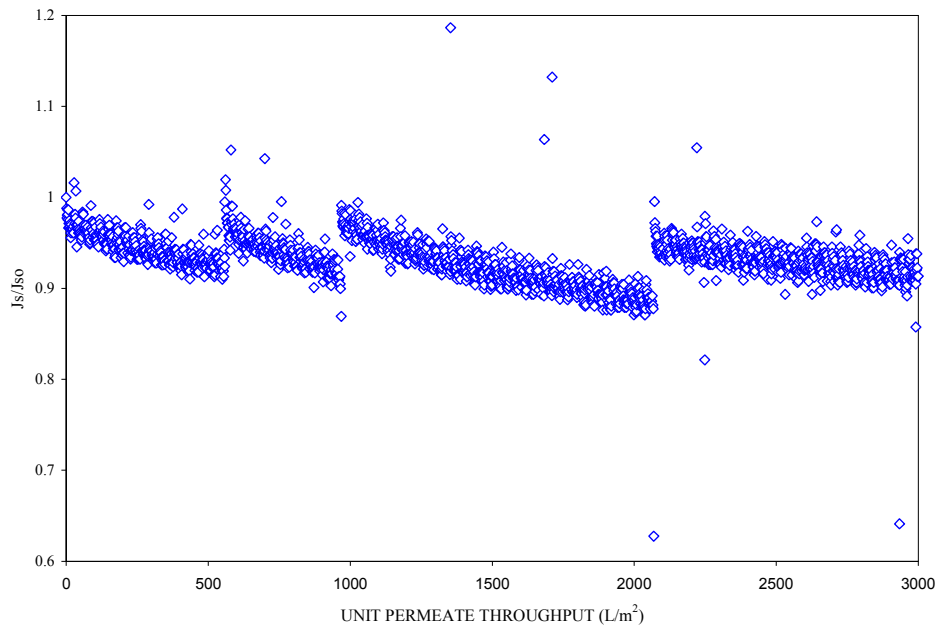


**Figure 6.37 Run 1 normalized net specific flux during Minneapolis pilot study**

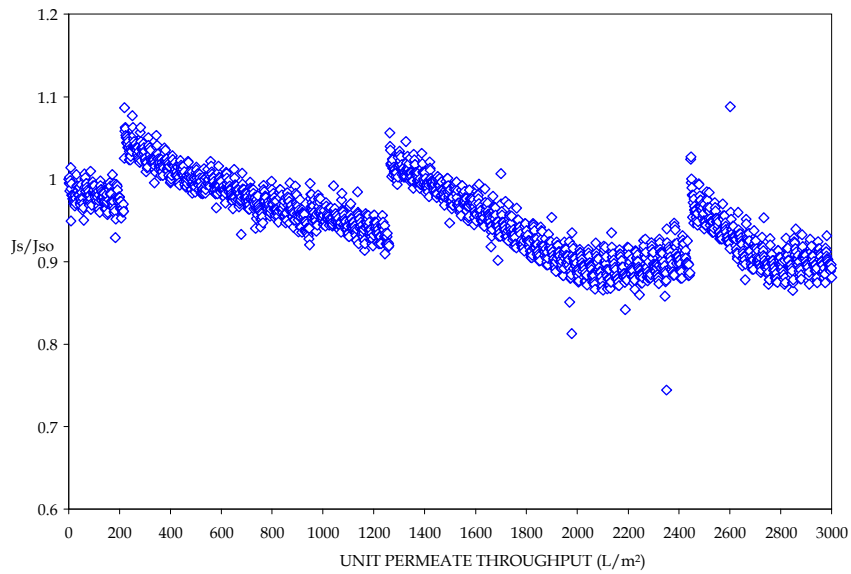


**Figure 6.38 Run 2 normalized net specific flux for Membrane C during Minneapolis pilot study**

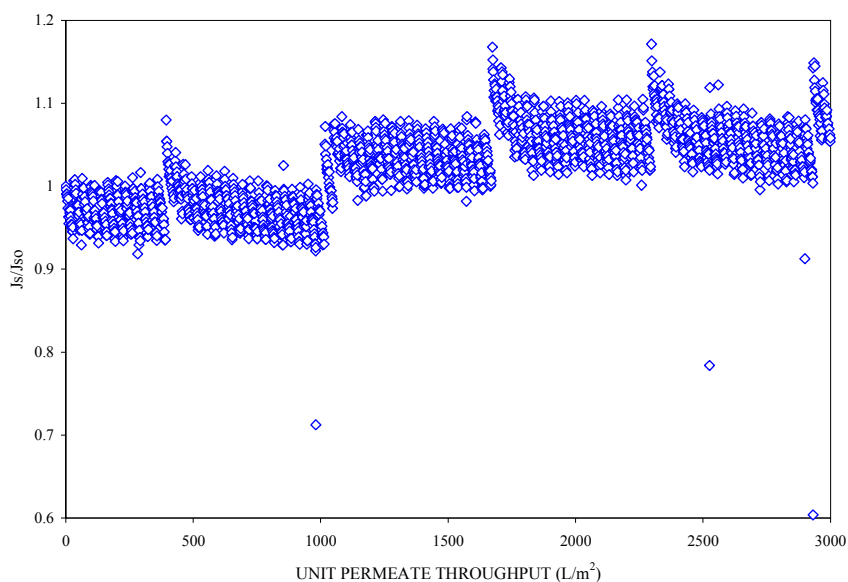


**Figure 6.39 Run 3 normalized net specific flux for Membrane C during Minneapolis pilot study**

Over the 3000  $L/m^2$  of permeate throughput, the rate of fouling, as evidenced by the slope of the  $J_s/J_{s0}$  curves between chemical wash events, was highest for Run 2 and lowest for Run 3. During this period, there were no significant variations in UF feed water turbidity, which ranged between 2 and 3 NTU. One set of samples were collected during each of the three runs for both the raw water (Mississippi River water) and UF feed water, and the NOM in each was characterized using SEC-DOC/UVA and XAD-4/-8 analyses. The SEC-DOC/UVA chromatograms for the raw water and UF feed are shown in Figures 6.40 and 6.41, respectively. The integrated SEC-DOC peaks for each, expressed as mg/L DOC are presented in Table 6.34, while the XAD results are shown in Table 6.35. Taken together, the NOM characterization data show that (1) lime softening/recarbonation and ferric clarification are effective in reducing DOC and the PS and HPO/TPI fractions of the river water NOM, and (2) NOM levels, particularly the PS fraction, are lowest during Run 1 when the rate of fouling was intermediate. The lower fouling rate experienced during Run 3 indicates that the greater frequency of chemical washes was effective in reducing the rate of flux decline despite the higher NOM levels present in the UF feed water during these runs. This beneficial impact was not evident during Run 2 when fouling rate was highest.

No permeate or backwash samples were analyzed by SEC-DOC/UVA; consequently, no conclusions can be drawn as to the partitioning of NOM fractions between feed, backwash, and chemical wash.

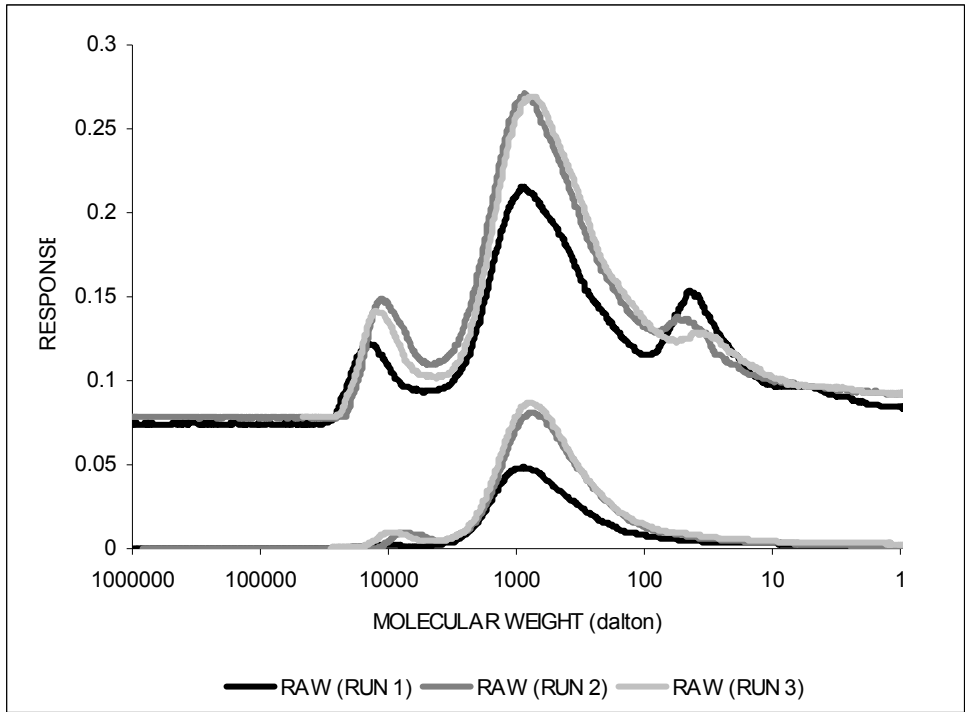


**Figure 6.40 SEC-DOC/UVA chromatogram for raw water for Runs 1, 2, and 3 - Minneapolis pilot study using Membrane C**

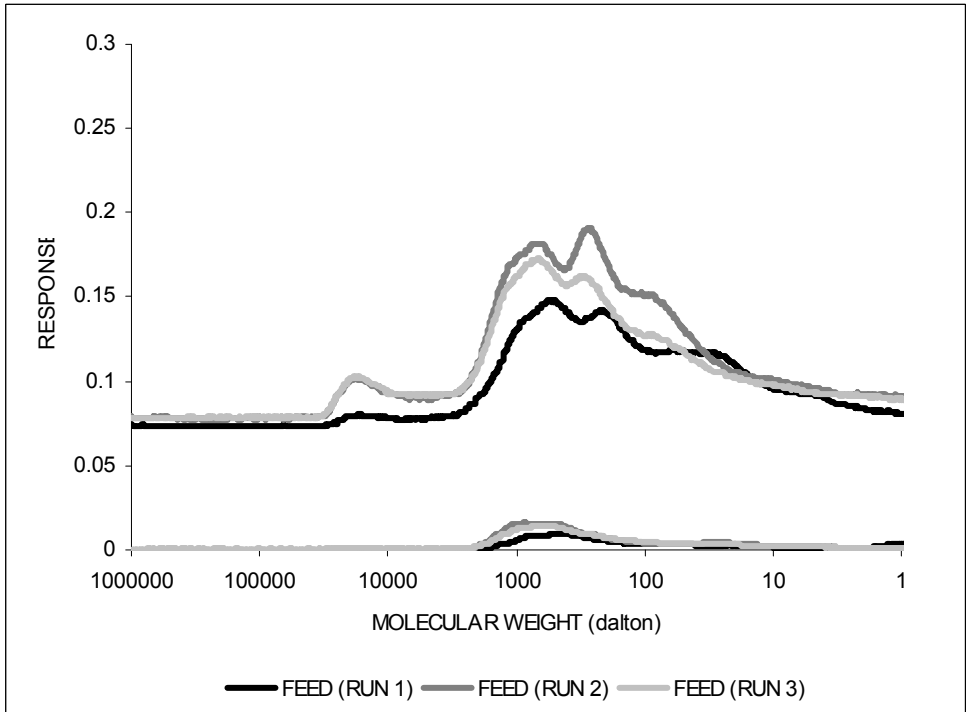


**Figure 6.41 SEC-DOC/UVA chromatogram for UF feed water for Runs 1, 2 and 3 - Minneapolis pilot study using Membrane C**

**Table 6.34**  
**DOC and NOM SEC-DOC fractions for Mississippi River water and UF feed**

Run	Process stream*	DOC (mg/L)	PS (mg/L)	HS (mg/L)	LMA (mg/L)
1	Raw	7.82	0.80	5.18	1.84
1	Feed	4.28	0.02	2.89	1.37
2	Raw	10.1	1.26	7.27	1.57
2	Feed	5.18	0.35	3.32	1.51
3	Raw	11.2	1.22	8.55	1.42
3	Feed	5.42	0.48	3.72	1.22

\*Raw = raw river water; feed = membrane feed after softening, recarbonation, and clarification

**Table 6.35**  
**XAD-8/-4 fractions for Mississippi River water and UF feed**

Run	Process stream*	HPO (%)	TPI (%)	HPI (%)
1	Raw	38	24	37
1	Feed	33	21	46
3	Raw	45	24	32
3	Feed	39	21	40

\*Raw = raw river water; feed = membrane feed after softening, recarbonation, and clarification

## North Bay

Trout Lake (feed to the Membrane A pilot unit) is characterized by low temperature, TDS and turbidity; and moderate TOC (see Appendix D). As such, the primary feed water component contributing to fouling of Membrane A is NOM.

Normalized net specific flux profile for the period of Membrane A pilot operation evaluated in this report is shown in [Figure 6.42](#). Over the 3000+ L/m<sup>2</sup> of permeate throughput, the rate of fouling was low when compared to that observed in the Tier 1 studies. The frequent chlorine wash regime employed with the pilot unit resulted in a relatively high CT (7650 mg/L-min), which was effective in reversing NOM fouling. This is consistent with the results from the bench and Tier 1 pilot studies, which showed that chlorine washes with high CT values were effective for specific flux recovery.

[Figure 6.43](#) presents the SEC-DOC/UVA chromatogram for feed, permeate, and backwash samples collected during the pilot operation. The plot shows the typical rejection of PS fraction and subsequent concentration of PS in the backwash sample. Unlike filtration of the Tier 1 source waters, however, the MF membrane also removed a significant portion of the HS fraction. Surprisingly, this rejected fraction did not appear in the backwash water.

[Table 6.36](#) presents the SEC-DOC peak integration data for the NOM samples. The integrated backwash peaks are shown as percentages only because no DOC value was available for this sample. The data in the table show a reduction in PS fraction and, to a lesser extent, HS fraction from feed to permeate. Although the change in concentration of each fraction from feed

to backwash cannot be determined, it can be stated with some confidence through mass balance considerations that the backwash water was enriched in both. The SEC-DOC results from this study are consistent with those from the bench and other pilot studies and reinforce the importance of the PS fraction as the primary contributor to NOM fouling.

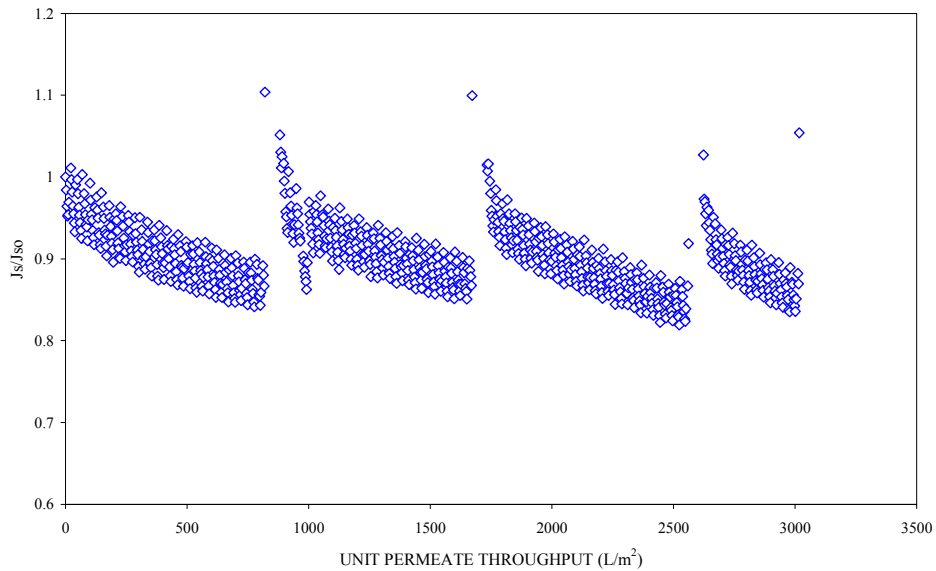


**Figure 6.42 Normalized net specific flux profile for the Membrane A pilot unit at North Bay, Ontario**

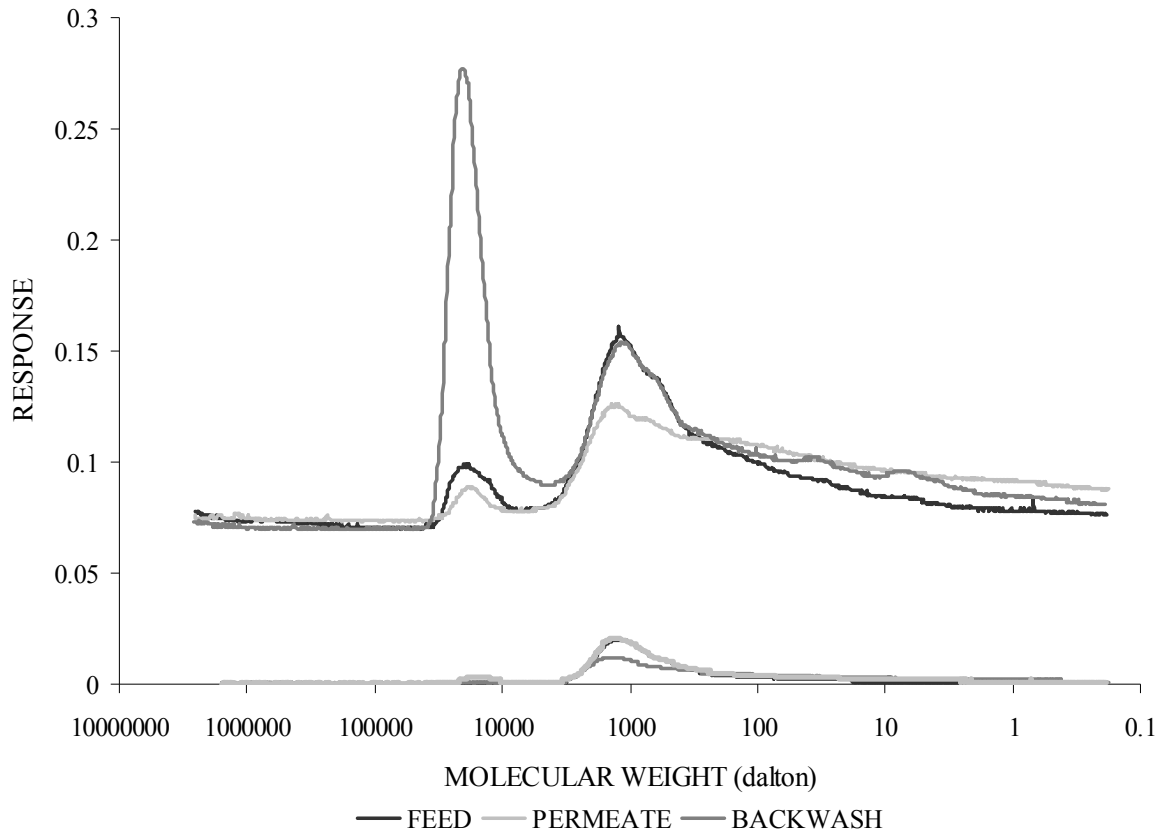


**Figure 6.43 SEC-DOC/UVA chromatogram for NOM samples collected during the Membrane A pilot study at North Bay, Ontario**

**Table 6.36  
DOC and NOM SEC-DOC fractions for North Bay pilot water samples**

Feed (mg/L)				Permeate (mg/L)				Backwash (% DOC)			
DOC	PS	HS	LMA	DOC	PS	HS	LMA	DOC	PS	HS	LMA
2.7	0.48	1.74	0.71	2.9	0.15	1.47	1.29	NA*	36.2	38.6	25.2

NA = not analyzed

## FULL-SCALE RESULTS

The purpose of including full-scale facilities in the study was to apply the analytical methodologies used for the NOM characterization of bulk water, membranes, and membrane foulants in the bench and pilot studies to selected operating plants to enhance the utilities' understanding of how the NOM in the plant's source water contributes to membrane fouling. The approach was to obtain basic source water quality information and performance data for an operating membrane unit at the plant and combine this information with the NOM characterization results. This knowledge could be used to develop more effective foulant management strategies.

This section presents information on source water quality, membrane unit performance, fouled membranes, and membrane foulants for the Parsons, Kan. and Manitowoc, Wis. facilities. Samples were also collected for bulk water NOM characterization; however, the SEC-DOC/UVA equipment was inoperable at the time the samples arrived at University of Colorado and could not be repaired quickly enough to be able to analyze the samples within an acceptable holding time. This delay limited the ability to link membrane performance with NOM fouling and to provide the intended insight into better fouling management approaches.

### Parsons, Kansas

Figure 6.44 shows the normalized net specific flux as a function of permeate throughput for one of the three Membrane E skids in operation at the Parsons treatment facility. The data in Figure 6.44 in which the Membrane E system was operated following a chemical clean, illustrate a moderate degree of fouling over the 3000 L/m<sup>2</sup> throughput period. Although no TOC or turbidity data was available on the MF feed water to determine the NOM and solids loading to the membrane, the rate of fouling was sufficiently low as to not require the MF skids to be cleaned very frequently (more than a 3-month interval), particularly in light of the absence of chemical washes to manage fouling. This suggests that coagulation with aluminum chlorohydrate was effective in reducing the PS (and HS) fraction in the creek water to levels that minimize NOM fouling.

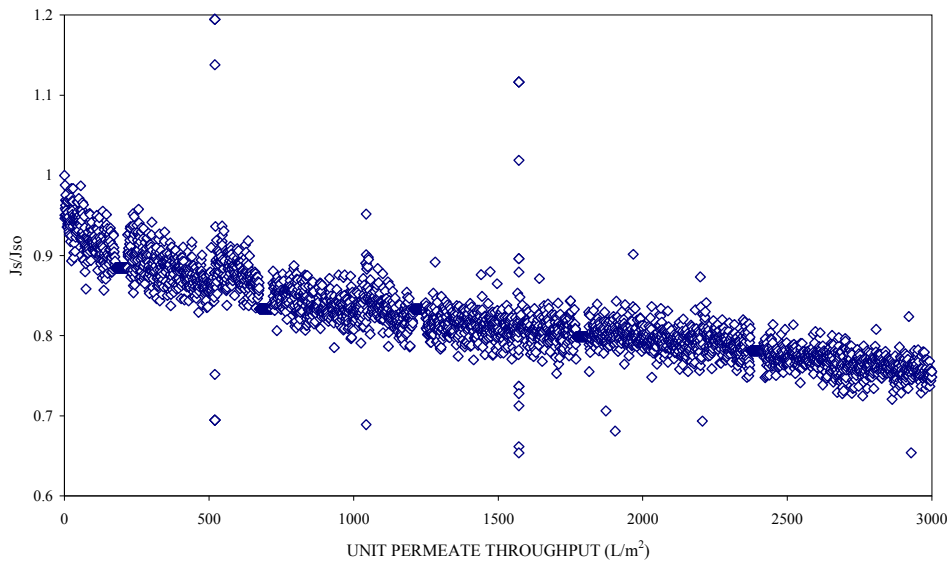


**Figure 6.44 Normalized net specific flux profile for one of the full-scale Membrane E units at Parsons, Kansas**

### Manitowoc

Figure 6.45 shows the normalized net specific flux as a function of permeate throughput for one of the thirteen Membrane F skids in operation at the Manitowoc water treatment facility. The data in Figure 6.45, which reflects operation directly following a CIP, is typical of the fouling profile for the Membrane F trains on Lake Michigan water. Relative to the profiles for Membrane E at Parsons, Kans. and those for the previously discussed pilots, the loss of membrane permeability shown in the figure is quite low ( $J_s > 90$  percent of  $J_{s0}$  after 2400  $L/m^2$  permeate throughput), illustrating a low rate of fouling despite the use of a highly hydrophobic membrane. Although NOM profiling by SEC-DOC was not conducted on the Lake Michigan water, the NOM in this source is relatively low (less than 2 mg/L TOC) compared to the other source waters used in this study. The low rate of fouling observed here suggests that the PS fouling NOM fraction may be very low in the Lake Michigan water.

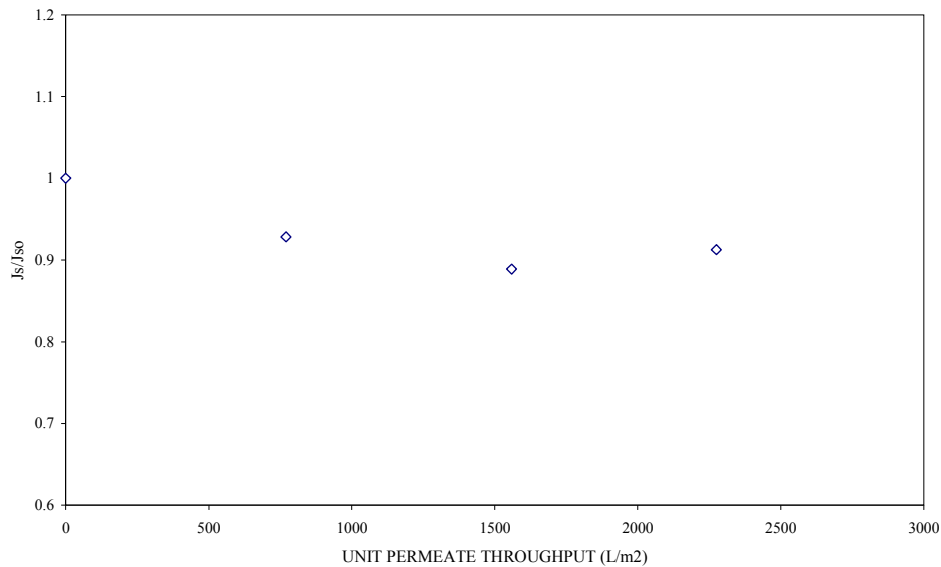


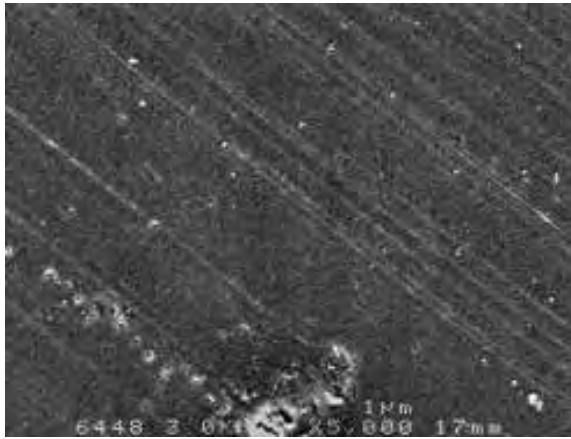
**Figure 6.45 Normalized net specific flux profile for the full-scale Membrane A skid at Manitowoc**

## **CHARACTERIZATION OF FOULED FIBERS FROM PILOT- AND FULL-SCALE MODULES**

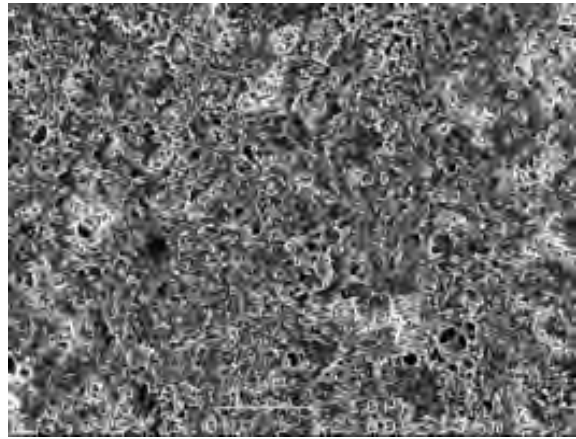
### **Morphology of Fouled Pilot- and Full-Scale Membrane Fibers**

FESEM images of the inner and outer surfaces of fouled fibers collected from the pilot modules following filtration runs at Tampa Bay, Indianapolis, and Scottsdale are presented in [Figures 6.46 through 6.49](#).

For the Membrane B fibers from Tampa Bay, FESEM images did not show clear evidence of organic deposit on the outer (filtration) surface of the fibers. For all Indianapolis runs (only the results of Run 3 and 7 are given) conducted with Membrane A, the results led to the same observation. Surprisingly, for both samples, a deposit was observed on the inner surface of the fibers. The deposit appeared to be relatively more abundant for Membrane A (associated with Indianapolis Run 7) with very distinct accumulation of spherical structures (grape-type structures). This material may correspond to microbial entities (algae and/or bacteria). Physical chemical characteristics of the feed water of Run 7 indicated a high concentration of algae during this period of the study.

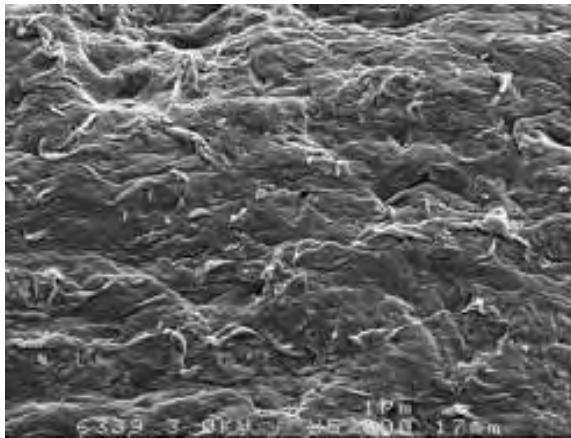


**Outer (feed) surface**

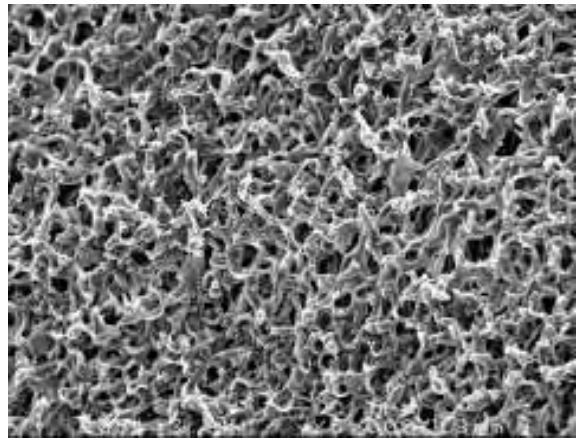


**Inner (permeate) surface**

**Figure 6.46 SEM of fouled Membrane B fiber from Tampa Bay pilot study (Run 9)**

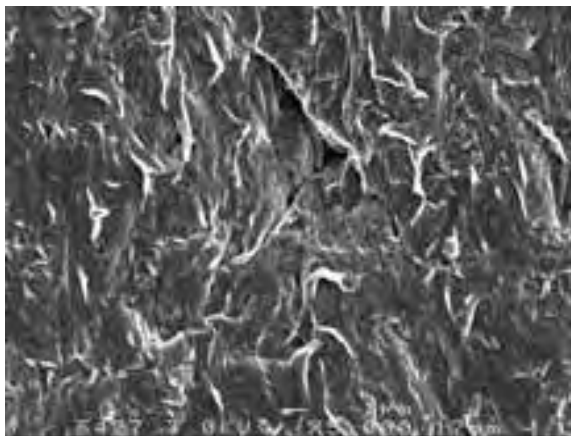


**Outer (feed) surface**

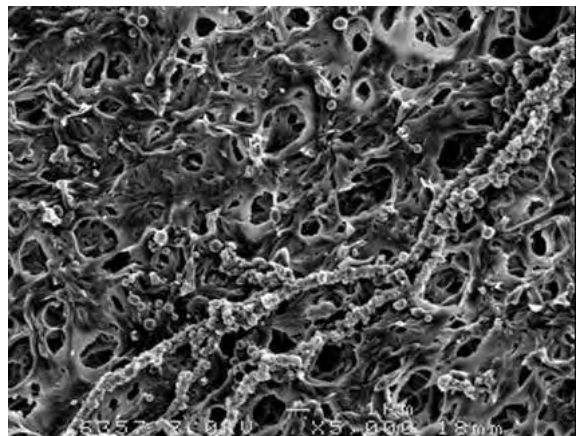


**Inner (permeate) surface**

**Figure 6.47 SEM of fouled Membrane A fiber from Indianapolis pilot study (Run 3)**

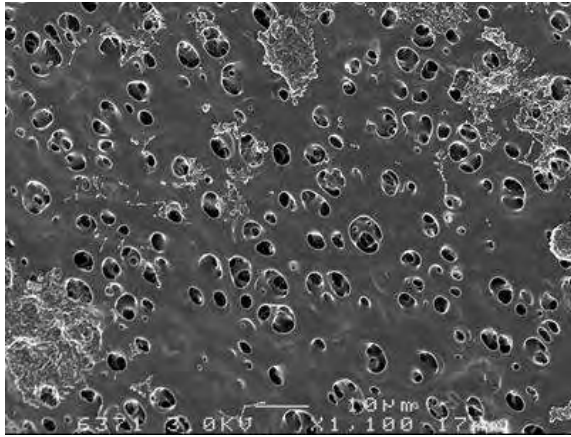


**Outer (feed) surface**

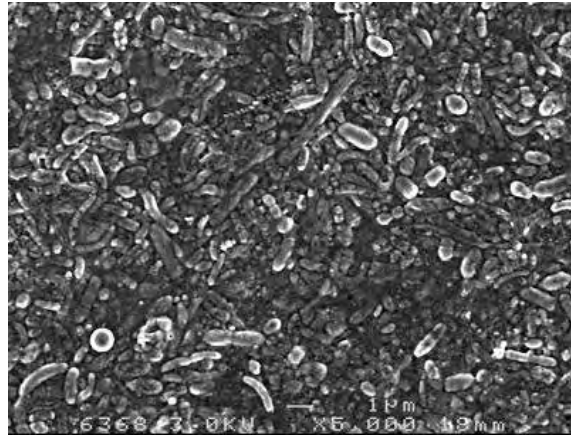


**Inner (permeate) surface**

**Figure 6.48 SEM of fouled Membrane A fiber from Indianapolis pilot study (Run 7)**



**Outer (permeate) surface**



**Inner (feed) surface**

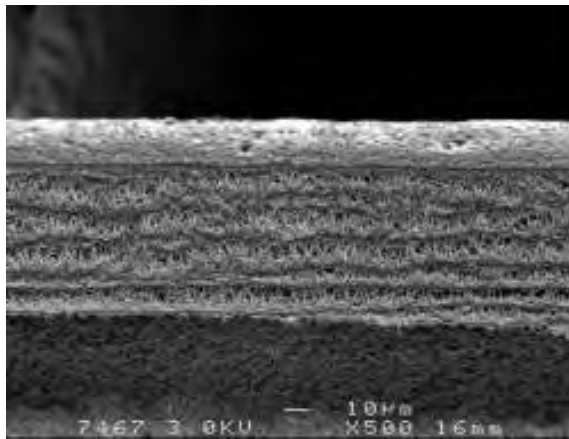
**Figure 6.49 SEM of fouled Membrane D1 PES fiber from Scottsdale pilot study (end of study, baseline conditions)**

The accumulation of material and microorganisms on the inner (feed-side) surface of Membrane D1 fibers operated on Scottsdale effluent can be clearly observed in [Figure 6.48](#). In contrast, the outer (permeate-side) surface of the fiber shows only minor amounts of material and no bacteria, indicating effective bacterial exclusion by the pores.

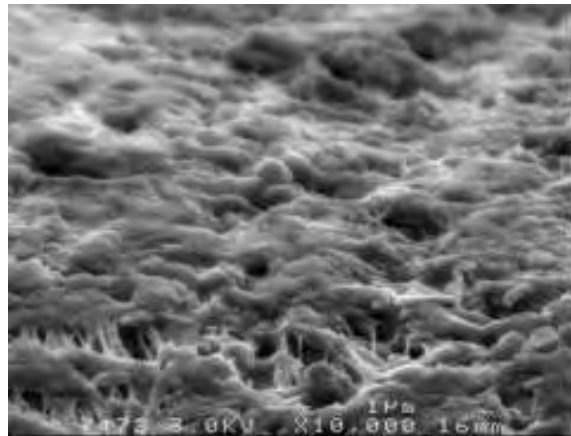
[Figure 6.50](#) presents an FESEM of a Membrane F fiber extracted from a full-scale module at the MPU MF plant operating on Lake Michigan water. Before the fiber specimens were harvested, the module was backwashed and washed successively with sulfuric acid and sodium hydroxide (the unit was run for 436 hours between the two last cleaning operations). These cleaning operations apparently did not affect the “sticky” material that can be observed at the outer surface of the membrane.

### **Contact Angle of Fouled Pilot- and Full-Scale Membranes**

[Table 6.37](#) shows the contact angle of the fibers harvested from fouled modules operated during the Tier 1 pilot studies. Contact angles for the virgin fibers, previously presented, as well as pertinent water quality data for membrane feed water for the Indianapolis pilot runs, are also shown for reference.



**Cross section**



**Outer (feed) surface**

**Figure 6.50 SEMs of Membrane F fiber from module treating Lake Michigan water**

**Table 6.37  
Contact angle of fouled membrane fibers from pilot-scale testing**

Source water	Indianapolis – White River Membrane A				Tampa Bay Membrane B	Scottsdale Membrane D1	
	Run 1	Run 3	Run 4	Run 7	Run 14	Run 9	
	Raw water				Coagula- ted water	Raw water	Tertiary effluent
Run condition	Baseline	High recovery	Acid wash	Coagu- lation		NaOCl wash	
Feed water TOC (mg/L)	3.47	3.5	4.6	3.4	3.2	4.38	
Feed water UVA (1/m)	9.2	17.9	17.4	5.7	6.8	12.1	
SUVA (L/m-mg)	2.65	5.11	3.78	1.68	2.12	2.76	
Turbidity (NTU)	6.5	4.2	38	0.87	4.7	2.24	
Contact angle (deg) (Virgin)			83°± 5			80°± 4	0°
Contact angle (Fouled)	109° ± 2	102° ± 2	101° ± 1	97° ± 1	94° ± 2	92°± 2	0°

Note: Contact angle measurements were made on feed side for Membranes A and B and permeate side for Membrane D1

For both Tampa Bay and Indianapolis, which utilized “outside-in” flow membranes, contact angle increases after fouling. The presence of foulants at the surface of the membrane or in the pores could be responsible for the modification of the membrane wetting properties. However, FESEM showed no evidence of the presence of deposit on the fouled PVDF membranes. Changes to the physical chemical properties of the membrane after several runs of operation due to chemical cleaning and backwashing could be the primary contributing factor to a higher contact angle.

The increase of the contact angle is more significant for Membrane A operated at Indianapolis than for Membrane B operated at Tampa Bay. For Indianapolis, a greater increase in contact angle was observed where no coagulation was employed. Coagulation was effective for reduction in hydrophobic NOM fraction, so the adsorption or accumulation of greater amounts of hydrophobic NOM at the surface of Membrane A during Runs 1, 3, and 4 correlate with greater increases in contact angle (hydrophobicity).

No change in permeate-side contact angle was observed for Membrane D1 (Scottsdale study). This would be expected because very little foulant was observed on the permeate side (Figure 6.48).

Fouled fibers from the full-scale Membrane F module operated on Lake Michigan water showed a strong hydrophobic character with a contact angle of 100° (data not shown in Table 4.8). Unfortunately, a virgin polypropylene membrane was not available for measurement of contact angle. Polypropylene membranes generally have a very high contact angle. Sainbayar et al. (2001) indicated a contact angle of 112 degrees for a virgin 0.2 μm polypropylene membrane. Kou, et al. (2003) published a contact angle of 120° for a microporous polypropylene hollow-fiber membrane. Based on literature data, the fouling material observed by FESEM made the membrane surface more hydrophilic.

### **AFM of Fouled Pilot- and Full-Scale Membranes**

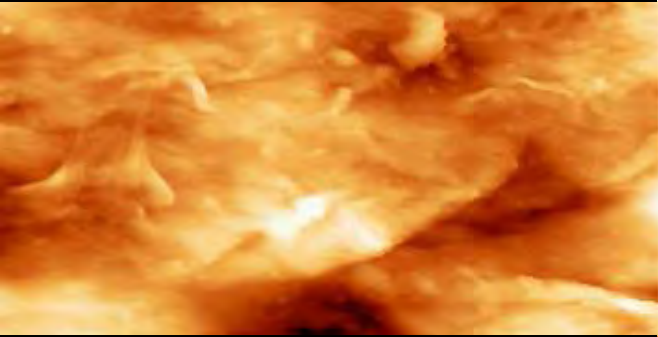
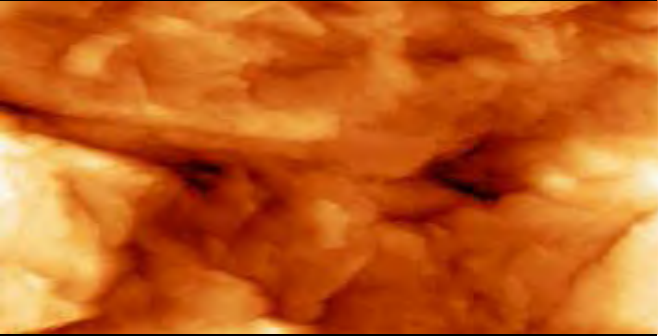
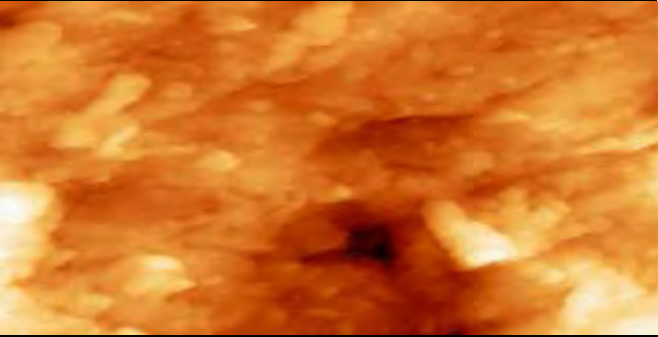
Tables 6.38 and 6.39 give the roughness characteristics (Ra and Rq) and the AFM 2D image of fouled membranes and the corresponding virgin (clean) membrane.

For all membranes studied and for all filtration conditions used, the roughness of the membrane surface increases significantly after filtration due to the accumulation of foulants. A larger increase in roughness was observed with the fibers from the fouled pilot module compared to the fouled bench modules. This reflects the greater degree of foulant deposition associated with the greater permeate throughput for the pilot studies.

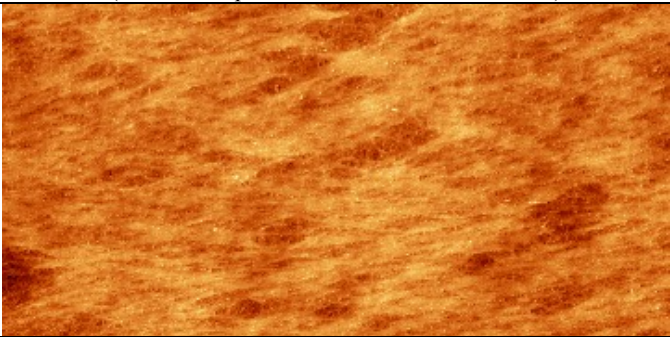
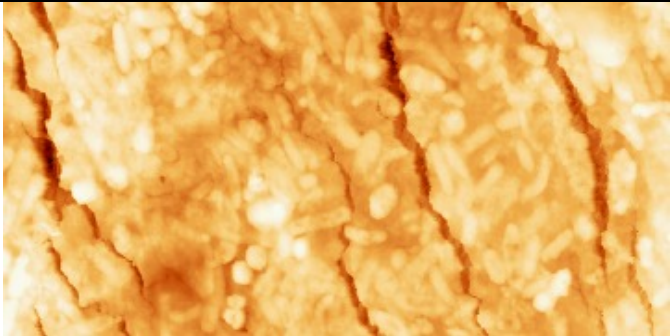
Regardless of the differences in characteristics of the membrane feed water used in Runs 1, 7, and 14 of the Indianapolis pilot study, the roughness of the feed surface of the fouled Membrane A fibers remains relatively similar (Ra = 80 to 110 nm as compared to 40 to 48 nm for the clean membrane) (Figure 6.41). For Run 1, roughness determined at different locations along the fiber varied significantly, corresponding to a heterogeneous fouling layer.

For Membrane D1, operated on Scottsdale effluent (Figure 6.42), AFM 2D images show that the deposit on the feed surface of the fiber had severely changed the initial topography of the membrane. The initial filamentous structure has disappeared with the accumulation of foulants. Roughness (Ra) significantly increased from 17 to 41 nm. The presence of bacteria (1-2 μm) can be observed on the fiber. Cracks observed on the AFM 2D image of the fouled membrane were probably generated when the fiber was sliced and installed on the imaging support.

**Table 6.38**  
**Roughness parameters (Ra and Rq) of fouled Membrane A fibers**  
**operated on White River water (Indianapolis)**

Membrane A	Rq (nm)	Ra (nm)	Topographic AFM 2D image (white area: protuberance/ back area: hollow)
Clean	60.9	48.2	
	61.8	48.5	
Outer surface	54.2	41.2	
Scan 5×2.5 μm <sup>2</sup>			
Run 1	112.3	82.8	
	81.5	63.0	
Outer surface	138.9	110.2	
Scan 5×2.5 μm <sup>2</sup>	110.9	88.0	
	92.3	73.2	
Run 7	141.5	110.3	
	105.8	82.0	
Outer surface	107.5	84.0	
Scan 5×2.5 μm <sup>2</sup>	126.1	104.3	
Run 14	110.8	83.1	
Outer surface			
Scan 5×2.5 μm <sup>2</sup>			

**Table 6.39**  
**Roughness parameters (Ra and Rq) of fouled Membrane D1 fibers**  
**operated on Scottsdale effluent**

Membrane D1	Rq (nm)	Ra (nm)	Topographic AFM 2D image (White area: protuberance/ Black area: hollow)
<b>Clean</b>			
Inner surface Scan 20×10 μm <sup>2</sup>	22.2	17.6	
<b>Fouled</b>			
Inner surface Scan 20×10 μm <sup>2</sup>	52.2	41.5	

### **Characterization of Foulant from Fouled Pilot- and Full-Scale Membrane Modules**

Fouling material recovered from pilot and full-scale modules were analyzed to characterize organic content.

#### ***Carbon and Nitrogen Content***

Solutions of foulant prepared in Milli-Q water were subjected to DOC and TN analyses after filtration through a 1.2-μm glass-fiber filter (GFF). (Results are provided in [Table 6.40](#).) The number of fibers received from Run 9 of the Tampa Bay pilot study did not provide enough material to conduct carbon and nitrogen analysis.

The first major observation is that material isolated from fouled membranes is relatively poor (low) in organic material. NOM isolated from natural waters typically has a carbon content ranging from 40 to 55 percent depending on the hydrophobic character of the fractions; the more hydrophilic, the lower the carbon content. Material isolated from fouled membranes did not exceed 14.5 percent of organic carbon. Complementary analyses (i.e., ICP analysis) showed that the material contained a large amount of sulfur present in a reduced form that corresponds to the excess of sodium bisulfite used to preserve the membranes against bacterial growth (difficult to remove from the inside of the hollow fiber). Depending on the concentration of bisulfite used and the efficacy of the rinsing step with Milli-Q water, the fouling material comprises more or less inorganics.

**Table 6.40**  
**Carbon and nitrogen content of foulants**  
**isolated from fouled fibers during pilot-scale and full-scale testing**

Sample	Mass of isolate (mg) in 25 mL of Milli-Q water	Concentration mg/L	DOC mg/L	DOC %	TN mg/L	C/N
Indianapolis Run 1	2.1 ± 0.1	84	7.90 ± 0.45	9.4	0.76 ± 0.05	10.39
Indianapolis Run 3	4.3 ± 0.1	172	10.75 ± 0.16	6.2	1.09 ± 0.02	9.86
Indianapolis Run 4	5.0 ± 0.1	200	3.43 ± 0.09	1.7	0.22 ± 0.01	15.59
Indianapolis Run 7	6.3 ± 0.1	252	2.84 ± 0.07	1.1	2.71 ± 0.05	1.05
Indianapolis Run 14	3.3 ± 0.1	132	19.17 ± 0.07	14.5	1.00 ± 0.02	19.17
Scottsdale	4.6 ± 0.1	184	5.22 ± 0.18	2.8	1.08 ± 0.03	4.83
Manitowoc	2.0 ± 0.1	80	10.14 ± 0.39	12.6	0.98 ± 0.04	10.34

The carbon/nitrogen (C/N) ratio is a good indicator of the nature of the deposit. It is well known that the higher the hydrophilic character of the natural organic material the higher the nitrogen content and the lower the C/N ratio (Aiken and Cotsaris, 1995). Typically, C/N ratio ranges from 4 to 5 to more than 20 in progressing from hydrophilic to hydrophobic NOM fraction (Croué et al., 1999a). Effluent organic matter is also more enriched in nitrogen as compared to NOM. Most of the isolated foulants show C/N ratio ranging from 10 to 20, typical of humic-type material. It is interesting to note that Indianapolis Run 7 and Scottsdale isolates have low C/N ratios. The low C/N ratio of Indianapolis Run 7 may correspond to very high algae levels (84,000 counts/mL). Also, the feed water of Run 7 corresponded to coagulated water with the lowest UVA. However, a C/N ratio of 1 cannot be observed unless inorganic nitrogen is present. If the period of Run 7 corresponds to algal bloom, the presence of inorganic nitrogen in the feed water is possible.

The Scottsdale effluent is enriched in organic and inorganic nitrogen compared to the natural (Marne River) water, which can explain the low C/N ratio of the former. The abundance of microbes observed at the membrane surface would also decrease the C:N ratio. With the exception of Indianapolis Run 7, the C:N ratios of the foulant isolates from the filtration of surface waters (Manitowoc and Indianapolis) are comparable.

### ***High-pressure size-exclusion chromatography analysis***

SEC/UV-260 nm analyses were conducted on solutions of foulants. The mobile phase was prepared with sodium acetate, which can provide a better resolution as compared to a phosphate mobile phase. Figure 6.51 shows the SEC/UV-260 normalized fingerprint of the Indianapolis Run 14, Scottsdale, and Lake Michigan foulants. The chromatograms are compared with the profile obtained with Marne River (France) NOM.

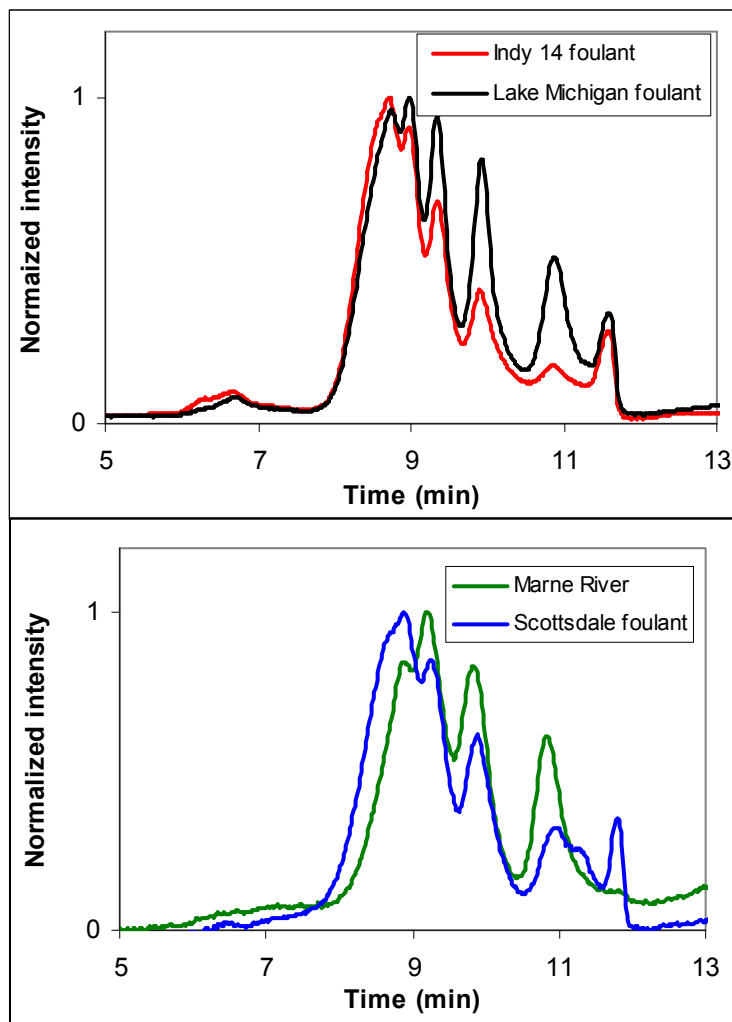


**Figure 6.51 HPSEC/UV-260 of foulant material isolated from Run 14 of Indianapolis (Run 14) and Scottsdale pilot studies, Manitowoc full-scale plant (Lake Michigan), and Marne River water**

Figure 6.52 compares the foulant profiles from Runs 1, 3, 4, and 7a of the Indianapolis pilot unit (Membrane A). It is important to notice that the chromatograms are not as well resolved as the ones shown in Figure 6.51. The presence of a high salt content in the foulant and/or the use of a column with less resolution efficacy could explain this observation. However, the normalized spectra are relatively similar, with possibly a more intense first band (before 7 min) for Run 3 that corresponds to a high recovery operational mode.

To conclude, the SEC/UV 260 profiles were not very informative. The profiles were relatively similar to the Marne River water profile, which indicates that foulants incorporate humic-type NOM material, an expected result. It is important to note that SEC was conducted with UV absorbance detection, rather than DOC detection (as used with the bulk water samples), and as such, does not capture the important high MW PS fraction that has been shown in elsewhere in this report to be preferentially adsorbed/retained by the low pressure membranes and would be expected to be present in the membrane foulants.

### ***FTIR Analysis***

The FTIR spectra recorded for the different isolates (Figures 6.55 to 6.57) show bands and peaks that are indicators of the presence of organic material. FTIR spectra were recorded in KBr pellets. The Tampa Bay isolate could not be analyzed because of insufficient foulant material. For comparison, Figure 6.53 presents the FTIR spectra of fractions of Marne River NOM. The four fractions presented in this figure represent the entire picture of NOM structures present in typical surface waters.

All of these spectra, with the exception of the (organic) colloids, show the predominantly acidic character of the isolates (carboxyl peak at  $1720\text{ cm}^{-1}$ ). The hydrophobic fraction HPO shows stronger aliphatic hydrocarbon prominent peaks ( $2960$ ,  $2920$ ,  $1440$ , and  $1380\text{ cm}^{-1}$ ) than does the transphilic fraction. Significant alcohol content (from carbohydrates) is indicated by the carbon-oxygen (C-O) stretching peak near  $1100\text{ cm}^{-1}$  in the transphilic and hydrophilic acids. The colloids spectrum is typical of N-acetyl aminosugars with the absence of a significant carboxyl peak, the abundance of carbohydrates (large C-O stretching peak near  $1100\text{ cm}^{-1}$ ) associated with the significant secondary amide content indicated by the amide 1 ( $1660\text{ cm}^{-1}$ ) and amide 2 ( $1550\text{ cm}^{-1}$ ) and a distinct methyl group at  $1380\text{ cm}^{-1}$ .

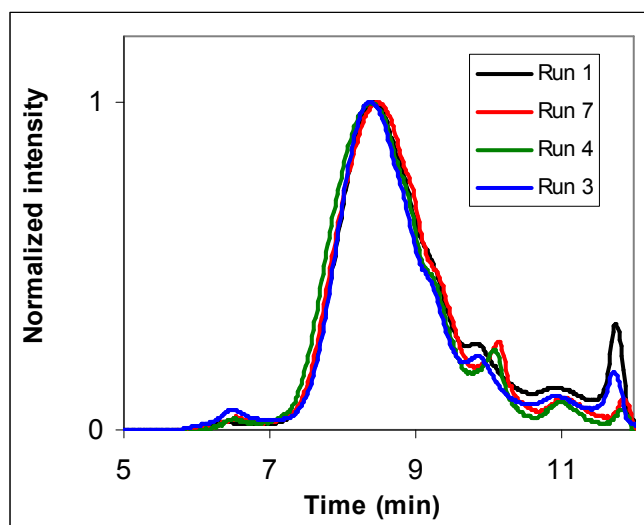


**Figure 6.52 SEC/UV 260 profiles of foulant harvested from membrane modules operated during Runs 1, 3, 4, and 7a of the Indianapolis pilot study (Membrane A)**

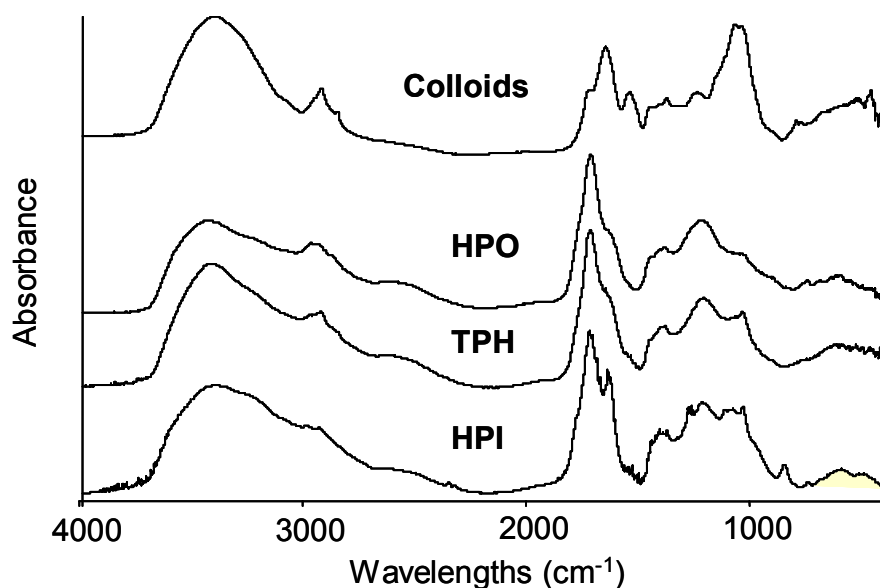


**Figure 6.53 FTIR spectra of NOM fractions isolated from Marne River water**

The FTIR spectra recorded for the different isolates (Figures 6.54 and 6.55) show bands and peaks that indicate organic material. However, as mentioned previously, some of the isolates contained large proportion of sodium bisulfite used as preservative. The presence of sodium bisulfite is clearly indicated by the peaks at 1150, 970, 635  $\text{cm}^{-1}$ . These peaks are predominant for the Indianapolis Runs 4 and 7a and Scottsdale isolates.

For all spectra, the large hydroxyl (OH) stretch near 3500  $\text{cm}^{-1}$  indicate adsorbed water as well as organic hydroxyl groups. Aliphatic hydrocarbon peaks (2960, 2920, 1440, and 1380  $\text{cm}^{-1}$ ) are also present in all spectra, indicating the presence of organic matter.

Indianapolis Runs 1, 3, and 14 spectra are characterized by a peak at 1700  $\text{cm}^{-1}$  that is probably derived from free carboxyl groups (Figure 6.54). The 1670  $\text{cm}^{-1}$  band is an amide band. For natural organic structures, amide bands that are not amino sugars include proteins and pyrrolidones (cyclic lactams from degraded porphyrins from algae). However, with the foulants extracted in this study, this band is more likely caused by the presence of pyrrolidinones, compounds used as a hydrophilic coating agent to reduce the contact angle of the feed surface of the membrane. (These compounds were also detected by pyrolysis GC/MS). The band at 1740  $\text{cm}^{-1}$  corresponds to ester that might come from triglyceride lipids (fatty acids were identified by thermochemolysis GC/MS). The band at 1380  $\text{cm}^{-1}$  could be methyls from N-acetyl groups because the presence of aminosugars was confirmed by pyrolysis GC/MS. For Indianapolis Runs 4 and 7 spectra, the large bands that are derived from excess sodium bisulfite mask the rest of the profile. However, the small band at 1650  $\text{cm}^{-1}$  confirms the presence of proteins and aminosugars in the foulant.

The large band at 1160  $\text{cm}^{-1}$  (bisulfite) for the Scottsdale isolate spectrum makes the interpretation difficult (Figure 6.55). The band at 1700  $\text{cm}^{-1}$  is not as pronounced as found for the Indianapolis isolates. The spectrum shows a broad band at 1740  $\text{cm}^{-1}$  derived from esters (lipids) and two distinct peaks at 1650 and 1580  $\text{cm}^{-1}$  associated with a small peak at 1380  $\text{cm}^{-1}$  that could be indicators of the presence of aminosugars (confirmed by pyrolysis GC/MS).

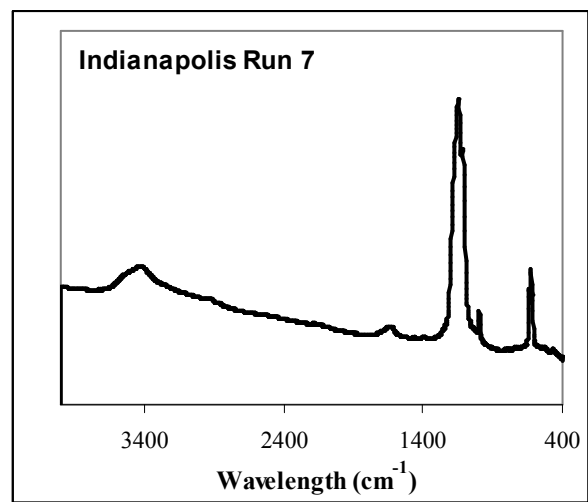
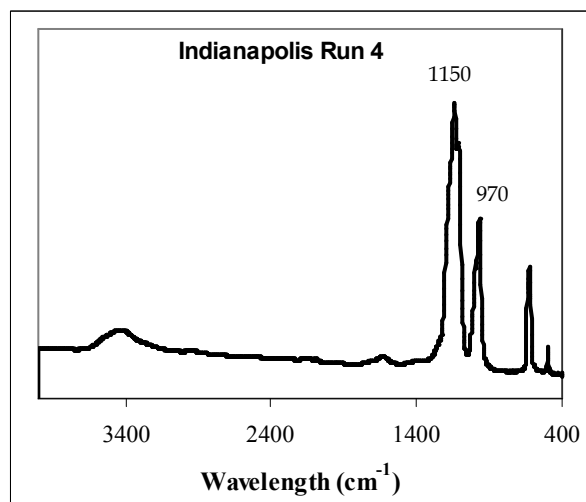
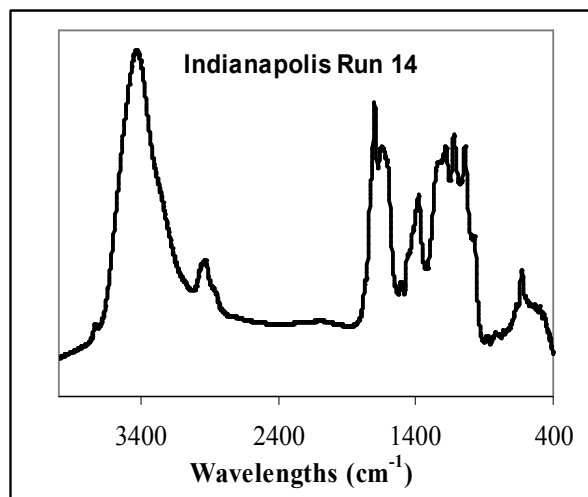
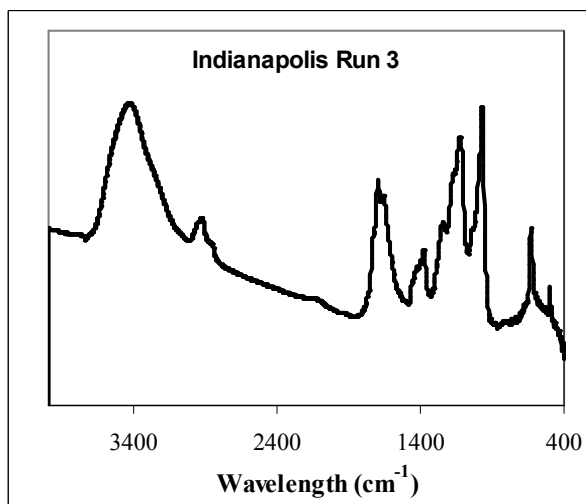
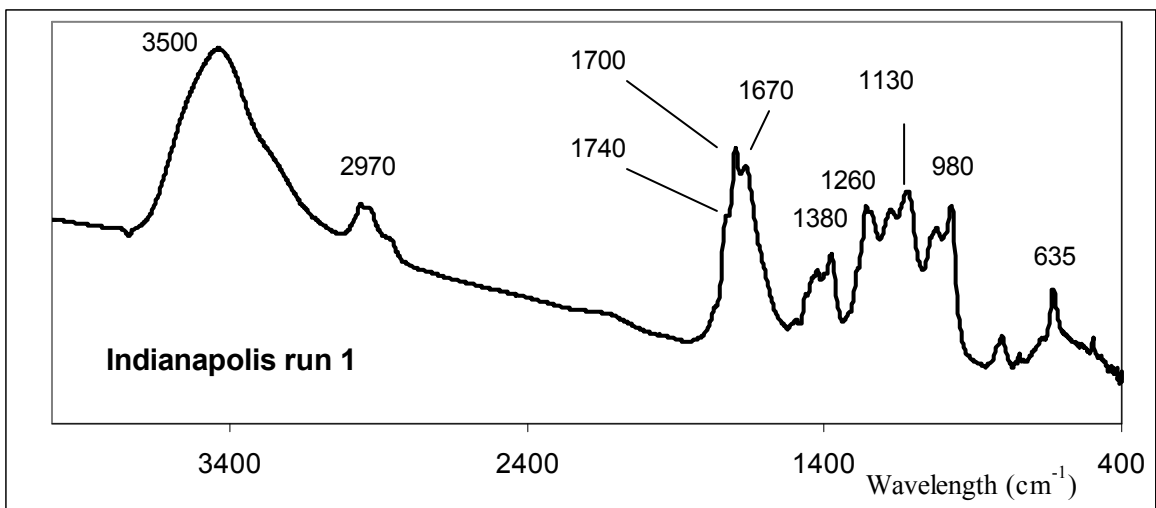
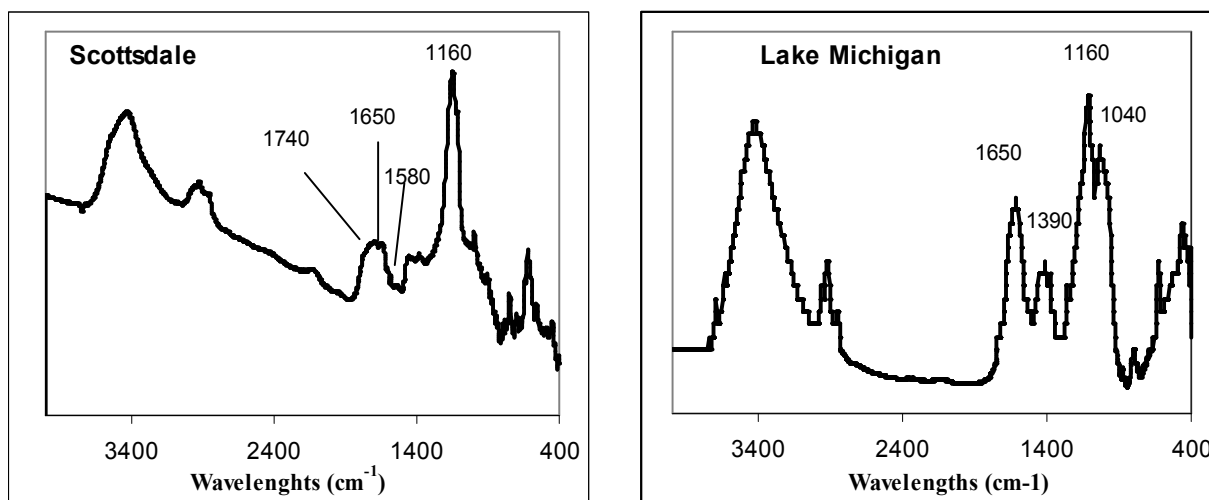


Figure 6.54 FTIR spectra of foulants isolated from Membrane A fibers operated during the Indianapolis pilot study



**Figure 6.55 FTIR spectra for foulants isolated from Membrane D1 fibers (Scottsdale) and Membrane F fibers (Manitowoc WTP [Lake Michigan])**

The Lake Michigan isolate spectrum (Figure 6.55) also indicates the presence of proteins with a broad band at  $1650\text{ cm}^{-1}$ . This band can be slightly shifted to lower frequencies if there are adjacent hydroxyl groups that hydrogen bond with the amide carbonyl group. The presence of aminosugars is difficult to confirm due to the absence of the amide 2 band near  $1550\text{ cm}^{-1}$ . However, the large and broad band at  $1040\text{ cm}^{-1}$  could be derived from sugars.

All of these FTIR spectra seem to indicate the presence of organic matter derived from bacterial origin (aminosugars, proteins, lipids). A more distinct peak attributed to carboxyl groups in the Indianapolis isolates is probably terrestrial from (allochthonous) NOM.

### ***Pyrolysis GC/MS***

At high temperature natural biopolymers and synthetic polymers are degraded to a large number of low-molecular-weight thermal decomposition products that are volatile enough to be separated and identified by GC/MS. Pyrochromatograms of NOM fractions isolated from rivers have been interpreted and discussed in previous AWWARF projects (Croué, et al. 1999b; Hwang, et al. 2001).

Figures 6.56 through 6.58 present the pyrochromatograms recorded for the foulants obtained from the different hollow fibers analyzed in this study.

While P-GC/MS cannot be used as a strictly quantitative analytical technique, it can provide a specific fingerprint of the organic material present.

All of the chromatograms showed the presence of natural biopolymers with peaks that are produced from the thermal degradation of proteins (pyridines, pyrroles), sugars (furfurals, ketones such as cyclopentenones), aminosugars (acetamide, propanamide) and lignin-type structures (phenols, methoxyphenols). Peaks produced from the degradation of membrane polymers (Membrane B used at Tampa Bay) and hydrophilic coating agents (Membrane A at Indianapolis) are also present, suggesting that ultrasound (used for foulant extraction) can potentially damage hollow fiber.

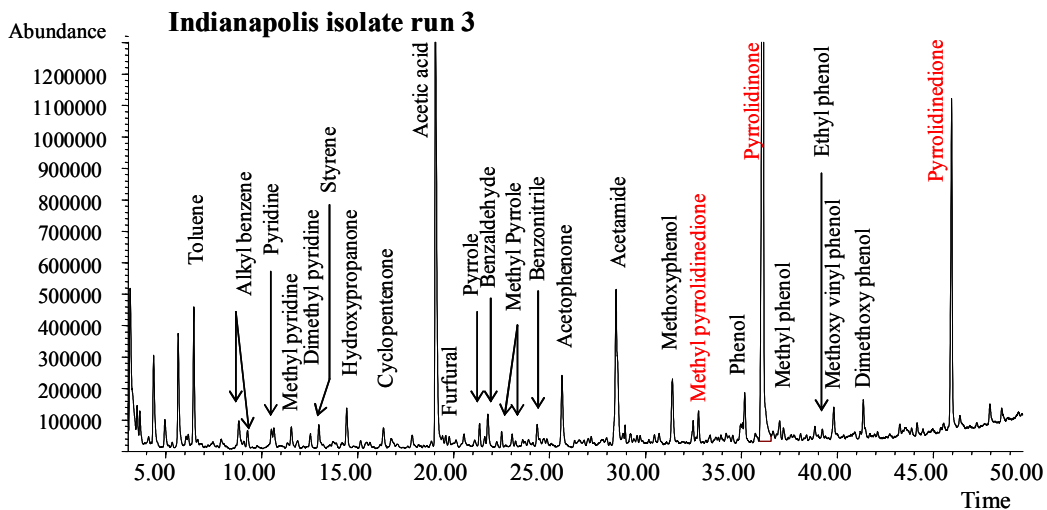
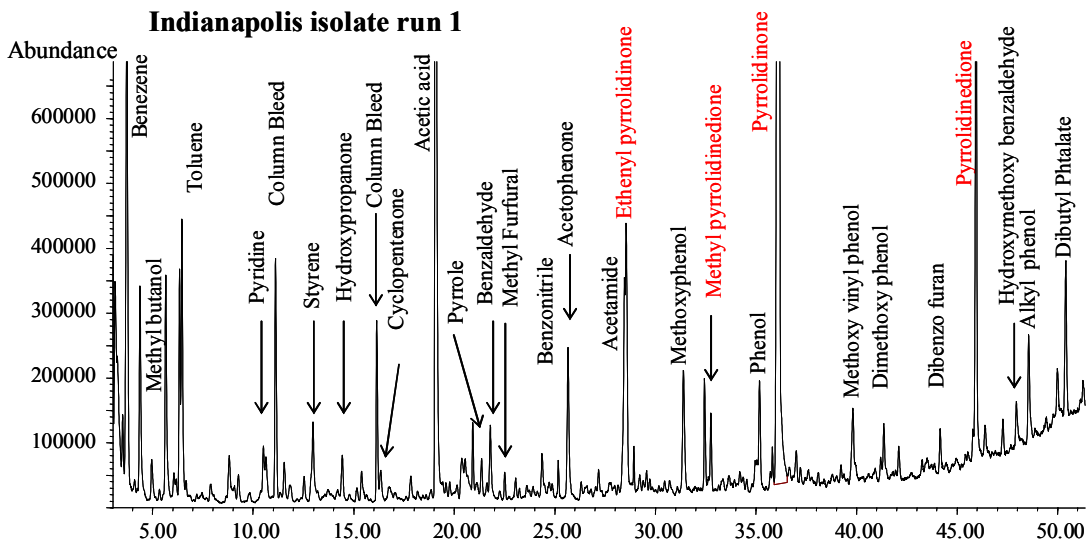
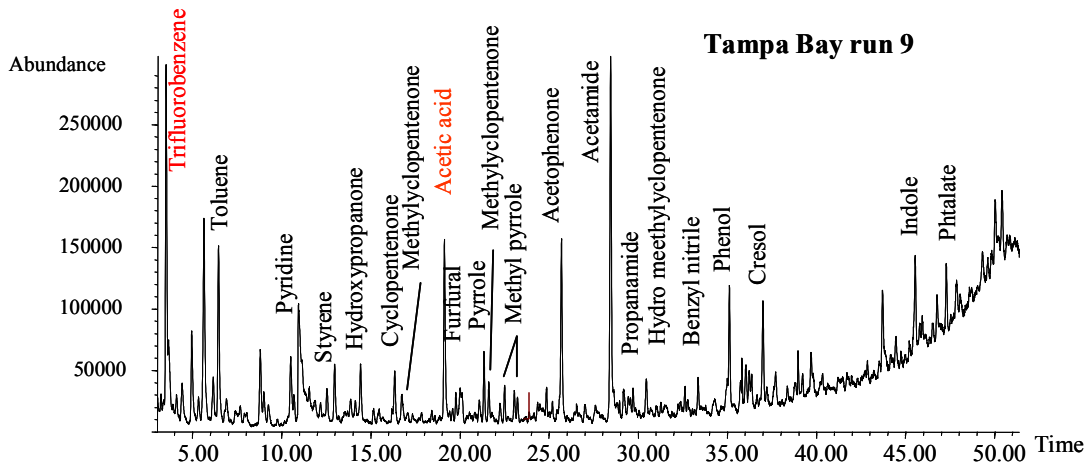


**Figure 6.56 Pyrochromatograms of foulant isolated from Membrane B (Tampa Bay) and Membrane A (Indianapolis) fibers**

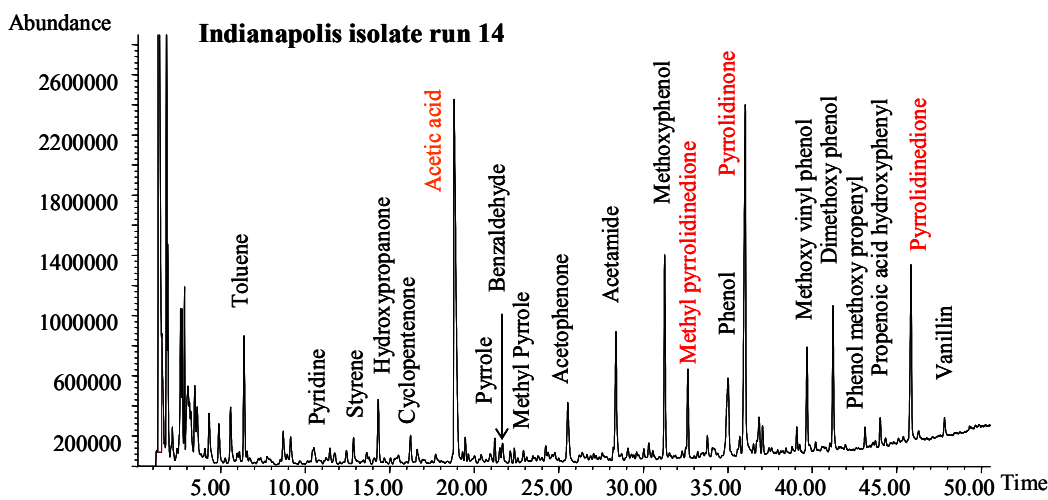
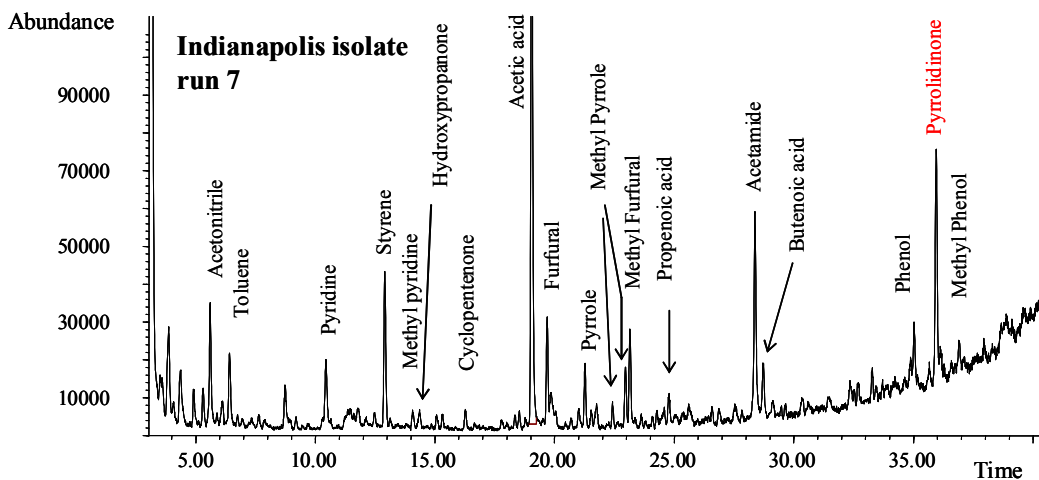
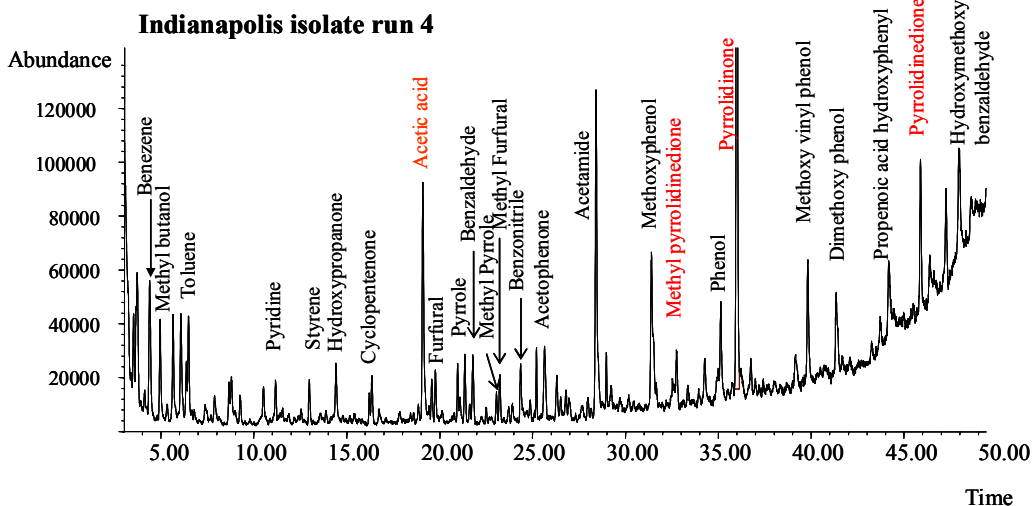


**Figure 6.57 Pyrochromatograms of foulant isolated from Membrane B (Indianapolis) fibers**

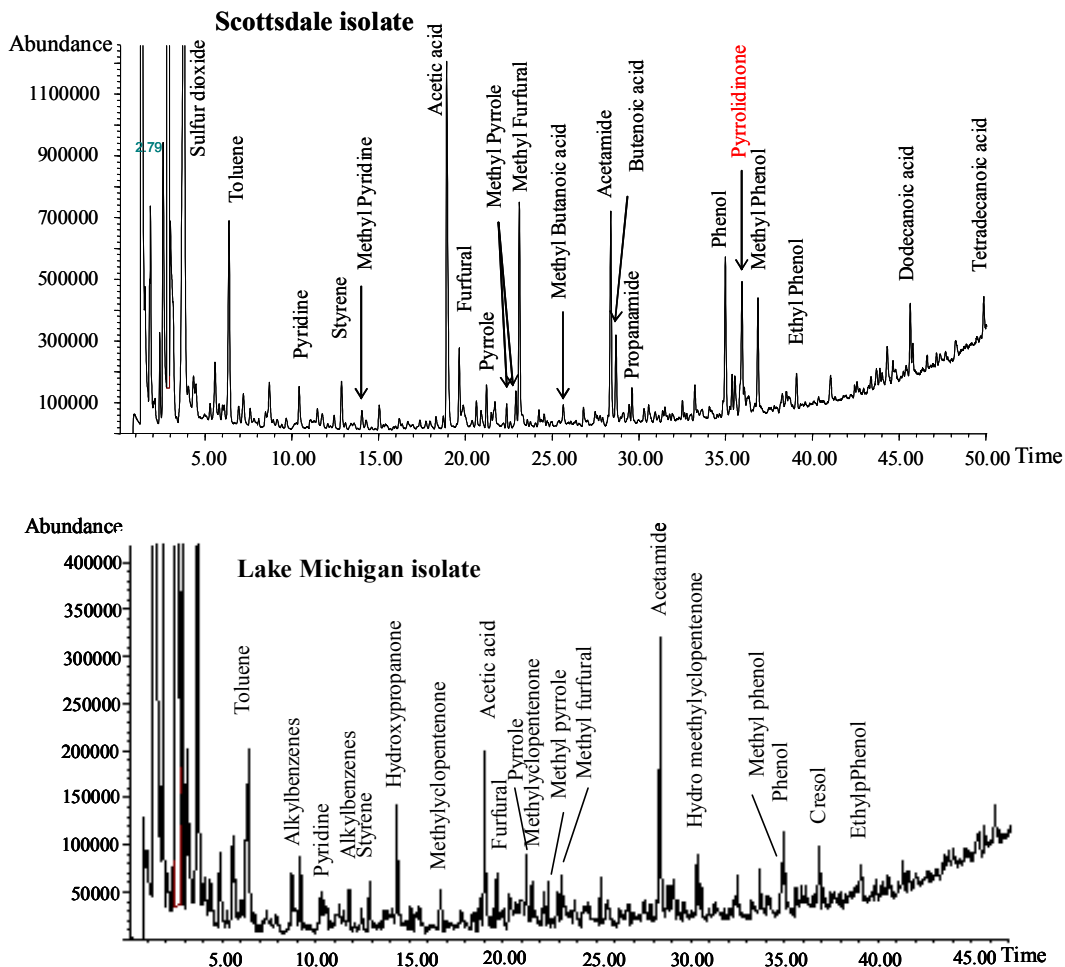


**Figure 6.58** Pyrochromatograms of foulant isolated from Membrane D1 (Scottsdale) and Membrane F (Manitowoc) fibers

Significant differences can be noticed between the fingerprints obtained for the foulants isolated from the different studies:

- Acetamide, an indicator of the presence of aminosugars (i.e., microbial residues) in the foulant, was detected in all chromatograms (minor peak in Indianapolis Run 1 isolate). It is a predominant peak in the pyrochromatograms of the material isolated from Tampa Bay (Membrane B) and Lake Michigan (Membrane F) modules.
- Foulants from Scottsdale and Indianapolis Run 7 show a significant acetamide peak associated with furfural derivatives, indicators of the presence of sugars, but also butenoic acid, an indicator of living or well-preserved biological organisms. (FESEM images of Scottsdale fibers clearly show the presence of microorganisms). The feed water of Indianapolis Run 7 was also characterized by high algae (microbial) activity.
- C<sub>12</sub> and C<sub>14</sub> fatty acids, indicators of bacterial activity, were detected in the Scottsdale isolate only, a finding consistent with an effluent source.

Methoxyphenol derivatives produced from the thermal degradation of lignin structures were only identified in foulants isolated from the Indianapolis fibers. These derivatives most likely come from the source water (White River); however, the hydrophobic character of the membrane (Membrane A PVDF) may also have played a significant role in the retention of such aromatic material. Methoxyphenols were not detected in Indianapolis Run 7 isolate. The abundance of algal organic matter in the feed water and the coagulation-flocculation treatment operated (expected to remove high MW lignin structures) prior to membrane filtration may explain this finding.

Natural organic matter from different origins produces similar sub-units under pyrolysis, but the amount of the sub-units varies significantly between samples, providing a specific fingerprint for a select organic material (Hwang, et al. 2001). The peak areas of select by-products in pyrochromatograms can also be used to estimate the relative proportion of the major biopolymers in the original organic matrix. The biopolymer distribution obtained by this approach should not be considered to reflect the “real” relative proportions of the main types of biopolymers present in the original samples. Different biopolymers exert different pyrolysis yields that were not considered in this project. However, this semi-quantitative approach can be used for a better comparison of the GC profiles.

Figure 6.59 summarizes the relative distribution of the main biopolymers identified in the pyrochromatograms. It is important to note that acetic acid was not taken into account in our calculation approach because this pyrolysis compound does not have a specific origin; also, it was found to be generated from the pyrolysis of PES. Phenol, which may originate from the decomposition of polyphenolic structures, can be produced from the decomposition of tyrosine-containing proteins. Based on the observations of Bruchet, et al. (1990), phenol derivatives analyzed in pyrochromatograms of this study were attributed to the pyrolysis of polyphenolic structures because ortho and meta cresols were identified in addition to phenol and para cresol. On the contrary, phenol derivatives can also be attributed to proteinaceous material containing tyrosine. For the Scottsdale (Membrane D1), the presence of phenol may also originate from the degradation of the membrane polymer during ultrasonic removal of the foulant, thus it was decided that the phenol peak not be considered when correlating observed biopolymers with source water foulants. Pyrolysis GC/MS is a semi-quantification approach and, as such, attempting to correct for phenol contribution from the virgin membrane through chromatogram subtraction to determine the relative phenol contribution from fouling was considered inappropriate.

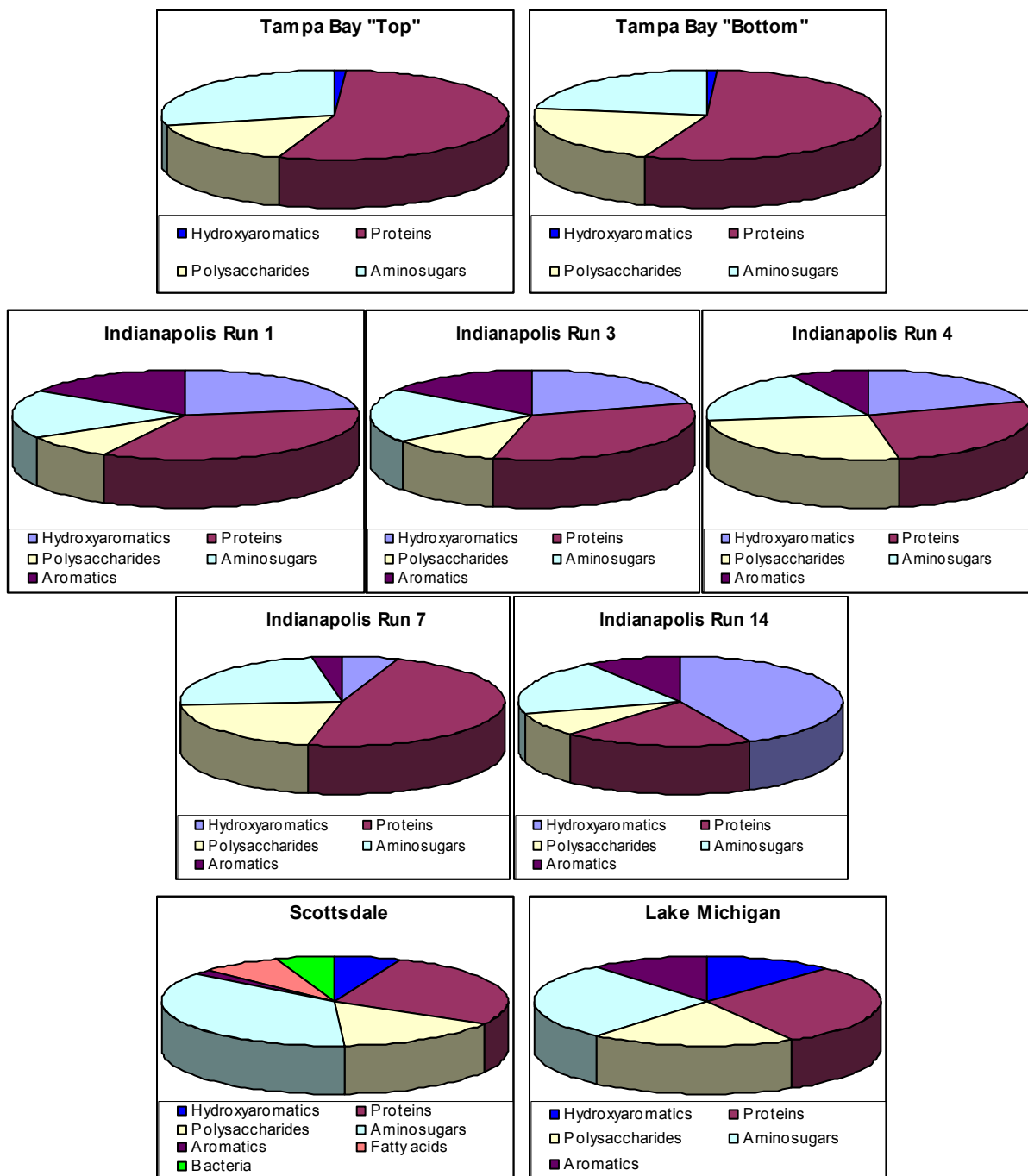


**Figure 6.59 Relative distribution of the main biopolymers present in the foulant material from isolate from Tampa Bay, Indianapolis, and Scottsdale pilot and Manitowoc (Lake Michigan) full-scale plant membrane fibers**

Foulant isolated from the Membrane B (Tampa Bay) shows a large predominance of sugars plus aminosugars and proteins as compared to other foulants. The distribution was found to be identical for fibers harvested from the top or the bottom of the module. This fingerprint seems to indicate that the foulant is mainly of bacterial origin. This is surprising given the high aromatic (humic substance) content of the water. However, it is important to note that the fibers from Tampa Bay were air-shipped to France without preservative. It is not certain, but always possible, that bacterial growth might have occurred to some extent during shipment.

Deposits isolated from the Membrane F fibers (Lake Michigan water) yield a similar distribution. However, aromatic derivatives are more abundant in the pyrochromatogram. The large presence of sugars and aminosugars correlates with the sticky material observed by FESEM on the membrane surface. Again, proteins and sugars plus aminosugars appeared to be the major foulant species accumulated on the surface of the Membrane F.

The biopolymer distribution of Membrane D1 (Scottsdale) foulant is quite unique with a predominance of aminosugars (bacterial cell wall) and the presence of fatty acids and butenoic acids, indicators of recent bacterial activity. The foulant material is definitely of bacterial origin and most likely incorporates living organisms.

The results obtained for the Indianapolis runs are different because aromatics represent a significant contribution of the biopolymer distribution. Run 1 (baseline conditions) and 3 (high recovery conditions) isolates show similar biopolymer distributions. Run 4 isolate obtained after acid wash seems to be characterized by a higher proportion of polysaccharides and a reduction of the protein content as compared to isolates obtained from the previous runs. Acid wash may have favored the removal of proteinaceous materials from the membrane foulant. Run 7 (alum coagulation) isolate provides a different profile with a distribution almost split between proteins and sugars plus aminosugars. Aromatic-type structures represent a minor part of the foulant. This distribution is relatively similar to the one that characterized the Tampa Bay isolates. The fact that the pilot unit feed water was treated by coagulation/flocculation has significantly changed the nature of the foulant during this period of the year. Surprisingly, the isolate obtained from fibers harvested after Run 14, where the pilot unit was operated on alum coagulated/flocculated/clarified water from the treatment plant, shows a biopolymer distribution similar to Runs 1 and 3, with even a higher contribution of the polyhydroxyaromatic moieties (i.e., lignin-type structures). It should be noted that for Runs 11 to 17, the source water to both the pilot unit and the treatment plant contained 20 to 30 percent groundwater, which has lower TOC and higher calcium hardness than White River water. The higher calcium levels could have caused more retention of humic substances, thereby increasing the aromaticity of the foulant.

### ***Thermochemolysis GC/MS***

It has been clearly demonstrated that benzenecarboxylic moieties undergo decarboxylation during conventional pyrolysis. New pyrolytic approaches using alkylated agents (i.e., tetra-alkyl ammonium hydroxide) has been developed during the past ten years to overcome this major limitation and improve the detection of polar compounds. Because evidence has been given that both hydrolysis and alkylation mechanisms occur at high temperature in the presence of alkylated agents such as tetramethyl ammonium hydroxide (TMAH) the procedure has therefore been termed thermally assisted hydrolysis and methylation (THM) (del Rio et al., 1996). Most of the results that have been published refer to humic substances. Flash heating in the presence of tetra-alkyl ammonium hydroxides avoids decarboxylation and releases carboxylic groups in aliphatic and aromatic structures. Comparing conventional pyrolysis and

pyrolysis/methylation experiments of an aquatic fulvic acid, Saiz-Jimenez (1994) considered that the most significant finding was the identification of furancarboxylic acids, benzene carboxylic acids and aliphatic dicarboxylic acids as their respective methyl esters in the methylated pyrolysate. Lethonen et al. (2000) confirmed that the most typical sub-units obtained by TMAH treatment for aquatic NOM isolates are phenols, alkylphenols, phenolic acids, aliphatic monocarboxylic acids and dicarboxylic acids. Similar conclusions were recently addressed by González-Vila et al. (2001), pyrolysis TMAH of aquatic humic substances providing information on the presence of lignin markers, and allowing the identification of dicarboxylic acids. It is important to point out that one of the major drawback of the TMAH technique is that it does not allow the differentiation between naturally occurring methyl ether or methyl esters and those formed by THM. The use of tetrabutyl ammonium hydroxide made it possible. Using different ammonium salts (hydroxide and acetate forms), it is now possible to estimate the free, esterified and total acid content (Ambles, 2001).

As a general observation, THM is considered to be a useful technique as it provides complementary information on the NOM structure, in particular the lignin moieties and to a lower extent the polysaccharide moieties.

Thermochemolysis GC/MS analysis was performed on the isolates to provide complementary insights on the nature of the foulants. Again, this approach cannot be used as a quantitative method but can bring some valuable qualitative information regarding the nature of complex organic matrix in particular those containing microbial by-products (i.e., fatty acids) and lignin derivatives containing carboxyl and OH groups.

The thermochemolysis chromatograms are shown in [Figures 6.60 and 6.61](#). Regarding the Indianapolis study, chromatograms of Run 7 and Run 14 isolates are only presented; the other profiles did not add any additional information and were found to be relatively similar to the Run 14 isolate.

The first major observation is that all thermochemolysis chromatograms exhibit a series of fatty acids (all are present in the ester form due to TMAH methylation) with the hexadecanoic acid methyl ester ( $C_{16}$ ) as the dominant peak, except for the Scottsdale isolate showing the unsaturated  $C_{16}$  (hexadecenoic acid methyl ester) as the major peak.  $C_{20}$  methyl ester was the longest chain fatty acid detected in the chromatograms recorded.

The identification of these fatty acids confirms that foulants recovered from the hollow-fiber membranes used in this study incorporate organic structures that are derived from microbial activity. The presence of the  $C_{15}$  iso and  $C_{15}$  anteiso fatty acids in all chromatograms is also a strong indicator of the bacterial input.

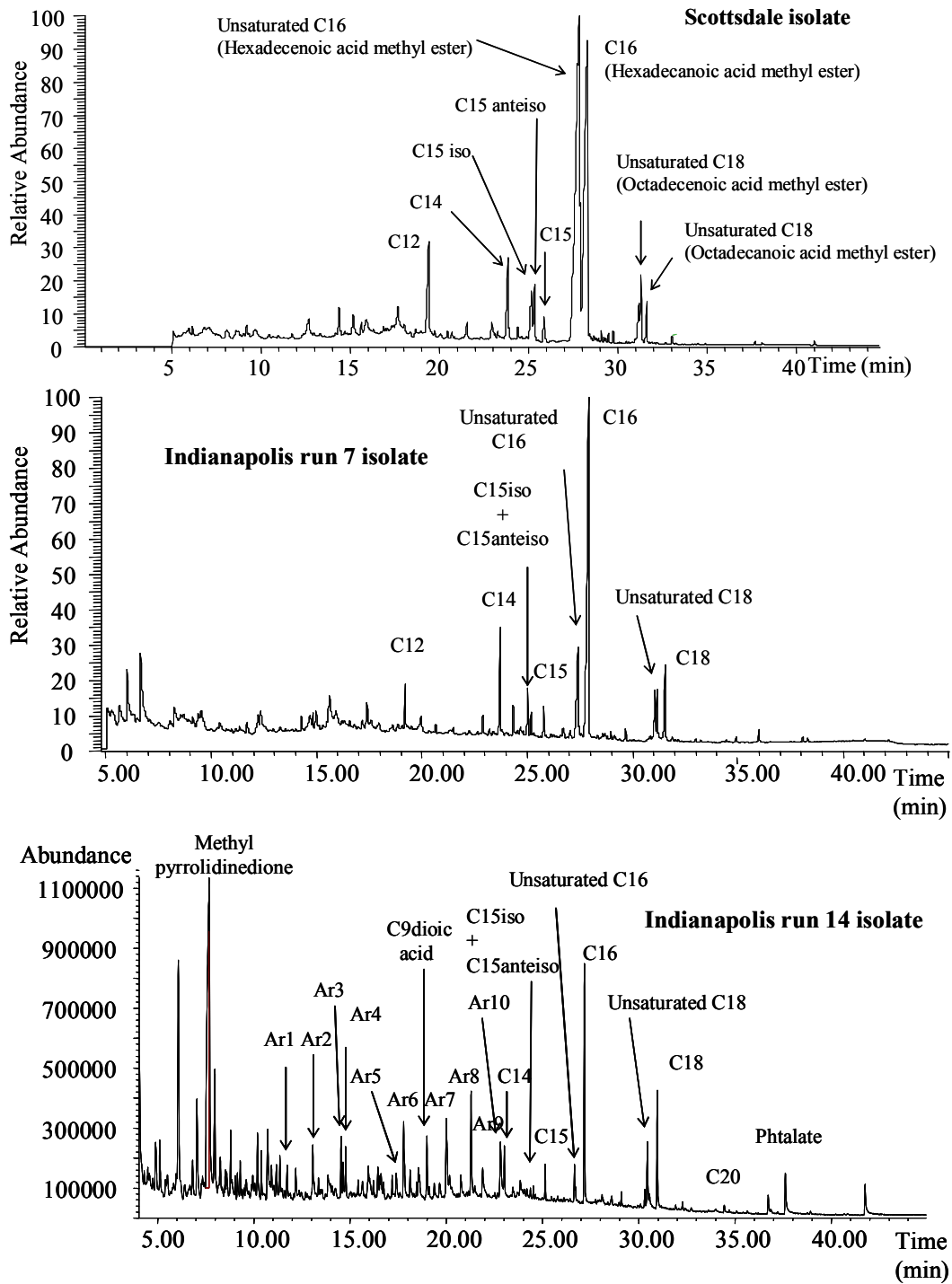


**Figure 6.60** Thermochemolysis–TMAH/GC–MS chromatograms of the hollow-fiber foulants

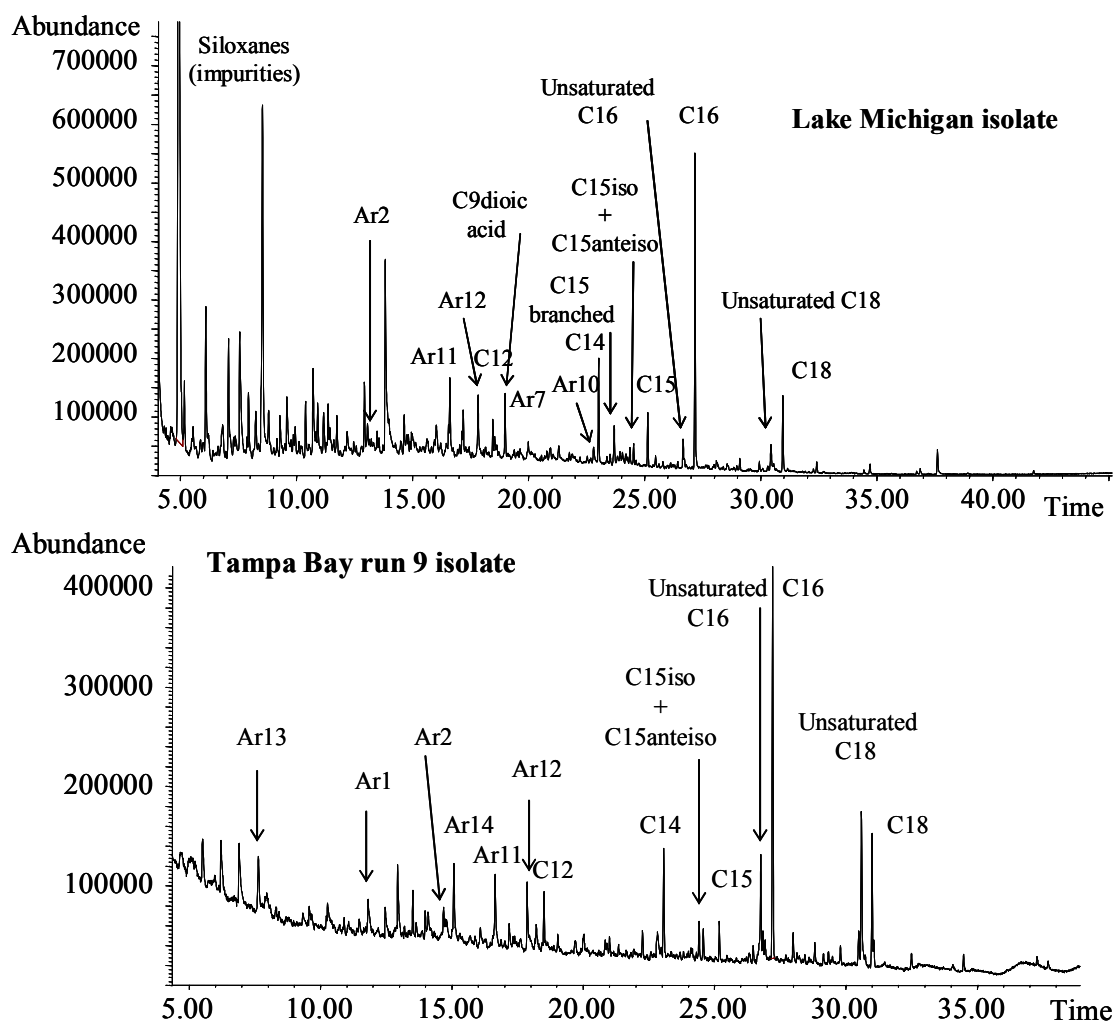


**Figure 6.61 Thermochemolysis –TMAH/GC-MS chromatograms of the hollow-fiber foulants (end)** (Ar1: Benzaldehyde, 4-methoxy; Ar2: Trimethoxybenzene; Ar3: Benzene, 4-ethenyl-1,2-dimethoxy; Ar4: Benzoic acid, 4-methoxy, methyl ester; Ar5: Benzaldehyde, 3,4-dimethoxy; Ar6: Benzene, 1,2-dimethoxy-4-(1-propenyl); Ar7: Benzoic acid, 3,4-dimethoxy, methyl ester; Ar8: Benzene 1,2,3-trimethoxy, propenyl; Ar9: Ethanone, 1-(3,4,5-trimethoxyphenyl); Ar10: Benzoic acid, 2,4,5-trimethoxy, methyl ester; Ar11: Dimethyl Phtalate; Ar12: Benzene dicarboxylic acid dimethyl ester; Ar13: Benzoic acid methyl ester; Ar14: Propenoic acid, 3-phenyl, methyl ester)

As mentioned above, the Scottsdale isolate exerts a unique profile with the predominance of the unsaturated form of the C<sub>16</sub> and C<sub>18</sub> fatty acids. This specificity confirms that the material recovered from Membrane D1 was “fresh material” and corresponds to living or well-preserved microorganisms. This conclusion agrees with the FESEM image and the results from the flash pyrolysis GC/MS. The chromatogram of the Tampa Bay isolate also gives a more abundant unsaturated C<sub>18</sub> compared to the saturated C<sub>18</sub>, which might also be an indicator of recently released microbial products. The absence of an abundant unsaturated C<sub>16</sub> may result from the presence of microorganisms with a different metabolism pathway.

The chromatogram for the Indianapolis Run 14 isolate shows a very different thermochemolysis profile from that of the Scottsdale isolate with the presence of numerous and abundant aromatic derivatives such as methoxybenzenes and methoxy benzoic acid methyl esters. The TMAH thermochemolysis is probably responsible for the methylation of the OH functional groups (carboxyls, OH phenolic). The presence of a large diversity of aromatic compounds is in accordance with the biopolymer distribution established from the flash pyrolysis profile. Lignin moieties are present at significant levels in the Indianapolis Run 14 foulant. The thermochemolysis profiles of the other Indianapolis isolates were similar; however, the relative abundance of the aromatic compounds was not as high. The presence of the methyl pyrrolidinedione peak in the thermochemolysis chromatogram may come from membrane hydrophilic additives. As expected from the flash pyrolysis pyrochromatogram, these aromatic components were not detected in the Indianapolis Run 7 foulant when thermochemolysis conditions were applied. This reinforces the hypothesis that the blending of calcium-rich groundwater with White River water led to increased humic substance retention on Membrane A through bridging and correlates well with the higher rate of fouling observed on the blended source.

The predominance of material of bacterial origin (presence of fatty acids) was observed in the Scottsdale isolate and that of Indianapolis Run 7. Some aromatic compounds were also detected in the chromatograms recorded for Lake Michigan and Tampa Bay isolates. The presence of lignin derivatives in these foulants is suggested.

### **Integration of Pilot- and Full-Scale Results via the UMFI Concept**

Figure 6.62 presents a cumulative frequency plot<sup>2</sup> of  $UMFI_i$ ,  $UMFI_{150}$  and  $UMFI_{3000}$  values calculated from the specific flux data of the Tier 1 and Tier 2 pilot runs presented in this chapter. The data in the plot resulted in the following findings:

- The  $UMFI_i$  values are the highest and most variable. This is to be expected because  $UMFI_i$  representing total fouling, will always be greater than short-term hydraulically reversible fouling represented by  $UMFI_r$  and  $UMFI_{150}$ . The greater variability indicates that there is more variation in the total versus hydraulically reversible fouling potential of the different source waters.
- $UMFI_{150}$  values are lower and have significantly less variability than  $UMFI_i$  but are generally greater and have more variability than  $UMFI_{3000}$ . The former ( $UMFI_{150}$ ) reflects the more consistent and lower degree of fouling that results when backwashing is employed compared to  $UMFI_i$ , while the latter ( $UMFI_{3000}$ ) reflects fouling at a greater permeate throughput where, compared to  $UMFI_i$ , there is a reduced non-linear fouling rate due to the characteristics of NOM fouling.
- The  $UMFI_{3000}$  values fall within a very narrow range, indicating that differences in membrane fouling rates, as measured by UMFI, become quite small after 5 to 7 days of pilot operation.

---

<sup>2</sup> A cumulative frequency distribution is a plot of the number of observations falling in or below an interval.

- An important finding is the degree of correlation between  $UMFI_{150}$  and  $UMFI_{3000}$  values. Despite greater variability, the hydraulically reversible fouling rate measured after only 1.5 to 2 hours of pilot operation is a reasonably accurate predictor of the fouling rate observed after 3 days of operation. This provides for the potential to utilize multi-cycle bench-scale experiments to predict longer-term (pilot-scale) fouling rates.

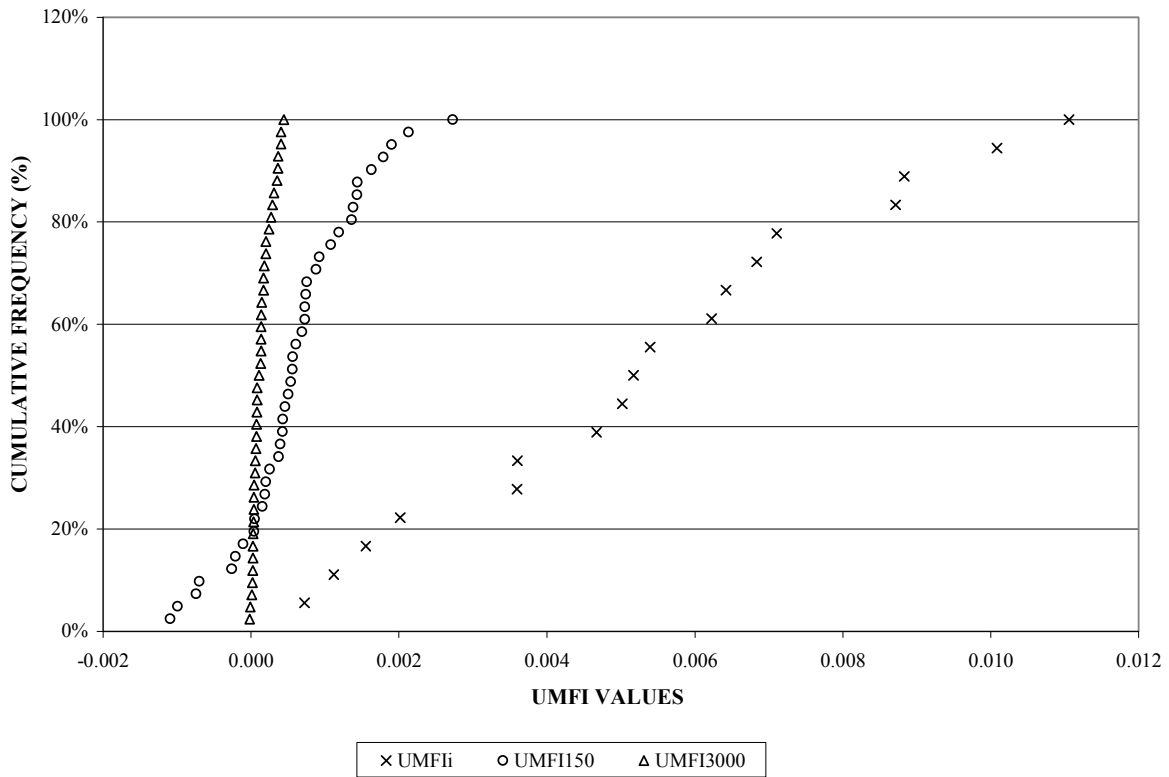


**Figure 6.62 Cumulative frequency distribution diagram of UMFI values for the pilot-scale studies**

## CHAPTER 7

# SYNTHESIS AND INTEGRATION OF ALL RESULTS

### STATISTICAL ANALYSES

From the different scales of the membrane filtration tests (stirred-cell tests, bench-scale hollow-fiber tests, and pilot tests), several parameters associated with NOM characteristics and membrane properties were derived and quantified for statistical analyses. Statistical analysis was employed to determine which parameters contribute most significantly to low-pressure membrane fouling by NOM. The statistical methods performed included simple linear correlation (correlation matrices), multiple linear regression, probability frequency distribution, and principal component analysis (PCA) using a software package, STATISTICA (Statsoft, Okla.).

#### Correlation Matrices

Simple linear correlations were employed to determine the correlations among all identified variables to one another. A linear correlation indicates the degree of (linear) relationship between two variables and, within a correlation matrix of all variables, it is described by “r,” the correlation coefficient. The correlation coefficient ( $r$ ) ranges from +1 to -1. As  $r$  approaches 1, the relationship between variables approaches a perfect linear relationship. A positive or negative sign means a direct or an inverse correlation, respectively. A correlation of “0” means that there is no linear relationship between the two variables.

The nomenclature of abbreviations/acronyms for the parameters used in the statistical analyses is summarized in [Table 7.1](#). Correlation matrices for stirred-cell tests, Hollow-Fiber Unit 1 tests, and pilot tests are tabulated in [Tables 7.2, 7.3, and 7.4](#), respectively (test results from the Hollow-Fiber Unit 2 and full-scale datasets were not included in the statistical analyses because of the limited amount of data). In the following discussion, those correlations exhibiting an  $r$  value of  $\geq 0.5$  are emphasized. In stirred-cell tests, PS-DOC and HPI-DOC are more highly correlated to UMFI ( $r = 0.61$  each) and  $J_S/J_{S0}$  at  $75\text{L}/\text{m}^2$  ( $-0.59$  and  $-0.58$ , respectively) than other variables. In contrast, HS-DOC and HPO-DOC do not correlate well to UMFI or either of the  $J_S/J_{S0}$  values. One possible explanation is that Ca can form complexes with humic substances (HS-DOC or HPO-DOC) and affect membrane fouling by charge neutralization and/or steric modification. Thus, the ratios of Ca/HS-DOC and Ca/HPO-DOC were examined and found to be inversely, although weakly ( $r < 0.5$ ), correlated to UMFI; this may be due to enhanced permeation of neutralized humic substances as opposed to their electrostatic rejection in the absence of Ca.

Hollow-Fiber Unit 1 bench tests demonstrated the highest correlation of zeta potential to both UMFI, an index of total fouling, and  $\text{UMFI}_R$ , an index of (short-term) hydraulically irreversible fouling. Among NOM characteristics, DON, SUVA, HS-DOC and HPO-DOC are positively related to  $J_S/J_{S0}$  at  $450\text{ mg C}/\text{m}^2$ , implying less fouling potential.

**Table 7.1**  
**Nomenclature of parameter abbreviations used in statistical analyses**

PS-DOC	DOC concentration of polysaccharides peak in SEC-DOC (mg/L)
HS-DOC	DOC concentration of humic substances peak in SEC-DOC (mg/L)
HPI-DOC	DOC concentration of hydrophilic fraction by XAD-8/-4 fractionation (mg/L)
HPO-DOC	DOC concentration of hydrophobic fraction by XAD-8/-4 fractionation (mg/L)
DON	Dissolved organic nitrogen concentration (mg/L)
SUVA	Specific UVA, = $UVA_{254}/DOC$ (L/mg·m)
FI	Fluorescence index (= fluorescence intensity ratio of Em 450 to Em 500 at Ex 370)
Pore Size	Membrane pore size suggested by manufacturer (nm)
Roughness	Roughness measured by AFM (nm)
PWP	Pure water permeability by MQ filtration test (L/m <sup>2</sup> -hr-kPa)
zeta potential	zeta potential measured by electrophoresis (mV)
Hydrophobicity	Determined by contact angle of membrane surface (1: hydrophilic, 2: hydrophobic)
UMFI	Unified membrane fouling index (m <sup>2</sup> /L)

The pilot test data are divided into two parts because of the available numbers of cases (N values) in data sets related to NOM characteristics (N = 18) versus those related to membrane properties (N = 10). HPO-DOC, Ca/HPO-DOC and HPI-DOC values are not included in this correlation matrix due to the limited number of cases. DON is highly correlated to HS-DOC, Ca/HS-DOC, and SUVA. Membrane properties are more correlated to UMFI<sub>3000</sub> than NOM characteristics. DON and SUVA are moderately and negatively correlated to UMFI<sub>3000</sub>, showing less fouling potential. PS-DOC and FI are negatively correlated to  $J_s/J_{s0}$  at 75 L/m<sup>2</sup>, indicating their high fouling potential.

**Table 7.2**  
**Correlation matrix (r values) for stirred-cell test data**

N=15	PS-DOC	HS-DOC	Ca/HS-DOC	HPI-DOC	HPO-DOC	Ca/HPO-DOC	DON	SUVA	FI	Pore size	Roughness	PWP	zeta potential	Hydrophobicity	UMFI	J <sub>s</sub> /J <sub>s0</sub> (75 L/m <sup>2</sup> )	J <sub>s</sub> /J <sub>s0</sub> (450 mg/m <sup>2</sup> )
PS-DOC	1.00	0.65	-0.22	0.98	0.59	-0.13	0.57	0.09	0.22	N/A*	N/A	N/A	N/A	N/A	0.61	-0.59	-0.07
HS-DOC		1.00	-0.57	0.77	0.99	-0.58	0.97	0.82	-0.50	N/A	N/A	N/A	N/A	N/A	0.36	-0.36	0.28
Ca/HS-DOC			1.00	-0.30	-0.48	0.99	-0.70	-0.57	0.35	N/A	N/A	N/A	N/A	N/A	-0.24	0.30	0.10
HPI-DOC				1.00	0.73	-0.22	0.69	0.27	0.09	N/A	N/A	N/A	N/A	N/A	0.61	-0.58	0.01
HPO-DOC					1.00	-0.50	0.92	0.84	-0.50	N/A	N/A	N/A	N/A	N/A	0.34	-0.33	0.33
Ca/HPO-DOC						1.00	-0.72	-0.65	0.48	N/A	N/A	N/A	N/A	N/A	-0.15	0.22	0.02
DON							1.00	0.84	-0.61	N/A	N/A	N/A	N/A	N/A	0.28	-0.31	0.25
SUVA								1.00	-0.84	N/A	N/A	N/A	N/A	N/A	-0.01	-0.01	0.44
FI									1.00	N/A	N/A	N/A	N/A	N/A	0.35	-0.30	-0.49
Pore Size										1.00	0.95	1.00	0.48	0.06	-0.31	0.29	0.25
Roughness											1.00	0.91	0.73	0.37	-0.40	0.33	0.29
PWP												1.00	0.40	-0.03	-0.28	0.27	0.23
zeta potential													1.00	0.90	-0.44	0.30	0.27
Hydrophobicity														1.00	-0.35	0.20	0.18
UMFI															1.00	-0.96	-0.67
J <sub>s</sub> /J <sub>s0</sub> (75L/m <sup>2</sup> )																1.00	0.72
J <sub>s</sub> /J <sub>s0</sub> (450mg/m <sup>2</sup> )																	1.00

\*N/A = not applicable

**Table 7.3**  
**Correlation matrix (r values) for Hollow-Fiber Unit 1 test data**

N=42	PS-DOC	HS-DOC	Ca/HS-DOC	HPI-DOC	HPO-DOC	Ca/HPO-DOC	DON	SUVA	FI	Pore size	Roughness	PWP	zeta potential	Hydrophobicity	UMFI	UMFI <sub>R</sub>	J <sub>s</sub> /J <sub>s0</sub> (75 L/m <sup>2</sup> )	J <sub>s</sub> /J <sub>s0</sub> (450 mg/m <sup>2</sup> )
PS-DOC	1.00	0.16	-0.09	0.12	0.20	-0.09	0.23	0.15	-0.04	N/A*	N/A	N/A	N/A	N/A	0.44	0.46	-0.01	-0.06
HS-DOC		1.00	-0.84	0.81	0.98	-0.91	0.95	0.90	-0.76	N/A	N/A	N/A	N/A	N/A	0.33	0.44	0.09	0.60
Ca/HS-DOC			1.00	-0.99	-0.75	0.98	-0.78	-0.53	0.39	N/A	N/A	N/A	N/A	N/A	-0.41	-0.36	0.22	-0.34
HPI-DOC				1.00	0.74	-0.96	0.80	0.48	-0.29	N/A	N/A	N/A	N/A	N/A	0.45	0.38	-0.26	0.29
HPO-DOC					1.00	-0.83	0.98	0.93	-0.75	N/A	N/A	N/A	N/A	N/A	0.33	0.46	0.14	0.61
Ca/HPO-DOC						1.00	-0.82	-0.66	0.55	N/A	N/A	N/A	N/A	N/A	-0.37	-0.37	0.11	-0.44
DON							1.00	0.84	-0.60	N/A	N/A	N/A	N/A	N/A	0.40	0.49	0.04	0.52
SUVA								1.00	-0.93	N/A	N/A	N/A	N/A	N/A	0.16	0.37	0.34	0.70
FI									1.00	N/A	N/A	N/A	N/A	N/A	0.00	-0.22	-0.42	-0.70
Pore Size										1.00	0.99	-0.66	0.61	0.21	-0.27	-0.20	-0.06	0.03
Roughness											1.00	-0.63	0.50	0.30	-0.17	-0.10	-0.14	-0.05
PWP												1.00	-0.83	-0.69	0.51	0.41	-0.07	-0.24
zeta potential													1.00	0.19	-0.72	-0.62	0.30	0.45
Hydrophobicity														1.00	-0.03	0.03	-0.20	-0.08
UMFI															1.00	0.92	-0.60	-0.48
UMFI <sub>R</sub>																1.00	-0.43	-0.31
J <sub>s</sub> /J <sub>s0</sub> (75L/m <sup>2</sup> )																	1.00	0.73
J <sub>s</sub> /J <sub>s0</sub> (450mg/m <sup>2</sup> )																		1.00

\*N/A = not applicable

**Table 7.4**  
**Correlation matrices (r values) for pilot test data\***

N=18	PS-DOC	HS-DOC	Ca/HS-DOC	DON	SUVA	FI	$J_s/J_{s0}$ (75 L/m <sup>2</sup> )	$J_s/J_{s0}$ (150 L/m <sup>2</sup> )	UMFI <sub>150</sub> (Method 2)	UMFI <sub>3000</sub> (Method 2)
PS-DOC	1.00	0.50	-0.54	0.00	-0.11	0.43	-0.53	-0.23	0.38	0.28
HS-DOC		1.00	-0.75	0.71	0.73	-0.38	0.07	0.18	0.07	-0.25
Ca/HS-DOC			1.00	-0.61	-0.46	0.06	0.20	-0.07	-0.33	0.27
DON				1.00	0.88	-0.71	0.32	0.30	-0.14	-0.44
SUVA					1.00	-0.84	0.30	0.12	-0.03	-0.40
FI						1.00	-0.47	-0.18	0.17	0.30
$J_s/J_{s0}$ (75L/m <sup>2</sup> )							1.00	0.84	-0.81	-0.41
$J_s/J_{s0}$ (150L/m <sup>2</sup> )								1.00	-0.77	-0.37
UMFI <sup>150</sup> Method 2									1.00	0.25
UMFI <sup>3000</sup> Method 2										1.00

N=10	Pore size	zeta potential	Roughness	PWP	$J_s/J_{s0}$ (150 L/m <sup>2</sup> )	$J_s/J_{s0}$ (75 L/m <sup>2</sup> )	UMFI <sub>150</sub> (Method 2)	UMFI <sub>3000</sub> (Method 2)
Pore size	1.0	1.0	1.0	-1.0	-0.09	-0.27	0.27	0.71
zeta potential		1.0	1.0	-1.0	-0.09	-0.27	0.27	0.71
Roughness			1.0	-1.0	-0.09	-0.27	0.27	0.71
PWP				1.0	0.09	0.27	-0.27	-0.71
$J_s/J_{s0}$ (150 L/m <sup>2</sup> )					1.00	0.89	-0.76	-0.25
$J_s/J_{s0}$ (75 L/m <sup>2</sup> )						1.00	-0.72	-0.41
UMFI <sup>150</sup> (Method 2)							1.00	0.60
UMFI <sup>3000</sup> (Method 2)								1.00

\*Tier 1 pilot data for Tampa Bay, Indianapolis, and Scottsdale.

## Probability Frequency Distribution Diagrams

Figure 7.1 provides a comparison of the cumulative frequency of UMFI values resulting from various filtration experiments; corresponding 50 and 90 percentile values are summarized in Table 7.5. A general definition of cumulative frequency distribution is a probability plot of the number of observations falling within a given interval. Pilot testing results show a more narrow distribution than stirred-cell or bench tests.

First, comparing bench-scale results, the cumulative frequency of UMFI values observed in stirred-cell tests and those of  $UMFI_r$  in Hollow-Fiber Unit 1 bench-scale (Unit 1) tests show very similar trends. Even though stirred-cell tests provide dead-end conditions for membrane fouling, hydraulic conditions induced by the stirrer inhibit greater deposition of foulant on the membrane surface. In the case of bench test with  $UMFI_r$ , the backwashing step reduces the ultimate deposition of foulant. Thus, the UMFI of stirred-cell tests is less than the UMFI of bench (Unit 1) tests and similar to  $UMFI_r$ .

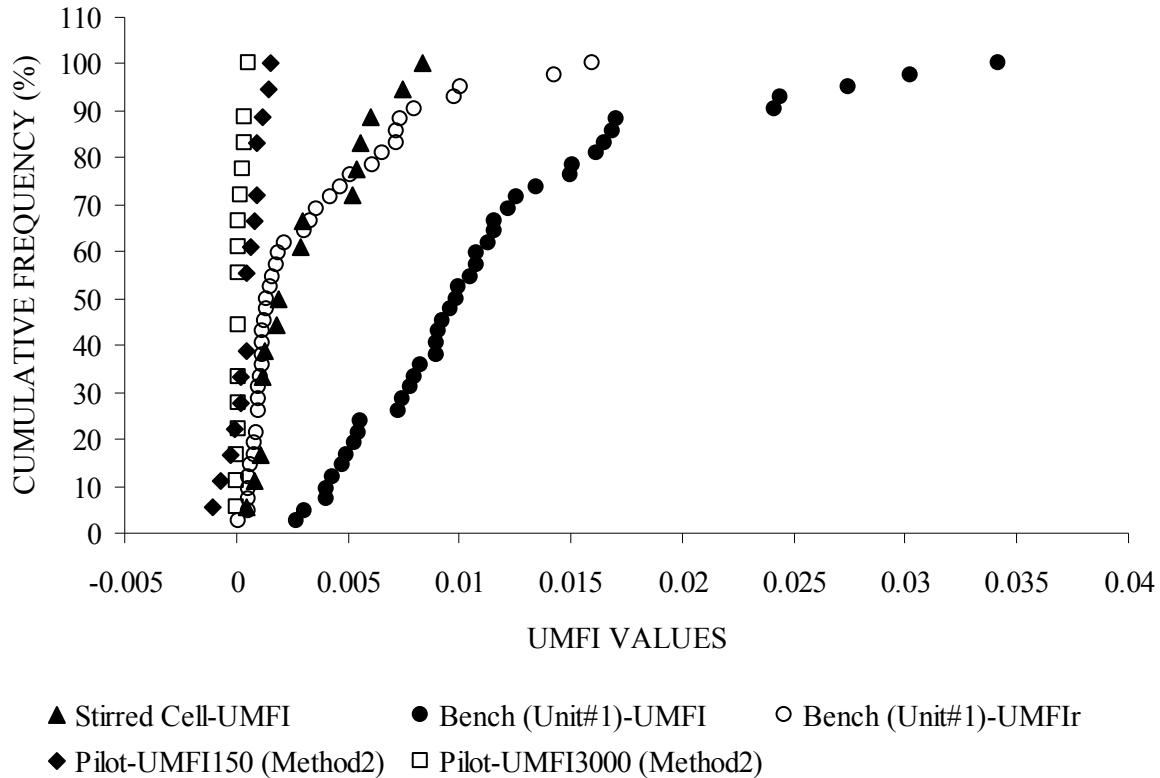


**Figure 7.1 Probability frequency distribution of various filtrations**

**Table 7.5**  
**Comparison of UMFI**  
**corresponding to 50 percentile and 90 percentile cumulative frequencies**

	Cumulative frequency (%)	UMFI value (m <sup>2</sup> /L)
Stirred-cell (UMFI)	50	1.9E-03
	90	6.0E-03
Hollow-Fiber Unit 1 (UMFI)	50	9.9E-03
	90	2.3E-02
Hollow-Fiber Unit 1 (UMFI <sub>r</sub> )	50	1.4E-03
	90	7.9E-03
Pilot UMFI <sub>150</sub>	50	5.5E-04
	90	1.6E-03
Pilot UMFI <sub>3000</sub>	50	1.1E-04
	90	3.6E-04

Pilot testing results show a more narrow distribution of UMFI values than stirred-cell or hollow-fiber bench scale tests in which end-of-run backwash was utilized (UMFI<sub>r</sub>). This reflects the fact that stirred-cell and hollow-fiber bench UMFI values represent total membrane fouling (which have higher values) versus pilot UMFI<sub>150</sub> and UMFI<sub>3000</sub> values, which represent hydraulically (and pneumatically) reversible fouling only. Hollow-fiber (bench) UMFI<sub>150</sub> values are intermediate because of shorter-term, hydraulically reversible fouling.

### Multiple Linear Regression Equations

Multiple linear regression analysis derives a relationship between several independent (or predictor) variables and a dependent (or criterion) variable at a given significance (p) level. It is used to estimate a value of the designated dependent variable as a function of the designated multiple independent variables through a linear predictive equation. The form of a linear equation is:

$$Y = a + b_1 \times X_1 + b_2 \times X_2 + \dots + b_n \times X_n$$

$b_1 \sim b_n$  are the regression coefficients that represent the weight for the contributions of each independent variable to the prediction of the dependent variable; “a” is a constant intercepting the y-axis, Y is the dependent variable, and  $X_1 \sim X_n$  are independent variables.  $R^2$  is the multiple correlation coefficient or, more specifically, the coefficient of multiple determination and is the percent of variance in the dependent variable explained collectively by all of the independent variables. A  $R^2$  value close to 1.0 indicates that almost all of the variability with the designated variables has been accounted for in the model.

The importance of certain variables in explaining other variables (i.e., correlation) was first revealed by the correlation matrices. Next, after identifying a dependent variable(s) of interest and considering all other potentially influential variables, multiple linear regression analysis was performed using a *step-wise* approach. The step-wise approach chooses a subset of the independent variables, one by one, that “best” explain the dependent variable until no variables “significantly” explain residual variation; variable inclusion is terminated after

reaching a threshold designated in terms of  $\Delta R^2$  (i.e., the incremental increase in  $R^2$  by including another independent variable). All thirteen independent variables (PS-DOC, HS-DOC, Ca/HS-DOC, HPI-DOC, HPO-DOC, Ca/HPO-DOC, DON, FI, SUVA, pore size, PWP, roughness, and zeta potential) used in stirred-cell tests were considered for selecting significant variables to explain UMFI (the designated dependent variable). Considering all candidate independent variables, PS-DOC, zeta potential, and FI were selected and introduced into the linear equation as follows:

$$\text{UMFI} = -0.017529 + 0.008869 \times \text{PS peak} - 0.000375 \times \text{zeta potential} + 0.002369 \times \text{FI}$$

$$(R^2 = 0.624, p < 0.011)$$

When only NOM characteristics (PS-DOC, HS-DOC, Ca/HS-DOC, HPI-DOC, HPO-DOC, Ca/HPO-DOC, DON, FI, and SUVA) are considered, PS-DOC peak, FI, and DON are selected and introduced into the linear equation as follows:

$$\text{UMFI} = -0.020203 - 0.000967 \times \text{PS peak} + 0.009018 \times \text{FI} + 0.015509 \times \text{DON}$$

$$(R^2 = 0.510, p < 0.043)$$

When only membrane characteristics (pore size, roughness, PWP, zeta potential, hydrophobicity) are considered, only zeta potential is selected as significant.

$$\text{UMFI} = -0.010754 - 0.000375 \times \text{zeta potential}$$

$$(R^2 = 0.195, p < 0.099)$$

Hollow-Fiber Unit 1 test results were also used for multiple regression analysis. All variables for bench tests were considered, and zeta potential, HPI-DOC and roughness were selected. The linear equation with these parameters is as follows:

$$\text{UMFI} = -0.012729 - 0.000121 \times \text{zeta potential} + 0.0003746 \times \text{HPI DOC} + 0.000018 \times \text{Roughness}$$

$$(R^2 = 0.683, p < 0.0000)$$

When only NOM characteristics (PS-DOC, HS-DOC, Ca/HS-DOC, HPI-DOC, HPO-DOC, Ca/HPO-DOC, DON, FI, and SUVA) are considered, HPI-DOC, PS-DOC, and Ca/HS-DOC are selected and introduced into the linear equation as follows;

$$\text{UMFI} = -0.037689 + 0.016109 \times \text{HPI DOC} + 0.001988 \times \text{PS peak} + 0.000372 \times \text{Ca/HS peak}$$

$$(R^2 = 0.37, p < 0.0004)$$

When only membrane characteristics (pore size, roughness, PWP, zeta potential, and hydrophobicity) are considered, only two variables, zeta potential and roughness, are selected and introduced into the linear equation as follows;

$$\text{UMFI} = -0.004246 - 0.000129 \times \text{zeta potential} + 0.000017 \times \text{Roughness}$$

$$(R^2 = 0.56, p < 0.0000)$$

Taken together, the multiple linear regression analyses indicate that NOM membrane fouling, as represented by UMFI, is most strongly influenced by the PS peak and HPI-DOC of the source water and membrane zeta potential, and secondarily influenced by the source water fluorescence index and the membrane surface roughness.

### **Principal Component Analysis**

PCA was performed to provide a comprehensive understanding of low-pressure membrane fouling related to NOM characteristics and membrane properties. While PCA is not a truly quantitative statistical analysis tool, its main attribute is as a cluster analysis, revealing clusters or patterns of data (e.g., UMFI values) according to common factors (e.g., NOM characteristics and/or membrane properties). While a detailed description of the underlying statistics is beyond the scope of this report, the following represents a concise summary.

The major functions of PCA are to discover or to reduce the dimensionality of the data set and to identify new meaningful underlying (composite) variables. PCA transforms the multivariate set into a set of artificial factors (principal components) based on the symmetric correlation matrix (e.g., [Tables 7.2](#) through [7.4](#)) or the symmetric covariance matrix. The procedure of PCA starts with assigning eigenvalues to each component for transforming a set of multiple variables into a set of components. Generally, the first two components account for meaningful amounts of variance and are interpreted for subsequent analyses. Next, the two components are loaded with variables depending on the scores of each variable. As the score of a variable comes close to 1, the variable contributes significantly to the component. To make a simple structure, the component loading is performed with rotation. A rotation is a linear transformation for the purpose of making the analysis easy to interpret, and a variance maximizing (varimax) rotation is applied. Varimax rotation is an orthogonal rotation that maximizes the variance of a column of the component matrix. The actual values of individual cases to the components can be estimated after the component loading.

The major role of PCA in this study is to help explain the relation of NOM characteristics and membrane properties to low-pressure membrane fouling (as represented by, for example, UMFI). Based on the database, several data sets were analyzed by PCA to address the following questions:

1. Which Feed-Water NOM Characteristics Affect Membrane Fouling?
2. Which Membrane Properties Influence Fouling?
3. Which Membrane Operating Conditions Influence Fouling?

Data derived from stirred-cell tests were used to answer questions 1 and 2 because these tests were performed under the same operating conditions and without any pretreatment. Data from Hollow-Fiber Units 1 and 2 tests were not used to answer questions 1 and 2 because the

limited data corresponding to various operational conditions were not amenable to statistical analysis. Data from pilot tests were used to address questions 1 and 3; the fouling influence by membrane properties could not be interpreted because each water source was tested with different membranes.

### ***Which Feed Water (NOM) Characteristics Affect Membrane Fouling?***

The parameters derived from NOM characteristics and filtration performances in stirred-cell tests are loaded into two components determined by eigenvalues in **Figure 7.2** (component loading plot). PS-DOC, HPI-DOC, and DON are directly related to component 1 (a composite variable embodying the indicated parameters), while Ca/HS-DOC and Ca/HPO-DOC are inversely related. FI and UMFPI are related to component 2 (a second composite variable) and SUVA,  $J_s/J_{s0}$  (75 L/m<sup>2</sup>), and  $J_s/J_{s0}$  (450 mg/m<sup>2</sup>) are inversely related. **Figure 7.3** (ordination plot) shows the distribution (clustering) of datasets with four different source waters. The Scottsdale and Twente Canal water are located (clustered) in the upper part of the graph (Quadrants 1 and 2) with higher UMFPI values than other waters, inferring higher fouling tendency.<sup>3</sup> The location of the Twente Canal water is situated (clustered) more to the right side of the x axis than the Scottsdale water due to its higher content of PS-DOC and HPI-DOC. Even though the Tampa Bay water has a high DOC concentration (~17 mg/L), its fouling tendency is less than the Scottsdale and Twente Canal waters. Thus, PS-DOC and HPI-DOC content are closely related to UMFPI values and related to significant membrane fouling.

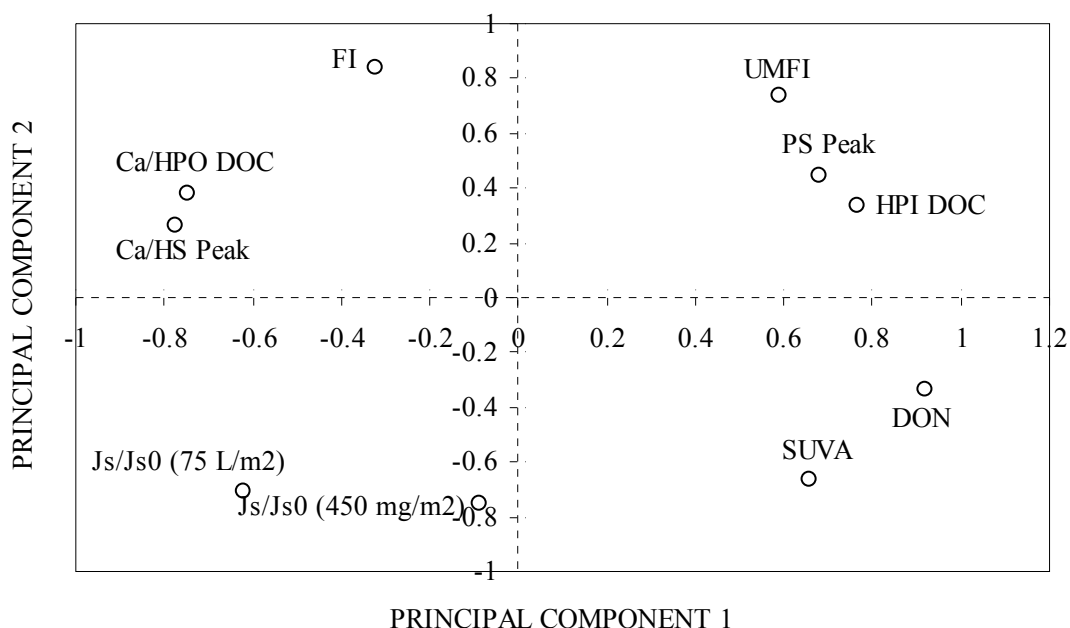


**Figure 7.2 Component loading (NOM characteristics and filtration performance) by stirred-cell test results**

<sup>3</sup> For each of the PCA quadrant plots, the upper right quadrant is designated as Quadrant 1, the upper left as Quadrant 2, the lower left as Quadrant 3, and the lower right as Quadrant 4.

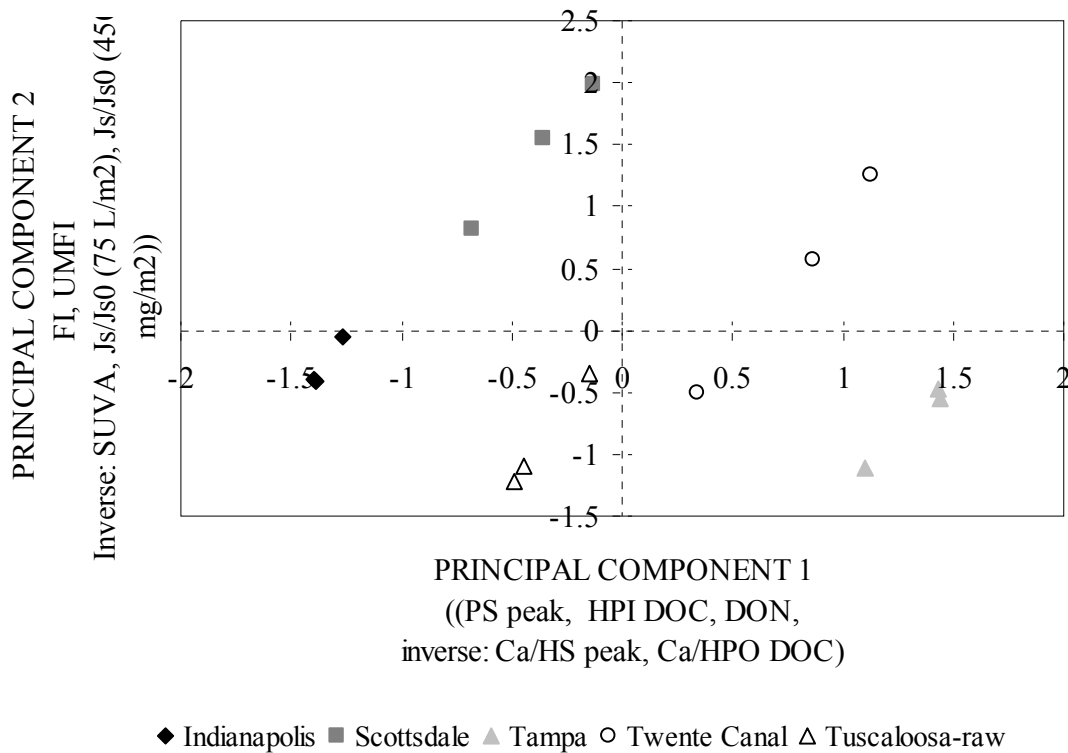


**Figure 7.3 Ordination results for stirred-cell test results with respect to NOM characteristics and filtration performance**

In the case of Hollow-Fiber Unit 1 tests, PS-DOC, UMF1, and UMF1<sub>R</sub> are inversely related to component 2, and HPI-DOC is inversely related to component 1 as well as DON and SUVA. Ca/HS-DOC and Ca/HPO-DOC are related to component 1 (Figure 7.4, component loading graph). The lower part of the ordination graph (Figure 7.5) represents a high fouling tendency with high UMF1 and UMF1<sub>R</sub> values. For this analysis, a location in Quadrant 4 (lower right) indicates a high fouling potential, and most data points of associated with the Scottsdale water are distributed in Quadrant 4.

The PCA with NOM characteristics for pilot tests is discussed in the answer to question 3.

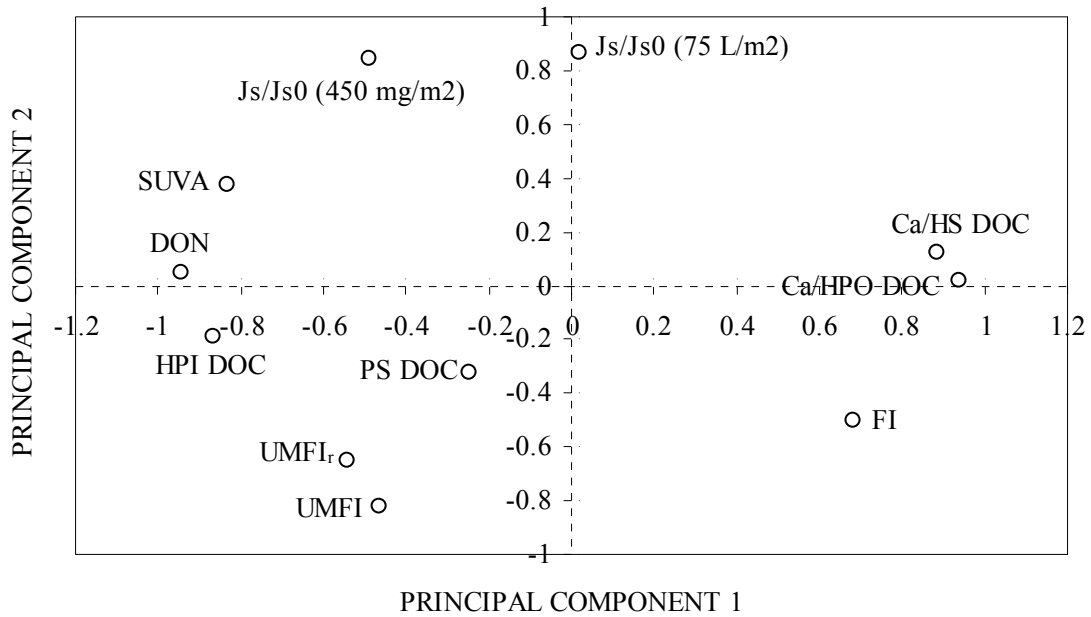


**Figure 7.4 Component loading (NOM characteristics and filtration performance) by the Hollow-Fiber Unit 1 bench test results**

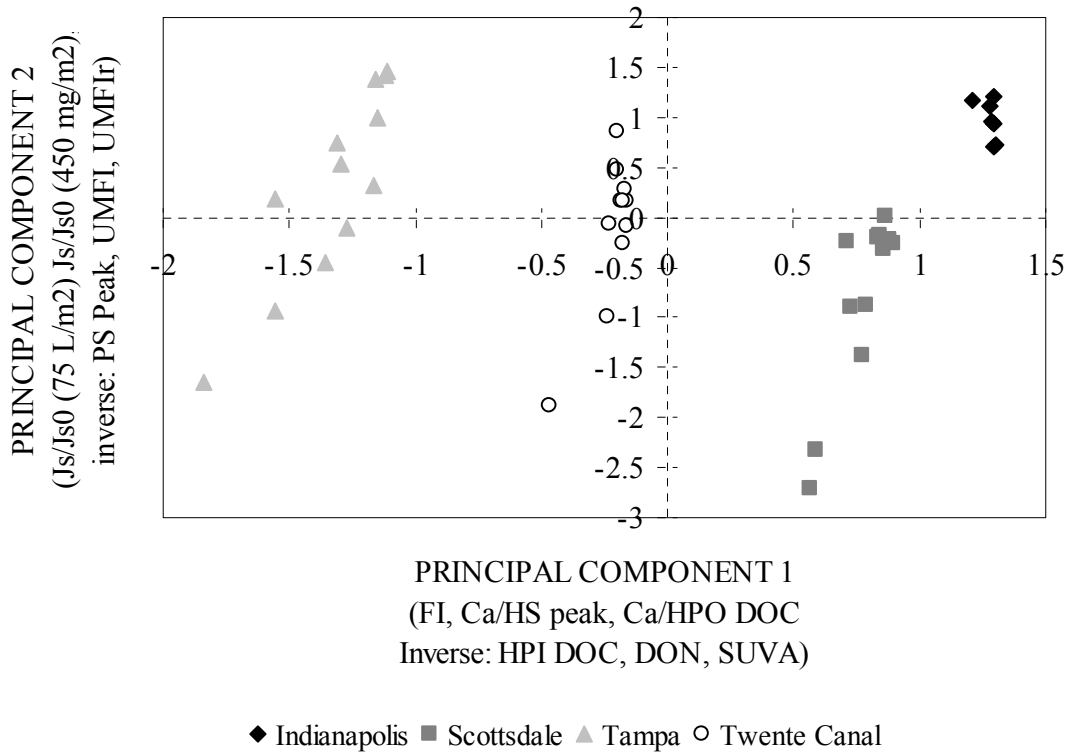


**Figure 7.5 Ordination results for Hollow-Fiber Unit 1 bench test results with respect to NOM characteristics and filtration performance**

### ***Which Membrane Properties Influence Fouling?***

To answer question 2, the parameters taken from membrane properties and filtration performance in stirred-cell tests are loaded in [Figure 7.6](#). All parameters representing membrane properties are inversely related to component 1, except UMFI. The PES UF and PAN MF/UF membrane show more fouling tendency than the PVDF MF membrane due to the larger pore size and higher PWP of the latter, although the different materials may also play a role. An interesting point is that the zeta potential is inversely related to UMFI. Generally, a positively charged membrane has a potential to bind with negatively charged molecules, such as humic substances, and cause fouling. The results reveal that other properties are likely more influential because the zeta potential of each of the three membranes are very similar in this case. [Figure 7.7](#) illustrates the ordination results. The PES UF membrane is located solely in Quadrant 4, indicating a higher fouling trend than the other membranes. Thus, fouling is likely to be dominantly affected by the pore size of the membrane in low-pressure membrane fouling.

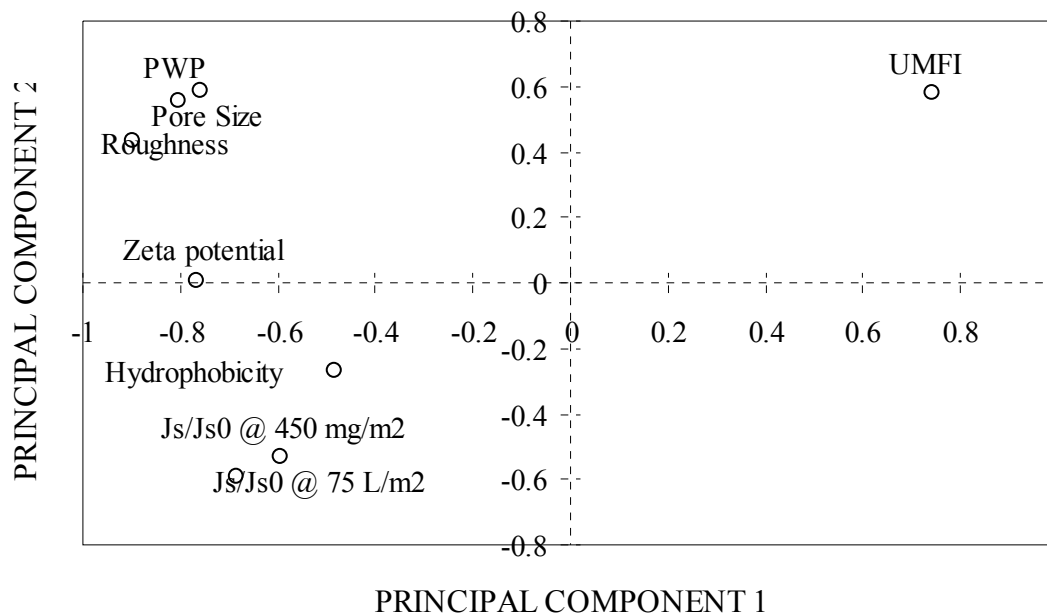


**Figure 7.6 Component loading (membrane property and filtration performance) by stirred-cell test results**

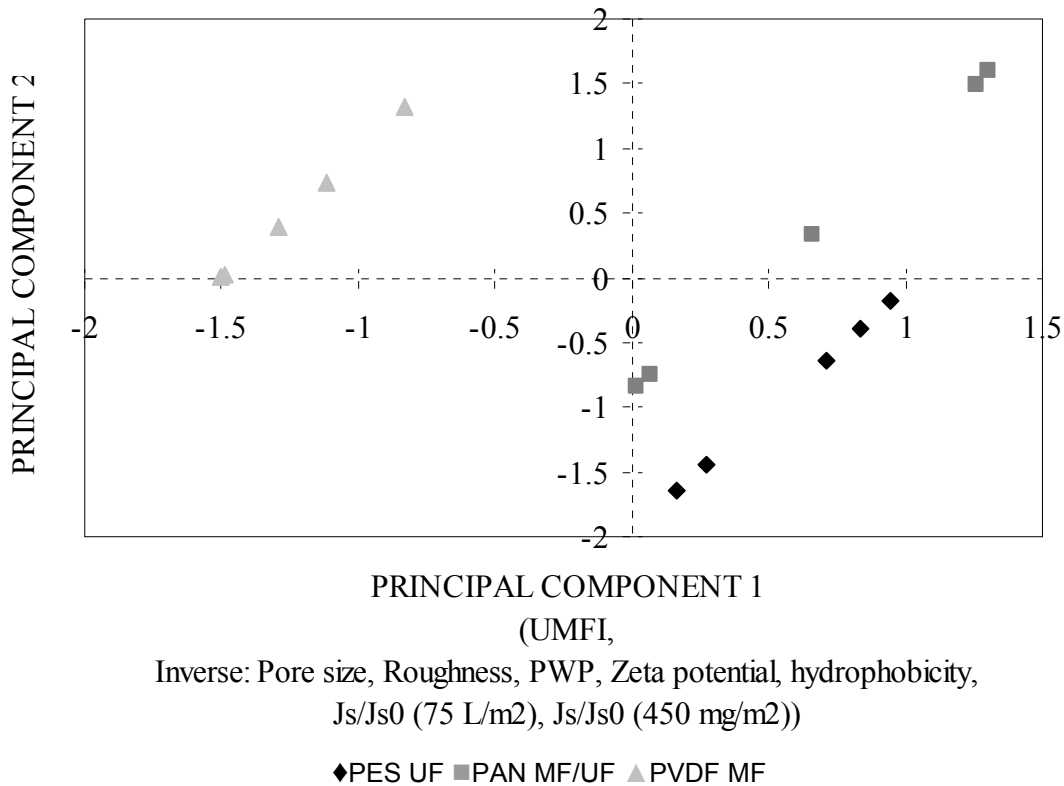


**Figure 7.7 Ordination results for stirred-cell test results with respect to membrane property and filtration performance**

Using a similar approach described above, [Figure 7.8](#) (component loading) and [Figure 7.9](#) (ordination) display PCA analysis of Hollow-Fiber Unit 1 test results. Smaller pore size, higher PWP, and a lower negatively charged membrane correspond to higher UMFI and UMFI<sub>R</sub> values, indicating a higher fouling tendency. Membrane D2 has the highest fouling tendency, as well as the smallest pore size (0.016  $\mu\text{m}$ ) and lowest zeta potential. In contrast, Membrane A provides the least fouling tendency, and has the largest pore size (0.1  $\mu\text{m}$ ) and the highest zeta potential.

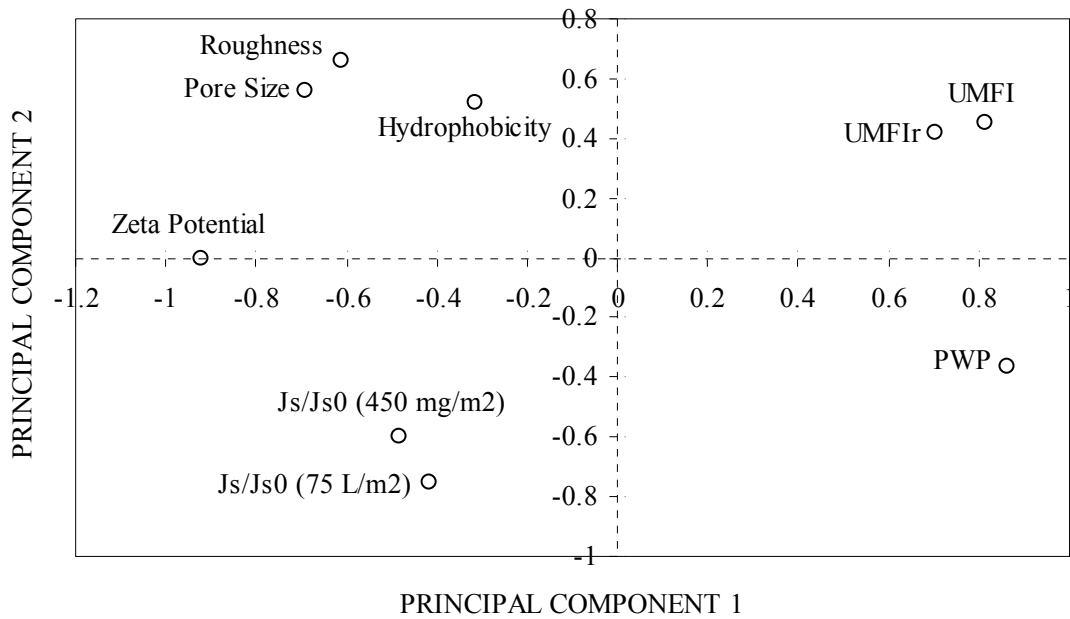


**Figure 7.8 Component loading (membrane property and filtration performance) for Hollow-Fiber Unit 1 bench test results**

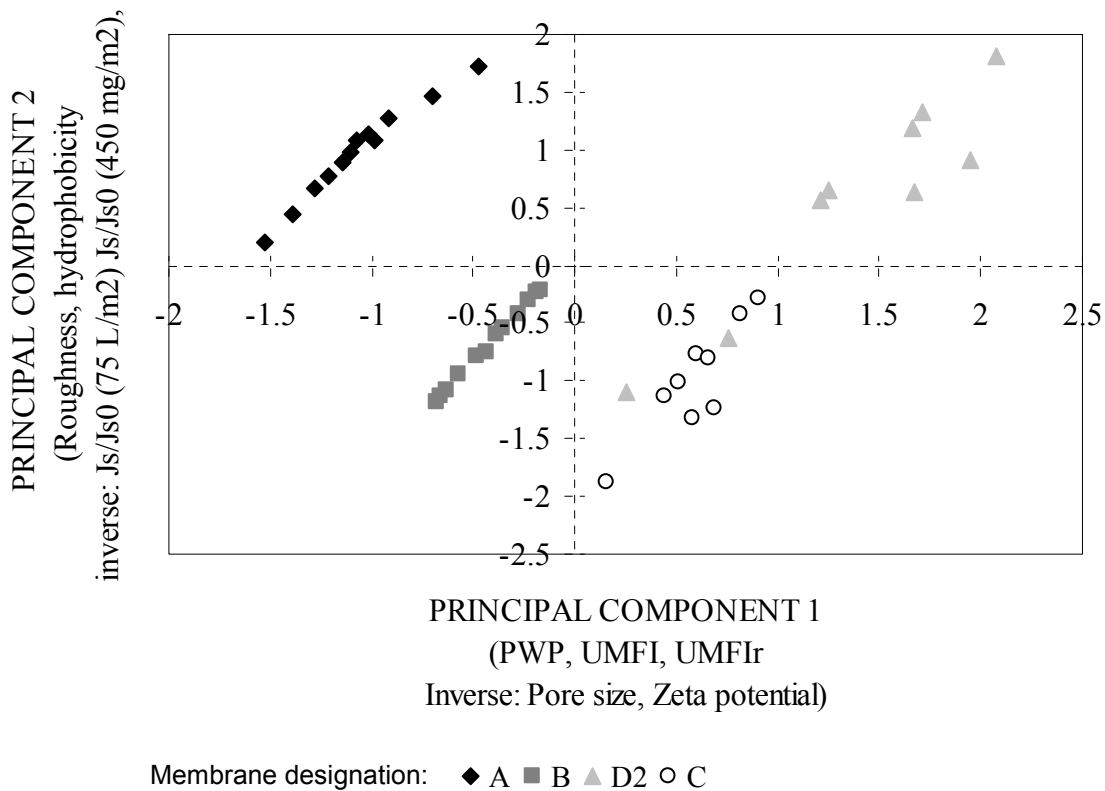


**Figure 7.9 Ordination results for Hollow-Fiber Unit 1 bench test results with respect to membrane property and filtration performance**

**Which Membrane Operating Conditions Influence Fouling?** This question can indirectly be answered by pilot test results. While each of the pilot tests embodied different operating conditions, each also employed a different feed water. Thus, it is not possible to separate operational conditions from feed water (NOM) characteristics. A decision was made to represent the components in terms of NOM characteristics, and then to emphasize the interpretation of the cluster analysis based on operational conditions. NOM characteristics were classified into components 1 and 2 (Figure 7.10). Different backwash flux (high and normal) conditions and pretreatments by alum coagulation and ferric coagulation were evaluated in Figure 7.11. The data points to the right side of the x axis (Quadrants 1 and 4) have high PS-DOC and high fouling potential (high UMFIs values). The circled data points with designation “A” represent high backwash flux (volume) operation, and lie to the left of the data points representing normal backwash flow operation. This spatial relationship indicates that high backwash flux reduces membrane fouling through more effective removal of a reversible cake layer from the membrane surface. The second set of circled data points (designated “B”) represents high recovery conditions. This group lies to the right of the data points representing normal recovery conditions, indicating that high recovery (i.e., increased organic and particulate loading) increases membrane fouling. Most data points corresponding to filtration with pretreated water are located in or close to Quadrant 2, revealing a low fouling tendency.

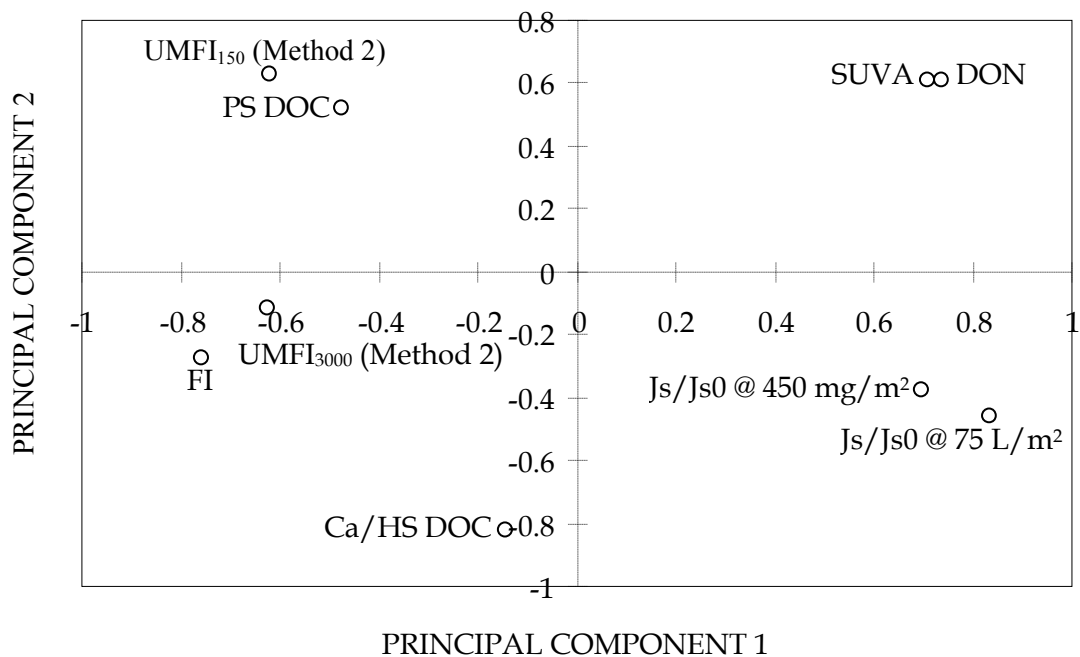


**Figure 7.10 Component loading by pilot test results**

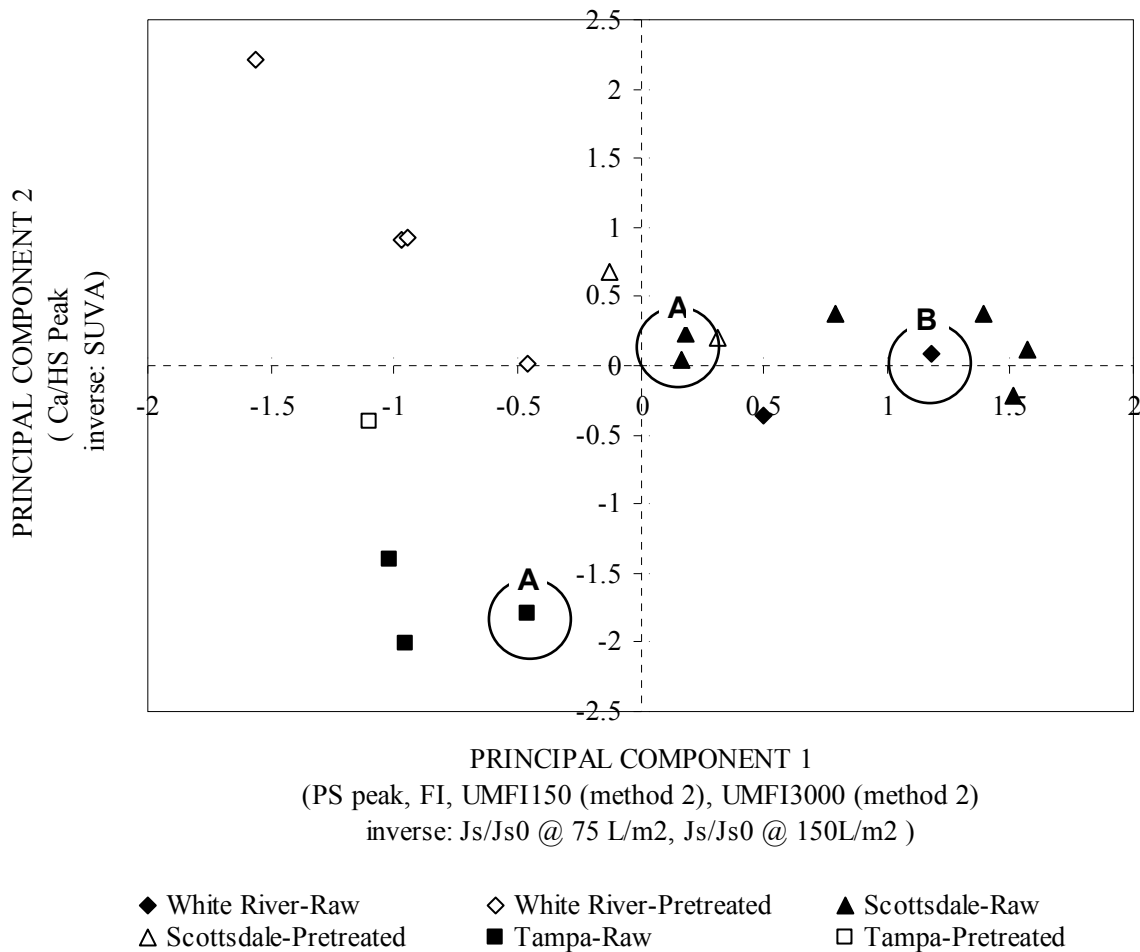


**Figure 7.11 Ordination results for pilot test results**

### SCALE-UP VIA UMF1 CONCEPT

The work done in this study encompassed experimentation at four scales in order of increasing operational complexity: bench-scale with flat-sheet membranes (i.e., stirred cells), bench-scale with hollow-fiber membranes, pilot scale, and full scale. Potentially, one of the major contributions of this study was the development of the UMF1 concept enabling the comparison of results between these differing levels (scales) of experimental complexity. The following discussion presents the findings for comparisons between the flat-sheet stirred-cell unit, the bench-scale hollow-fiber tests, and pilot tests.

### Matched Pair Data Analysis: Stirred-cell versus Bench-Scale Hollow-Fiber Tests

Matched pair analysis was used to compare UMF1 results from stirred-cell experiments using flat-sheet membranes with Hollow-Fiber Unit 1 end-of-run backwash experiments for runs conducted with the four Tier 1 source waters. Three sets of comparisons were performed, based on hollow-fiber and flat-sheet membrane type, respectively. Membrane pairings were

(1) Membrane A with the PVDF MF, (2) Membrane B with the PAN MF/UF, and (3) Membranes C and D1, with the PES UF. The highest flux run for each membrane water combination in the Hollow-Fiber Unit 1 baseline testing was used for comparison, as it best approximated the range in flux during the constant pressure operation of the flat-sheet stirred-cell unit. For each corresponding pair of experiments the UMF<sub>I</sub> for the flat-sheet test was subtracted from UMF<sub>I</sub> of the hollow-fiber test. In the case of the two hollow-fiber PES membranes (C and D1), the UMF<sub>I</sub> values were averaged to obtain one value for comparison. Hollow-fiber and flat-sheet comparisons can be considered to be statistically different if the 95 percent confidence interval about the mean does not encompass the origin. Figure 7.12 shows the matched pairs for each comparison. The hollow-fiber and flat-sheet tests were found to be statistically different in all cases. The Membrane B versus PAN MF/UF comparison showed the greatest similarity, although the results are still statistically different. These comparisons support the assertion that flat-sheet membranes chosen for this research do not serve as good surrogates of the hollow-fiber membranes at the bench scale. However, part of this disparity may be attributed to the different membranes used in stirred-cell versus hollow-fiber bench testing. This is not unexpected when trying to simulate performance of hollow-fiber Membrane B (PVDF UF) with the PAN MF/UF membrane because of the different membrane material (the original pairing was based on comparable pore sizes). However, better simulation was anticipated with the PVDF MF versus Membrane A, and PES UF versus Membranes C and D2. Part of the disparity may be attributed to the different modes of filtration (dead end with stirring in the stirred cell versus dead end along the hollow fiber).

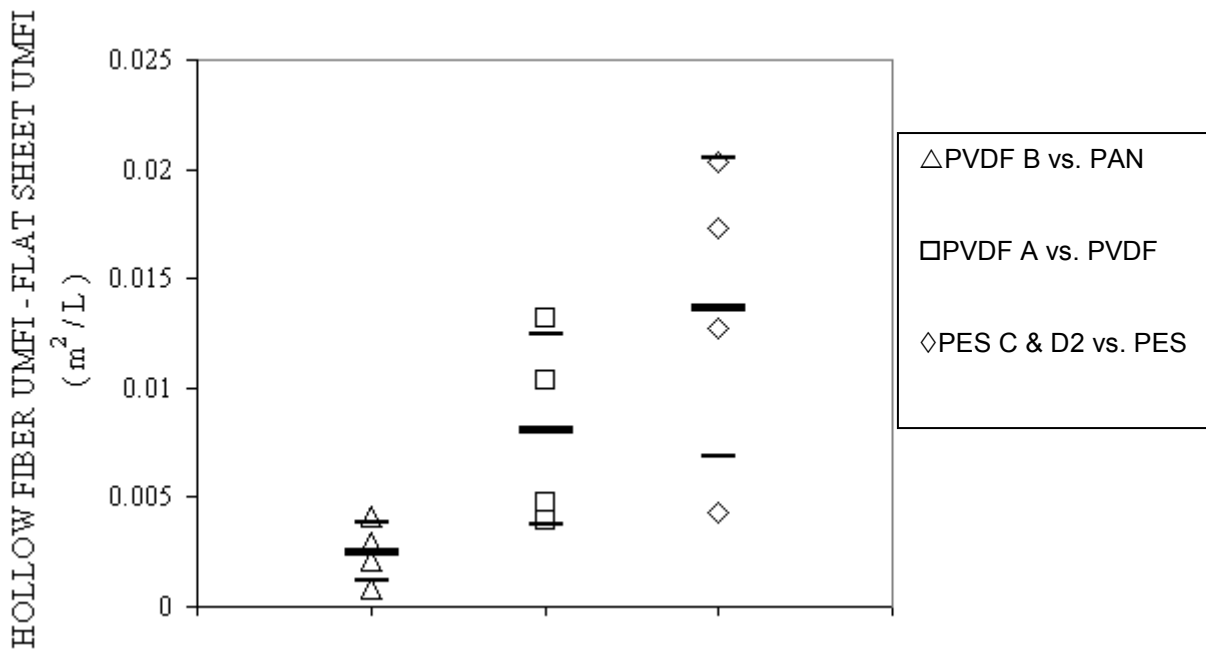


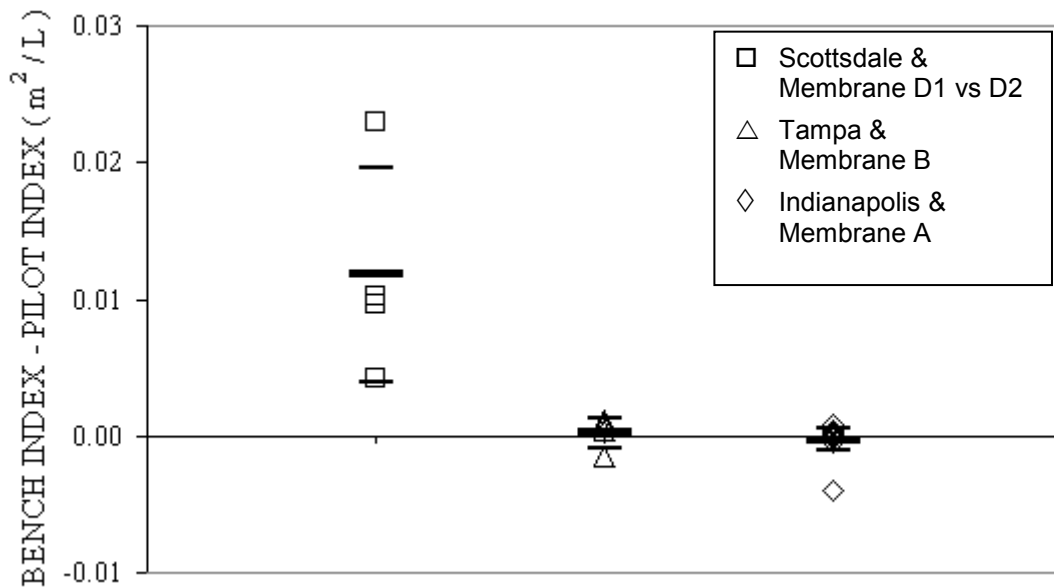
**Figure 7.12 Matched pair analysis of UMF<sub>I</sub> results between flat-sheet and bench-scale Hollow-Fiber Unit 1 end-of-run backwash tests. Matched pairs for three membrane comparisons are shown for the end-of-run backwash hollow-fiber and flat-sheet stirred-cell operational modes. Each membrane was tested with four natural waters. The mean and 95 percent confidence interval are shown for each comparison with heavy and light bars respectively. The legend lists the hollow-fiber membrane material and letter code, followed by the flat-sheet membrane material.**

## Matched Pair Data Analysis: Bench-Scale Hollow-Fiber versus Pilot Tests

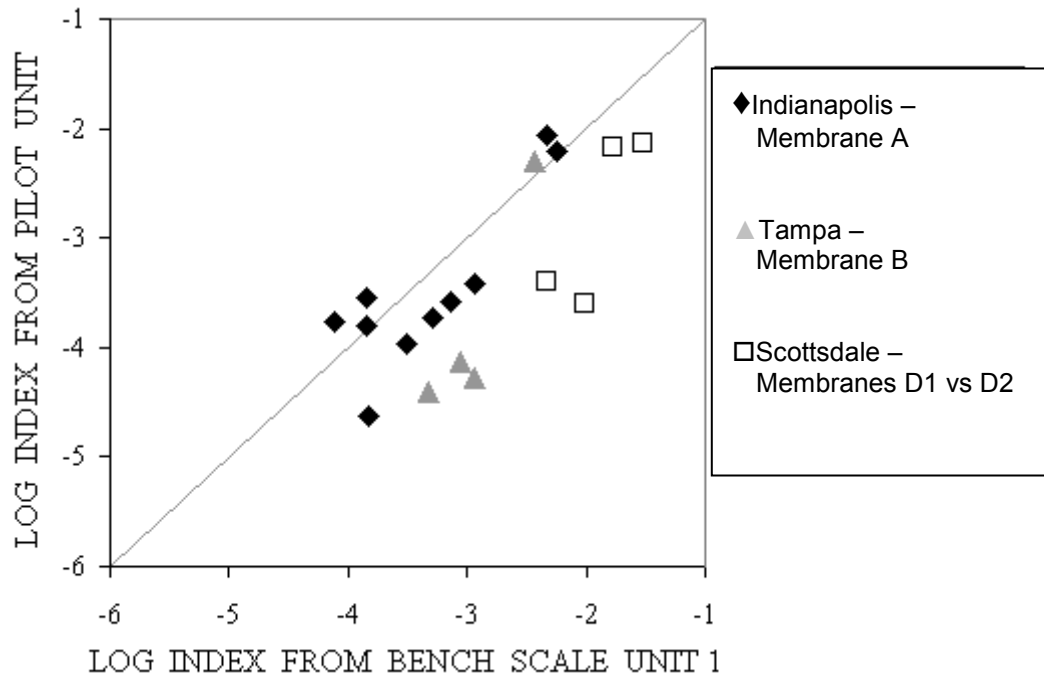
Matched pair analysis was used to compare Hollow-Fiber Unit 1 and pilot-scale results for each of three water-membrane combinations. The analysis consists of defining pairs of experiments for each water-membrane combination that is comparable. The fouling index for the pilot test was subtracted from the fouling index of the bench-scale test. Comparisons consisted of the following: (1) total fouling  $UMFI - UMFI_i$ , (2) hydraulically irreversible fouling  $UMFI_R - UMFI_{3000}$  Method 2, and (3) chemically irreversible fouling  $UMFI_{cleaning} - UMFI_{3000}$  Method 2. Of the four measures of hydraulically irreversible fouling at pilot scale,  $UMFI_{3000}$  Method 2 was chosen because it was available for the majority of runs and because it encompassed at least one chemical wash cycle. In the case of replicate test runs, the indices from each experiment were averaged to provide one value for comparison. Pilot and bench comparisons can be considered to have no statistical difference if the 95 percent confidence interval about the mean encompasses the origin.

Figure 7.13 shows the results of the matched pair analysis for the Scottsdale – Membrane D1 vs. D2, Tampa – Membrane B, and Indianapolis – Membrane A pilot experiments versus the corresponding Hollow-Fiber Unit 1 experiments. The experiments with Scottsdale water show a distinct difference between pilot and Hollow-Fiber Unit 1, with consistently higher index values for the bench-scale unit. This difference is likely attributable to the differences in properties of the D1 and D2 membranes used at pilot- and bench-scale, respectively, particularly with respect to the presence and absence of the PVP hydrophilizing agent (see Table 4-6).

No difference was observed between pilot and bench scale for the both the Tampa Bay – B and Indianapolis – A water-membrane combinations. The best correspondence between bench and pilot was observed in the Indianapolis – Membrane A tests. This relationship can be seen in Figure 7.14, in which the log-transformed indices for each match pair are plotted against each other. The Indianapolis – A comparisons (black diamonds) cluster around the one-to-one ( $45^\circ$ ) line shown in light gray. Except for a slight overestimation of the index at bench scale, the two operational modes compare favorably in the Indianapolis – A experiments. The results from the bench to pilot comparisons support the premise that bench-scale testing can be used to successfully predict fouling behavior at the pilot scale.



**Figure 7.13 Matched pair analysis for three membrane-water combinations between Hollow-Fiber Unit 1 and the corresponding pilot-scale units. Expressed as the difference between the bench-scale index (UMFI, UMFI<sub>R</sub> or UMFI<sub>cleaning</sub>) and pilot-scale index (UMFI<sub>i</sub> or UMFI<sub>3000</sub> Method 2).**



**Figure 7.14 Correspondence between Hollow-Fiber Unit 1 and pilot-scale operation for three membrane-water combinations. The log transformed bench-scale index (UMFI, UMFI<sub>R</sub>, or UMFI<sub>cleaning</sub>) is plotted versus the log transformed pilot-scale index (UMFI<sub>i</sub> or UMFI<sub>3000</sub> Method 2) for each comparable run at pilot scale. A light gray line with slope = 1 is shown for reference.**

## CHAPTER 8

# SUMMARY AND APPLICATION TO UTILITIES

### SUMMARY OF PROJECT RESULTS

The overall goal of this project was to investigate the specific contributions of the different types and properties of NOM to MF/UF fouling with the intent to develop a surrogate test and/or index that could be used to predict NOM fouling through a combination of source water characterization and rapid bench-scale testing at low cost. Specific objectives included identifying and quantifying problematical NOM foulant(s); differentiating between hydraulically reversible versus irreversible fouling; determining the influence of membrane properties on fouling; evaluating pretreatment options to reduce NOM-related fouling; determining how membrane operating conditions influence fouling; and developing a predictive tool(s), either a surrogate parameter(s) or a fouling index, to estimate fouling potential.

#### Feed Water Characteristics

A number of different feed waters were selected for membrane testing, primarily based on different types of NOM: (1) allochthonous (terrestrially derived) NOM, (2) autochthonous (microbially derived) NOM, and 3) wastewater EfOM. These different NOM types were distinguished through analytical *signatures* including (1) DOC; (2) DON; (3) SUVA; (4) SEC-DOC, providing MW distribution and classification according to PS-DOC, HS-DOC, and LMA-DOC; (5) fluorescence excitation emission matrix, differentiating humic-like NOM from protein-like NOM and providing an FI distinguishing allochthonous NOM from autochthonous NOM; and (6) XAD-8/-4 resin chromatography, fractionating NOM according to HPO-DOC, TPI-DOC, and HPI-DOC. The hypothesis to be tested was that NOM character is more important than NOM amount and that foulant attributes correspond to higher DON, lower SUVA, higher PS-DOC, greater protein-like NOM, higher FI, and higher HPI-DOC (i.e., non-humic NOM).

Source waters included (1) the White River (Indianapolis), (2) a clarified, filtered secondary effluent (Scottsdale), (3) the Hillsborough River<sup>4</sup> (Tampa Bay); and (4) the Twente Canal (Netherlands); a more limited amount of testing was done with Lake Nicol (Tuscaloosa). Based on the hypothesis, the secondary effluent (low SUVA, high FI, high HPI-DOC) was deemed to have a high fouling potential as an EfOM source; the Hillsborough River (high DON) and Twente Canal (high PS-DOC) were deemed to have a medium fouling potential; and the White River was deemed to have a low fouling potential (this source was originally selected as a potential autochthonous source, but an anticipated algal bloom did not occur to the desired degree during the period of testing). While NOM characteristics are influential, NOM amount also plays a role in terms of the Hillsborough River (high DOC). Moreover, while a high DOC source (e.g., Hillsborough River) may have a low percentage of PS-DOC, the amount of PS-DOC can be significant.

---

<sup>4</sup>This source includes contributions from the Alafia River and the Tampa Bypass Canal.

## Membrane Properties

Three flat-sheet membranes were tested as disk specimens in stirred-cell testing; properties that were determined included (1) pore size/MWCO; (2) PWP; (3) contact angle, an index of surface hydrophobicity; (4) zeta potential, an index of surface charge; and (5) surface roughness by AFM. The specific membranes—a PVDF MF, a PAN MF/UF, and a PES UF—were selected as flat-sheet analogs of hollow-fiber membranes tested at both bench- and pilot-scales. The PVDF MF membrane exhibited the largest pore size, highest PWP, greatest contact angle, and highest roughness. The PAN MF/UF membrane exhibited a pore size intermediate to classical definitions of MF and UF, and the highest zeta potential.

Four hollow-fiber membranes were tested at both bench- and pilot-scale: (1) Membrane A (a PVDF MF), (2) Membrane B (a PVDF UF), (3) Membrane C (a PES/PVP UF), and (4) Membrane D (a PES UF) tested in earlier (D1) and later (D2) product forms. These membranes were also characterized according to pore size/MWCO, PWP, contact angle, and roughness. Streaming current was used to estimate IEP, and material composition was probed by pyrolysis GS/MS. Membrane A exhibited the largest pore size and greatest roughness; Membranes A and B exhibited the lowest IEP, corresponding to the greatest (negative) charge; and Membranes C and D1 exhibited the most hydrophilic character. Given a comparison of the properties of flat-sheet versus hollow-fiber properties, it was thought that the flat-sheet PVDF MF was a good analog of Membrane A; the bench-scale PAN MF/UF was a poor analog of the Membrane B; and the bench-scale PES UF was a fair analog of Membranes C and D. The hypothesis was that attributes of a low-fouling membrane would include higher surface charge and lower contact angle. Prediction of the impact of membrane pore size on NOM fouling tendency was not determined and was not a priority in this study.

## Unified Modified Fouling Index Concept

Because the traditional MFI was developed for constant pressure filtration, the concept of a UMFI was derived to quantify the fouling rate encountered not only in constant pressure, but also in constant flux filtration. The UMFI provides a basis for comparison of results derived from different units (e.g., stirred-cell versus hollow-fiber bench-scale units) and different scales (e.g., bench- versus pilot-scale). A value of UMFI ( $\text{m}^2/\text{L}$ ) is estimated from a data plot of inverse normalized specific flux versus hydraulic throughput ( $\text{L}/\text{m}^2$ ). There are several versions of the UMFI, as discussed below.

The general UMFI is calculated for experiments with a single, long period of filtration, specifically bench-scale testing with the flat-sheet stirred-cell unit and the hollow-fiber unit with a single end-of-run backwash operational mode. The UMFI is a measure of the total fouling capacity, but does not take the effects of hydraulic backwashing or chemical washing into account. The  $\text{UMFI}_i$  is used to assess the total fouling potential of a water for operational protocols involving multiple short periods of filtration, specifically hollow-fiber bench scale multi-cycle tests with multiple backwashes as well as pilot- and full-scale operation. The  $\text{UMFI}_i$  is calculated for the first filtration cycle of an experiment; the  $\text{UMFI}_i$  and UMFI are equivalent except that  $\text{UMFI}_i$  represents a shorter period of filtration. The short-term hydraulically irreversible portion of fouling is described by the  $\text{UMFI}_{150}$ , corresponding to results over a volumetric throughput of  $150 \text{ L}/\text{m}^2$ , for operational protocols involving multiple cycles of filtration interspersed by backwashing, namely multi-cycle bench scale as well as pilot- and full-scale operation. Long-term hydraulically irreversible fouling is described by the  $\text{UMFI}_{3000}$  for

pilot- and full-scale operation;  $UMFI_{3000}$  is similar to  $UMFI_{150}$ , except that the volumetric throughput is  $3000 \text{ L/m}^2$ . A major advantage of the  $UMFI_{3000}$  is that it includes at least one cleaning cycle for pilot-scale runs for which chemical washing was performed; the  $UMFI_{150}$  does not. Short-term hydraulically irreversible fouling in the hollow-fiber bench-scale tests with a single end-of-run backwash operational mode is described by the  $UMFI_R$ , and is comparable to the  $UMFI_{150}$  or  $UMFI_{3000}$  of multi-cycle bench-, pilot-, and full-scale operation. Chemically irreversible fouling is described by the  $UMFI_{\text{cleaning}}$  for the bench-scale end-of-run backwash operational mode. The  $UMFI_{\text{cleaning}}$  can be compared to the  $UMFI_{3000}$  for multi-cycle runs with chemical washing included their protocols.

## **Bench-Scale Membrane Filtration Tests**

Bench-scale membrane tests were performed using two approaches: stirred-cell tests with disk specimens of flat-sheet membranes operated under a constant pressure/declining flux mode of operation, and hollow-fiber tests using two different units (1 and 2) operated under an increasing pressure/constant flux mode of operation. Fouling trends were defined in terms of a UMFI as a means of comparing different units and scales of testing.

### ***Stirred-Cell Tests***

Stirred-cell experiments were performed with five source waters (Indianapolis, Scottsdale, Tampa Bay, Twente Canal, and Tuscaloosa) and one clarified water (Tuscaloosa), under a constant pressure/declining flux mode of operation using three membranes (PVDF MF, PAN MF/UF, and PES UF). For all three membranes evaluated as a function of volumetric throughput ( $\text{L/m}^2$ ), the Scottsdale, Tampa Bay, and Twente Canal waters showed significant flux decline while the Indianapolis water and both the untreated and clarified Tuscaloosa waters showed less flux decline. These results may be due to the high amount of DOC in the Tampa Bay water and the presence of problematical components in the Scottsdale and Twente Canal waters (PS-DOC and/or HPI-DOC). Among the three membranes, the PVDF MF membrane showed the least flux decline. Little benefit was realized in clarification because one water subjected to pretreatment (Tuscaloosa) contained low foulant levels. For all three membranes evaluated as a function of delivered DOC ( $\text{mg/m}^2$ ), the same general trends were observed with the following exceptions: (1) a lesser degree of fouling for the (high DOC) Tampa Bay water except for the PAN MF/UF membrane where Tampa Bay still showed significant fouling, and (2) a benefit of clarification was observed for the PVDF MF membrane with the Tuscaloosa water. An evaluation of fouling mechanisms showed a dominance of cake formation. In all cases, cake formation dominated for the PES UF membrane while, in several cases, pore constriction played a role in fouling of the PVDF MF membrane and, to a lesser extent, the PAN MF/UF. The PES UF and PAN MF/UF membranes showed that high molecular weight components were accumulated in the cell as a retentate during filtration or on the membrane surface and later recovered in a simulated backwash. The PVDF MF membrane did not indicate significant accumulation of high molecular components, likely because of its relatively larger pore size.

The qualitative trends indicated above were supported by corresponding UMFI values ( $\text{m}^2/\text{L}$ ) and trends. More than an order of magnitude in difference was observed for UMFI values, with higher values for the Scottsdale, Twente Canal, and Tampa Bay source waters, and the PES UF and PAN MF/UF membranes.

## ***Hollow-Fiber Unit 1***

The experimental matrix tested with Hollow-Fiber Unit 1 included four source waters (Scottsdale, Tampa Bay, Indianapolis, and Twente Canal) and four membranes (A, B, C, and D2). Regardless of the permeate flux, UMFI values were the greatest for Membranes A and C when the Tampa Bay water was filtered, and the least when the Indianapolis water was filtered. For Membranes B and D2, the Indianapolis water also gave the lowest UMFI for the four waters tested. However, the greatest UMFI values for Membrane B were observed with the Scottsdale water, not the Tampa Bay water. In comparison, UMFI values were similar and the greatest when the Scottsdale and Tampa Bay waters were filtered by Membrane D2. The results suggest that Scottsdale water and/or Tampa Bay water in general caused the greatest total fouling for all four membranes tested, while the Indianapolis water caused the least.

The trend for  $UMFI_R$  was somehow different from that for UMFI. The  $UMFI_R$  was the greatest for the Tampa Bay water and the least for the Indianapolis water with all membranes except Membrane B.  $UMFI_R$  values for Membrane A did not differ extensively with the four waters studied, although the values were slightly higher with the Scottsdale water. These results indicate that the hydraulically irreversible fouling was the worst for all membranes when the Tampa Bay water was filtered under the hydraulic conditions investigated, except for Membrane B. Interestingly, the Tampa Bay water appeared to be extremely problematic for Membrane A, the only microfiltration membrane tested in the study.

However, because the natural waters tested contained different concentrations of DOC, membrane-fouling trends were also examined in terms of delivered DOC ( $mg/m^2$ ) in addition to volumetric throughput ( $L/m^2$ ) that serves as the basis for the UMFI concept. Unlike the difference in UMFI and  $UMFI_R$  observed with different membranes, consistency in the relationship between total fouling and NOM source was found with all membranes tested from the perspective of delivered DOC. Regardless of the type of membrane, the Scottsdale water NOM resulted in the most severe fouling; the Tampa Bay water NOM produced the least. Considering the dominant NOM component of the waters, these data suggest that, under conditions employed in the study, EfOM exhibited the highest fouling potential, allochthonous NOM had the lowest fouling potential, and autochthonous NOM usually lay between the two. Given the Tampa Bay source, NOM amount (concentration) is also influential.

An increase of permeate flux usually resulted in a slight increase of UMFI and  $UMFI_R$ , indicating a positive relationship between membrane fouling (both total and hydraulically irreversible) and the permeate flux. However, the type or source of the NOM had a greater impact on membrane fouling than operating fluxes. This finding is different from earlier studies in regard to the importance of critical flux in membrane fouling, a result likely attributable to differences in the properties of the major foulants.

The hydraulic reversibility of NOM fouling reflects the possibility of fouling reduction using permeate backwash with an operational definition of hydraulically irreversible fouling.  $UMFI_R$  values were calculated based on the recovery of the permeate flux immediately after the first hydraulic backwash of a single-cycle experiment. In these and subsequent backwash flux experiments, the restoration of specific flux varied to different extents according to NOM source. Experiments were conducted to evaluate the effects on membrane fouling by single versus multiple backwash cycles. Generally, multi-cycle backwashing yielded similar levels of hydraulically irreversible fouling compared to single-cycle backwashing. The similarity in the permeability of the membranes after the first minute of filtration following backwash of the single cycle and the first minute of filtration of the final cycle in the multi-cycle experiments

suggest that the simpler single-cycle end-of-run backwash protocol can be used to simulate multi-cycle results.

Further assessment of the similarity of multi- and single-cycle bench-scale operations was performed by comparing various UMFI<sub>s</sub>. The total fouling is described by UMFI for single cycle and UMFI<sub>i</sub> for multi-cycle experiments. The hydraulically irreversible portion of the fouling is expressed as UMFI<sub>R</sub> for single-cycle and UMFI<sub>150</sub> for multi-cycle experiments. There was a good correspondence observed between each pair of UMFI values, furthering supporting the proposition that the bench-scale end-of-run backwash protocol does an equally good job of estimating hydraulically irreversible fouling as does the multi-cycle operation.

### ***Hollow-Fiber Unit 2***

Hollow-Fiber Unit 2 was used to test four source waters (primarily Twente Canal with limited work on Scottsdale, Tampa Bay, and Indianapolis) and three membranes (primarily Membrane C, with limited work on Membranes A, B, and D2). The main attribute of unit D2 versus D1 is its fully automated backwash capabilities; its major deficiency compared to unit D1 is that it can be operated only at a single flux (120 L/m<sup>2</sup>-hr).

Based on work with Membrane C and the four source waters, the fouling rate was lowest for the secondary effluent of the Scottsdale Wastewater Treatment Plant, was higher for the Twente Canal and the White River (Indianapolis) waters, and highest for the Tampa Bay water. These results differ from other bench-scale results in terms of a lower relative fouling potential for the Scottsdale water and a higher relative fouling potential for the Indianapolis water, possibly an artifact of shipping these waters across the Atlantic for testing in the Netherlands (only the Twente Canal water was a local source). Based on work with the Twente Canal water and the four membranes, it was observed that the two PVDF-membrane types (A and B) have similar fouling properties. However, the fouling rate of the two PES membranes (C and D2) is very different, likely due to a difference in material composition (Membrane C is made with a blend of PES and PVP, whereas Membrane D2 is only PES). These results are generally similar to results observed in other bench-scale testing. In evaluating pretreatment, the fouling properties of the Twente Canal water tested with Membrane C revealed an optimum coagulant dose of 2.5 mg Fe/L; at this concentration, there was hardly any irreversible fouling.

## **Pilot-Scale Testing and Full-Scale Plant Operations**

### ***Tier 1 Pilot Studies***

Tier 1 pilot-scale testing was performed at three sites in North America using three of the four source waters and hollow-fiber membrane types evaluated in this project: (1) Tampa Bay/Hillsborough River - PVDF UF (Membrane B); (2) Indianapolis/White River – PVDF MF (Membrane A); (3) Scottsdale/secondary effluent – PES UF (Membrane D1); and Vitens/Twente Canal – PES UF (Membrane C). Tampa Bay testing included raw and coagulated waters, and different flux rates, backwash flows, feedwater recoveries, and chemical wash regimes. Indianapolis testing included raw, coagulated, and clarified waters, and different flux rates, feedwater recoveries, coagulant doses and chemical wash regimes. Scottsdale testing comprised raw and coagulated waters, and different flux rates, feedwater recoveries, coagulants, coagulant doses and chemical wash regimes. The observed differences across the various pilot tests reflect both differences in operating conditions and feed water (NOM) characteristics.

At baseline flux and recovery conditions (90 L/m<sup>2</sup>-hr and 95 percent recovery at Tampa Bay and Indianapolis; 80 L/m<sup>2</sup>-hr and 90 percent recovery at Scottsdale; 50 L/m<sup>2</sup>-hr and 60 percent recovery at Vitens), the rate of fouling was highest at Scottsdale despite the less challenging operating conditions and lower DOC when compared to Tampa Bay. Similarly, the fouling rate was next highest at Vitens despite the least challenging operating conditions of flux and recovery. These results are generally consistent with the greater fouling potential of the polysaccharide, hydrophilic NOM fractions present in the Scottsdale effluent, White River, and Twente Canal waters, although the lower fouling potential result for Tampa Bay differs from that observed in the bench tests. Calcium, which has been shown to increase NOM fouling, was significantly higher in the Scottsdale, Indianapolis (White River), and Vitens (Twente Canal) sources.

Increasing flux and feedwater recovery for tests conducted on raw water increased fouling rate in all studies except Vitens, with the greatest impact observed at Scottsdale. At Tampa Bay and Indianapolis (both tested with PVDF membranes), increased flux and recovery caused comparable loss of flux, but the benefit was temporary; the long-term fouling rate was comparable to baseline conditions. Backwash flowrate (at equal recovery) did not materially improve rate of fouling. For PES Membrane D1 tested at Scottsdale, higher recovery caused a much greater rate of fouling than did higher flux, suggesting the backwash regime used with the inside-out flow configuration (no air scour) is not as effective in managing fouling from solids accumulation. For PES Membrane C piloted at Vitens, no increase in fouling rate was observed when flux was increased by 50 percent (from 50 to 75 L/m<sup>2</sup>-hr).

Of the different chemical wash regimes evaluated with Tampa, Indianapolis, and Scottsdale studies, the most significant reduction in fouling was observed using chlorine (sodium hypochlorite), followed by caustic (in combination with acid). Acid (citric) alone provided little or no impact. An evaluation of different CT conditions (combinations of chlorine dose and contact [soak] time) during chemical washing showed a non-linear relationship between flux recovery and CT, with a ten-fold increase in CT (from 1500 to 15,000 mg min/L) required to achieve a doubling of flux recovery at Indianapolis. The greater effectiveness of chlorine (which oxidizes a range of NOM compounds) versus caustic (which is effective in solubilizing the humic substance fraction) is consistent with industry's predominant use of hypochlorite chemical washes. The single chemical wash regime (HCl followed by caustic) was not employed on a fixed permeate throughput basis, but instead at a trigger TMP (30 kPa) and was effective in stabilizing flux when used with increasing frequency.

Coagulation had a beneficial effect on NOM fouling in all studies, but the effect was dependent on coagulant dose and feedwater recovery. For Tampa Bay, ferric coagulation reduced flux decline at 90 percent recovery, but increased it at 95 percent recovery. Incorporating a phosphoric chemical wash with coagulation allowed for improved performance at the higher recovery. For Indianapolis, alum coagulation reduced fouling at low dose (5-15 mg/L) but increased it at high dose (30 mg/L). At Scottsdale, coagulation using PACl was beneficial at low and high doses (15 and 85 mg/L), with the larger dose providing the greatest fouling reduction. Ferric coagulation (25 mg/L) provided a reduction intermediate to the two PACl doses. Considering the high solids loading resulting from 85 mg/L PACl dosing, it is surprising the (inside-out) PES membrane showed such a significant fouling reduction considering the negative impact observed when this membrane was operated at high (95 percent) recovery. For Vitens, a very low dose of coagulant (1 mg/L Al) showed only a temporary benefit (300 L/m<sup>2</sup> permeate throughput on specific flux).

As expected, clarification (alum coagulation, flocculation, and sedimentation) was more effective in reducing NOM fouling than coagulation alone (at Indianapolis [PVDF]). Specific flux loss was more than 50 percent lower at 5000 L/m<sup>2</sup> of permeate throughput. However, the reduction in fouling caused by increased flux and increased recovery was more severe with lower solids clarified water than with raw water. When clarification was coupled with chemical washing, the relative benefits of acid, caustic, and chlorine washing on flux recovery were similar to that observed with raw water; however, the degree of benefits derived from chlorine washing was reduced.

Vitens testing examined the impact of flux, coagulation, and chemical wash regimes on NOM fouling rate. Operation at 50 percent higher flux (with 1 mg/L Al coagulation) showed no benefit on fouling; likewise, operation at baseline with the absence of coagulation had little impact after a low coagulant dose (1 mg/L Al) showed decreased fouling rate in the short term (initial 300 L/m<sup>2</sup>).

NOM characterization by SEC-DOC of feed, permeate, and backwash from the three pilot studies showed similar and consistent results. PS is the only NOM fraction appreciably retained by the MF and UF membranes. Upon backwashing, this fraction is readily displaced and highly concentrated in the backwash water, indicating that PS fouling is largely hydraulically reversible. Coagulation is effective in converting a significant portion of all three fractions (PS, HS, and LMA) from soluble to particulate, thereby reducing the amount of soluble NOM available to cause membrane fouling.

### ***Tier 2 Pilot Studies***

Tier 2 pilot studies were limited to three locations (Tuscaloosa, Ala.; Minneapolis, Minn.; and North Bay, Ont.) where testing was conducted with either multiple (two MF and one UF PVDF at Tuscaloosa) or single membrane types (PES UF at Minneapolis and PVDF MF at North Bay). The source waters at these locations contained predominantly allochthonous NOM. At Tuscaloosa, the tighter UF membrane showed a higher rate of fouling than the two MF membranes, possibly due to a greater amount of PS retention. SEC-DOC analyses showed significant PS and lesser HS retention by the UF membrane, with both fractions highly concentrated in the backwash water. At Minneapolis, the treatment sequence of lime softening/recarbonation/ferric coagulation/clarification was effective in reducing all three SEC-DOC NOM fractions, but reduction was greatest for PS, considered to be the most fouling. Increased frequency of chemical washing was shown to be beneficial in reducing the rate of fouling. For North Bay, the use of high CT chlorine washes was very effective in reversing NOM flux loss. SEC-DOC NOM fractionation results were consistent with those from other bench and pilot studies; the PS fraction was well retained by the MF membrane and effectively removed during backwashing.

### ***Full-Scale Plant Operations***

Evaluation of NOM fouling contribution and impacts on performance of full-scale MF plants at Manitowoc, Wis. and Parsons, Kan. was constrained by the absence of NOM characterization data. Rates of fouling in both plants were low, however. Although NOM levels in Parson's raw water supply are significant (8 to 12 mg/L), chemical clarification reduces these levels significantly (to < 2 mg/L). Although no SEC-DOC characterization was performed on MF process samples, it is anticipated that with this level of DOC removal, that PS fraction

removal is very high, thereby resulting in a low NOM fouling potential for the clarified water. NOM (DOC) levels in the Manitowoc plant feed (Lake Michigan) are low (< 2 mg/L), suggesting that NOM fouling potential is low.

## MEMBRANE AUTOPSIES

Autopsies were performed on membrane fibers harvested from both bench- and pilot-scale testing of hollow-fiber membranes. Autopsy tools included (1) contact angle, (2) FESEM, providing a visualization of foulant deposition, (3) FTIR, (4) pyrolysis GC/MS of extracted foulant, and (5) elemental (C and N) composition of extracted foulant.

As a general rule, there were only small changes (increases) in contact angle before and after fouling. In bench-scale testing with less severely fouled membranes, the contact angle slightly decreased when fouled with autochthonous NOM or EfOM for more hydrophobic membranes. A slight increase was observed when membranes were fouled with allochthonous NOM. In pilot testing with more severely fouled membranes, contact angle slightly increased for a hydrophobic membrane and either an autochthonous or an allochthonous NOM source. It was concluded that contact angle is not a very revealing autopsy tool.

FESEM images were made of both the external and internal surfaces of the fibers autopsied after fouling. For Membrane B (outside-in configuration) with an allochthonous source, FESEM images did not show clear evidence of an organic deposit at the external (filtration) surface of the fibers. For an autochthonous source filtered with Membrane A (outside-in configuration), the results led to the same observation. More surprisingly, for both the allochthonous and autochthonous sources, a deposit was observed at the inner surface of the fibers, with material possibly corresponding to microbial entities (algae and/or bacteria), particularly for the autochthonous source where algae were observed during the period of testing. For Membrane D1 (inside-out configuration), there was some evidence of microbial accumulation on the inner (filtration) surface.

Fouling material was recovered from the hollow fibers using sonication in Milli-Q water and lyophilisation. Material isolated from fouled membranes was found to be relatively poor in organic material. NOM present in natural waters typically has a carbon content ranging from 40 to 55 percent; material isolated from fouled membranes did not exceed 15 percent of organic carbon. A high N/C ratio was found in foulant extracted from Membrane D1, fouled with secondary effluent.

Most of the FTIR spectra of extracted foulant indicated the presence of organic matter derived from bacterial origin (aminosugars, proteins, lipids).

All of the pyrochromatograms of extracted foulant showed strong indicators of the presence of natural biopolymers with the presence of peaks that are produced from the thermal degradation of proteins, sugars, aminosugars, and lignin-type structures.

The autopsy results are generally supportive of the findings related to feed-water NOM composition in which EfOM or autochthonous NOM characteristics were found to correspond to a higher fouling potential.

## STATISTICAL ANALYSES

From the different scales of membrane filtration tests (stirred-cell tests, bench-scale Hollow-Fiber Unit 1 tests, and pilot tests), several parameters associated with NOM characteristics and membrane properties were identified and quantified for statistical analyses.

Statistical analysis was employed to identify the parameters that contribute most significantly to low-pressure membrane fouling by NOM. Methods used for the statistical analyses included simple linear correlation/correlation matrix, probability frequency distribution, multiple linear regression, and PCA.

### **Simple Linear Correlation/Correlation Matrices**

Correlation matrices based on stirred-cell test data showed that PS-DOC and HPI-DOC are more highly correlated to UMFI than other independent variables. HS-DOC and HPO-DOC are poorly correlated with UMFI. These results confirm the greater influence of non-humic over humic NOM in low-pressure membrane fouling. No clear trends emerged in term of the influence of membrane properties on UMFI. Correlation matrices based on hollow-fiber bench-scale tests demonstrated the highest (inverse) correlation between zeta potential and both UMFI, an index of total fouling, and  $UMFI_R$ , an index of (short-term) hydraulically irreversible fouling. This inverse relationship suggests the merits of a (negatively) charged membrane. No clear trends emerged from correlation matrices based on data from pilot tests.

### **Probability Frequency Distributions**

Probability frequency distributions of UMFI values among the various tests revealed that pilot testing results show a more narrow distribution of UMFI than stirred-cell or hollow-fiber bench tests. This reflects the fact that stirred-cell and hollow-fiber (bench-scale) UMFI values represent total membrane fouling (which have higher values) versus pilot  $UMFI_{150}$  and  $UMFI_{3000}$  values, which represent hydraulically reversible fouling only. Hollow-fiber (bench-scale)  $UMFI_{150}$  values are intermediate because of shorter-term, hydraulically reversible fouling. The narrower distribution for pilot-scale results indicate that reversible fouling is quite consistent (in terms of fouling rate) across all the source water types.

### **Multiple Linear Regression**

Multiple linear regression analysis based on stirred-cell tests showed that UMFI is best explained by PS-DOC, FI (a higher FI value reflects autochthonous [microbially derived] NOM), and (inverse) zeta potential. These results confirm some of the correlation matrix trends. Multiple regression analysis based on hollow-fiber bench-scale tests indicates that HPI-DOC, (inverse) zeta potential, and surface roughness best explain UMFI.

### **Principal Component Analysis**

PCA was used to address three questions:

- Which feed water NOM characteristics most affect membrane fouling?
- Which membrane properties most influence fouling?
- Which membrane operating conditions most influence fouling?

The Scottsdale and Twente Canal feed waters clustered together and corresponded with higher UMFI values, inferring higher fouling tendency. These waters reflect significant levels of PS-DOC, HPI-DOC, and/or DON. Even though the Tampa Bay feed water has a high DOC concentration (~17 mg/L), its fouling tendency is less than the Scottsdale and Twente Canal

waters. Thus, PS-DOC and HPI-DOC are closely related to UMFI values, and related to significant membrane fouling. This is consistent with the multiple linear regression analysis.

Based on PCA analysis of membranes tested in stirred-cell tests, clustering of results suggest that the PES UF exhibited the highest fouling tendency followed by the PAN MF/UF and the PVDF MF membrane, with the progression toward a larger pore size. Zeta potential appears to be inversely related to UMFI. Thus, fouling appears to be dominantly affected by pore size of the membrane in stirred-cell tests (without backwashing). Based on membranes tested in hollow-fiber membranes, smaller pore size and a less negatively charged membrane correspond to higher UMFI and  $UMFI_R$  values, indicating a higher fouling tendency. Membrane D2 has the highest fouling tendency, and also has the smallest pore size and the lowest zeta potential. In contrast, Membrane A provides the least fouling tendency, and has the largest pore size (0.1  $\mu\text{m}$ ) and the highest zeta potential.

Based on PCA analysis of pilot test results, different backwash flux (high and normal) conditions and pretreatments by alum coagulation and ferric coagulation were evaluated. Data clustering suggested that high backwash flux reduces membrane fouling through removal of a reversible cake layer from the membrane surface, and a high recovery condition increases membrane fouling. Most data points corresponding to filtration with treated water were clustered in regions corresponding to low fouling tendency.

## **UMFI COMPARABILITY AND SCALE-UP**

Matched paired analyses was used to address important scale-up questions:

- Do UMFI values derived from stirred-cell tests simulate (predict) UMFI trends based on Hollow-Fiber Unit 1 bench-scale test?
- Do UMFI values derived from Hollow-Fiber Unit 1 bench-scale tests simulate (predict) UMFI trends based on pilot-scale tests?

## **Stirred-Cell versus Hollow-Fiber Bench-Scale Results**

Matched pair analysis was used to compare stirred-cell flat-sheet results and hollow-fiber bench-scale results corresponding to end-of-run backwash experiments. Three sets of comparisons were performed, based on membrane type. Membrane pairings were (1) PVDF Membrane B with the PAN MF/UF, (2) PVDF Membrane A with the PVDF MF, and (3) PES Membranes C and D1 with the PES UF. The highest flux run for each membrane/source water combination in Hollow-Fiber Unit 1 baseline testing was used for comparison as it best approximated the flux range used in the constant pressure/declining flux operational mode of the flat-sheet stirred-cell unit. The hollow-fiber and flat-sheet tests were found to be statistically different in all cases. The PVDF Membrane B versus PAN MF/UF comparison showed the greatest similarity, although still not statistically different. These comparisons support the assertion that flat-sheet membranes chosen for this research do not serve as good surrogates of the hollow-fiber membranes tested at bench scale.

## Hollow-Fiber Bench-Scale versus Pilot-Scale Results

Matched pair analysis was used to compare UMFI results from hollow-fiber bench-scale versus pilot-scale experiments for each of three membrane/source water combinations. The experiments with Scottsdale water showed a distinct difference between pilot and bench scale, with consistently higher index values for the bench-scale unit. This difference is likely attributable to differences in the properties of Membranes D2 and D1, used at the pilot and bench scales, respectively, with Membrane D2 exhibiting higher fouling potential due to the absence of the PVP co-polymer. No difference was observed between bench-and pilot-scale for the Tampa Bay/Membrane B combination. The best correspondence between bench- and pilot-scales was observed with the Indianapolis water/Membrane A tests. The results from the bench- to pilot-scale comparisons generally support the premise that bench-scale testing incorporating backwashing can be used to successfully predict longer-term fouling behavior at the pilot scale.

## APPLICATION TO UTILITIES

One of the major outcomes of this research was the demonstration of the importance of the high molecular weight PS fraction, and to a lesser extent, HS fraction, to the fouling of MF/UF membranes. While the historical perspective has been that humic substances cause fouling, HS fouling is only significant in the cases of very high concentrations (e.g., the Tampa Bay water) and/or the presence of high levels of calcium. The use of SEC in combination with DOC measurement provides a valuable analytical tool for the water industry by allowing quantification of these fouling fractions in the context of the overall DOC level of a given source water. Although SEC-DOC analysis is not a routine analytical procedure, when used in conjunction with more conventional treatment process evaluation techniques such as jar testing, it can provide a valuable means to quickly assess the NOM fouling potential of a source water and the effectiveness of different preliminary treatment processes (i.e., coagulation, coagulation/sedimentation, powdered activated carbon) to reduce this fouling potential. Clearly, the presence of high PS-DOC, that is, an attribute of a eutrophic (algal-impacted) source, a wastewater effluent, or wastewater-impacted source, is a warning sign about the fouling potential of a source water.

A second and probably more important outcome of this research is the development of a quantitative unified modified fouling index that can be used to measure the fouling potential of a source water rapidly at relatively low cost. The research reported herein has shown that measurement of the short-term, hydraulically reverse fouling rate (e.g.,  $UMFI_{150}$ ) using a bench-scale apparatus employing hollow-fiber membranes can predict the longer-term fouling rate of similar membranes observed at pilot scale with reasonable accuracy. The use of  $UMFI_{150}$  represents an important advancement in predicting NOM fouling of low-pressure membranes and provides a cost-effective means of evaluating different approaches to reducing such fouling and improving the economics of low-pressure membrane implementation when coupled with conventional process evaluation tools such as jar testing.

To make full use of the UMFI<sub>150</sub> as a predictive fouling tool, it will be necessary for the manufacturers of hollow-fiber membranes currently used for drinking water production and wastewater reuse to manufacture modules of a size that is compatible with a bench-scale testing apparatus. This will enable standardization of testing techniques and more precise and reproducible fouling measurements.

## **APPLICATIONS POTENTIAL**

The UMFI is a concept that can potentially be embraced by the membrane industry, both manufacturers and end-users, as a predictive tool for fouling, much like the silt density index is now used widely for RO fouling prediction. However, a necessary first step will be standardization of the protocol.

With the recent commercialization of the SEC-DOC approach (marketed as liquid chromatography with organic carbon detection [LC-OCD]), this innovative technique will become more common at both commercial and utility laboratories over the next decade. Given its spectrophotometric basis, there is an opportunity for fluorescence EEM to evolve into an on-line technique for process control.

## **RECOMMENDATIONS FOR FUTURE RESEARCH**

Additional research is recommended to more fully demonstrate the efficacy of the UMFI concept through a more comprehensive evaluation of coupled bench-, pilot-, and full-scale parallel testing on a common source using membranes have similar materials and characteristics (pore size, zeta potential, contact angle). Such research should examine a wider range of commercially available hollow-fiber membranes and explore the feasibility of incorporating backwashing into the stirred-cell test protocol in combination with flat-sheet membranes that are better hollow-fiber analogs, particularly for PES UF membranes. This testing should be accompanied by comprehensive characterization of NOM, using the methods employed in this research as well as more typical analyses for particulate and inorganic contaminants.

## **WHAT IS THE TAKE HOME MESSAGE?**

The primary objective of this study was to develop an analytical protocol consisting of a suite of tools and/or a surrogate test to provide a basis for understanding, and potentially predicting, NOM-related fouling.

The analytical tools provide quantitative and qualitative measures of NOM constituents and/or properties: DOC (NOM amount), SUVA (NOM character), DON (NOM N-content), SEC-DOC fractions (PS-DOC, HS-DOC, and LMA-DOC), XAD-8/-4 DOC fractions (HPO-DOC, TPI-DOC, and HPI-DOC), and fluorescence. EEM spectral trends (protein-like NOM, humic-like NOM, and FI) can potentially describe NOM-related foulants according to their size, structure, and functionality, as well as source (origin).

The surrogate test corresponds to various versions of a UMFI derived from bench-scale membrane filtration tests, with those tests based on a hollow-fiber (as opposed to stirred-cell) protocol representing the recommended surrogate test. The resultant UMFI<sub>i</sub> is a measure of total fouling capacity, but it does not account for the effects of hydraulic backwashing or chemical cleaning that are typically incorporated into pilot- and full-scale systems. The UMFI<sub>150</sub> describes the short-term hydraulically irreversible portion of fouling for multiple cycles of filtration over a

designated volumetric throughput (150 L/m<sup>2</sup>), while the UMFI<sub>R</sub> represents the short-term hydraulically irreversible fouling for a single end-of-run backwash. Ideally, a feed water with a low NOM-fouling potential would reflect low values of all UMFI indices. However, a feed water with a high value of UMFI<sub>i</sub>, regardless of corresponding values of UMFI<sub>150</sub> and UMFI<sub>R</sub>, is problematical because it reflects poor filterability; statistical analysis revealed a strong correlation between UMFI<sub>i</sub> and UMFI<sub>R</sub>, implying that poor filterability leads to hydraulically irreversible fouling.

### **What is/are the problematical NOM foulant(s)?**

Polysaccharide- and protein-like NOM, analytically revealed by both SEC-DOC and fluorescence EEM, represent the most problematical foulants, occurring in both macromolecular and colloidal forms. Feed waters dominated by these NOM constituents generally exhibit lower SUVA values than those dominated by humic substances; thus, a first warning sign of fouling potential is a low SUVA value. Protein-like NOM also is manifested in a higher DON level while polysaccharide-like NOM is also captured by a higher HPI-DOC level. While these foulants are partially amenable to hydraulic reversibility, they adversely affect the feed-water *filterability*, adversely affecting the length of a filtration cycle (between backwashes) and the associated loss of permeability during a cycle. The presence of calcium, unlike its adverse effect on NOM fouling of high pressure membranes, does not appear to be an influential factor in NOM fouling of low-pressure membranes, most likely because it is not inherently retained by the MF/UF membranes.

### **What is the NOM-related fouling potential of different types of waters?**

The presence of polysaccharide-like and/or protein-like foulants is more pronounced in NOM of a microbial origin, i.e., autochthonous/algal organic matter or effluent organic matter than in allochthonous (terrestrial) NOM. While NOM *character* is more important than amount, allochthonous sources with a high DOC level (e.g., the Tampa Bay source) can cause significant fouling.

### **Which foulant(s) contribute(s) to hydraulically reversible versus irreversible fouling?**

The highest degree of hydraulically irreversible fouling was observed for an allochthonous NOM source (Tampa Bay); however, it is difficult to generalize this trend to allochthonous sources in general because of the very high DOC of this source. It is noteworthy that UMFI<sub>R</sub> and UMFI<sub>150</sub> values generally showed some correlation, implying that the magnitude of hydraulically irreversible fouling is not affected by the number of backwash cycles; however, frequent backwashing is necessary to maintain adequate permeability.

### **Which foulant(s) contribute(s) to chemically reversible versus irreversible fouling?**

Polysaccharide-like foulants are neutral in character and interact with a membrane through either hydrogen bonding (a weak association) or, in a colloidal form, contribute to a cake/gel/layer. Protein-like foulants are amphoteric (possessing both negatively and positively charged functional groups) and interact with a membrane surface through either dipole interactions or, in colloidal form, contribute to a cake/gel layer. The definition of chemical reversibility is operationally defined in terms of the specific cleaning agent(s) employed, with chlorine generally being more effective than caustic. The traditional NOM cleaning agent, caustic, would be more appropriate for desorbing humic-like foulants, although some benefit may be realized for protein-like foulants that become more negative at higher pH. Otherwise, there are clear merits to chlorine as an oxidizing agent in targeting polysaccharide (neutral) foulants. If NOM foulants are present in a colloidal form, hydraulic backwashing alone may be adequate.

### **How do membrane properties affect fouling?**

While this issue was not a primary focus of the study, it appears that a negative zeta potential (surface charge) is a positive attribute of a lower fouling membrane. Pore size also appears to have an effect on fouling mechanism, with greater hydraulically irreversible fouling observed for smaller pore size, implying that UF is more prone to hydraulically irreversible fouling than MF. Caution is urged in interpreting this trend because the two membranes with the smallest pore size were PES versus PVDF for the two membranes with the largest pore size. Consequently, the ability to distinguish between the impact of membrane material and pore size could not be adequately determined.

### **What pretreatment options can reduce NOM fouling?**

Coagulation/flocculation can remove polysaccharide- and protein-like NOM; at high coagulant doses, clarification may be necessary. However, if NOM fouling is hydraulically reversible, then coagulant addition may simply lead to added resistance and an associated decrease in permeability. Although only limited bench testing was done, there appears to be little benefit of powdered activated carbon (PAC).

### **How do membrane operating conditions affect NOM fouling?**

As expected, higher flux and/or recovery can exacerbate NOM fouling. Given the moderately favorable hydraulic reversibility of polysaccharide- and protein-like foulants, higher backwash rates are beneficial. Given the neutral (polysaccharide) or amphoteric (protein) character of NOM foulants, caustic cleaning, more appropriate for humic substances, is less effective than chlorine. However, the type or source of the NOM has a greater impact on membrane fouling than operating fluxes. NOM-related fouling can be minimized by conservative operation in terms of flux, recovery, and backwash flux; however, such conservatism increases membrane system capital and operating costs.

## **APPENDIX: PROJECT DATABASE**

The project database is provided as an electronic file included in the CD provided with this document.



## REFERENCES

- Aiken, G.R., F.H. Frimmel, and R.F. Christman. 1988. A Critical Evaluation of the Use of Macroporous Resins for the Isolation of Aquatic Humic Substances. *Humic Substances and Their Role in the Environment*, John Wiley & Sons Limited, 15-28.
- Aiken, G., and Cotsaris, E. 1995. Soil and Hydrology: Their Effect on NOM. *Journal AWWA*, 87:1:36-45.
- Aiken, G.R., and J. Leenheer. 1993. Isolation and chemical characterization of dissolved and colloidal organic matter, *Chemistry and Ecology*, 8:135-151.
- Aiken, G.R., D.M. McKnight, K.A. Thorn, and E.M. Thurman. 1992. Isolation of hydrophilic organic acids from water using nonionic macroporous resins. *Organic Geochemistry*, 18(4):567-573.
- Aiken, G.R., E.M. Thurman, and R.L. Malcolm. 1979. Comparison of XAD Macroporous Resins for the Concentration of Fulvic Acid from Aqueous Solution. *Analytical Chemistry*, 51(11):1799-1803.
- Ambles, A. 2001. Methods to Reveal the Structure of Humic Substances. *Biopolymers*. Wiley-VCH Publisher, 325-348.
- American Public Health Association. 2005. Standard Methods for the Examination of Water and Wastewater. 21<sup>st</sup> edition.
- Amy, G. 2000. Class Note: Dept. of Civil, Environmental, Architectural Engineering, University of Colorado at Boulder.
- Amy, G., J. Cho, Y. Yoon, S. Wright, M.M. Clark, E. Molis, C. Combe, Y. Wang, P. Lucas, Y. Lee, M. Kumar, K. Howe, K-S Kim, J. Pellegrino, and S. Irvine. 2001. *NOM Rejection by, and Fouling of, NF and UF Membranes*. Denver, Colo.: AwwaRF and AWWA.
- Aptel, P., and C.A. Buckley. 1996. *Categories of Membrane Operations in Water Treatment-Membrane Processes*. McGraw-Hill, New York.
- Averett, R.C., J.A. Leenheer, D.M. McKnight, and K.A. Thorn. 1994. U.S. Geological Survey Water-Supply paper. 2373.
- Baker, A. 2001. Fluorescence excitation-emission matrix characterization of some sewage impacted rivers. *Environ. Sci. Tech.*, 35(5):948-953.
- Belfer, S., R. Fainchtain, Y. Purinson, and O. Kedem. 2000. Surface characterization by FTIR-ATR spectroscopy of polyethersulfone membranes-unmodified, modified and protein fouled. *J. of Mem. Sci.*, 172(1-2):113-124.
- Bian, R., Y. Watanabe, N. Tambo, and G. Ozawa. 1999. Removal of Humic Substances by UF and NF Membrane Systems. *Wat. Sci. Tech.*, 40(9):121-129.
- Bowen W., J. Calvo, and A. Hernandez. 1995. Steps of membrane blocking in flux decline during protein microfiltration. *J. of Mem. Sci.*, 101(1-2):153-165.
- Bowen, W.R., N. Hilal, R.W. Lovitt, and P.M. Williams. 1996. *Journal of Colloid and Interface Science*, 180(2):50-359.
- Braghetta, A., F.A. DiGiano, and W.P. Ball. 1997. Nanofiltration of Natural Organic Matter: pH and Ionic Strength Effects. *Journal of Environmental Engineering*: 123(7):628-641.
- Bruchet, A., C. Rousseau, and J. Mallevialle. 1990. Pyrolysis GC-MS for Investigating High Molecular Weight THM Precursors and Other Refractory Organics. *Journal AWWA*, 82(9):66-74.

- Carroll, T., S. King, S.R. Gray, B.A. Bolto, and N.A. Booker. 2000. The Fouling of Microfiltration Membranes by NOM after Coagulation Treatment. *Wat. Res.*, 34(11):2861-2868.
- Chan, R., V. Chen, and M. Bucknall. 2002. Ultrafiltration of Protein Mixtures: Measurement of Apparent Critical Flux, Rejection Performance, and Identification of Protein Deposition. *Desalination*. 146(1-3):83-90.
- Cho, J. 1998. Natural Organic Matter (NOM) Rejection by, and Flux-Decline of, Nanofiltration (NF) and Ultrafiltration (UF) Membranes. Ph.D diss. University of Colorado at Boulder.
- Cho, J., G. Amy, and J. Pellegrino, 1999. Membrane Filtration of natural organic matter: initial comparison of rejection and flux decline characteristics with ultrafiltration and nanofiltration membrane, *Wat. Res.*, 33(11):2517-2526.
- Cho, J., G. Amy, and J. Pellegrino. 2000. Membrane filtration of natural organic matter: factors and mechanisms affecting rejection and flux decline with charged ultrafiltration (UF) membrane. *J. of Mem. Sci.*, 164:89-110.
- Cho, J., G. Amy, J. Pellegrino, and Y. Yoon. 1998. Characterization of clean and natural organic matter (NOM) fouled NF and UF membranes, and foulants characterization. *Desalination*, 118(1-3):101-108.
- Combe, C., E. Molis, P. Lucas, R. Riley, and M. Clark. 1999. The effect of CA membrane properties on adsorptive fouling by humic acid. *J. of Mem. Sci.*, 154(1):73-87.
- Croué, J-P, G.V. Korshin, and M. Benjamin. 1999a. *Isolation, Fractionation and Characterization of Natural Organic Matter in Drinking Water*. Denver, Colo.: AwwaRF and AWWA.
- Croué, J-P, J-F Debroux, G. Aiken, J.A. Leenheer, and G.L. Amy. 1999b. Natural Organic Matter Isolates and Fractions: Structural Characteristics and Reactive Properties. In *Formation and Control of Disinfection By-Products in Drinking Water*, Edited by P.C. Singer. Denver, Colo.:AWWA.
- Croué, J-P, L. Grasset, S. Bacle, and V. Jacquemet. 2003. Nanofiltration Membrane Autopsy of a Full-Scale Unit: Characterization of the Organic and Inorganic Foulants. Presented at Membrane Technology Conference, Atlanta, Ga., March 2-5, 2003.
- Del Rio J.C., F. Martin, and F.J. González-Vila. 1996. Thermally assisted hydrolysis and alkylation as a novel pyrolytic approach for the structural characterization of natural biopolymers and geomacromolecules. *Trends in Analytical Chemistry*, 15(2): 70-79.
- Dietz, P., P.K. Hansma, O. Inacker, H.D. Lehmann, and K.H. Herrmann. 1992. Surface pore structures of micro- and ultrafiltration membranes imaged with the atomic force microscope. *J. of Mem. Sci.*, 65(1-2):101-111.
- Esparza-Soto, M. and P.K. Westerhoff. 2001. Fluorescence spectroscopy and molecular weight distribution. *Wat. Sci. Tech.*, 43(6):87-95.
- Fan, L., J. Harris, F. Roddick, and N. Booker. 2001. Influence of Natural Organic Matter Characteristics on the Fouling of Microfiltration Membranes. *Wat. Res.*, 35(18):4455-4463.
- Frimmel, F.H., Christman, R.F., Eds. 1998. *Humic Substances and Their Role in the Environment*. Chichester:Wiley-Interscience.
- Gonzalez-Vila, F.J., U. Lakes, and H-D Lüdemann. 2001. Comparison of the Information Gained by Pyrolytic Techniques and NMR Spectroscopy on the Structural Features of Aquatic Humic Substances. *Journal of Analytical and Applied Pyrolysis*, 8-59:349-359

- Gray, S., T. Tran, B. Bolto, and C. Ritchie. 2005. NOM composition: effect on microfiltration fouling. Presented at Membrane Technology Conference. Phoenix, Ariz., March 6-9, 2005.
- Habarou, H., J-P Croué, G. Amy, and H. Suty. 2005. Using HPSEC and Pyrolysis GC/MS to Characterize Organic Foulants from MF and UF Membranes During Algal Bloom. Presented at Membrane Technology Conference. Phoenix, Ariz., March 6-9, 2005.
- Her, N. 2002. Identification and Characterization of Foulants and Scalants on NF Membrane. Ph.D diss., University of Colorado at Boulder.
- Her, N., G. Amy, and C. Jarusutthirak. 2000. Seasonal Variations of Nanofiltration (NF) Foulants: Identification and Control. *Desalination*, 132 (1-3):143-160.
- Her, N., G. Amy, D. Foss, J. Cho, Y. Yoon, and P. Kosenka. 2002. Optimization of Method for Detecting and Characterizing NOM by HPLC-Size Exclusion Chromatography with UV and On-Line DOC Detection. *Environ. Sci. Tech.*, 36(5):1069-1076.
- Hermia, J. 1982. Constant Pressure Blocking Filtration Laws-Application to Power-Law Non-Newtonian Fluids. *Trans IChemE.*, 50:183-187
- Ho, C. 2001. Effects of membrane morphology and structure on protein fouling during microfiltration. Ph.D diss., University of Delaware.
- Ho, C. and A.L. Zydney. 2000. A Combined Pore Blockage and Cake Filtration Model for Protein Fouling during Microfiltration. *Journal. of Colloid and Interface Science*, 232(2):389-399.
- Hong, S. and M. Elimelech. 1997. Chemical and Physical Aspects of Natural Organic Matter (NOM) Fouling of Nonfiltration Membranes. *J. of Mem. Sci.*, 132 (2):159-181.
- Huber, S.A. and M. Gluschke. 1998. Instruments-Chromatographic Characterization of TOC in Process Water Treatment. *Ultrapure water*. 15(3):48-52.
- Hwang, C.J., S.W. Krasner, G.L. Amy, A. Bruchet, J-P Croué, and J.L. Leenheer. 2001. Polar NOM: Characterization, DBPs, Treatment. Denver, Colo.: AwwaRF and AWWA.
- Itoh, M., and Y. Magara. 2004. Accelerated Fouling Test of NF Membrane and Foulant Characteristics Using Small-Scale Pilot Plant. Presented at International Conference on Water Environmental Membrane Technology (WEMT), Seoul, Korea, June 7-10, 2004.
- Jacangelo, J.G., and C.A. Buckley. 1996. *Water Treatment Membrane Processes*. New York, McGraw-Hill.
- Jarusutthirak, C. 2002. Fouling and Flux Decline of Reverse Osmosis (RO), Nanofiltration (NF) and Ultrafiltration (UF) Membranes Associated with Effluent Organic Matter (EfOM) during Wastewater Reclamation/Reuse. Ph.D diss., University of Colorado at Boulder.
- Jones, K. and C. O'Melia. 2000. Protein and Humic Acid Adsorption onto Hydrophilic Membrane Surfaces: Effects of pH and Ionic Strength. *J. of Mem. Sci.*, 165(1):31-46.
- Jonsson, A. and B. Jonsson. 1995. Concentration Polarization and Fouling During Ultrafiltration of Colloidal Suspensions and Hydrophobic Solutes. *Separation Science and Technology*, 30(2):301-312.
- Jucker, C., and M.M. Clark. 1994. Adsorption of Aquatic Humic Substances on Hydrophobic Ultrafiltration Membranes. *J. of Mem. Sci.* 97:37-52.
- Kim, J.Y., H.K. Lee, and S.C. Kim. 1999. Surface Structure and Phase Separation Mechanism of Polysulfone Membranes by Atomic Force Microscopy. *J. of Mem. Sci.*, 163(2):159-166.
- Kou, R-Q, Z-K Xu, H-T Deng, Z-M Liu, P. Seta, and Y. Xu. 2003. Surface Modification of Microporous Polypropylene Membranes by Plasma-Induced Graft Polymerization of Alpha Allyl Glucoside. *Langmuir*, 19(17):6869-6875.

- Lee, N., G. Amy, H. Habarou, and J-C Schrotter. 2002. Identification and Control of Fouling of Low-Pressure (MF and UF) Membranes by Drinking-Water Natural Organic Matter (NOM). Presented at Membranes in Drinking and Industrial Water Production (MDIW) conference. Mülheim an de Ruhr, Germany, September 22-26, 2002.
- Lee, N., G. Makdissy, G. Amy, J-P Croué, H. Buisson, and J-C Schrotter. 2003. Morphological analysis of low-pressure membranes (MF/UF) fouled by NOM. Presented at AWWA Mem. Tech. Conf. (MTC), Atlanta, Ga., March 2-5, 2003.
- Lehtonen T., J. Peuravuori, and K. Pihlaja. 2000. Characterisation of Lake-Aquatic Humic Matter Isolated with Two Different Sorbing Solid Techniques: Tetramethylammonium Hydroxide Treatment and Pyrolysis-Gas Chromatography/Mass Spectrometry. *Analytica Chimica Acta*, 424:91-103.
- Lin, C.F., T.Y. Lin, and O.J. Hao. 2000. Effects of Humic Substance Characteristics on UF performance. *Wat. Res.*, 34(4):1097-1106.
- Maartens, A., P. Swart, and E.P. Jacobs. 1999. Feed-Water Pretreatment: Methods to Reduce Membrane Fouling by Natural Organic Matter. *J. of Mem. Sci.*, 163(1):51-62.
- Madaeni, S.S. 1997. An Investigation of the Mechanism of Critical Flux in Membrane Filtration Using Electron Microscopy. *Journal of Porous Materials*, 4(4):239-244.
- Makdissy, G., J-P Croué, H. Buisson, G. Amy, B. Legube. 2003. Organic Matter Fouling of Ultrafiltration Membranes. *Water Science and Technology: Water Supply*, 3(5/6):175-182.
- Marwah, A., K. Howe, K. Chiu, and S. Adham. 2005. Effect of Pretreatment on MF/UF Fouling by Foulants in Specific Size Ranges. Presented at Membrane Technology Conference. Phoenix, Ariz., March 6-9, 2005.
- McKnight, D.M., E.W. Boyer, P.K. Westerhoff, P.T. Doran, T. Kulbe, and D.T. Anderson. 2001. Spectrofluorometric Characterization of Dissolved Organic Matter for Indication of Precursor Organic Material and Aromaticity, *Limnol. Oceanogr.* 46(1):38-48.
- Neumann A.W., and R.J. Good. 1972. Thermodynamics of contact angles: I-Heterogeneous solid Surfaces. *Journal of Colloid and Interface Science*, 38(2):341-358.
- Ng, H.Y., Q. Li, and M. Elimelech. 2004. Organic Fouling of RO Membranes for Water Reuse: Role of Proteins and Polysaccharides. Presented at Water Environmental Membrane Technology (WEMT), Seoul, Korea, June 7-10, 2004.
- O'Melia, C.R., W. Becker, and K. Au. 1999. Removal of Humic Substances by Coagulation. *Wat. Sci. Tech.*, 40(9):47-54.
- Sainbayar, A., J.S. Kim, W.J. Jung, Y.S. Lee, and C.H. Lee. 2001. Application of Surface Modified Polypropylene Membranes to an Aerobic Membrane Bioreactor. *Environmental Technology*, 22(9):1035-1042.
- Saiz-Jimenez, C. 1994. Analytical Pyrolysis of Humic Substances: Pitfalls, Limitations and Possible Solutions. *Environ. Sci. Tech.*, 28(11):1773-1780.
- Schäfer, A.I., A.G. Fane, and T.D. Waite. 2000. Fouling Effects on Rejection in the Membrane Filtration of Natural Waters. *Desalination*, 131(1-3):215-224.
- Singer, P.C. 1999. Humic Substances as Precursors for Potentially Harmful Disinfection By-Products. *Wat. Sci. Tech.*, 40(9):25-30.
- Thurman, E.M. 1985. *Organic Geochemistry of Natural Waters*. Boston: Martinus Nijhoff/Dr. W. Junk Dordrecht, 497.

- Thurman, E.M., R. Malcolm, and G.R. Aiken. 1978. Prediction of Capacity Factors for Aqueous Organic Solutes Adsorbed on a Porous Acrylic Resin. *Analytical Chemistry*, 50(6): 775-779.
- U.S. Environmental Protection Agency. 1999. EPA Methods and Guidance for Analysis of Water, Version 2.0. EPA 821-C-99-004. June.
- Vrijenhoek, E.M., S. Hong, and M. Elimelech. 2001. Influence of Membrane Surface Properties on Initial Rate of Colloidal Fouling of Reverse Osmosis and Nanofiltration Membranes. *J. of Mem. Sci.* 188(1):115-128.
- Waite T.D., A.I. Schäfer, A.G. Fane, and A. Heuer. 1999. Colloidal Fouling of Ultrafiltration Membranes: Impact of Aggregate Structure and Size. *Journal of Colloid and Interface Science*, 212(2):264-274.
- Wiesner, M.R., and P. Aptel. 1996. *Water Treatment Membrane Processes*. New York: McGraw-Hill.
- Yuan, W., and A. Zydney. 1999. Humic acid fouling during microfiltration. *J. of Mem. Sci.*, 157:1-12.
- Zeman, L., and A. Zydney. 1996. *Microfiltration and Ultrafiltration Principles and Application*. New York:Marcel Dekker, Inc.
- Zeng, Y., Z. Wang, L. Wan, Y. Shi, G. Chen, and C. Bai. 2003. Surface Morphology and Nodule Formation Mechanism of Cellulose Acetate Membranes by Atomic Force Microscopy. *Journal of Applied Polymer Science*, 88(5):1328-1335.



## ABBREVIATIONS

Actiflo	sand-ballasted clarification process
ACS	American Chemical Society
AFM	atomic force microscopy
Ag-AgCl	silver-silver chloride
Al	aluminum
amu	atomic mass unit
AOM	algal organic matter
ATR-FTIR	Attenuated Total Reflection-Fourier Transform Infrared Spectroscopy
AWWA	American Water Works Association
AwwaRF	Awwa Research Foundation
$\alpha$ -Al <sub>2</sub> O <sub>3</sub>	alpha alumina
Br	bromine
BSA	bovine serum albumin
BW	backwash
° C	degrees Celsius
C	carbon
C-O	carbon-oxygen
C/min	degrees Celsius per minute
C/ms	Celsius per millisecond
C/N	carbon/nitrogen
C <sub>x</sub> (1, 2, 3, etc.)	conductivity element
Ca	calcium
Ca <sup>2+</sup>	calcium ion
CaCO <sub>3</sub>	calcium carbonate
CeO <sub>2</sub>	ceria
CH <sub>2</sub> -CF <sub>2</sub>	1,1-difluoroethylene
CIP	clean-in-place, cleaning-in-place
Cl <sub>2</sub>	chlorine
cm	centimeter
CMF-L	continuous microfiltration-low pressure
C-MF	coagulation-microfiltration
CT	product of chlorine dose times contact time
Cu <sup>2+</sup>	copper
CW	chemical wash
°	degrees
Da	Dalton
DBP	disinfection byproduct
DI	de-ionized
DOC	dissolved organic carbon
DOM	dissolved organic matter
DON	dissolved organic nitrogen

EEM	excitation emission matrix
EFM	enhanced flux maintenance
EfOM	effluent organic matter
Em	emission
<i>Environ. Sci. Tech.</i>	<i>Environmental Science &amp; Technology</i>
EPA	U.S. Environmental Protection Agency
EPS	extracellular polymer substances
eV	electron volt
Ex	excitation
Fe	iron
Fe <sub>2</sub> (SO <sub>4</sub> ) <sub>3</sub>	ferric sulfate
FeCl <sub>3</sub>	ferric chloride
FESEM	field emission scanning electron microscopy
FI	fluorescence index
FNU	Formazin Nephelometric Unit
ft	foot, feet
FTIR	Fourier Transformed Infrared (spectroscopy)
gal	gallon
GC	gas chromatography
GCD	gas chromatography detector
gfd	gallon per square foot per day
gff	glass fiber filter
γ-Al <sub>2</sub> O <sub>3</sub>	gamma alumina
h	hour
HCl	hydrochloric acid
HIF	hydraulically irreversible fouling
HP	Hewlett Packard
HPC	heterotrophic plate count
HPI	hydrophilic
HPLC	high-performance liquid chromatography, high-performance liquid chromatograph
HPO	hydrophobic
HS	humic substances
Hz	Hertz
IEP	isoelectric point
ICP	inductively coupled plasma
in	inch
JHU	Johns Hopkins University
<i>J. of Mem. Sci.</i>	<i>Journal of Membrane Science</i>
J <sub>s</sub>	Permeate Specific Flux
J <sub>s0</sub>	Initial Permeate Specific Flux

KBr	Potassium Bromide
KCl	potassium chloride
kD	kilo Dalton
kg	kilogram
kPa	kiloPascal
KHP	potassium hydrogen phthalate
L	liter
LC-OCD	liquid chromatography-organic carbon detection
LC-OND	liquid chromatography-organic nitrogen detection
<i>Limnol. Oceanogr.</i>	<i>Limnology and Oceanography</i>
LMA	low molecular weight acids
LPHF	low-pressure, hollow-fiber
L/m <sup>2</sup> -hr	liter per square meter per hour
ML/d	megaliters per day
M	molar
m	meter
m <sup>2</sup>	square meter
MF	microfiltration
MFI	membrane fouling index
MG	magnesium
mg	milligram
mgd	million gallons per day
MIB	2-Methylisoborneol
min	minute
mL	milliliter
ML	megaliter
mm	millimeter
mM	millimolar
Mn	manganese
MPa	megaPascal
MPU	Manitowoc Public Utility
MS	mass spectrometry
MV	millivolt
MW	molecular weight
MWCO	molecular weight cut off
μL	microliter
μm	micrometer
N	nitrogen
NaCl	sodium chloride
NaOCl	sodium hypochlorite
NaOH	sodium hydroxide
ND	not detected
NF	nanofiltration
NH <sub>4</sub>	ammonium

NIST	National Institute of Standards and Technology
nm	nanometer
NMR	nuclear magnetic resonance
NO <sub>2</sub>	nitrite
NO <sub>3</sub>	nitrate
NOM	natural organic matter
NTU	Nephelometric Turbidity Unit
OCWA	Ontario Clean Water Agency
OH	hydroxyl
OM	optical microscopy
o-PO <sub>4</sub> <sup>3-</sup> (PO <sub>4</sub> <sup>3-</sup> )	ortho phosphate ion
P-GC/MS	pyrolysis-gas chromatography/mass spectrometry
PAC	powdered activated carbon
PACl	polyaluminum chloride
PAN	polyacrylonitrile
PC	polycarbonate
PCA	principal component analysis
PCU	platinum cobalt unit
PE	polyethylene
PEG	polyethylene glycol
PES	polyethersulphone
PLC	programmable logic controller
POC	particulate organic carbon
POM	particulate organic matter
PP	polypropylene
ppb	parts per billion
ppm	parts per million
PS	polysaccharide
PSF	polysulphone
psi	pounds per square inch
psig	pounds per square inch gauge
PTFE	polytetrafluoroethylene
PVD	polyvinylidene
PVDF	polyvinylidene fluoride
PVP	polyvinyl pyrrolidene
PWP	pure water permeability
Ra	surface roughness based on arithmetic average calculation
RMS	root mean squared
RO	reverse osmosis
rpm	revolutions per minute
Rq	surface roughness based on root mean squared calculation
SASRF	simultaneous air scrubbing and reverse filtration
SCFM	standard cubic feet per minute

SEC	size-exclusion chromatography
SEC-DOC	size-exclusion chromatography with on-line dissolved organic carbon detection
SEC-DOC/UV	size-exclusion chromatography with an online connection of DOC and UV detectors
SEM	scanning electron microscopy
Si	silicon
SiO <sub>2</sub>	silicon dioxide
SO <sub>4</sub>	sulfate
SMP	soluble microbial products
SO <sub>2</sub>	sulfur dioxide
SO <sub>4</sub> <sup>2-</sup>	sulfate ion
STW	sewage treatment works
SU	standard units
SUVA	specific ultraviolet absorbance
SWC	Scottsdale Water Campus
TBRWTP	Tampa Bay Regional Water Treatment Plant
TDS	total dissolved solids
TEM	transmission electron microscopy
THM	thermally assisted hydrolysis and methylation
TiO <sub>2</sub>	titania
TMAH	tetramethyl ammonium hydroxide
TMP	transmembrane pressure
TN	total nitrogen
TOC	total organic carbon
TOM	total organic matter
torr	unit of pressure equal to one centimeter of mercury at 0 degrees Celsius
TPI	transphilic
<i>Trans IChemE</i>	<i>Korean Journal of Chemical Engineering</i>
2D	two-dimensional
3D	three-dimensional
UF	ultrafiltration
UMFI	Unified Modified Fouling Index
UV	ultraviolet
UVA	ultraviolet absorbance
v/v	by volume
V <sub>s</sub>	unit permeate throughput
varimax	variance maximizing
VVLP	hydrophilic polyvinylene difluoride disc membrane manufactured by Millipore Corp. under the brand name Durapore®

w/w	weight-by-weight
<i>Wat. Res.</i>	<i>Water Research</i>
<i>Water Sci. Tech.</i>	<i>Water Science and Technology</i>
WTP	water treatment plant
XAD	stryenic-macroporous-polymeric adsorbent resin manufactured by Rohm and Haas
ZrO <sub>2</sub>	zirconia
ZW	ZeeWeed





6666 West Quincy Avenue  
Denver, CO 80235-3098 USA  
P 303.347.6100  
[www.awwarf.org](http://www.awwarf.org)  
email: [info@awwarf.org](mailto:info@awwarf.org)

**Sponsors Research**  
**Develops Knowledge**  
**Promotes Collaboration**

**1P-2.25C-91208-04/08-NH**

ISBN 978-1-60573-007-3



9 781605 730073